LIMNOLOGY AND RESERVOIR DETENTION STUDY OF SAN VICENTE RESERVOIR

INTRODUCTION AND CONTENTS

San Vicente Reservoir (SVR) is located near Lakeside, California, and is used as a source of drinking water supply by the City of San Diego (City), its owner and operator. The reservoir currently has a capacity of about 90,000 acre-feet. It is undergoing an expansion that will raise the dam 117 feet and increase the reservoir's storage capacity to 247,000 acre-feet at the spillway level. The City is considering an option to augment the SVR supply by bringing advanced treated recycled water (*i.e*., purified water) from an advanced water purification facility to SVR. This would be an Indirect Potable Reuse / Reservoir Augmentation (IPR/RA) project. The purified water would be blended with other water in the reservoir. The current project – the Water Purification Demonstration Project (Demonstration Project) – will not actually put any purified water into the reservoir; rather it will study and model the reservoir augmentation process.

A component of the Demonstration Project is the Limnology and Reservoir Detention Study of San Vicente Reservoir (Limnology Study). For the Limnology Study, Flow Science Incorporated (FSI) has employed a numerical three-dimensional water quality model that is used to evaluate hydrodynamic and water quality effects of using purified water to augment SVR. The Limnology Study consists of four technical memoranda or TMs:

- TM #1 – calibration of the model
  (*Reservoir Augmentation Demonstration Project: Limnology and Reservoir Detention Study of San Vicente Reservoir - Calibration of the Water Quality Model, May 1, 2012*)
- TM #2 – hydrodynamic modeling
  (*Water Purification Demonstration Project: Limnology and Reservoir Detention Study of San Vicente Reservoir - Hydrodynamic Modeling Study, May 1, 2012*)
- TM #3 – nutrients and algae modeling results
  (*Water Purification Demonstration Project: Limnology and Reservoir Detention Study of San Vicente Reservoir – Nutrient and Algae Modeling Results, May 1, 2012*)
- TM #4 – proposed water quality monitoring plan
  (*San Vicente Reservoir Proposed Water Quality Monitoring Program, July 10, 2012*)

Flow Science Incorporated (FSI) began by developing [i.e., customizing or tailoring] the three-dimensional water model to conditions at SVR. The model was calibrated using measured data from SVR. After the model was developed its results were compared to existing field data. The results of this analysis were documented in a Technical Memorandum (TM #1) submitted to the City in 2010 and finalized in May 2012 (FSI, 2012a). TM #1 has been peer-reviewed by the National Water Research Institute Independent Advisory Panel (IAP) that was assembled for the review of the City's Demonstration Project. After implementing suggestions proposed by the IAP, the model was deemed by IAP to be "an effective and robust tool, for 1) simulating

thermoclines and hydrodynamics of the San Vicente Reservoir; 2) assessing biological water quality for nutrients; 3) assessing options for the purified water inlet location" (NWRI, 2010).

Upon completion of the SVR model calibration and validation, FSI conducted simulations of purified water delivery to the expanded SVR under various projected future operating conditions using the calibrated and validated model. The simulation results and findings are presented in two separate Technical Memorandums. TM #2 summarizes the hydrodynamic aspects of the modeling results, focusing on density stratification, mixing, and dilution in the reservoir. TM #2 was submitted to the City on November 28, 2011 and finalized in May 2012 (FSI, 2012b). TM #3 focuses on the water quality aspects of the modeling results and findings, with emphasis on nutrients (phosphorus and nitrogen), dissolved oxygen (DO), and algal productivity, and was submitted to the City on February 24, 2012 and finalized in May 2012 (FSI, 2012c). Both TM#2 and TM#3 have been peer-reviewed by the IAP (NWRI, 2012 a, b).

If SVR is augmented by purified water in the future, the three-dimensional model developed for the Limnology Study is expected to provide a tool for evaluating various reservoir management options, assessing residence time and dilution of the purified water within SVR, determining optimal reservoir operations for maximizing water quality, and minimizing any potential short-circuiting between the inlet and outlet. It is expected that the model will be updated on a yearly basis using new data collected each year. In order to update the model and maintain it as a tool for assessing reservoir water quality and operations, data collection in the reservoir, as well as its inflows and outflows, will be needed. TM #4 provides an outline of a reservoir monitoring plan to obtain these necessary data and was submitted to the City on June 21, 2012 and finalized in July 2012 (FSI, 2012d). Another goal of the monitoring plan is to identify monitoring efforts that may be needed to enhance water treatability and address future water quality regulatory issues.

REFERENCES

Flow Science Incorporated (2012a). "Reservoir Augmentation Demonstration Project: Limnology and Reservoir Detention Study of San Vicente Reservoir – Calibration of the Water Quality Model", FSI Project V094005, Pasadena, CA.

Flow Science Incorporated (2012b). "Water Purification Demonstration Project: Limnology and Reservoir Detention Study of San Vicente Reservoir – Hydrodynamic Modeling Study", FSI Project V094005, Pasadena, CA.

Flow Science Incorporated (2012c). "Water Purification Demonstration Project: Limnology and Reservoir Detention Study of San Vicente Reservoir – Nutrient and Algae Modeling Results", FSI Project V094005, Pasadena, CA.

Flow Science Incorporated (2012d). “San Vicente Reservoir Proposed Water Quality Monitoring Plan”, FSI Project V094005, Pasadena, CA.

National Water Research Institute (2010). “Findings and Recommendations of the Limnology and Reservoir Subcommittee Meeting for the Reservoir Augmentation Demonstration Project’s ‘Limnology and Reservoir Detention Study of the San Vicente Reservoir’ ” Memorandum from NWRI Independent Advisory Panel for the City of San Diego’s Indirect Potable Reuse/Reservoir Augmentation Demonstration Project, June 7, 2010.

National Water Research Institute (2012a). “Findings and Recommendations of the Limnology and Reservoir Subcommittee Meeting for the Reservoir Augmentation Demonstration Project’s ‘Limnology and Reservoir Detention Study of the San Vicente Reservoir’ ” Memorandum from NWRI Independent Advisory Panel for the City of San Diego’s Indirect Potable Reuse/Reservoir Augmentation Demonstration Project, February 22, 2012.

National Water Research Institute (2012b). “Findings and Recommendations of the Limnology and Reservoir Subcommittee Meeting for the Reservoir Augmentation Demonstration Project’s ‘Limnology and Reservoir Detention Study of the San Vicente Reservoir’ ” Memorandum from NWRI Independent Advisory Panel for the City of San Diego’s Indirect Potable Reuse/Reservoir Augmentation Demonstration Project, April 24, 2012.

Flow Science Incorporated
420 Neff Avenue, Suite 230, Harrisonburg, VA 22801
(540) 442-8433 • FAX (540) 442-8863

Reservoir Augmentation Demonstration Project: Limnology and Reservoir Detention Study of San Vicente Reservoir - Calibration of the Water Quality Model

Prepared for
City of San Diego
600 B Street, Suite 600,
San Diego, CA 92101

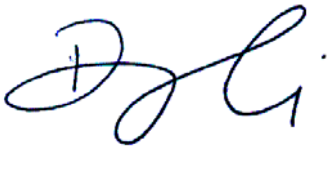

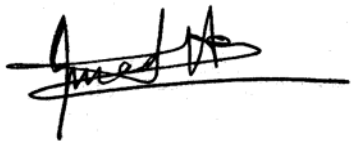

Prepared By
Li Ding, Ph.D., P.E. (VA)
Senior Engineer

Reviewed By
Imad A. Hannoun, Ph.D., P.E. (VA)
President

Reviewed By
E. John List, Ph.D., P.E.
Principal Consultant

FSI V094005
May 01, 2012

Table of Contents

SUMMARY **1**

1. INTRODUCTION **4**

1.1 Background and Objectives 4
1.2 Previous Studies 5
1.3 Technical Memorandum Organization 6

2. MODELING APPROACH AND SETUP **7**

2.1 ELCOM and CAEDYM Description 7
2.2 Approach 8
2.3 Model setup 8
2.3.1 Model Domain and Grid 8
2.3.2 Modeling Period 9
2.3.3 Model Inputs 9

3. ELCOM CALIBRATION **10**

3.1 Overview 10
3.2 ELCOM Calibration Setup 10
3.2.1 Computational Grid Setup and Initial Conditions 10
3.2.2 Flow Rate Inputs 11
3.2.3 Inflow Temperatures and Conductivity Inputs 12
Aqueduct Inflows 12
Runoff Inflows 12
Sutherland Reservoir Inflows 13
3.2.4 Meteorological Inputs 13
3.2.5 Outflow Port Openings 15
3.3 Calibration Results 17
3.3.1 Water Surface Elevation 17
3.3.2 Temperature 18
3.3.3 Conductivity 18
3.3.4 Animation of Aqueduct Tracer 19

4. ELCOM VALIDATION **20**

4.1 Field Tracer Studies 20
4.2 Model Validation Setup 20
4.2.1 Computational Grid and Model Inputs 20
4.2.2 Particle Settling 21
4.3 validation results 23

5. CAEDYM CALIBRATION **25**

5.1 Overview 25
5.2 CAEDYM Calibration Setup 25
5.2.1 Computational Grid Setup and Initial Conditions 25
5.2.2 Inflow Water Quality Inputs 26
Aqueduct Inflows 26
Runoff Inflows 27
Sutherland Reservoir Inflows 27
5.3 Calibration Results 28
5.3.1 Dissolved Oxygen 28
5.3.2 pH 29

5.3.3 Nutrients 29
5.3.4 Chlorophyll a and Secchi Depth 30
6. CONCLUSIONS AND DISCUSSION 33
7. REFERENCES 36
FIGURES 38
APPENDIX A: DESCRIPTION OF ELCOM/CAEDYM MODELS AND EVIDENCE OF VALIDATION A-1
APPENDIX B: HISTORICAL RESRVOIR DATA B-1
APPENDIX C: INPUTS FOR CALIBRATION - CALIBRATION/VALIDATION RESULTS C-1
APPENDIX D: LIST OF ANIMATIONS D-1

List of Tables

Chapter 3

Table 1 Details on the Composite Meteorological Data Used in the Model
Table 2 Available Withdrawal Elevations on Existing Outlet Tower
Table 3 Temperature Calibration Metrics
Table 4 Conductivity Calibration Metrics

Chapter 4

Table 5 Summary of Information on Tracer Studies
Table 6 Settling Velocity for Simulated Particle Groups

Chapter 5

Table 7 Dissolved Oxygen Calibration Metrics
Table 8 pH Calibration Metrics
Table 9 Secchi Depth Calibration Metrics

List of Figures

Figure 1 San Vicente Reservoir Plan View of Existing and Expanded Reservoir and Inflow/Outflow Locations
Figure 2 ELCOM-CAEDYM Schematic of Processes Modeled in ELCOM-CAEDYM
Figure 3 San Vicente Reservoir 5-m ELCOM Computational Grid
Figure 4 San Vicente Reservoir Measured/Modeled Inflow Volumes
Figure 5 San Vicente Reservoir Measured/Modeled Outflow Volumes
Figure 6 Map of Meteorological Stations
Figure 7 San Vicente Reservoir Station A – Simulated Temperature
Figure 8 San Vicente Reservoir Station A – Temperature Calibration
Figure 9 San Vicente Reservoir Station A – Measured Temperature Contours (2000-2007)
Figure 10 San Vicente Reservoir – Comparison of 2006 and 2007 Measured Aqueduct Inflow Rates and Temperatures
Figure 11 San Vicente Reservoir Station A – 2006-2007 Measured Temperature Profiles
Figure 12 San Vicente Reservoir Measured/Modeled Outflow Volumes
Figure 13 San Vicente Reservoir Station A – Temperature Calibration
Figure 14 San Vicente Reservoir Measured vs Simulated Water Surface Elevation
Figure 15 San Vicente Reservoir Station A – Water Temperature Calibration
Figure 16 San Vicente Resevoir Station A – Water Temperature Calibration
Figure 17 San Vicente Reservoir Scatter Plot of Measured vs Simulated Temperature
Figure 18 San Vicente Reservoir Station A – Conductivity Calibration
Figure 19 San Vicente Reservoir Station A – Conductivity Calibration
Figure 20 San Vicente Reservoir Scatter Plot of Measured vs Simulated Conductivity
Figure 21 San Vicente Reservoir 1995 Tracer Study Monitoring Stations
Figure 22 San Vicente Reservoir 1995 Tracer Studies – Percent of Total Initial Mass of Lanthanum in the Reservoir vs Time
Figure 23 San Vicente Reservoir a995 Tracer Studies – Simulated Mass Distribution of Particles
Figure 24 San Vicente Reservoir 1995 Tracer Studies – Percent of Total Initial Mass of Lanthanum in the Reservoir vs Time
Figure 24 San Vicente Reservoir Station A – Water Temperature in 1995 Winter Tracer Study
Figure 25 San Vicente Reservoir 1995 Tracer Winter Study – Measured vs Simulated Lanthanum Concentrations
Figure 26 San Vicente Reservoir 1995 Tracer Winter Study – Measured vs Simulated Lanthanum Concentrations
Figure 27 San Vicente Reservoir 1995 Winter Tracer Study – Measured vs Simulated Lanthanum Concentrations

Figure 28 San Vicente Reservoir 1995 Winter Tracer study – Measured vs Simulated Lanthanum Concentrations
Figure 29 San Vicente Reservoir Station A – Water Temperature Calibration
Figure 30 San Vicente Reservoir – Measured vs Simulated Lanthanum Concentrations
Figure 31 San Vicente Reservoir 1995 Tracer Study – Measured vs Simulated Lanthanum Concentrations
Figure 32 San Vicente Reservoir 1995 Summer Tracer Study – Measured vs Simulated Lanthanum Concentrations
Figure 33 San Vicente Resevoir 1995 Summer Tracer Study – Measured vs Simulated Lanthanum Concentrations
Figure 34 San Vicente Reservoir 100-m ELCOM-CAEDYM Computational Grid
Figure 35 San Vicente Reservoir Station A – Water Temperature Simulation
Figure 36 San Vicente Reservoir Station A – Conductivity Simulation
Figure 37 San Vicente Reservoir Station A – Dissolved Oxygen Calibration
Figure 38 San Vicente Reservoir Station A – Dissolved Oxygen Calibration
Figure 39 San Vicente Reservoir Scatter Plot of Measured vs Simulated Dissolved Oxygen
Figure 40 San Vicente Reservoir Station A – pH Calibration
Figure 41 San Vicente Reservoir Station A – pH Calibration
Figure 42 San Vicente Reservoir Scatter Plot of Measured vs Simulated pH
Figure 43 San Vicente Reservoir Station A – Soluble Reactive Phosphorus
Figure 44 San Vicente Reservoir Station A – Total Phosphorus
Figure 45 San Vicente Reservoir Station A – Ammonia
Figure 46 San Vicente Reservoir Station A – Nitrate
Figure 47 San Vicente Reservoir Station A – Total Nitrogen
Figure 48 San Vicente Reservoir Station A – Chlorophyll *a* Concentrations
Figure 49 San Vicente Resevoir Station A – Secchi Depth Calibration
Figure 50 San Vicente Reservoir Scatter plot of Measured vs Simulated Secchi Depth

SUMMARY

San Vicente Reservoir (SVR) is located near Lakeside, California, and is used as a source of drinking water supply by the City of San Diego (City), its owner and operator. The reservoir currently has a capacity of about 90,000 acre-feet. San Vicente Reservoir is undergoing an enlargement that will raise the dam 117 feet and increase the reservoir's storage to 247,000 acre-feet at the spillway level (or 242,000 acre-feet at the maximum operation level).

A water reuse project, entitled Reservoir Augmentation, is being studied by the City. If implemented at full-scale, Reservoir Augmentation would bring advanced treated recycled water from the North City Water Reclamation Plant to SVR via a pipeline. The advanced treated recycled water would be blended with other water in the reservoir. The current project – the Reservoir Augmentation Demonstration Project – will not actually put any advanced treated recycled water into the reservoir; rather it will study and demonstrate the Reservoir Augmentation process. A component of the Reservoir Augmentation Demonstration Project (Demonstration Project) is the Limnology and Reservoir Detention Study of San Vicente Reservoir.

As part of the Limnology Study, the City has requested that Flow Science Incorporated (FSI) develop a three-dimensional water quality model that can accurately predict hydrodynamics and water quality of the existing and expanded SVR. It is anticipated that this model will be utilized to (1) establish residence time requirement for advanced treated recycled water in the reservoir and assess the short-circuiting of the advanced treated recycled water to the outlet structure; and (2) evaluate the effects of the advanced treated recycled water on water quality and eutrophication in the reservoir. This Technical Memorandum focuses on the development, calibration and validation of the three-dimensional water quality model for SVR.

Flow Science used two comprehensive and coupled three-dimensional computer models to simulate the hydrodynamics and water bio-chemistry of SVR. The models include a three-dimensional hydrodynamic module (Estuary Lake and Coastal Ocean Model, or ELCOM) and a water quality module (Computational Aquatic Ecosystem DYnamics Model, or CAEDYM). ELCOM simulates water velocities, temperatures, concentrations of salinity (*i.e.*, conductivity) and tracers; CAEDYM computes changes in dissolved oxygen (DO), nutrients, organic matter, pH and chlorophyll *a*. The coupled models are used to study the spatial and temporal relationships between physical, biological, and chemical variables in SVR.

The modeling domain includes the existing portion of the reservoir as well as the proposed expanded portion of the reservoir. A fine grid with a horizontal resolution of 50 × 50 m was used in the ELCOM calibration while a coarse grid with a horizontal resolution of 100 × 100 m was used in the CAEDYM calibration. This was necessitated by the large computer requirements and the desire to limit computation time to several

days per model run for a two-year simulation. A variable grid size was used in the vertical dimension with a grid size of 1.64 ft (0.5 m) near the surface, and expanding in size with depth. The calibration was conducted for the two-year period of 2006-2007. The input data required by the calibration were either based on measured data or derived from these data. ELCOM requires limited calibration effort in that the physical aspects of water movements in reservoirs are fairly well understood. The CAEDYM model was calibrated by adjusting some model bio-chemical parameters so that the simulation results best match measured field data.

The calibrated/validated ELCOM model shows good agreement with the measured data for both water temperature and conductivity. The calibration involved reconstruction of some meteorological data during periods where data were unavailable. It also involved an adjustment for the outlet port openings during the second half of 2007. As will be discussed in detail in the report, the City-specified field reports of the ports open during a portion of 2007 are at variance with the basic thermodynamics of the system. It is demonstrated later in this report that the open ports must have been at or above the thermocline level and not in the hypolimnion, as specified. In the future, it is recommended that outflow temperatures from SVR be recorded so that they can provide verification of the field record of port openings.

The onset and duration of thermal stratification as well as the deepening rate of the thermocline were predicted accurately by the model. Furthermore, the water conductivity, a measure of salinity, was well predicted by the model. It is noted that future modeling of the hydrodynamics at SVR would benefit from a full set of meteorological data gathered at SVR (the City stopped gathering on-site meteorological data in March 2007). An analysis presented herein shows that the meteorological data measured at the nearby California Irrigation Management Information System (CIMIS) station in Escondido differ in significant aspects from data gathered at SVR.

After the model was calibrated, a validation was performed to compare the model against the results of previous field studies. The field studies involved two separate episodes of tracer injection in the reservoir (winter 1995 and summer 1995). The field studies clearly showed the impacts of stratification (or lack thereof) on the mixing and dispersion of the tracer. The ELCOM model was capable of replicating the main features of the tracer study. Due to the nature of the tracer used in those studies (Lanthanum Chloride), a significant amount of tracer was lost due to coagulation/flocculation and subsequent settling. A simple coagulation/settling model was added to ELCOM. After the implementation of the coagulation/settling model, very good agreement between the model and the data was obtained. This validation provides strong verification and assurance that the model performance is accurate.

The calibration of the water quality model CAEDYM was carried out after the ELCOM calibration and verification process. The comparison between simulation results and measured in-reservoir field data involved water quality parameters including

dissolved oxygen (DO), pH, nutrients (nitrogen and phosphorus), chlorophyll *a* and Secchi depth. It is noted that some assumptions had to be made in order to calibrate the model. For example, assumptions on nutrient levels for the Aqueduct inflows during the "Bypassing Period" were needed to characterize nutrient loadings because there are only limited nutrient data available for the Aqueduct inflow.

The calibrated CAEDYM model shows overall good agreements with measured data. The simulated DO concentrations capture the major trends in the measured DO concentrations, including the onset, duration, and magnitude of periods of anoxia in the hypolimnion, the depth to the top of the anoxic (*i.e.,* "without oxygen") region, the DO decay rate in the spring in the hypolimnion, and the high surface DO concentrations in the spring (and sometimes fall) that are due to algae blooms. The simulated pH values closely match the measured data and are on average within 0.3 of the measured values. The calibrated model also replicates the major trends in the measured nutrient (phosphorus and nitrogen) concentrations. It is noted, however, that some of the field data are below the detection limit. The available in-reservoir chlorophyll *a* data were qualitatively measured using a fluorometer that has not been calibrated. The calibration of chlorophyll *a* had to be conducted indirectly through the calibration of Secchi depth. The final calibration run shows a fairly good agreement with the measured Secchi depths, indicating a fairly good calibration for chlorophyll *a*.

At this point, it is believed that the model calibration/validation is nearly complete. The calibrated/validated model will undergo peer review. After that, the model will be applied to the study of the expanded reservoir as well as the evaluation of the mixing of the advanced treated recycled water within the reservoir. The planned modification of Aqueduct release locations/facilities into the expanded SVR and outlet structure/port depths will be incorporated into the model.

Finally, it is noted that future evaluations of water quality at SVR would benefit from more frequent sampling of nutrients and chlorophyll *a* within the reservoir, lower nutrient detection limits, and an increased use of duplicate samples or periodic sampling audits. It is recommended that nutrient samples be collected more frequently for the inflows and within the water column. It is further recommended that the collection of chlorophyll *a* samples be resumed. Composite samples should be collected from the reservoir surface in order to analyze chlorophyll *a* concentrations in the laboratory. This would allow for calibration of the optical fluorometer data and improve the usefulness and interpretation of those data.

1. INTRODUCTION

1.1 BACKGROUND AND OBJECTIVES

San Vicente Reservoir (SVR) is located near Lakeside, California, and is used as a drinking water supply by the City of San Diego (City), its owner and operator (**Figure 1**). The reservoir currently has a capacity of about 90,000 acre-feet. San Vicente Reservoir is undergoing an enlargement that will raise the dam by 117 feet and increase the reservoir's storage to 247,000 acre-feet at the spillway level (or 242,000 acre-feet at the maximum operation level).

A water reuse project, entitled Reservoir Augmentation, is being studied by the City. If implemented at full-scale, Reservoir Augmentation would bring advanced treated recycled water from the North City Water Reclamation Plant to SVR via a pipeline. The City's Reservoir Augmentation program consists of three phases (Welch, 1997; City of San Diego, 2008).

- In Phase One, a comprehensive evaluation of all viable options to maximize the amount of water reuse in San Diego was undertaken. It included analysis and research on the health effects of reuse options, and included a public participation process. The Reuse Study's stakeholders identified Reservoir Augmentation at the City's San Vicente Reservoir to be the preferred reuse strategy.

- Phase Two is the Reservoir Augmentation Demonstration Project (Demonstration Project). The Demonstration Project will: (1) design, construct, operate, and test a demonstration-scale advanced water treatment (AWT) plant at the North City Water Reclamation Plant which will produce advanced treated recycled water; (2) conduct a limnology study of SVR to evaluate the water quality effects of bringing advanced treated recycled water into the reservoir, establish residence time and assess short-circuiting for advanced treated recycled water in the reservoir; (3) convene an Independent Advisory Panel (IAP) to provide independent expert oversight of the Demonstration Project; (4) define the State's regulatory requirements for the Reservoir Augmentation program; (5) perform an independent energy and economic analysis for the Reservoir Augmentation program; (6) and conduct a public outreach and education program regarding Reservoir Augmentation.

- If the Demonstration Project meets regulatory requirements and provides evidence of the viability of the Reservoir Augmentation process, the City could choose to proceed with Phase Three, the full-scale Reservoir Augmentation Project. Phase Three would create a new potable water supply for the City of San Diego and the region from advanced treated recycled water.

A component of the Demonstration Project is the Limnology and Reservoir Detention Study of San Vicente Reservoir (Limnology Study). As part of the Limnology Study, the City has requested that Flow Science Incorporated (FSI) develop a three-dimensional water quality model that can accurately predict hydrodynamics and water quality of the existing and expanded SVR. It is anticipated that this model will be utilized to (1) establish residence time requirement for advanced treated recycled water in the reservoir and assess the short-circuiting of the advanced treated recycled water to the outlet structure; and (2) evaluate the effects of the advanced treated recycled water on water quality and eutrophication in the reservoir.

This Technical Memorandum (TM) focuses on the development, calibration and validation of the three-dimensional water quality modeling for SVR. This work has been performed by Flow Science Incorporated (FSI) of Pasadena, California, under contract to the City of San Diego, California.

1.2 PREVIOUS STUDIES

FSI has previously performed various hydraulic and water quality modeling evaluations of SVR. The current work builds on these previous evaluations.

In the early 1990s, FSI conducted an analysis to evaluate the feasibility of introducing some highly-treated tertiary effluent into SVR (FSI, 1994). The study comprised one-dimensional reservoir modeling, a field study and data analysis. In 1995, the City conducted two field tracer studies in SVR that were completed in the winter and summer of 1995 (FSI, 1995). The work was used to enhance understanding of the water circulation patterns in the reservoir and help identify the fate and transport of the Aqueduct inflow. The results of that work have been used here to validate the three-dimensional water quality model developed in this study.

In 1997, FSI evaluated the hypolimnetic oxygen demand in SVR (FSI, 1997). As part of that project, FSI developed calibrated models of temperature and DO in SVR for 1992-1994 using the one-dimensional Dynamic Reservoir Simulation Model – Water Quality (DYRESM-WQ). In 2001, FSI revised the estimated hypolimnetic oxygen demand for SVR based on more extensive reservoir profiling data from 1992-2000. These data were used to develop recommendations for sizing a diffused oxygen input system and to develop performance specifications and design criteria for such a system (FSI, 2001).

In 2005, FSI developed a calibrated one-dimensional DYRESM-WQ model of temperature, conductivity (*i.e.,* salinity), and dissolved oxygen (DO) for SVR for the period 1999-2000 (FSI, 2005a). The model was then used to perform an assessment of water quality in the reservoir after the proposed dam raise and expansion. The purpose of the modeling work was to identify the effects of the reservoir expansion and new inlet and outlet facilities on water quality and possible design and management options for

maintaining or enhancing water quality. In particular, the focus of the work was on identifying the optimum elevations for the seven ports in the outlet tower that is being constructed as part of the dam-raise project. The work defined the port elevations so that the City and the Water Authority can selectively withdraw the best-available water in the reservoir at different lake elevations and for different operating conditions.

Most recently, in 2009, FSI re-calibrated the SVR one-dimensional DYRESM-WQ model developed in 2005 for the period 2006-2007 (FSI, 2009) using newly-obtained in-reservoir nutrient and chlorophyll *a* data that were either insufficient, or non-existent, for the previous calibration period (1999-2000). The calibrated DYRESM-WQ model was then used to evaluate water quality effects within the reservoir during dam construction drawdown conditions, when the water surface elevation levels (WSELs) in the reservoir would be reduced from around 620 ft to around 590 ft during the dam-raise construction.

The current project builds upon knowledge gained from the development of these models and analysis and the associated database of information on SVR.

1.3 TECHNICAL MEMORANDUM ORGANIZATION

This TM provides a detailed description of the three-dimensional water quality modeling performed for SVR. **Chapter 2** of the report provides details of the modeling approach and setup, including a description of the computer code used in the model and its required inputs. **Chapter 3** describes the calibration of the hydrodynamic part of the model, including details on the calibration setup and field data used for the calibration. Then, the calibration validation of the hydrodynamic part of the model (ELCOM) is presented in **Chapter 4**. **Chapter 5** provides details of the calibration of the water quality part of the model (CAEDYM). Conclusions and discussion are provided in **Chapter 6**.

2. MODELING APPROACH AND SETUP

2.1 ELCOM AND CAEDYM DESCRIPTION

FSI used comprehensive computer modeling to simulate the hydrodynamics and water quality for this study. The models used include a three-dimensional hydrodynamic module (Estuary Lake and Costal Ocean Model, or ELCOM) and a water quality module (Computational Aquatic Ecosystem DYnamics Model, or CAEDYM). ELCOM simulates water velocities, temperatures, concentrations of salinity (*i.e.*, conductivity) and tracers; CAEDYM computes changes in dissolved oxygen (DO), nutrients, organic matter, pH and chlorophyll *a*. By coupling these two modules, the models can be used to study the spatial and temporal relationships between physical, biological, and chemical variables in San Vicente Reservoir (see **Figure 2**[1]).

Both the ELCOM and CAEDYM models were developed at the Centre for Water Research at the University of Western Australia. They have been used in predicting water quality in many lakes and reservoirs throughout the world and a more detailed description of them is included in **Appendix A**.

Compared to the one-dimensional DYRESM-WQ model used in the previous studies of SVR, both ELCOM and CAEDYM are more advanced computer models that are capable of simulating sophisticated hydrodynamic and biogeochemical processes in three dimensions. More importantly, as three-dimensional models, they can track the horizontal and vertical movement of the advanced treated recycled water in the reservoir. Therefore, water quality effects induced by the advanced treated recycled water can be evaluated both temporally and spatially. By comparison, DYRESM-WQ is a one-dimensional model that focuses on identifying the vertical gradients in the reservoir.

ELCOM can run independently of CAEDYM to predict only reservoir hydrodynamics and parameters such as water velocities, temperatures and tracer concentrations. However, CAEDYM needs to be run coupled with ELCOM because it relies on ELCOM to provide the hydrodynamic "driver" to transport and mix the biological and chemical water quality parameters that are the essence of CAEDYM.

[1] Note that Figure 2 illustrates some processes that do not occur or are not modeled in SVR and are therefore not included in the modeling.

2.2 APPROACH

The approach to studying water quality effects of the advanced treated recycled water using a computer model consists of the following steps:

- Select an appropriate hydrodynamic and water quality computer models for the SVR model, which in this case are ELCOM and CAEDYM;
- Obtain and assemble existing data for calibration and validation of the SVR model;
- Set up the SVR model and associated input data files;
- Perform ELCOM simulations necessary to calibrate and validate the hydrodynamic part of the SVR model;
- Perform ELOCM-CAEDYM simulations necessary to calibrate the water quality part of the SVR model;
- Extend the model to the enlarged reservoir;
- Determine the future scenarios and associated input data;
- Apply the calibrated SVR model to different future scenarios and evaluate water quality changes induced by the Demonstration Project.

This report focuses on the first five steps, which involve the calibration and validation of the SVR water quality model.

2.3 MODEL SETUP

2.3.1 Model Domain and Grid

The model domains include the existing portion of the reservoir (WSEL = 650 ft) and the expanded portion of the reservoir (WSEL = 780 ft) (see **Figure 1**). However, the calibration/validation work discussed herein only considers the existing reservoir.

Bathymetry contour data for the reservoir were provided by the City with contour intervals varying from 2 ft to 10 ft, from which the model computational grid was created. The horizontal resolution of the grid for the ELCOM runs is 50 × 50 m (see **Figure 3**). The model grid was rotated 42 degrees counter-clockwise from North in order to align the major channels of the reservoir with the model grid axes to reduce numerical

errors. A two-year ELCOM simulation using this grid takes approximately 7 days on a fast personal computer. In order to control the run time for ELCOM-CAEDYM, a 100 × 100 m grid was used, as will be discussed in **Chapter 5**.

A variable grid size was used in the vertical dimension. A vertical grid size of 1.64 ft (0.5 m) was used near the top of the reservoir in order to provide a high resolution for resolving vertical stratification in the reservoir. Below this a stretched grid was used in order to decrease the number of cells needed and to improve computational efficiency. Each stretched cell is 6 percent larger in the vertical direction than the cell directly above it (i.e., stretch ratio or the ratio of grid sizes for adjacent cells = 1.06). This is possible because vertical gradients of water parameters such as temperature and conductivity within the hypolimnion tend to be small. The same vertical resolution was used for both ELCOM and ELCOM-CAEDYM.

2.3.2 Modeling Period

The period of 2006-2007 was chosen as the model calibration period for the following reasons:

- Measurements of daily Aqueduct inflow volumes began in late 2006;
- It had as dense a data set as other years since nutrient sampling began in 2003;
- Most data sets in this period have been evaluated, cleaned (by removing seemingly erroneous data), and verified in the most recent SVR study conducted by FSI (FSI, 2009) and are ready to use;
- Field data in 2007 showed faster rates of DO decay and smaller Secchi depths than in previous years, which provided a more conservative basis for the calibration.

2.3.3 Model Inputs

The input data required by the modeling include flow rates for inflows and outflows, inflow water quality, and meteorological forcing functions (rainfall, air temperature, wind speed and direction, relative humidity, solar influx) over the modeling period. The input data used in this study were either based on measured data or derived from these data. The sources and derivation of these data are discussed in more detail in the next three chapters.

3. ELCOM CALIBRATION

3.1 OVERVIEW

Model calibration is the process of adjusting some model parameters and sometimes correcting seemingly erroneous input data in an attempt to match the simulation results with measured field data. In this study, the calibration of the hydrodynamic model ELCOM was carried out first. The comparison between simulation results and measured in-reservoir field data involved the following parameters: water surface elevation (WSEL), water temperature and conductivity.

The in-reservoir field data were measured and provided by the City. **Appendix B** includes plots of the historical in-reservoir water temperature data since 1992 and conductivity data since 1999, as well WSEL data since 1990. During the calibration period (year 2006-2007), WSELs were measured daily while temperature and conductivity profiles were measured weekly. Most of these inputs were obtained by FSI for the recent study in 2009 (FSI, 2009).

3.2 ELCOM CALIBRATION SETUP

3.2.1 Computational Grid Setup and Initial Conditions

As described in **Chapter 2**, the model grid with a constant horizontal grid size of 50 × 50 m and a variable vertical grid size was used for ELCOM calibration (see **Figure 3**).

The initial reservoir temperature profile at the beginning of 2006 was based on in-reservoir measured data from Station A (near the outlet tower, see **Figure 1**) on January 3, 2006, as shown in **Appendix B**.

Since ELCOM requires salinity as an input, but only conductivity is generally measured in the reservoir and in the inflows, salinity values were estimated from the conductivity data. The in-reservoir salinity is estimated to be approximately equal to the total dissolved solids (TDS) concentration, and the TDS concentration and salinity can be estimated according to the following formula developed from comparisons of available measured TDS and conductivity data using a least squares best fit to a linear relation (FSI, 2009):

$$\text{TDS (mg/L)} = \text{Salinity (mg/L)} = 0.65 * \text{Conductivity (}\mu\text{S/cm)} \qquad \text{[Eqn. 1]}$$

As suggested in the previous SVR modeling study (FSI, 2009), conductivity data from January 9, 2006, were used for the initial conditions for the computation. The calibration was performed as one continuous two-year simulation,

3.2.2 Flow Rate Inputs

Three surface inflows were included in the model calibration. These include the First San Diego Aqueduct (Aqueduct), stream inflows (Runoff), and water transfers from Sutherland Reservoir. The Aqueduct consists of two pipelines that extend from the Metropolitan Water District of Southern California's (MWD's) Colorado River Aqueduct near San Jacinto, California, and terminate at the north-west corner of SVR (**Figure 1**). The Aqueduct inflow cascades down a steep, natural channel and enters the reservoir at the surface. Runoff enters the reservoir as a surface inflow through several tributaries, with San Vicente Creek being the dominant Runoff inflow. When water is transferred from Sutherland Reservoir, it enters San Vicente Reservoir at the north end of the reservoir via San Vicente Creek.

The only modeled outflow in the calibration is the withdrawal from the existing outlet tower located near the center of the upstream face of the dam (see **Figure 1**). It consists of a vertical outlet tower with six tiers, three of which can also be equipped with an optional 20 ft riser. The multiple tier elevations allow for selective withdrawal of the water at desired depths. A detailed discussion of modeled withdrawal elevations is included in **Section 3.2.5**.

Total monthly flow volumes for each of the three inflows and the outflow were provided by the City. In addition, daily Aqueduct inflow volumes were provided starting in November 2006, and daily outflow (draft) volumes were provided for the entire calibration period. During those times when daily Aqueduct inflow volumes were not available, the monthly inflow data were used for the average daily inflow volumes. The monthly inflow data were also used for the average daily inflow volumes for the Runoff and Sutherland Reservoir inflows. Note that the Runoff volumes are not measured directly; instead, they are determined from other known values based on a mass balance computation.

However, the calculated reservoir storage using the inflow/outflow rates provided by the City does not match the measured storage volumes and it varied by as much as 40 Million Gallon (MG) (about 0.2% of the total reservoir volume) from the measured volumes in June 2006 and April, May, and December 2007. Thus, as part of WSEL calibration, a correction was made to the Aqueduct inflow or outlet flows (depending upon whether additional inflows or outflows were needed to correct the storage) to improve the WSEL results. Details on the correction method can be found in the previous SVR model calibration study (FSI, 2009). A plot of the resulting inflow and outflow volumes used in the model calibration, as compared to the measured volumes, is included in **Figures 4** and **5**.

As shown, the Aqueduct comprises the major inflow source to SVR with maximum flow rates generally occurring in the winter and spring. Runoff inflows were much less

than the Aqueduct inflows during this period, with maximum Runoff occurring in the winter and spring. The controlled inflows from Sutherland Reservoir occurred in March, November, and December 2007.

3.2.3 Inflow Temperatures and Conductivity Inputs

Temperature and salinity of all inflows are the parameters required as inputs in the ELCOM calibration; but these data were not available at all times for all inflows. Therefore several assumptions and estimates were made when preparing these input files for the calibration. A brief description of these assumptions is provided below for each inflow and details can be found in the previous SVR model calibration study (FSI, 2009). **Appendix C** (see **Figures C-1** through **C-6**) includes plots of the measured data and input data used in the model calibration for each inflow.

Aqueduct Inflows

Discharges from Lake Skinner generally supply the Aqueduct. Therefore, since Aqueduct temperature and conductivity data are not measured at the inlet to SVR, data measured at the Lake Skinner outlet (located 80 miles upstream) were used to characterize the Aqueduct inflow for most of the 2006-2007 calibration period under the assumption that these parameters in the Aqueduct do not change significantly from the Lake Skinner discharge to SVR. These data at Lake Skinner were obtained directly from MWD and included approximately bi-weekly temperature and conductivity (and some TDS data).

During the period from approximately October 2006 through January 2007, about 80% of the water in the Aqueduct was being supplied directly from the San Diego Canal while the remaining water was supplied by Lake Skinner (verbal communication with Dr. Rich Losee of MWD on June 4, 2008). Based on limited data obtained from MWD for the San Diego Canal, temperature and conductivity (*i.e.*, salinity) values during the "Bypassing Period" are comparable to data measured at the Lake Skinner outflow, so the more dense Lake Skinner outflow data were used. The final temperature and conductivity input values for the Aqueduct inflow as well as all the measured data were presented in **Figures C-1** and **C-2**.

Runoff Inflows

Temperature and conductivity data for the local tributaries to SVR were obtained from the City and sampled as often as monthly since 2003. Data were measured in San Vicente Creek (SV Creek) - both upstream and downstream of the confluence with the Sutherland Reservoir inflow - and in Barona Creek, Aqueduct Creek, Kimball Creek, and Tool Road Creek. Due to the lack of data for other tributaries, data measured in SV Creek were used to estimate the model inputs for other tributaries.

The Runoff conductivity can vary significantly depending upon whether it is composed of a small or large rain event, and stream data are not collected frequently enough to characterize the complex relationship between conductivity and flow rate. However, stream conductivity generally decreases with increasing flow rates. As suggested in the previous SVR model calibration study (FSI, 2009), salinity values were reduced in February 2006, March 2006, December 2007 for possible sustained runoff events that were not captured by monthly sampling data (per statements made by City and Water Authority personnel during 9/23/08 conference call). Otherwise there is no conductivity drop as demonstrated in the measured conductivity profile data. The final temperature and conductivity input values for the runoff as well as all the measured data are presented in **Figures C-3** and **C-4**.

Sutherland Reservoir Inflows

Water from Sutherland Reservoir is intermittently released from the hypolimnion and travels through an approximately 12-mile pipeline before discharging into SV Creek about 4.5 miles upstream of SVR. During the calibration period, inflows from Sutherland Reservoir occurred in March 2006 and November-December 2007. In-reservoir temperature and conductivity data were obtained from the City for Sutherland Reservoir. The temperature and conductivity values of inflows from Sutherland Reservoir were in general assumed to be equal to the values from the in-reservoir profile data measured from within the hypolimnion near the elevation of the sole Sutherland outlet located at EL 1940 ft.

As suggested in the previous SVR model calibration study (FSI, 2009), inflow temperatures in March 2007 were adjusted in order to decrease the density of the inflow relative to San Vicente Reservoir so that the Sutherland Reservoir inflow would insert at the surface as indicated by conductivity profile data taken from San Vicente Reservoir. This correction may be related to the heating of the water while it travels between the two reservoirs. The final temperature and conductivity input values for the Sutherland reservoir inflow as well as all the measured data are presented in **Figures C-5** and **C-6**.

3.2.4 Meteorological Inputs

The meteorological inputs required for the model, which features a complete thermodynamic calculation, include measurements of solar radiation, air temperature, wind speed, wind direction, relative humidity, and rainfall. The meteorological data at SVR are only available from January 1, 2006, through December 11, 2006, and January 1, 2007, through March 15, 2007, which were measured every 10 minutes by the City at a monitoring station on Lowell Island within San Vicente Reservoir (see **Figure 1**).

Initially, the remaining meteorological data for 2006 and 2007 were filled by data obtained from the California Irrigation Management Information System (CIMIS). Hourly CIMIS data were measured at Station 153 in Escondido, California, which is the closest operational CIMIS station during the calibration period and is more than 10 miles from SVR (see **Figure 6**). The ELCOM calibration run using this composite data set shows that the simulated temperature profiles track closely to the measured value in 2006 when the meteorological data from the City were used, while the model overestimates thermocline depths in the summer of 2007 when the CIMIS data were mostly used (see **Figure 7**). Several attempts were made to adjust the CIMIS data based on an evaluation of the overlapping City and CIMIS data, but they all failed to accurately reproduce the measured thermocline depths in the summer of 2007. It was concluded that the CIMIS meteorological data do not represent meteorological conditions at SVR, even with the adjustments, probably because of distance between these two places and the complex terrain surrounding SVR. In particular, it is noted that the wind velocity can have a significant impact on lake mixing and the depth of the thermocline, and as a result, using wind speed from a remote location with different wind patterns can lead to erroneous modeling results.

Due to the inadequacy of using the meteorological data from Escondido, the approach used herein involved constructing a composite meteorological data set by filling in the missing 2007 meteorological data from SVR with the corresponding 2006 data gathered by the City. For an approximately three-week period in December 2006 and 2007, there were no meteorological data available from the City. This period was filled by using the CIMIS data from Escondido (see **Table 1)**. Using this composite data set, the simulation results show very good agreement between the simulated and measured water temperatures between April and June 2007, but the model results start to deviate from the measured data after July 2007 (see **Figure 8**). As described later, the deviation in the second half of 2007 can be attributed to issues other than meteorological data. As a result, this composite meteorological data set was used in all the calibration runs. Graphical plots of the final meteorological data inputs are included in **Appendix C** (see **Figures C-7** through **C-12**).

Table 1. Details on the Composite Meteorological Data Used in the Model

Period	Data Source	Measured Location
1/1/2006 – 12/11/2006	City	Lowell Island
12/12/2006-12/31/2006	CIMIS	Escondido
1/1/2007 – 3/15/2007	City	Lowell Island
3/16/2007 – 12/11/2007	Using data between 3/16/2006 – 12/11/2006 from the City	Lowell Island
12/12/2007 – 12/31/2007	Using data between 12/12/2006 – 12/31/2006 from CIMIS	Escondido

3.2.5 Outflow Port Openings

The existing reservoir outlet tower consists of six tiers, three of which are also equipped with an optional 20 ft riser. A summary of the available withdrawal elevations from the ports on the current tower is included in **Table 2**.

Table 2. Available Withdrawal Elevations on Existing Outlet Tower

Port	Withdrawal Elevation
1	493 ft
2	510 ft
2 w/ 20 ft riser	530 ft
3	540 ft
3 w/20 ft riser	560 ft
4	570 ft
4 w/20 ft riser	590 ft
5	600 ft
6	630 ft

Based on records obtained from the City, outflows were withdrawn from Port No. 3 with a 20-ft riser (560 ft EL) and Port No. 4 (570 ft EL) from January through mid-June 2006. From mid-June 2006 through mid-September 2007, outflows were withdrawn from Port No. 2 with a 20-ft riser (530 ft EL) and Port No. 3 (540 ft EL). Starting in mid-September 2007, outflow withdrawal switched back to Port No. 3 with a 20-ft riser (560 ft EL) and Port No. 4 (570 ft EL).

The ELCOM calibration run using the outflow port openings described above shows that simulated thermocline depths match well with measured data in 2006 and the first half of 2007, but it predicted much deeper thermocline levels than shown by the in-reservoir data from July 2007 onward (see **Figures 7** and **8**). Historical temperature data between 2000 and 2007 (**Figure 9**) reveal that the thermocline depth in the summer of 2007 resided around 20 ft below the surface and is much shallower than those in previous years. However, there is no evidence indicating that meteorological conditions in 2007 at SVR, which was believed to be not much different from previous years (verbal communication with Jeff Pasek of the City), could lead to such a shallow thermocline depth.

This initial finding led to a more careful examination of the effect of inflows and outflows on thermocline depths at SVR. In the summers of 2006 and 2007, the Aqueduct flow was the major inflow source at SVR and entered the reservoir at the surface. Temperatures for the Aqueduct inflow were between 20 and 28 ^{o}C between early June and later September in both 2006 and 2007 (see **Figure 10**). If the 18 ^{o}C isotherm (see **Figure 11**) is used to represent the thermocline, the Aqueduct inflow should reside above the defined thermocline, given that it enters the reservoir at the surface with a relatively high temperature. The City reported withdrawal levels during this period were below the observed thermocline. As a result, the increase in thickness of epilimnion (the layer above the thermocline) at SVR would be expected to be greater than the thickness of the layer formed by the Aqueduct inflow during the same period (making due allowance for evaporation losses). For 2006, the thermocline (defined as the 18 ^{o}C isotherm) is observed to deepen by about 9.5 ft between early June and early September. During the same period, the thickness of the layer formed by the Aqueduct inflow would be 2.6 ft and the evaporation loss is calculated to be about 2 ft. The net thermocline deepening in this time period due to external forcing (wind, heating and cooling, etc.) can be calculated using the following equation:

Deepening due to external forcing (m) = Net observed thermocline deepening (m)
- Deepening due to inflow insertion (m)
+ Loss due to withdrawal above thermocline (m)
+ Loss due to evaporation (m) [Eqn. 2]

From Eqn. 2, the deepening of the thermocline due to external forcing is estimated to be 8.9 ft, calculated as 9.5 less 2.6 plus 2 ft. However, for 2007, the thermocline (defined as the 18 ^{o}C isotherm) is observed to deepen by about 6.6 ft between early June and early September, while the thickness of the layer formed by the Aqueduct inflow is 11 ft. Applying Eqn. 2, the deepening of the thermocline due to external forcing in 2007 is therefore estimated to be -2.4 ft, which is a clearly unrealistic answer. If the mixing in

2007 is considered to actually have deepened the thermocline by the same amount as 2006 (*i.e.*, 8.9 ft which is a reasonable assumption[2]), then the thermocline depth would be 11.3 ft deeper than observed (calculated using Eqn. 2).

It is therefore apparent that the measured depth of the thermocline in the summer of 2007 is not reasonable unless some outflows were withdrawn from the epilimnion during this period[3] (about 11.3 ft worth of outflow). During this time period, the recorded outflows were from Port No. 2 with a 20-ft riser (530 ft EL) and Port No. 3 (540 ft EL), at a depth of 60 and 50 ft below the observed thermocline, respectively. The total water withdrawn from the reservoir during this time was 3,300 MG, corresponding to a reservoir layer of 11 ft (at the level of the thermocline). The only explanation of the above discrepancy is that the recorded open ports during this period were not correct, and that an approximately 11.3 ft thick layer of water was withdrawn at or above the thermocline level. It is noted that the recorded open ports show a switch to higher ports (Port No. 3 with a 20-ft riser at 560 ft EL and Port No. 4 at 570 ft EL) in mid-September 2007. However, these recorded open ports were too deep (both were below the thermocline) and the switch was too late to explain the above-mentioned discrepancy. To correct for the discrepancy it was considered in the model that the switch to the upper ports occurred earlier (in mid-June 2007) and the switch was to the shallower ports (Port No. 4 with a 20-ft riser at 590 ft EL and Port No. 5 at 600 ft EL) (see **Figure 12**), both of which were above the observed thermocline in the summer of 2007. The corresponding model results incorporating this change show good agreement in matching the measured data regarding thermocline depth (see **Figure 13**).

3.3 CALIBRATION RESULTS

3.3.1 Water Surface Elevation

Figure 14 shows the measured versus simulated water surface elevations for the calibration based on the flow data provided by the City. As shown, the simulated water surface elevations are generally within 1 ft of the measured WSELs.

---

[2] We have conducted a few sensitivity test runs and the results indicated that reducing the wind speed by 30%, or decreasing sunlight penetration depth (due to higher algae concentrations) only reduced the thermocline deepening due to external forcing by 1-2 ft.

[3] It is noted here that the thermocline depth measurements were performed using three different instruments at different times, and all the instruments produced similar results, thus ruling out instrument error as a source of the discrepancy.

3.3.2 Temperature

Figure 15 shows a time series plot of the simulated versus measured temperatures for both 2006 and 2007 at the surface and bottom of the reservoir. **Figure 16** shows color contours of the simulated water temperatures in comparison to the measured data. In addition, comparisons of simulated and measured temperature profiles at selected dates are included in **Appendix C** (see **Figures C-13** through **C-15**). As presented, the simulated temperatures closely match the measured data and accurately predict the onset and duration of thermal stratification, as well as the depth of the thermocline.

A scatter plot of the measured and simulated temperature for years 2006 and 2007 is provided in **Figure 17**. The plot includes only surface and bottom temperature. In the plot, the 45-degree theoretical line with zero intercept represents what would be a "perfect" correlation between the simulated and measured data. Therefore, the nearer the plotted points are to the 45-degree line, the better is the simulation. The graph indicates a good calibration in temperature.

A statistical analysis of the calibration results versus the measured temperature produced the metrics presented in **Table 3**. These metrics quantitatively summarize the accuracy of the calibration results. For example, the computed Root Mean Square Errors (RMSE) indicate that the calibrated temperatures in 2006 are on average within 0.60 ^{o}C of the measured data, corresponding to 3.6% of the range in measured temperatures (relative RMSE = RMSE / $|T_{max} - T_{min}|$); and the calibrated temperatures in 2007 are on average within 1.03 ^{o}C of the measured data, corresponding to 6.2% of the range in measured temperatures. Mean error calculates the average of difference between the measured and simulated values. Thus, the model on average overestimates temperatures by 0.17 ^{o}C in 2006 and on average underestimates temperatures by 0.1 ^{o}C in 2007. These metrics indicate a good calibration.

Table 3. Temperature Calibration Metrics

PARAMETER	2006 RESULTS			2007 RESULTS		
	ROOT MEAN SQUARE ERROR (RMSE)	RELATIVE RMSE	MEAN ERROR	ROOT MEAN SQUARE ERROR (RMSE)	RELATIVE RMSE	MEAN ERROR
Surface and Bottom Temperature	0.60 °C	3.6 %	-0.17 °C	1.03 °C	6.2 %	0.1 °C

3.3.3 Conductivity

Figures 18 and **19** are comparison plots (time series and color contours, respectively) for the simulated and measured conductivities (*i.e.*, salinities). The simulated

conductivity data plotted in the figures are computed based on the in-reservoir relationships between conductivity, salinity, and TDS as given in Eqn. 1.

The resulting simulated conductivities capture the seasonal trends in both the surface and bottom conductivity values; the magnitudes of the simulated and measured conductivity data also track closely, particularly in 2006.

A scatter plot of the measured and simulated conductivity values for years 2006 and 2007 is provided in **Figure 20**. Statistical metrics are included in **Table 4**. The RMSE indicate that the calibrated conductivity values are on average within 15-30 µS/cm of the measured, corresponding to 10 – 20% of the range in measured conductivity. These indicate a good conductivity calibration for both years, especially given that an error of 30 µS/cm is common in field-measured conductivity (FSI, 2005b).

Table 4. Conductivity Calibration Metrics

PARAMETER	2006 RESULTS			2007 RESULTS		
	ROOT MEAN SQUARE ERROR (RMSE)	RELATIVE RMSE	MEAN ERROR	ROOT MEAN SQUARE ERROR (RMSE)	RELATIVE RMSE	MEAN ERROR
Surface and Bottom Conductivity	14.9 µS/cm	10.7 %	8.6 µS/cm	29.7 µS/cm	19.7 %	2.8 µS/cm

3.3.4 Animation of Aqueduct Tracer

An animation that shows transport and mixing of a conservative tracer injected into the Aqueduct inflow on July 1, 2006 is included in **Appendix D**. The tracer was added at a constant concentration of 100 to the Aqueduct inflow. The plan view plots the maximum value of the tracer concentrations for each vertical water column within the model domain. Two cross sections plot the tracer concentrations on the section connecting between Aqueduct inflow and the Dam and the section connecting between Kimball Arm and the Dam.

4. ELCOM VALIDATION

4.1 FIELD TRACER STUDIES

Model validation presented here involves simulating the periods of the tracer studies completed in 1995 using the previously-calibrated SVR model (**Chapter 3**). The ability of the calibrated model to reproduce observed field data in these tracer studies provides assurance of the predictive capability of the model.

Two tracer field studies were conducted by the City of San Diego in 1995: the winter study that was completed in January and February and the summer study that was completed between July and early September. In each study, a lanthanum (lanthanide) chloride solution was injected as a tracer into the Aqueduct inflow just before it enters the reservoir. Over the period of each study, tracer concentrations and other water quality parameters such as temperature, salinity and pH were measured at various reservoir stations (see **Figure 21**). **Table 5** presents a summary of information on field studies. A detailed description and analysis of the tracer studies can be found in the FSI report titled "San Vicente Water Reclamation Project: Results of Tracer Studies" (FSI, 1995).

Table 5. Summary of Information on Tracer Studies

Name	Injection Date	Injected Lanthanum Mass	Lake Condition	Sampling Period
Winter study	9:00 AM, 1/4/95-9:00 AM, 1/5/95	77.9 kg	Weak Stratification	1/6/95 – 2/7/95
Summer Study	10:00 AM, 7/24/95-10:00 AM, 7/25/95	154.5 kg	Strong Stratification	7/31/95 – 9/5/95

4.2 MODEL VALIDATION SETUP

4.2.1 Computational Grid and Model Inputs

The approach to setting up grid and input files for the model validation run is similar to that used in setting up the calibration run, except that 1995 data (inflows, outflow, meteorology) were used.

Since no meteorological data were collected at SVR in 1995, data at CIMIS Ramona Station (#98) were used as input in the validation run. Ramona Station is about 6 miles away from SVR. Note that the Ramona station was only in operation before 1999, and thus could not be used in the 2006/07 calibration to reconstruct missing meteorological data.

The winter validation run simulated a 45-day period starting on January 3, 1995 (1 day prior to the tracer injection) and ending on February 18, 1995. The initial conditions for the winter run were based on data measured at Station A on January 3, 1995.

The summer validation run simulated a 50-day period starting on July 21, 1995 (3 days prior to tracer injection) and ending on September 9, 1995. The initial conditions for the summer run were based on data measured at Station A on July 21, 1995.

4.2.2 Particle Settling

Both winter and summer tracer studies used lanthanum chloride as the tracer. Lanthanum, a coagulant used in the wastewater treatment, can bind with phosphate in water and form insoluble particles (Niquette, *et al.,* 2004, Recht, *et al*., 1970). After the particles are formed, they grow in size by attaching themselves to other large particles in the water (*i.e.,* "flocculation") and then settle within the water column and may deposit on the sediment. This lanthanum removal process by settling is evidenced in the exponential loss of total measured lanthanum mass in the reservoir over the time during the tracer studies (see **Figure 22**). For example, after 35 days from the initial injection of the lanthanum, there was about 15% of the lanthanum mass left in the water column for the winter tracer study (illustrated as red diamonds in **Figure 22**) and about 50% of the lanthanum remained in the water column in the summer tracer study (illustrated as green squares in **Figure 22**). These figures were obtained based on integrating the in-reservoir measured lanthanum concentration data at all stations. In contrast, after 35 days there would have been about 95% and 99% of the lanthanum left for the winter and summer studies, respectively, if the lanthanum were a conservative tracer (the contour plots for these runs are include in **Figures C-16** through **C-22** of **Appendix C**). This indicates that less than 5% of the lanthanum was withdrawn through outlets during the 35-day period and significant portion of the total injected lanthanum was lost through settling. It is also noted that the volume of water withdrawn from the reservoir during the winter and summer studies was approximately 4 and 10 % of the reservoir volume, respectively. Therefore, it is more appropriate to model lanthanum as particles that grow in size and settle rather than a conservative tracer.

Lanthanum chloride usually bonds with phosphate to form insoluble particles. In the winter study, most of injected lanthanum chloride was observed to reside close to the bottom of the reservoir, where phosphate is ample due to sediment release and lack of algae consumption at depth. In the summer study, most of lanthanum chloride resides in the epilimnion or at the level of the thermocline where phosphate level is low due to algae consumption. Therefore, more insoluble lanthanum phosphate particles are expected to form in the winter than in the summer. In addition, more large suspended particles in the reservoir were expected in the winter due to winter storms and runoff. These particles provide the medium to which lanthanum phosphate can attach.

Therefore, it is reasonable to apply different particle distributions and flocculation rates in the summer and winter simulations as described above.

In the validation run, the lanthanum coagulation/flocculation was modeled using a simplified representation as follows:

- Nine (9) different-sized particle groups (leading to different settling velocities) were used to represent the lanthanum in the reservoir. The settling velocity of each particle size group was calculated according to Stokes's Law, which suggests that the settling velocity increases in proportion to the square of the particle diameter. A summary of settling velocity for each particle size group is listed in **Table 6**.

- In the winter study, starting with the initial distribution among the particle size groups, it is assumed that 8% mass of each group particle moves to the next group with larger size daily (*i.e.*, a flocculation rate equal to 8% of mass / day). The simulated mass distributions of the particle groups on the sampling dates in the winter study are presented in **Figure 23**.

- In the summer study, two flocculation rates were used for each particle size group: 60% mass of each group has the flocculation rate of 0.9% of mass / day (*i.e.*, 0.9% mass of each group moves to the next group with larger size daily); and 40% mass of each group has the flocculation rate of 28% of mass / day (*i.e.*, 28% mass of each group moves to the next group with larger size daily). The simulated mass distributions of particle groups on the sampling dates in the summer study are presented in **Figure 23**. The use of different flocculation rates in summer and winter is discussed further below.

- These flocculation rates were selected mainly because they produce the best match to the rate of decrease in measured total lanthanum mass over the whole reservoir (see **Figure 24**).

Table 6. Settling Velocity for Simulated Particle Groups

Particle Size Group	Settling Velocity (m/day)
1	0.0
2	0.1
3	0.2
4	0.3
5	0.5
6	1.0
7	1.5
8	2.5
9	5.0

4.3 VALIDATION RESULTS

Figure 25 presents color contours of the simulated water temperature in comparison to the measured temperature data during the period of the winter tracer study. Note that the simulated temperature shows more diurnal fluctuations because the simulation results were plotted based on three-hour sampling, while the field data were measured once every few days. During the winter study, the reservoir was well-mixed initially and started to develop a weak stratification later. As presented, the simulated temperatures match well with the measured data and the model accurately predicts the onset and development of thermal stratification.

Figures 26 through **28** show color contours of measured and simulated lanthanum profiles in the winter tracer study along a continuous path joining Stations I, B, K, L, A, L, M, C, D, G, Q, and R as shown in **Figure 21**. The majority of the lanthanum stays close to the bottom of the reservoir and was rarely mixed to the surface (probably due to the settling of lanthanum and a weak stratification). This indicates that the Aqueduct inflows dove to the bottom of the reservoir in the winter after entering from the surface. (The inflow was slightly colder and therefore denser than the reservoir water during winter.) As presented, both the fate of the Aqueduct inflow and decrease of lanthanum concentrations over the time are well captured by the model.

Figures 29 through **33** are comparison plots of the simulated and measured temperatures and lanthanum concentrations for the summer tracer study. Due to the strong temperature stratification in the summer, the Aqueduct inflow, with its relatively higher temperature, stayed above the colder and denser water in the hypolimnion after entering at the surface as shown in the measured field data. Then, lanthanum started to settle as evidenced by the layer of lanthanum expanding vertically toward the bottom. Without the formation of lanthanum particles and subsequently settling, the lanthanum

would have mostly remained trapped at the thermocline and eventually mixed to the surface by wind (see **Figures C-16** through **C-22** of **Appendix C)**. Both the insertion level and settling were well captured by the model. The model was also able to accurately predict the horizontal extent of lanthanum plume in the reservoir.

The validation presented here introduced additional assumptions, such as particle distributions and flocculation rates other than those made in the calibration. However, both the particle distributions and flocculation rates were determined solely based on the measured decreasing mass of total lanthanum over the whole reservoir. The model was able to reproduce the three-dimensional details in measured lanthanum concentrations such as the insertion, horizontal extent and dilution of the plume, as well as the settling. This provides verification and confidence in the model performance.

5. CAEDYM CALIBRATION

5.1 OVERVIEW

The calibration of the water quality model CAEDYM was carried out after the ELCOM calibration was completed. The comparison between simulation results and measured in-reservoir field data involved the following water quality parameters: DO, pH, nutrients, chlorophyll *a* and Secchi depth.

The in-reservoir water quality data were obtained by the City and plots of these data are included in **Appendix B**. Secchi depths and DO profiles are measured weekly. Nutrients are measured monthly at the surface (*i.e.*, epilimnion) and 1 meter above the reservoir bottom (*i.e.*, within the hypolimnion). Surface grab samples of chlorophyll *a* were measured monthly through 2003 (**Figure B-21**); since 2004, chlorophyll *a* concentration profiles have been estimated using an optical fluorometer (**Figure B-11** through **B-15**). These in-reservoir data were used to specify the initial profile concentrations at the start of the calibration period as well as for comparison against the simulated results for CAEDYM calibration.

5.2 CAEDYM CALIBRATION SETUP

5.2.1 Computational Grid Setup and Initial Conditions

A grid with a horizontal resolution of 100 × 100 m as shown in **Figure** 34 (compared to the finer grid with a horizontal resolution of 50 × 50 m used in the ELCOM calibration) was used for the CAEDYM calibration in order to complete the two-year run in reasonable computation time (4 days on a fast PC). The vertical grid is the same as that in the ELCOM calibration. The ELCOM calibration run was conducted on both grids to evaluate any difference in the predicted hydrodynamic conditions. **Figure 35** shows a comparison of the predicted temperature profiles at Station A using the fine and coarse grids. **Figure 36** shows a time series of predicted surface and bottom conductivity using these two grids. The results indicate that using either the fine or coarse grids will result in almost the same predicted conductivity and very similar predicted temperature profiles. Therefore, it is appropriate to use the coarse grid in the CAEDYM calibration to provide both reasonable model run times as well as adequate model resolution.

The initial reservoir DO and pH concentrations at the beginning of 2006 were based on in-reservoir measured data from Station A (see **Figure 1**) on January 3, 2006, as shown in **Appendix B**. The initial conditions for nutrients were based on the first available measured data (*i.e.*, on January 26, 2006).

5.2.2 Inflow Water Quality Inputs

Water quality parameters such as pH, DO, nutrients and chlorophyll *a* of all inflows are required as inputs in the CAEDYM calibration; but these data were not measured at all times for all inflows. In the previous SVR modeling study (FSI, 2009), a lot of effort has been put into preparing and testing the input files for the water quality calibration based on several assumptions and estimates. These assumptions and estimates have been through peer review in the previous study and were adopted directly in this calibration. A brief description of these assumptions is provided below for each inflow and details can be found in the previous SVR model calibration study (FSI, 2009). **Appendix C** (see **Figures C-23** through **C-40**) includes plots of the measured data and input data used in the model calibration for each inflow.

Aqueduct Inflows

Similar to the ELCOM calibration, water quality data measured at the Lake Skinner outlet were used to characterize the Aqueduct inflow for most of the 2006-2007 calibration period. These data were obtained directly from MWD and included approximately bi-weekly total phosphate (TP), and nitrate for at least 2006-2007. Ortho-phosphate (OPO4, used interchangeably with soluble reactive phosphate, or SRP here) data were only available for 2001-2004, ammonia data were only available for 2000-2004, and total nitrogen (TN) data were not available at all. Assumptions made in developing the Aqueduct water quality input files (**Figures C-23** through **C-29**) are noted below:

- DO concentrations were assumed to be 100% saturated based on water temperature.
- Chlorophyll *a* concentrations were assumed to be 0 µg/L since releases from Lake Skinner are generally at depth.
- Concentrations of SRP were estimated as 40 percent of the TP concentrations based on comparisons of the limited OP data from 2001-2004 with the TP data.
- Ammonia concentrations were estimated as 20 percent of the nitrate concentrations based on comparisons of the limited ammonia data from 2000-2004 with the nitrate data.
- TN concentrations were estimated as 120 percent of the sum of the nitrate and ammonia concentrations

During the "Bypassing Period" (October 2006 through January 2007), about 80% of the water in the Aqueduct was being supplied directly from the San Diego Canal while

the remaining water was supplied by Lake Skinner. During this period, limited TP and nitrate, but not SRP, ammonia, and TN, data were obtained from MWD for the San Diego Canal. Assumptions made in developing the Aqueduct input data files during the Bypassing Period are noted below:

- DO concentrations were assumed to be 100 percent saturated based on water temperature.
- Chlorophyll *a* concentrations were assumed to be 0 µg/L.
- TP and nitrate concentrations measured at the San Diego Canal were used to represent those in the Aqueduct inflow. Concentrations of SRP were estimated as 40 percent of the TP concentrations. Ammonia concentrations were estimated as 20 percent of the nitrate concentrations. TN concentrations were estimated as 1.2 mg/L to reflect the fact that a majority of the water in the San Diego Canal at that time was from the State Water Project (SWP), and SWP water generally has high nutrient concentrations (verbal communication with Bill Taylor of MWD and Jeffery Pasek of the City).

Runoff Inflows

Water quality data for the local tributaries to SVR were obtained from the City and included DO, TP, OPO4, TN, nitrate, and ammonia data, measured as often as monthly since 2003. Similar to the ELCOM calibration, data measured in SV Creek were used to estimate the model inputs for other tributaries (**Figures C-30** through **C-36**).

Sutherland Reservoir Inflows

Due to the limited nutrient data available during the months in which the Sutherland Reservoir inflows occurred (**Figure C-37**), TP, SRP, and TN concentrations were estimated by computing the average concentrations from measurements taken within Sutherland Reservoir when destratified in the winter, a period when nutrients are generally not being quickly consumed. Nitrate data were all below the detection limit, so nitrate concentrations were estimated to be equal to the detection limit. Since ammonia concentration data were not collected, ammonia concentrations were estimated as 20% of the TN.

The pH, DO and chlorophyll *a* values of inflows from Sutherland Reservoir were assumed to be equal to the profile data measured within the hypolimnion near the elevation of the outlet (**Figures C-38** through **C-40**).

5.3 CALIBRATION RESULTS

5.3.1 Dissolved Oxygen

Comparison plots for the simulated and measured DO concentrations are provided in **Figures 37** and **38**. The measured data show that DO concentrations at the surface remained high throughout the years because of the supply of oxygen directly from the atmosphere by diffusion and because of oxygen produced by photosynthetic activity of algae at surface. At high rates of photosynthesis, oxygen production by algae exceeded the diffusion of oxygen out of the system and resulted in occasional oxygen supersaturation in the spring of 2006 and 2007. The DO at bottom was replenished through vertical mixing with the surface water with high DO concentrations during the reservoir destratified periods in the winter of 2006 and 2007. However, during the summer, strong stratification at SVR prevented such vertical mixing and DO at the bottom was quickly depleted by the decay of algae and other organic matter in the sediment (*i.e.*, Sediment Oxygen Demand or SOD). The water conditions in the hypolimnion became anoxic (*i.e.*, dissolved oxygen concentrations are 0 mg/L) in the spring and anoxia lasted through the fall for both years, until the reservoir became destratified in the winter.

The simulated DO concentrations capture the major trends in the measured DO concentrations, including the onset, duration, and magnitude of periods of anoxia in the hypolimnion, the depth to the top of the anoxic (*i.e.*, "without oxygen") region, and the high surface DO concentrations in the spring (and sometimes fall) that are due to algae blooms. A value of 1.5 g/m^2/day was used for SOD in the calibration as it achieved the best match to the rate of decrease in DO measured at bottom during the stratified periods. This value is at the high end of the range of 0.1 – 1.75 g/m^2/day for sediment oxygen demand measured at SVR in 2001 (Beutel, 2001), but is consistent with historic DO profile data (**Appendix B**) that show faster rates of DO decay at the bottom in 2006-2007 than in 2001 due to more algal productions in the reservoir evidenced by relatively smaller Secchi depths in 2006-2007.

A scatter plot of the measured and simulated DO concentrations for years 2006 and 2007 is provided in **Figure 39**. A statistical analysis of the calibration results versus the measured data produced the metrics presented in **Table 7**. The computed Root Mean Square Errors (RMSE) indicate that the calibrated DO concentrations are on average within 1.3 mg/L of the measured data, corresponding 7-9% of the range in measured DO concentrations. These indicate a good calibration for DO for both years.

Table 7. Dissolved Oxygen Calibration Metrics

PARAMETER	2006 RESULTS			2007 RESULTS		
	ROOT MEAN SQUARE ERROR (RMSE)	RELATIVE RMSE	MEAN ERROR	ROOT MEAN SQUARE ERROR (RMSE)	RELATIVE RMSE	MEAN ERROR
Surface and Bottom Dissolved Oxygen	1.26 mg/L	9.0 %	0.76 mg/L	1.03 mg/L	7.4 %	0.45 mg/L

5.3.2 pH

Figures 40 and **41** show comparison plots for the simulated and measured pH. The measured data show that pH increased in the spring and summer of each year when inorganic carbon was consumed by the photosynthetic activity of algae; pH values were reduced in the winter because of the release of CO_2 as a byproduct of algae respiration. The model accurately captures major trends in the measured pH and the simulated pH closely tracks measured data. It is noted in these figures that the measured surface pH on 11/5/07 and the measured bottom pH on 6/16/06, 4/23/07, 4/30/07, 7/16/07, 7/30/07, 11/5/07 and 11/19/07 are unusually low compared to other data. Thus, these data are considered as outliers and were excluded from the analysis described next. A scatter plot of the measured and simulated pH for years 2006 and 2007 is provided in **Figure 42**. A statistical analysis of the calibration results versus the measured data produced the metrics presented in **Table 8**. The computed Root Mean Square Errors (RMSE) indicates that the calibrated pH are on average within 0.3 of the measured data, corresponding to 10-15% of the range in measured pH values. These indicate a good pH calibration for both years, especially considering the small variation of pH during the two-year calibration period.

Table 8. pH Calibration Metrics

PARAMETER	2006 RESULTS			2007 RESULTS		
	ROOT MEAN SQUARE ERROR (RMSE)	RELATIVE RMSE	MEAN ERROR	ROOT MEAN SQUARE ERROR (RMSE)	RELATIVE RMSE	MEAN ERROR
Surface and Bottom pH	0.19	9.7 %	0.03	0.28	14.3 %	0.05

5.3.3 Nutrients

Figures 43 and 44 are plots of the simulated and measured SRP and TP concentrations, respectively. The measured surface SRP and TP data are usually below

the detection limits (*i.e.*, 0.008 and 0.08 mg/L P, respectively), and the bottom SRP and TP data are also below the detection limits in the winter and spring. Despite that, general trends in the measured phosphorus data can still be observed. At the surface, phosphorus levels were usually low due to consumption by algae. At the bottom, phosphorus concentrations were low at the beginning of 2006 when the reservoir was fully mixed. As the reservoir became stratified in the early spring of 2006, phosphorus concentrations started to increase due to the release of phosphorus from the sediment caused by anoxic conditions in the hypolimnion. However, after June 2006, phosphorus concentrations stayed relatively constant until the reservoir was fully mixed again in January 2007. This is due to the fact that the sediment release of phosphorus in spring probably exhausts the phosphorus storage in the sediments. In 2007, phosphorus concentrations increased slowly at the bottom through the year. As shown, the model captures these trends fairly well although the simulated bottom concentrations are slightly higher than the measured data.

Comparison plots of the simulated and measured ammonia, nitrate, and TN concentrations are provided in **Figures 45** through **47**, respectively. In these figures, ammonia concentrations are below the detection limit (*i.e.*, 0.04 mg/L N) at the surface throughout the year and at the bottom during the destratified period. The nitrate concentrations are below the detection limit (*i.e.*, 0.02 mg/L N) from about July through January of each year. The observed trends in measured ammonia data are similar to those in measured phosphorus data. However, the trends of nitrate concentrations at the bottom are the reverse of those in ammonia concentrations: nitrate concentrations are high when the reservoir is destratified and DO at bottom is high; nitrate concentrations decrease when the reservoir is stratified and DO at bottom is low. This is because ammonia in the sediment can convert to nitrate through a nitrification process if oxygen is present and, consequently, the sediment releases nitrate instead of ammonia. Once the bottom of the reservoir becomes anoxic, nitrate is depleted slowly by denitrification. As shown, the simulated ammonia and nitrate match the trends and magnitude of the measured data fairly well.

The simulated TN concentrations match the measured concentrations during the destratified periods and follow the general trends of the data, although the simulated TN concentrations are significantly lower than a few measured data points during the summer of 2006. These measured TN concentrations in the summer of 2006 are very high compared to those in summer of 2007. There are no evident sources of nitrogen that can explain such spikes.

5.3.4 Chlorophyll *a* and Secchi Depth

There are no measured chlorophyll *a* concentrations available in years 2006-2007 at SVR. Instead, chlorophyll *a* concentration profiles were estimated using an optical fluorometer and were provided by the City (**Figure B-11** through **B-15**). The optical

fluorometer measures fluorescence and, if calibrated, can make an estimate of relative chlorophyll *a* concentrations because algae fluoresce at characteristic wavelengths. Optical fluorometers can be used to collect profile measurements similar to a temperature or conductivity probe. Thus, they could provide more data (albeit of lower quality) more economically than could be obtained with grab samples and laboratory analysis. However, fluorometer readings can be corrupted by other particles present in the water column and indicate "false" algae blooms. For example, in SVR, the algae bloom that starts from August 2007 is probably a "false" algae bloom because the data show extremely high chlorophyll *a* concentrations (> 100 µg/L) at the depth below the thermocline but measured DO profiles show no evidence of high oxygen spikes/production at that depth to support the existence of such algae bloom (**Figure 48**). These high readings of fluorescence below the thermocline could, for example, be caused by the accumulation of surface algae and other particles at the thermocline due to settling flocculants such as manganese and iron hydroxides formed in the epilimnion. Manganese and iron hydroxides are insoluble under high DO conditions (*e.g.* in the epilimnion) and soluble under low DO conditions (*e.g.* in the hypolimnion). Therefore, if water is rich in manganese and iron hydroxides which are flocculants, they form flocs in the epilimninon under high DO conditions. These flocs catch algae and other particles as they settle at the thermocline, leading to concentrated algae and particles (thus high readings of fluorescence) at the thermocline. Similar processes involved in arsenic accumulation at the thermocline have been reported at Halls Brook Pond, Massachusetts (Ford, *et al.,* 2005 and 2006)

Since a fluorometer calibration had not been conducted at SVR, the simulated chlorophyll *a* concentrations by the SVR model were not compared directly against chlorophyll *a* data estimated using fluorometer data. Instead, the calibration of chlorophyll *a* was conducted through a "simulated" Secchi depth derived from a correlation between the simulated chlorophyll *a* concentrations and Secchi depth.

Secchi depth is a measure of the degree of transparency at the reservoir surface and, in a water body like SVR, is generally strongly correlated (for water with low inorganic turbidity) with chlorophyll *a* concentration since algae growth affects water clarity. Based on a study by Rast and Lee (1978) on various reservoirs, the following relationship was suggested:

$$\text{Log (Secchi Depth in m)} = -0.473 \text{ Log (Chlorophyll } a \text{ in } \mu g/L) + 0.803 \qquad \text{[Eqn. 4]}$$

Although CAEDYM does not simulate Secchi depth directly, the "simulated" Secchi depths can be derived from the simulated surface chlorophyll *a* concentrations using this formula. Therefore, a good calibration for Secchi depth can be translated into a good calibration for chlorophyll *a* concentrations.

The "simulated" Secchi depths are plotted against the measured Secchi depths in **Figure 49**. The measured Secchi depths are generally in the range of 3 to 5 m from

January through September 2006. However, between October and December 2006, the Secchi depths decreased significantly and remained low through June 2007. This period of small Secchi depth corresponds to the Bypassing Period when 80% of flow into the Aqueduct was coming directly from the San Diego Canal that has higher nutrient levels as discussed in **Section 5.2.2**. It is believed that the decrease in Secchi depth starting in October 2006 is predominantly due to chlorophyll *a* growth (verbal communication with Jeffery Pasek of the City) caused by a large influx of nutrient from the water in the San Diego Canal during the Bypassing Period.

The Secchi depth data in **Figure 49** suggest that the calibrated chlorophyll *a* concentrations during the Bypassing Period and through June 2007 are still a little lower than the data. But without more detailed information on the Aqueduct source water quality and direct chlorophyll *a* measurements, it was difficult to obtain a better correlation. A scatter plot of the measured and simulated Secchi depth for years 2006 and 2007 is provided in **Figure 50**. A statistical analysis of the calibration results versus the measured data produced the metrics presented in **Table 9**. The computed Root Mean Square Errors (RMSE) indicate that the calibrated Secchi depths are on average within 1.2 m of the measured data, corresponding to about 20% of the range in measured Secchi depth. These indicate a fairly good calibration for both Secchi depth and chlorophyll *a*, especially considering the unknown nutrient loadings during the Bypassing Period.

Table 9. Secchi Depth Calibration Metrics

PARAMETER	2006 RESULTS			2007 RESULTS		
	ROOT MEAN SQUARE ERROR (RMSE)	RELATIVE RMSE	MEAN ERROR	ROOT MEAN SQUARE ERROR (RMSE)	RELATIVE RMSE	MEAN ERROR
Secchi Depth	1.06 m	20.8 %	0.18 m	1.14 m	22.3 %	-0.87 m

6. CONCLUSIONS AND DISCUSSION

A three-dimensional water quality model has been applied, calibrated and verified for SVR. It is anticipated that this model will be used to study the dynamics, mixing, and residence time of advanced treated recycled water and its effects on eutrophication in the expanded SVR.

The modeling domain includes the existing portion of the reservoir as well as the proposed expanded portion of the reservoir. A fine grid with a horizontal resolution of 50 × 50 m was used in the ELCOM calibration while a coarse grid with a horizontal resolution of 100 × 100 m was used in the CAEDYM calibration. This was necessitated by the large computer requirements and the desire to limit computation time to several days per model run for a two-year simulation. A variable grid size was used in the vertical dimension with a grid size of 1.64 ft (0.5 m) near the surface, and expanding in size with depth. The calibration was conducted for the two-year period of 2006-2007. The input data required by the calibration were either based on measured data or derived from these data. ELCOM requires limited calibration effort in that the physical aspects of water movements in reservoirs are fairly well understood. The CAEDYM model was calibrated by adjusting some model bio-chemical parameters so that the simulation results best match measured field data.

The calibrated/validated ELCOM model shows good agreement with the measured data for both water temperature and conductivity. The calibration involved reconstruction of some meteorological data during periods where data were unavailable. It also involved an adjustment for the outlet port openings in the second half of 2007. As discussed in detail in the report, the City-specified field reports of the ports open during a portion of 2007 are at variance with the basic thermodynamics of the system. It is demonstrated later in this report that the open ports must have been at or above the thermocline level and not in the hypolimnion, as specified. In the future, it is recommended that outflow temperatures from SVR be recorded so that they can provide verification of the field record of port openings.

The onset and duration of thermal stratification as well as the deepening rate of the thermocline were predicted accurately by the model. Furthermore, the water conductivity, a measure of salinity, was well predicted by the model. It is noted that future modeling of the hydrodynamics at SVR would benefit from a full set of meteorological data gathered at SVR (the City stopped gathering on-site meteorological data in March 2007). An analysis presented herein shows that the meteorological data measured at the nearby California Irrigation Management Information System (CIMIS) station in Escondido differ in significant aspects from data gathered at SVR.

After the model was calibrated, a validation was performed to compare the model against the results of previous field studies. The field studies involved two separate episodes of tracer injection in the reservoir (winter 1995 and summer 1995). The field

studies clearly showed the impacts of stratification (or lack thereof) on the mixing and dispersion of the tracer. The ELCOM model was capable of replicating the main features of the tracer study. Due to the nature of the tracer used in those studies (Lanthanum Chloride), a significant amount of tracer was lost due to coagulation/flocculation and subsequent settling. A simple coagulation/settling model was added to ELCOM. After the implementation of the coagulation/settling model, very good agreement between the model and the data was obtained. This validation provides strong verification and assurance that the model performance is accurate.

The calibration of the water quality model CAEDYM was carried out after the ELCOM calibration and verification process. The comparison between simulation results and measured in-reservoir field data involved water quality parameters including dissolved oxygen (DO), pH, nutrients (nitrogen and phosphorus), chlorophyll *a* and Secchi depth. It is noted that some assumptions had to be made in order to calibrate the model. For example, assumptions on nutrient levels for the Aqueduct inflows during the "Bypassing Period" were needed to characterize nutrient loadings because there are only limited nutrient data available for the Aqueduct inflow.

The calibrated CAEDYM model shows overall good agreements with measured data. The simulated DO concentrations capture the major trends in the measured DO concentrations, including the onset, duration, and magnitude of periods of anoxia in the hypolimnion, the depth to the top of the anoxic (*i.e.*, "without oxygen") region, the DO decay rate in the spring in the hypolimnion, and the high surface DO concentrations in the spring (and sometimes fall) that are due to algae blooms. The simulated pH values closely match the measured data and are on average within 0.3 of the measured values. The calibrated model also replicates the major trends in the measured nutrient (phosphorus and nitrogen) concentrations. It is noted, however, that some of the field data are below the detection limit and real values of the nutrient concentrations on these days are unknown. The available in-reservoir chlorophyll *a* data were qualitatively measured using a fluorometer that has not been calibrated. The calibration of chlorophyll *a* had to be conducted indirectly through the calibration of Secchi depth. The final calibration run shows a fairly good agreement with the measured Secchi depths, indicating a fairly good calibration for chlorophyll *a*.

At this point, it is believed that the model calibration/validation is nearly complete. The calibrated/validated model will undergo peer review. After that, the model will be applied to the study of the expanded reservoir as well as the evaluation of the mixing of the advanced treated recycled water within the reservoir. The planned modification of Aqueduct release locations/facilities into the expanded SVR and outlet structure/port depths will be incorporated into the model.

Future evaluations and modeling of water quality at SVR would benefit from more frequent sampling of nutrients and chlorophyll *a* within the reservoir, also from lower nutrient detection limits, and an increased use of duplicate samples or periodic sampling

audits. It is recommended that nutrient samples be collected more frequently and at additional depths throughout the water column. This would increase the data resolution and reliability, improve understanding of the reservoir behavior, and allow for a more precise water quality calibration. It is further recommended that the collection of chlorophyll *a* samples be resumed. Composite samples should be collected from the reservoir surface in order to analyze chlorophyll *a* concentrations in the laboratory. This would allow for calibration of the optical fluorometer data and improve the usefulness and interpretation of that data. Finally, it is recommended that more frequent sampling of nutrients and other parameters be conducted for the inflows (especially the Runoff, and the Aqueduct inflow during bypassing conditions).

7. REFERENCES

Beutel, M. (2001). "San Vicente Reservoir: Sediment-Water Interface Study," dated July 2001 and submitted to the San Diego Water Department.

City of San Diego (2008). "IPR Description for BOR Grant 122208 MS," obtained from Jeffery Pasek of the City of San Diego through email on December 23, 2008

Flow Science Incorporated (1994). "Water Recycling Conceptual Feasibility Study, San Vicente Reservoir, prepare for Montgomery Watson on behalf of Water Authority," FSI Project No. C938088, Pasadena, CA

Flow Science Incorporated (1995). "San Vicente Water Reclamation Project: Results of Tracer Studies, prepared for Montgomery Watson," FSI Project No. P941003, Pasadena, CA.

Flow Science Incorporated (1997). "San Vicente Reservoir Hypolimnetic Oxygenation System Design Support, prepared for Boyle Engineering Corp. on behalf of City of San Diego Water Department," FSI Project No. P974005, Pasadena, CA.

Flow Science Incorporated (2001). "Analysis and Modeling For San Diego Reservoir Oxygenation System, prepared for Boyle Engineering Corp. on behalf of City of San Diego Water Department," FSI Project No. V044091, Pasadena, CA.

Flow Science Incorporated (2005a). "Water Quality Assessment For San Vicente Reservoir Enlargement, prepared for GEI Consultants, Inc. on behalf of Water Authority," FSI Project No. V044091, Pasadena, CA.

Flow Science Incorporated (2005b). "Lake Mead ELCOM/CAEDYM Modeling, prepared for Black & Veatch on behalf of Clean Water Coalition," FSI Project No. S014004, Pasadena, CA.

Flow Science Incorporated (2009). "Water Quality Assessment of San Vicente Reservoir During Construction Drawdown Conditions, prepared for GEI Consultants, Inc. on behalf of Water Authority," FSI Project No. V074117, Pasadena, CA.

Ford, R.G., R.T. Wilkin, C.J. Paul, F. Beck and T. Lee (2005). "Field Study of the Fate of Arsenic, Lead, and Zinc at the Ground-Water/Surface-Water Interface," EPA/600/R-05/161, U.S. Environmental Protection Agency, Ada, Oklahoma.

Ford, R.G., R.T. Wilkin and G. Hernandez (2006). "Arsenic Cycling within the Water Column of a Small Lake Receiving Contaminated Ground-water Discharge," Chemical Geology, Vol. 228. No.1-3, p137-155.

Niquette, P., F. Monette, A. Azzouz and H. Hausler (2004). "Impacts of Substituting Aluminum-Based Coagulants in Drinking Water Treatment," Water Quality Research Journal of Canada, Vol. 39, No.3 p303-310.

Rast, W. and G.F. Lee (1978). "Summary Analysis of the North American (U.S. portion) OECD Eutrophycation Project: Nutrient loading – lake response relationships and trophic state indices," Ecological Research Serries, No. EPA-600/3-78-008, U.S. Environmental Protection Agency, Corvallis, Oregon, 454p.

Recht, H.L., M. Ghassemi and E.V. Kleber (1970). "Percipitation of Phosphate from Water and Wastewater using Lanthanum Salts," Presented at the 5th International Water Polluation Research Conference, San Francisco, California. P.I-17/1-I-17/12, July-August.

Welch, M.R. (1997). "Draft Report: San Vicente Reservoir Management Program – Water Repurification Project, prepare for Montgomery Watson on behalf of City of San Diego", dated on November 1997 and submitted to the City of San Diego.

FIGURES

San Vicente Reservoir

Plan View of Existing and Expanded Reservoir and Inflow/Outflow Locations

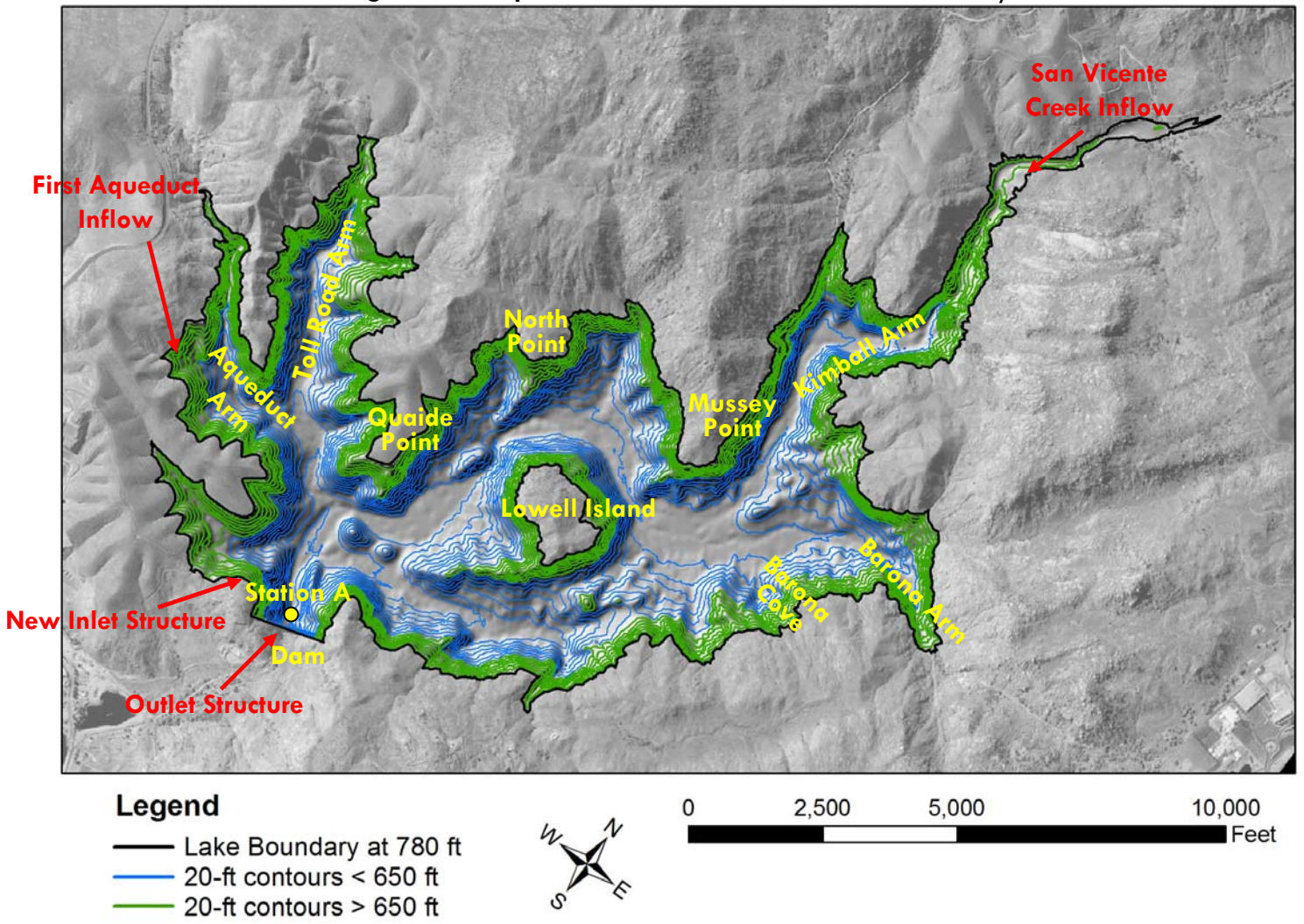

FSI V094005
May 01, 2012

Figure 1

FLOW SCIENCE®

ELCOM-CAEDYM

Schematic of Processes Modeled in ELCOM-CAEDYM

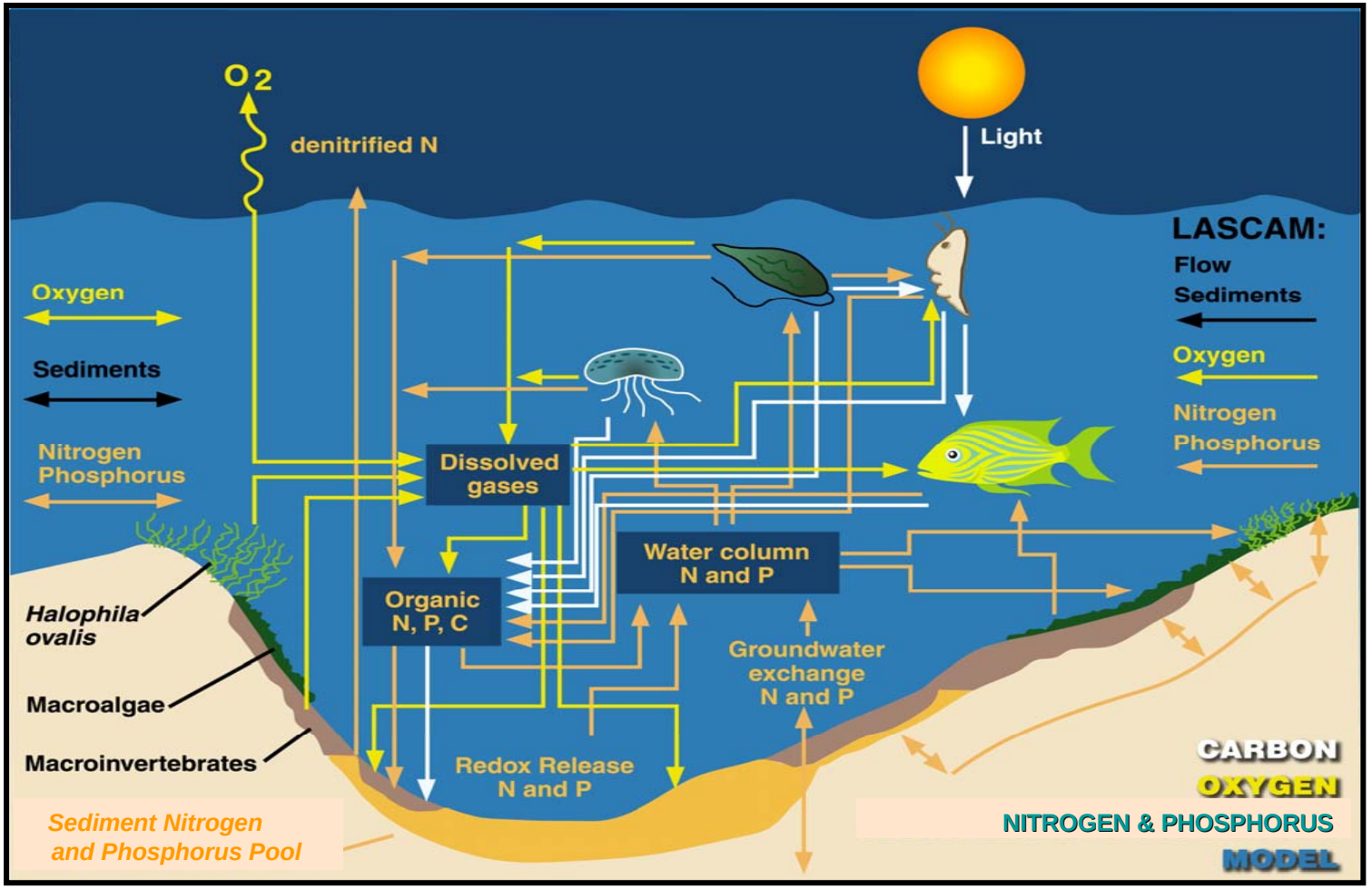

FSI V094005
May 01, 2012

Figure 2

FLOW SCIENCE®

San Vicente Reservoir 50-m ELCOM Computational Grid

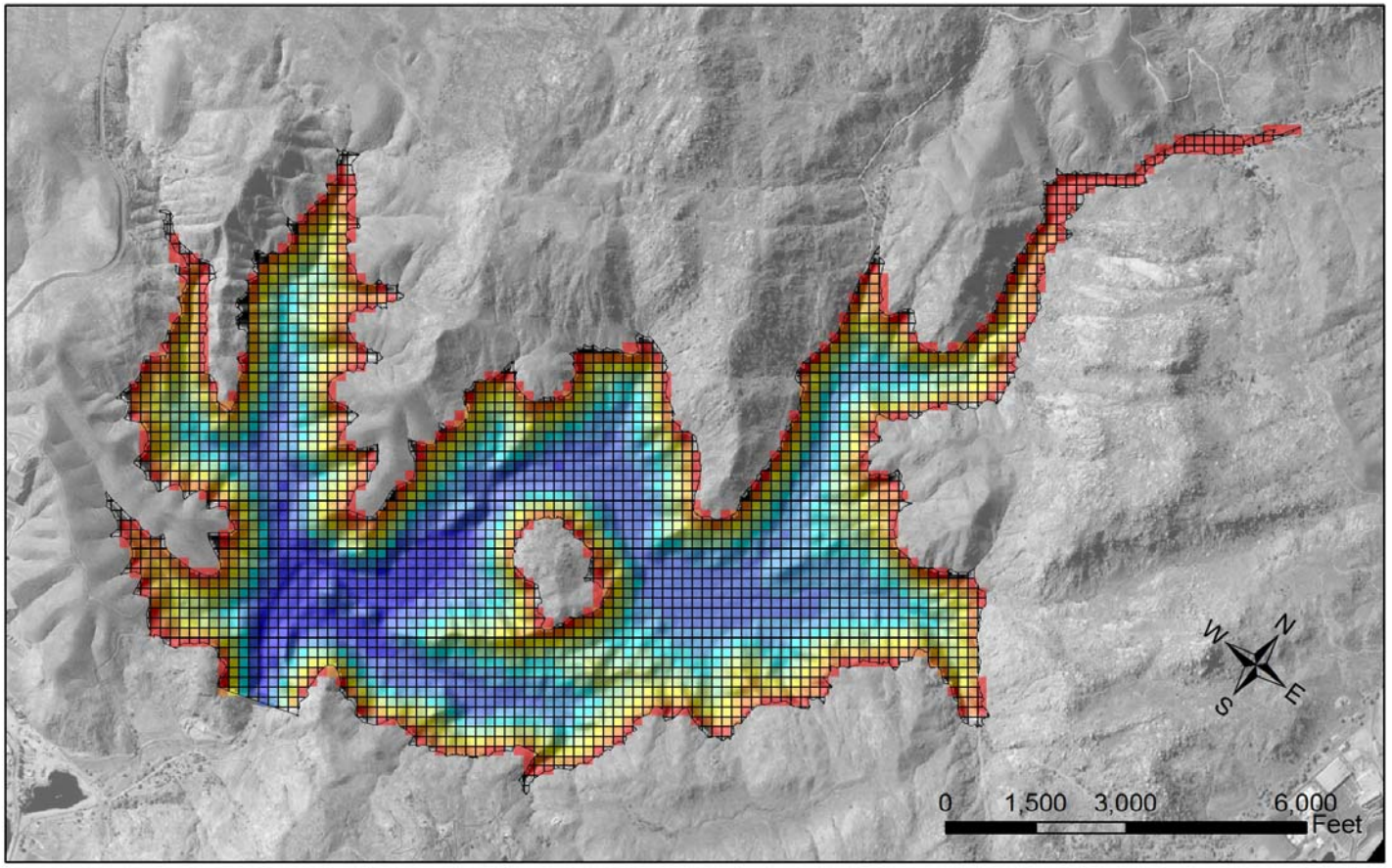

San Vicente
50-m ELCOM Grid

Legend

Lake Boundary at 780 ft

Elevation (ft)			
480 - 510	541 - 569	630 - 659	719 - 748
511 - 540	570 - 599	660 - 689	749 - 778
	600 - 629	690 - 718	

Figure 3

FSI V094005
May 01, 2012

FLOW SCIENCE®

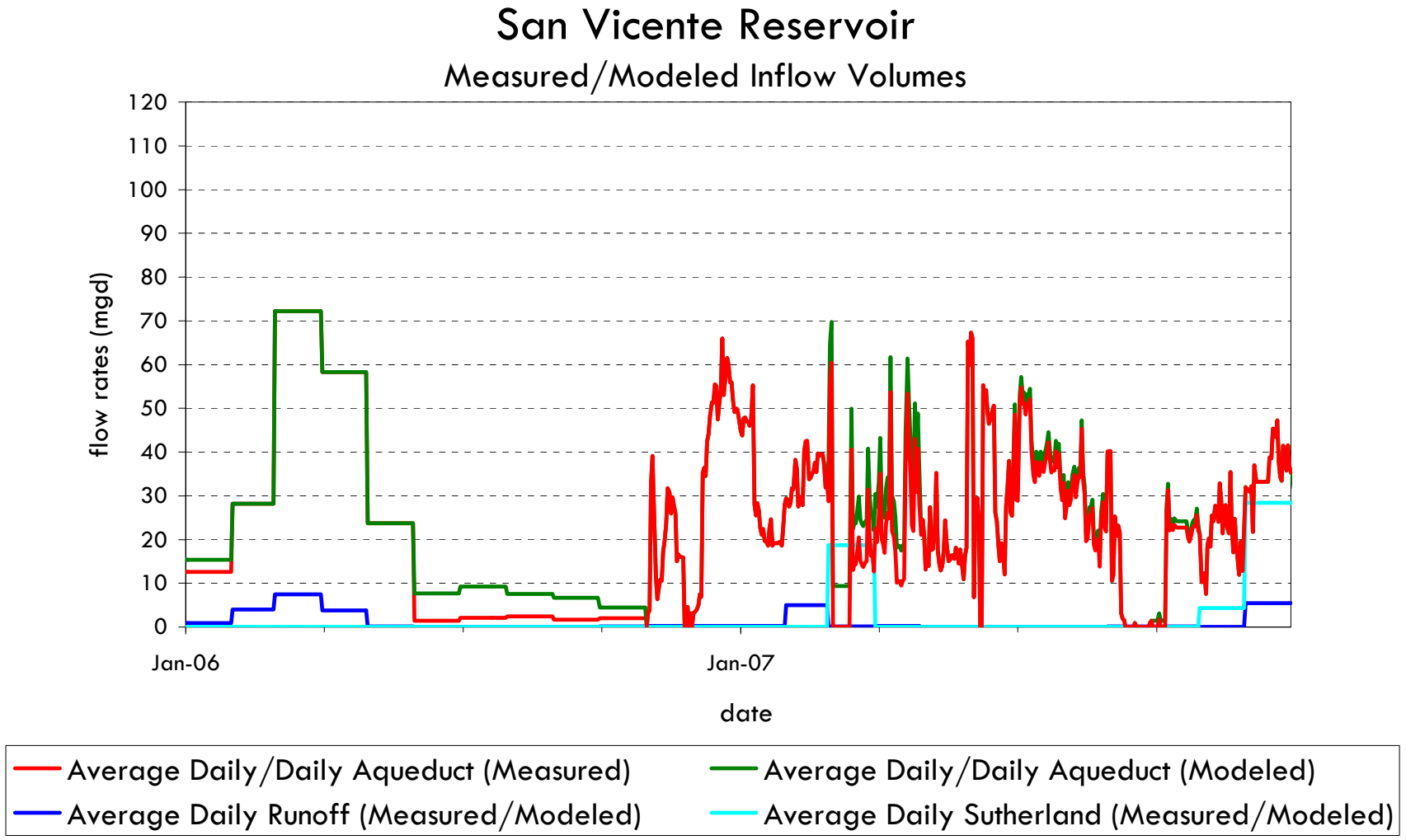

FSI V094005
May 01, 2012

Figure 4

FLOW SCIENCE®

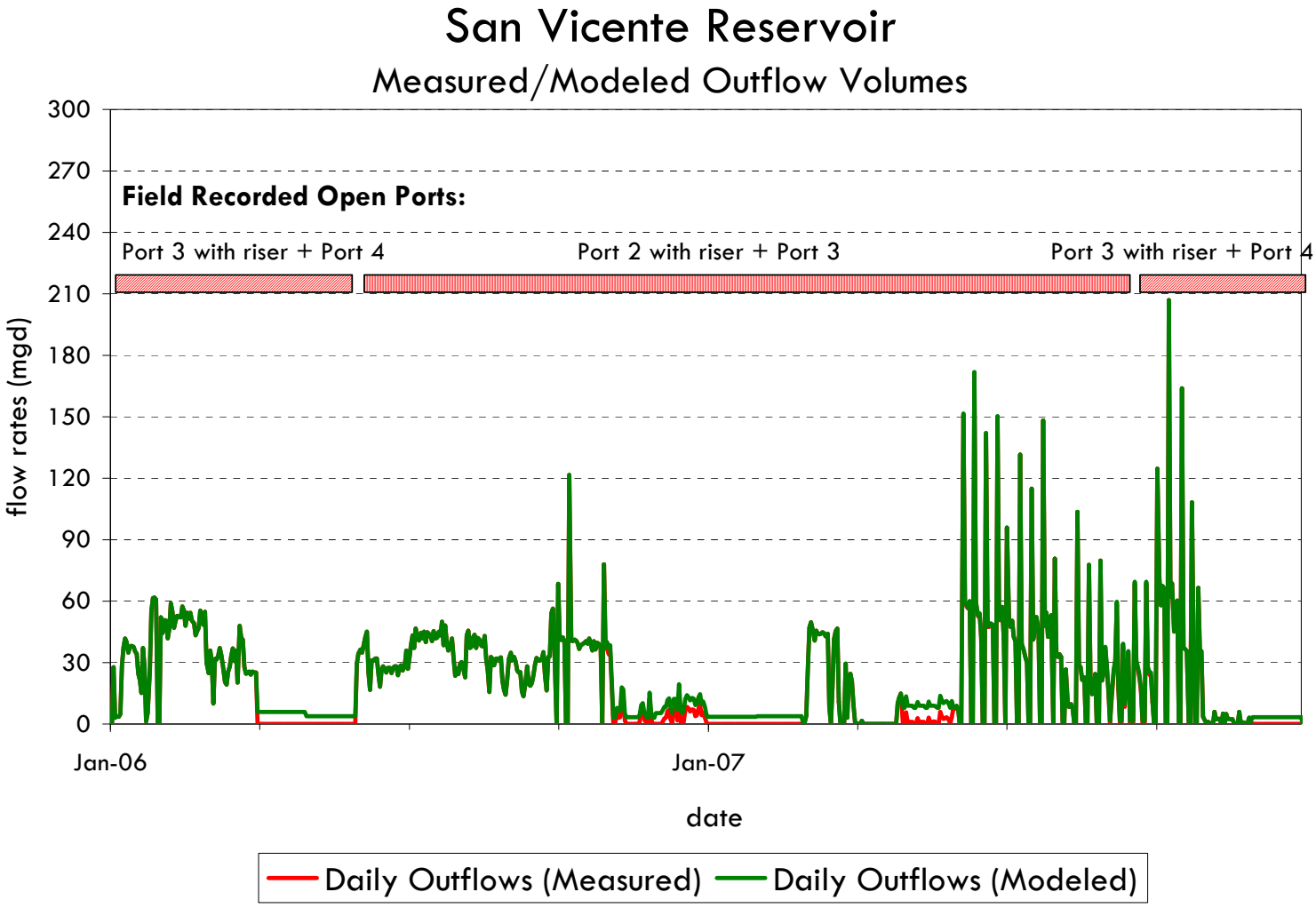

FSI V094005
May 01, 2012

Figure 5

FLOW SCIENCE®

Map of Meteorological Stations

FSI V094005
May 01, 2012

Figure 6

FLOW SCIENCE®

San Vicente Reservoir

Station A – Simulated Temperature Using CIMIS Meteorological Data After March 2007

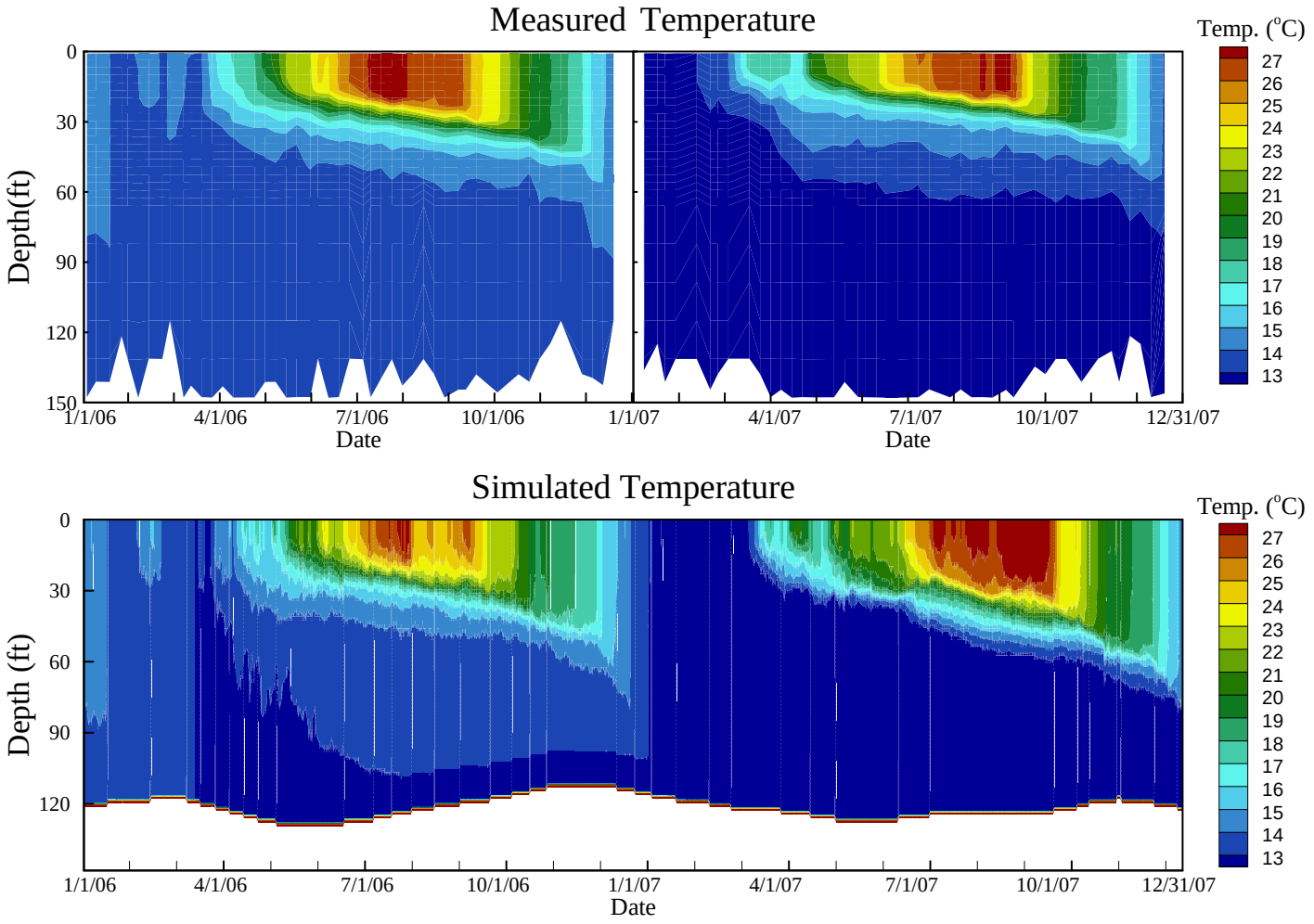

Figure 7

FSI V094005
May 01, 2012

FLOW SCIENCE®

San Vicente Reservoir - Station A Temperature Calibration

Impact of Using Different Meteorological Inputs

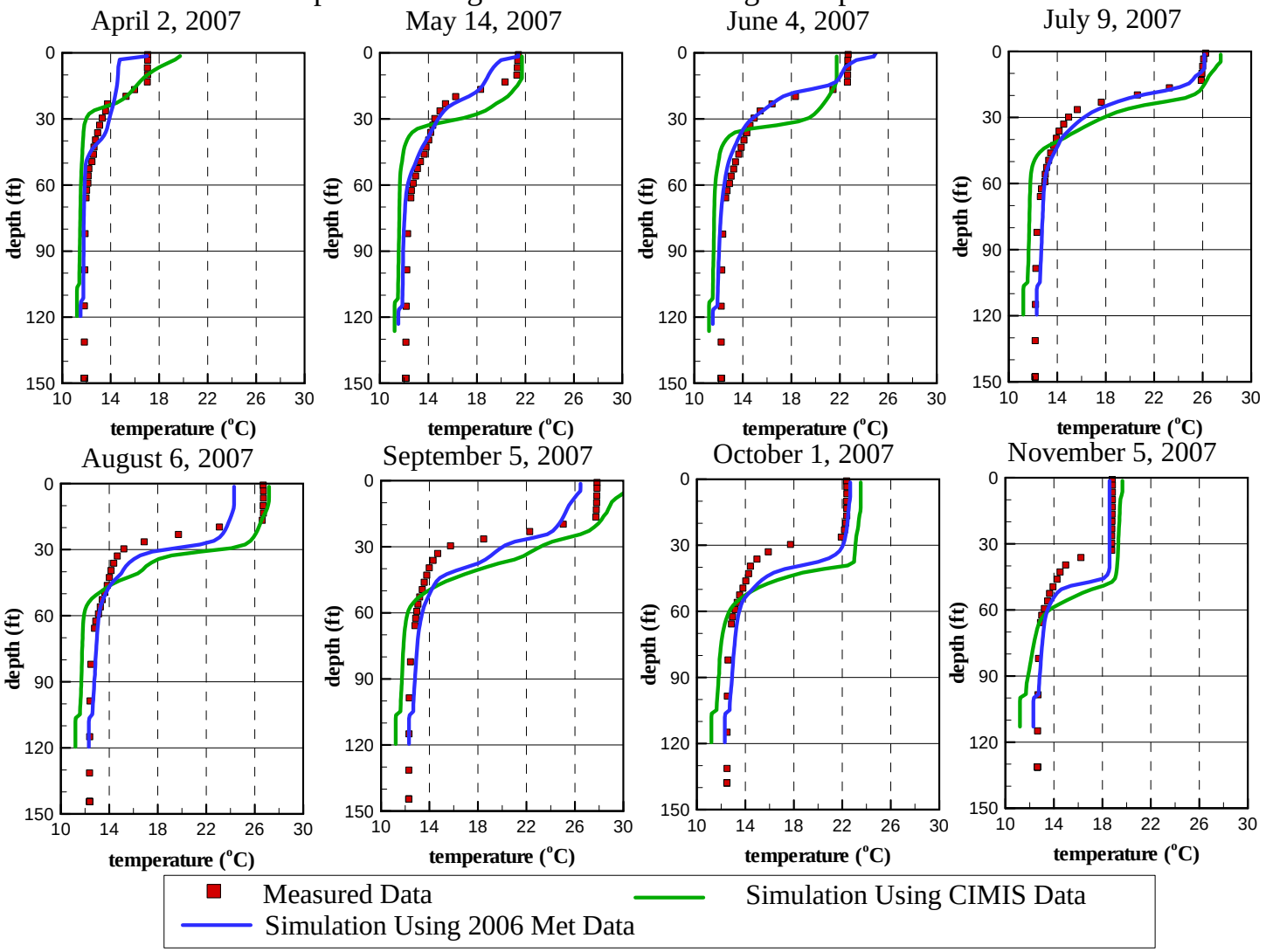

FSI V094005
May 01, 2012

Figure 8

FLOW SCIENCE®

San Vicente Reservoir

Station A - Measured Temperature Contours (2000-2007)

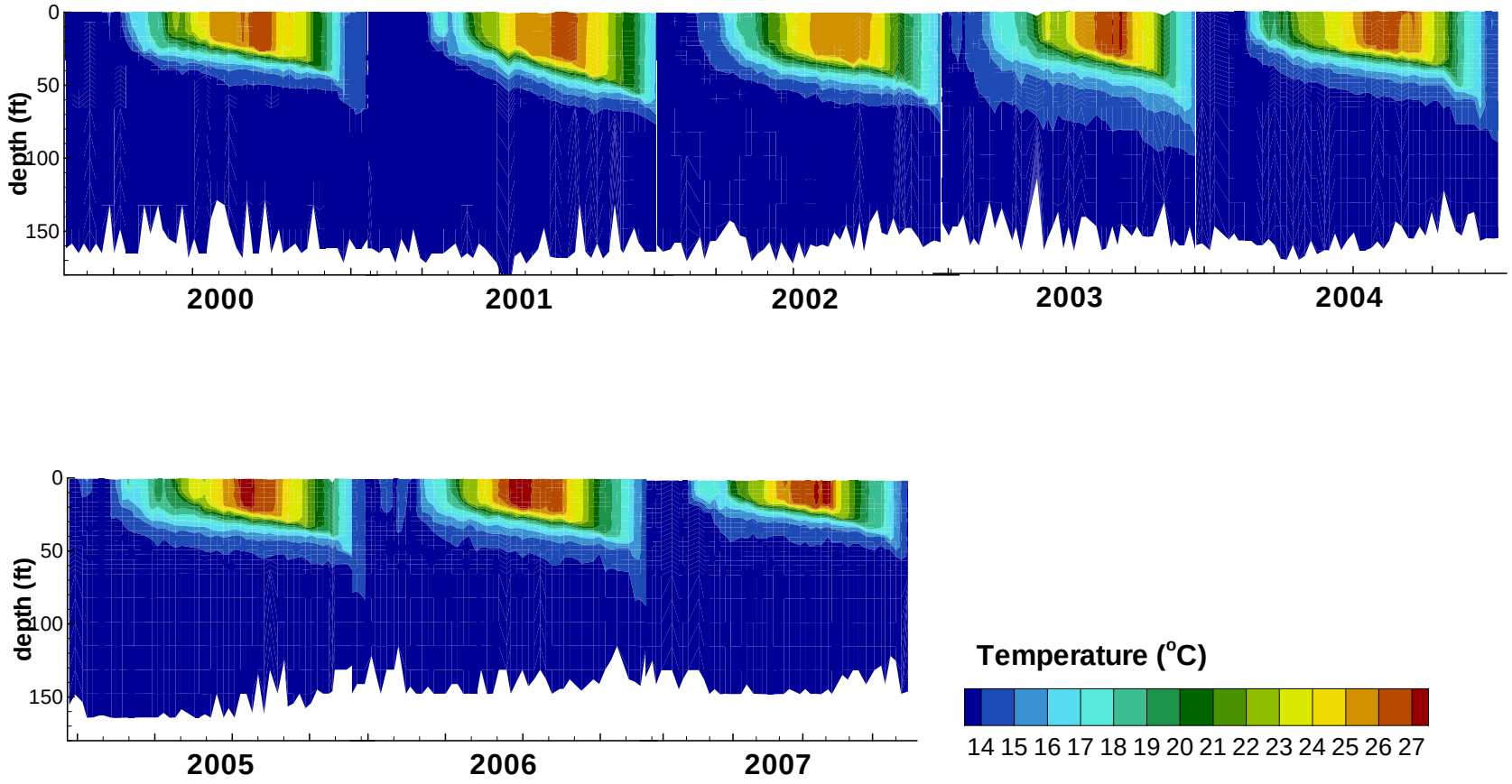

FSI V094005
May 01, 2012

Figure 9

FLOW SCIENCE®

San Vicente Reservoir

Comparison of 2006 and 2007 Measured Aqueduct Inflow Rates and Temperatures

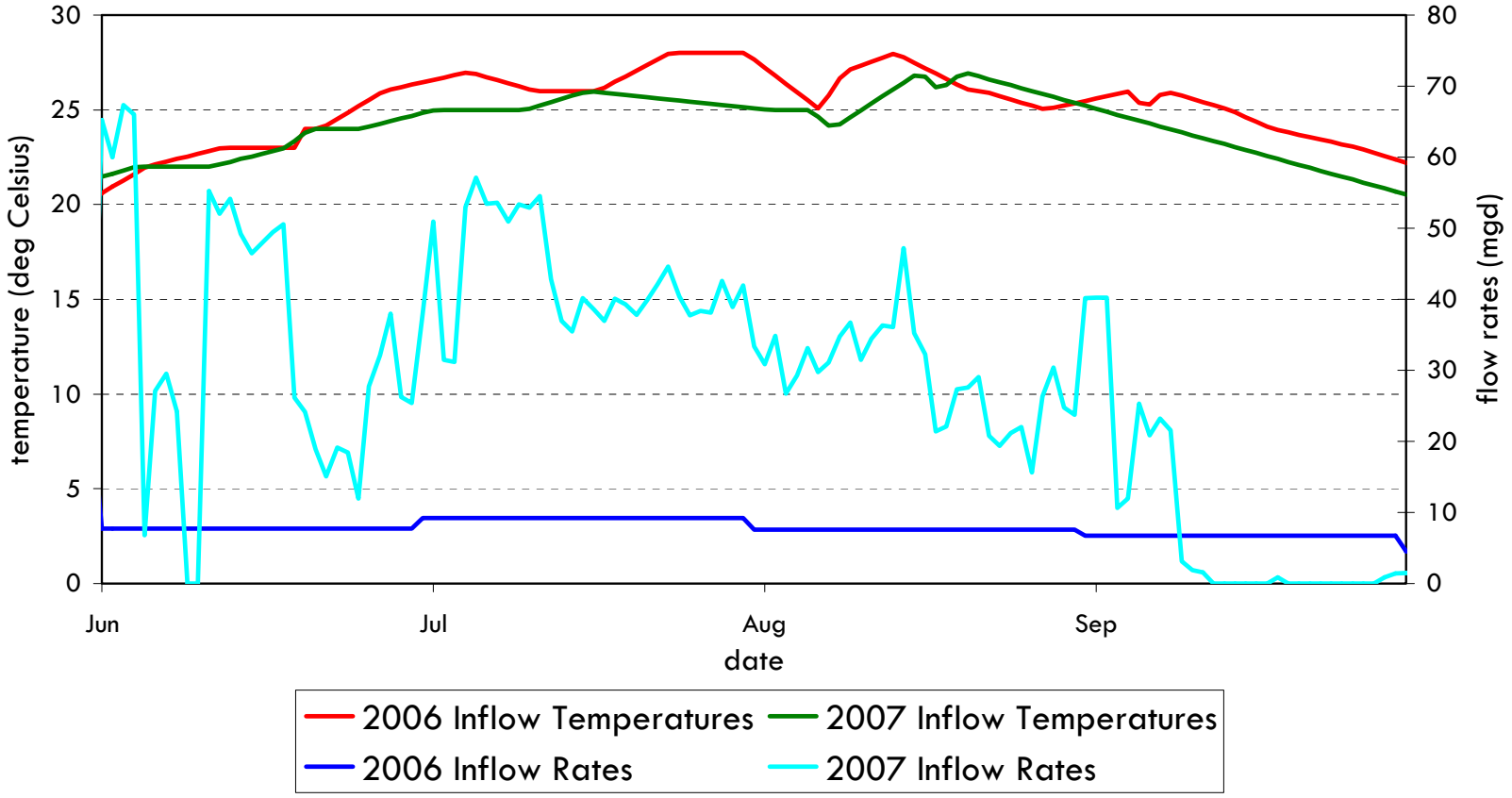

FSI V094005
May 01, 2012

Figure 10

FLOW SCIENCE®

San Vicente Reservoir

Station A - 2006-2007 Measured Temperature Profiles

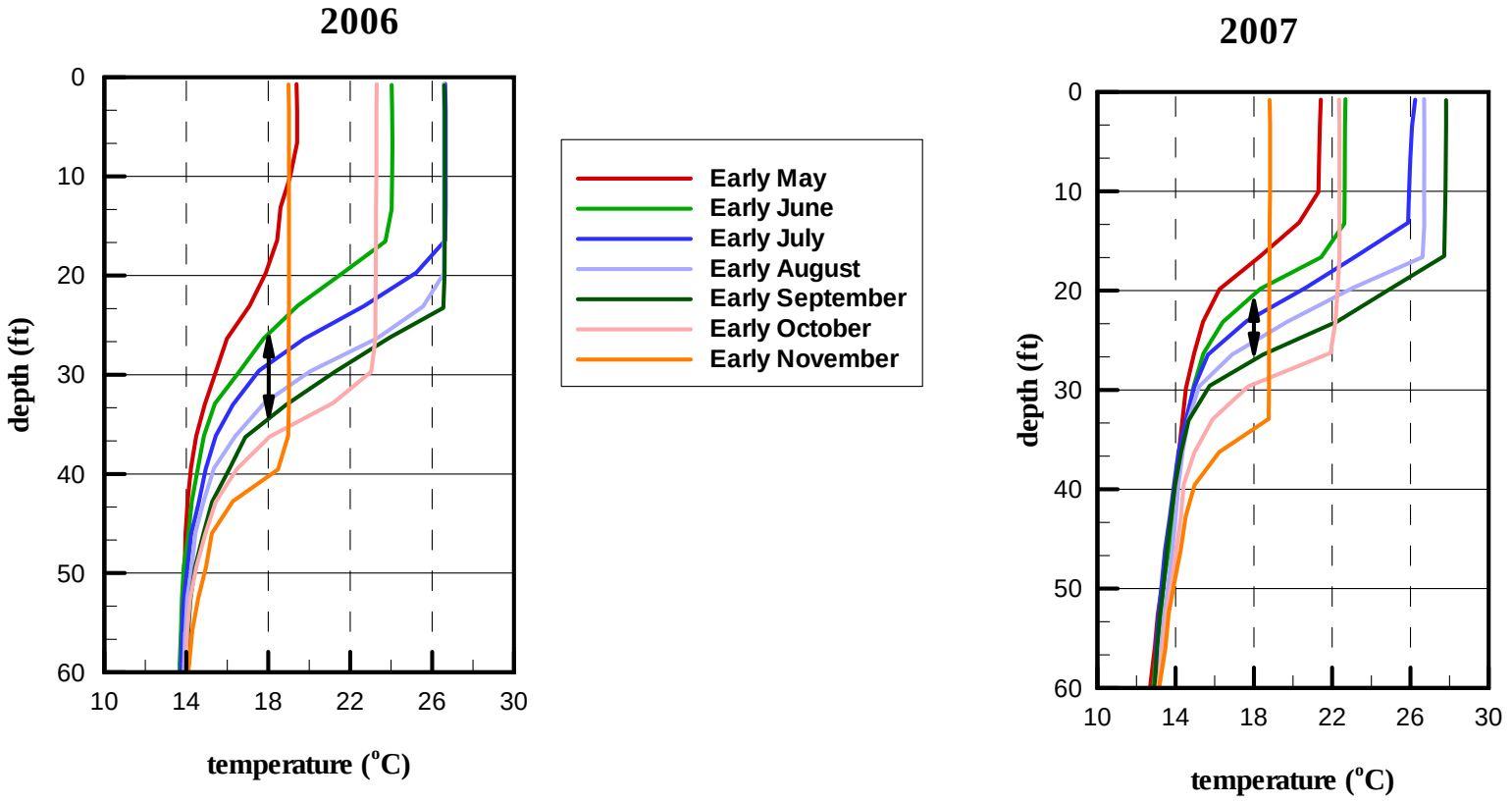

↔ Thermocline Deepening Between Early June and Early September

FSI V094005
May 01, 2012

Figure 11

FLOW SCIENCE®

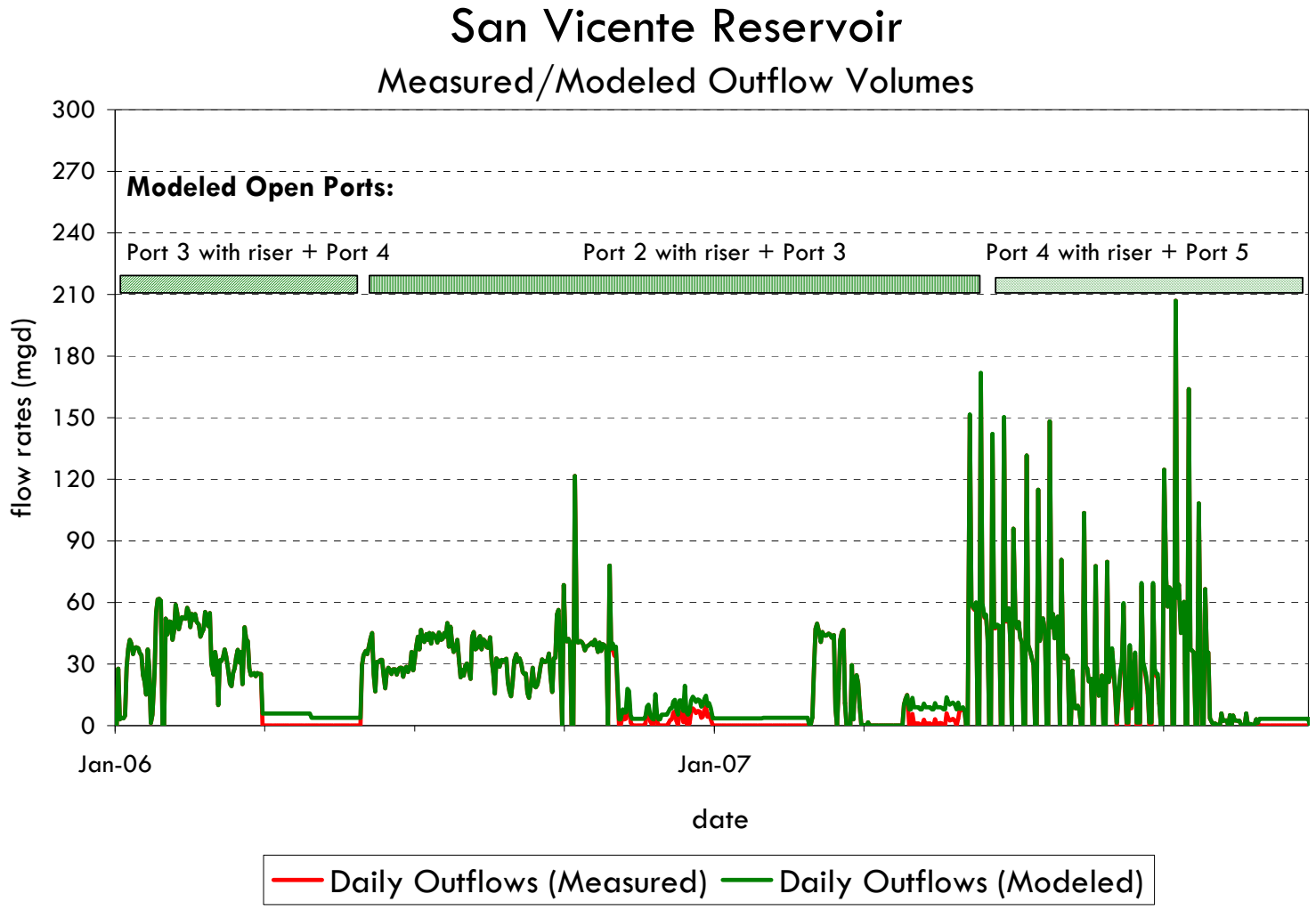

FSI V094005
May 01, 2012

Figure 12

FLOW SCIENCE®

San Vicente Reservoir - Station A Temperature Calibration

Impact of Opening Different Outlet Ports

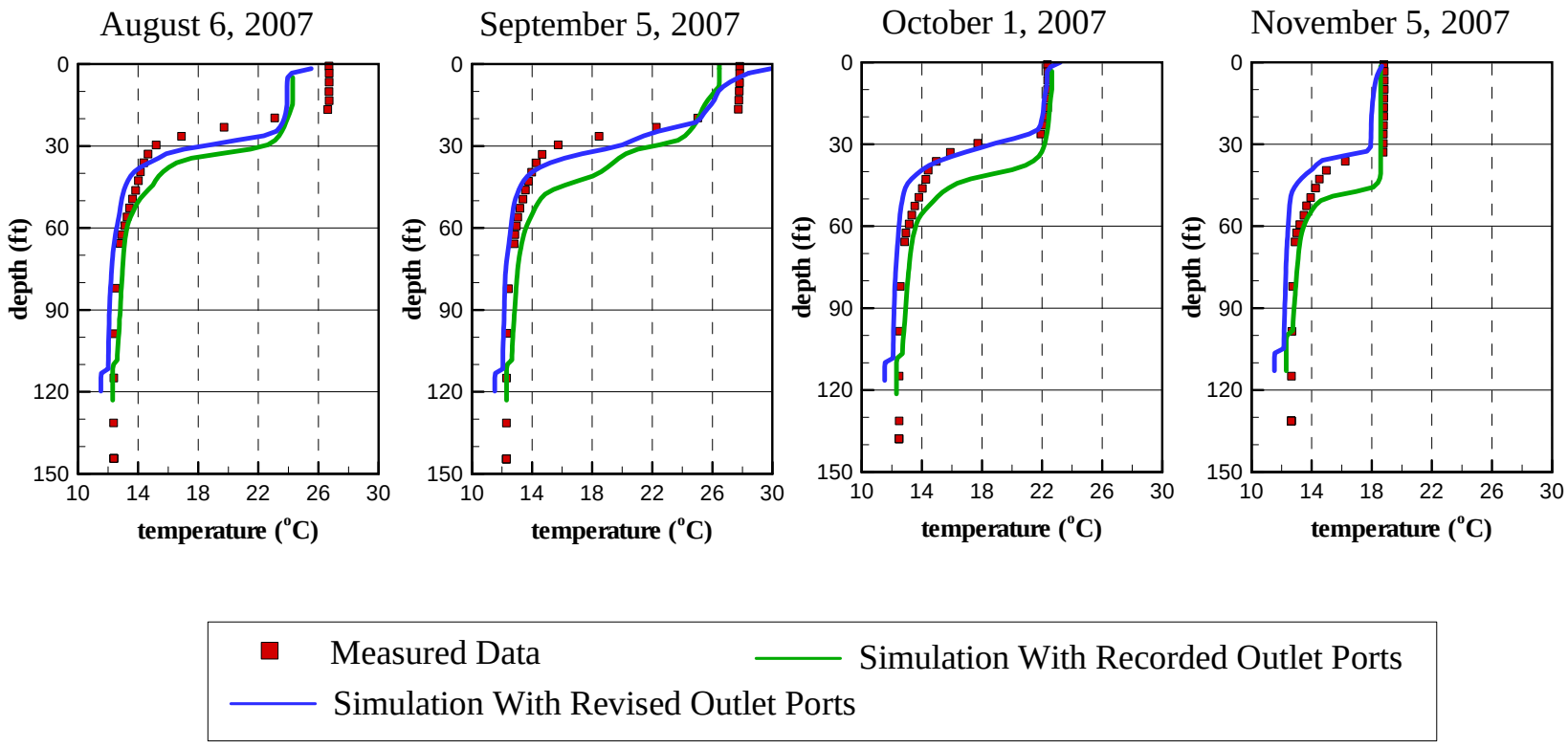

FSI V094005
May 01, 2012

Figure 13

FLOW SCIENCE®

San Vicente Reservoir

Measured vs Simulated Water Surface Elevations

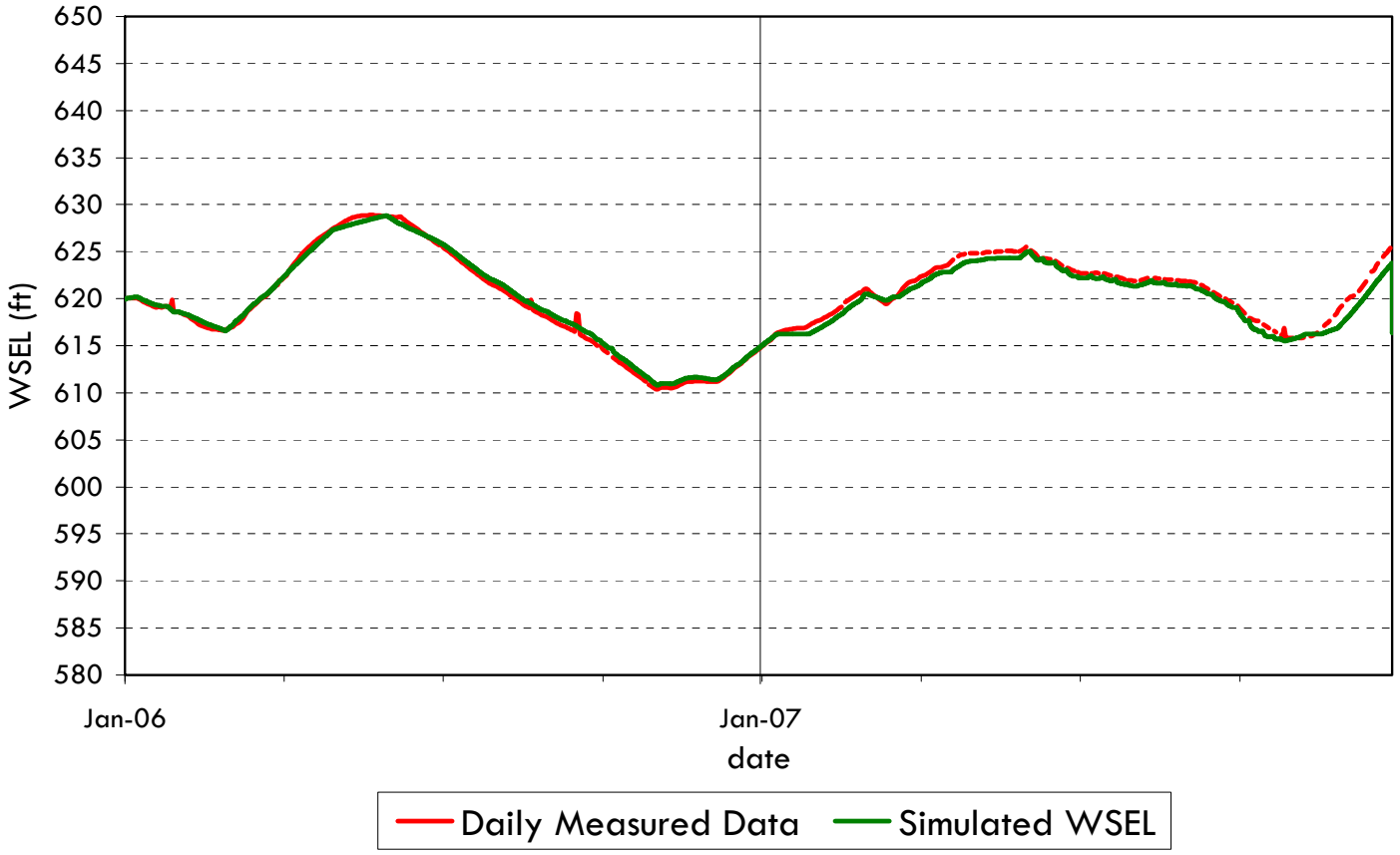

FSI V094005
May 01, 2012

Figure 14

FLOW SCIENCE®

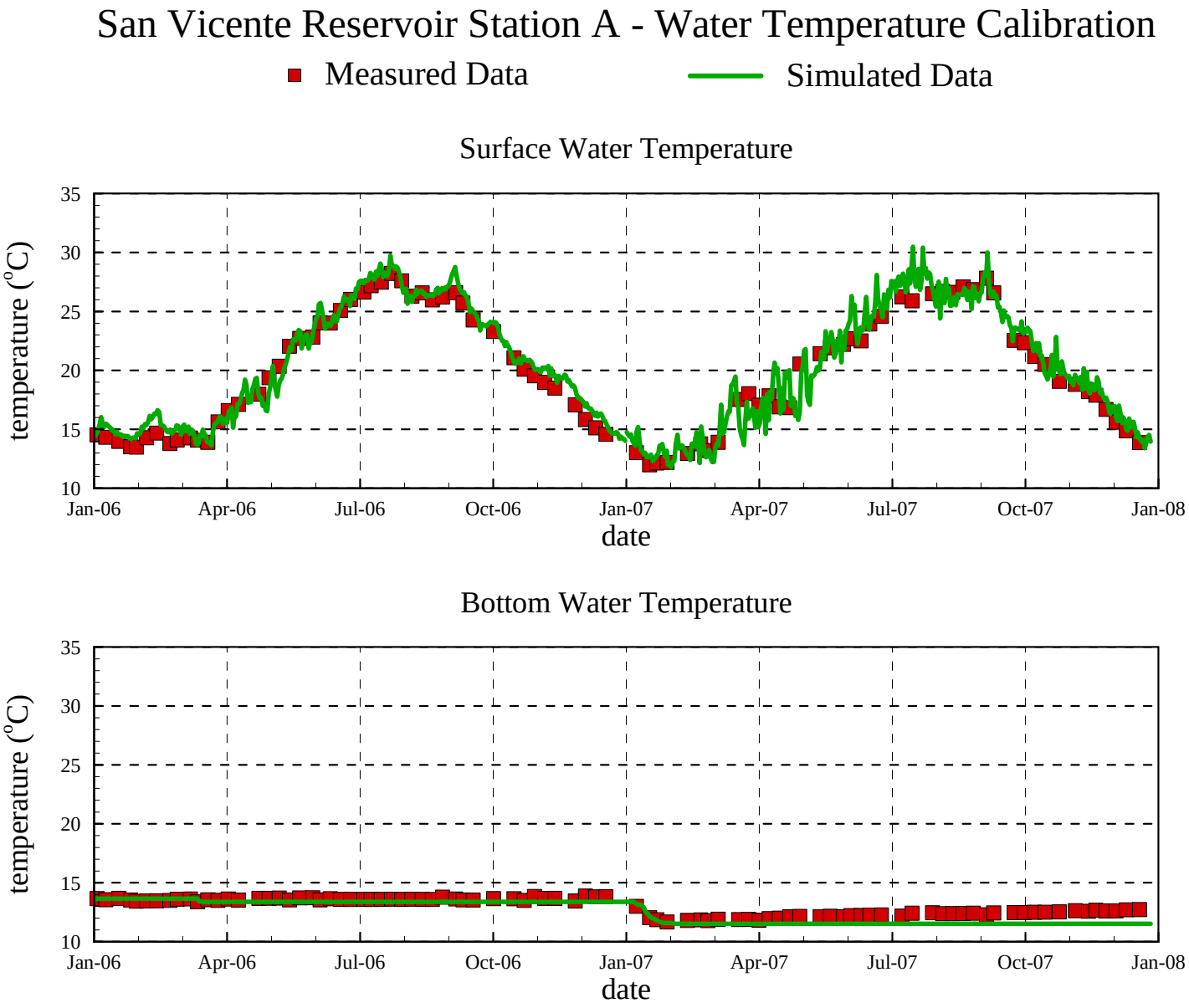

FSI V094005
May 01, 2012

Figure 15

FLOW SCIENCE®

San Vicente Reservoir

Station A - Water Temperature Calibration

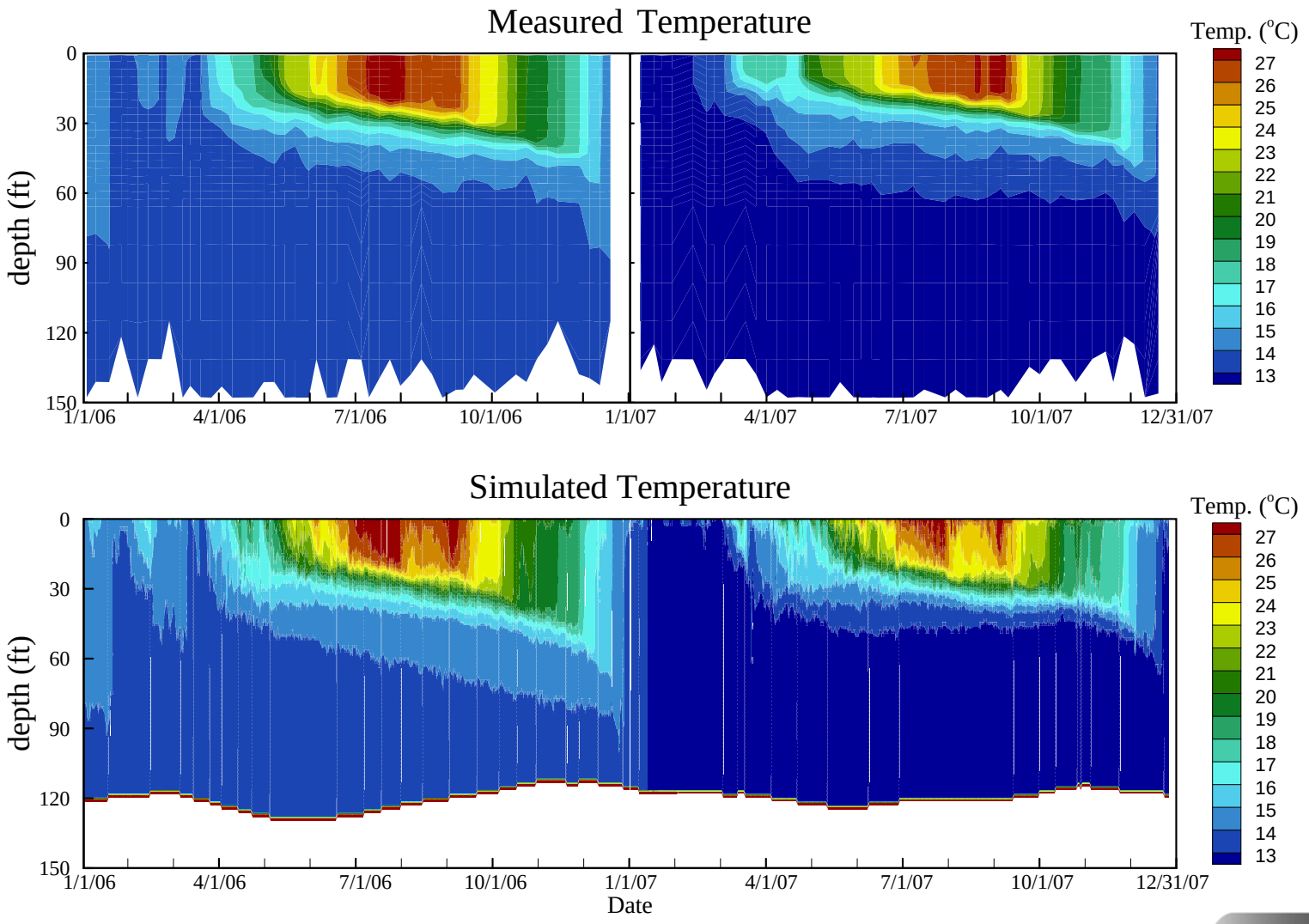

Figure 16

FSI V094005
May 01, 2012

FLOW SCIENCE®

San Vicente Reservoir

Scatter Plot of Measured vs. Simulated Temperature

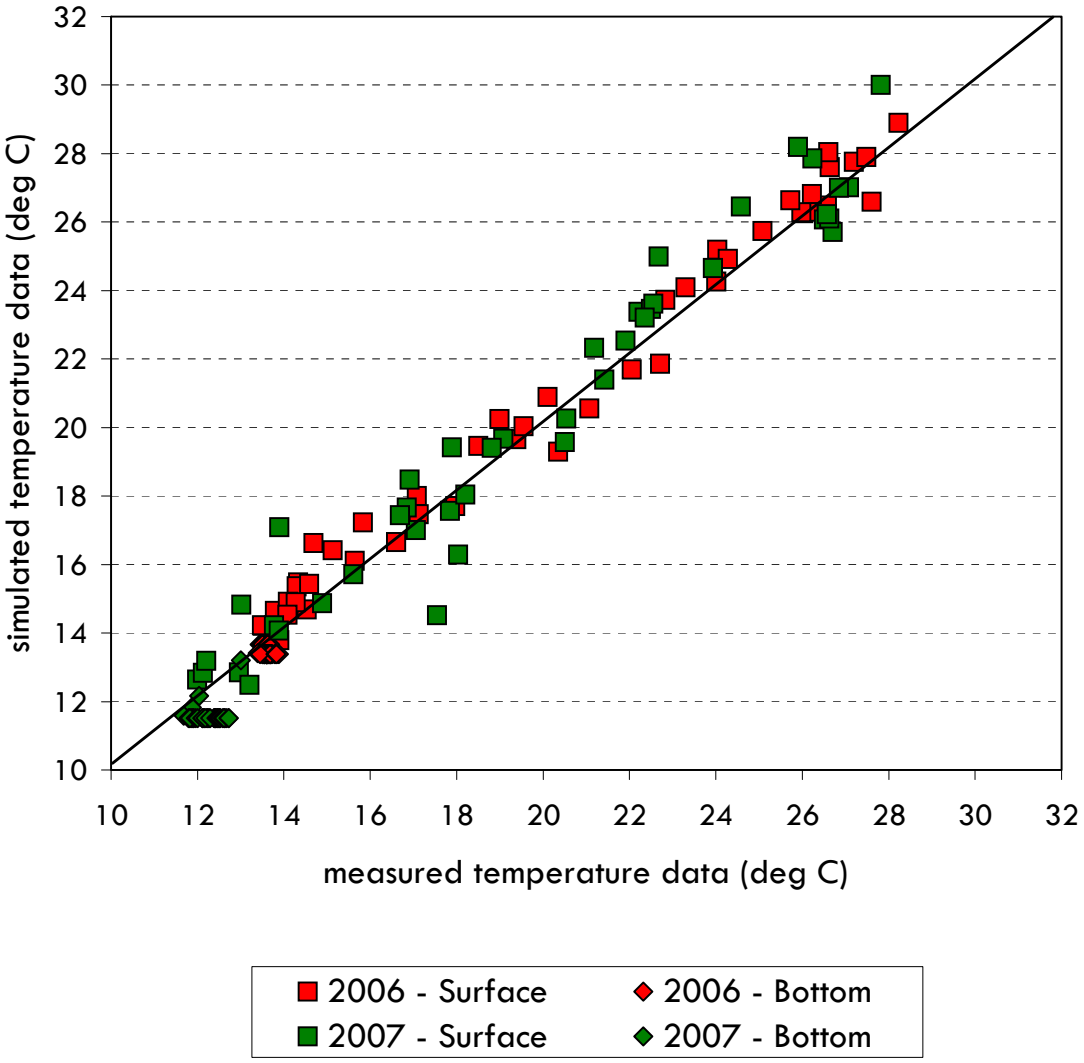

Figure 17

FSI V094005
May 01, 2012

FLOW SCIENCE®

San Vicente Reservoir Station A - Conductivity Calibration

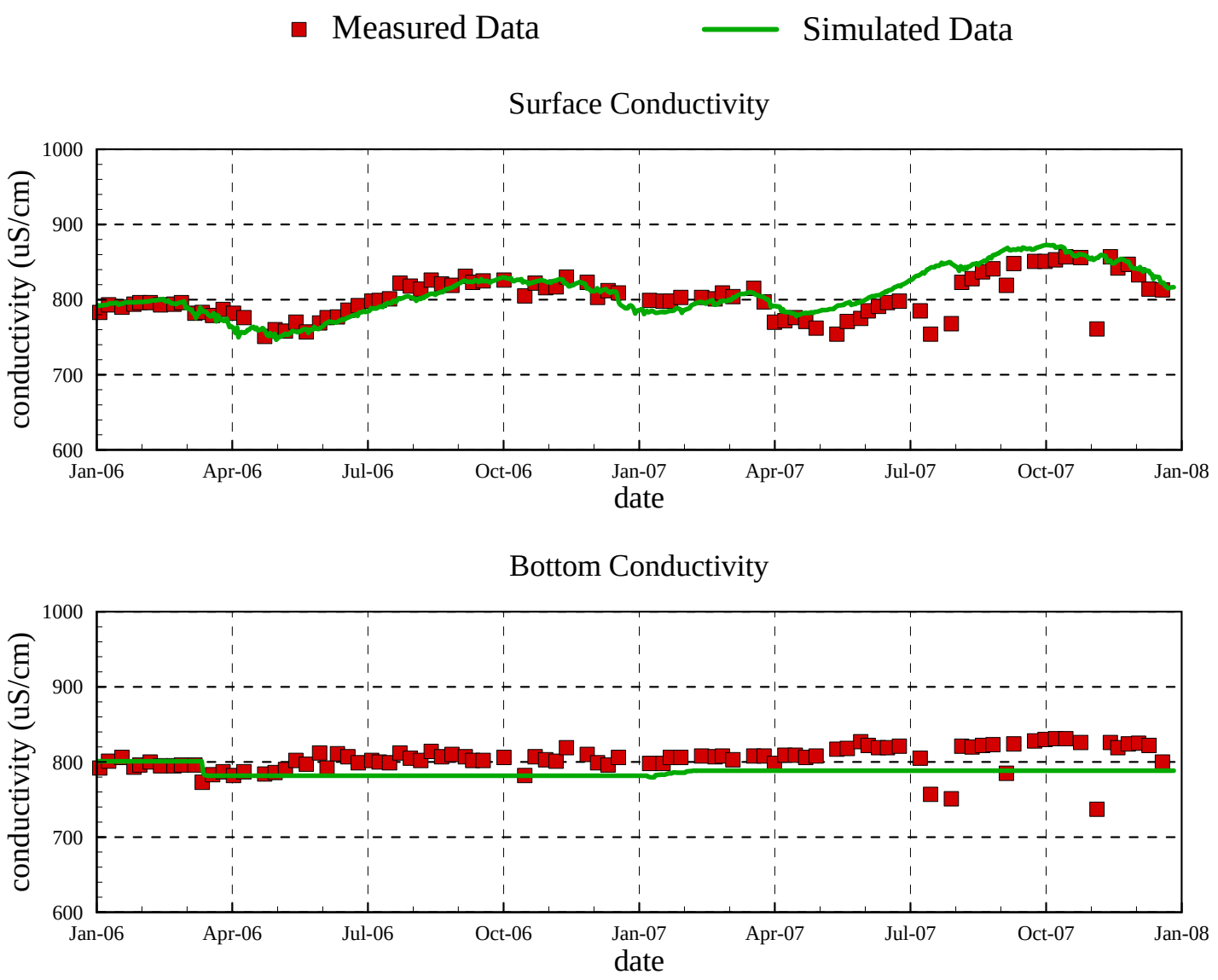

FSI V094005
May 01, 2012

Figure 18

FLOW SCIENCE®

San Vicente Reservoir
Station A - Conductivity Calibration

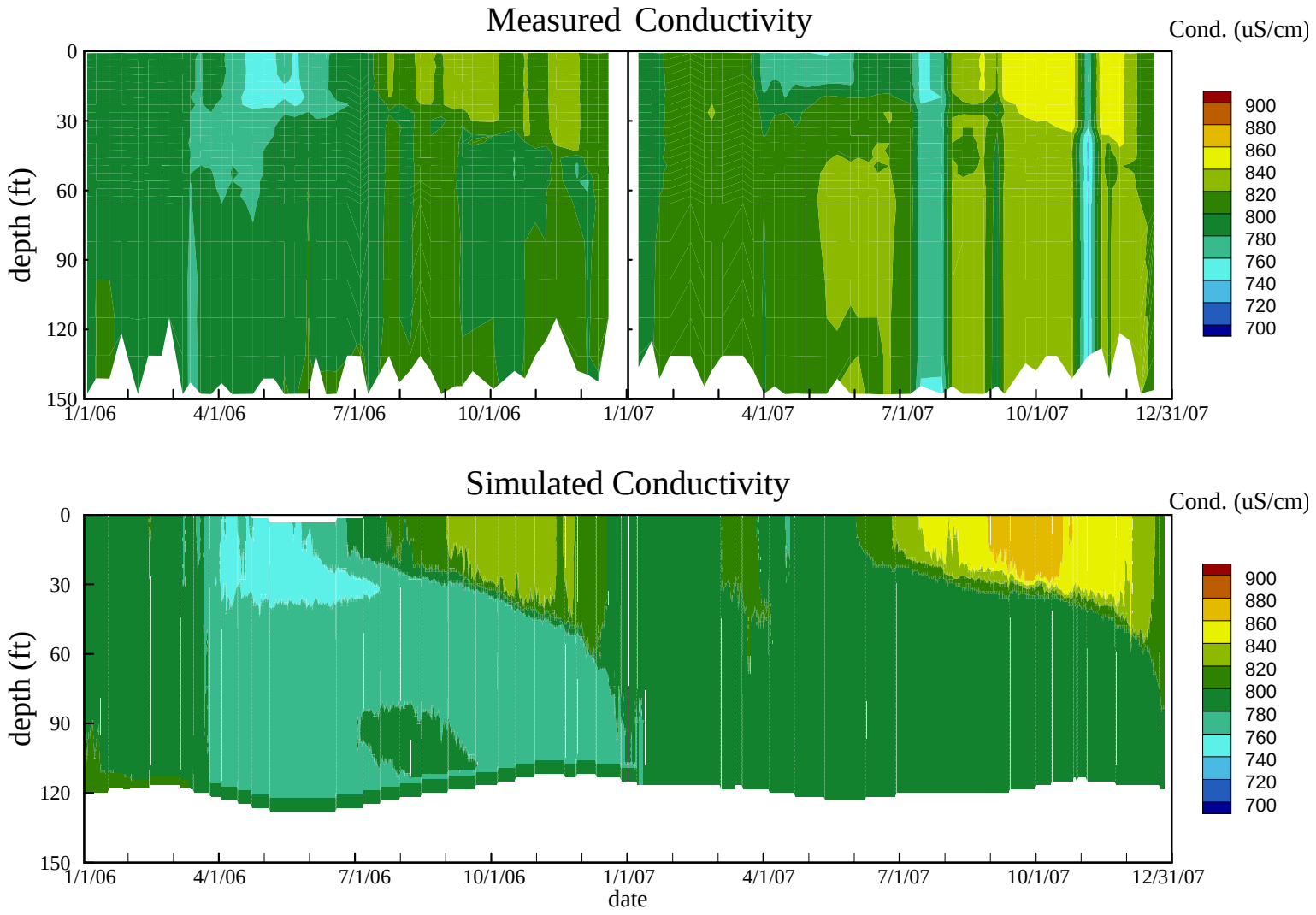

FSI V094005
May 01, 2012

Figure 19

FLOW SCIENCE®

San Vicente Reservoir

Scatter Plot of Measured vs. Simulated Conductivity

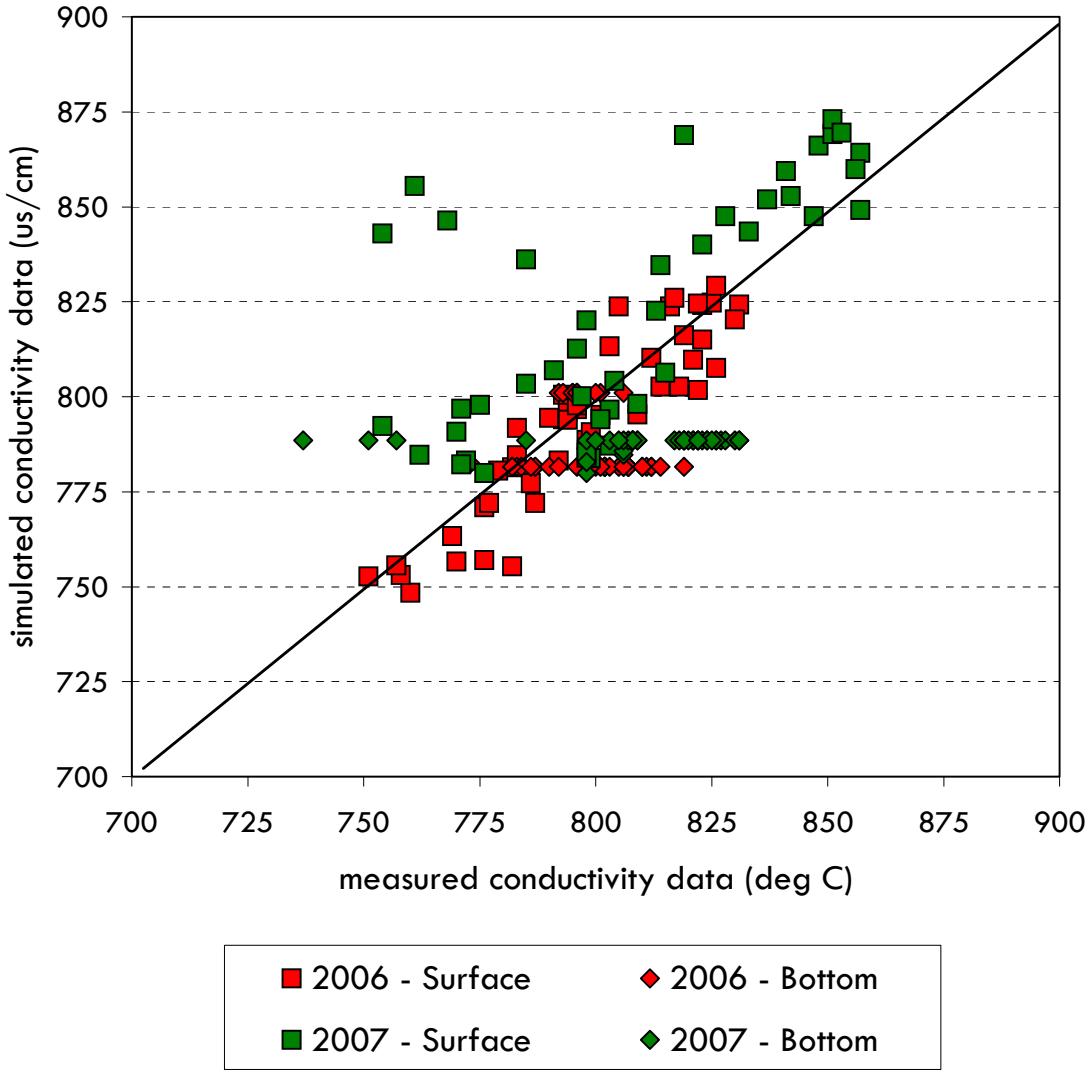

Figure 20

FSI V094005
May 01, 2012

FLOW SCIENCE®

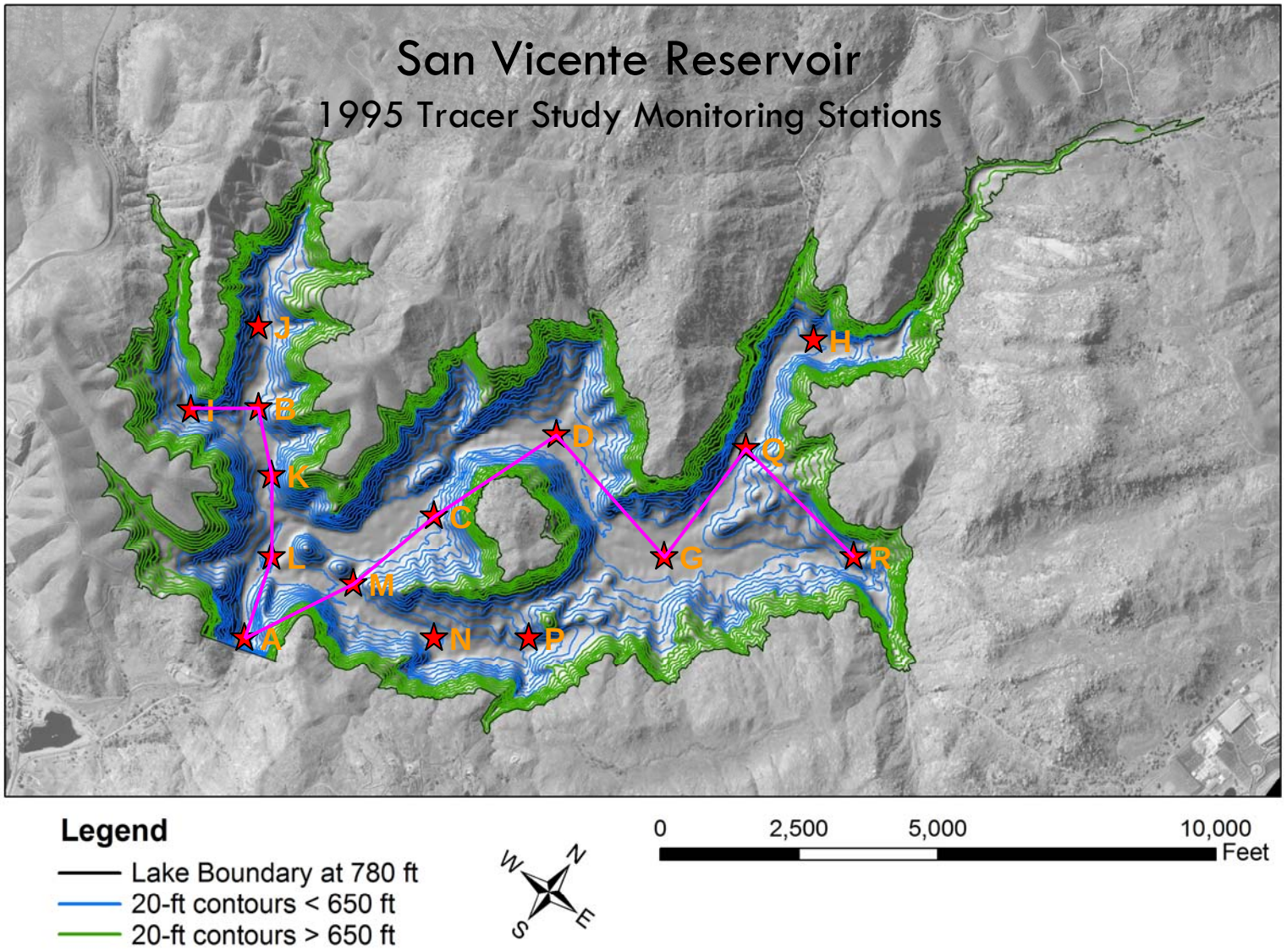

FSI V094005
May 01, 2012

Figure 21

FLOW SCIENCE®

San Vicente Reservoir

1995 Tracer Studies - Percent of Total Initial Mass of Lanthanum in the Reservoir versus Time

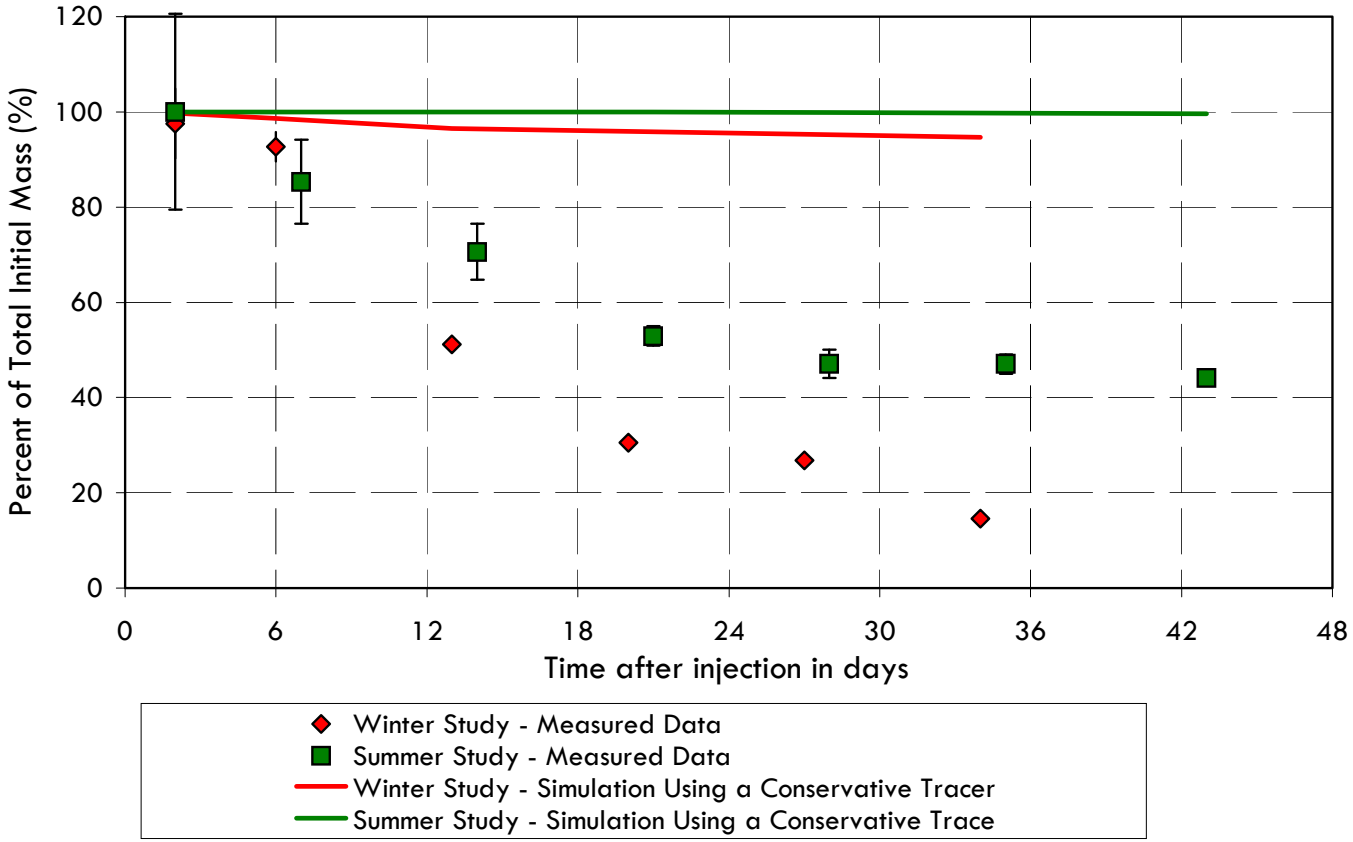

FSI V094005
May 01, 2012

Figure 22

FLOW SCIENCE®

San Vicente Reservoir

1995 Tracer Studies – Simulated Mass Distribution of Particles

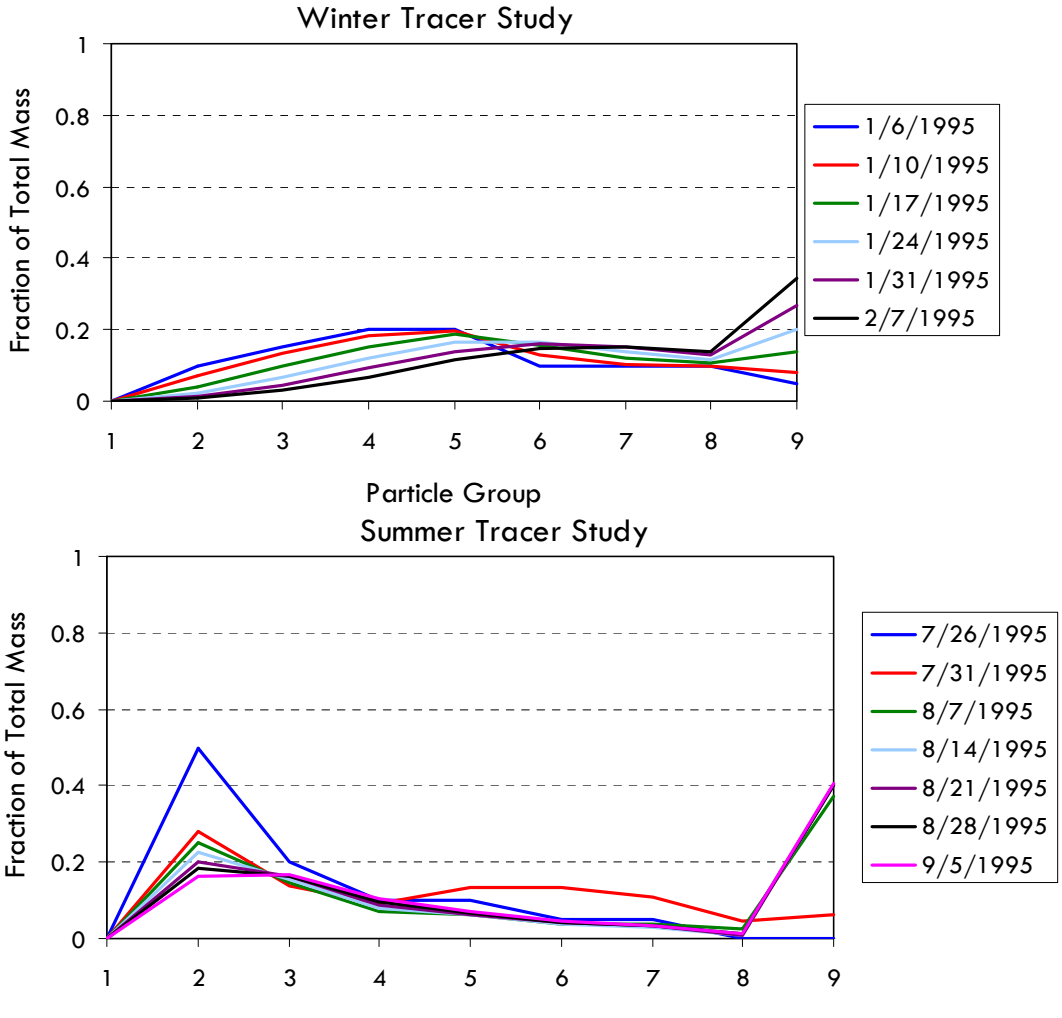

Figure 23

FSI V094005
May 01, 2012

FLOW SCIENCE®

San Vicente Reservoir

1995 Tracer Studies - Percent of Total Initial Mass of Lanthanum in the Reservoir versus Time

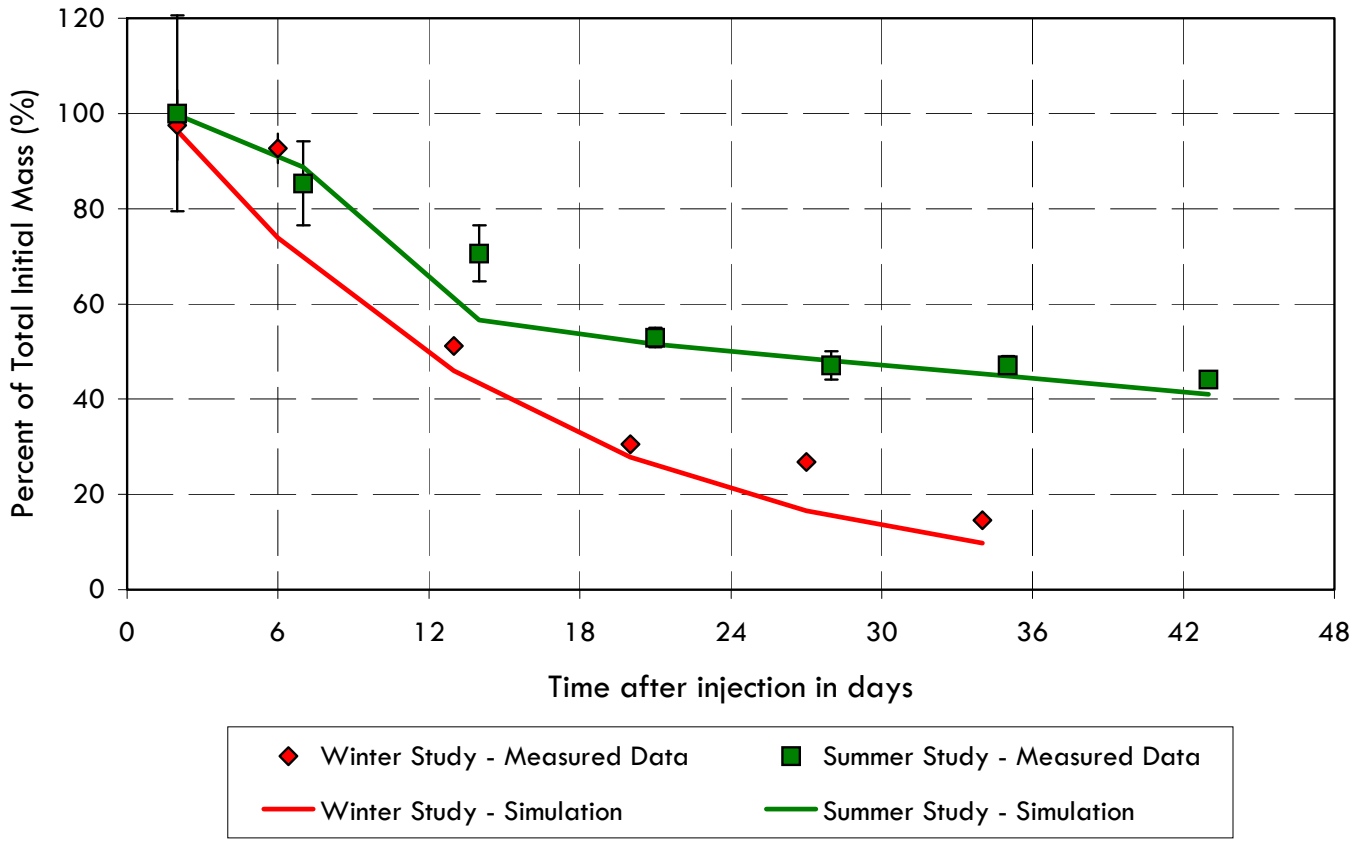

FSI V094005
May 01, 2012

Figure 24

FLOW SCIENCE®

San Vicente Reservoir
Station A - Water Temperature in 1995 Winter Tracer Study

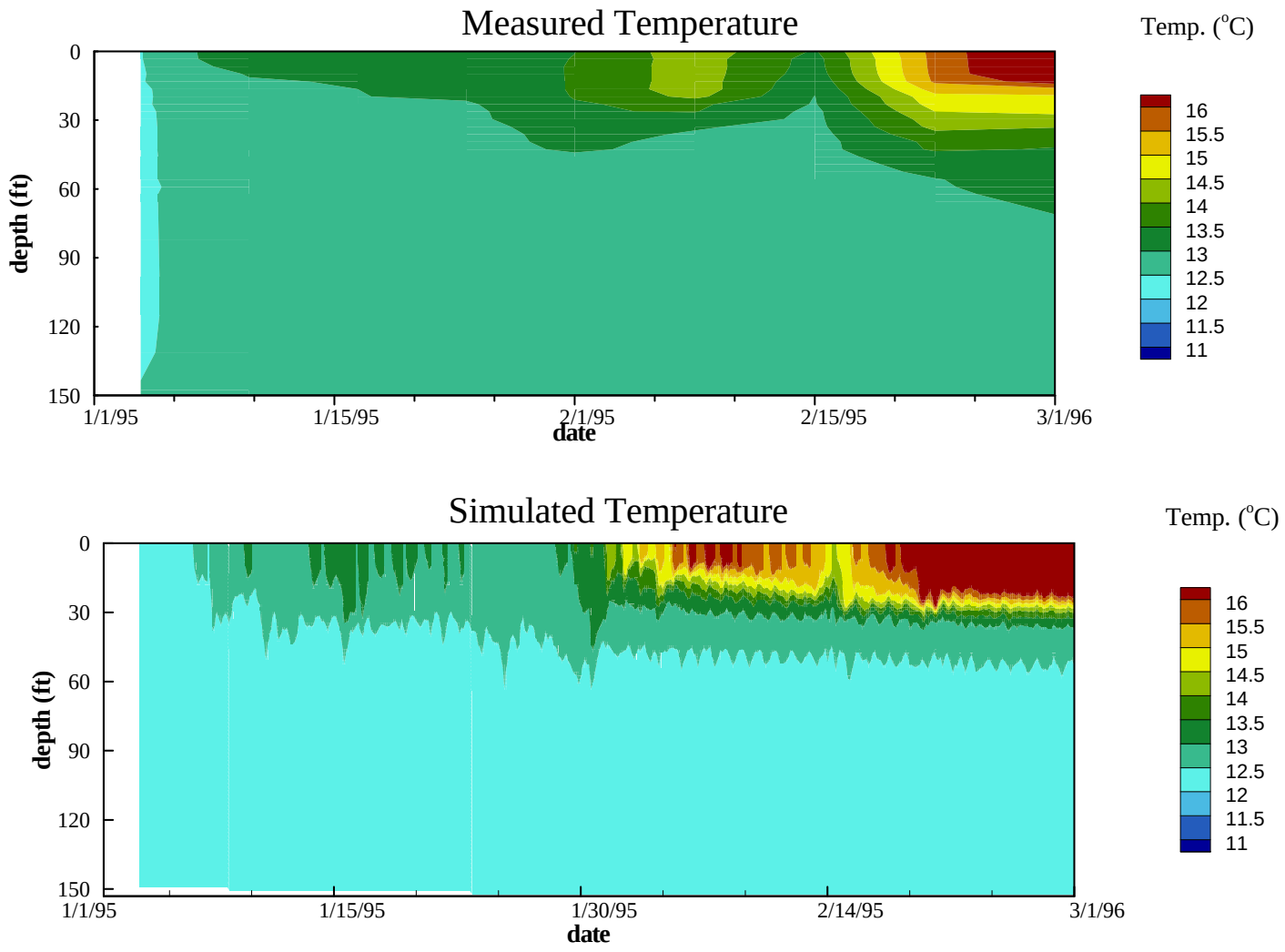

FSI V094005
May 01, 2012

Figure 25

FLOW SCIENCE®

San Vicente Reservoir

1995 Tracer Winter Study – Measured versus Simulated Lanthanum Concentrations

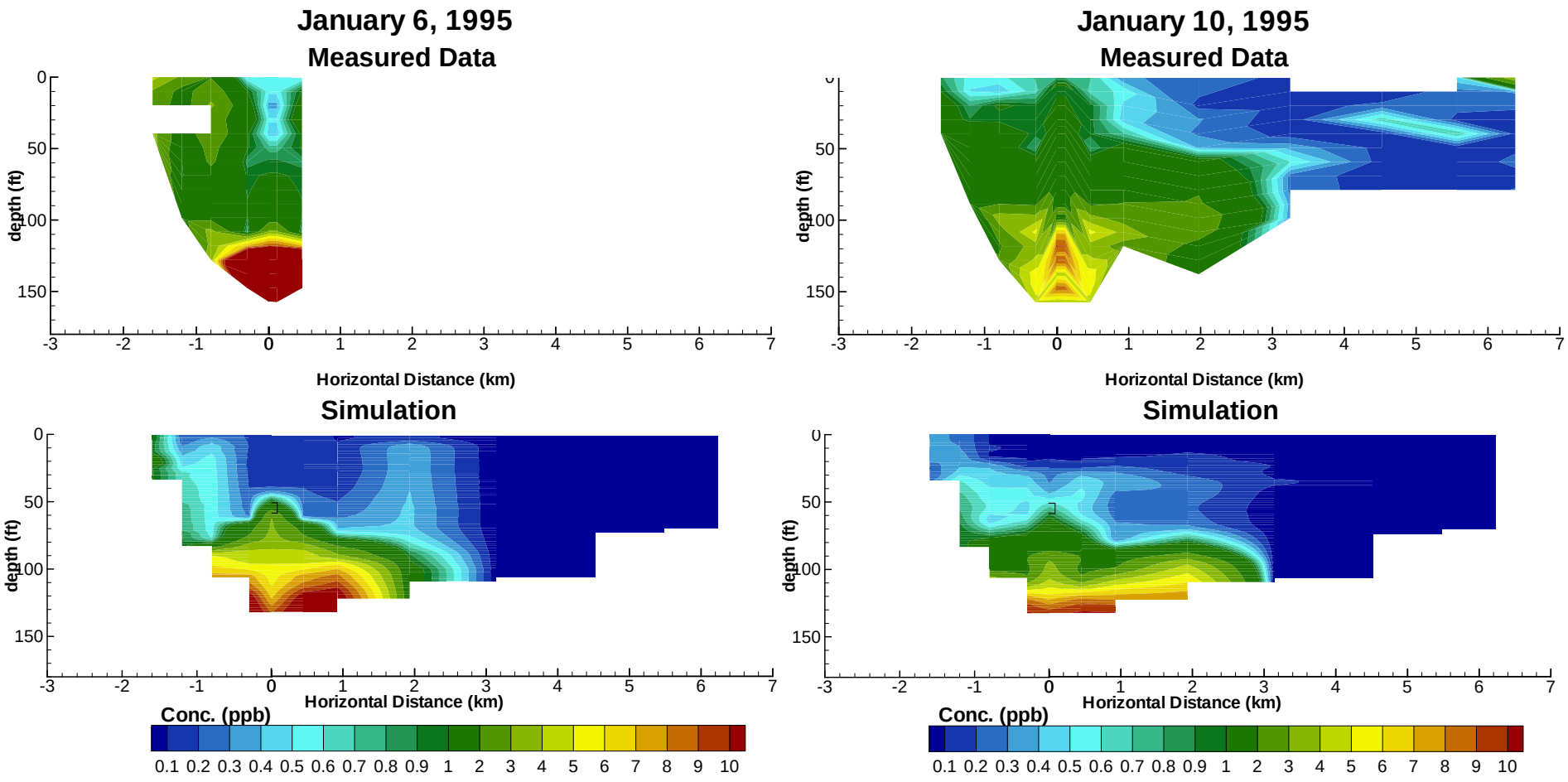

FSI V094005
May 01, 2012

Figure 26

FLOW SCIENCE®

San Vicente Reservoir

1995 Winter Tracer Study – Measured versus Simulated Lanthanum Concentrations

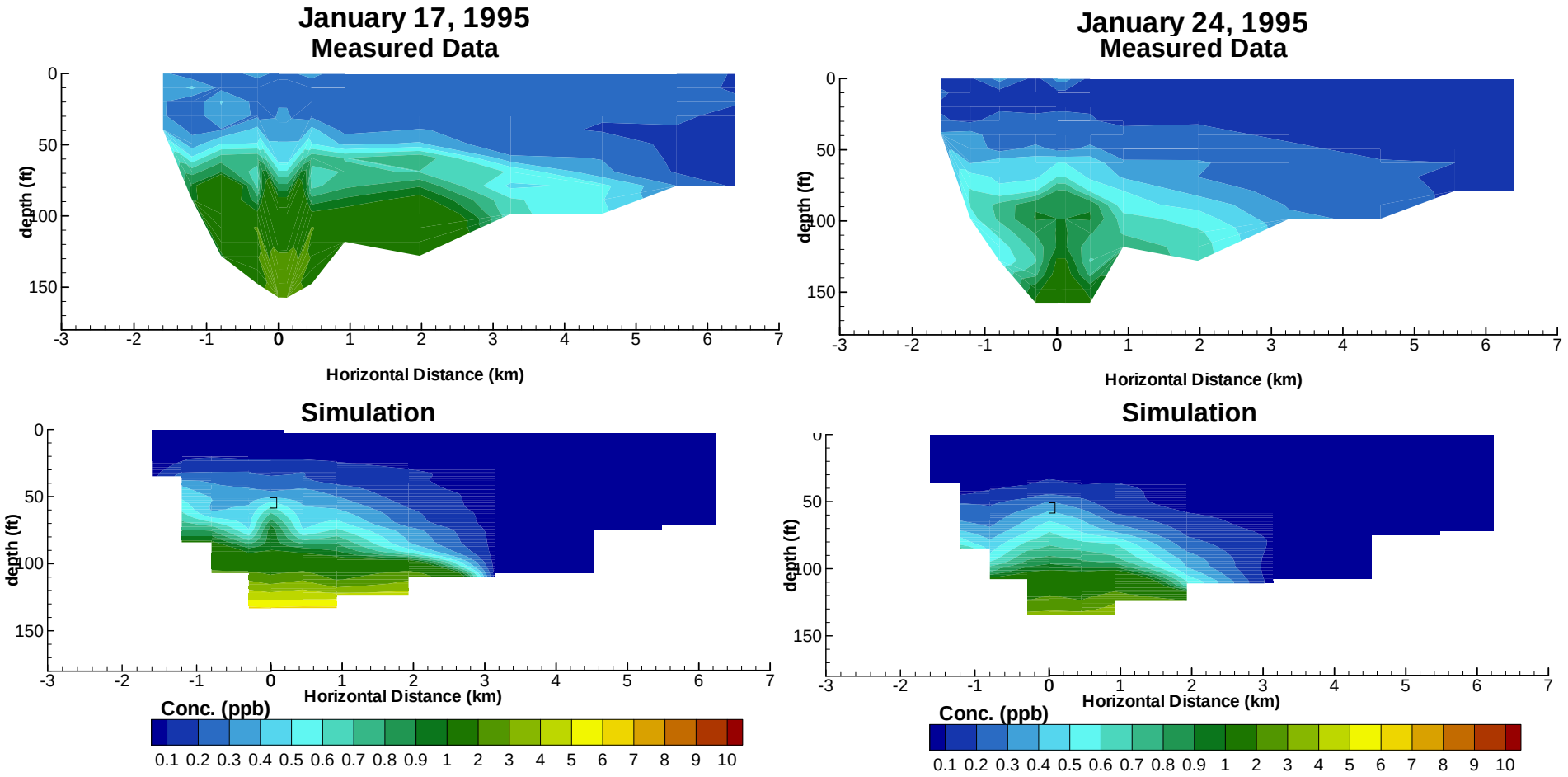

FSI V094005
May 01, 2012

Figure 27

FLOW SCIENCE®

San Vicente Reservoir

1995 Winter Tracer Study – Measured versus Simulated Lanthanum Concentrations

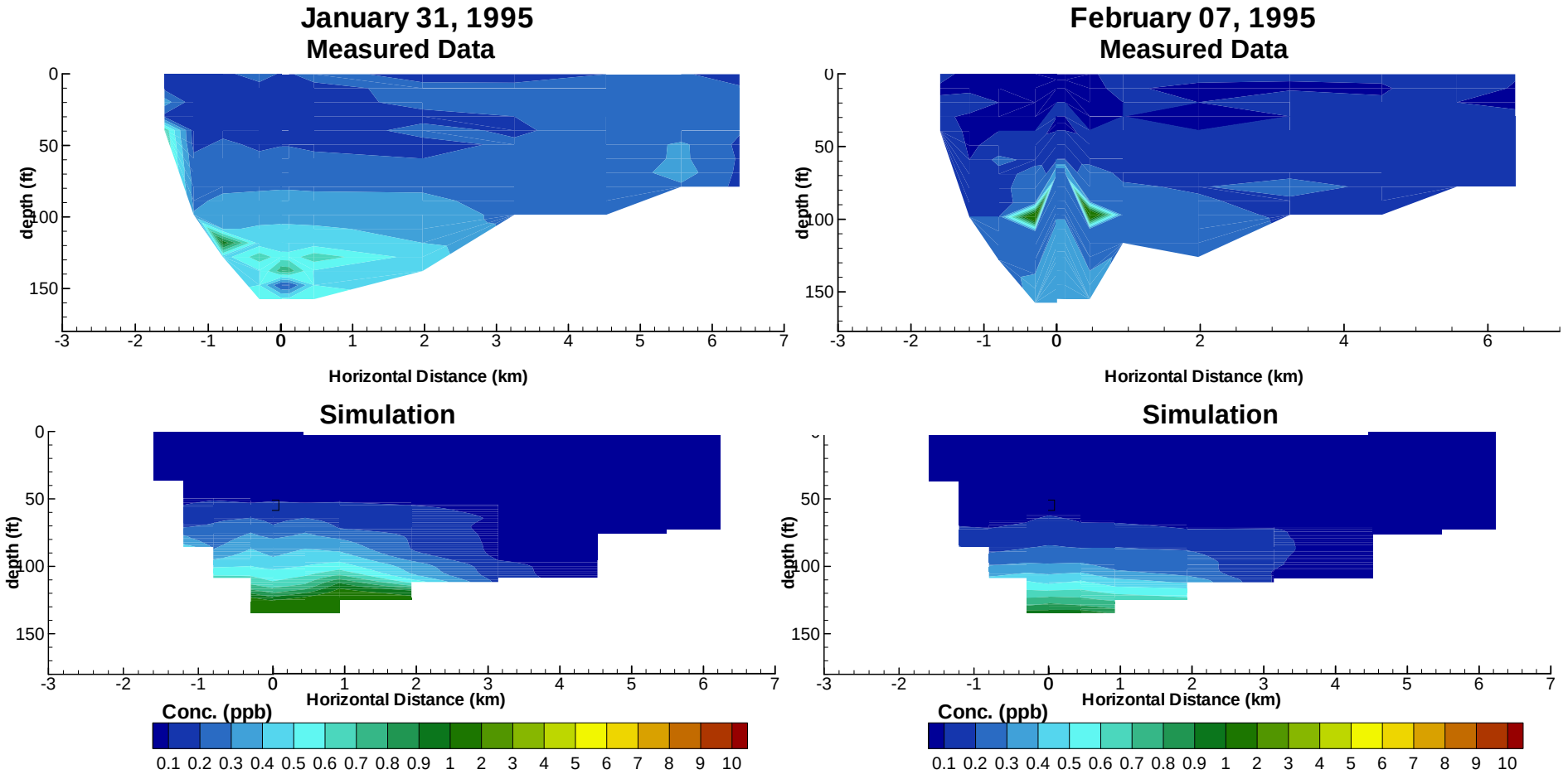

FSI V094005
May 01, 2012

Figure 28

FLOW SCIENCE®

San Vicente Reservoir
Station A - Water Temperature Calibration

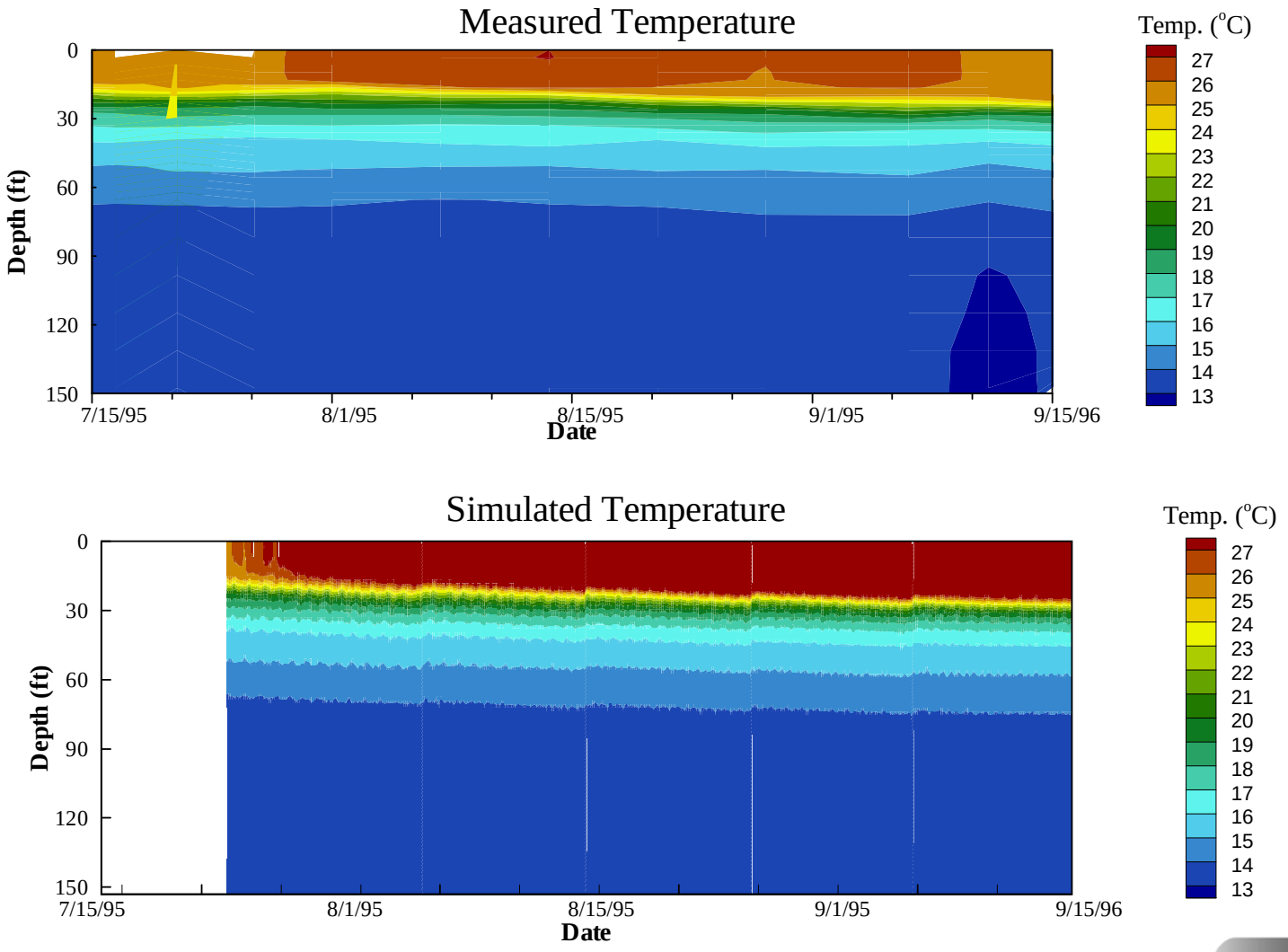

Figure 29

FSI V094005
May 01, 2012

FLOW SCIENCE®

San Vicente Reservoir

1995 Summer Tracer Study – Measured versus Simulated Lanthanum Concentrations

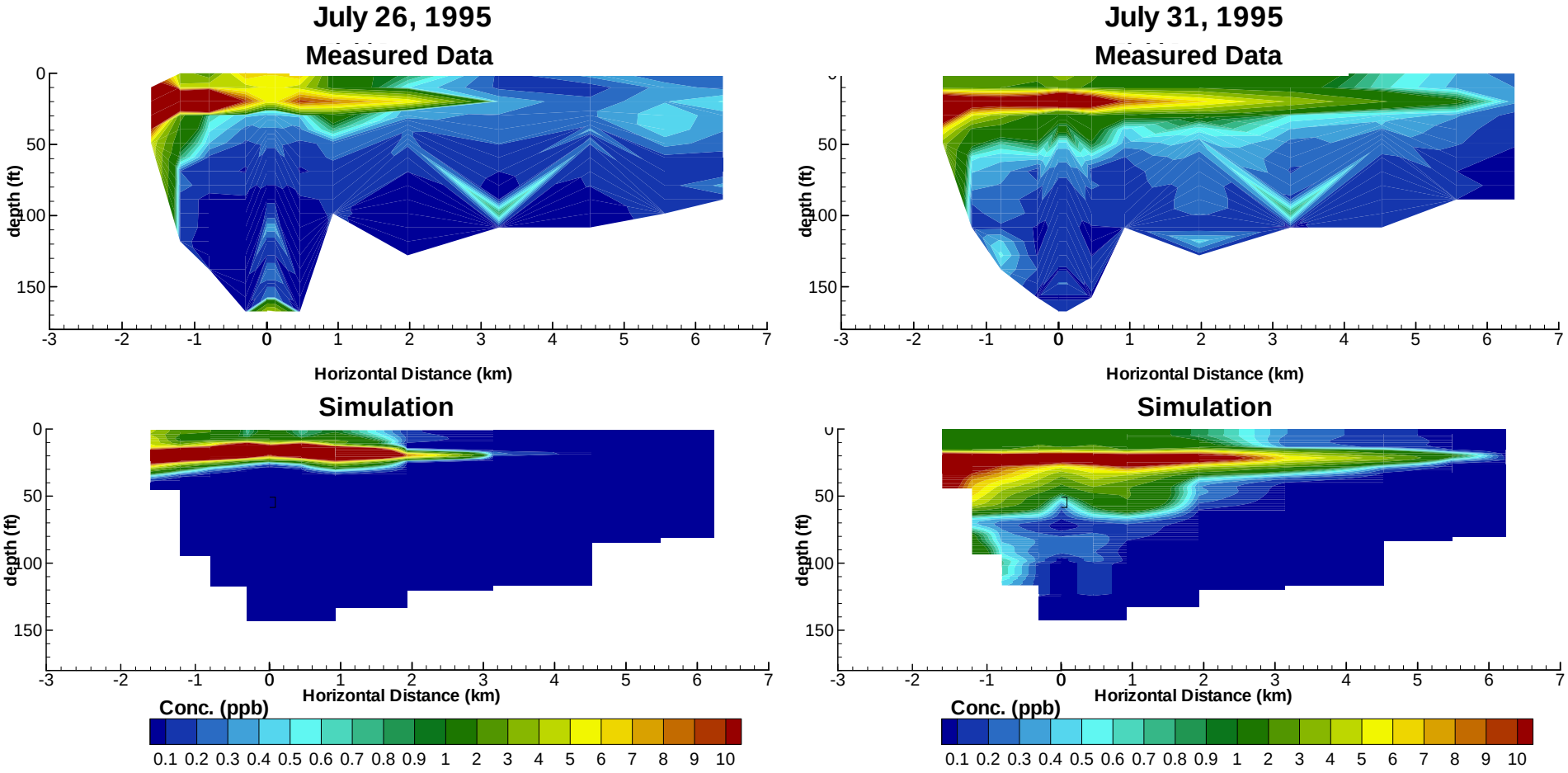

FSI V094005
May 01, 2012

Figure 30

FLOW SCIENCE®

San Vicente Reservoir

1995 Summer Tracer Study – Measured versus Simulated Lanthanum Concentrations

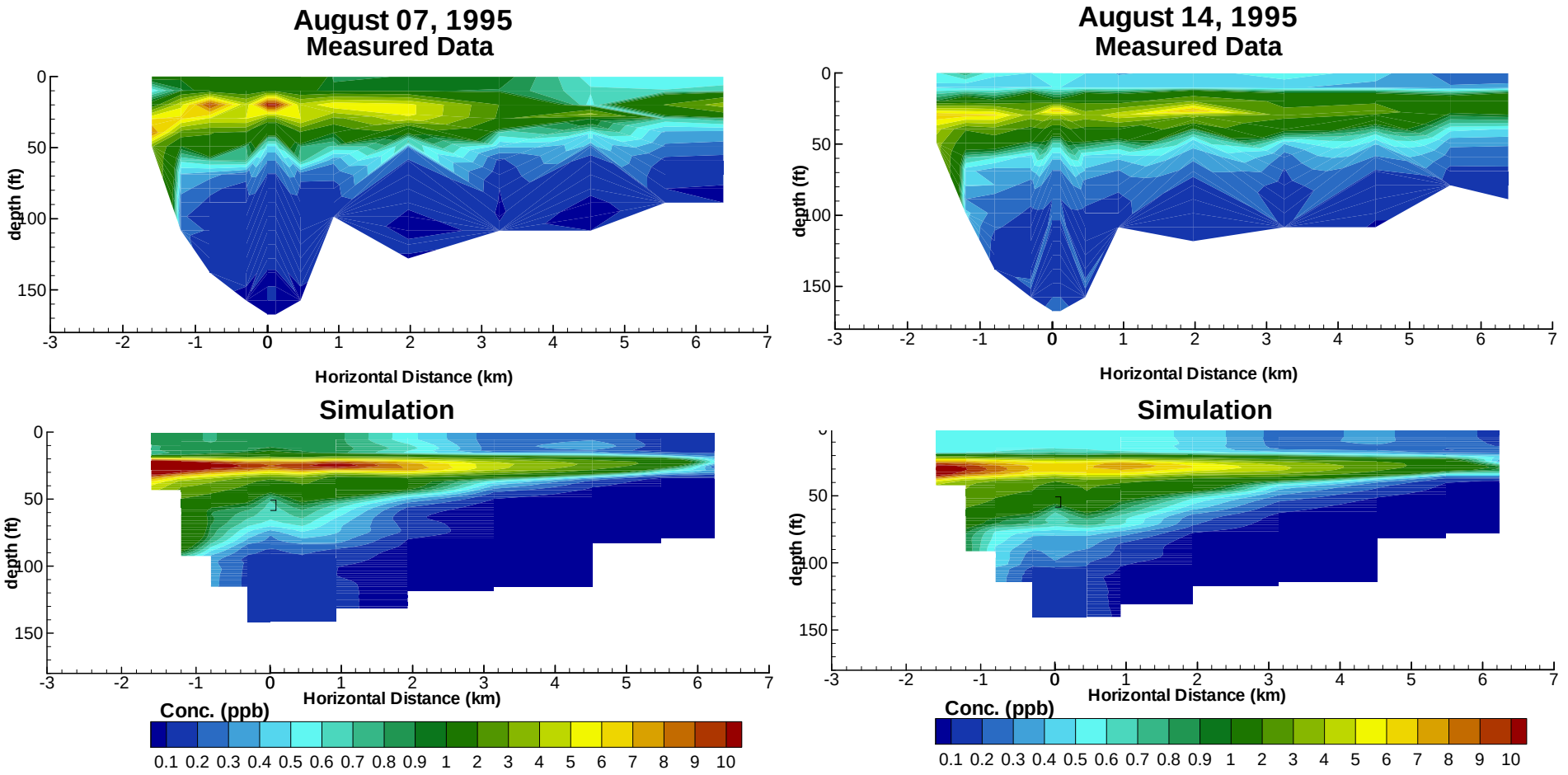

FSI V094005
May 01, 2012

Figure 31

FLOW SCIENCE®

San Vicente Reservoir

1995 Summer Tracer Study – Measured versus Simulated Lanthanum Concentrations

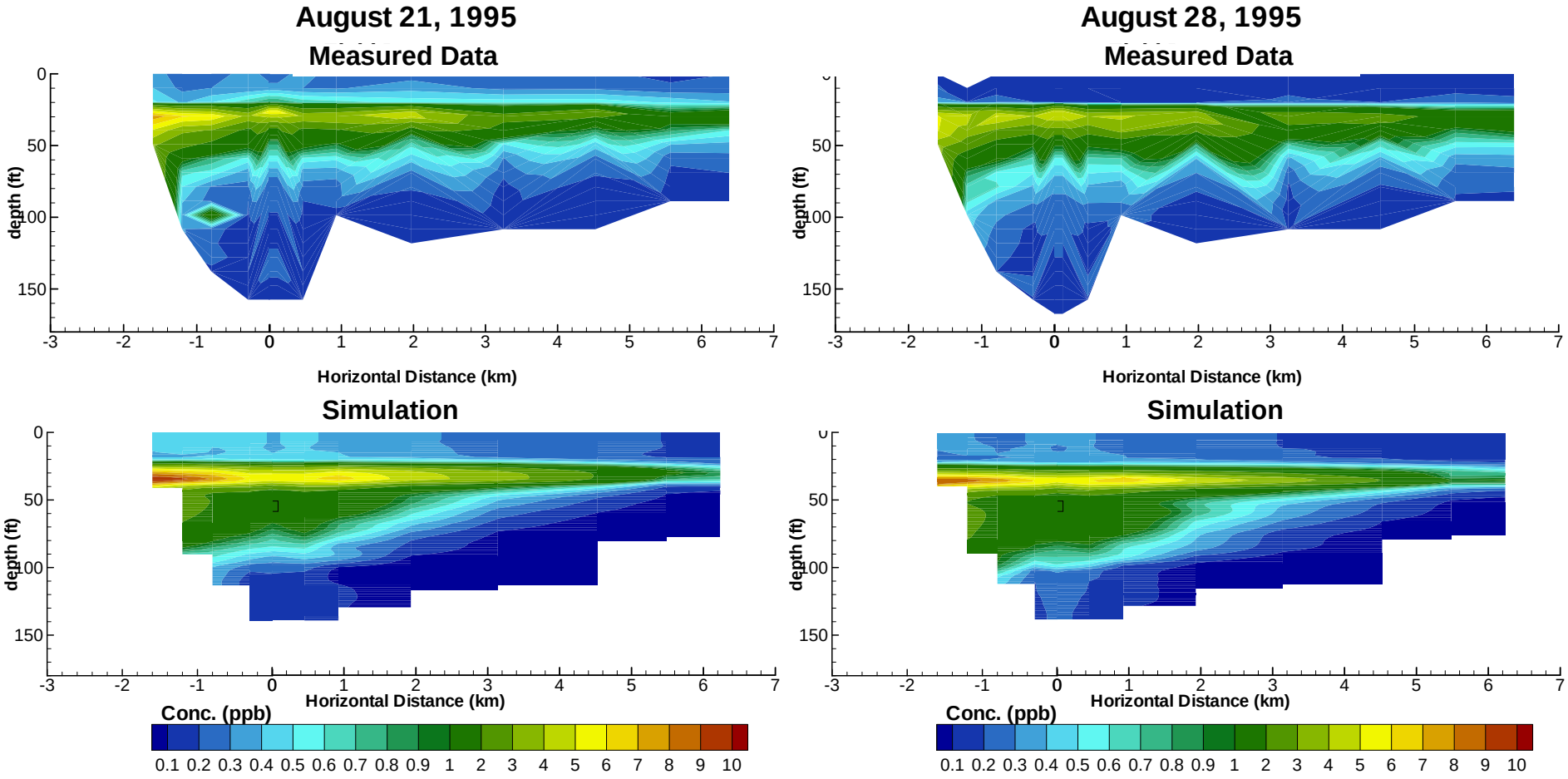

FSI V094005
May 01, 2012

Figure 32

FLOW SCIENCE®

San Vicente Reservoir

1995 Summer Tracer Study – Measured versus Simulated Lanthanum Concentrations

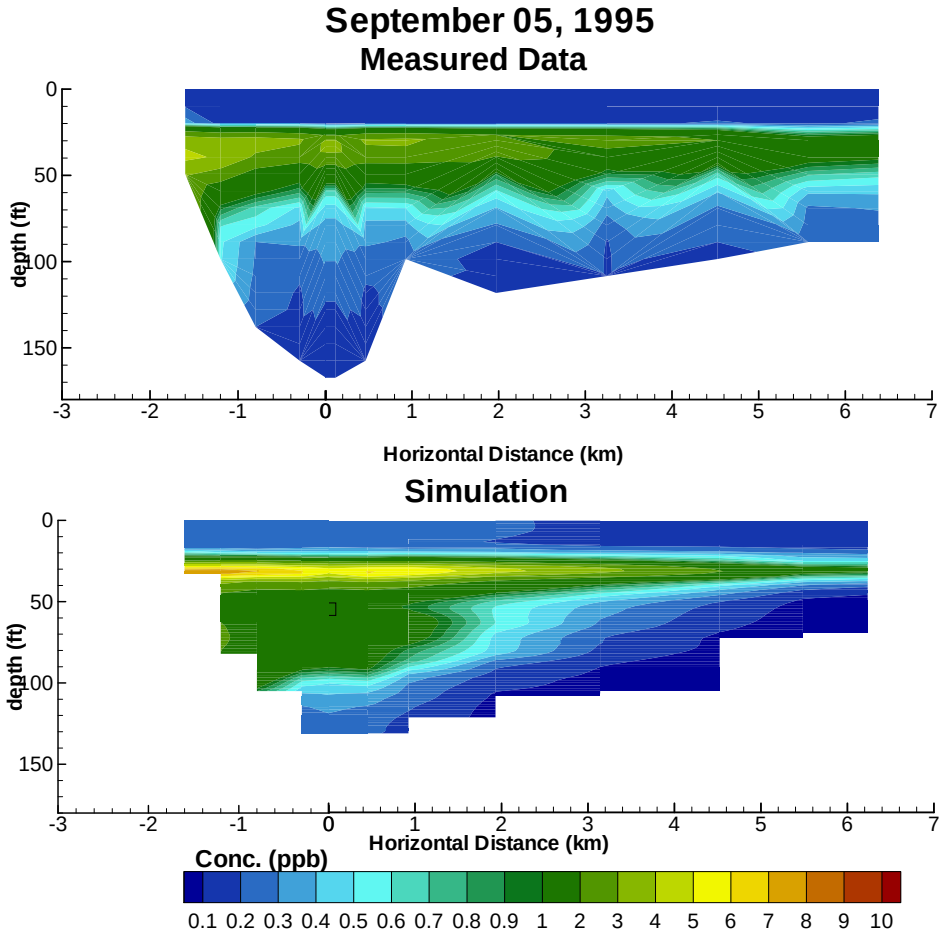

FSI V094005
May 01, 2012

Figure 33

FLOW SCIENCE®

San Vicente Reservoir 100-m ELCOM-CAEDYM Computational Grid

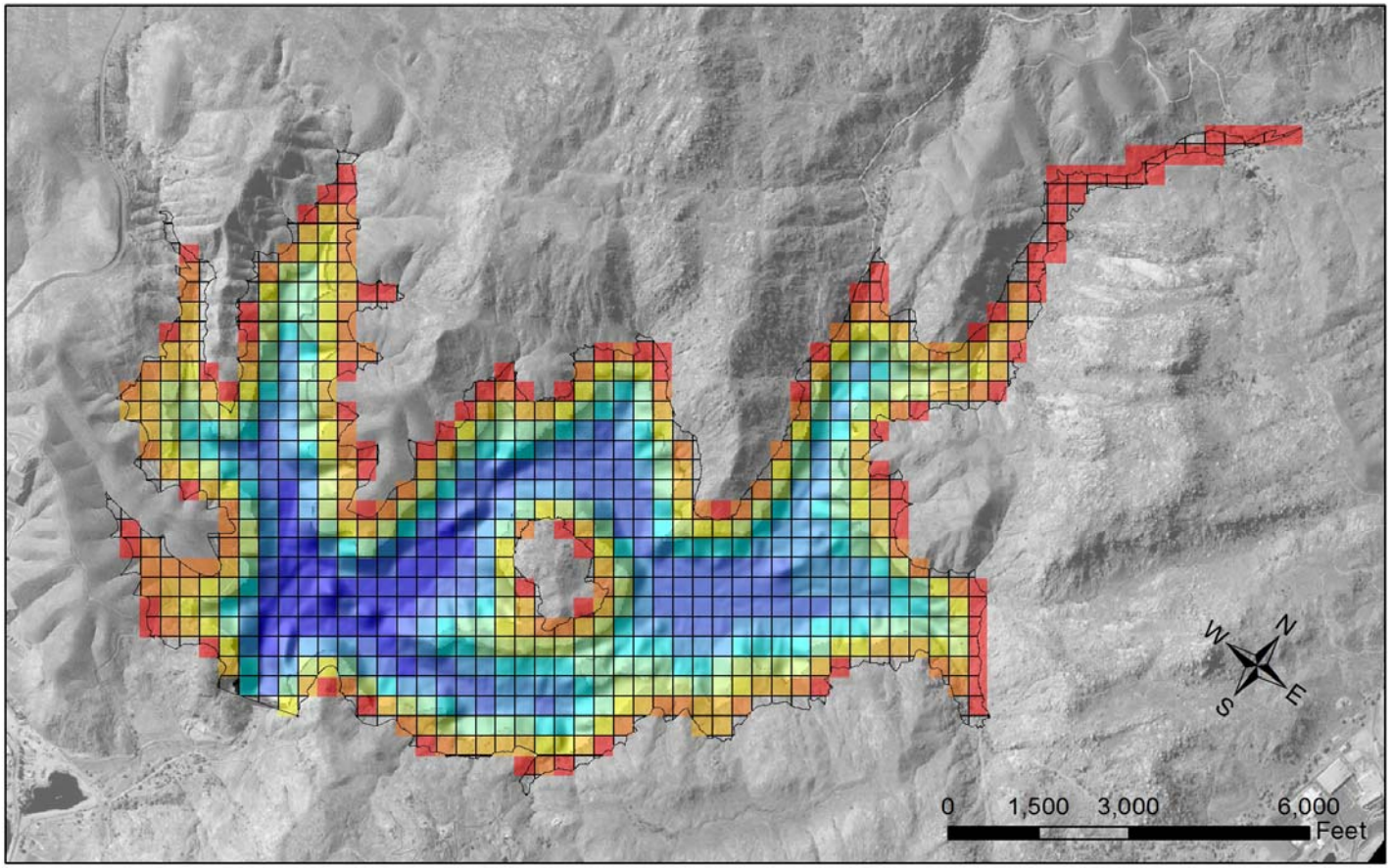

San Vicente
100-m ELCOM Grid

Legend

Lake Boundary at 780 ft

Elevation (ft)

480 - 510	541 - 569	630 - 659	719 - 748
511 - 540	570 - 599	660 - 689	749 - 778
	600 - 629	690 - 718	

FSI V094005
May 01, 2012

Figure 34

FLOW SCIENCE®

San Vicente Reservoir Station A - Water Temperature Simulation

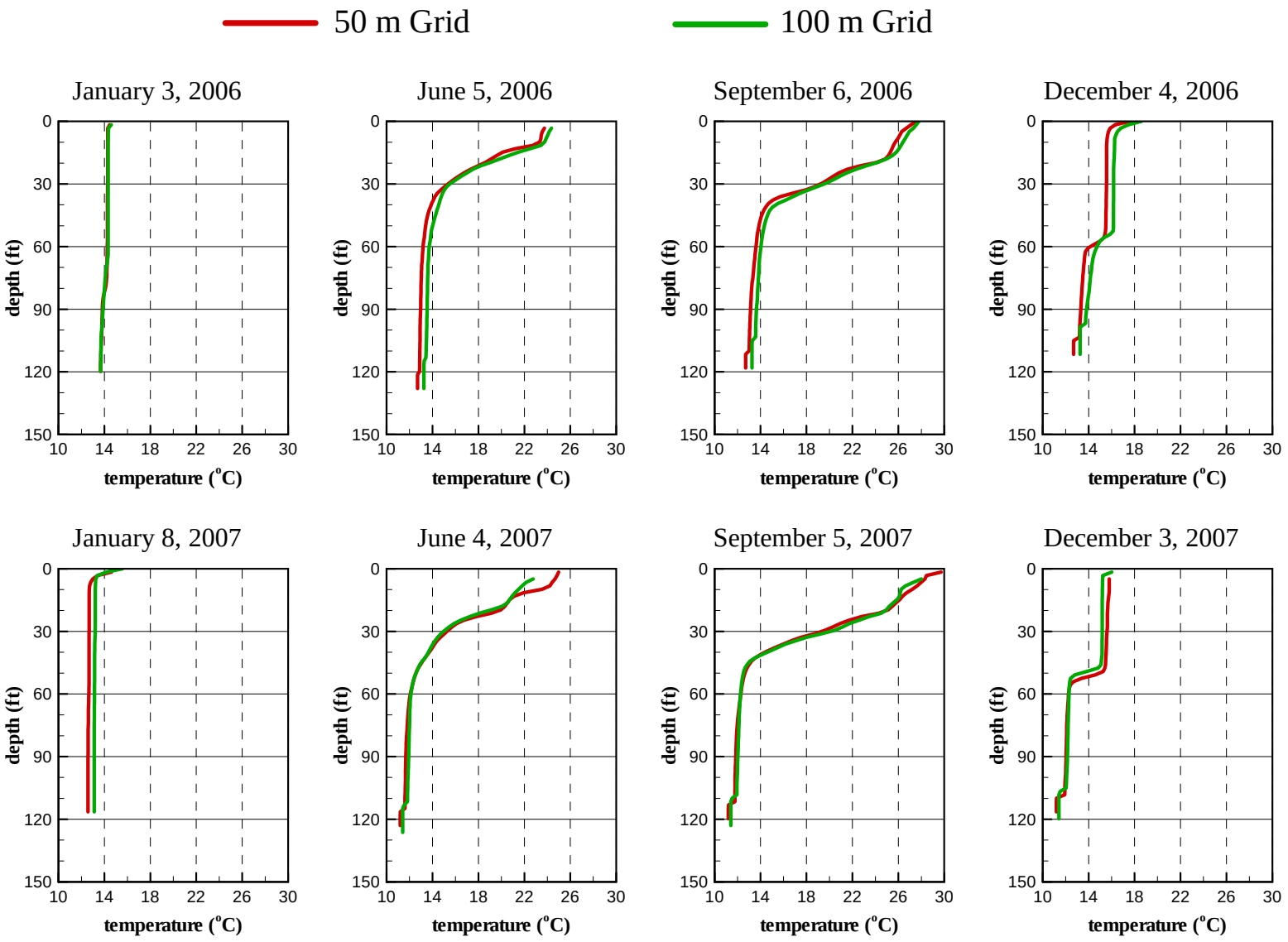

FSI V094005
May 01, 2012

Figure 35

FLOW SCIENCE®

San Vicente Reservoir Station A - Conductivity Simulation

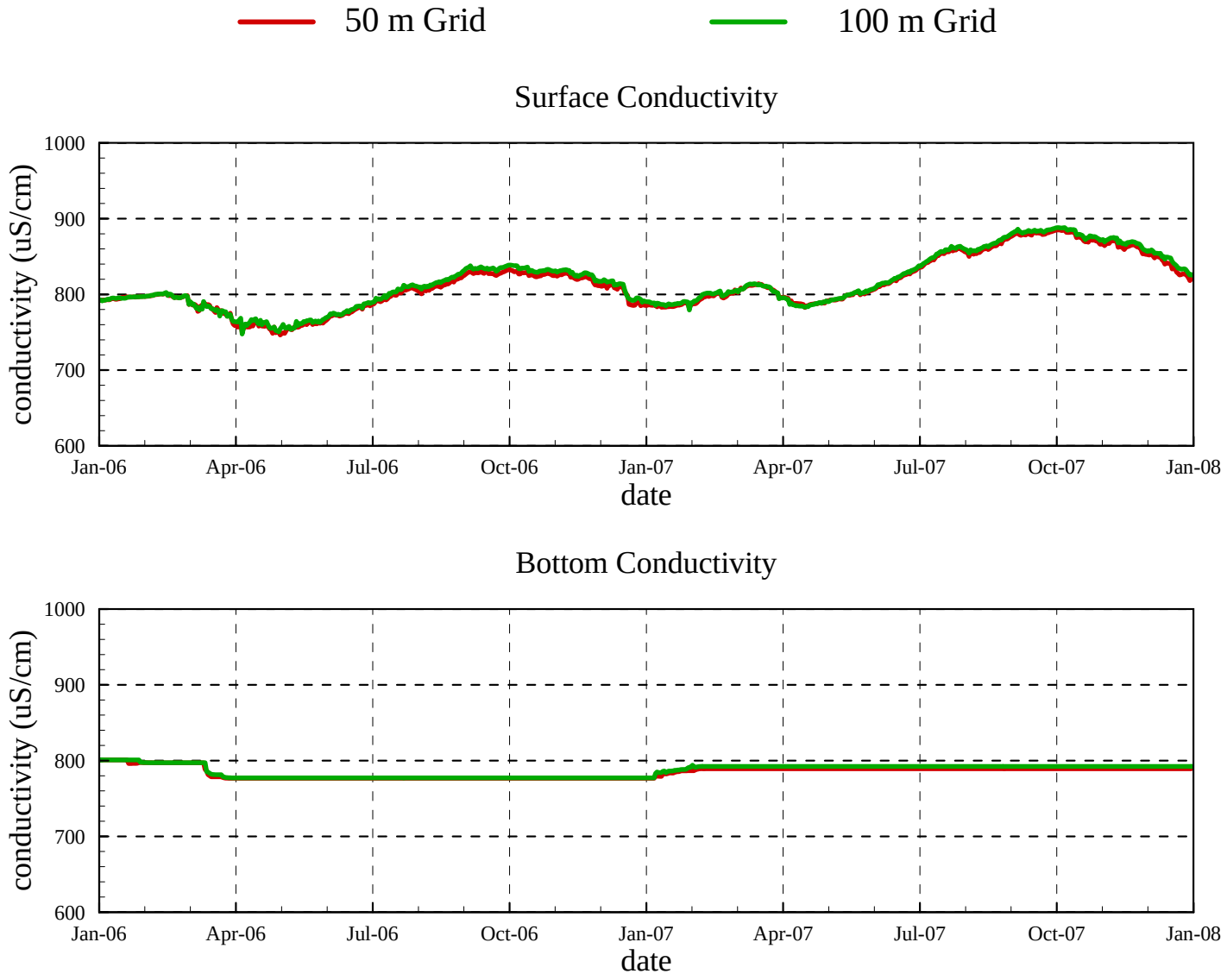

FSI V094005
May 01, 2012

Figure 36

FLOW SCIENCE®

San Vicente Reservoir Station A - Dissolved Oxygen Calibration

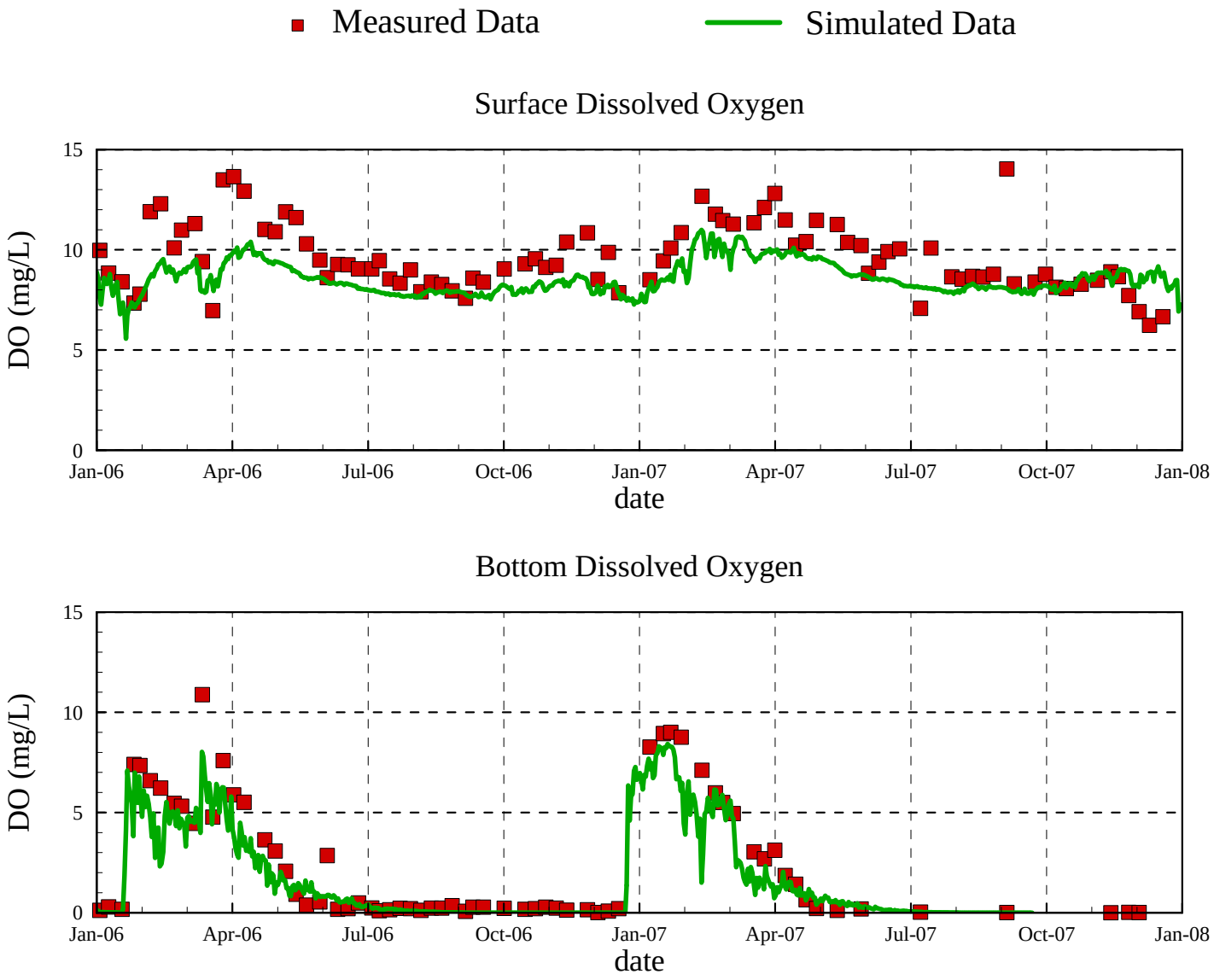

FSI V094005
May 01, 2012

Figure 37

FLOW SCIENCE®

San Vicente Reservoir

Station A - Dissolved Oxygen Calibration

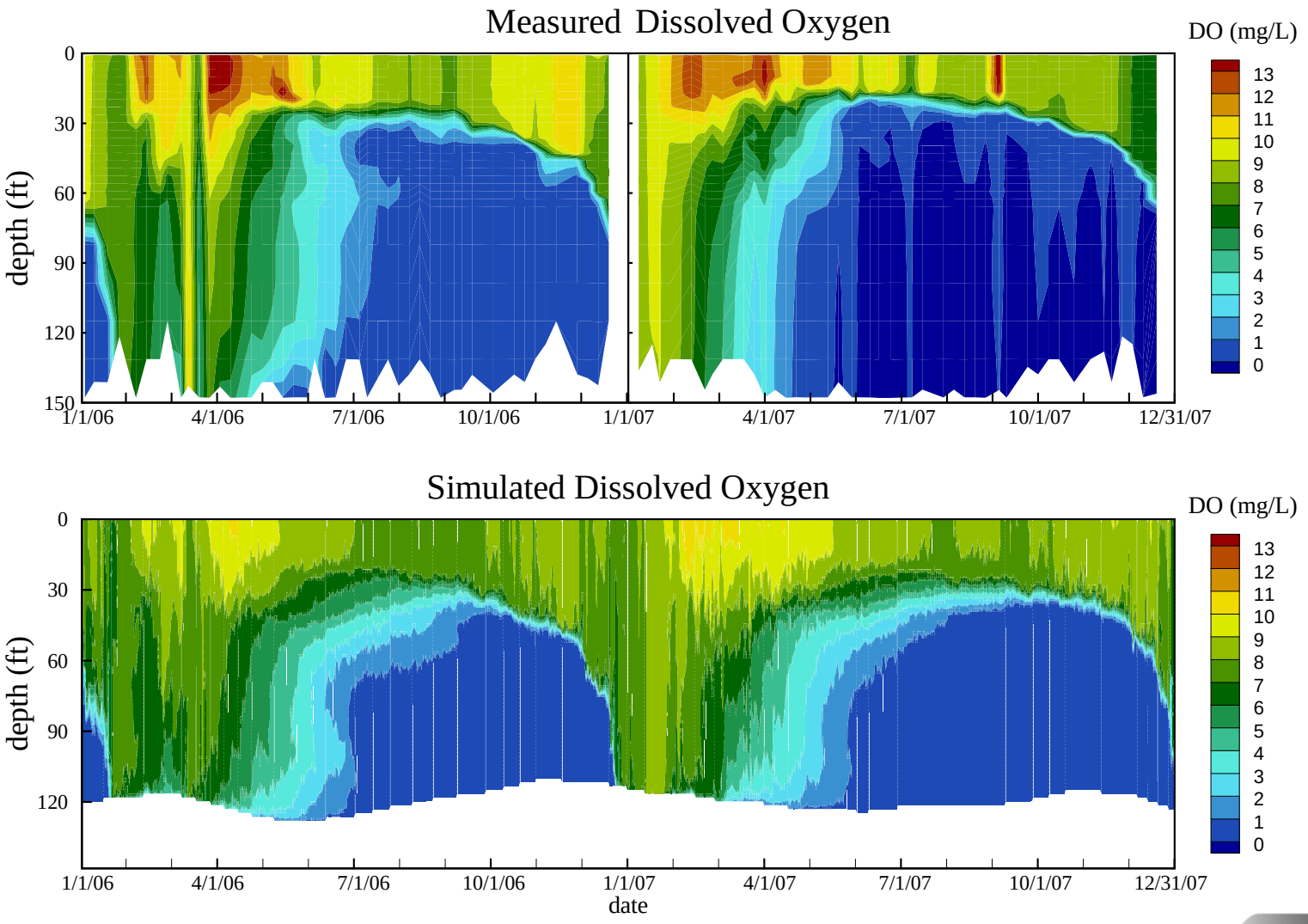

Figure 38

FSI V094005
May 01, 2012

FLOW SCIENCE®

San Vicente Reservoir

Scatter Plot of Measured vs. Simulated Dissolved Oxygen

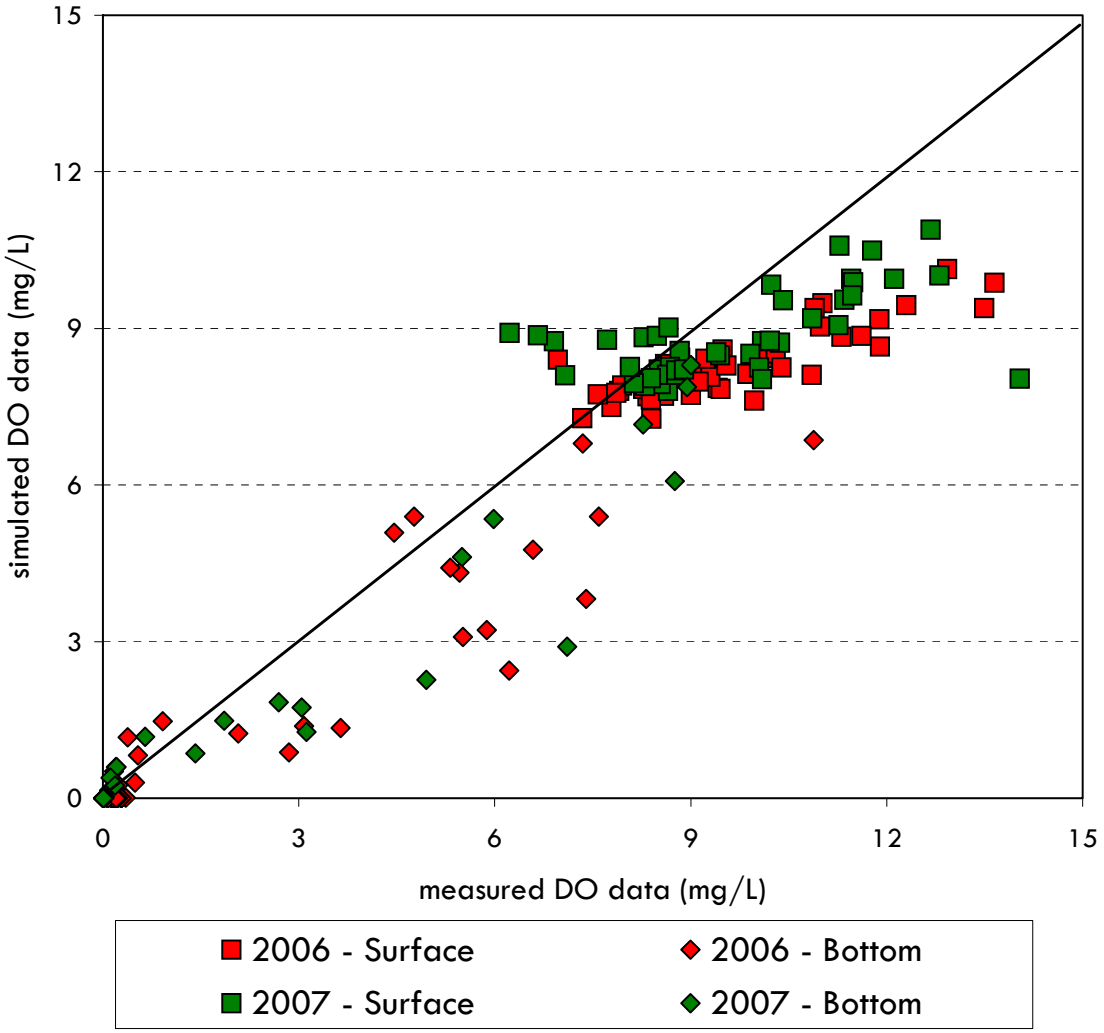

Figure 39

FSI V094005
May 01, 2012

FLOW SCIENCE®

San Vicente Reservoir Station A - pH Calibration

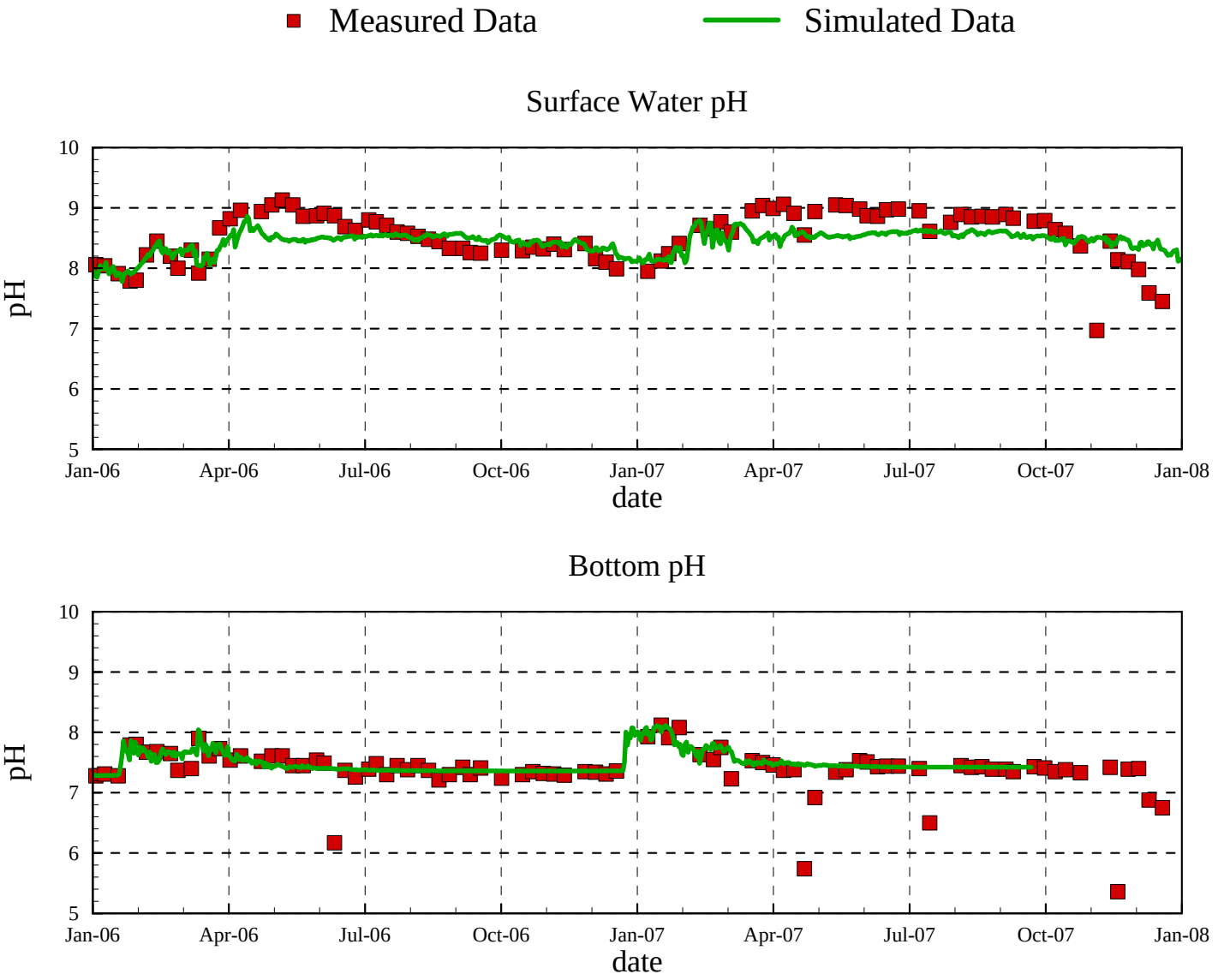

Figure 40

FSI V094005
May 01, 2012

FLOW SCIENCE®

San Vicente Reservoir

Station A - pH Calibration

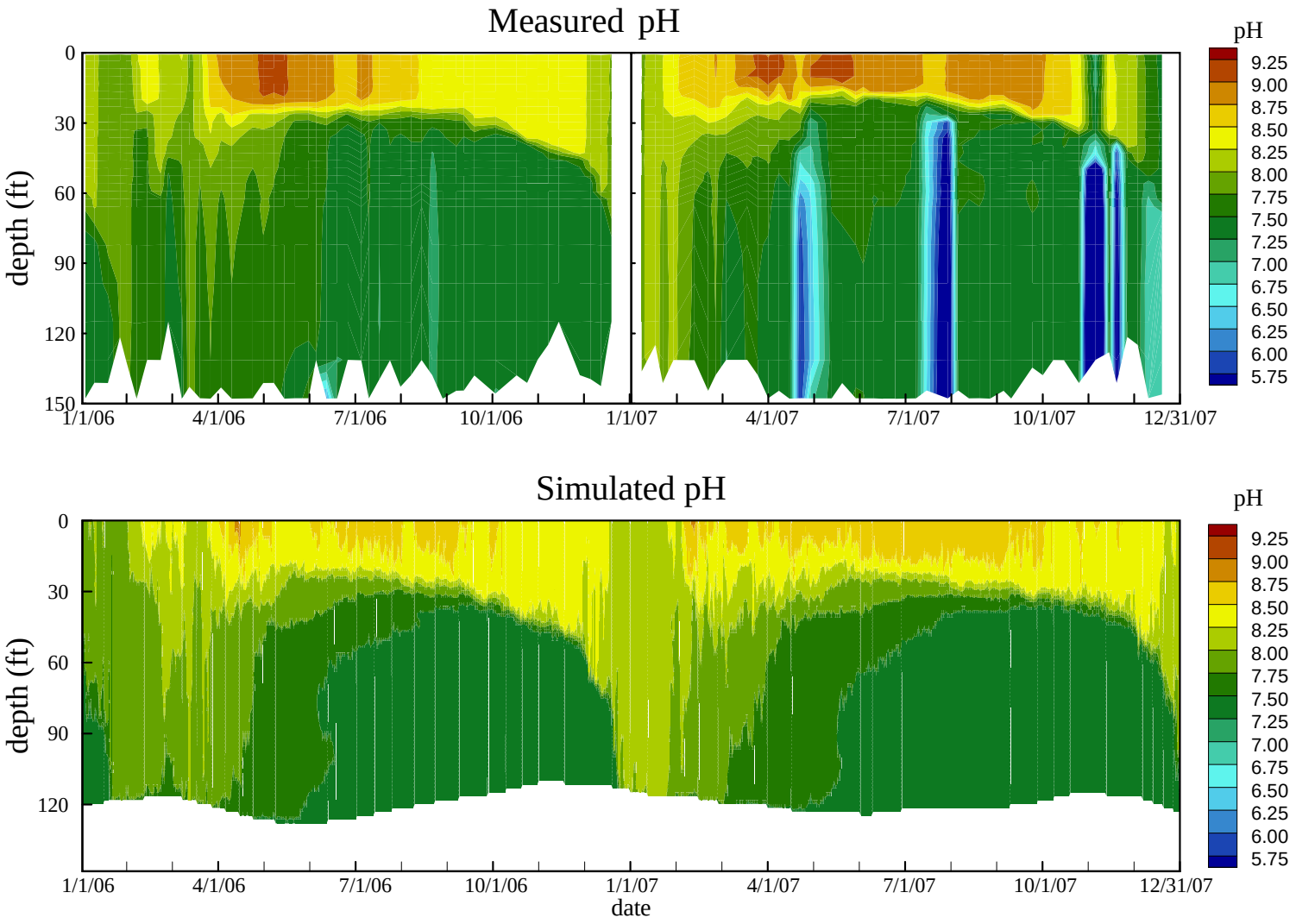

FSI V094005
May 01, 2012

Figure 41

FLOW SCIENCE®

San Vicente Reservoir

Scatter Plot of Measured vs. Simulated pH

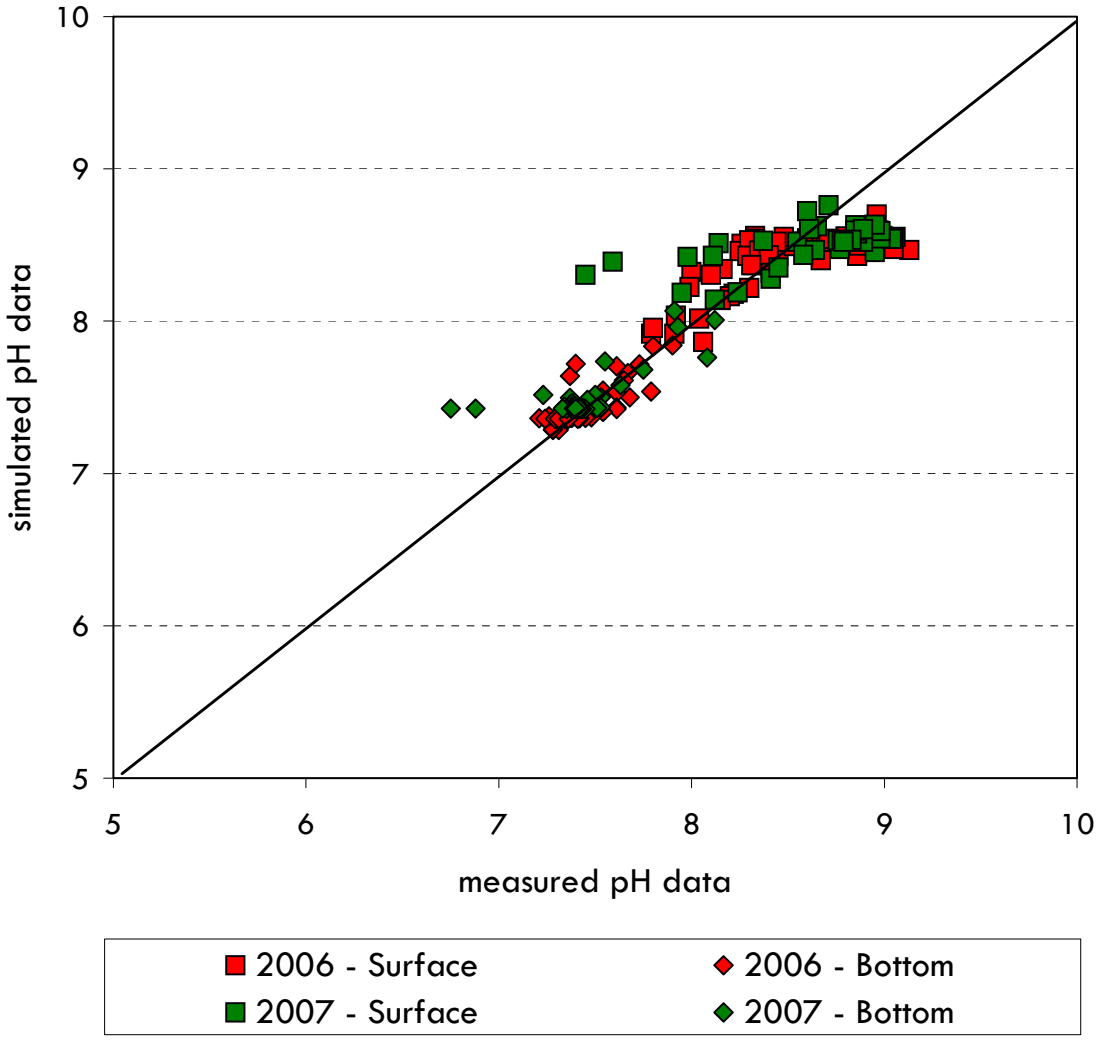

Figure 42

FSI V094005
May 01, 2012

FLOW SCIENCE®

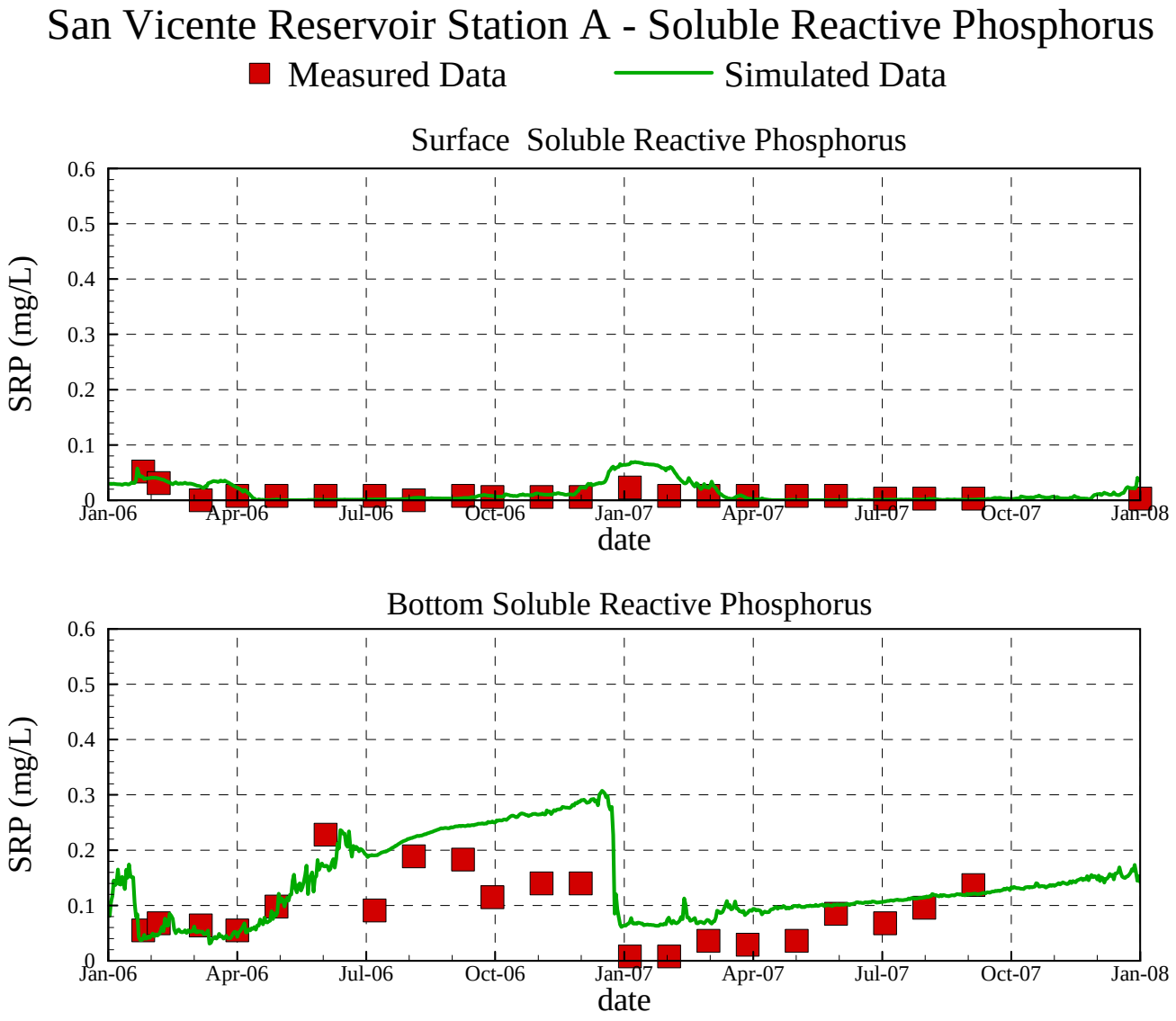

FSI V094005
May 01, 2012

Figure 43

FLOW SCIENCE®

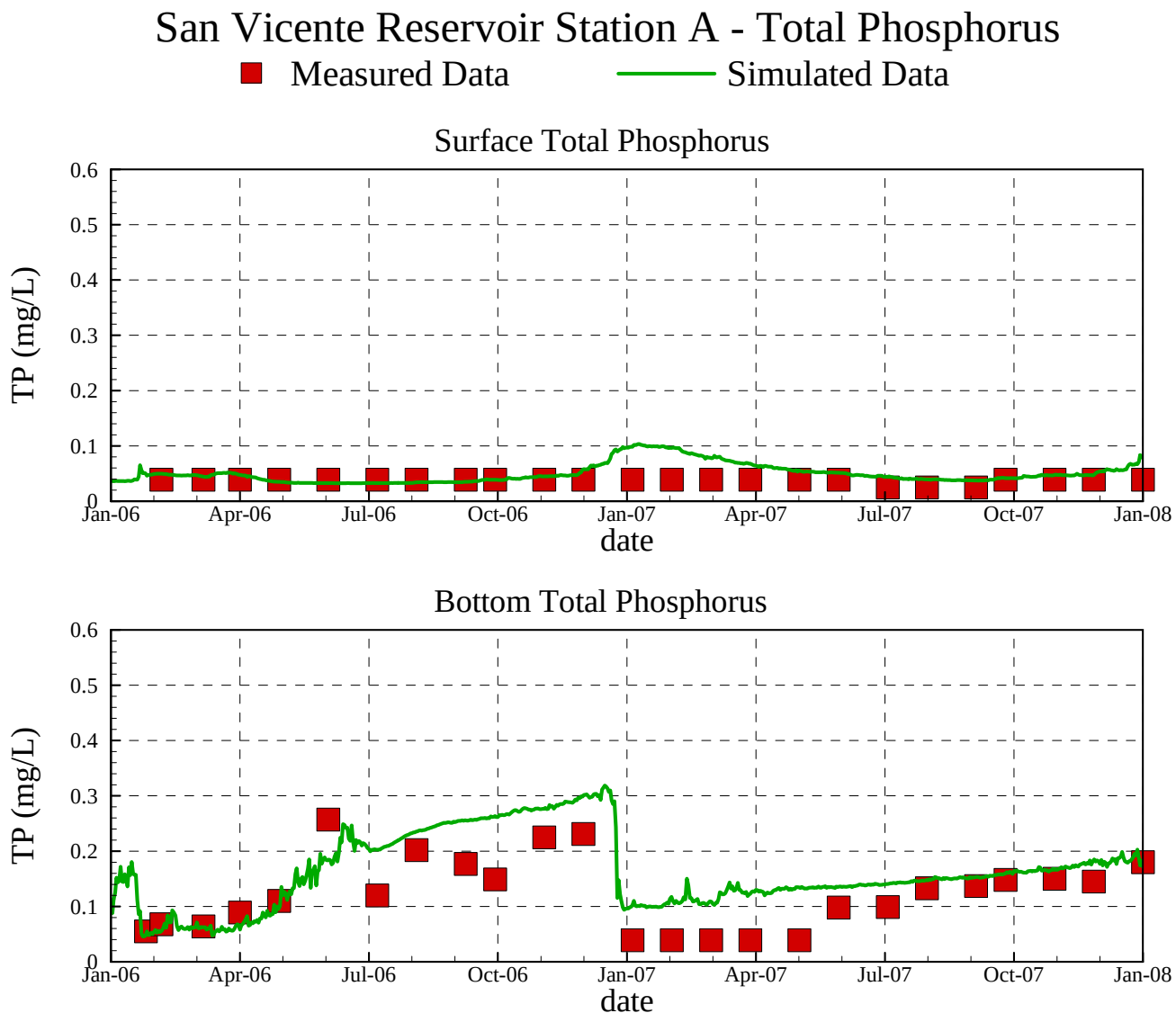

FSI V094005
May 01, 2012

Figure 44

FLOW SCIENCE®

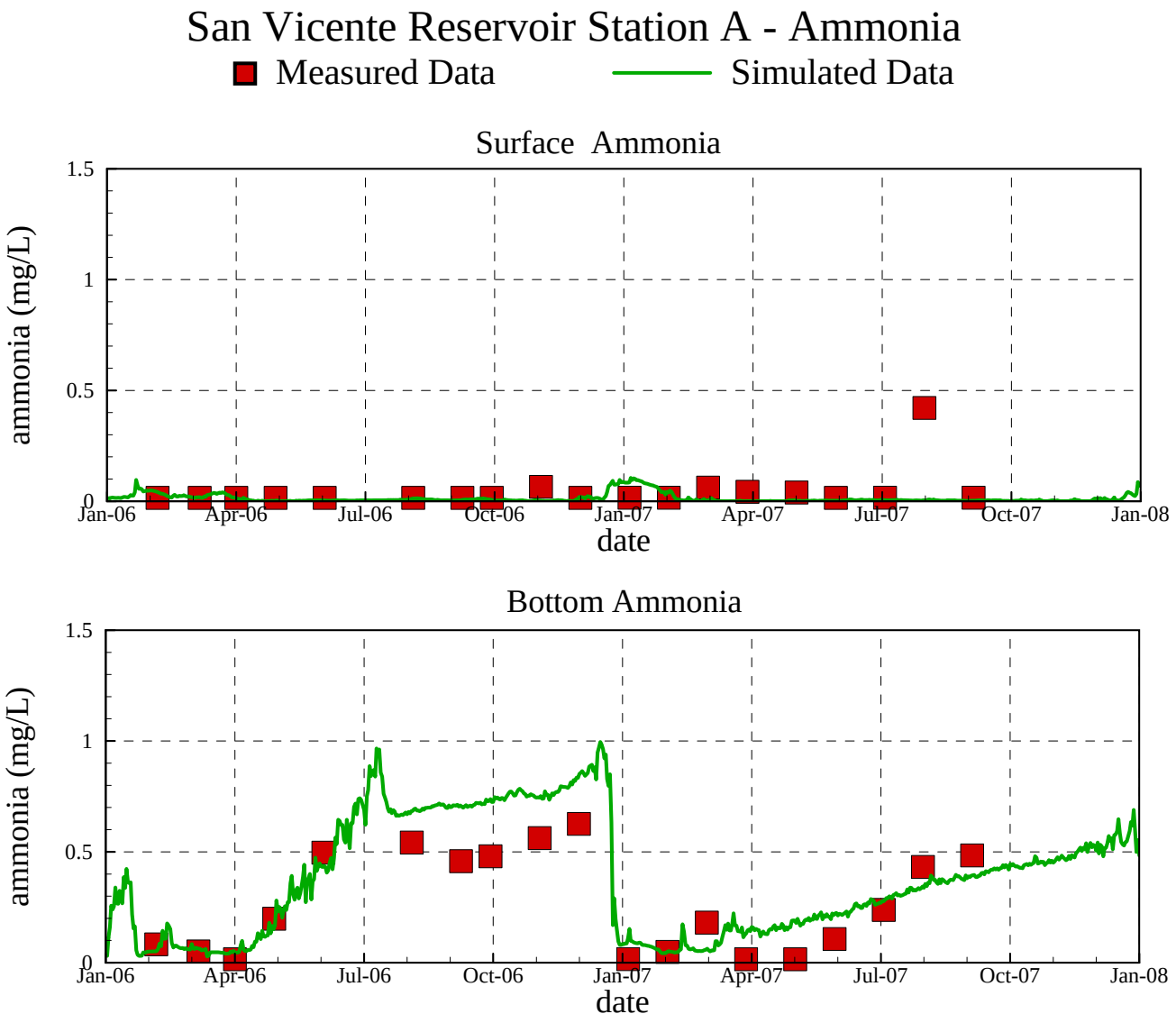

FSI V094005
May 01, 2012

Figure 45

FLOW SCIENCE®

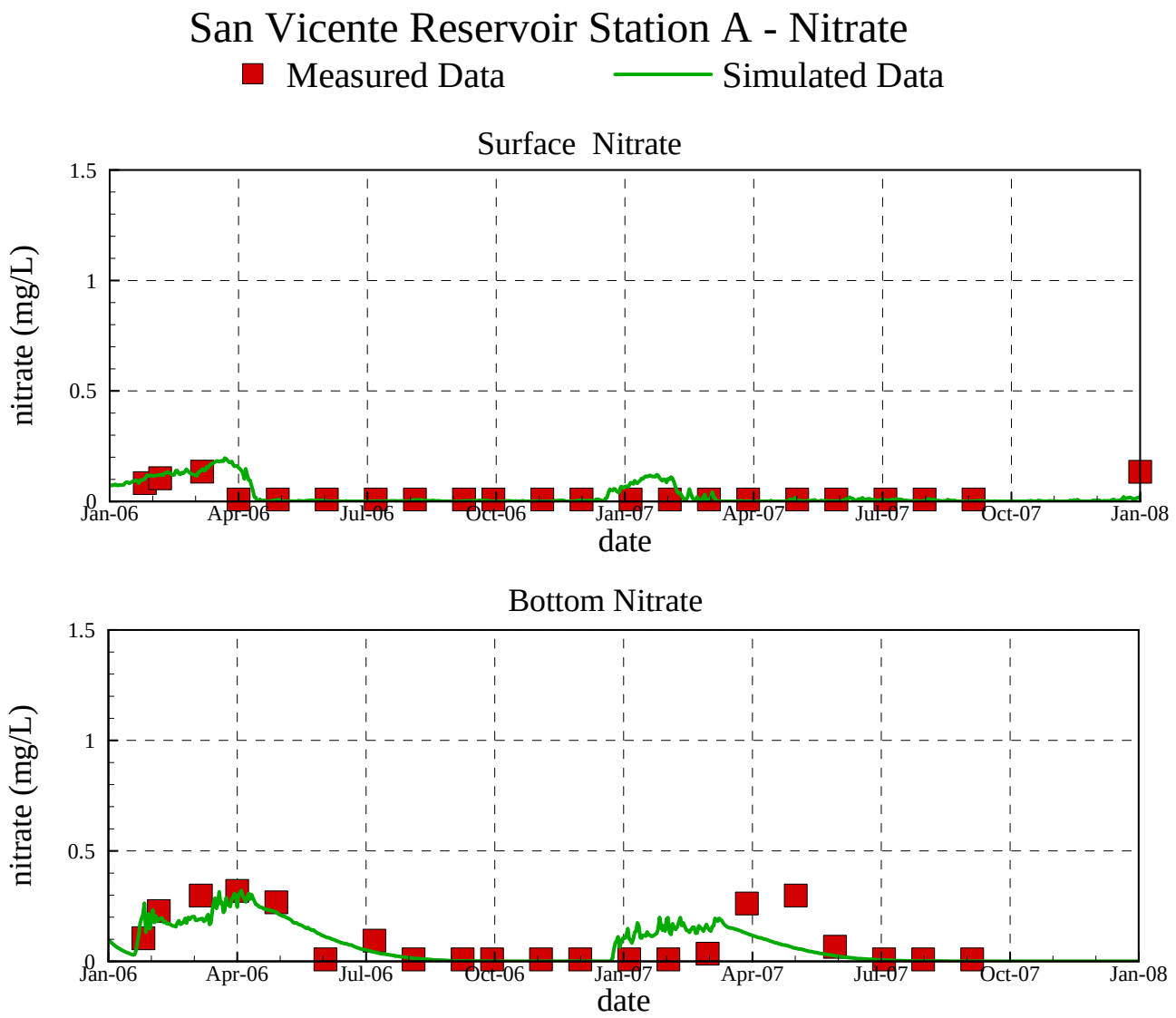

FSI V094005
May 01, 2012

Figure 46

FLOW SCIENCE®

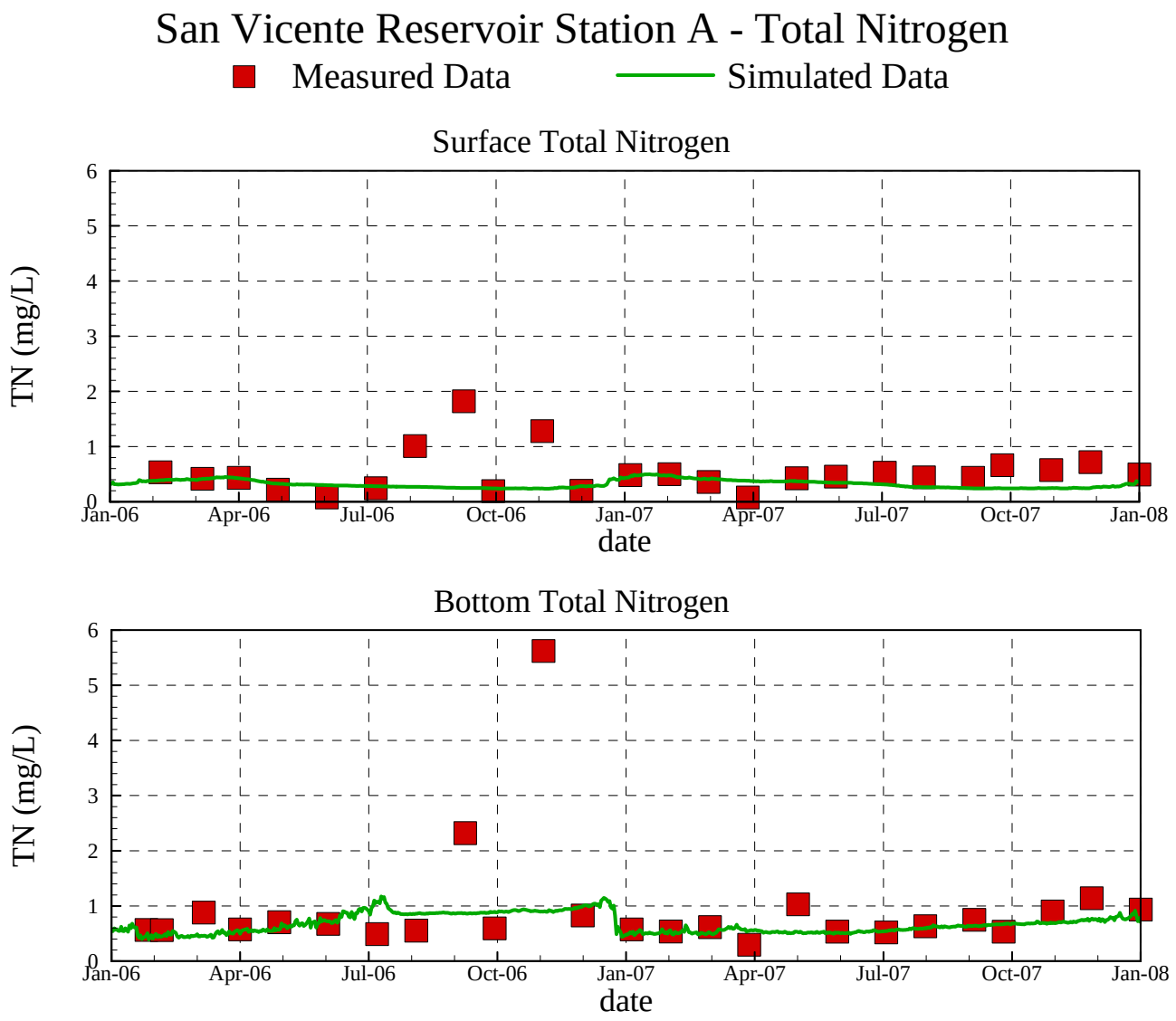

FSI V094005
May 01, 2012

Figure 47

FLOW SCIENCE®

San Vicente Reservoir

Station A – Chlorophyll a Concentrations

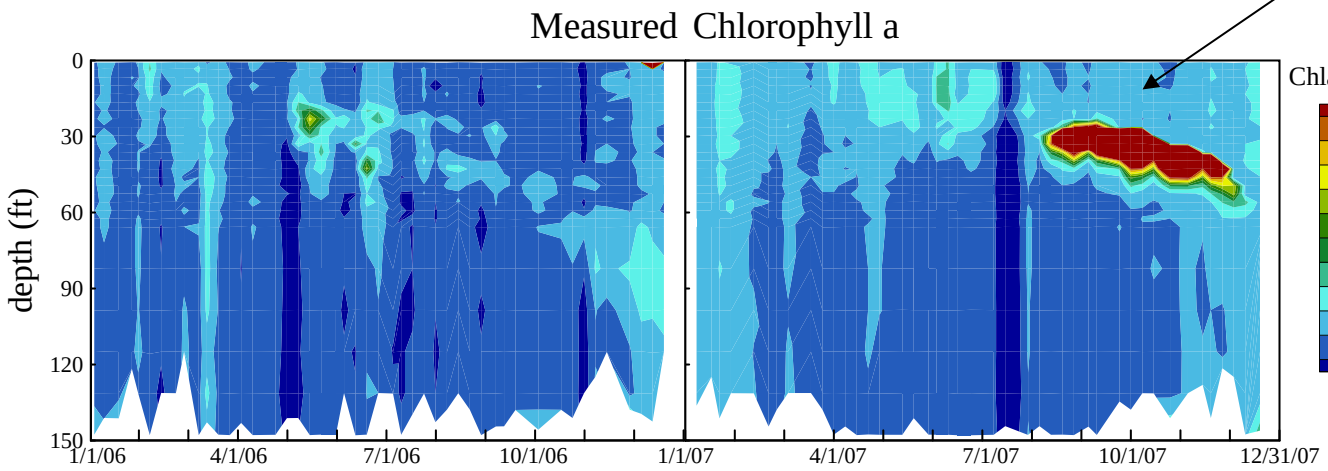

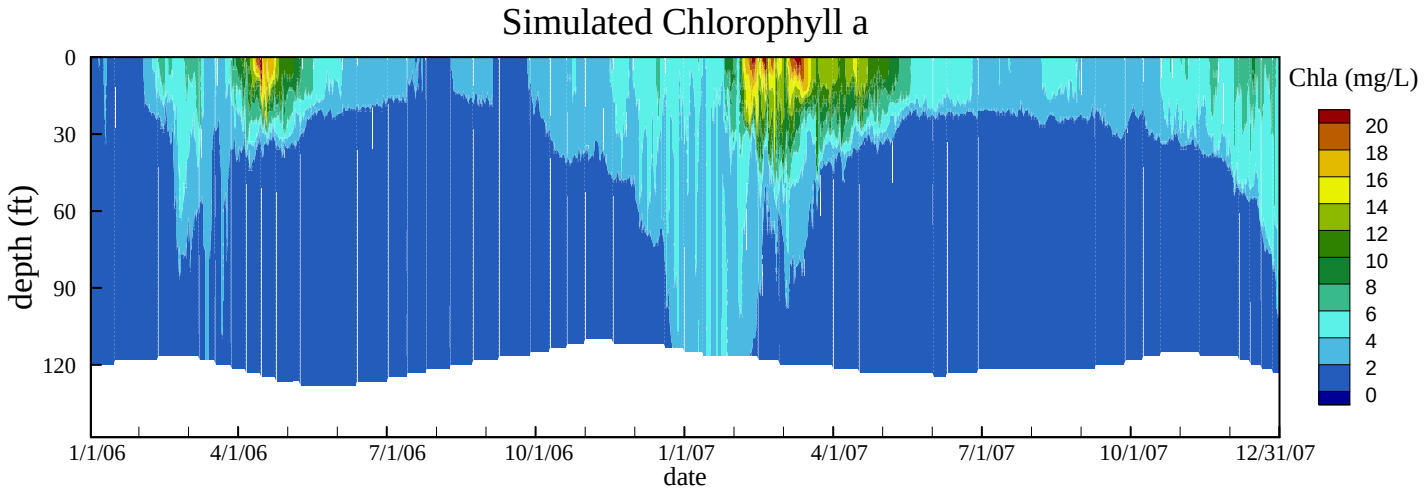

Measured DO, chlorophyll a and temperature profiles on 9/24/2007

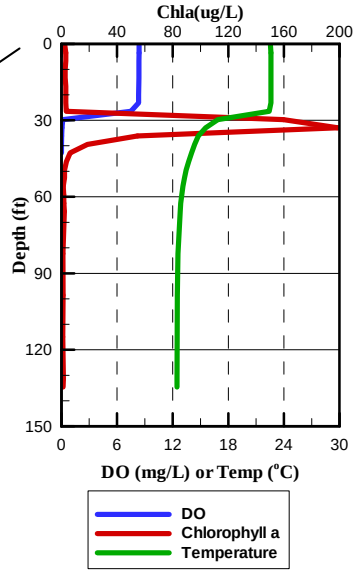

FSI V094005
May 01, 2012

Figure 48

FLOW SCIENCE®

San Vicente Reservoir Station A - Secchi Depth Calibration

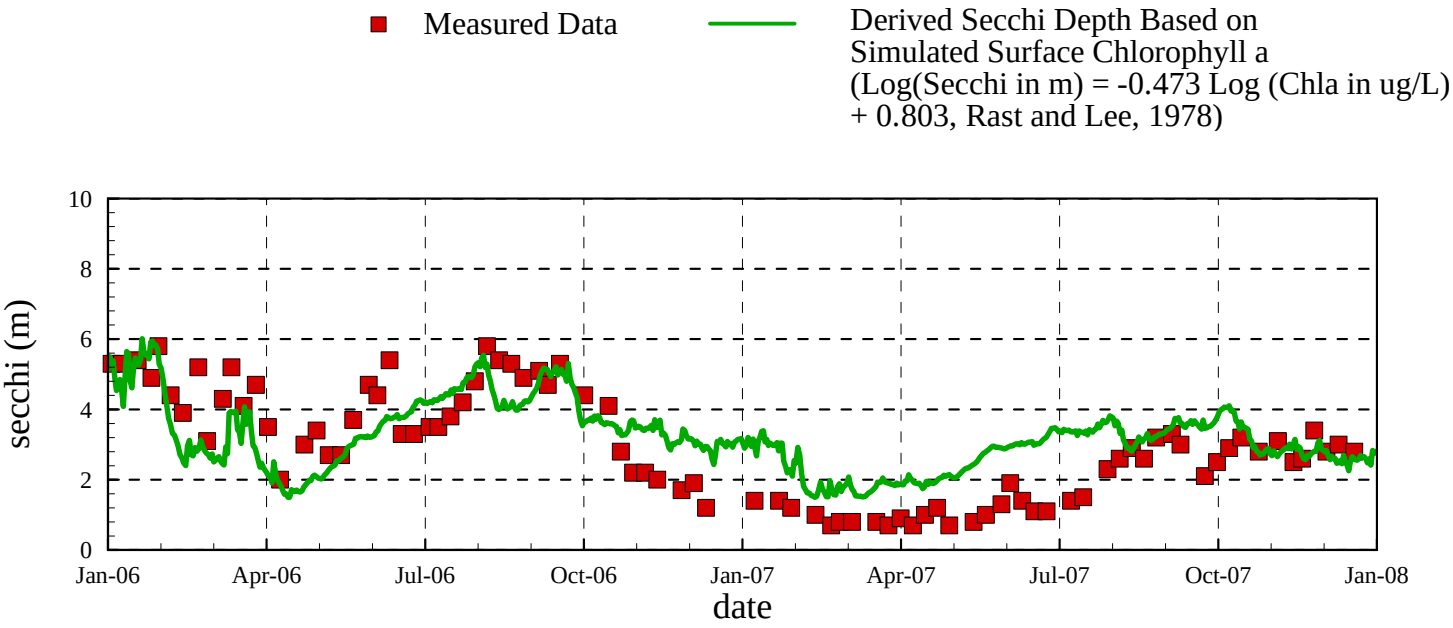

FSI V094005
May 01, 2012

Figure 49

FLOW SCIENCE®

San Vicente Reservoir

Scatter Plot of Measured vs. Simulated Secchi Depth

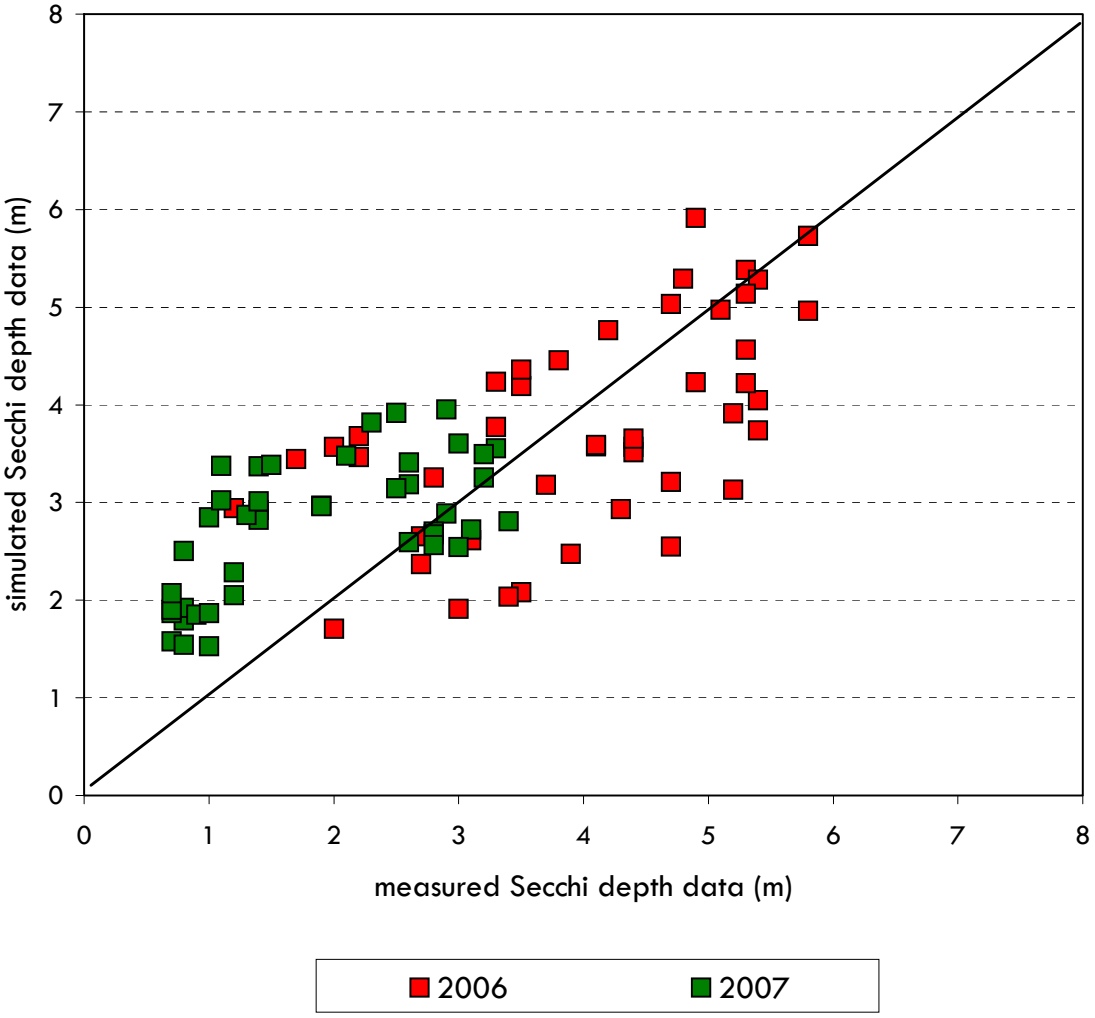

Figure 50

FSI V094005
May 01, 2012

FLOW SCIENCE®

APPENDIX A

DESCRIPTION OF ELCOM/CAEDYM MODELS AND EVIDENCE OF VALIDATION

DESCRIPTION OF ELCOM/CAEDYM MODELS AND EVIDENCE OF VALIDATION

1.0 INTRODUCTION

The coupling of biogeochemical and hydrodynamic processes in numerical simulations is a fundamental tool for research and engineering studies of water quality in coastal oceans, estuaries, lakes, and rivers. A modeling system for aquatic ecosystems has been developed that combines a three-dimensional hydrodynamic simulation method with a suite of water quality modules that compute interactions between biological organisms and the chemistry of their nutrient cycles. This integrated approach allows for the feedback and coupling between biogeochemical and hydrodynamic systems so that a complete representation of all appropriate processes can be included in an analysis. The hydrodynamic simulation code is the Estuary and Lake Computer Model (ELCOM) and the biogeochemical model is the Computational Aquatic Ecosystem Dynamics Model (CAEDYM).

The purpose of this document is to demonstrate that ELCOM and CAEDYM are accepted models that have been systematically tested and debugged, and then successfully validated in numerous applications. A history of the models is provided, followed by an outline of the general model methodology and evolution that emphasizes the basis of the ELCOM/ CAEDYM codes in previously validated models and research. Then the process of code development, testing, and validation of ELCOM/CAEDYM is detailed. Specific model applications are described to illustrate how the ELCOM/CAEDYM models have been applied to coastal oceans, estuaries, lakes, and rivers throughout the world and the results successfully validated against field data. Finally, a general description of the governing equations, numerical models, and processes used in the models is provided along with an extensive bibliography of supporting material.

A comprehensive description of the equations and methods used in the models is provided in the "The CWR Estuary and Lake Computer Model, User Guide" by Hodges (1999), "Estuary and Lake Computer Model, ELCOM Science Manual Code Version 1.5.0" by Hodges and Dallimore (2001), "Computational Aquatic Ecosystem Dynamics Model, CAEDYM: User Manual" (1999), and the "Computational Aquatic Ecosystem Dynamics Model (CAEDYM), An Ecological Water Quality Model Designed for Coupling with Hydrodynamic Drivers, Scientific Manual" by Hamilton and Herzfeld (1999).

2.0 MODEL HISTORY

The ELCOM/CAEDYM models were originally developed at the Centre for Water Research (CWR) at the University of Western Australia, although the hydrodynamics code ELCOM is an outgrowth of a hydrodynamic model developed earlier by Professor Vincenzo Casulli in Italy and now in use at Stanford University under the name TRIM-3D. The CAEDYM model was essentially developed at CWR as an outgrowth of earlier water quality modules used in the one-dimensional model, Dynamic Reservoir Simulation Model - Water Quality (DYRESM-WQ, Hamilton and Schladow, 1997).

The original ELCOM/CAEDYM models, as developed by CWR, were implemented in Fortran 90 (with F95 extensions) on a UNIX computer system platform. In 2001, the codes for both models were ported to a personal computer (PC) platform through an extensive recompiling and debugging effort by Flow Science Incorporated (Flow Science) in Pasadena, California.

3.0 MODEL METHODOLOGY

ELCOM is a three-dimensional numerical simulation code designed for practical numerical simulation of hydrodynamics and thermodynamics for inland and coastal waters. The code links seamlessly with the CAEDYM biogeochemical model undergoing continuous development at CWR, as shown graphically in **Figure 1**. The combination of the two codes provides three-dimensional simulation capability for examination of changes in water quality that arise from anthropogenic changes in either quality of inflows or reservoir operations.

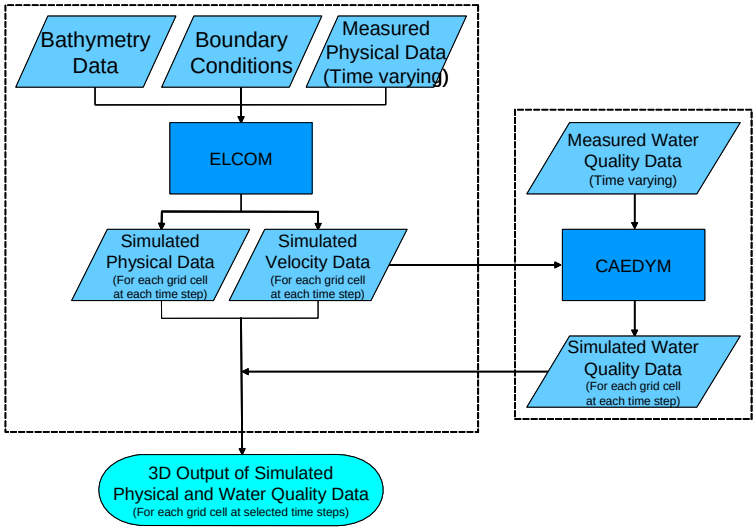

Figure 1 Flow chart showing the integration of the linked ELCOM/CAEDYM models.

The numerical method used in ELCOM is based on the TRIM-3D model scheme of Casulli and Cheng (1992) with adaptations made to improve accuracy, scalar conversion, numerical diffusion, and implementation of a mixed-layer model. The ELCOM model also extends the TRIM-3D scheme by including conservative advection of scalars. The unsteady Reynolds-averaged, Navier-Stokes equations, and the scalar transport equations serve as the basis of ELCOM. The pressure distribution is assumed hydrostatic and density changes do not impact the inertia of the fluid (the Boussinesq approximation), but are considered in the fluid body forces. There is an eddy-viscosity approximation for the horizontal turbulence correlations that represent the turbulent momentum transfer. Vertical momentum transfer is handled by a Richardson number-based diffusion coefficient. Since numerical diffusion generally dominates molecular processes, molecular diffusion in the vertical direction is neglected in ELCOM.

Both ELCOM and TRIM-3D are three-dimensional, computational fluid dynamics (CFD) models. CFD modeling is a validated and well-established approach to solving the equations of fluid motions in a variety of disciplines. Prior to the development of TRIM-3D, there were difficulties in modeling density stratified flows and such flows required special numerical methods. With TRIM-3D, Casulli and Cheng (1992) developed the first such successful method to model density-stratified flows, such as occur in the natural environment. Since then, TRIM-3D has been validated by numerous publications. ELCOM is based on the same proven method, but incorporates additional improvements as described above. Furthermore, the ELCOM model is based on governing equations and numerical algorithms that have been used in the past (e.g., in validated models such as TRIM-3D), and have been validated in refereed publications. For example:

- The hydrodynamic algorithms in ELCOM are based on the Euler-Lagrange method for advection of momentum with a conjugate gradient solution for the free-surface height (Casulli and Cheng, 1992).
- The free-surface evolution is governed by vertical integration of the continuity equation for incompressible flow applied to the kinematic boundary condition *(e.g.*, Kowalik and Murty, 1993).
- The numerical scheme is a semi-implicit solution of the hydrostatic Navier-Stokes equations with a quadratic Euler-Lagrange, or semi-Lagrangian (Staniforth and Côté, 1991).
- Passive and active scalars (*i.e.*, tracers, salinity, and temperature) are advected using a conservative ULTIMATE QUICKEST discretization (Leonard, 1991). The ULTIMATE QUICKEST approach has been implemented in two-dimensional format and demonstration of its effectiveness in estuarine flows has been documented by Lin and Falconer (1997).

- Heat exchange is governed by standard bulk transfer models found in the literature (*e.g.*, Amorocho and DeVries, 1980; Imberger and Patterson, 1981; Jacquet, 1983).
- The vertical mixing model is based on an approach derived from the mixing energy budgets used in one-dimensional lake modeling as presented in Imberger and Patterson (1981), Spigel *et al* (1986), and Imberger and Patterson (1990). Furthermore, Hodges presents a summary of validation using laboratory experiments of Stevens and Imberger (1996). This validation exercise demonstrates the ability of the mixed-layer model to capture the correct momentum input to the mixed-layer and reproduce the correct basin-scale dynamics, even while boundary-induced mixing is not directly modeled.
- The wind momentum model is based on a mixed-layer model combined with a model for the distribution of momentum over depth (Imberger and Patterson, 1990).

The numerical approach and momentum and free surface discretization used in ELCOM are defined in more detail in Hodges, Imberger, Saggio, and Winters (1999). Similarly, the water quality processes and methodology used in CAEDYM are described in more detail in Hamilton and Schladow (1997). Further technical details on ELCOM and CAEDYM are provided in Sections 5.0 and 6.0 below.

4.0 VALIDATION AND APPLICATION OF ELCOM/CAEDYM

Since initial model development, testing and validation of ELCOM and/or CAEDYM have been performed and numerous papers on model applications have been presented, written, and/or published as described in more detail below. In summary:

- ELCOM solves the full three-dimensional flow equations with small approximations.
- ELCOM/CAEDYM was developed, tested, and validated over a variety of test cases and systems by CWR.
- Papers on ELCOM/CAEDYM algorithms, methodology, and applications have been published in peer reviewed journals such as the *Journal of Geophysical Research*, the *Journal of Fluid Mechanics*, the *Journal of Hydraulic Engineering*, the *International Journal for Numerical Methods in Fluids*, and *Limnology and Oceanography*.
- ELCOM/CAEDYM was applied by Flow Science to Lake Mead, Nevada. As part of this application, mass balances were verified and results were presented to a model review panel over a two-year period. The model review panel, the National Park Service, the Bureau of Reclamation, the Southern Nevada Water Authority, and the Clean Water Coalition (a

consortium of water and wastewater operators in the Las Vegas, Nevada, region) all accepted the ELCOM/CAEDYM model use and validity.

- There are numerous applications of ELCOM/CAEDYM in the literature that compare the results to data, as summarized in Section 3.2.

The process of code development, testing, and validation of ELCOM/CAEDYM by CWR, and the ongoing validation and refinement of the codes through further application of the models are detailed in the following subsections. The major components of the development, testing, and validation process are summarized in **Figure 2**.

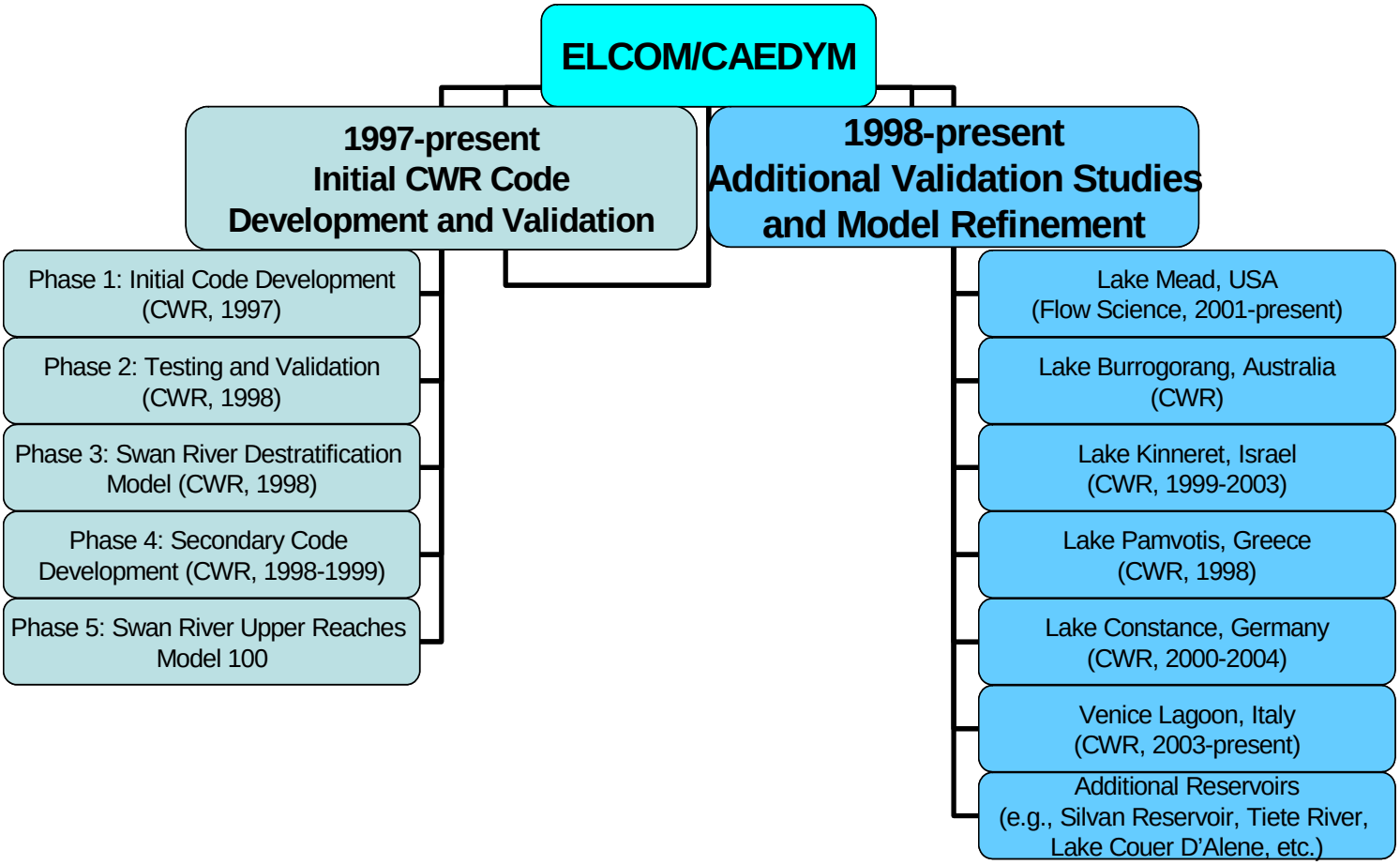

Figure 2 ELCOM/CAEDYM code development, testing, validation, and applications by CWR and Flow Science Incorporated.

4.1 CWR CODE DEVELOPMENT, TESTING, AND VALIDATION

Initial development of the code by CWR occurred from March through December 1997 (Phase 1), followed by a period of testing and validation from January through April 1998 (Phases 2 and 3). Secondary code development by CWR occurred from September 1998 through February 1999 (Phase 4). Testing and validation were performed over a variety of test cases and systems to ensure that all facets of the code were tested. In addition, Phase 5 modeling of the Swan River since 1998 has been used to gain a better understanding of the requirements and limitations of the model (Hodges *et al*, 1999).

4.1.1 Phase 1: Initial Code Development

The ELCOM code was initially conceived by CWR as a Fortran 90/95 adaptation of the TRIM-3D model of Casulli and Cheng (1992) in order to: 1) link directly to the CAEDYM water quality module developed concurrently at CWR and 2) provide a basis for future development in a modern programming language. Although written in Fortran 77, TRIM-3D is considered a state-of-the-art numerical model for estuarine applications using a semi-implicit discretization of the Reynolds-averaged hydrostatic Navier-Stokes equations and an Euler-Lagrange method for momentum and scalar transport.

During development of ELCOM, it became clear that additional improvements to the TRIM-3D algorithm were required for accurate solution of density-stratified flows in estuaries. After the basic numerical algorithms were written in Fortran 90, subroutine-by-subroutine debugging was performed to ensure that each subroutine produced the expected results. Debugging and testing of the entire model used a series of test cases that exercised the individual processes in simplified geometries. This included test cases for the functioning of the open boundary condition (tidal forcing), surface wave propagation, internal wave propagation, scalar transport, surface thermodynamics, density underflows, wind-driven circulations, and flooding/drying of shoreline grid cells. Shortcomings identified in the base numerical algorithms were addressed during secondary code development (Phase 4).

Towards the end of the initial code development, ELCOM/CAEDYM were coupled and test simulations were run to calibrate the ability of the models to work together on some simplified problems. Results showing the density-driven currents induced by phytoplankton shading were presented at the Second International Symposium on Ecology and Engineering (Hodges and Herzfeld, 1997). Further details of modeling of density-driven currents due to combinations of topographic effects and phytoplankton shading were presented at a joint meeting of the American Geophysical Union (AGU) and the American Society of Limnology and Oceanography (ASLO) by Hodges *et al*. (1998), and at a special seminar at Stanford University (Hodges 1998).

Additionally, presentations by Hamilton (1997), Herzfeld *et al*. (1997), and Herzfeld and Hamilton (1998) documented the concurrent development of the CAEDYM ecological model.

4.1.2 Phase 2: Testing and Validation

The simplified geometry tests of Phase I revealed deficiencies in the TRIM-3D algorithm including the inability of the TRIM-3D Euler-Lagrange method (ELM) to provide conservative transport of scalar concentrations (e.g., salinity and temperature). Thus, a variety of alternate scalar transport methods were tested, with the best performance being a flux-conservative implementation of the ULTIMATE filter applied to third-order QUICKEST discretization based on the work of Leonard (1991).

Model testing and validation against simple test cases was again undertaken. In addition, a simulation of a winter underflow event in Lake Burragorang in New South Wales, Australia, was performed to examine the ability of the model to capture a density underflow in complex topography in comparison to field data taken during the inflow event. These tests showed that the ability to model underflows is severely constrained by the cross-channel grid resolution.

4.1.3 Phase 3: Swan River Destratification Model

Phase 3 involved examining a linked ELCOM/CAEDYM destratification model of the Swan River system during a period of destratification in 1997 when intensive field monitoring had been conducted. The preliminary results of this work were presented at the Swan-Canning Estuary Conference (Hertzfeld *et al*, 1998). More comprehensive results were presented at the Western Australian Estuarine Research Foundation (WAERF) Community Forum (Imberger, 1998).

4.1.4 Phase 4: Secondary Code Development

In conducting the Phase 3 Swan River destratification modeling, it became clear to CWR that long-term modeling of the salt-wedge propagation would require a better model for mixing dynamics than presently existed. Thus, the availability of an extensive field data set for Lake Kinneret, Israel, led to its use as a test case for development of an improved mixing algorithm for stratified flows (Hodges *et al*, 1999).

A further problem appeared in the poor resolution of momentum terms using the linear ELM discretization (*i.e.*, as used in the original TRIM-3D method). Since the conservative ULTIMATE QUICKEST method (used for scalar transport, see Phase 1 above) does not lend itself to efficient use for discretization of momentum terms in a semi-implicit method, a quadratic ELM approach was developed for more accurate discretization of the velocities.

4.1.5 Phase 5: Swan River Upper Reaches Model

Phases 1-4 developed and refined the ELCOM code for accurate modeling of three-dimensional hydrodynamics where the physical domain is well resolved. Phase 5 is an ongoing process of model refinement that concentrates on developing a viable approach to modeling longer-term evolution hydrodynamics and water quality in the Swan River where fine-scale resolution of the domain is not practical. The Swan River application is also used for ongoing testing and calibration of the CAEDYM water quality module.

The Swan River estuary is located on the Swan Coastal Plain, Western Australia. It is subject to moderate to high nutrient loads associated with urban and agricultural runoff and suffered from *Microcystis aeruginosa* blooms in January 2000. In an effort to find a viable means of conducting seasonal to annual simulations of the Swan River that retain the fundamental along-river physics and the cross-channel variability in water quality parameters, CWR has developed and tested ELCOM/CAEDYM extensively. A progress report by Hodges *et al* (1999) indicates that ELCOM is capable of accurately reproducing the hydrodynamics of the Swan River over long time scales with a reasonable computational time.

Furthermore, studies conducted by Robson and Hamilton (2002) proved that ELCOM/CAEDYM accurately reproduced the unusual hydrodynamic circumstances that occurred in January 2000 after a record maximum rainfall, and predicted the magnitude and timing of the *Microcystis* bloom. These studies show that better identification and monitoring procedures for potentially harmful phytoplankton species could be established with ELCOM/CAEDYM and will assist in surveillance and warnings for the future.

4.2 MODEL APPLICATIONS

In addition to the initial code development, testing, and validation by CWR, numerous other applications of ELCOM/CAEDYM have been developed by CWR and validated against field data. Additionally, Flow Science has applied ELCOM/CAEDYM extensively at Lake Mead (USA) and validated the results against measured data. The results of numerous ELCOM/CAEDYM model applications are presented below.

4.2.1 Lake Mead (Nevada, USA)

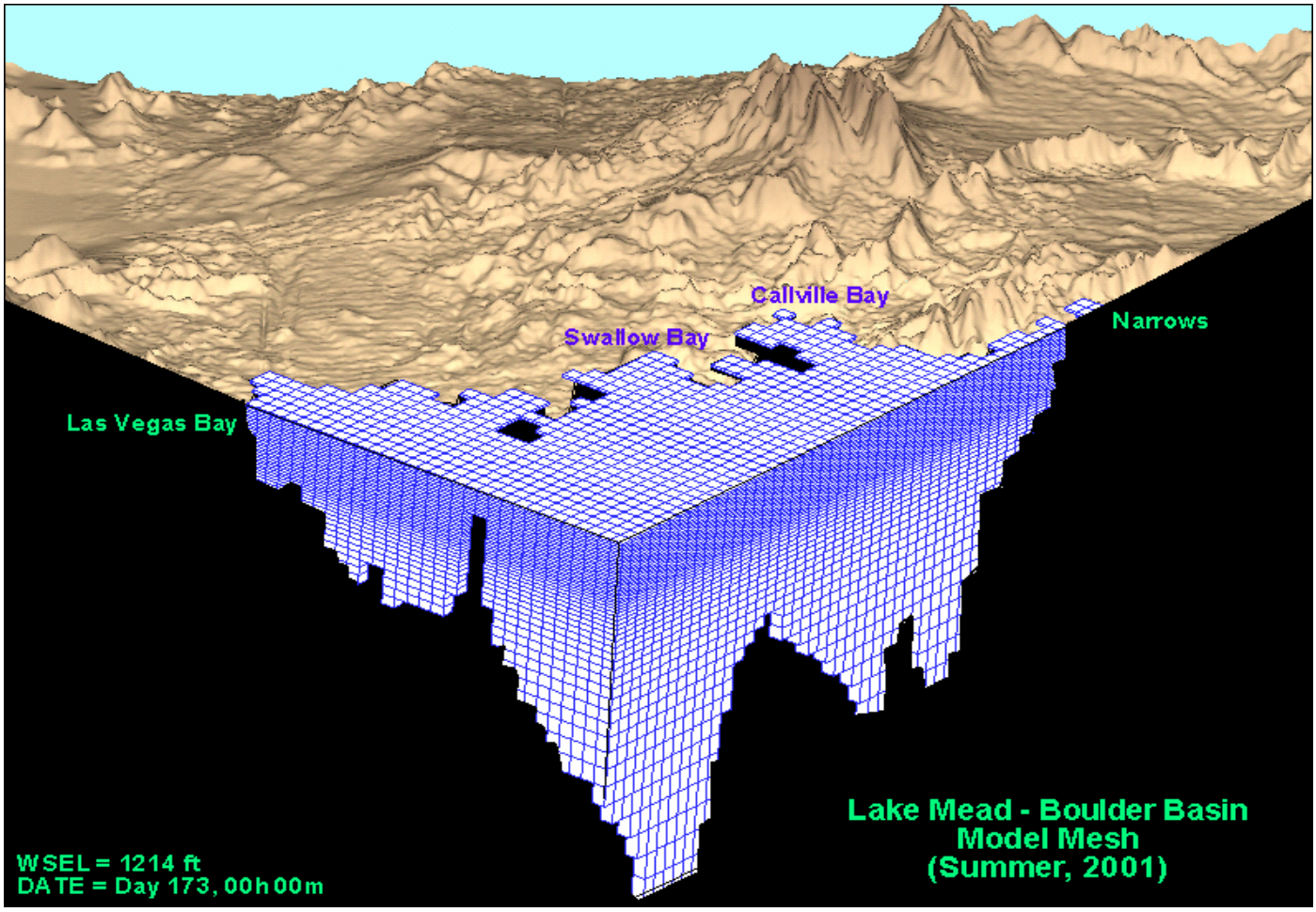

Figure 3 Model Grid for Lake Mead.

An ELCOM/CAEDYM model of Lake Mead near Las Vegas, Nevada, is being used to evaluate alternative discharge scenarios for inclusion in an Environmental Impact Statement (EIS) for the Clean Water Coalition (CWC), a consortium of water and wastewater operators in the Las Vegas region. **Figure 3** is a cut-away of the three-dimensional model grid used for Lake Mead, showing the varying grid spacing in the vertical direction. **Figure 4** is an example of the model output, showing the isopleths of a tracer plume within the reservoir for a sample case.

As part of the EIS process, a model review panel met monthly for two years to review the validation of the ELCOM/CAEDYM model, its calibration against field data, and its application. The modeling committee approved the use of the model.

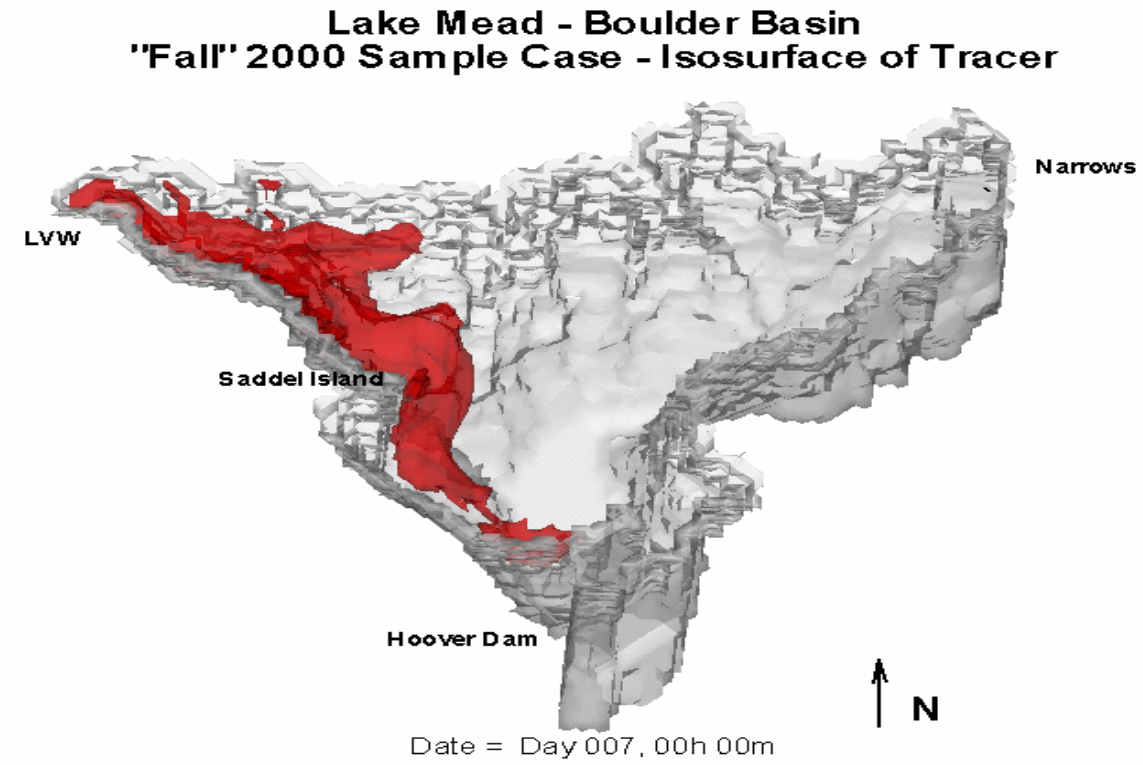

Figure 4 Lake Mead isopleths of tracer for a fall 2000 sample case.

Subsequently, a scientific Water Quality Advisory Panel concluded that the ELCOM/CAEDYM model was applicable and acceptable. The members of the Water Quality Advisory Panel were diverse and included Jean Marie Boyer, Ph.D., P.E. (Water Quality Specialist/Modeler, Hydrosphere), Chris Holdren, Ph.D., CLM (Limnologist, United States Bureau of Reclamation), Alex Horne, Ph.D. (Ecological Engineer, University of California Berkeley), and Dale Robertson, Ph.D. (Research Hydrologist, United States Geological Survey).

More specifically, the Water Quality Advisory Panel agreed on the following findings:

- The ELCOM/CAEDYM model is appropriate for the project.
- There are few three-dimensional models available for reservoirs. ELCOM is one of the best hydrodynamic models and has had good success in Lake Mead and other systems.
- The ELCOM model accurately simulates most physical processes.
- The algorithms used in CAEDYM are widely accepted (a biological consultant, Professor David Hamilton of The University of Waikato, New Zealand, has been retained to review the CAEDYM coefficients and algorithms).

The Lake Mead ELCOM/CAEDYM model was calibrated against four years of measured data for numerous physical and water quality parameters including temperature, salinity, conductivity, dissolved oxygen, pH, nutrients (nitrogen and phosphorus), chlorophyll *a*, perchlorate, chloride, sulfate, bromide, and total organic carbon. Detailed results of this calibration and the subsequent evaluation of alternative discharge scenarios will be made available in late 2005 in the CWC EIS that is currently being prepared for this project. An example of the calibration results for chlorophyll *a* for 2002 is presented in **Figure 5** below. In this figure, simulated concentrations are compared against field data measured in the lake by the United States Bureau of Reclamation (USBR) and the City of Las Vegas (COLV).

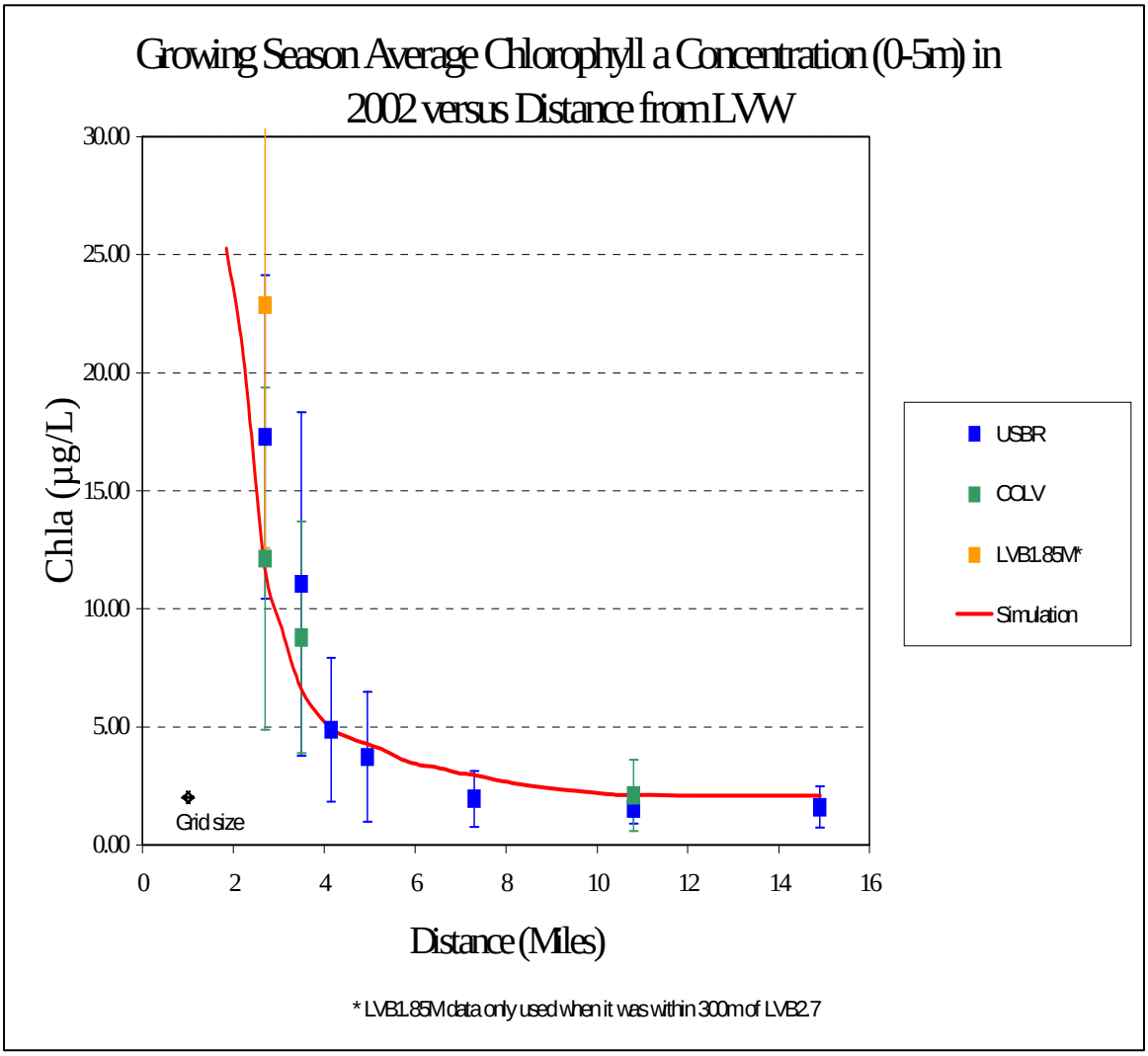

Figure 5 ELCOM/CAEDYM calibration results for chlorophyll a for 2002 as a function of distance from the inflow at Las Vegas Wash.

In addition to the good agreement between the model and field data and the acceptance of the model by the review committees, Flow Science also performed a mass balance on the model to ensure conservation of tracer materials. As a result of such tests and debugging, Flow Science and the CWR have made continuous improvements to the model as necessary including refinements to the ULTIMATE QUICKEST scheme and boundary cell representations.

4.2.2 Lake Burragorang (New South Wales, Australia)

ELCOM was applied and validated for Lake Burragorang in order to rapidly assess the potential impacts on water quality during an underflow event (CWR). Underflows usually occur during the winter when inflow water temperature is low compared to the reservoir. This causes the upheaval of hypolimnetic water at the dam wall, and as a result it transports nutrient rich waters into the euphotic zone.

The thermal dynamics during the underflow event were reproduced accurately by ELCOM for the case with idealized bathymetry data with coarse resolutions (straightened curves and rotating the lake in order to bypass the resolution problem), but not for the simulation with the complex, actual bathymetry. This is because the model tests showed that the ability to model underflows is severely constrained by the cross-channel grid resolution. When the cross-channel direction is poorly resolved at bends and curves, an underflow is unable to propagate downstream without a significant loss of momentum. Nevertheless, the simulations with the coarse idealized domain certainly can be used as aids and tools to visualize the behavior of reservoirs. Particularly, ELCOM was able to capture the traversal of the underflow down the length of Lake Burragorang and then had sufficient momentum to break against the wall causing the injection of underflow waters into the epilimnion near the dam. This simulated dynamic was in agreement with what was measured in the field.

4.2.3 Lake Kinneret (Israel)

ELCOM was applied to model basin-scale internal waves that are seen in Lake Kinneret, Israel, since understanding of basin-scale internal waves behaviors provide valuable information on mixing and transport of nutrients below the wind-mixed layer in stratified lakes. In studies done by Hodges *et al*. (1999) and Laval *et al* (2003), the ELCOM simulation results were compared with field data under summer stratification conditions to identify and illustrate the spatial structure of the lowest-mode basin-scale Kelvin and Poincare waves that provide the largest two peaks in the internal wave energy spectra. The results demonstrated that while ELCOM showed quantitative differences in the amplitude and steepness of the waves as well as in the wave phases, the basin-scale waves were resolved very well by ELCOM. In particular, the model captures the qualitative nature of the peaks and troughs in the thermocline and the depth of the wind-mixed layer at relatively coarse vertical grid resolutions (Hodges *et al*, 1999).

4.2.4 Lake Pamvotis (Greece)

ELCOM/CAEDYM was applied to Lake Pamvotis, a moderately sized (22 km^2), shallow (4 m average depth) lake located in northwest Greece. Since the lake has undergone eutrophication over the past 40 years, many efforts are directed at understanding the characteristics of the lake and developing watershed management and restoration plans.

Romero and Imberger (1999) simulated Lake Pamvotis over a one month period during May to June, 1998, and compared the simulated thermal and advective dynamics of the lake with data obtained from a series of field experiments. The simulation results over-predicted heating; however, diurnal fluctuations in thermal structures were similar to those measured. Since the meteorological site was sheltered from the winds, the wind data used in the simulation was believed to be too low, causing insufficient evaporative heat-loss and subsequent over-heating by ELCOM. An increase in the wind speed by a factor of three gave temperature profiles in agreement with the field data. Moreover, the study demonstrated that the model is capable of predicting the substantial diurnal variations in the intensity and direction of both vertical and horizontal velocities. Romero and Imberger were also able to illustrate the functionality of ELCOM when coupled to the water quality model, CAEDYM, and confirmed that the model could be used to evaluate the effect of various strategies to improve poor water quality in localized areas in the lake.

4.2.5 Lake Constance (Germany, Austria, Switzerland)

Appt (2000) and Appt *et al*. (2004) applied ELCOM to characterize the internal wave structures and motions in Lake Constance since internal waves are a key factor in understanding the transport mechanisms for chemical and biological processes in a stratified lake such as Lake Constance. Lake Constance is an important source of drinking water and a major tourism destination for its three surrounding countries of Germany, Austria, and Switzerland. Due to anthropogenic activities and climatic changes, Lake Constance water quality has deteriorated and its ecosystem has changed.

It was shown that ELCOM was able to reproduce the dominant internal wave and major hydrodynamic processes occurring in Lake Constance. For instance, three types of basin-scale waves were found to dominate the wave motion: the vertical mode-one Kelvin wave, the vertical mode-one Poincare waves, and a vertical mode-two Poincare wave. Moreover, an upwelling event was also reproduced by ELCOM suggesting that the width and length ratio of the basin, spatial variations in the wind, and Coriolis effects play critical roles in the details of the upwelling event. This on-going research has shown that ELCOM can be used as a tool to predict and understand hydrodynamics and water quality in lakes.

4.2.6 Venice Lagoon (Italy)

ELCOM/CAEDYM is being used to develop a hydrodynamic and sediment transport model of Venice Lagoon, Italy, since future gate closures at the mouth of the lagoon are likely to impact flushing patterns. This project is an integral part of the Venice Gate Projects in Italy that was launched in May 2003 to prevent flooding.

ELCOM was validated for the tidal amplitude and phase using the data obtained from 12 tidal stations located throughout the lagoon (Yeates, 2004). Remaining tasks include model validation of temperature, salinity, and velocity against measurements made in the major channels of the lagoon.

4.2.7 Silvan Reservoir (Australia)

ELCOM is currently being applied to reproduce the circulation patterns observed in Silvan Reservoir, Australia, during a field experiment that was conducted in March 2004 to determine the transport pathways in the lake. This experiment confirmed the upwelling behavior of the lake and the strong role of the inflows in creating hydraulic flows in the reservoir (Antenucci, 2004).

4.2.8 Billings and Barra Bonita Reservoirs (Brazil)

ELCOM/CAEDYM is being applied to Billings and Barra Bonita Reservoirs in Brazil. Billings Reservoir is an upstream reservoir that feeds Barra Bonita via the Tiete River. The objective of the project is to develop an integrated management tool for these reservoirs and river reaches for use in the future planning of water resource utilization in Sao Paulo, Brazil (Romero and Antenucci, 2004).

4.2.9 Lake Coeur D'Alene (Idaho, USA)

ELCOM/CAEDYM is being applied to investigate the trade-off between reducing heavy metal concentrations and a potential increase in eutrophication due to remediation procedures in Lake Coeur D'Alene, Idaho. In order to investigate heavy metal fate and transport, CAEDYM is being improved further to include heavy metals and a feedback loop to phytoplankton based on metal toxicity (Antenucci, 2004).

4.2.10 Lake Perris (California, USA)

ELCOM was applied to Lake Perris in order to compare the impacts of several recreational use strategies on measured fecal coliform concentrations at the outlet tower. The physical results of the simulation were validated against measured temperature and salinity data over a one-year period. The comparison of fecal coliform concentrations

against measured data was fair due to a lack of data describing the timing and magnitude of loading and the settling and re-suspension of fecal matter.

4.2.11 Other Applications

Other ELCOM/CAEDYM applications and development in on-going research at CWR include:

- Plume dynamics and horizontal dispersion (Marmion Marine Park, Australia).
- Inflow and pathogen dynamics (Helena, Myponga and Sugarloaf Reservoirs, Australia).
- Mixing and dissipation in stratified environments (Tone River, Japan, and Brownlee Reservoir, USA).
- Tidally forced estuaries and coastal lagoons (Marmion Marine Park and Barbamarco Lagoon, Italy).
- Three-dimensional circulation induced by wind and convective exchange (San Roque Reservoir, Argentina, and Prospect Reservoir, Australia).
- Sea-surface temperature fluctuation and horizontal circulation (Adriatic Sea).
- Response of bivalve mollusks to tidal forcing (Barbamarco Lagoon, Italy).
- Impacts of the additional withdrawals and brine discharge into the ocean from a proposed desalination facility co-located with an existing power plant in the City of Carlsbad (California, USA).

5.0 TECHNICAL DESCRIPTION OF ELCOM

As outlined above, ELCOM solves the unsteady, viscous Navier-Stokes equations for incompressible flow using the hydrostatic assumption for pressure. ELCOM can simulate the hydrodynamics and thermodynamics of a stratified system, including baroclinic effects, tidal forcing, wind stresses, heat budget, inflows, outflows, and transport of salt, heat and passive scalars. Through coupling with the CAEDYM water quality module, ELCOM can be used to simulate three-dimensional transport and interactions of flow physics, biology, and chemistry. The hydrodynamic algorithms in ELCOM are based upon the proven semi-Lagrangian method for advection of momentum with a conjugate-gradient solution for the free-surface height (Casulli and Cheng, 1992) and a conservative ULTIMATE QUICKEST transport of scalars (Leonard, 1991). This approach is advantageous for geophysical-scale simulations since the time step can be allowed to exceed the Courant-Friedrichs-Lewy (CFL) condition for the velocity without producing instability or requiring a fully-implicit discretization of the Navier-Stokes equations.

5.1 GOVERNING EQUATIONS

Significant governing equations and approaches used in ELCOM include:

- Three-dimensional simulation of hydrodynamics (unsteady Reynolds-averaged Navier-Stokes equations).
- Advection and diffusion of momentum, salinity, temperature, tracers, and water quality variables.
- Hydrostatic approximation for pressure.
- Boussinesq approximation for density effects.
- Surface thermodynamics module accounts for heat transfer across free surface.
- Wind stress applied at the free surface.
- Dirichlet boundary conditions on the bottom and sides.

5.2 NUMERICAL METHOD

Significant numerical methods used in ELCOM include:

- Finite-difference solution on staggered-mesh Cartesian grid.
- Implicit volume-conservative solution for free-surface position.
- Semi-Lagrangian advection of momentum allows time steps with CFL > 1.0.
- Conservative ULTIMATE QUICKEST advection of temperature, salinity, and tracers.
- User-selectable advection methods for water quality scalars using upwind, QUICKEST, or semi-Lagrangian to allow trade-offs between accuracy and computational speed.
- Solution mesh is uniform in horizontal directions but allows non-uniformity in vertical direction.

The implementation of the semi-Lagrangian method in Fortran 90 includes sparse-grid mapping of three-dimensional space into a single vector for fast operation using array-processing techniques. Only the computational cells that contain water are represented in the single vector so that memory usage is minimized. This allows Fortran 90 compiler parallelization and vectorization without platform-specific modification of the code. A future extension of ELCOM will include dynamic pressure effects to account for nonlinear dynamics of internal waves that may be lost due to the hydrostatic approximation.

Because the spatial scales in a turbulent geophysical flow may range from the order of millimeters to kilometers, it is presently impossible to conduct a Direct Navier-Stokes (DNS) solution of the equations of motion (*i.e.* an exact solution of the equations).

Application of a numerical grid and a discrete time step to a simulation of a geophysical domain is implicitly a filtering operation that limits the resolution of the equations. Numerical models (or closure schemes) are required to account for effects that cannot be resolved for a particular grid or time step. There are four areas of modeling in the flow physics: (l) turbulence and mixing, (2) heat budgets, (3) hydrodynamic boundary conditions, and (4) sediment transport.

5.3 TURBULENCE MODELING AND MIXING

ELCOM presently uses uniform fixed eddy viscosity as the turbulence closure scheme in the horizontal plane (in future versions a Smagorinsky 1963 closure scheme will be implemented to represent subgrid-scale turbulence effects as a function of the resolves large-scale strain-rates). These methods are the classic "eddy viscosity" turbulence closure. With the implementation of the Smagorinsky closure, future extensions will allow the eddy-viscosity to be computed on a local basis to allow improvements in modeling local turbulent events and flow effects of biological organisms (e.g., drag induced by macroalgae or seagrass).

In the present code, the user has the option to extend the eddy-viscosity approach to the vertical direction by setting different vertical eddy-viscosity coefficients for each grid layer. However, in a stratified system, this does not adequately account for vertical turbulent mixing that may be suppressed or enhanced by the stratification (depending on the stability of the density field and the magnitude of the shear stress). To model the effect of density stratification on turbulent mixing the CWR has developed a closure model based on computation of a local Richardson number to scale. The latter is generally smaller than the time step used in geophysical simulations, so the mixing is computed in a series of partial time steps. When the mixing time-scale is larger than the simulation time step, the mixing ratio is reduced to account for the inability to obtain mixing on very short time scales. This model has the advantage of computing consistent mixing effects without regard to the size of the simulation time-step (*i.e.* the model produces mixing between cells that is purely a function of the physics and not the numerical step size).

5.4 HEAT BUDGET

The heat balance at the surface is divided into short-wave (penetrative) radiation and a heat budget for surface heat transfer effects. The surface heat budget requires user input of the net loss or gain through conduction, convection, and long wave radiation in the first grid layer beneath the free surface. The short wave range is modeled using a user-prescribed input of solar radiation and an exponential decay with depth that is a function of a bulk extinction coefficient (a Beer's law formulation for radiation absorption). This coefficient is the sum of individual coefficients for the dissolved organics ("gilvin"), phytoplankton biomass concentration, suspended solids, and the

water itself. The extinction coefficients can either be computed in the water quality module (CAEDYM) or provided as separate user input.

5.5 HYDRODYNAMIC BOUNDARY CONDITIONS

The hydrodynamic solution requires that boundary conditions on the velocity must be specified at each boundary. There are six types of boundary conditions: (1) free surface, (2) open edge, (3) inflow-outflow, (4) no-slip, (5) free-slip, and (6) a Chezy-Manning boundary stress model (the latter is presently not fully implemented). For the free surface, the stress due to wind and waves is required. The user can either input the wind/wave stress directly, or use a model that relates the surface stress to the local wind speed and direction *via* a bulk aerodynamic drag coefficient. Open boundaries (e.g. tidal inflow boundaries for estuaries) require the user to supply the tidal signature to drive the surface elevation. Transport across open boundaries is modeled by enforcing a Dirichlet condition on the free-surface height and allowing the inflow to be computed from the barotropic gradient at the boundary. Inflow-outflow boundary conditions (e.g. river inflows) are Dirichlet conditions that specify the flow either at a particular boundary location *or inside the domain*. Allowing an inflow-outflow boundary condition to be specified for an interior position (*i.e.* as a source or sink) allows the model to be used for sewage outfalls or water outlets that may not be located on a land boundary. Land boundaries can be considered zero velocity (no-slip), zero-flux (free-slip) or, using a Chezy-Manning model, assigned a computed stress.

5.6 SEDIMENT TRANSPORT

While sediment transport is fundamentally an issue of flow physics, the algorithms for the sediment transport are more conveniently grouped with the water quality algorithms in CAEDYM. Settling of suspended particulate matter is computed using Stokes law to obtain settling velocities for the top and bottom of each affected grid cell. This allows the net settling flux in each cell to be computed. A two-layer sediment model has been developed that computes resuspension, deposition, flocculation, and consolidation of sediment based on (1) the shear stress at the water/sediment interface, (2) the type of sediment (cohesive/non-cohesive), and (3) the thickness of the sediment layer. Determination of the shear stress at the water/sediment interface requires the computation of bottom shear due to current, wind, and waves. A model has been developed to account for the effects of small-scale surface waves that cannot be resolved on a geophysical-scale grid. This model computes the theoretical wave height and period for small-scale surface waves from the wind velocity, water depth, and domain fetch. From these, the wavelength and orbital velocities are calculated. The wave-induced shear stress at the bottom boundary resulting from the wave orbital velocities is combined with a model for the current-induced shear stress to obtain the total bottom shear that effects sediment resuspension. The cohesiveness of the sediment determines the critical shear stresses that are necessary to resuspend or deposit the sediments. A model of

consolidation of the sediments is used to remove lower sediment layers from the maximum mass that may be resuspended.

6.0 TECHNICAL DESCRIPTION OF CAEDYM

CAEDYM is an outgrowth of previous CWR water quality modules in DYRESM-WQ and the Estuary Lake Model - Water Quality (ELMO-WQ) codes. CAEDYM is designed as a set of subroutine modules that can be directly coupled with one, two, or three-dimensional hydrodynamic "drivers", catchment surface hydrological models, or groundwater models. Additionally, it can be used in an uncoupled capacity with specification of velocity, temperature, and salinity distributions provided as input files rather than as part of a coupled computation. The user can specify the level of complexity in biogeochemical process representation so both simple and complex interactions can be studied. Direct coupling to a hydrodynamic driver (*e.g.* ELCOM) allows CAEDYM to operate on the same spatial and temporal scales as the hydrodynamics. This permits feedbacks from CAEDYM into ELCOM for water quality effects such as changes in light attenuation or effects of macroalgae accumulation on bottom currents. **Figure 6** shows an illustration of the interactions of modeled parameters in CAEDYM. Being an “N-P-Z” (nutrient-phytoplankton-zooplankton) model, CAEDYM can be used to assess eutrophication. Unlike the traditional general ecosystem model, CAEDYM serves as a species- or group-specific model (*i.e.* resolves various phytoplankton species). Furthermore, oxygen dynamics and several other state variables are included in CAEDYM.

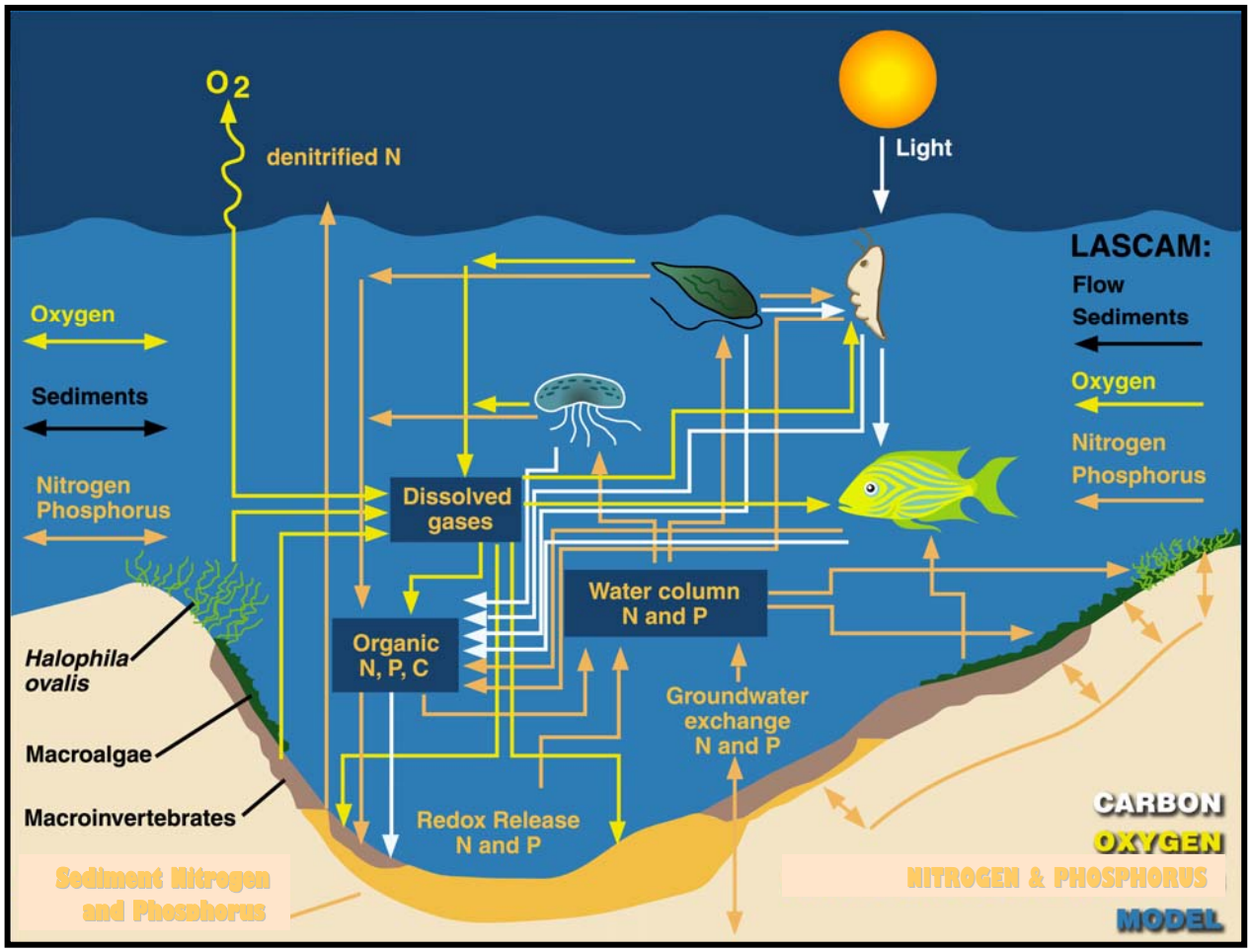

Illustration of interactions of modeled parameters in CAEDYM.

The representation of biogeochemical processes in ecological models has, historically, been treated in a simple manner. In fact, the pioneering work on modeling marine ecosystems (Riley *et al*, 1949; Steel, 1962) is still used as a template for many of the models that are currently used (Hamilton and Schladow, 1997). The level of sophistication and process representation included in CAEDYM is of a level hitherto unseen in any previous aquatic ecosystem model. This enables many different components of the system to be examined, as well as providing a better representation of the dynamic response of the ecology to major perturbations to the system (e.g. the response to various management strategies). **Figure 7** shows the major state variables included in the CAEDYM model. Using CAEDYM to aid in management decisions and

system understanding requires (1) a high level of process representation, (2) process interactions and species differentiation of several state variables, and (3) applicability over a spectrum of spatial and temporal scales. The spectrum of scales relates to the need for managers to assess the effects of temporary events, such as anoxia at specific locations, through to understanding long-term changes that may occur over seasons or years. There is considerable flexibility in the time step used for the ecological component. Long time steps (relative to the hydrodynamic advective scale) may be used to reduce the frequency of links to ELCOM when long-term (*i.e.* seasonal or annual) simulations are run.

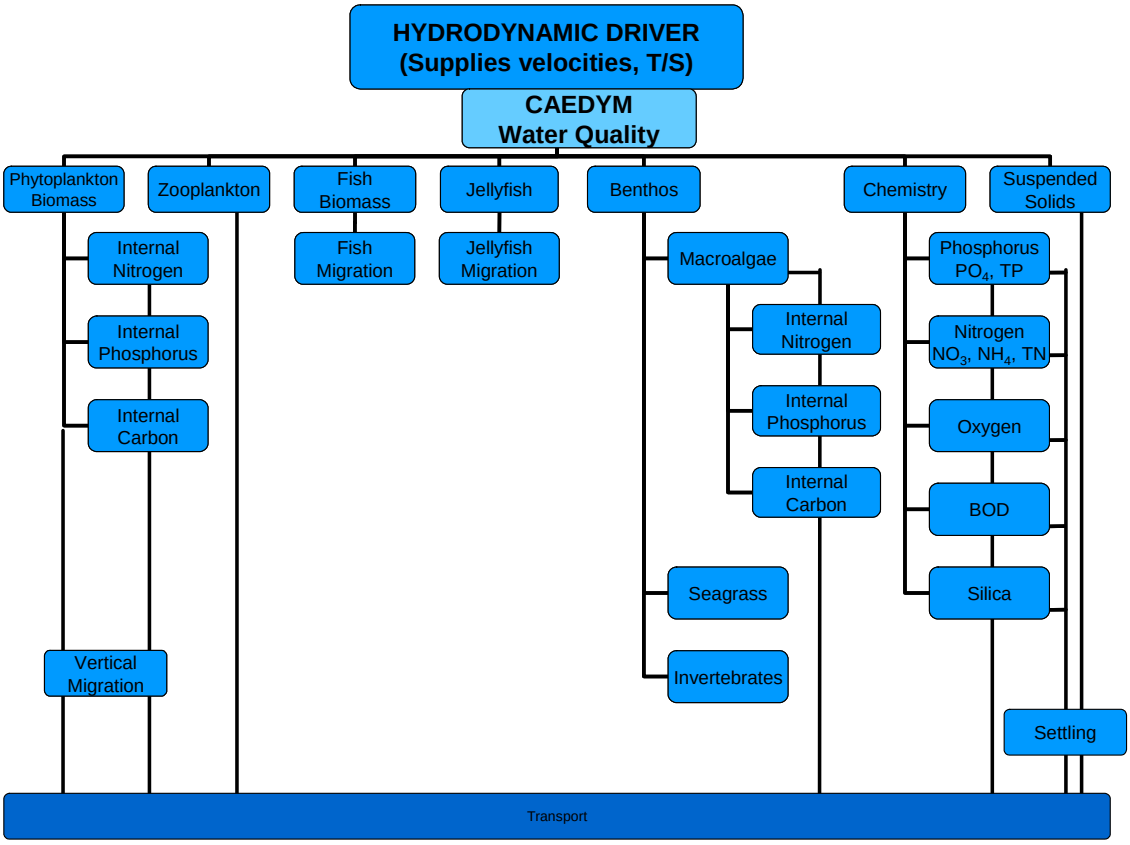

Figure 7 Major state variables included in the CAEDYM model.

6.1 BIOLOGICAL MODEL

The biological model used in CAEDYM consists of seven phytoplankton groups, five zooplankton groups, six fish groups, four macroalgae groups and three invertebrate groups, as well as models of seagrass and jellyfish. This set will be expanded as biological models are developed, tested, and calibrated to field data. There is flexibility for the user in choosing which species to include in a simulation. Vertical migration is simulated for motile and non-motile phytoplankton, and fish are migrated throughout the model domain according to a migration function based on their mortality. A weighted grazing function is included for zooplankton feeding on phytoplankton and fish feeding on zooplankton. The biomass grazed is related to both food availability and preference of the consumer for its food supply. Improved temperature, respiration and light limitation functions have been developed to represent the environmental response of the organisms. The benthic processes included a self-shading component and beach wrack function for macroalgae, sediment bioturbation and nutrient cycling by polychaetes, and effects of seagrass on sediment oxygen status.

In particular, the seven phytoplankton groups modeled are dinoflagellates, freshwater diatoms, marine/estuarine diatoms, freshwater cyanobacteria, marine estuarine cyanobacteria, chlorophytes, and cryptophytes. Phytoplankton biomass is represented in terms of chlorophyll *a*. Phytoplankton concentrations are affected by the following processes:

- Temperature growth function
- Light limitation
- Nutrient limitation by phosphorus and nitrogen (and when diatoms are considered, silica)
- Loss due to respiration, natural mortality, excretion, and grazing
- Salinity response
- Vertical migration and settling

6.2 NUTRIENTS, METALS, AND OXYGEN DYNAMICS

The transport and chemical cycling of nutrients is an important part of simulating the interaction of biological organisms in an ecosystem. CAEDYM includes as state variables the following:

- Nutrients (dissolved inorganic phosphorus, total phosphorus, total nitrogen, ammonium nitrate, and silica).
- Dissolved oxygen and biochemical oxygen demand.
- Metals (dissolved and particulate forms of iron and manganese).

- Suspended sediment (the particulate and colloidal fractions).
- pH

The model incorporates oxygen dynamics and nutrient cycling in both the sediments and water column. A sediment pool of organic detritus and inorganic sediments, both of which may be resuspended into the water column, is included. Redox-mediated release of dissolved nutrients is simulated from the sediments to the water column.

Processes included in the water and sediment oxygen dynamics include:

- Atmospheric exchange (Wanninkhof, 1992).
- Oxygen production and consumption through phytoplankton, macroalgae, and seagrass/macrophyte photosynthesis and respiration, respectively.
- Utilization of dissolved oxygen due to respiration of higher organisms such as zooplankton and fish and due to photosynthesis and respiration in jellyfish
- Water column consumption of oxygen during nitrification.
- Biochemical oxygen demand due to mineralization of organic matter in the water column and in the sediments.
- Oxygen flux from the water column to the sediments, sediment oxygen demand (SOD), as developed from Fick's law of diffusion.

The last two processes are used together with a sediment porosity and diffusion coefficient (Ullman and Aller, 1982) in order to define the depth of the toxic layer in the sediments.

Nutrient processes included in the sediment and water column dynamics include:

- Phytoplankton nutrient uptake, with provision for luxury storage of nutrients.
- Release of dissolved inorganic nutrients from phytoplankton excretion.
- Excretion of nutrients as fecal material by zooplankton.
- Nitrification and denitrification by bacterial mediated action.
- Generation of inorganic nutrients from organic detritus.
- Transfer of nutrients through the food chain (*e.g.* phytoplankton--zooplankton--fish).
- Uptake of nutrients by macroalgae and seagrasses.
- Adsorption/desorption of nutrients from inorganic suspended sediments.
- Sediment/water transfer of nutrients (*via* such processes as sediment resuspension, sedimentation, redox-mediated nutrient release, and bioturbation).

In essence, CAEDYM represents the type of interactive processes that occur amongst the ecological and chemical components in the aquatic ecosystem. As a broad generalization, one component of the system cannot be manipulated or changed within the model without affecting other components of the system. Similarly in nature, changing an integral component in the aquatic system will have wide-ranging and follow-on effects on many of the other system components. CAEDYM is designed to have the complexity and flexibility to be able to handle the continuum of responses that will be elicited as components of a system that are manipulated. Thus, the model represents a valuable tool to examine responses under changed conditions, as for example, when new approaches to managing an ecosystem are adopted.

7.0 BIBLIOGRAPHY

7.1 REFERENCED IN TEXT

(1999), "Computational aquatic ecosystem dynamics model, CAEDYM: User manual," TTF/4/Nov99, Centre for Water Research, University of Western Australia, 51pp.

Amorocho, J. and DeVries, J.J. (1980). "A new evaluation of the wind stress coefficient over water surfaces," Journal of Geophysical Research, 85:433-442.

Antenucci, Jason (2004). "Tracing Short-Circuiting Potential," from CWR Models: Bytes and Nybbles, Autumn 2004, Issue 10, page 2.

Antenucci, Jason (2004). "New Metals Model for CAEDYM," from CWR Services: Bytes and Nybbles, December 2004, Issue 11, page 1.

Appt, Jochen (January 2000), "Review on the modeling of short period internal waves in lakes with focus on Lake Constance," Pfaffenwaldring 61, D-70550 Stuttgart, Universität Stuttgart, Institut für Hydraulik und Grundwasser, Stuttgart.

Appt, J., Imberger, J., Kobus, H. (2004), "Basin-scale motion in stratified Upper Lake Constance," Limnology and Oceanography, 49(4), 919-933

Casulli, Vincenzo and Cheng, Ralph T. (1992), "Semi-implicit finite difference methods for three-dimensional shallow water flow," *International Journal for Numerical Methods in Fluids*, **15**, 629-48.

CWR, "Limnological Study of Lake Burragorang," Centre For Water Research, The University of Western Australia, Chapter 4 excerpt from report, pp. 104-126.

Hamilton, D. (1997). "An integrated ecological model for catchment hydrology and water quality for the Swan and Canning Rivers," presented at the 2nd International

Symposium on Ecology and Engineering, 10-12 November 1997, Freemantle, Australia. IAHR Eco-Hydraulics section.

Hamilton, David and Herzfeld, Michael (November 11, 1999), "Computational aquatic ecosystem dynamics model (CAEDYM), An ecological water quality model designed for coupling with hydrodynamic drivers, Scientific manual," Centre for Water Research, The University of Western Australia, Nedlands, Australia, 101pp.

Hamilton, D.P. and S.G. Schladow (1997), "Prediction of water quality in lakes and reservoirs: Part I: Model description," *Ecological Modelling, 96,* 91-110.

Herzfeld, M. and Hamilton, D. (1998), "A computational aquatic ecosystem dynamics model for the Swan River," *EOS Trans. AGU*, **79**(1), Ocean Sciences Meet. Suppl. OS11P-02.

Herzfeld, M.; Hodges, B.R.; and Hamilton, D. (1998), "Modelling the Swan River on small temporal and spatial scales," The Swan Canning Estuary conference, York, Australia, Apr., 1998.

Herzfeld, M.; Hamilton, D.; and Hodges, B.R. (1997), "Reality vs. management: The role of ecological numerical models," *2nd International Symposium on Ecology and Engineering*, 10-12 November 1997, Fremantle, Australia, IAHR Eco-Hydraulics section.

Hodges, B.R. (1998), "Hydrodynamics of differential heat absorption," *Environmental Mechanics Laboratory Seminar*, Dept. of Civil Eng., Stanford University, Feb. 1998.

Hodges, B.R. and Dallimore C. (2001), "Estuary and lake computer model, ELCOM Science Manual Code Version 1.5.0," Centre for Water Research, The University of Western Australia.

Hodges, B.R. and Herzfeld, M. (1997), "Coupling of hydrodynamics and water quality for numerical simulations of Swan River," *2nd International Symposium on Ecology and Enginnering*, 10-12 November, Fremantle, Australia, IAHR Eco-Hydraulics section.

Hodges, B.R.; Herzfeld, M.; Winters, K.; and Hamilton, D. (1998), "Coupling of hydrodynamics and water quality in numerical simulations," *EOS Trans. AGU*, **79**(1), Ocean Sciences Meet. Suppl. OS11P-01.

Hodges, Ben R. (May 25, 1999), "The CWR estuary and lake computer model, User guide," Centre for Water Research, The University of Western Australia, 47pp.

Hodges, B.R., Imberger, J., Saggio, A., and K. Winters (1999), "Modeling basin-scale internal waves in a stratified lake," *Limnology and Oceanography*), **45**(7), 1603-20.

Hodges, B.R., Yue, N., and Bruce, L. (May 27, 1999), "Swan River hydrodynamic model progress report," Centre For Water Research, The University of Western Australia, 14pp.

Jacquet, J. (1983). "Simulation of the thermal regime of rivers," In Orlob, G.T., editor, Mathematical Modeling of Water Quality: Streams, Lakes and Reservoirs, pages 150-176. Wiley-Interscience.

Kowalik, Z. and Murty, T.S. (1993). "Numerical Modeling of Ocean Dynamics," World Scientific.

Laval, B., Imberger, J., Hodges, B.R., and Stocker, R. (2003), "Modeling circulation in lakes: spatial and temporal variations," Limnology and Oceanography 48(3), 983-994.

Leonard, B.P. (1991), "The ULTIMATE conservative difference scheme applied to unsteady one-dimensional advection," *Computational Methods in Applied Mechanics and Engineering*, **88**, 17-74.

Lin, B. and Falconer, R.A. (1997). "Tidal flow and transport modeling using ULTIMATE QUICKEST," Journal of Hydraulic Engineering, 123:303-314.

Robson, B.J. and Hamilton, D. P. (2002). "Three-Dimensional Modeling of a Microcystis bloom event in a Western Australian Estuary." Centre For Water Research, The University of Western Australia, 491- 496 pp.

Romero, J.R. and Antenucci, J. (2004). "The Tiete River: Supply for Sao Paolo, Brazil," from CWR Models: Bytes and Nybbles, Autumn 2004, Issue 10, page 4.

Romero, J.R. and Imberger, J. (1999). "Lake Pamvotis Project-Final report", ED report WP 1364 JR, Centre for Water Research, Crawley, Western Australia, Australia.

Spigel, R.H.; Imberger, J.; and Rayner, K.N. (1986), "Modeling the diurnal mixed layer," *Limnology and Oceanography,* **31**, 533-56.

Staniforth, A. and Côté, J. (1991). "Semi-Lagrangian integration schemes for atmospheric models – a review," Monthly Weather Review, 119:2206-2223.

Stevens, C. and Imberger, J. (1996). "The initial response of a stratified lake to a surface shear stress," Journal of Fluid Mechanics, 312:39-66.

Ullman, W.J. and R.C. Aller (1982), "Diffusion coefficients in nearshore marine sediments," *Limnol. Oceanogr., 27,* 552-556.

Wanninkhof, R. (1992), "Relationship between wind speed and gas exchange over the ocean," *J. Geophys. Res., 97(C5)*, 7373-7382.

Yeates, Peter (2004). "ELCOM in the Venice Lagoon," from CWR Models: Bytes and Nybbles, Autumn 2004, Issue 10, page 2.

7.2 SUPPLEMENTAL REFERENCES

(November 1999), "Course notes, Computational aquatic ecosystem dynamics model, CAEDYM, Special introduction work session," TTF/3/Nov99, Centre for Water Research, University of Western Australia, 51pp.

(January 2000), "Course notes, Estuary & lake computer model, ELCOM, Special introduction training session," TTF/3/JAN2000, Centre for Water Research, University of Western Australia, 21pp+app.

(January 21, 2000) "Instructions for the use of the graphical user interface *modeler* in the configuration & visualization of DYRESM-CAEDYM," Draft version 2, 42pp.

Antenucci, J. and Imberger, J. (1999), "Seasonal development of long internal waves in a strongly stratified lake: Lake Kinneret," *Journal of Geophysical Research* (in preparation).

Antenucci, J. and Imberger, J. (2000), "Observation of high frequency internal waves in a large stratified lake," *5th International Symposium on Stratified Flows, (ISSF5)*, Vancouver, July 2000, **1**, 271-6.

Bailey, M.B. and Hamilton, D.H. (1997), "Wind induced sediment re-suspension: a lake wide model," *Ecological Modeling*, **99**, 217-28.

Burling, M.; Pattiaratchi, C.; and Ivey, G. (1996), "Seasonal dynamics of Shark Bay, Western Australia," *3rd National AMOS Conference*, 5-7 February 1996, University of Tasmania, Hobart, 128.

Chan, C.U.; Hamilton, D.P.; and Robson, B.J. (2001), "Modeling phytoplankton succession and biomass in a seasonal West Australian estuary," *Proceedings, SIL Congress XXVIII* (in press).

Chan, T. and Hamilton, D.P. (2001), "The effect of freshwater flow on the succession and biomass of phytoplankton in a seasonal estuary," *Marine and Freshwater Research* (in press).

De Silva, I.P.D.; Imberger, J.; and Ivey, G.N. (1997), "Localized mixing due to a breaking internal wave ray at a sloping bed," *Journal of Fluid Mechanics*, **350**, 1-27.

Eckert, W.; Imberger, J.; and Saggio, A. (1999), "Biogeochemical evolution in response to physical forcing in the water column of a warm monomictic lake," *Limnology and Oceanography* (submitted).

Gersbach, G.; Pattiaratchi, C.; Pearce, A.; and Ivey, G. (1996), "The summer dynamics of the oceanography of the south-west coast of Australia – The Capes current" *3rd National AMOS Conference*, 5-7 February 1996, University of Tasmania, Hobart, 132.

Hamilton, D.P. (1996), "An ecological model of the Swan River estuary: An integrating tool for diverse ecological and physico-chemical studies," *INTECOL's V International Wetlands Conference 1996 "Wetlands for the Future,"* September 1996, Perth, Australia.

Hamilton, D.P.; Chan, T.; Hodges, B.R.; Robson, B.J.; Bath, A.J.; and Imberger, J. (1999), "Animating the interactions of physical, chemical and biological processes to understand the dynamics of the Swan River Estuary," Combined Australian-New Zealand Limnology Conference, Lake Taupo.

Hamilton, D.P. (2000), "Record summer rainfall induces first recorded major cyanobacterial bloom in the Swan River," *The Environmental Engineer*, **1**(1), 25.

Hamilton, D.; Hodges, B.; Robson, B.; and Kelsey, P. (2000), "Why a freshwater blue-green algal bloom occurred in an estuary: the Microcystis bloom in the Swan River Estuary in 2000," Western Australian Marine Science Conference 2000, Path, Western Australia.

Hamilton, D.P.; Chan, T.; Robb, M.S.; Pattiaratchi, C.B.; Herzfeld, M.; and Hodges, B. (2001), "Physical effects of artificial destratification in the upper Swan River Estuary," *Hydrological Processes*.

Heinz, G.; Imberger, J.; and Schimmele, M. (1990), "Vertical mixing in Überlinger See, western part of Lake Constance," *Aquat. Sci.*, **52**, 256-68.

Herzfeld, M. (1996), "Sea surface temperature and circulation in the Great Australian bight," Ph.D. Thesis, School of Earth Science, Flinders University, South Australia.

Herzfeld, M. and Hamilton, D. (1997), "A computational aquatic ecosystem dynamics model for the Swan River, Western Australia," *MODSIM '97, International Congress on Modeling and Simulation Proceedings*, 8-11 December, 1997, University of Tasmania, Hobart, **2**, 663-8.

Herzfeld, Michael (May 28, 1999), "Computational aquatic ecosystem dynamics model (CAEDYM), An ecological water quality model designed for coupling with

hydrodynamic drivers, Programmer's guide," Centre for Water Research, The University of Western Australia, Nedlands, Australia, 133pp.

Hodges, Ben R. (July 1991), "Pressure-driven flow through an orifice for two stratified, immiscible liquids," M.S. thesis, The George Washington University, School of Engineering and Applied Science.

Hodges, Ben R. (March 1997), "Numerical simulation of nonlinear free-surface waves on a turbulent open-channel flow," Ph.D. dissertation, Stanford University, Dept. of Civil Engineering.

Hodges, Ben R. (June 9, 1998), "Heat budget and thermodynamics at a free surface: Some theory and numerical implementation (revision 1.0c)," Working manuscript, Centre for Water Research, The University of Western Australia, 14pp.

Hodges, Ben R. (1999), "Numerical techniques in CWR-ELCOM," Technical report, Centre for Water Research, The University of Western Australia. (in preparation)

Hodges, Ben R. (2000), "Recirculation and equilibrium displacement of the thermocline in a wind-driven stratified lake," *5th International Symposium on Stratified Flows, (ISSF5)*, Vancouver, July 2000, **1**, 327-30.

Hodges, B.R., Herzfeld, M., and Hamilton, D. (1998), "A computational aquatic ecosystem dynamics model for the Swan River," *EOS Trans. AGU*, **79**(1), Ocean Sciences Meet. Suppl. OS11P-02.

Hodges, B.; Herzfeld, M.; Winters, K.; and Hamilton, D. (1998), "Interactions of a surface gravity waves and a sheared turbulent current," *EOS Trans. AGU*, **79**(1), Ocean Sciences Meet. Suppl. OS53.

Hodges, B.R. and Street, R.L. (1999), "On simulation of turbulent nonlinear free-surface flow," *Journal of Computational Physics*, **151**, 425-57.

Hodges, B.R.; Imberger, J.; Laval, B.; and Appt, J. (2000), "Modeling the hydrodynamics of stratified lakes," *Fourth International conference on HydroInformatics*, Iowa Institute of Hydraulic Research, Iowa City, 23-27 July 2000.

Hodges, B.R. and Imberger, J. (2001), "Simple curvilinear method for numerical methods of open channels," *Journal of Hydraulic Engineering*, **127**(11), 949-58.

Hodges, Ben R. and Street, Robert L. (1996), "Three-dimensional, nonlinear, viscous wave interactions in a sloshing tank," *Proceedings of the Fluid Engineering Summer Meeting 1996*, Vol. **3**, FED-Vol. **238**, ASME, 361-7.

Hodges, Ben R. and Street, Robert L. (1998), "Wave-induced enstrophy and dissipation in a sheared turbulent current," *Proceedings of the Thirteenth Australian fluid Mechanics Conference*, M.C. Thompson and K. Hourigan (eds.), Monash University, Melbourne, Australia, 13-18 December 1998, Vol. **2**, 717-20.

Hodges, B.R., Street, R.L., and Zang, Y. (1996), "A method for simulation of viscous, non-linear, free-surface flows," *Twentieth Symposium on Naval Hydrodynamics*, National Academy Press, 791-809.

Hollan, E. (1998), "Large inflow-driven vortices in Lake Constance," in J. Imberger (ed.), *Physical Processes in Lakes and Oceans. Coastal and Estuarine Studies*, **54,** American Geophysical Union, 123-36.

Hollan, E.; Hamblin, P.F.; and Lehn, H. (1990), "Long-term modeling of stratification in Large Lakes: Application to Lake Constance," in: Tilzer, M.M. and C. Serruya (eds.). *Large Lakes, Ecological Structure and Function***,** Berlin: Springer Verlag, 107-24.

Horn, D.A.; Imberger, J.; and Ivey, G.N. (1999), "Internal solitary waves in lakes – a closure problem for hydrostatic models," *Proceedings of 'Aha Halikoa Hawaiian Winter Workshop*, January 19-22, 1999, University of Hawaii, Manoa.

Horn, D.A.; Imberger, J.; and Ivey, G.N. (1999), "The degeneration of large-scale interfacial gravity waves in lakes," under consideration for publication in *Journal of Fluid Mechanics*.

Horn, D.A.; Imberger, J.; Ivey, G.N.; and Redekopp, L.G. (2000), "A weakly nonlinear model of long internal waves in lakes," *5th International Symposium on Stratified Flows, (ISSF5)*, Vancouver, July 2000, **1**, 331-6.

Imberger, J. (1985), "The diurnal mixed layer," *Limnology and Oceanography*, **30**(4), 737-70.

Imberger, J. (1985), "Thermal characteristics of standing waters: an illustration of dynamic processes," *Hydrobiologia*, **125,** 7-29.

Imberger, J. (1994), "Mixing and transport in a stratified lake," Preprints of *Fourth International Stratified on Flows Symposium*, Grenoble, France, June-July 1994, **3** 1-29.

Imberger, J. (1994), "Transport processes in lakes: a review," in R. Margalef (ed.), *Limnology Now: A Paradigm of Planetary Problems*, Elsevier Science, 99-193.

Imberger, J. (1998), "Flux paths in a stratified lake: A review," in J. Imberger (ed.), *Physical Processes in Lakes and Oceans. Coastal and Estuarine Studies,* **54,** American Geophysical Union, 1-18.

Imberger, J. (1998), "How does the estuary work?" WAERF Community Forum, 25 July 1998, The University of Western Australia.

Imberger, J.; Berman, T; Christian, R.R.; Sherr, E.B.; Whitney, D.E.; Pomeroy, L.R.; Wiegert, R.G.; and Wiebe, W.J. (1983), "The influence of water motion on the distribution and transport of materials in a salt marsh estuary," *Limnology and Oceanography,* **28**, 201-14.

Imberger, J. and Hamblin, P.F. (1982), "Dynamics of lakes, reservoirs, and cooling ponds," *Journal of Fluid Mechanics,* **14**, 153-87.

Imberger, J. and Head, R. (1994), "Measurement of turbulent properties in a natural system," reprinted from *Fundamentals and Advancements in Hydraulic Measurements and Experimentation*.

Imberger, J. and Ivey, G.N. (1991), "On the nature of turbulence in a stratified fluid. Part II: Application to lakes," *Journal of Physical Oceanography,* **21**(5), 659-80.

Imberger, J. and Ivey, G.N. (1993), "Boundary mixing in stratified reservoirs," *Journal of Fluid Mechanics,* **248**, 477-91.

Imberger, J. and Patterson, J.C. (1981), "A dynamic reservoir simulation model – DYRESM: 5," In H.B. Fischer (ed.) *Transport Models for Inland and Coastal Waters,* Academic Press, 310-61.

Imberger, J. and Patterson, J.C. (1990), "Physical limnology," In: *Advances in Applied Mechanics,* **27**, 303-475.

Ivey, G.N. and Corcos, G.M. (1982), "Boundary mixing in a stratified fluid," *Journal of Fluid Mechanics,* **121**, 1-26.

Ivey, G.N. and Imberger, J. (1991), "On the nature of turbulence in a stratified fluid. Part I: The energetics of mixing," *Journal of Physical Oceanography,* **21**(5), 650-8.

Ivey, G.N.; Imberger, J.; and Koseff, J.R. (1998), "Buoyancy fluxes in a stratified fluid," in J. Imberger (ed.), *Physical Processes in Lakes and Oceans. Coastal and Estuarine Studies,* **54,** American Geophysical Union, 377-88.

Ivey, G.N.; Taylor, J.R.; and Coates, M.J. (1995), "Convectively driven mixed layer growth in a rotating, stratified fluid," *Deep-Sea Research I.,* **42**(3), 331-49.

Ivey, G.N.; Winters, K.B; and De Silva; I.P.D. (1998), "Turbulent mixing in an internal wave energized benthic boundary layer on a slope," submitted to *Journal of Fluid Mechanics*.

Jandaghi Alaee, M.; Pattiaratchi, C.; and Ivey, G. (1996), "The three-dimensional structure of an island wake," *8th International Biennial Conference. Physics of Estuaries and coastal Seas (PECS)* 9-11 September 1996, the Netherlands, 177-9.

Javam, A; Teoh, S.G.; Imberger, J.; and Ivey, G.N. (1998), "Two intersecting internal wave rays: a comparison between numerical and laboratory results," in J. Imberger (ed.), *Physical Processes in Lakes and Oceans. Coastal and Estuarine Studies*, **54,** American Geophysical Union, 241-50.

Kurup, R.; Hamilton, D.P.; and Patterson, J.C. (1998), "Modeling the effects of seasonal flow variations on the position of a salt wedge in a microtidal estuary," Estuarine Coastal *and Shelf Science*, **47**(2), 191-208.

Kurup, R.G.; Hamilton, D.P.; and Phillips, R.L. (2000), "Comparison of two 2-dimensional, laterally averaged hydrodynamic model applications to the Swan River Estuary," *Mathematics and Computers in Simulation*, **51**(6), 627-39.

Laval, B.; Hodges, B.R.; and Imberger, J. (2000), "Numerical diffusion in stratified lake," *5th International Symposium on Stratified Flows, (ISSF5)*, Vancouver, July 2000, **1**, 343-8.

Lemckert, C. and Imberger, J. (1995), "Turbulent benthic boundary layers in fresh water lakes," Iutam Symposium on Physical Limnology, Broome, Australia, 409-22.

Maiss, M.; Imberger, J.; and Münnich, K.O. (1994), "Vertical mixing in Überlingersee (Lake Constance) traced by SF6 and heat," *Aquat. Sci.*, **56**(4), 329-47.

Michallet, H. and Ivey, G.N. (1999), "Experiments on mixing due to internal solitary waves breaking on uniform slopes," *Journal of Geophysical Research*, **104**, 13467-78.

Nishri, A; Eckert, W.; Ostrovosky, I.; Geifman, J.; Hadas, O.; Malinsky-Rushansky, N.; Erez, J.; and Imberger, J. (1999), "The physical regime and the respective biogeochemical processes in Lake Kinneret lower water mass," *Limnology and Oceanography*, (in press).

Ogihara, Y.; Zic, K.; Imberger, J.; and Armfield, S. (1996), "A parametric numerical model for lake hydrodynamics," *Ecological Modeling*, **86**, 271-6.

Patterson, J.C; Hamblin, P.F.; and Imberger, J. (1984), "Classification and dynamic simulation of the vertical density structure of lakes," *Limnology and Oceanography*, **29**(4), 845-61.

Pattiaratchi, C.; Backhaus, J.; Abu Shamleh, B.; Jandaghi Alaee, M.; Burling, M.; Gersbach, G.; Pang, D.; and Ranasinghe, R. (1996), "Application of a three-dimensional numerical model for the study of coastal phenomena in south-western Australia," *Proceedings of the Ocean & Atmosphere Pacific International Conference*, Adelaide, October 1995, 282-7.

Riley, G.A., H. Stommel and D.F. Bumpus, "Quantitative ecology of the plankton of the Western North Atlantic," *Bull. Bingham Oceanogr. Coll., 12(3)*, 1-69, 1949.

Robson, B.J.; Hamilton, D.P.; Hodges, B.R.; and Kelsey, P. (2000), "Record summer rainfall induces a freshwater cyanobacterial bloom in the Swan River Estuary," *Australian Limnology Society Annual Congress*, Darwin, 2000.

Saggio, A. and Imberger, J. (1998), "Internal wave weather in a stratified lake," *Limnology and Oceanography*, **43**, 1780-95.

Schladow, S.G. (1993), "Lake destratification by bubble-plume systems: Design methodology," *Journal of Hydraulic Engineering*, **119**(3), 350-69.

Smagorinsky, J. (1963) "General circulation experiments with the primitive equations, ´*Monthly Weather Review, 91*, 99-152.

Spigel, R.H. and Imberger, J. (1980), "The classification of mixed-layer dynamics in lakes of small to medium size," *Journal of Physical Oceanography*, **10**, 1104-21.

Steele, J.H. (1962), "Environmental control of phytosynthesis in the sea," *Limnol. Oceanogr., 7*, 137-150.

Taylor, J.R. (1993), "Turbulence and mixing in the boundary layer generated by shoaling internal waves," *Dynamics of Atmospheres and Oceans*, **19**, 233-58.

Thorpe, S.A. (1995), "Some dynamical effects of the sloping sides of lakes," *IUTAM Symposium on Physical Limnology*, Broome, Australia, 215-30.

Thorpe, S.A. (1998), "Some dynamical effects of internal waves and the sloping sides of lakes," in J. Imberger (ed.), *Physical Processes in Lakes and Oceans. Coastal and Estuarine Studies*, **54,** American Geophysical Union, 441-60.

Thorpe, S.A. and Lemmin, U. (1999), "Internal waves and temperature fronts on slops," *Annales Geophysicae*, **17**(9), 1227-34.

Unlauf, L; Wang, Y.; and Hutter, K. (1999), "Comparing two topography-Following primitive equation models for lake circulation," *Journal of Computational Physics*, **153**, 638-59.

Winter, K.B. and Seim, H.E. (1998), "The role of dissipation and mixing in exchange flow through a contracting channel," submitted to *Journal of Fluid Mechanics*.

Winter, K.B.; Seim, H.E.; and Finnigan, T.D. (1998), "Simulation of non-hydrostatic, density-stratified flow in irregular domains," submitted to *International Journal of Numerical Methods in Fluids*.

Zhu, S. and Imberger, J. (1994) "A three-dimensional numerical model of the response of the Australian North West Shelf to tropical cyclones," in: *J. Austral. Math. Soc. Ser.***, B 36,** 64-100.

APPENDIX B

HISTORICAL RESERVOIR DATA

San Vicente Reservoir

Measured Water Surface Elevations

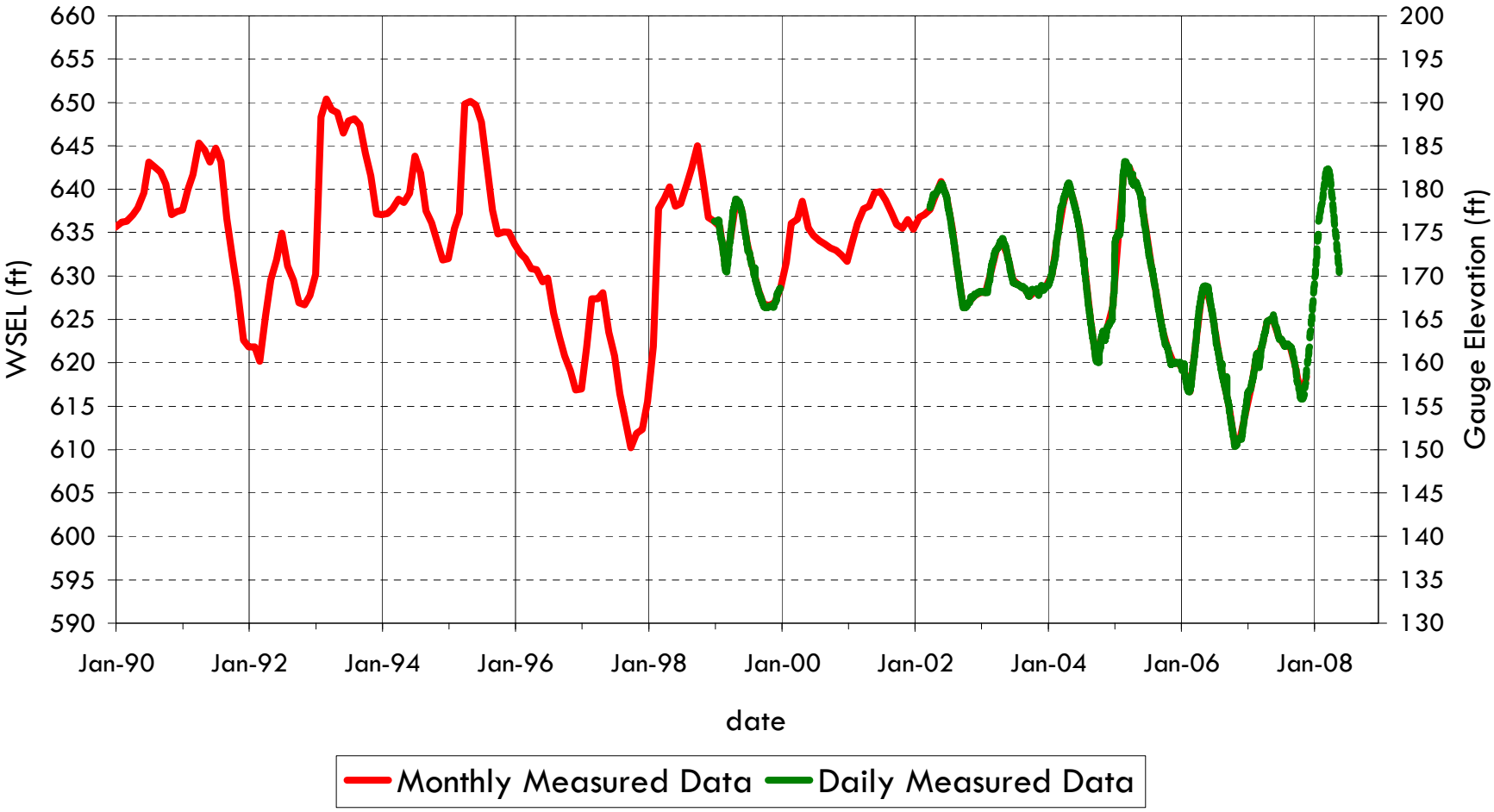

FSI V094005
May 01, 2012

Figure B-1

FLOW SCIENCE®

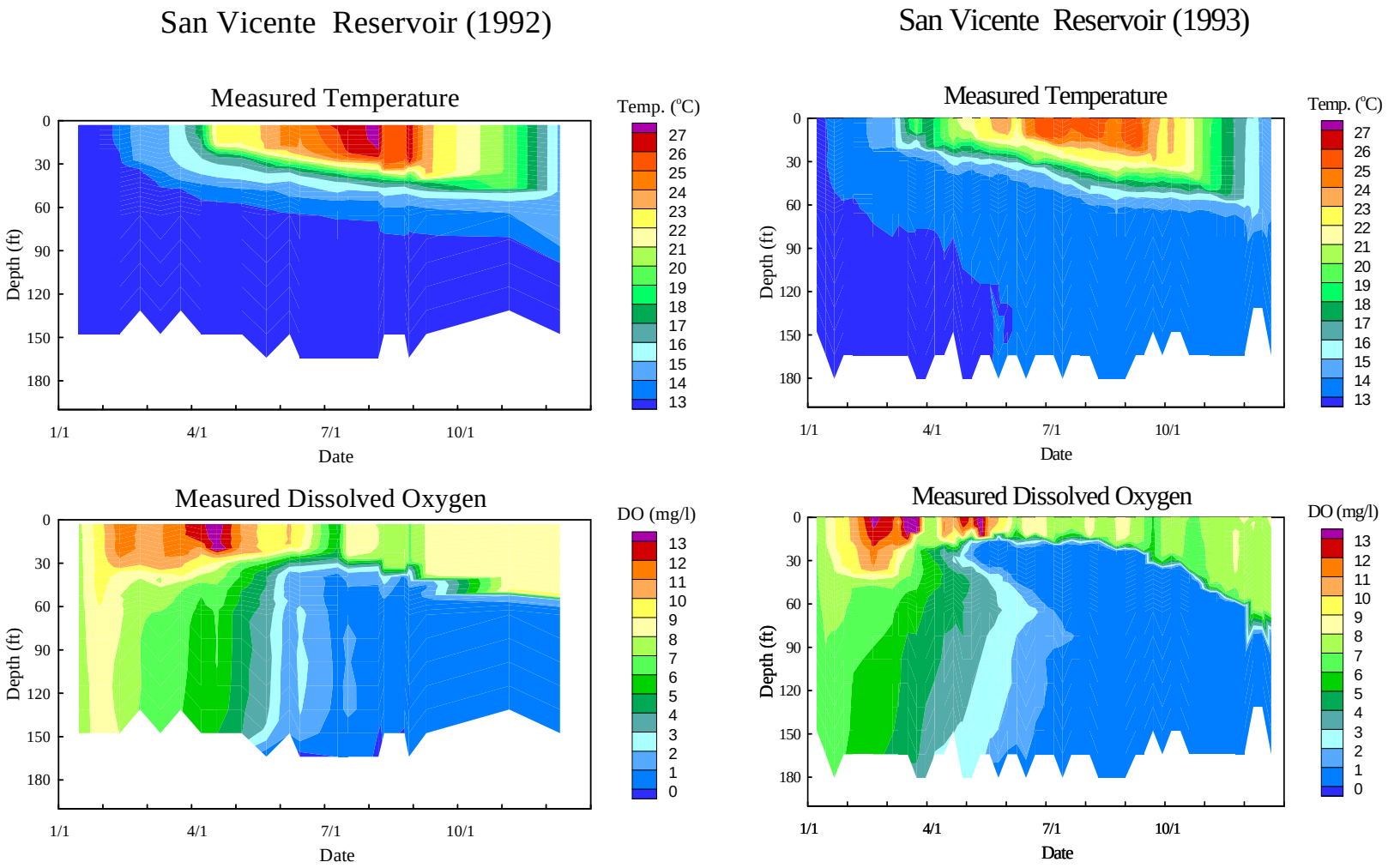

FSI V094005
May 01, 2012

Figure B-2

FLOW SCIENCE®

San Vicente Reservoir (1994)

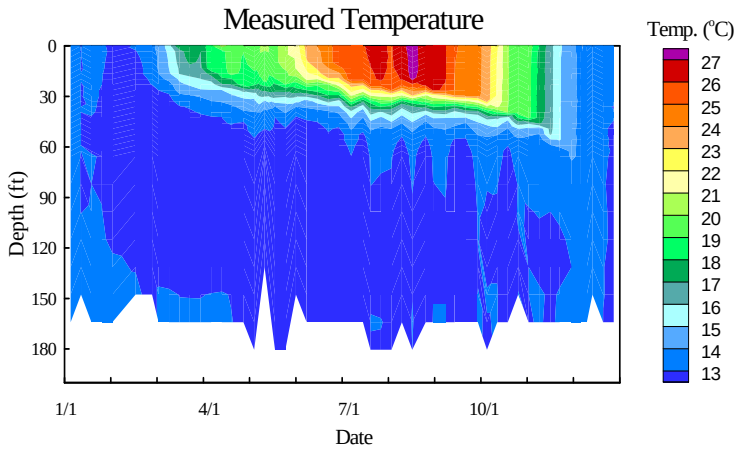

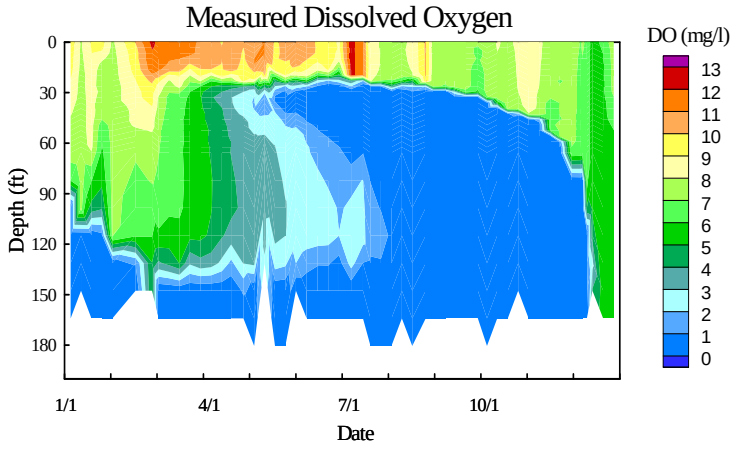

San Vicente Reservoir (1995)

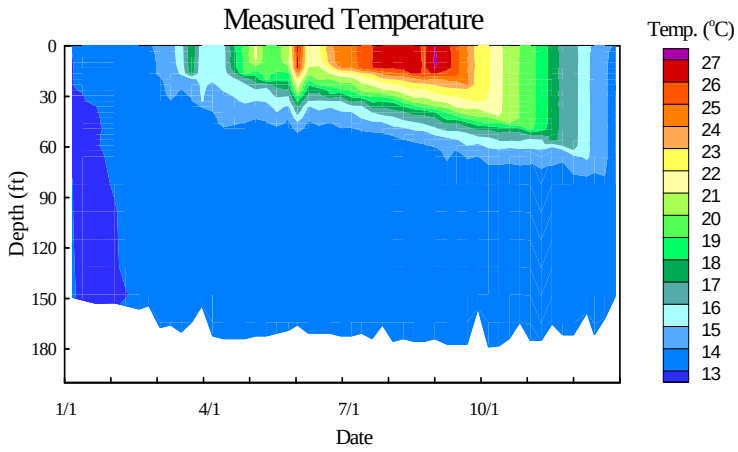

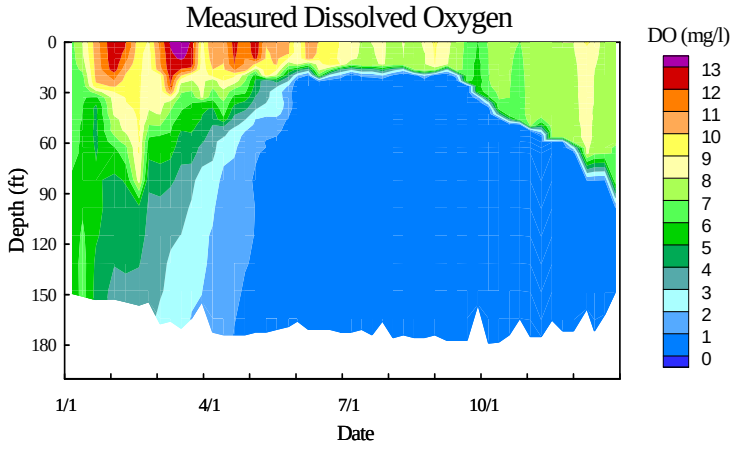

FSI V094005
May 01, 2012

Figure B-3

FLOW SCIENCE®

San Vicente Reservoir (1996)

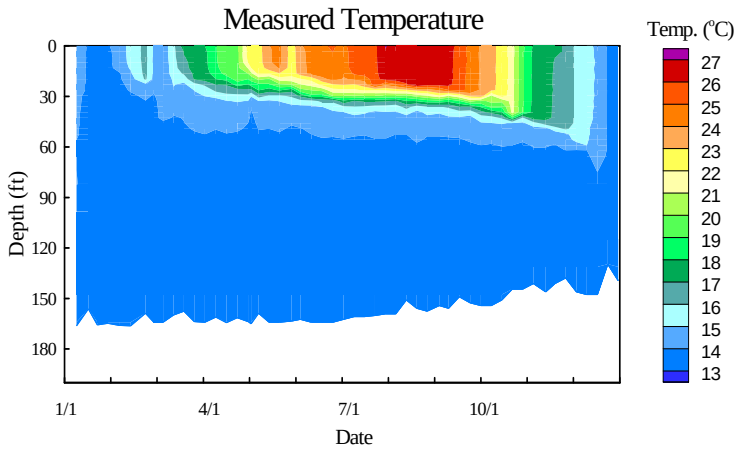

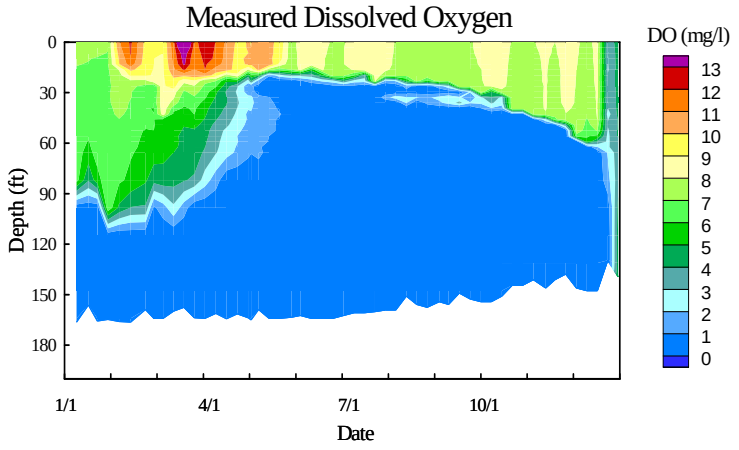

San Vicente Reservoir (1997)

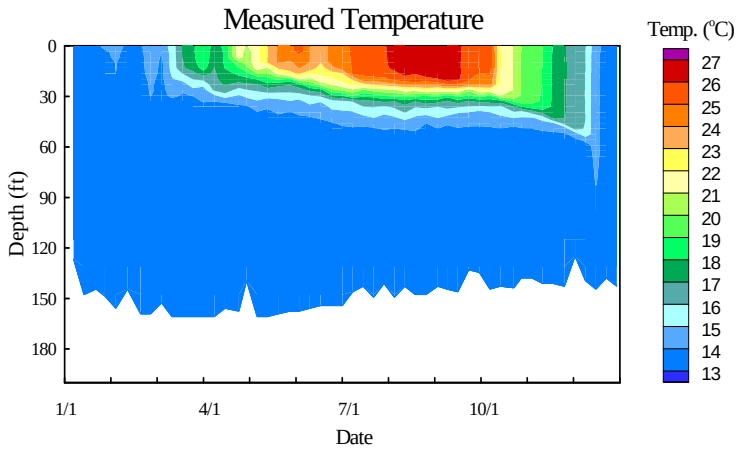

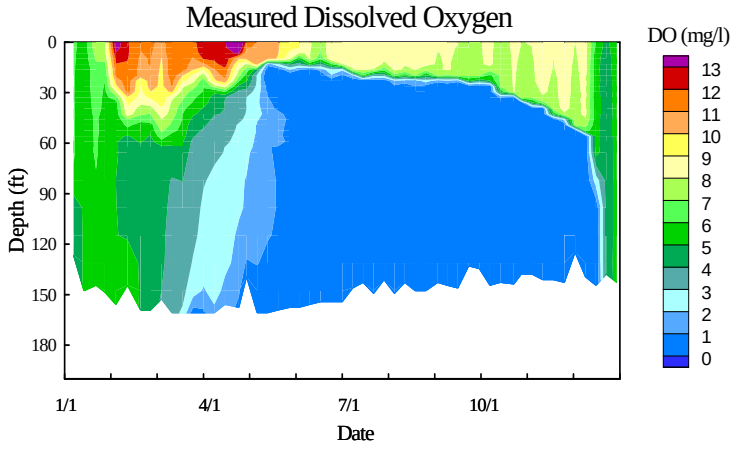

FSI V094005
May 01, 2012

Figure B-4

FLOW SCIENCE®

San Vicente Reservoir (1998)

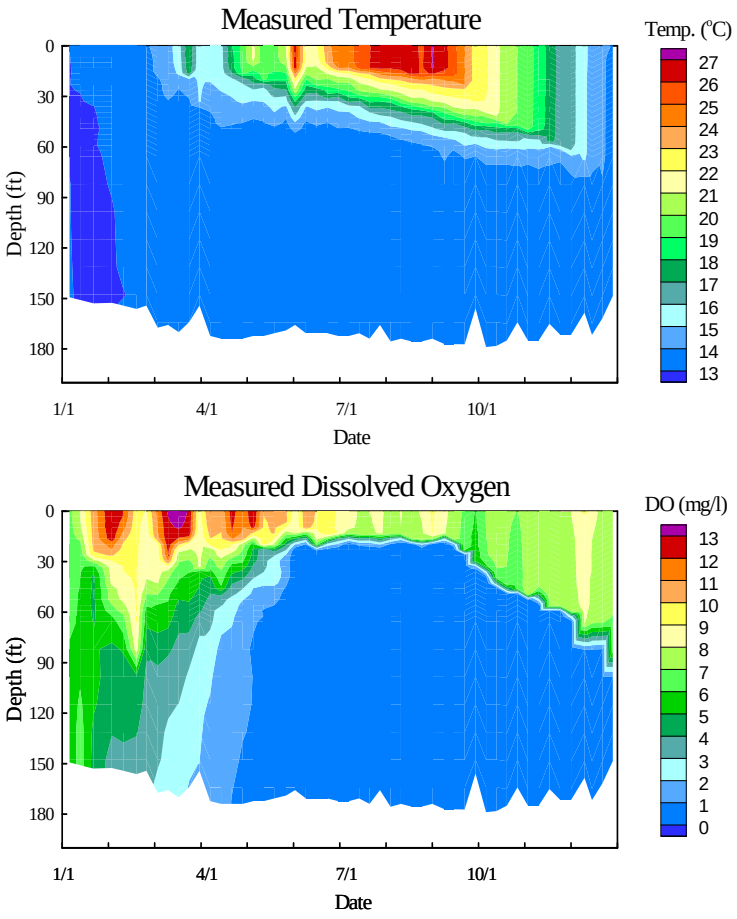

FSI V094005
May 01, 2012

Figure B-5

FLOW SCIENCE®

San Vicente Reservoir (1999)

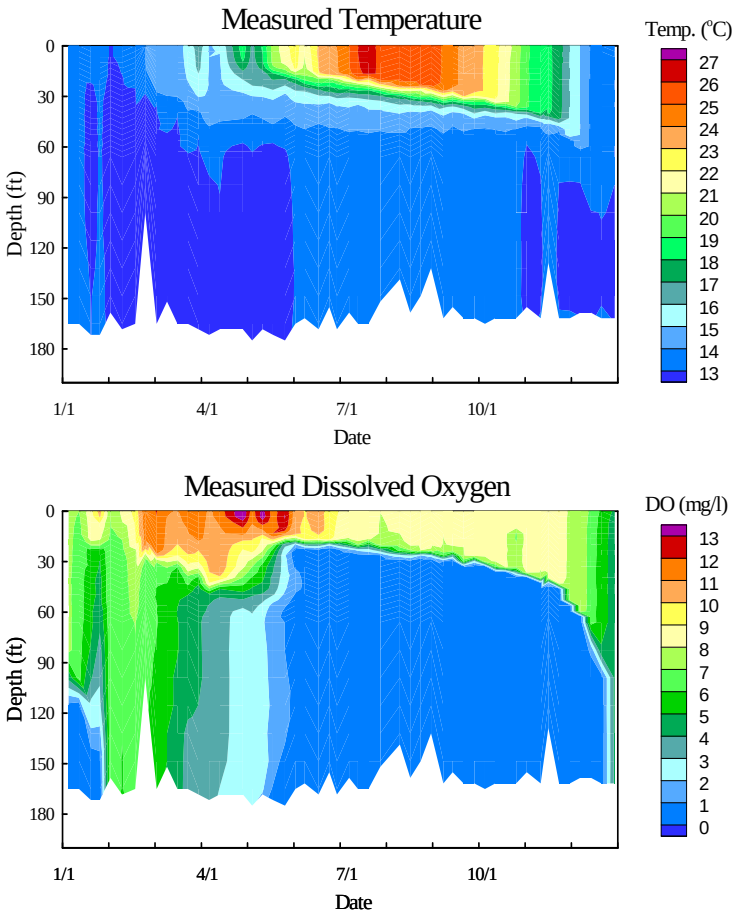

San Vicente Reservoir (1999)

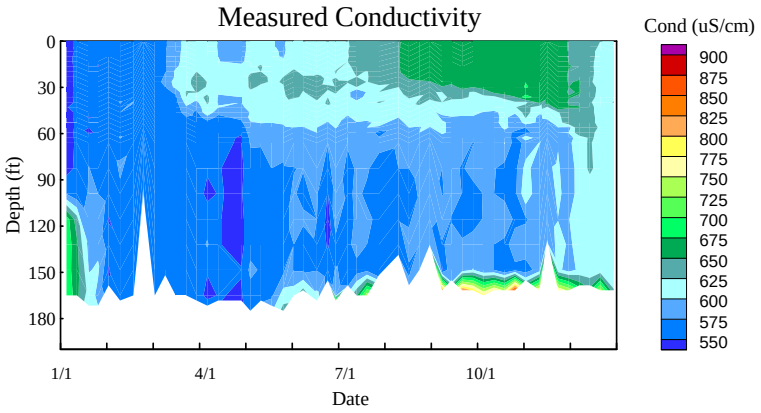

FSI V094005
May 01, 2012

Figure B-6

FLOW SCIENCE®

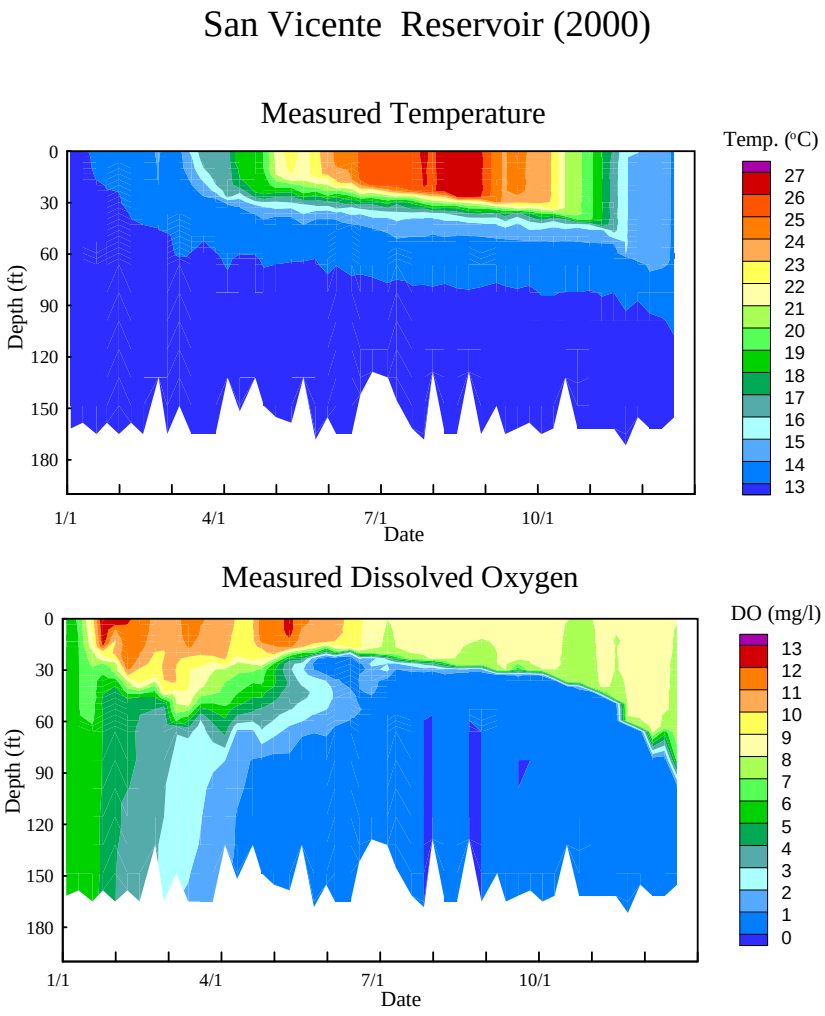

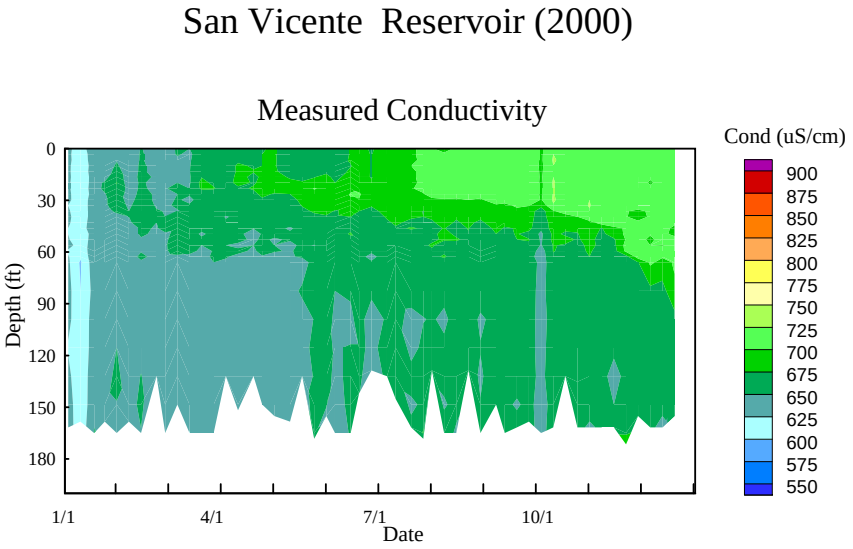

FSI V094005
May 01, 2012

Figure B-7

FLOW SCIENCE®

San Vicente Reservoir (2001)

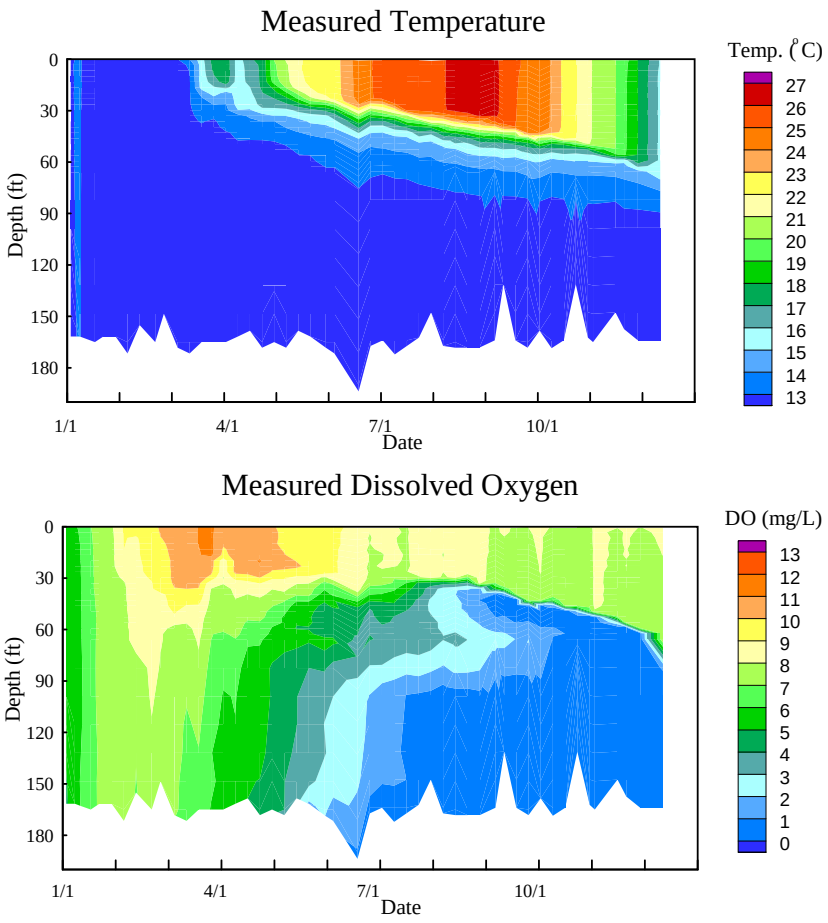

San Vicente Reservoir (2001)

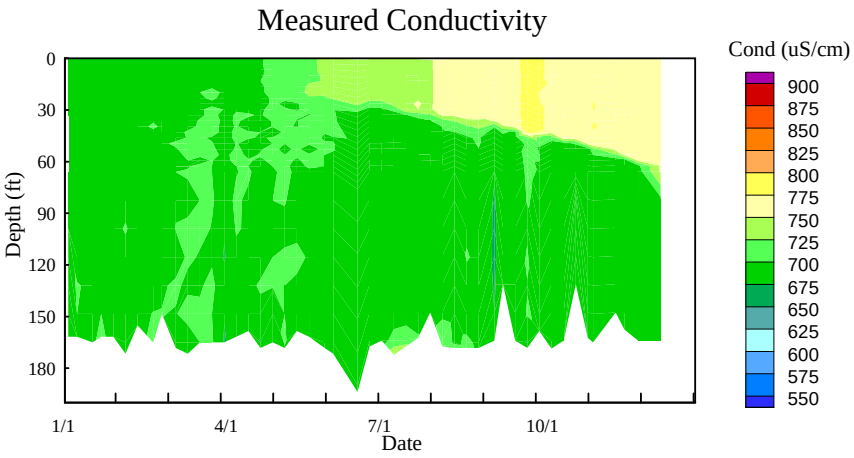

FSI V094005
May 01, 2012

Figure B-8

FLOW SCIENCE®

San Vicente Reservoir (2002)

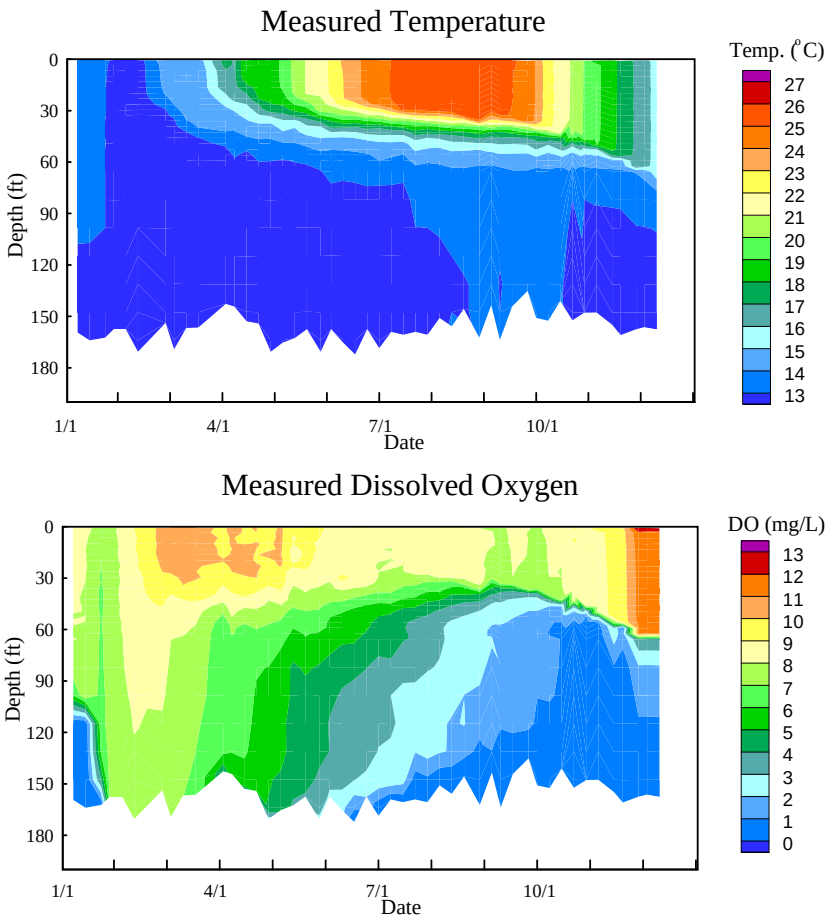

San Vicente Reservoir (2002)

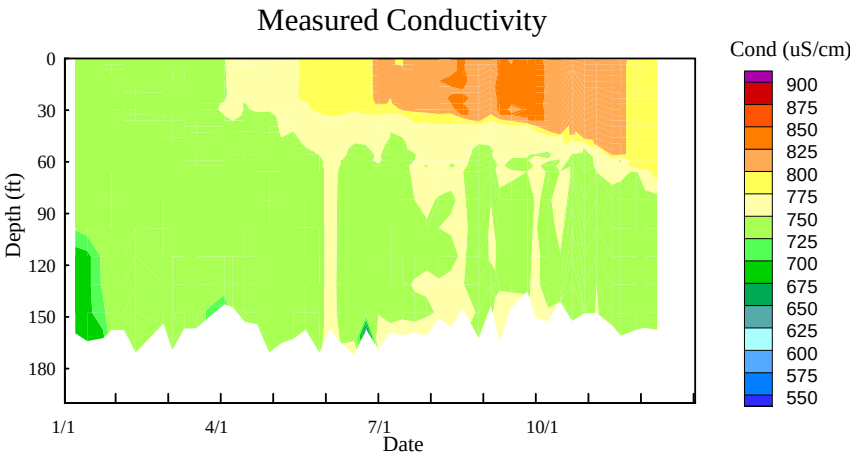

FSI V094005
May 01, 2012

Figure B-9

FLOW SCIENCE®

San Vicente Reservoir (2003)

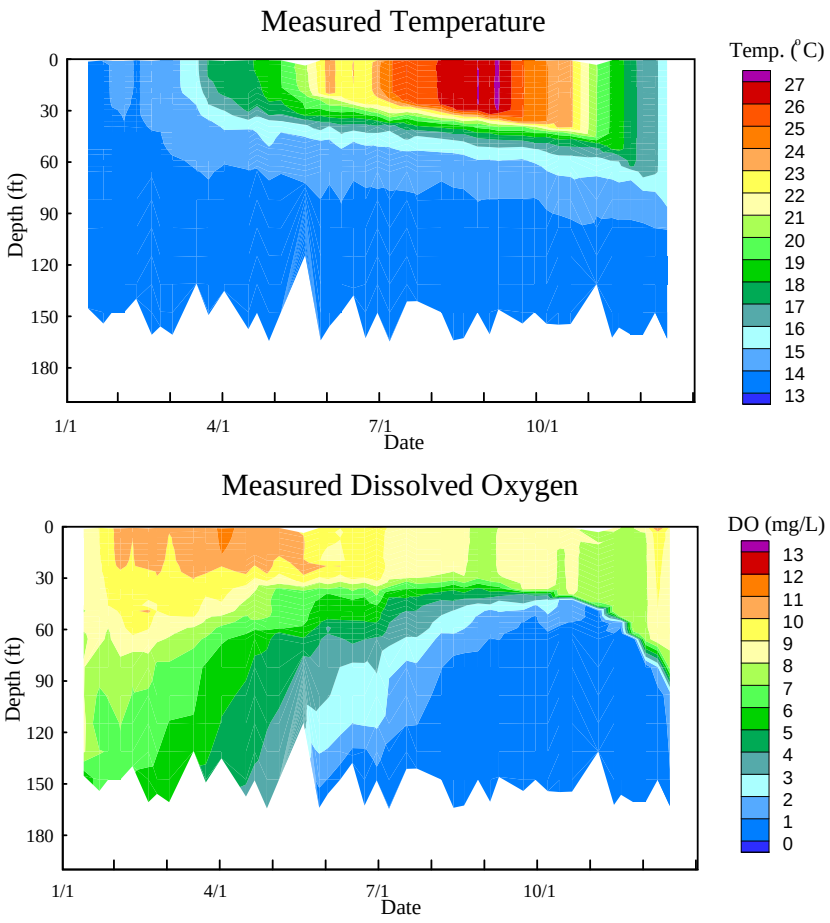

San Vicente Reservoir (2003)

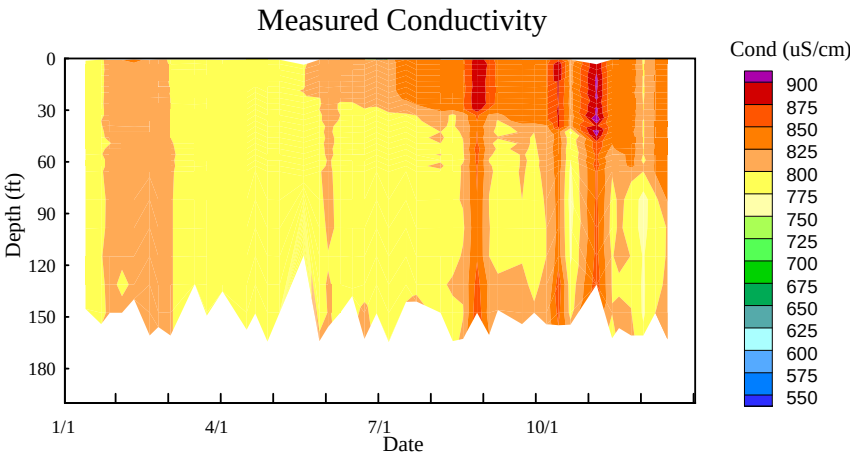

FSI V094005
May 01, 2012

Figure B-10

FLOW SCIENCE®

San Vicente Reservoir (2004)

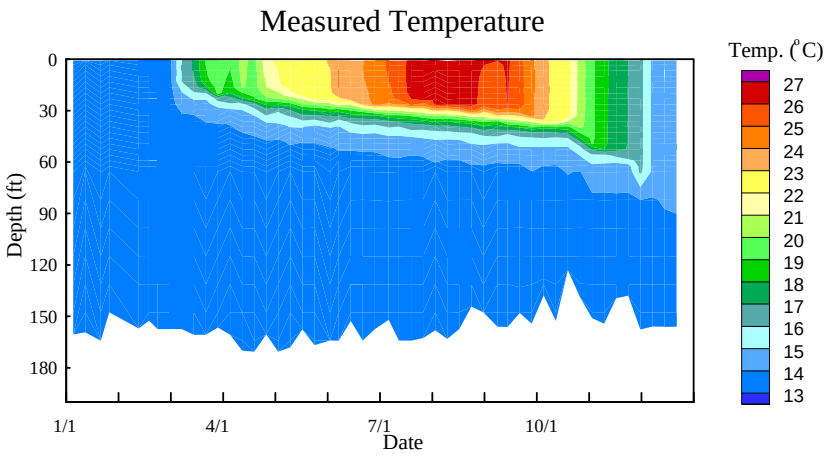

San Vicente Reservoir (2004)

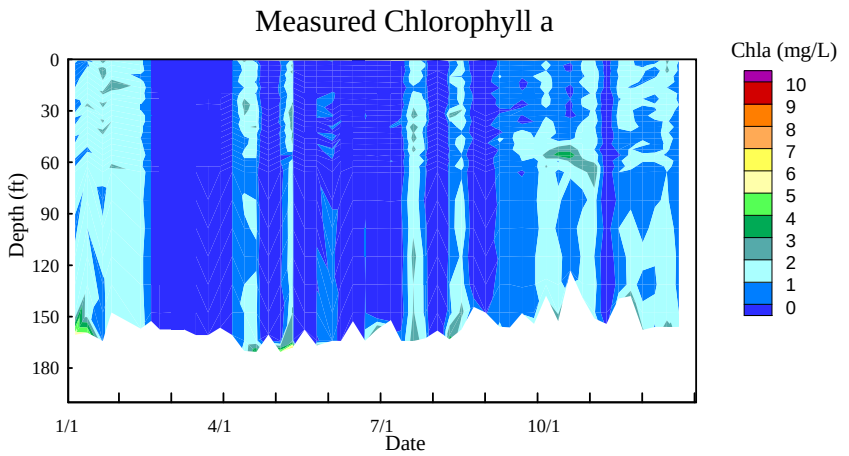

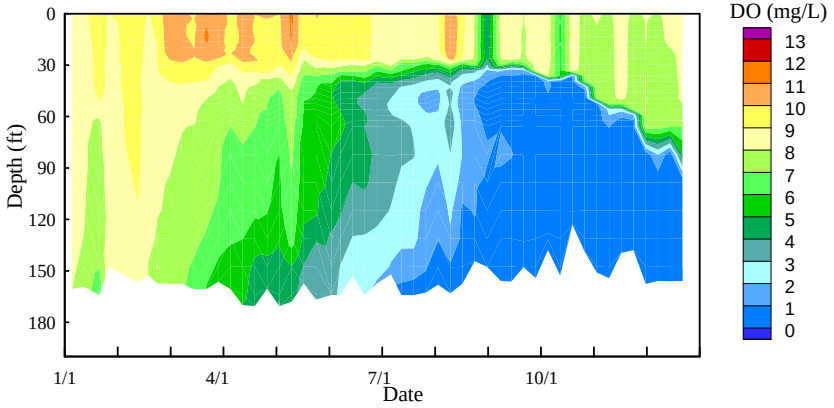

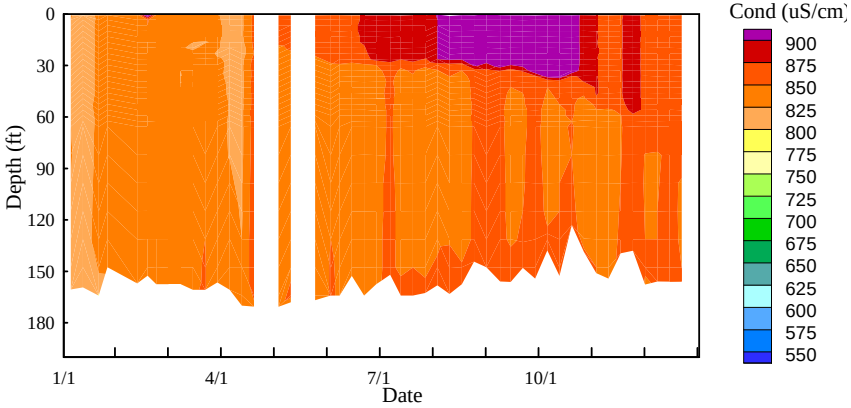

FSI V094005
May 01, 2012

Figure B-11

FLOW SCIENCE®

San Vicente Reservoir (2005)

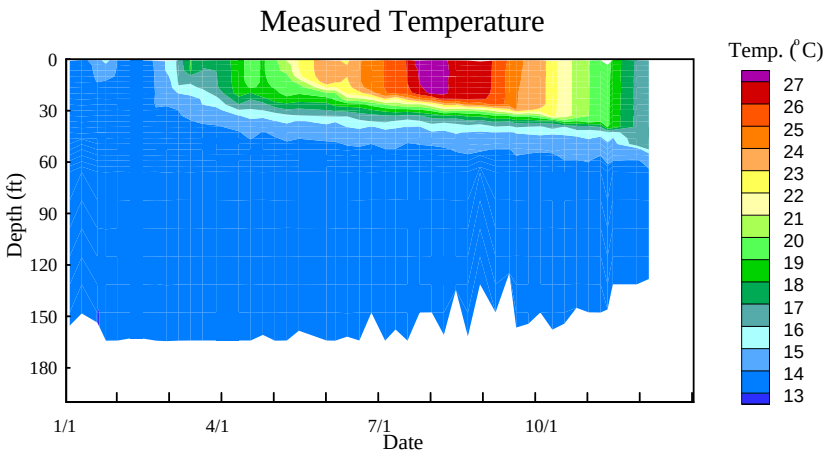

San Vicente Reservoir (2005)

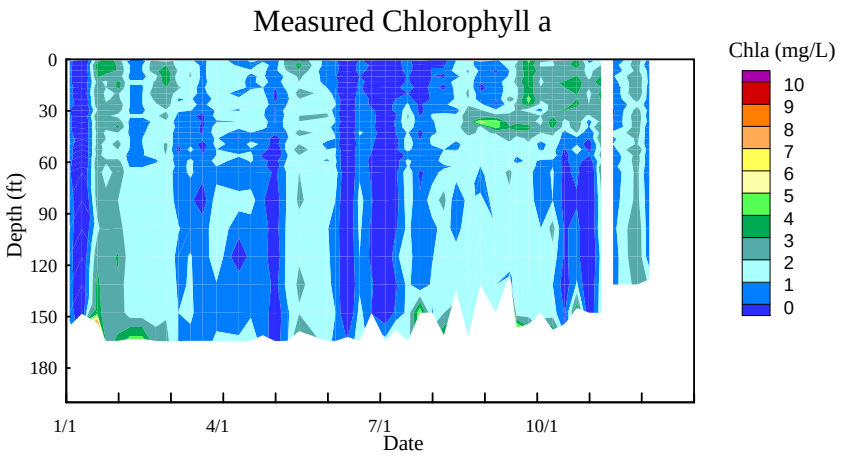

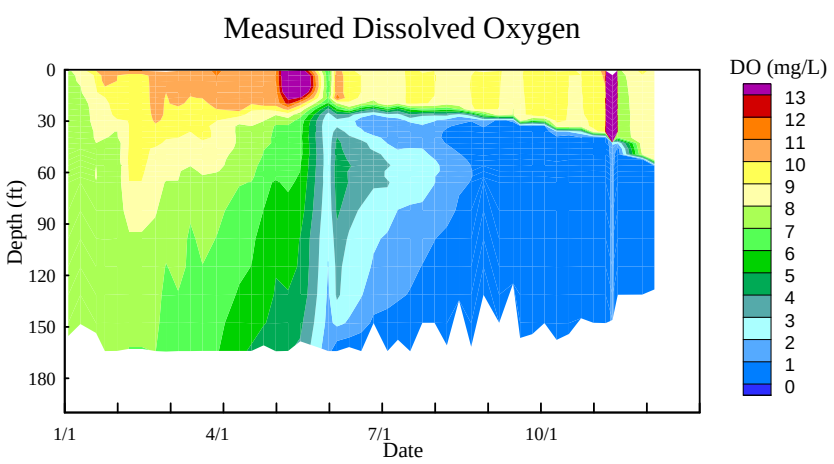

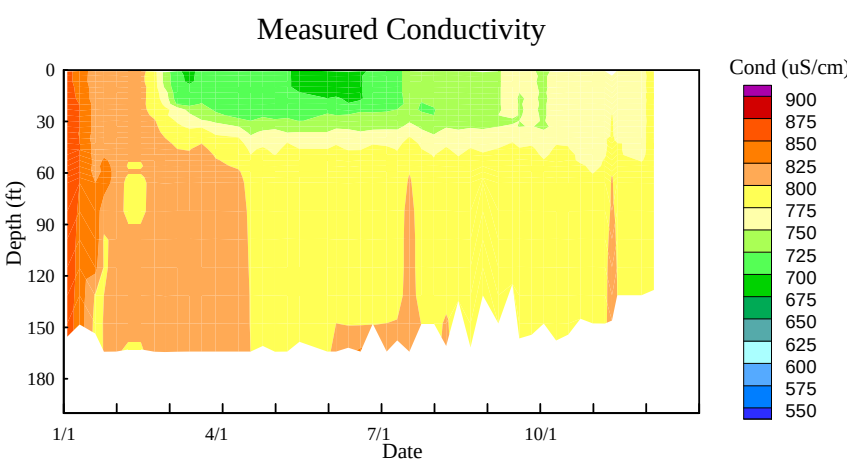

FSI V094005
May 01, 2012

Figure B-12

FLOW SCIENCE®

San Vicente Reservoir (2006)

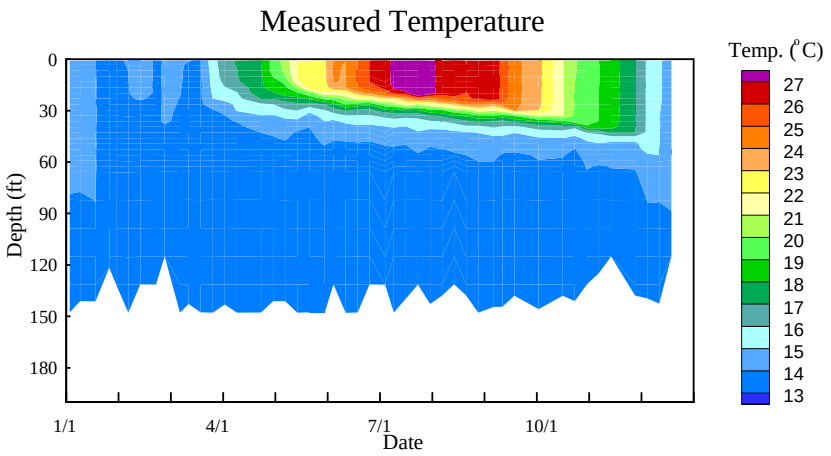

San Vicente Reservoir (2006)

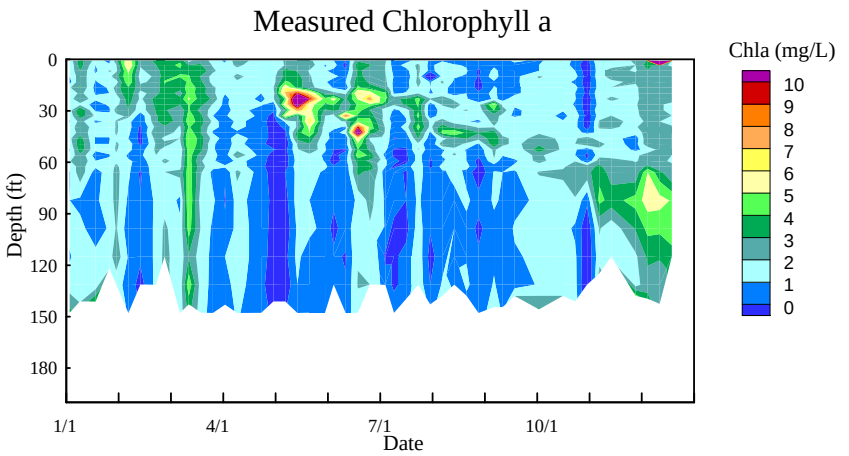

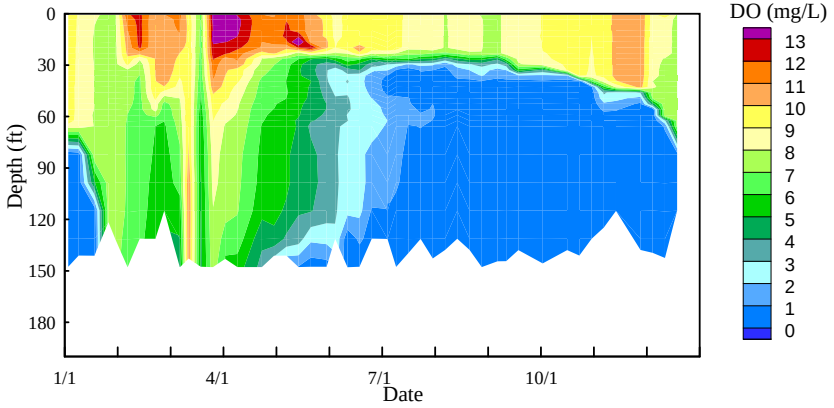

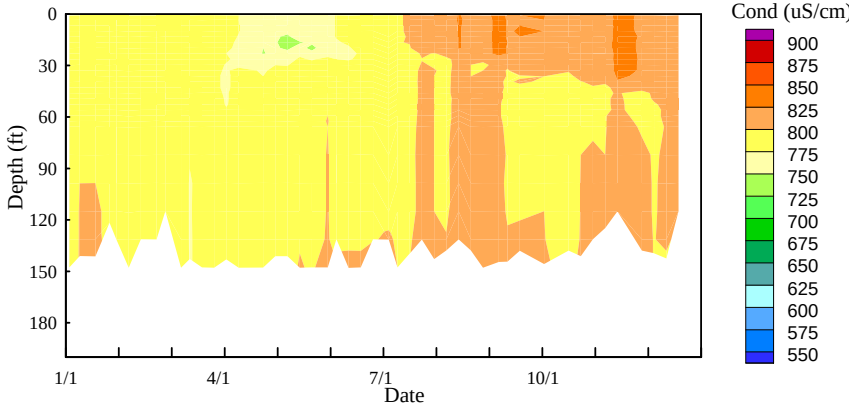

FSI V094005
May 01, 2012

Figure B-13

FLOW SCIENCE®

San Vicente Reservoir (2007)

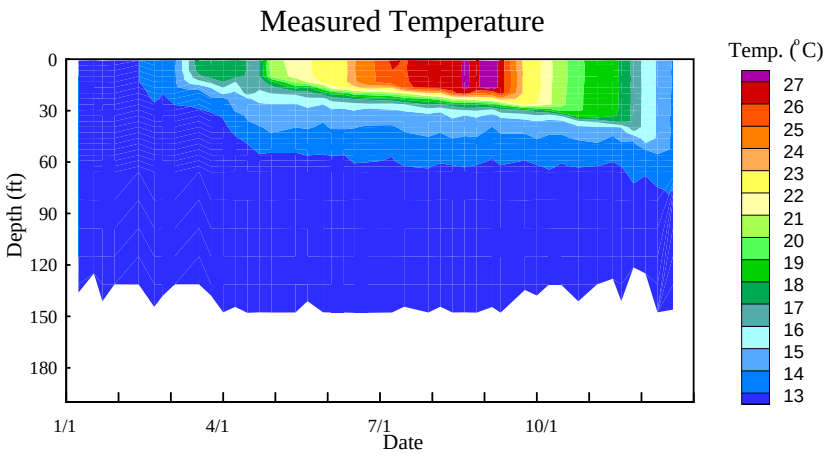

San Vicente Reservoir (2007)

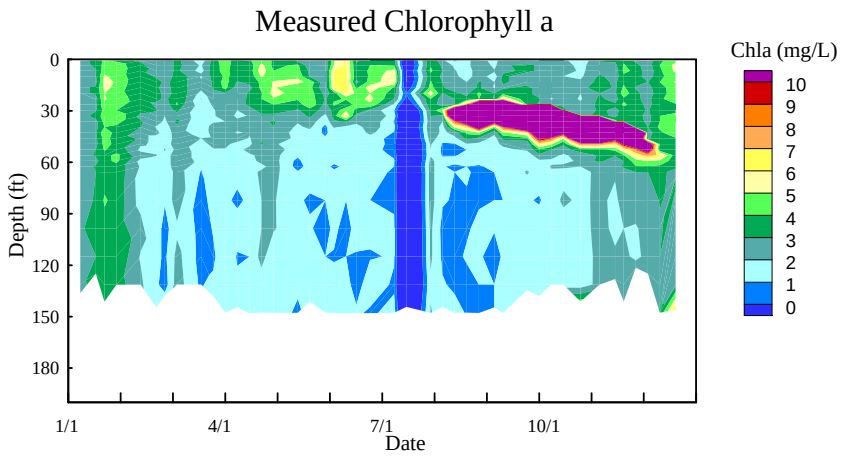

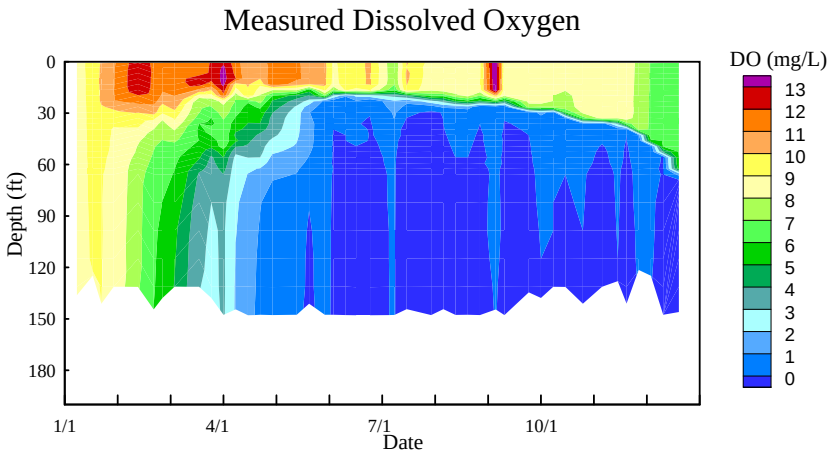

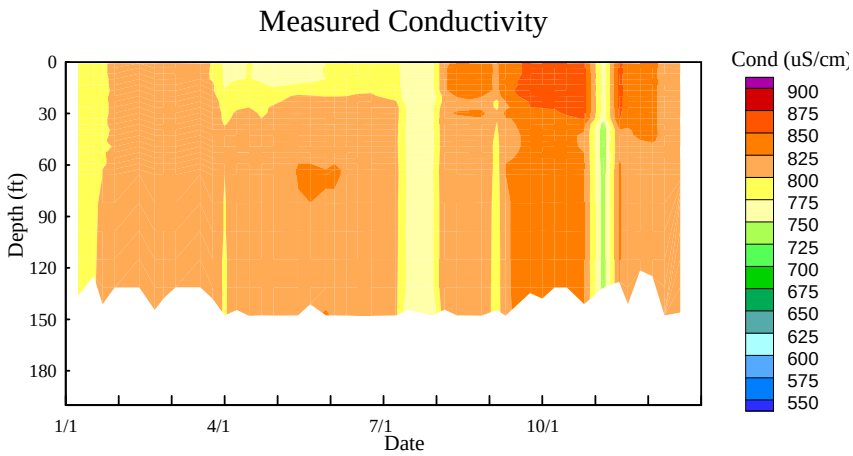

FSI V094005
May 01, 2012

Figure B-14

FLOW SCIENCE®

San Vicente Reservoir (2008)

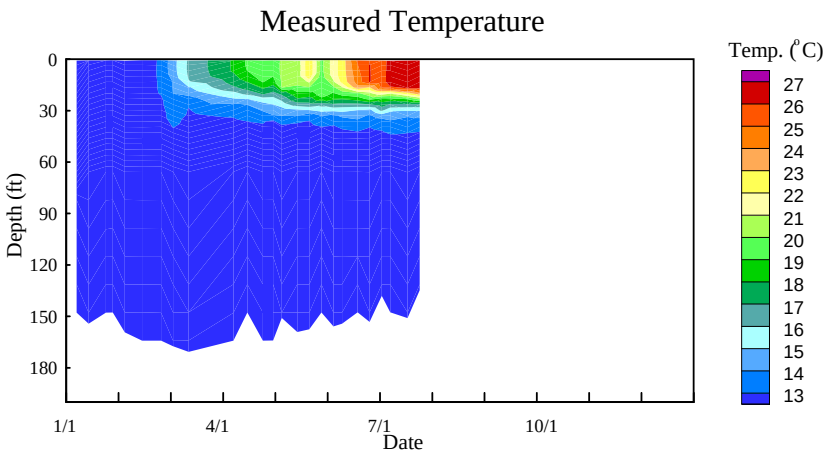

San Vicente Reservoir (2008)

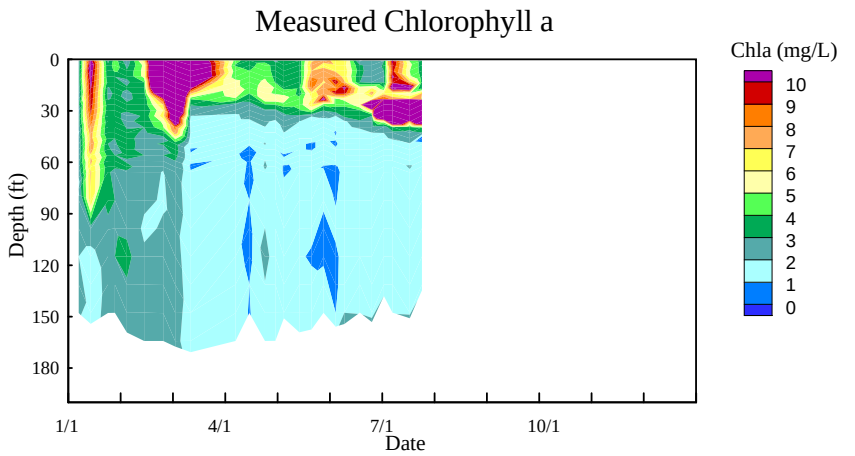

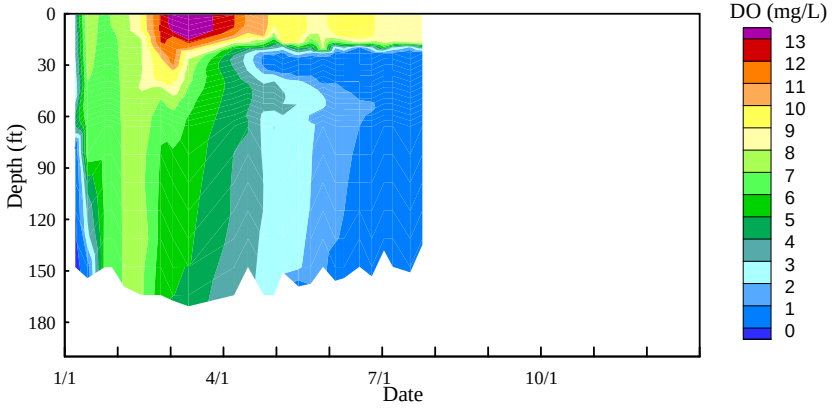

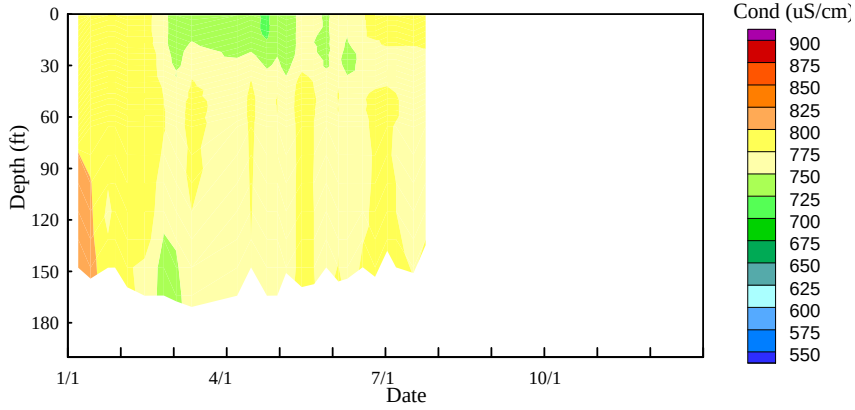

FSI V094005
May 01, 2012

Figure B-15

FLOW SCIENCE®

San Vicente Reservoir

In Reservoir Total Phosphorus Data

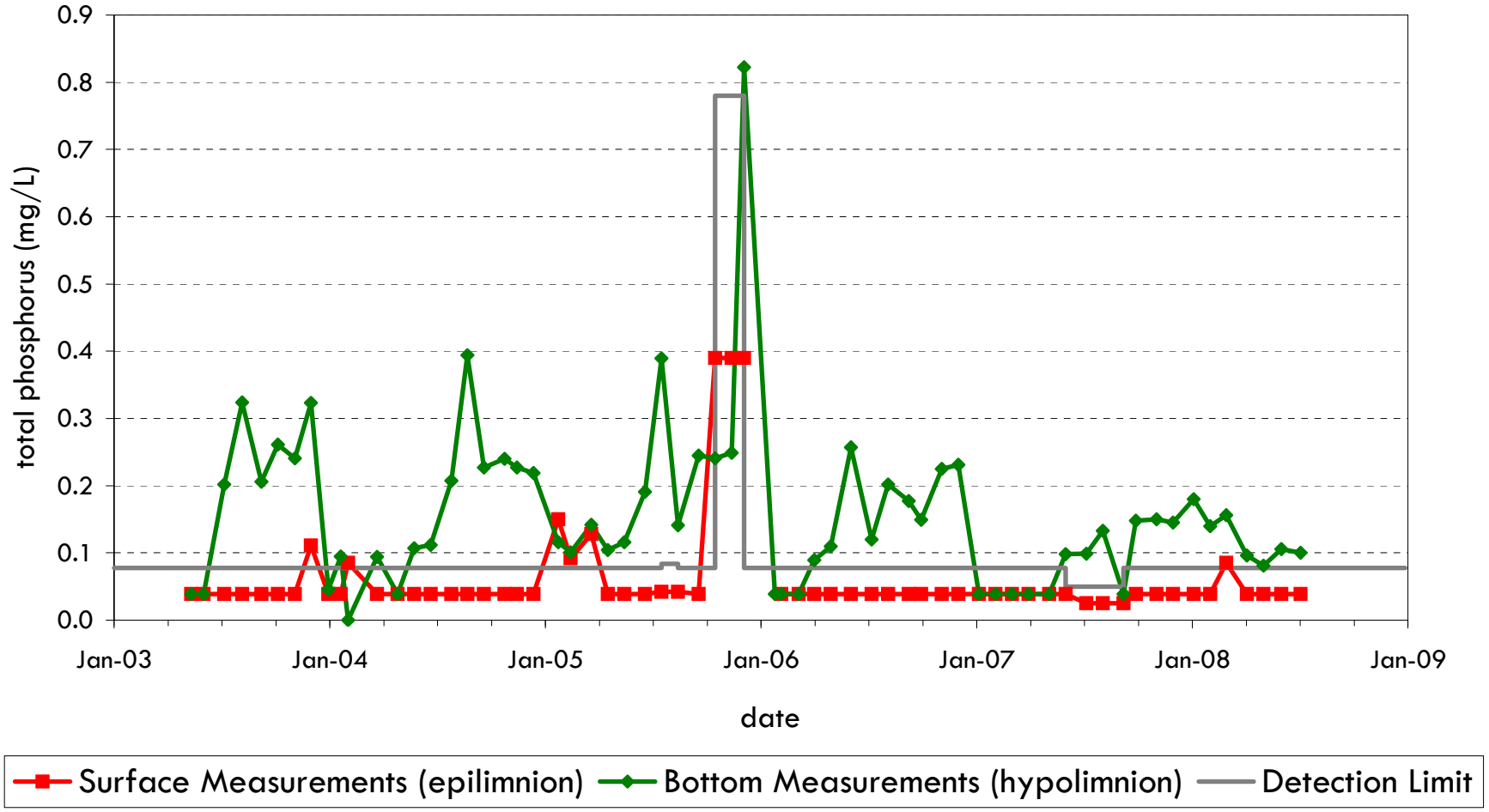

FSI V094005
May 01, 2012

Figure B-16

FLOW SCIENCE®

San Vicente Reservoir

In Reservoir Soluble Reactive Phosphorus Data

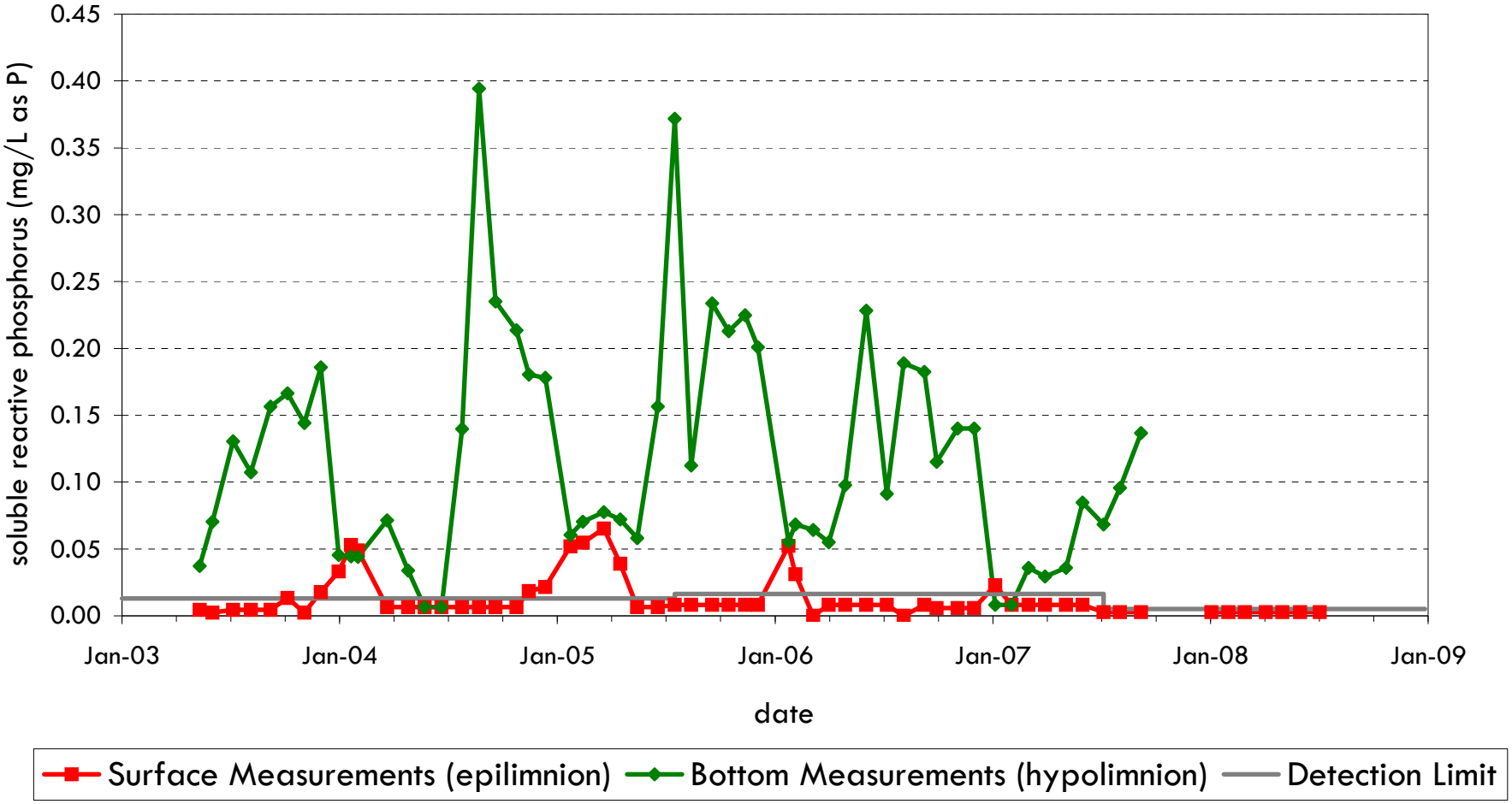

FSI V094005
May 01, 2012

Figure B-17

FLOW SCIENCE®

San Vicente Reservoir

In Reservoir Total Nitrogen Data

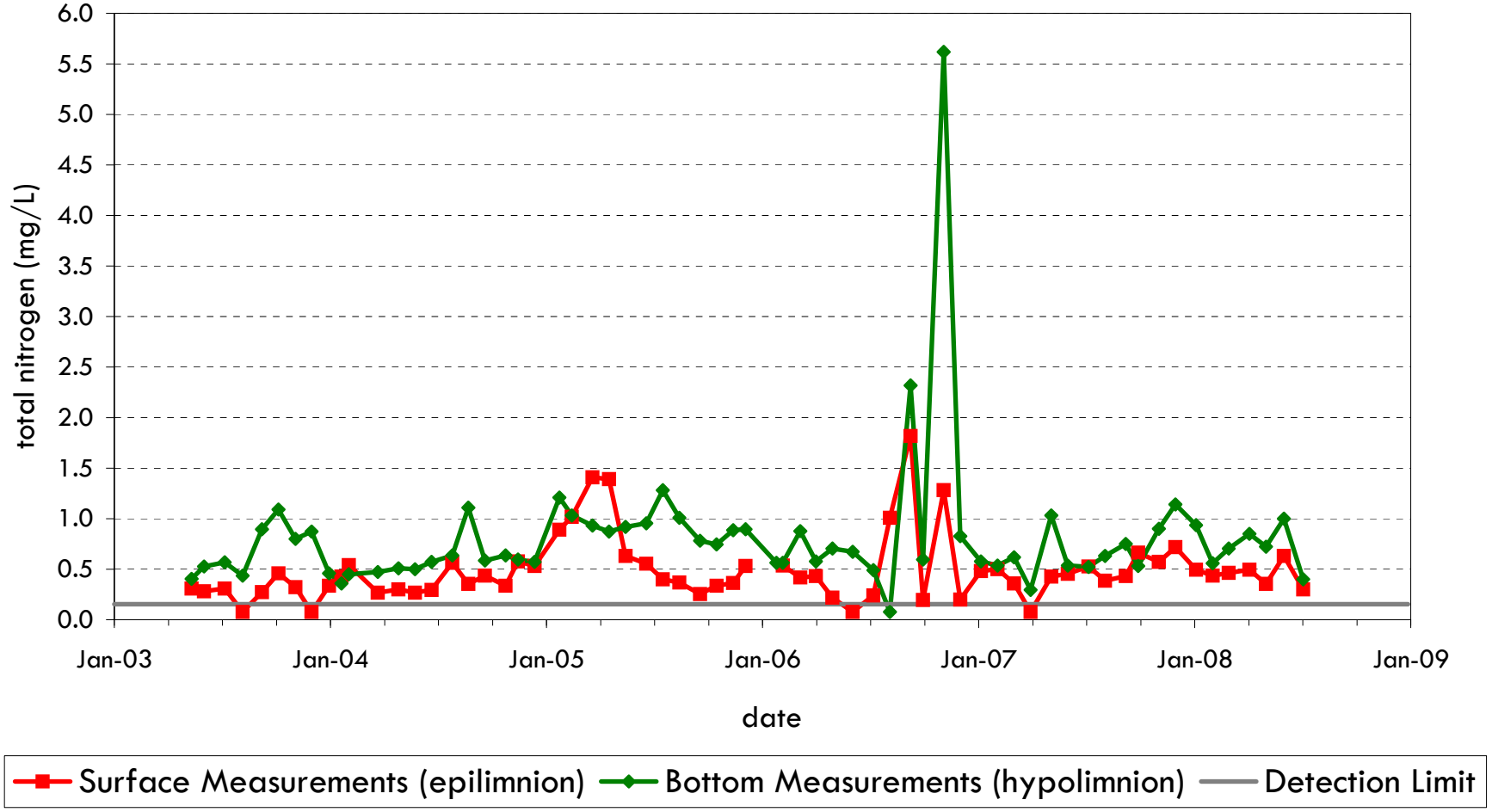

FSI V094005
May 01, 2012

Figure B-18

FLOW SCIENCE®

San Vicente Reservoir

In Reservoir Nitrate Data

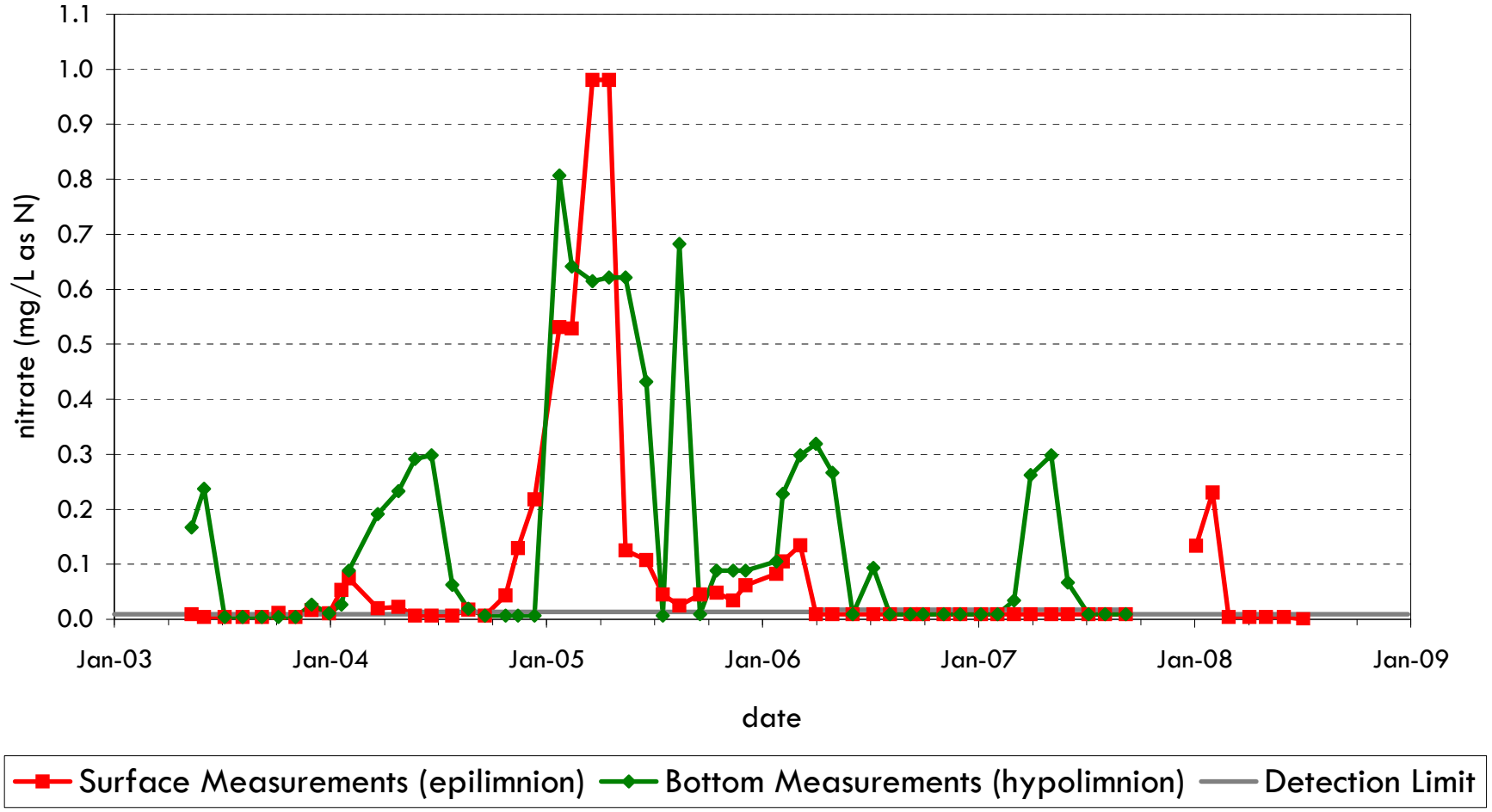

FSI V094005
May 01, 2012

Figure B-19

FLOW SCIENCE®

San Vicente Reservoir

In Reservoir Ammonia Data

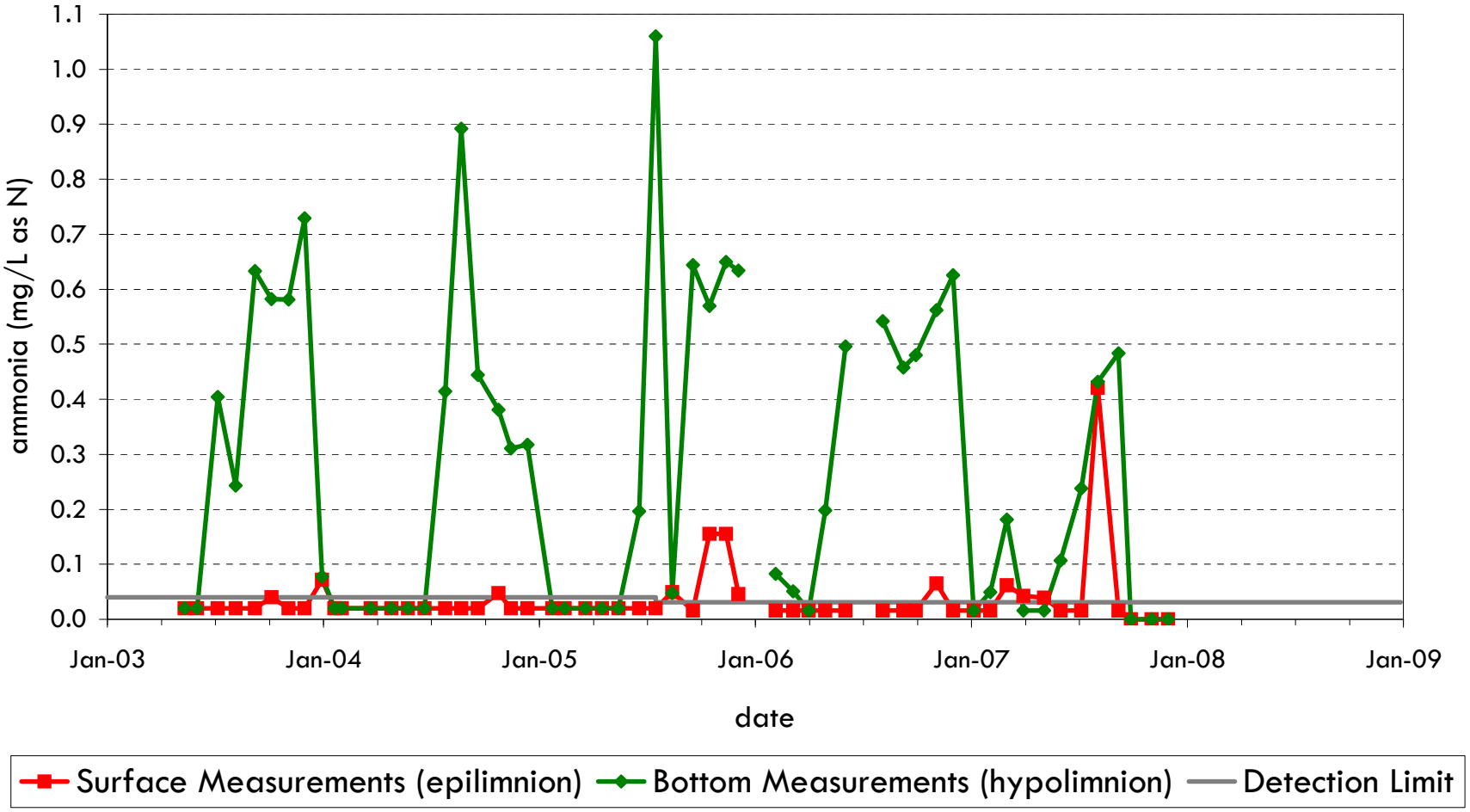

FSI V094005
May 01, 2012

Figure B-20

FLOW SCIENCE®

San Vicente Reservoir

In Reservoir Chlorophyll a Data

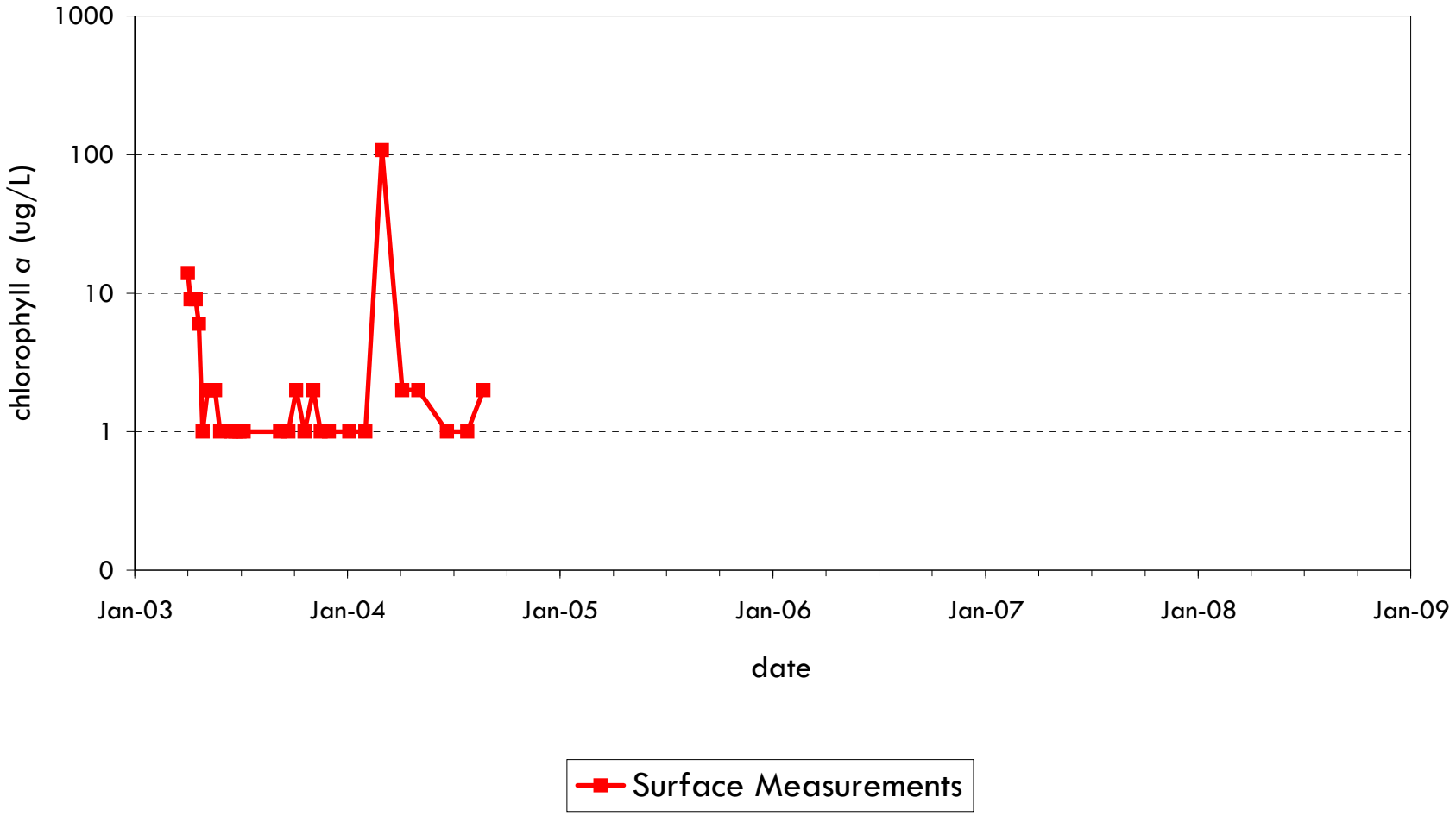

FSI V094005
May 01, 2012

Figure B-21

FLOW SCIENCE®

San Vicente Reservoir

In Reservoir Transparency Data

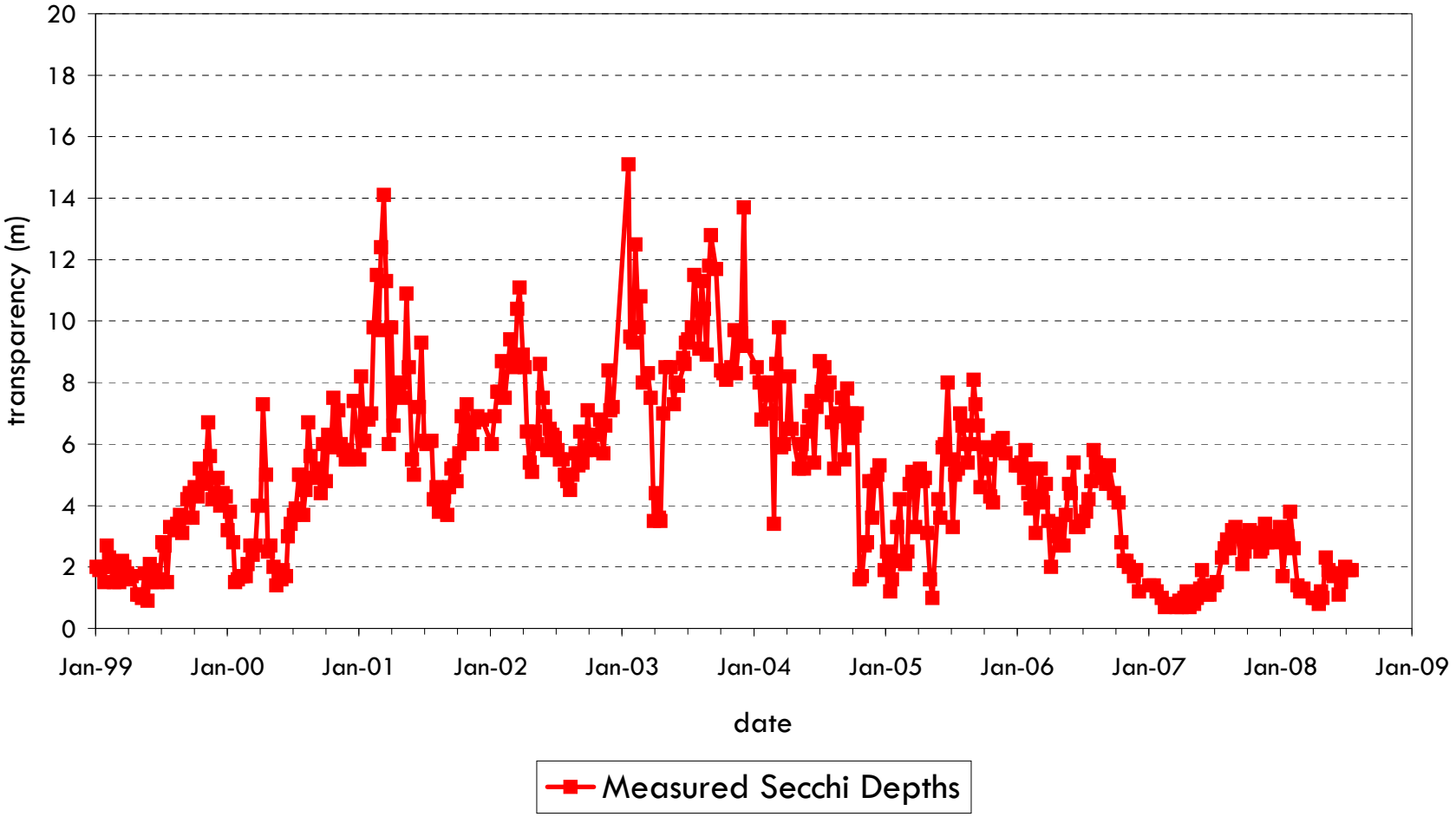

FSI V094005
May 01, 2012

Figure B-22

FLOW SCIENCE®

APPENDIX C

INPUTS FOR CALIBRATION
CALIBRATION/VALIDATION RESULTS

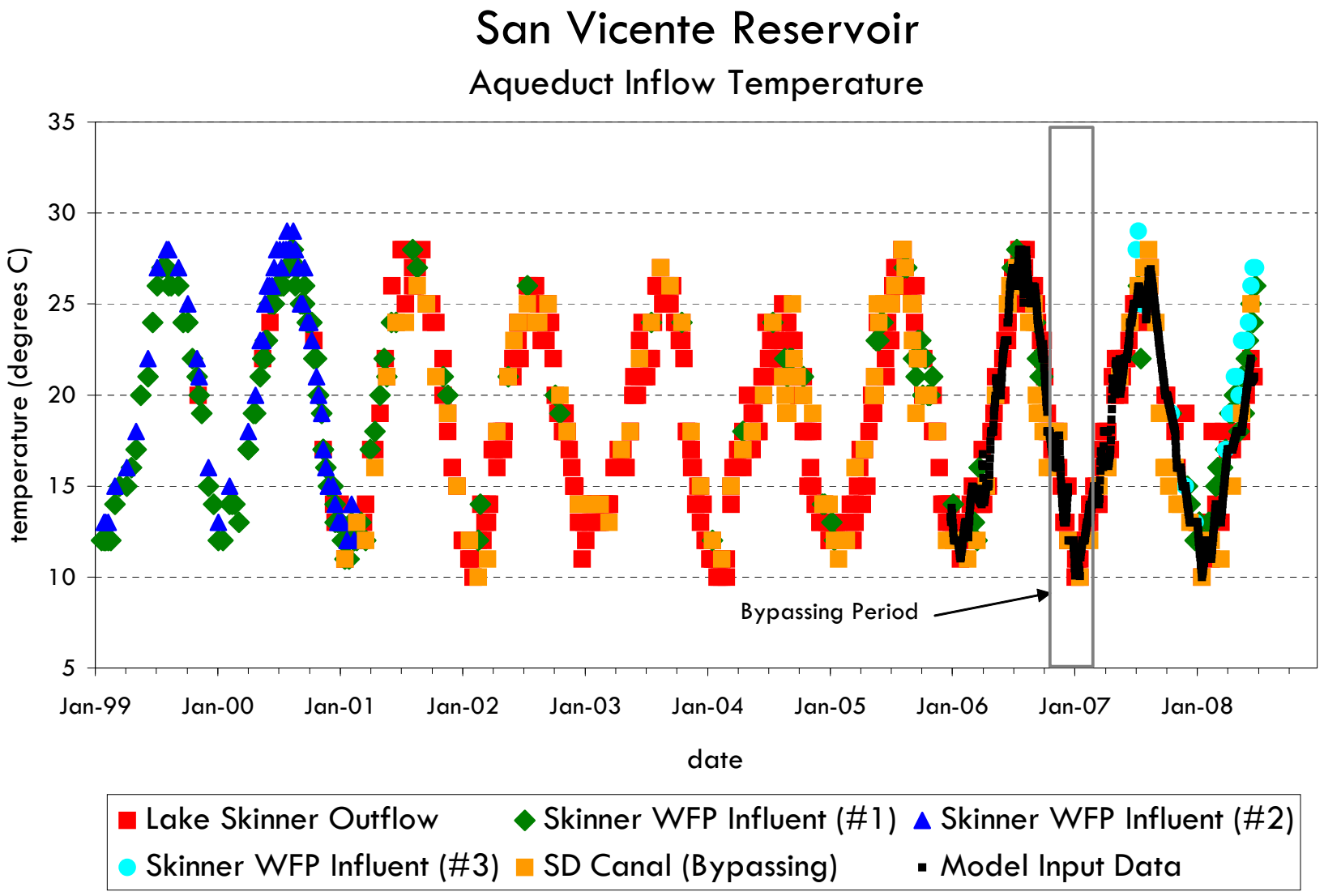

FSI V094005
May 01, 2012

Figure C-1

FLOW SCIENCE®

San Vicente Reservoir

Aqueduct Inflow Salinity/TDS

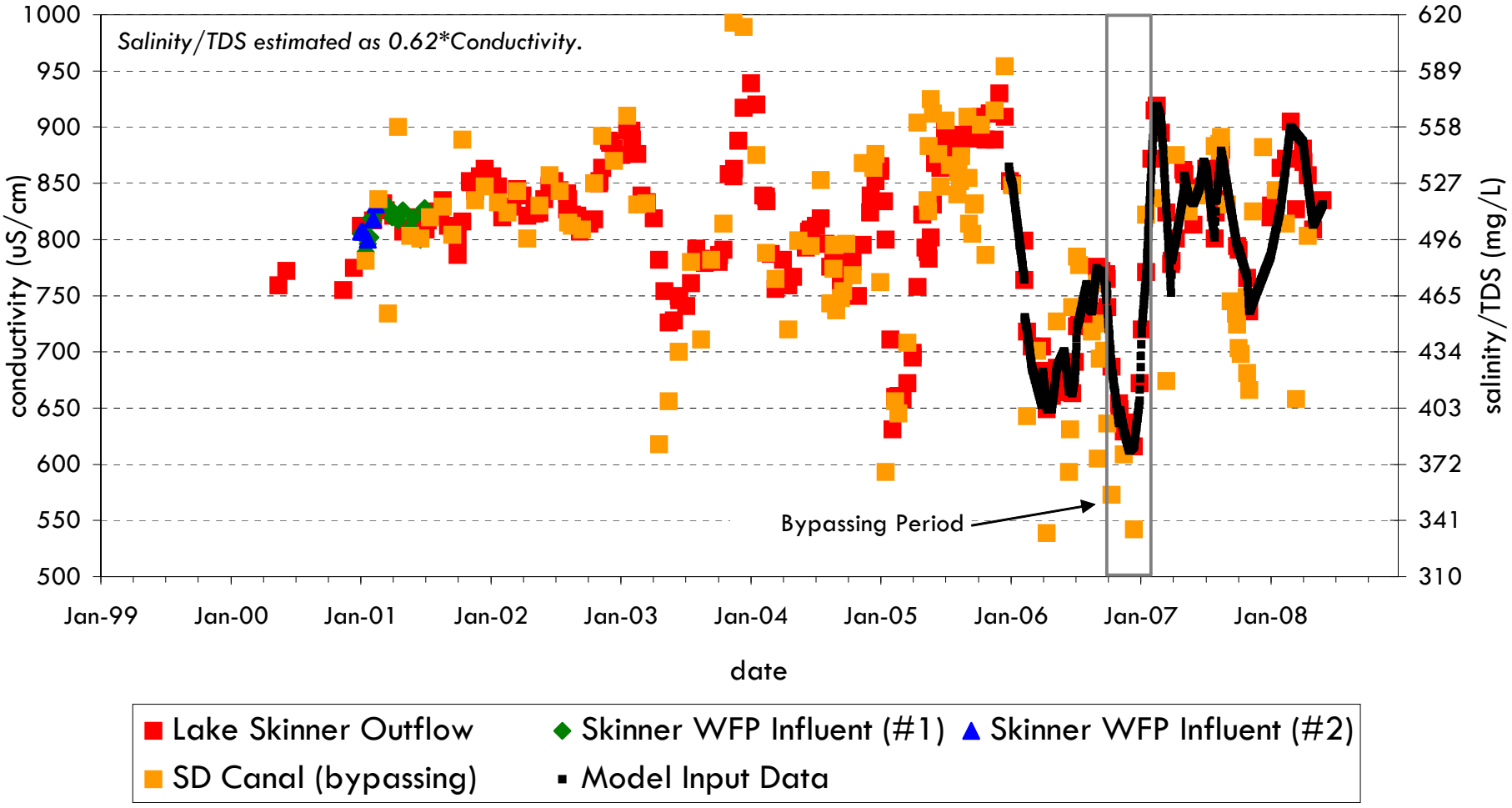

FSI V094005
May 01, 2012

Figure C-2

FLOW SCIENCE®

San Vicente Reservoir

Runoff Inflow Temperature

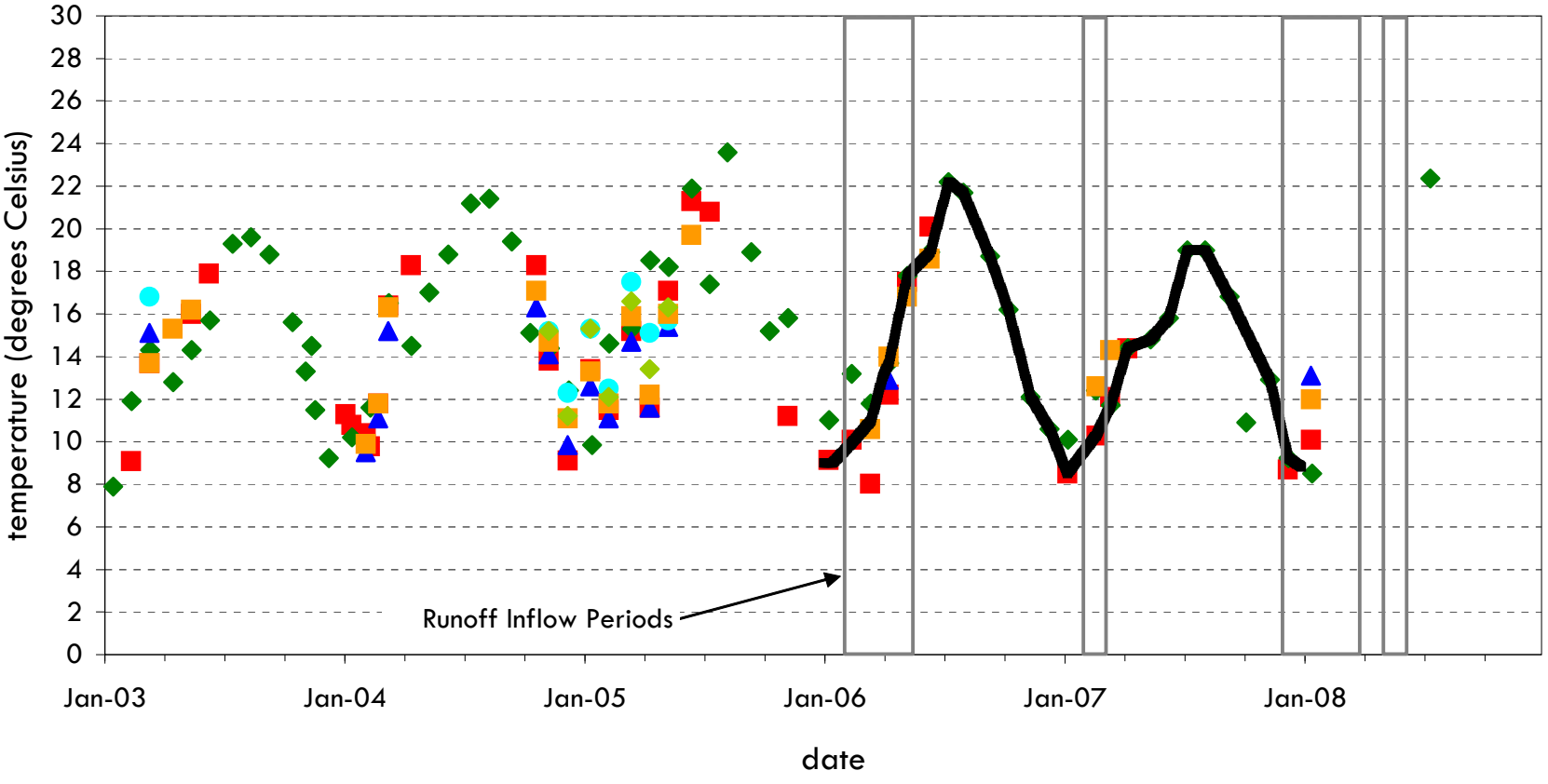

SV Creek (Blw Confluence) ◆ SV Creek (Abv Confluence) ▲ Barona Creek ● Aqueduct Creek

■ Kimball Creek ◆ Tool Road Creek ▪ Model Input Data

FSI V094005
May 01, 2012

Figure C-3

FLOW SCIENCE®

San Vicente Reservoir

Runoff Inflow Salinity/TDS

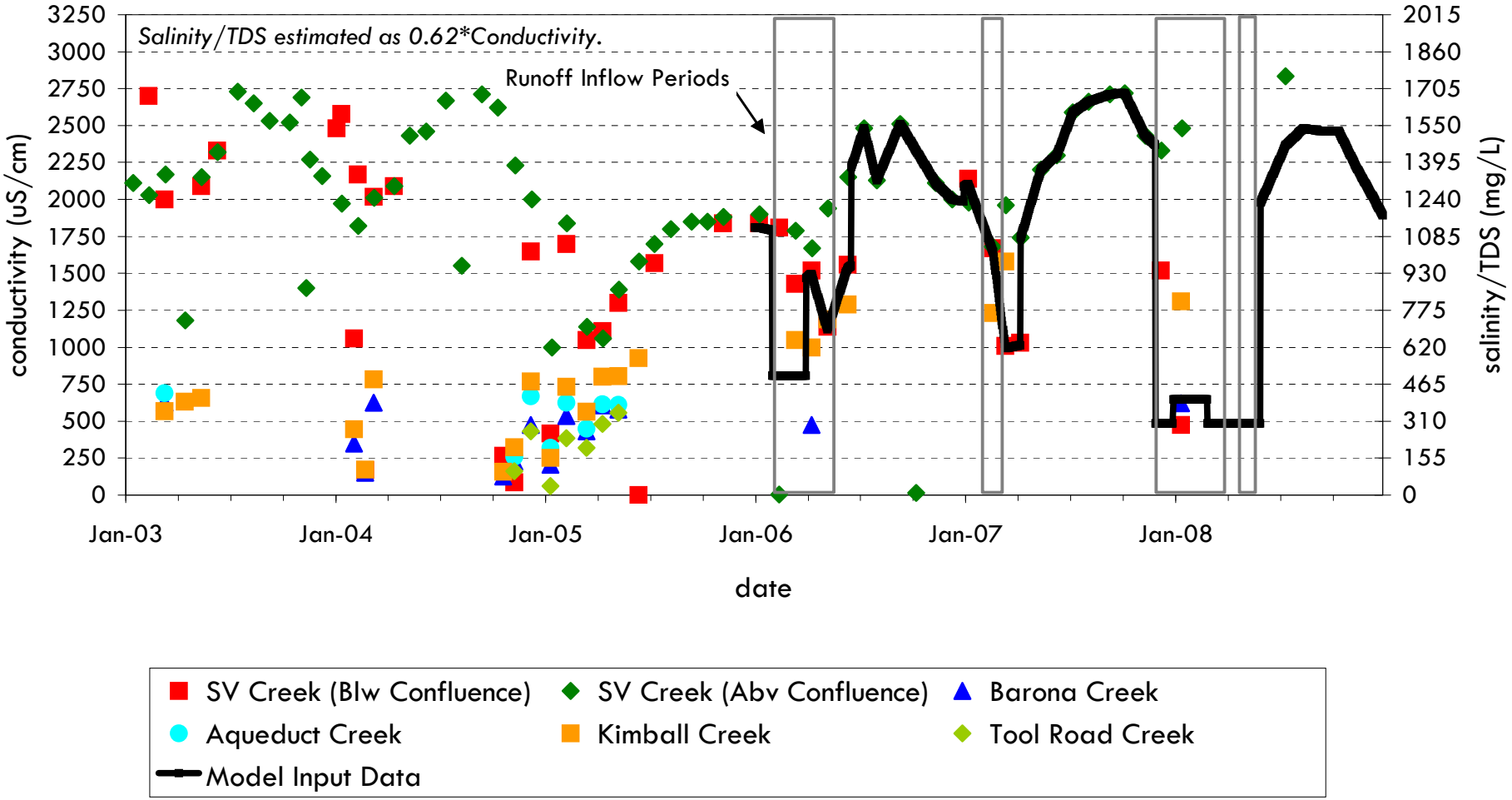

FSI V094005
May 01, 2012

Figure C-4

FLOW SCIENCE®

San Vicente Reservoir

Sutherland Reservoir Temperatures Near Outlet (El 1940 ft)

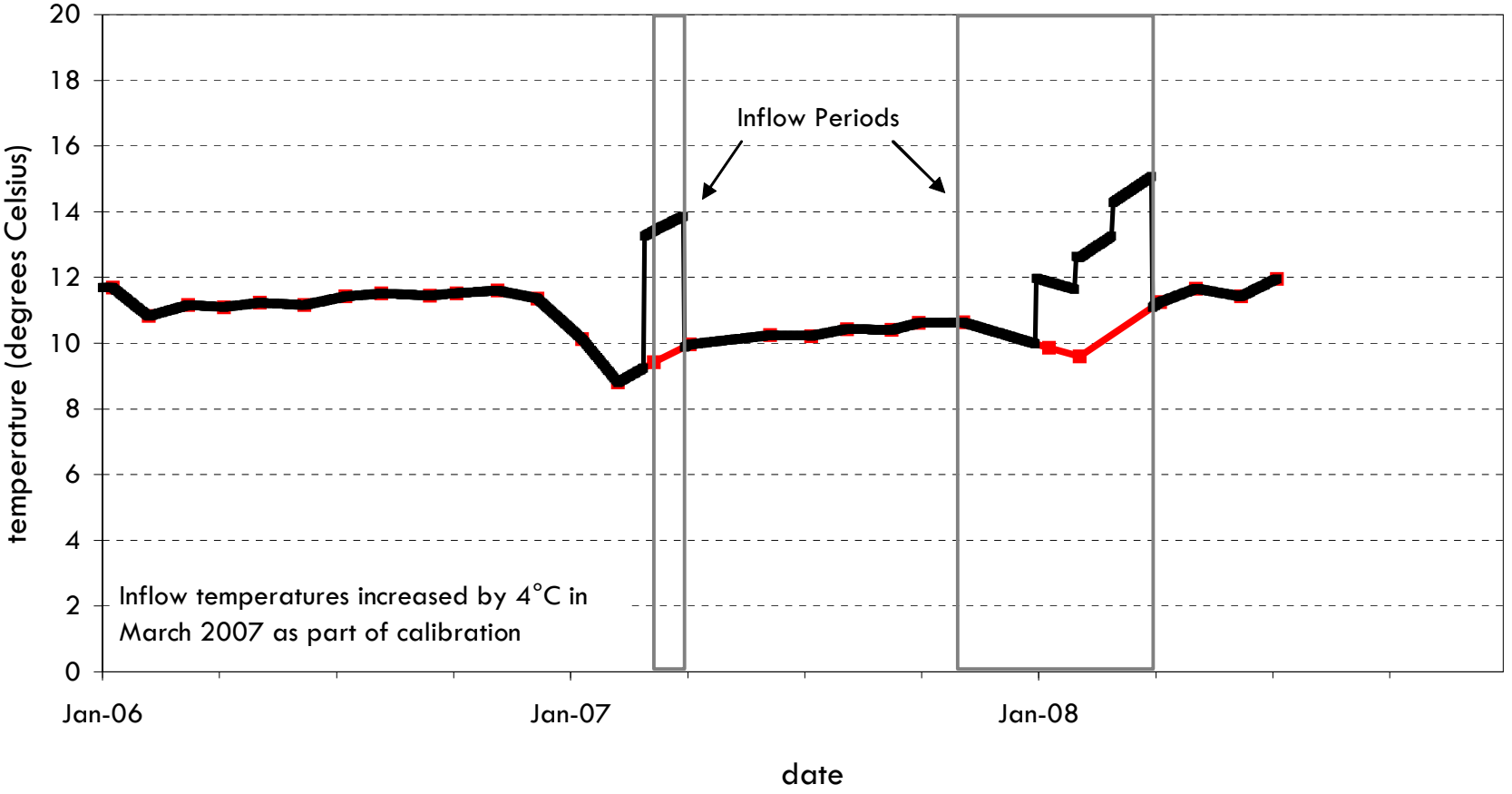

FSI V094005
May 01, 2012

Figure C-5

FLOW SCIENCE®

San Vicente Reservoir

Sutherland Reservoir Salinity/TDS Near Outlet (El 1940 ft)

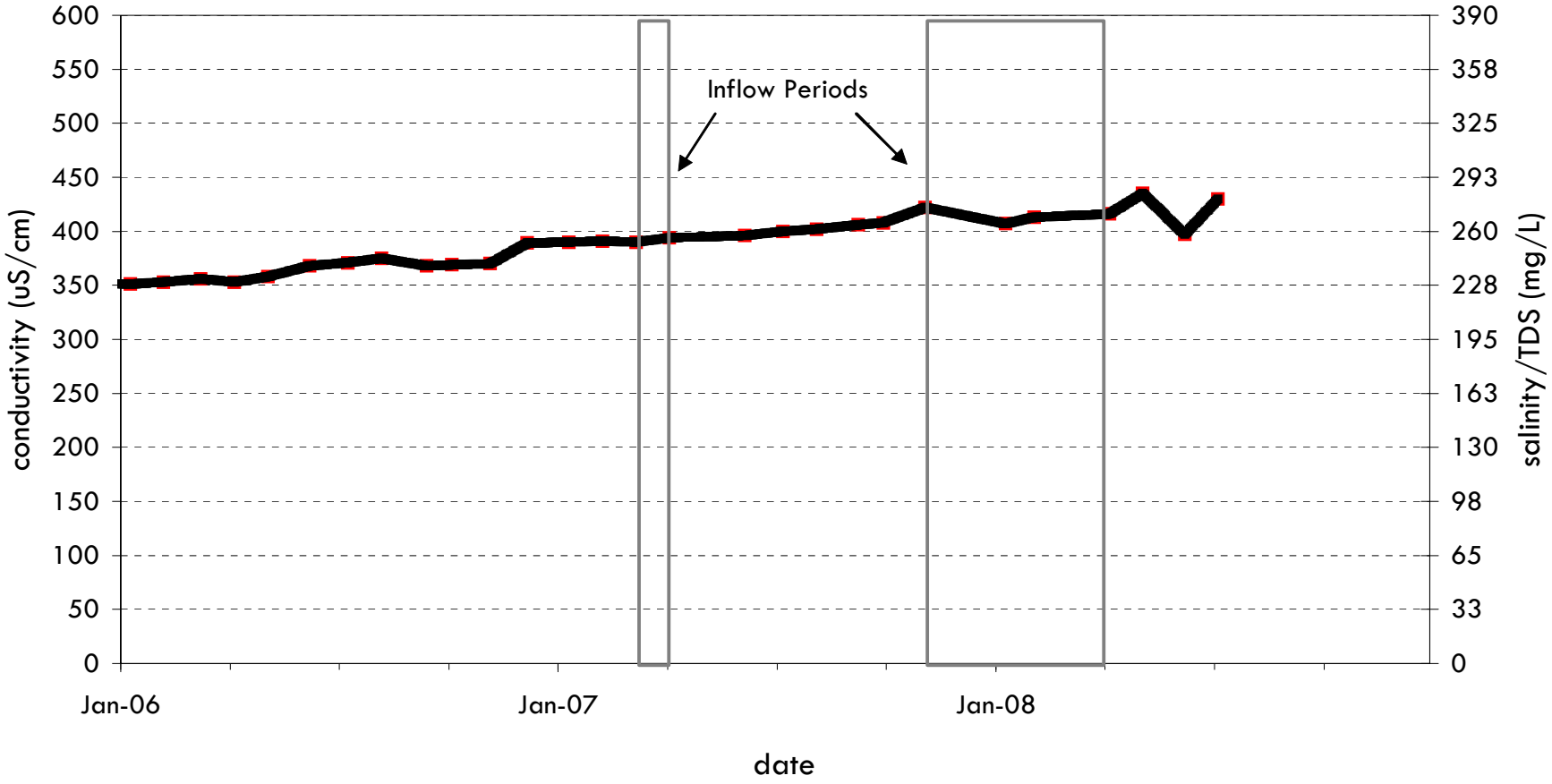

FSI V094005
May 01, 2012

Figure C-6

FLOW SCIENCE®

San Vicente Reservoir

Input Meteorological Data - Solar Radiation

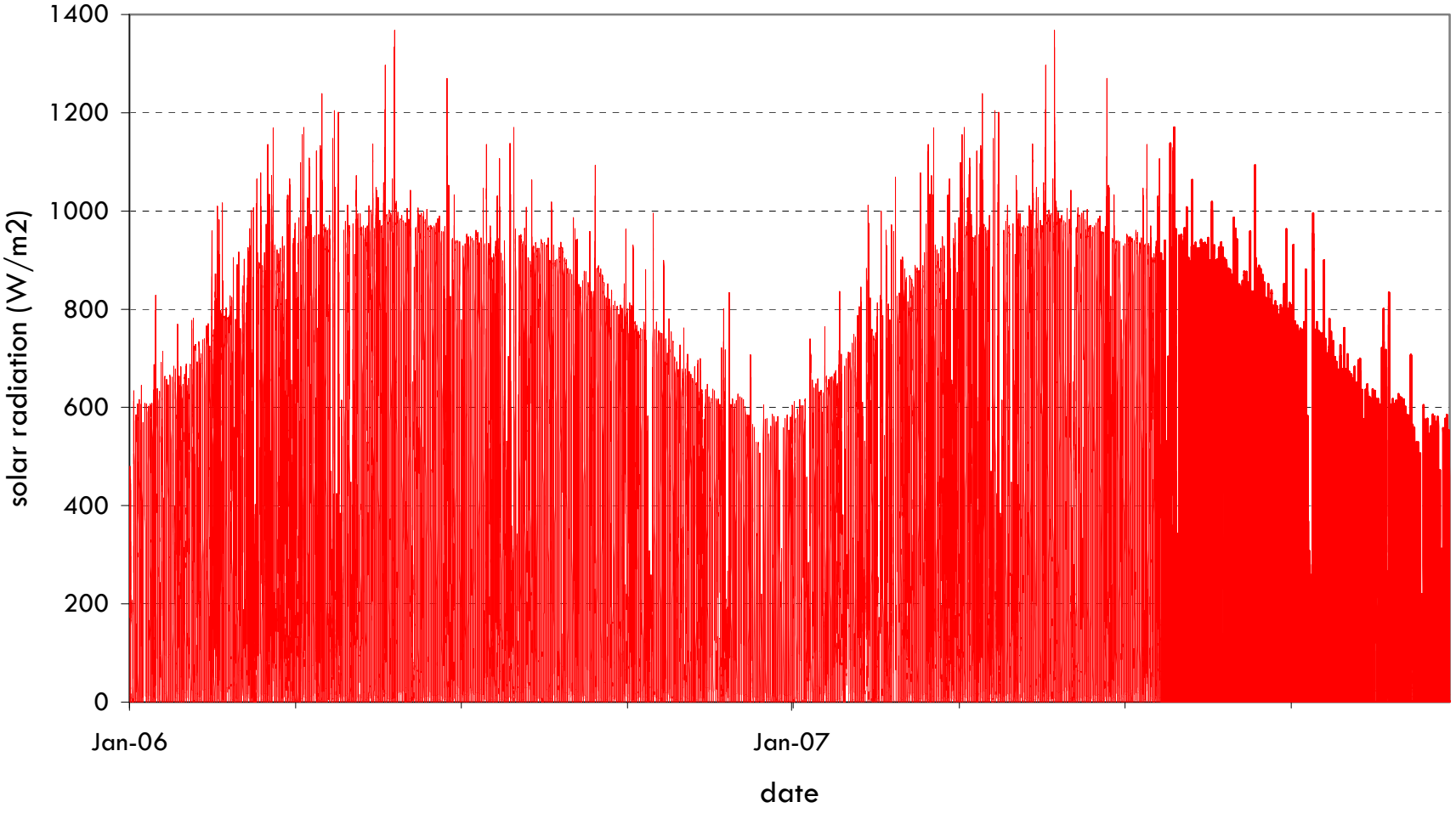

FSI V094005
May 01, 2012

Figure C-7

FLOW SCIENCE®

San Vicente Reservoir

Input Meteorological Data - Air Temperature

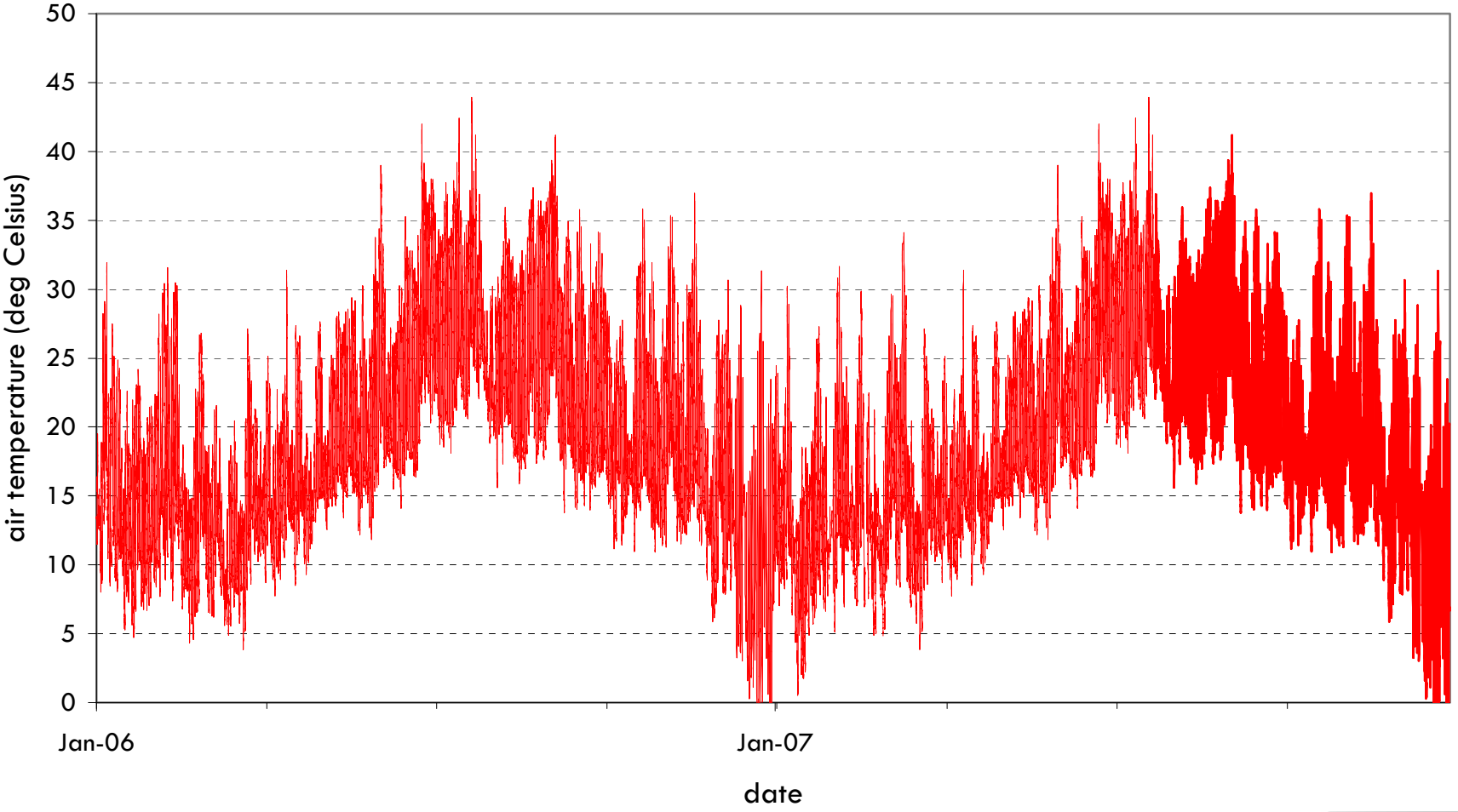

Figure C-8

FSI V094005
May 01, 2012

FLOW SCIENCE®

San Vicente Reservoir

Input Meteorological Data - Wind Speed

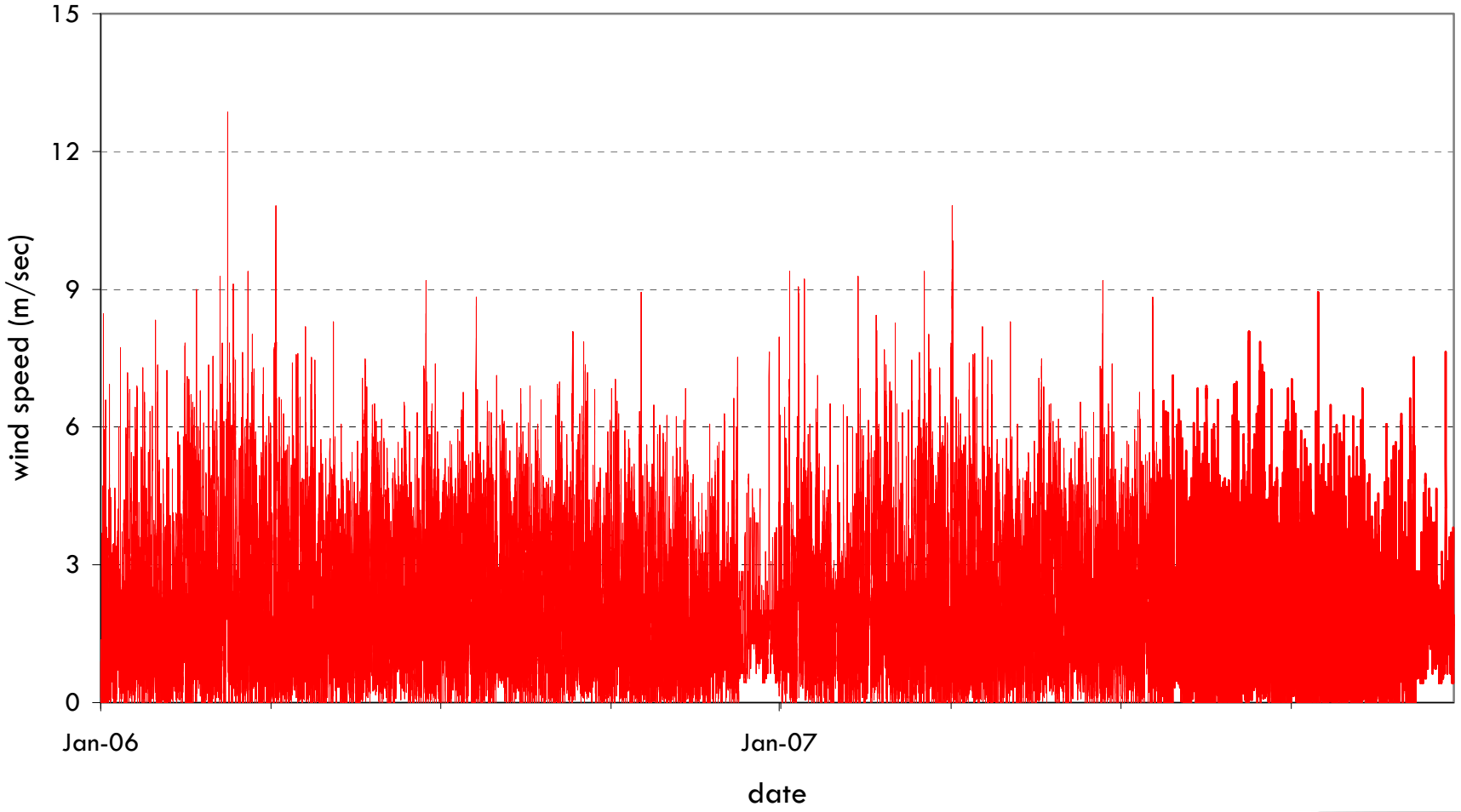

Figure C-9

FSI V094005
May 01, 2012

FLOW SCIENCE®

San Vicente Reservoir

Input Meteorological Data - Wind Direction

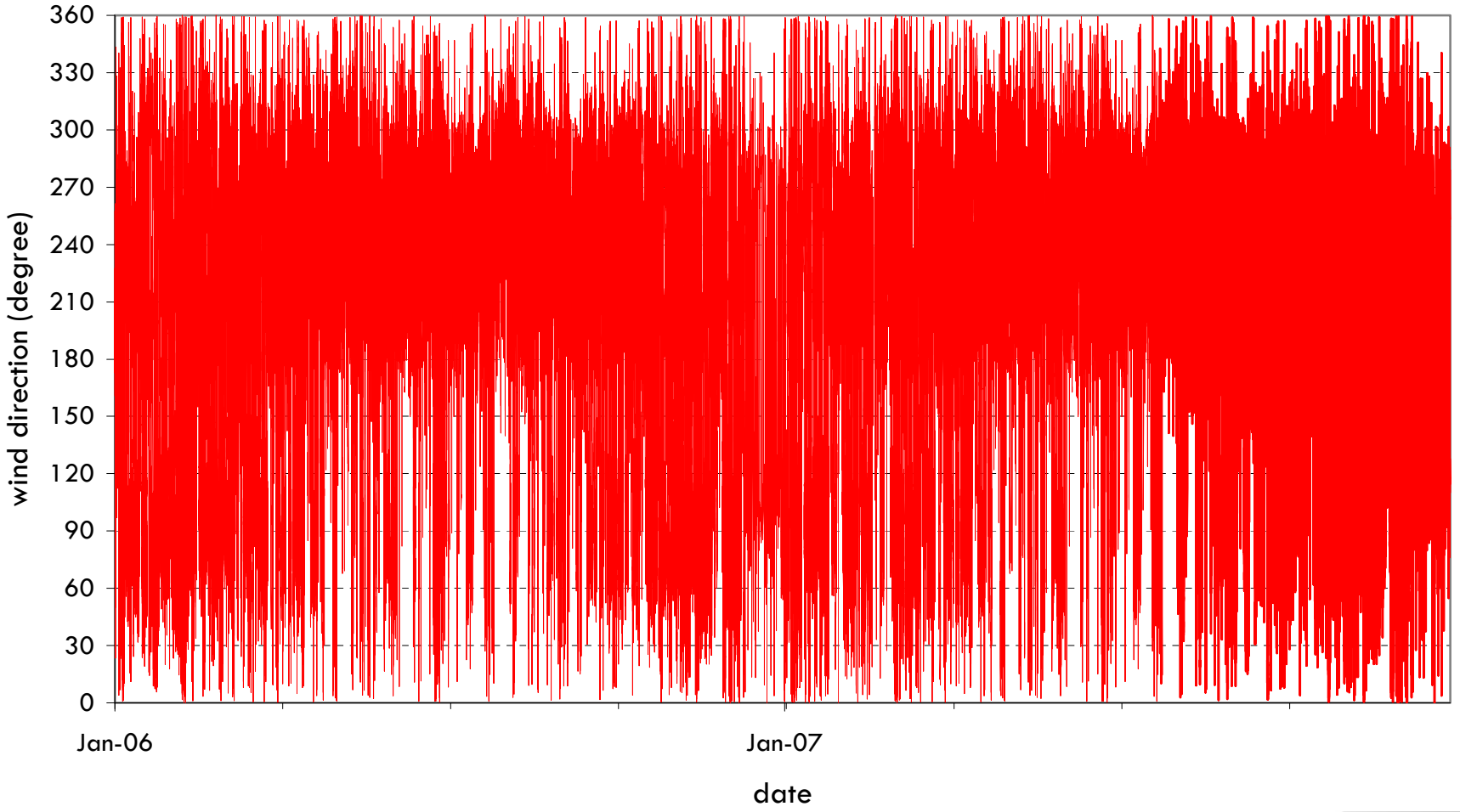

Figure C-10

FSI V094005
May 01, 2012

FLOW SCIENCE®

San Vicente Reservoir

Input Meteorological Data - Relative Humidity

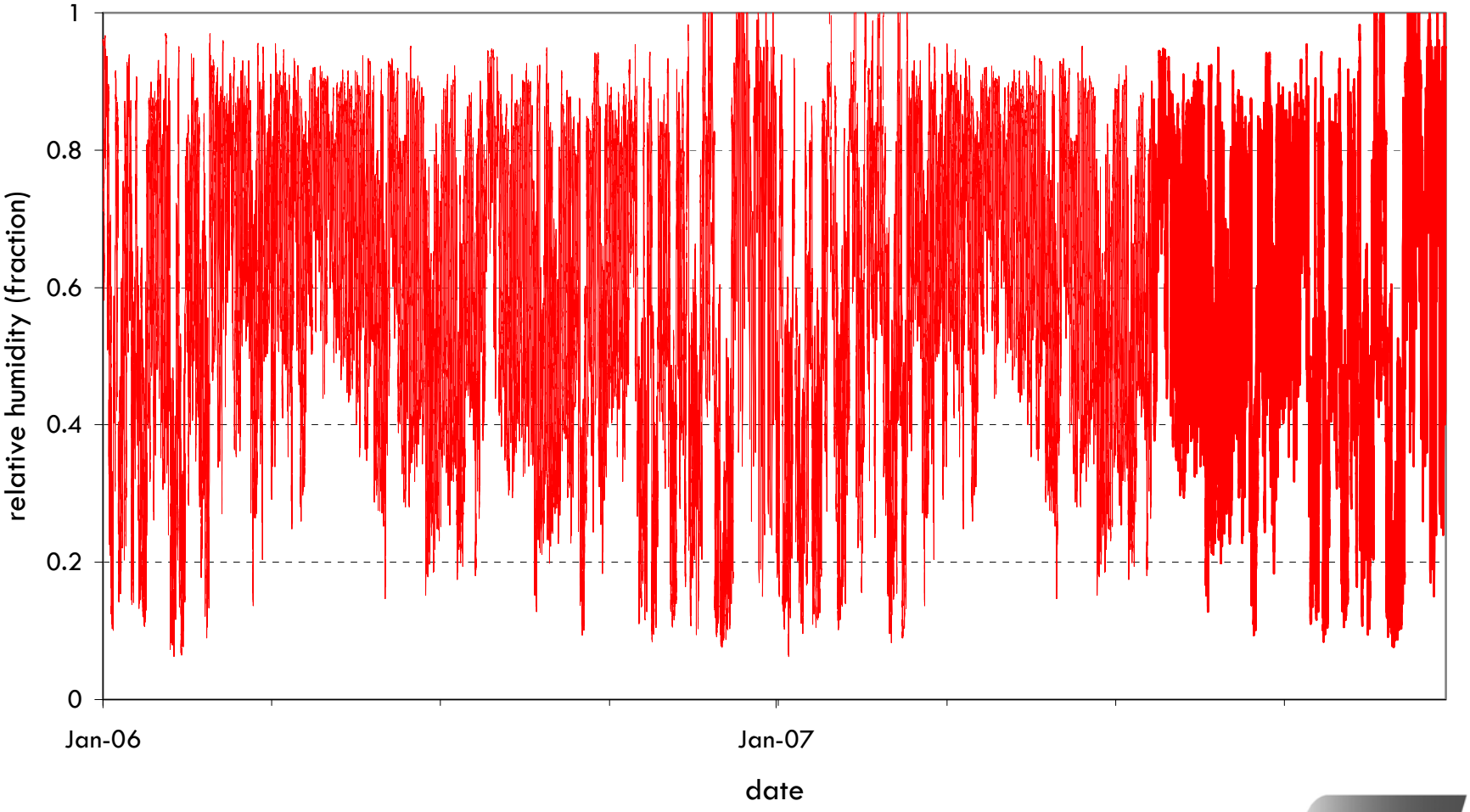

FSI V094005
May 01, 2012

Figure C-11

FLOW SCIENCE®

San Vicente Reservoir

Input Meteorological Data - Precipitation Rate

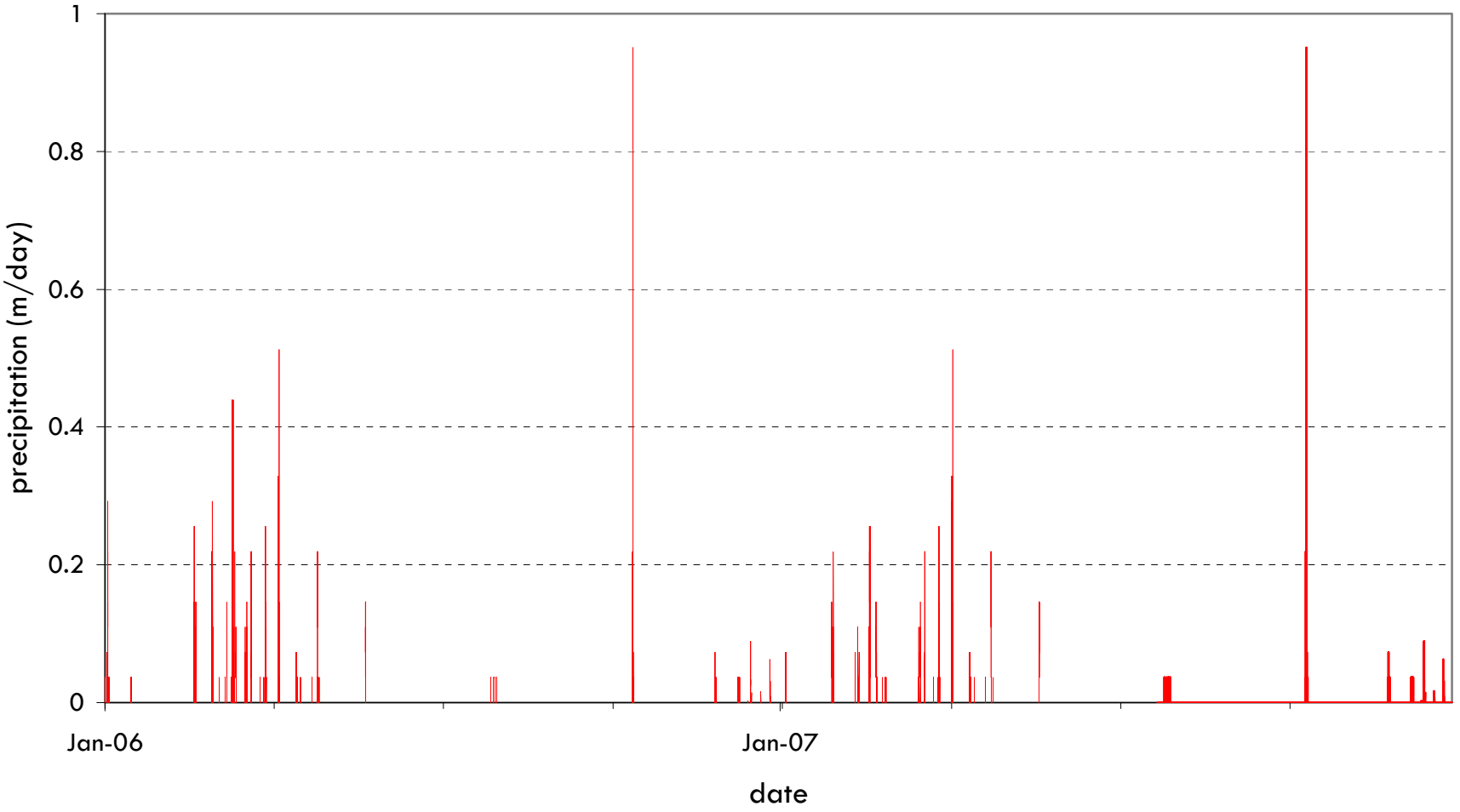

FSI V094005
May 01, 2012

Figure C-12

FLOW SCIENCE®

San Vicente Reservoir Station A - Water Temperature Calibration

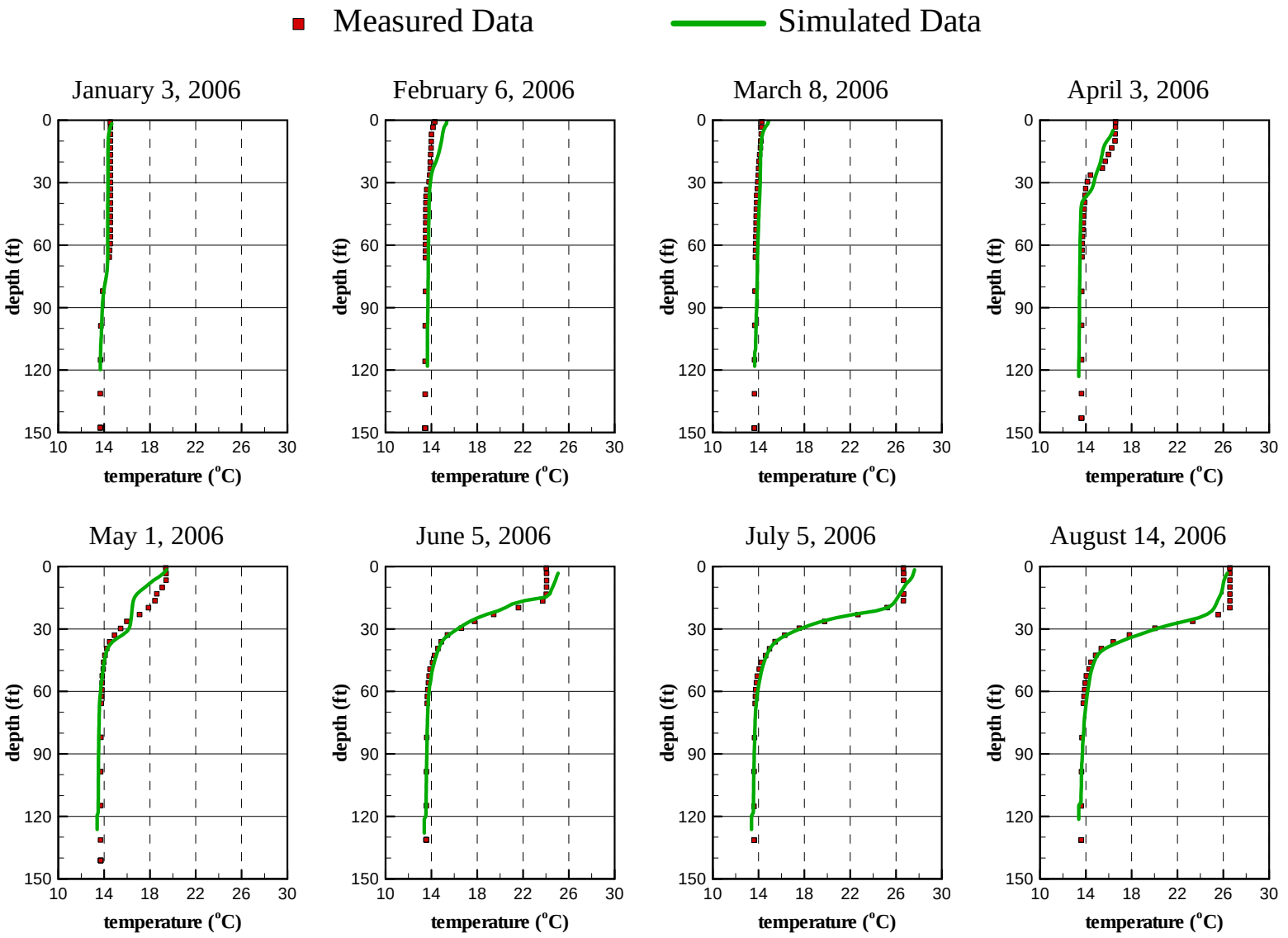

FSI V094005
May 01, 2012

Figure C-13

FLOW SCIENCE®

San Vicente Reservoir Station A - Water Temperature Calibration

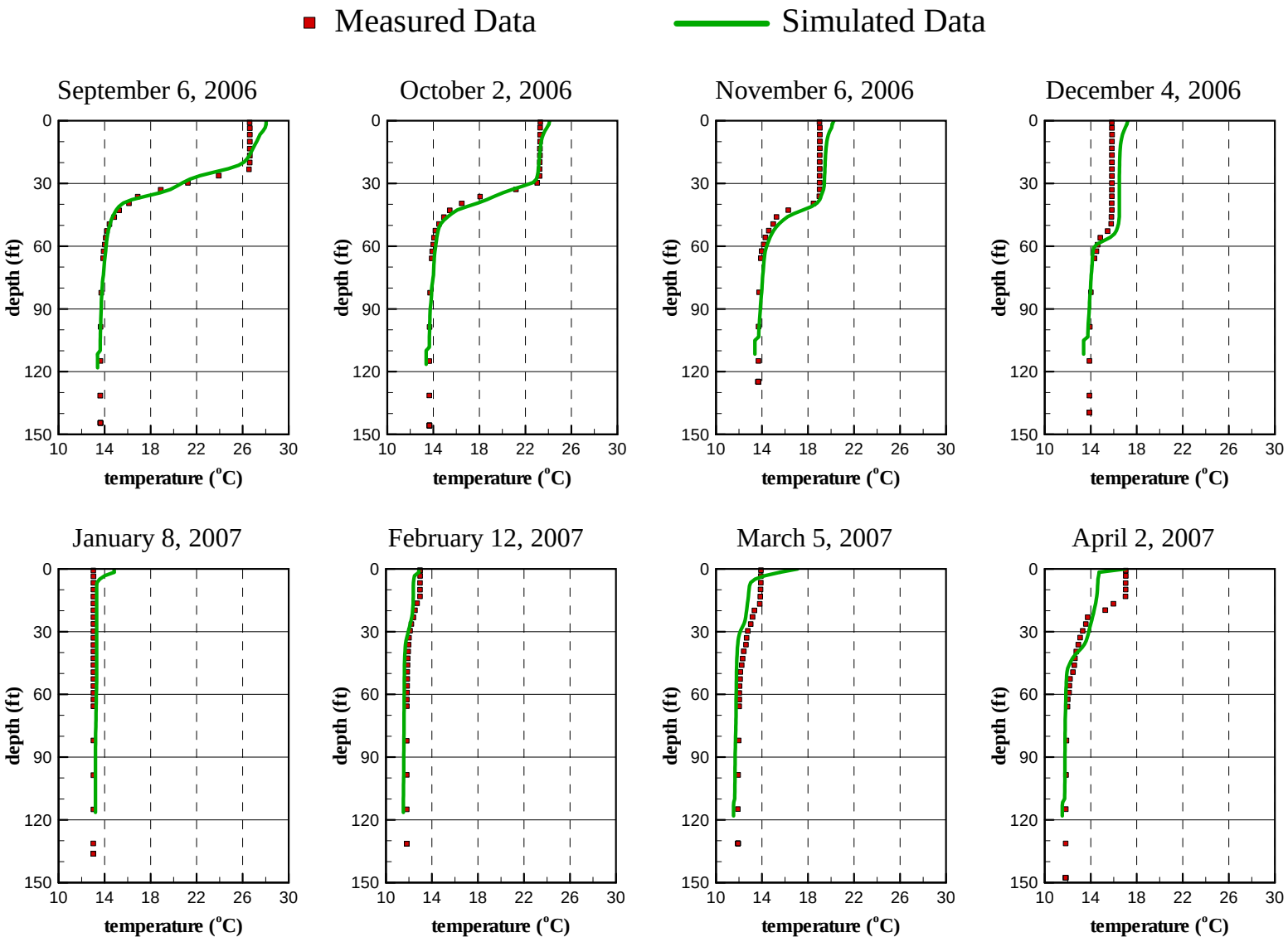

FSI V094005
May 01, 2012

Figure C-14

FLOW SCIENCE®

San Vicente Reservoir Station A - Water Temperature Calibration

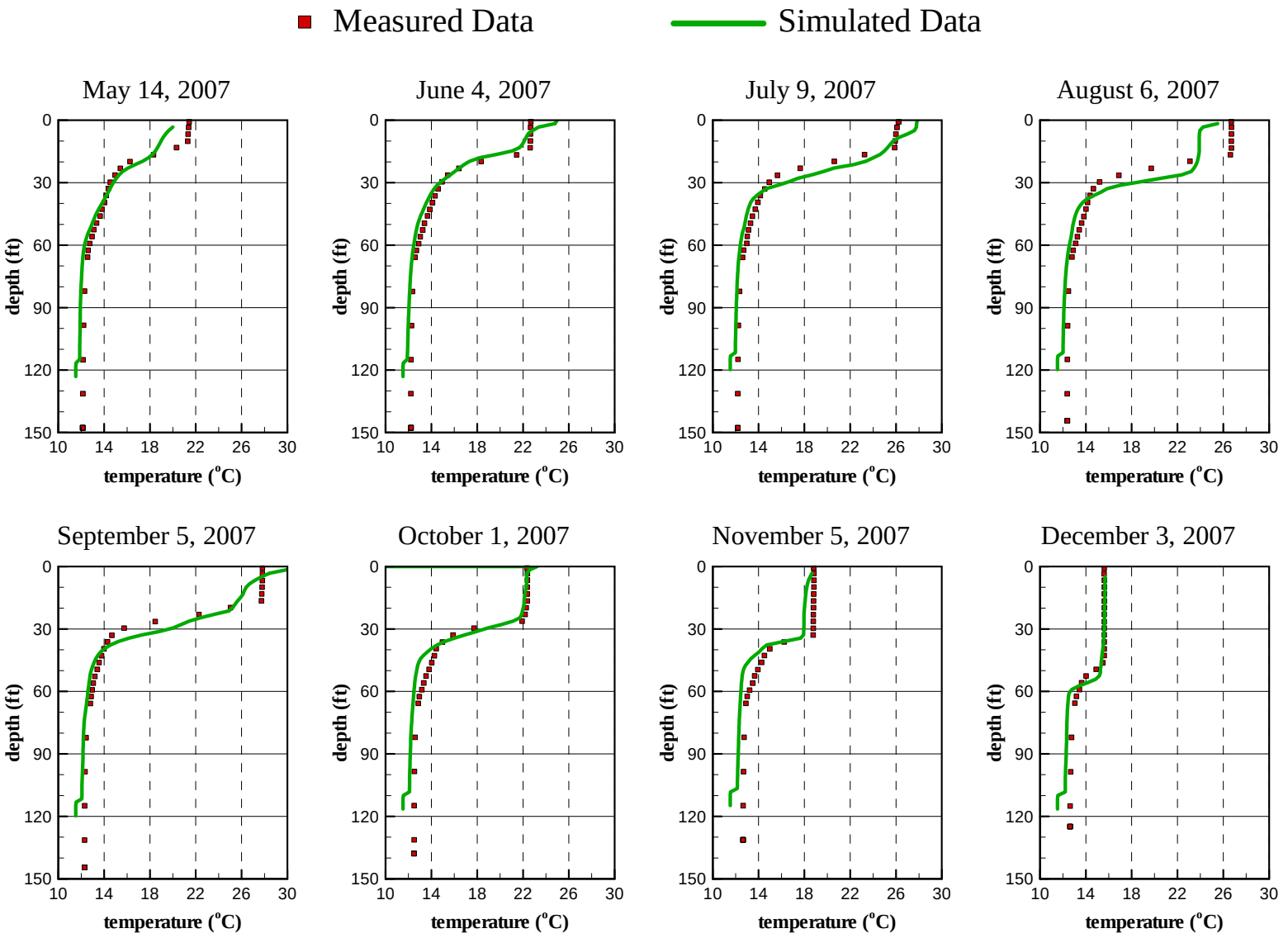

FSI V094005
May 01, 2012

Figure C-15

FLOW SCIENCE®

San Vicente Reservoir

1995 Tracer Winter Study – Measured Tracer versus Simulated Conservative Tracer

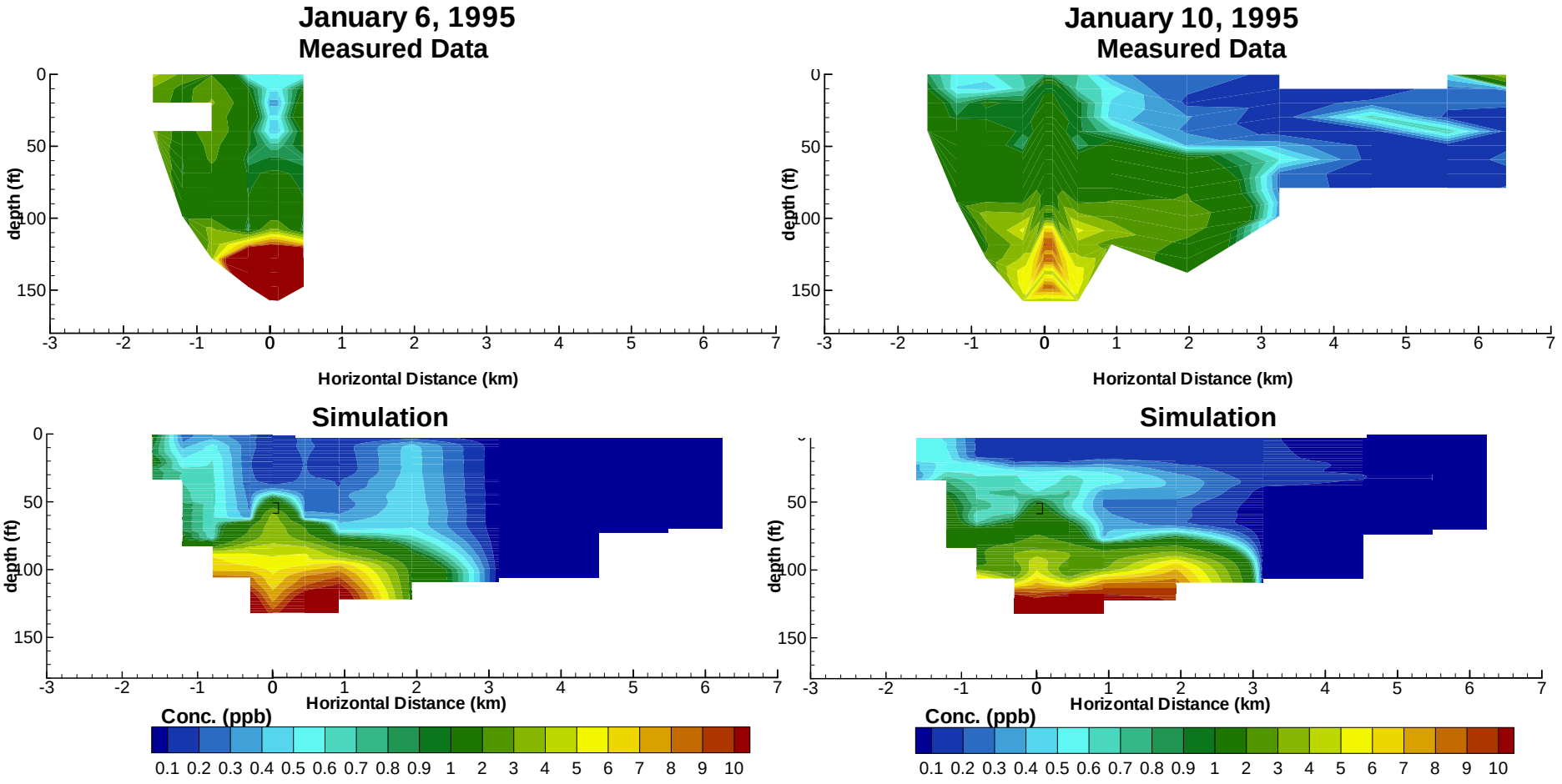

FSI V094005
May 01, 2012

Figure C-16

FLOW SCIENCE®

San Vicente Reservoir

1995 Tracer Winter Study – Measured Tracer versus Simulated Conservative Tracer

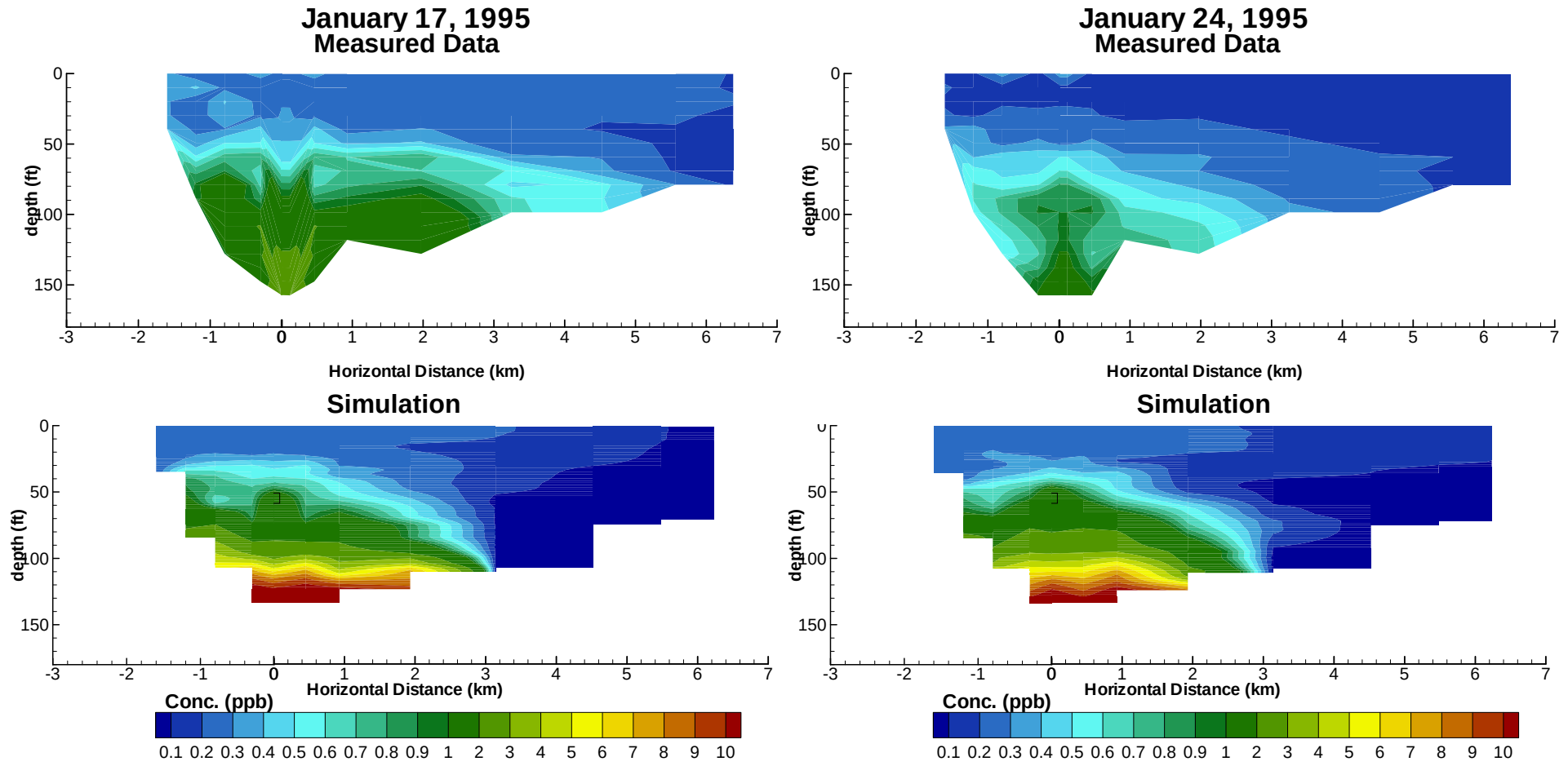

FSI V094005
May 01, 2012

Figure C-17

FLOW SCIENCE®

San Vicente Reservoir

1995 Tracer Winter Study – Measured Tracer versus Simulated Conservative Tracer

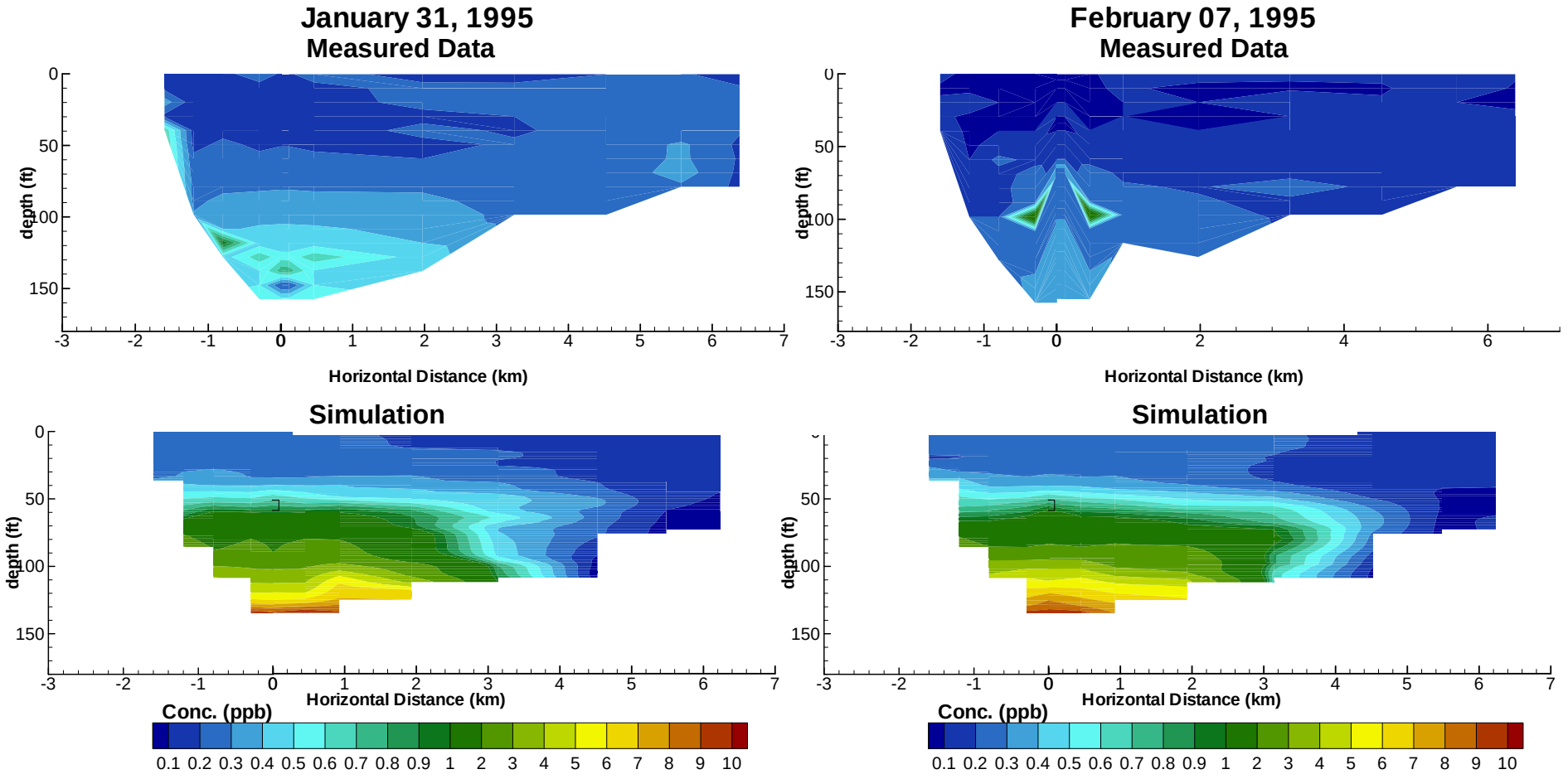

FSI V094005
May 01, 2012

Figure C-18

FLOW SCIENCE®

San Vicente Reservoir

1995 Tracer Summer Study – Measured Tracer versus Simulated Conservative Tracer

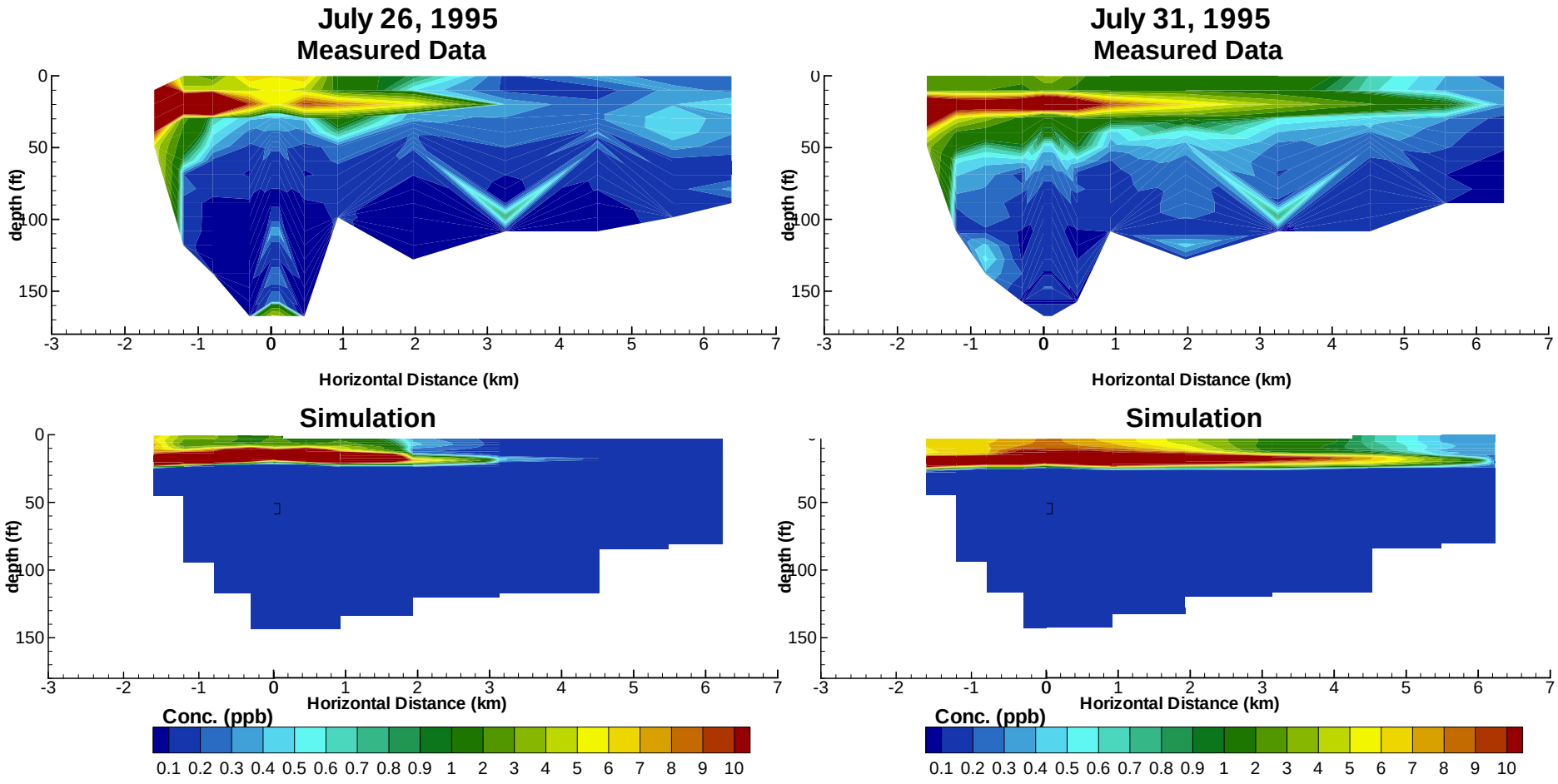

FSI V094005
May 01, 2012

Figure C-19

FLOW SCIENCE®

San Vicente Reservoir

1995 Tracer Summer Study – Measured Tracer versus Simulated Conservative Tracer

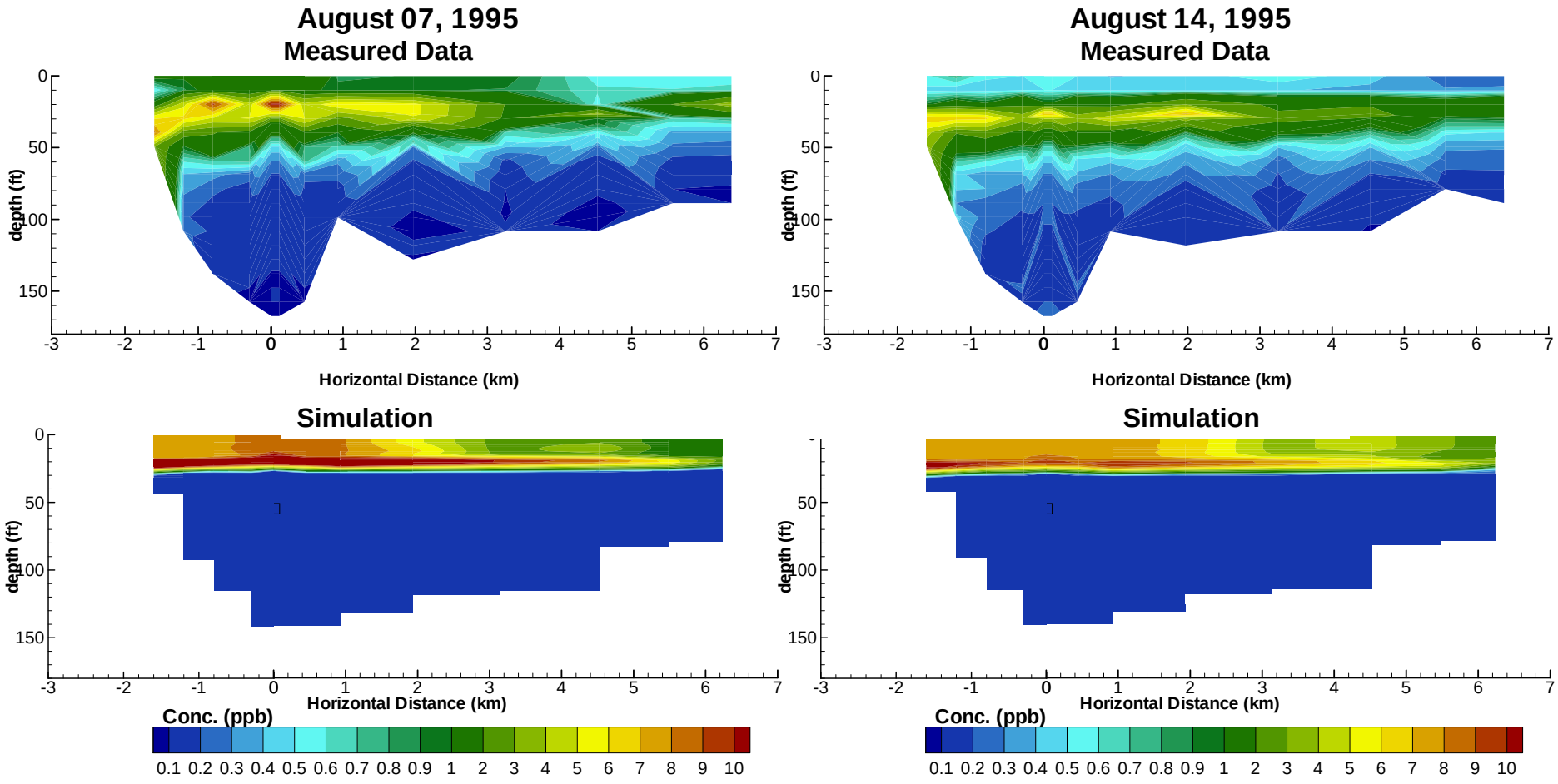

FSI V094005
May 01, 2012

Figure C-20

FLOW SCIENCE®

San Vicente Reservoir

1995 Tracer Summer Study – Measured Tracer versus Simulated Conservative Tracer

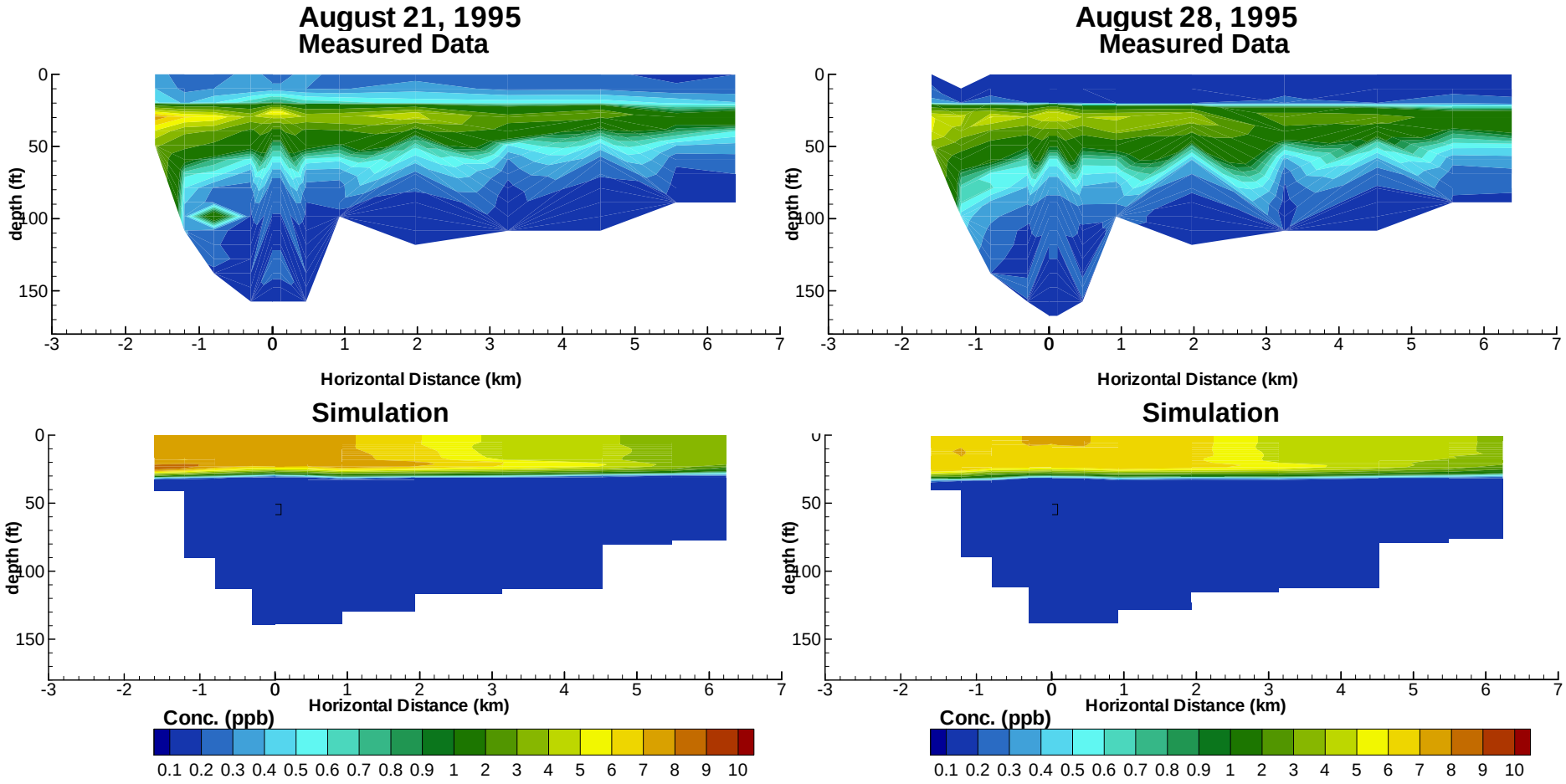

FSI V094005
May 01, 2012

Figure C-21

FLOW SCIENCE®

San Vicente Reservoir

1995 Tracer Summer Study – Measured Tracer versus Simulated Conservative Tracer

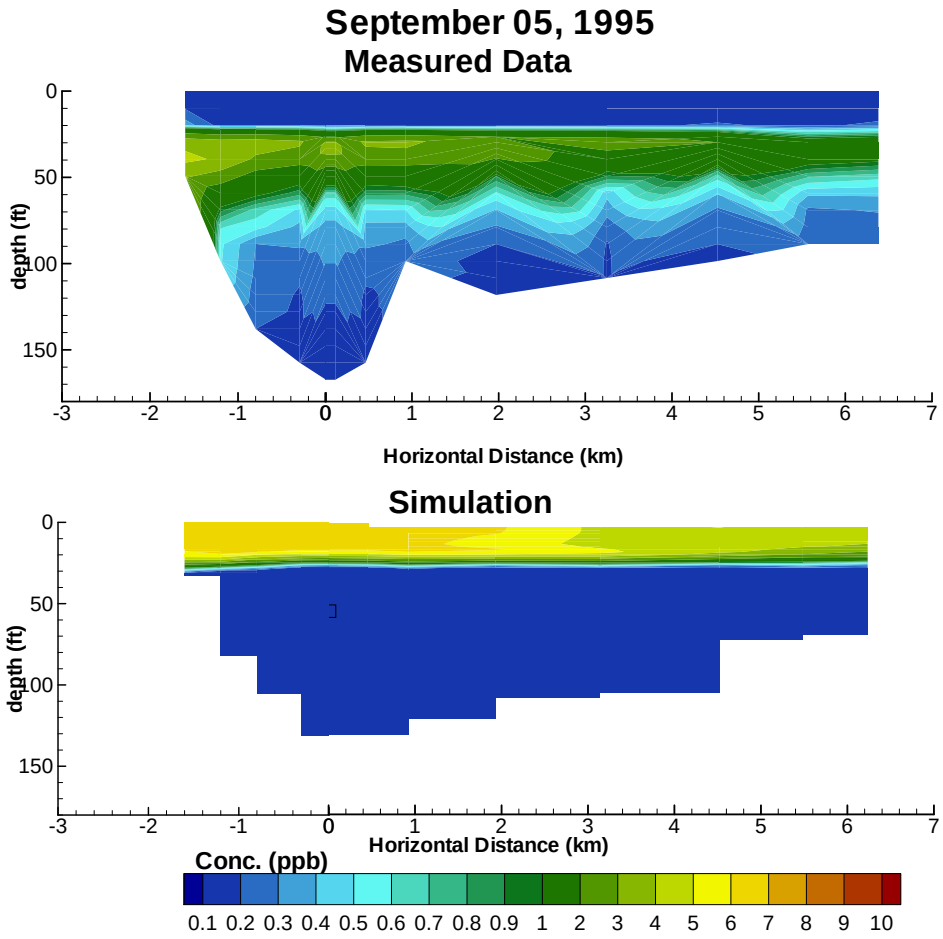

FSI V094005
May 01, 2012

Figure C-22

FLOW SCIENCE®

San Vicente Reservoir

Aqueduct Inflow Ammonia Data

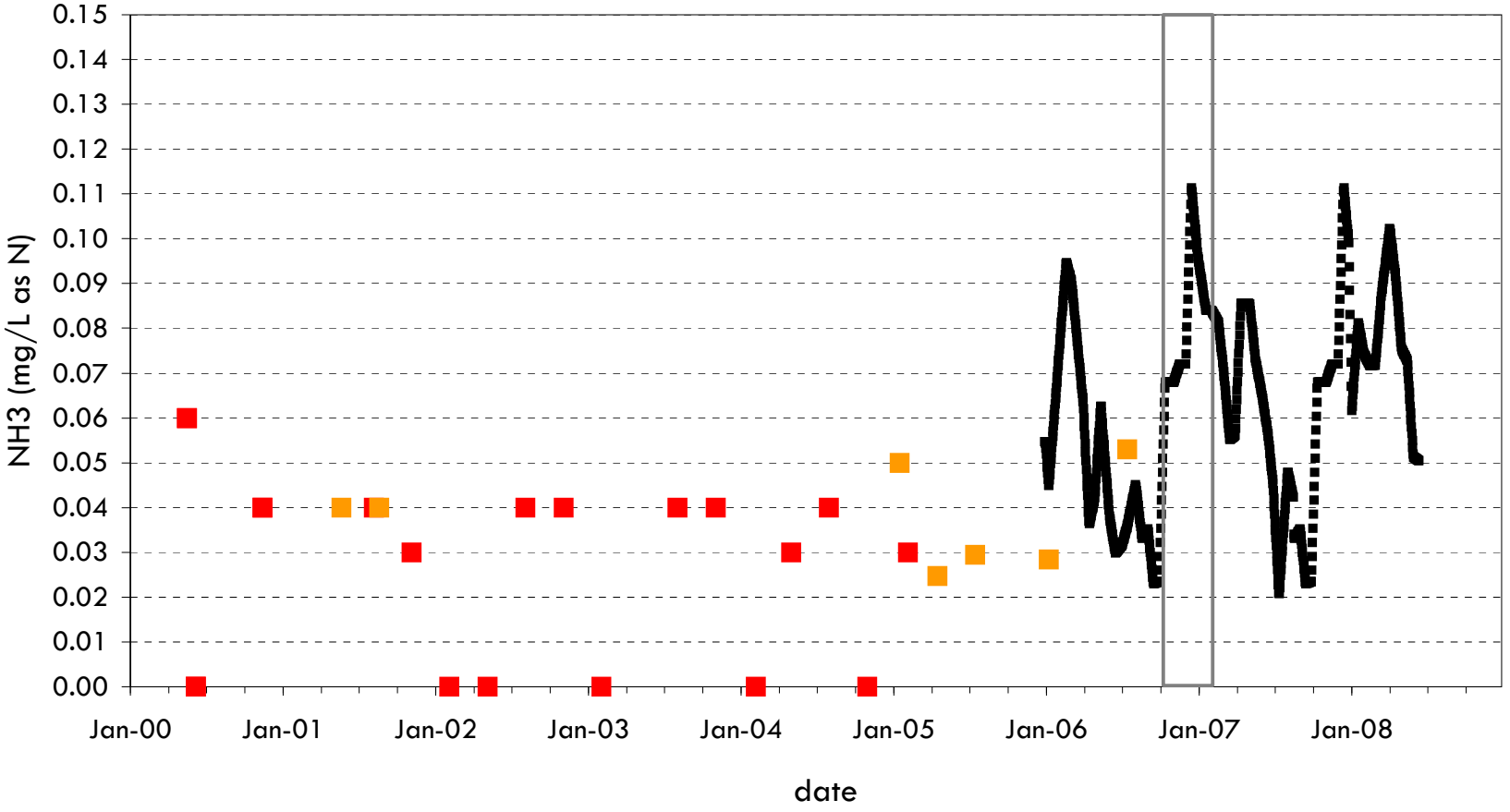

FSI V094005
May 01, 2012

Figure C-23

FLOW SCIENCE®

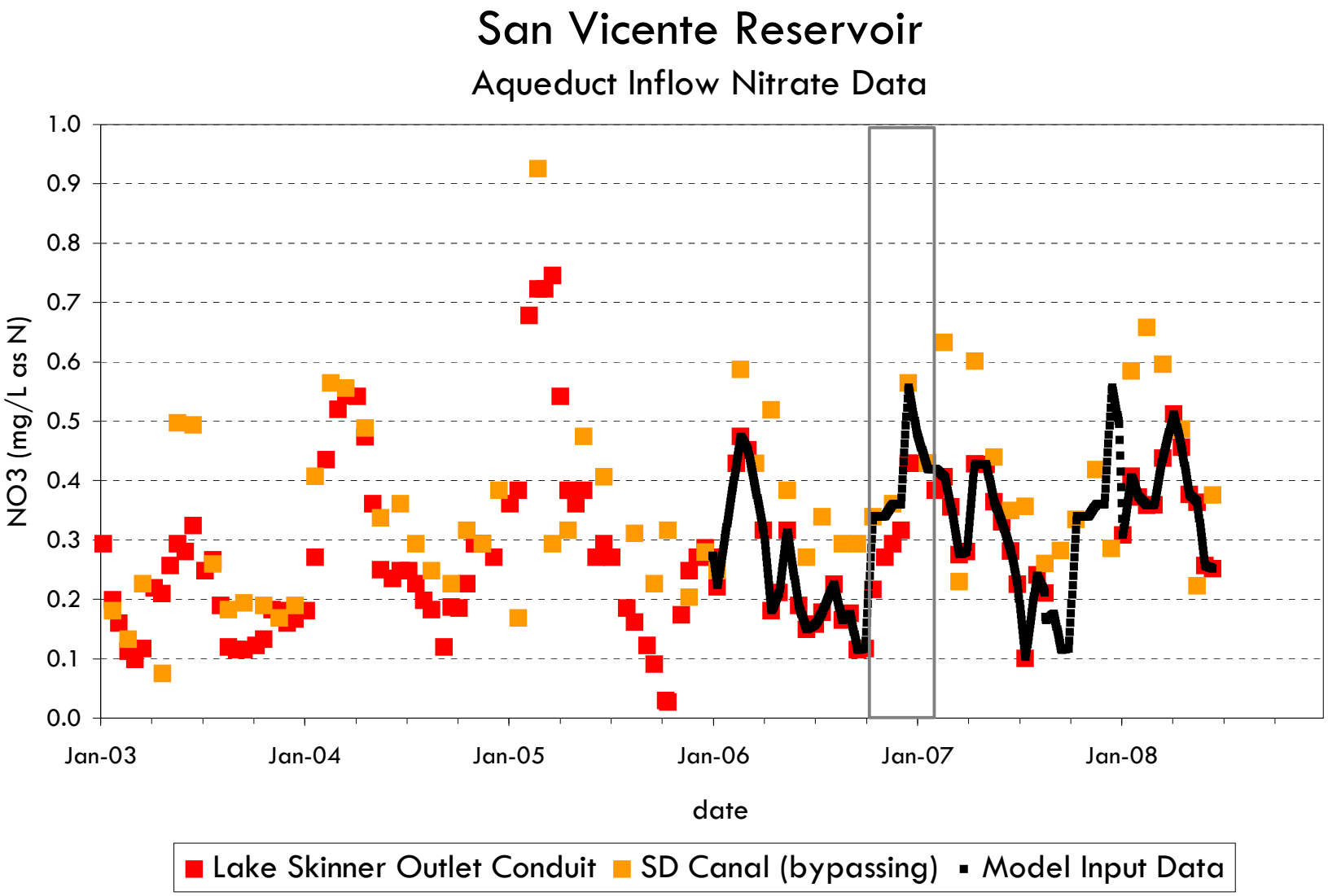

FSI V094005
May 01, 2012

Figure C-24

FLOW SCIENCE®

San Vicente Reservoir

Aqueduct Inflow Total Nitrogen Estimate

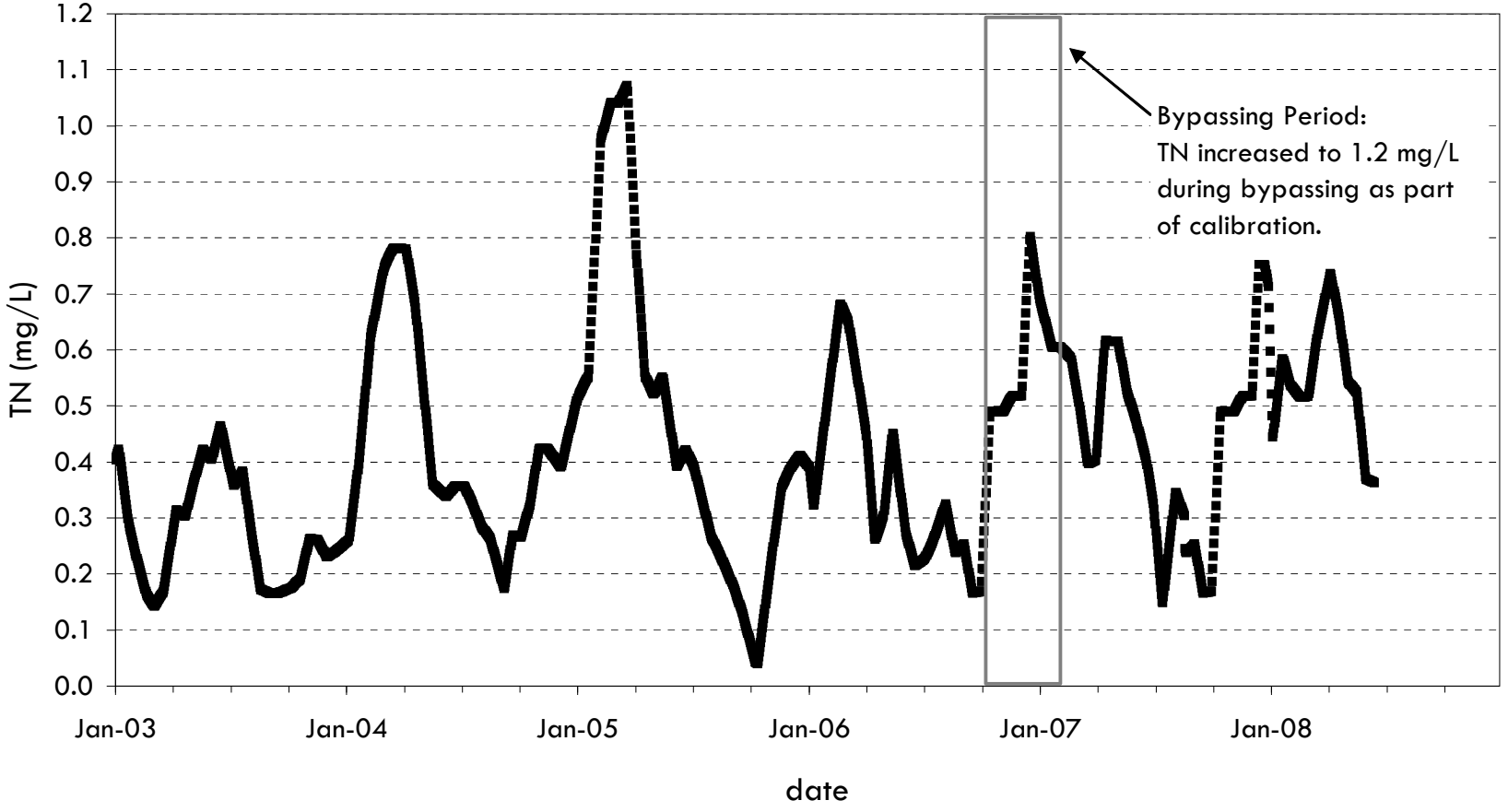

FSI V094005
May 01, 2012

Figure C-25

FLOW SCIENCE®

San Vicente Reservoir

Aqueduct Inflow Ortho-Phosphate Data

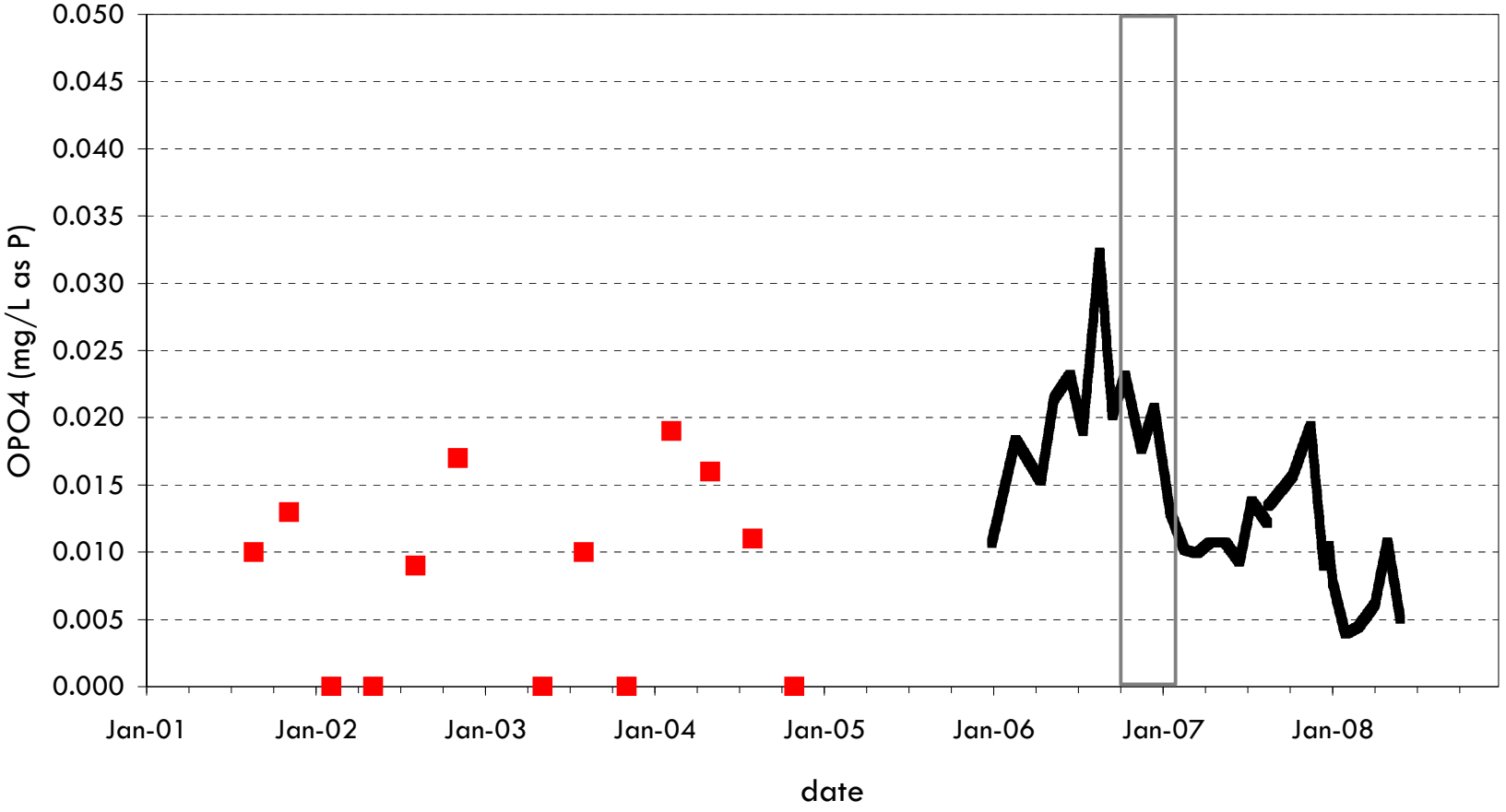

FSI V094005
May 01, 2012

Figure C-26

FLOW SCIENCE®

San Vicente Reservoir

Aqueduct Inflow Total Phosphorus Data

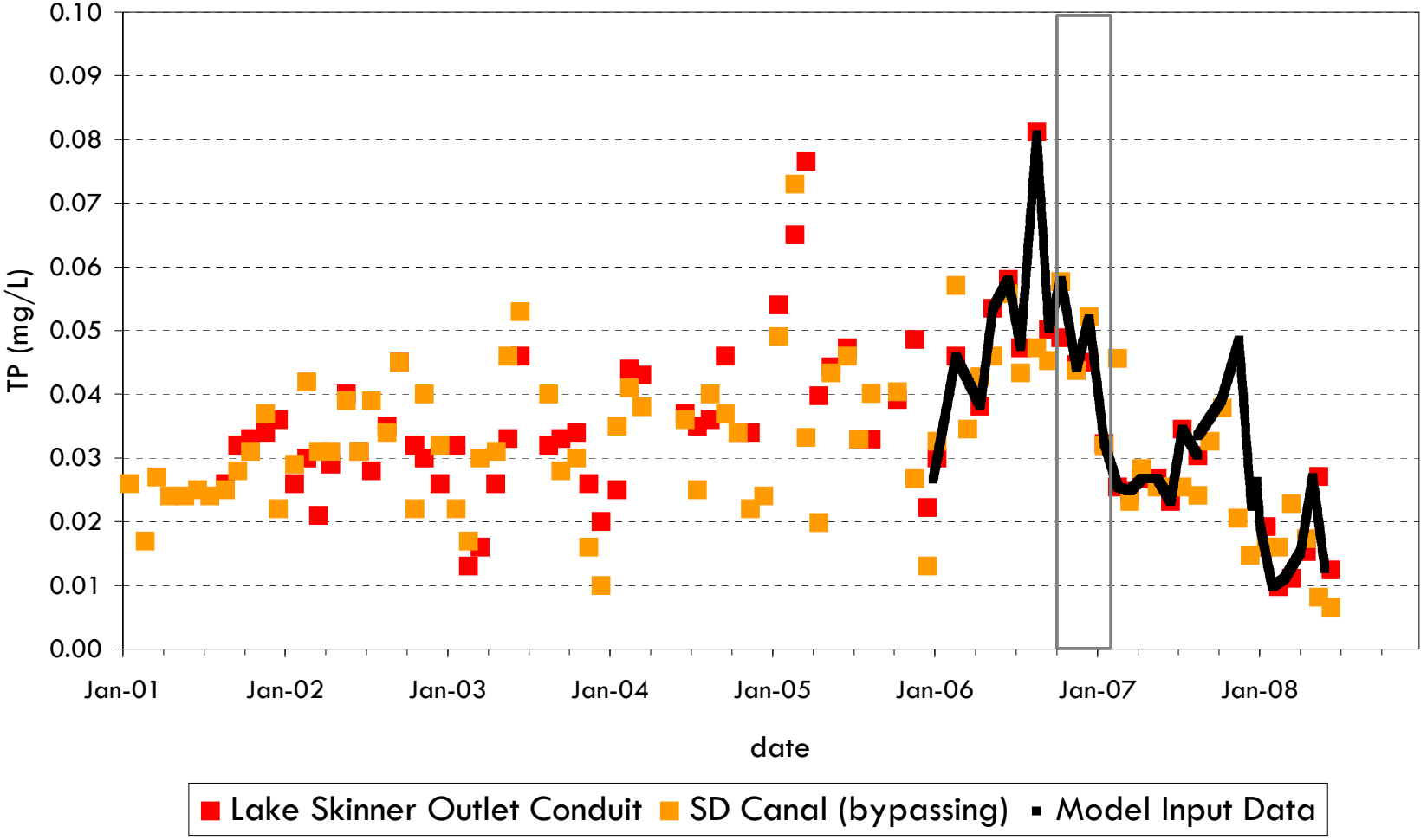

FSI V094005
May 01, 2012

Figure C-27

FLOW SCIENCE®

San Vicente Reservoir

Aqueduct Inflow Dissolved Oxygen

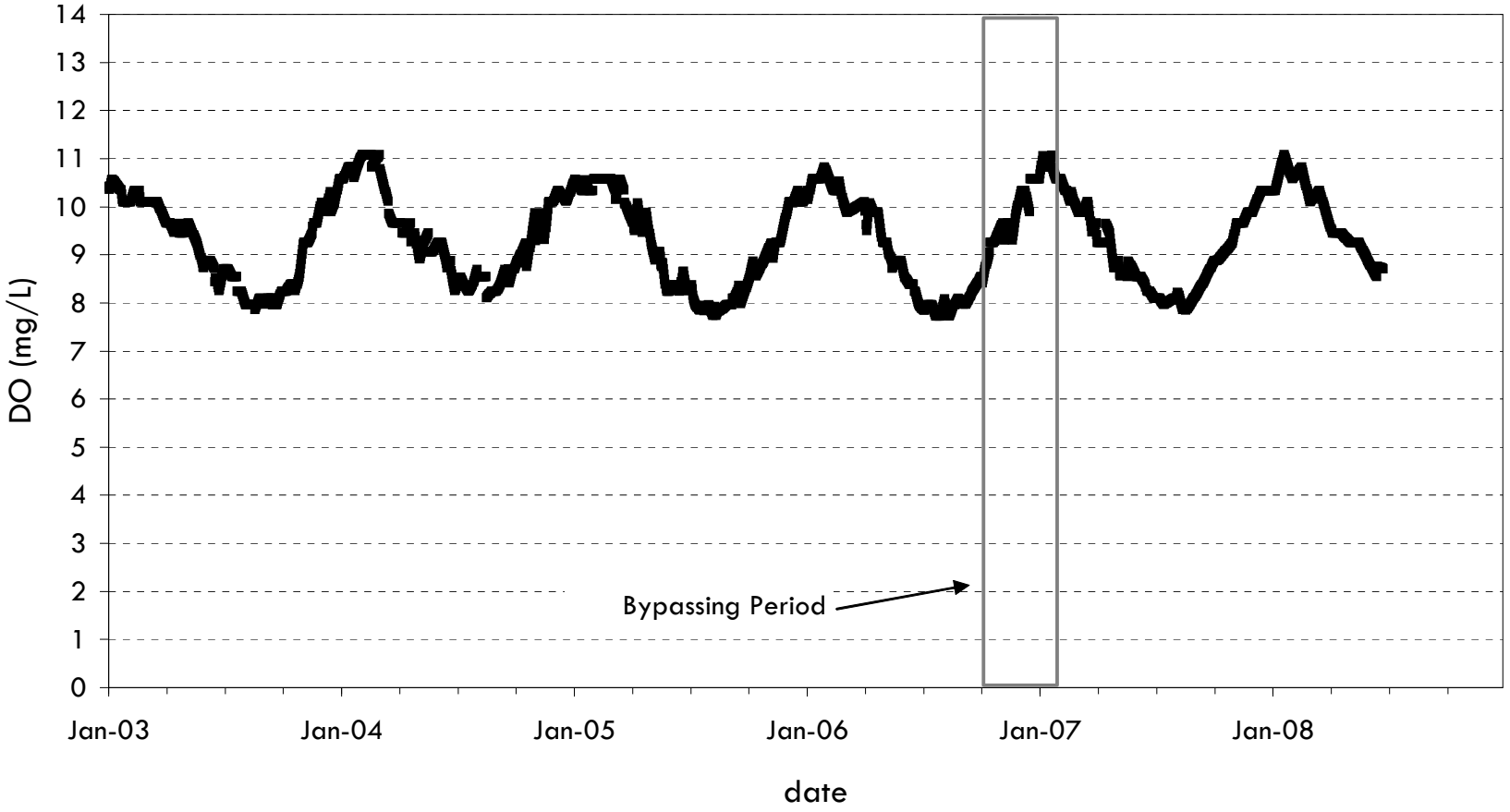

▪ Model Input Data (estimated based on temperature - 100% saturation)

FSI V094005
May 01, 2012

Figure C-28

FLOW SCIENCE®

San Vicente Reservoir

Aqueduct Inflow pH Data

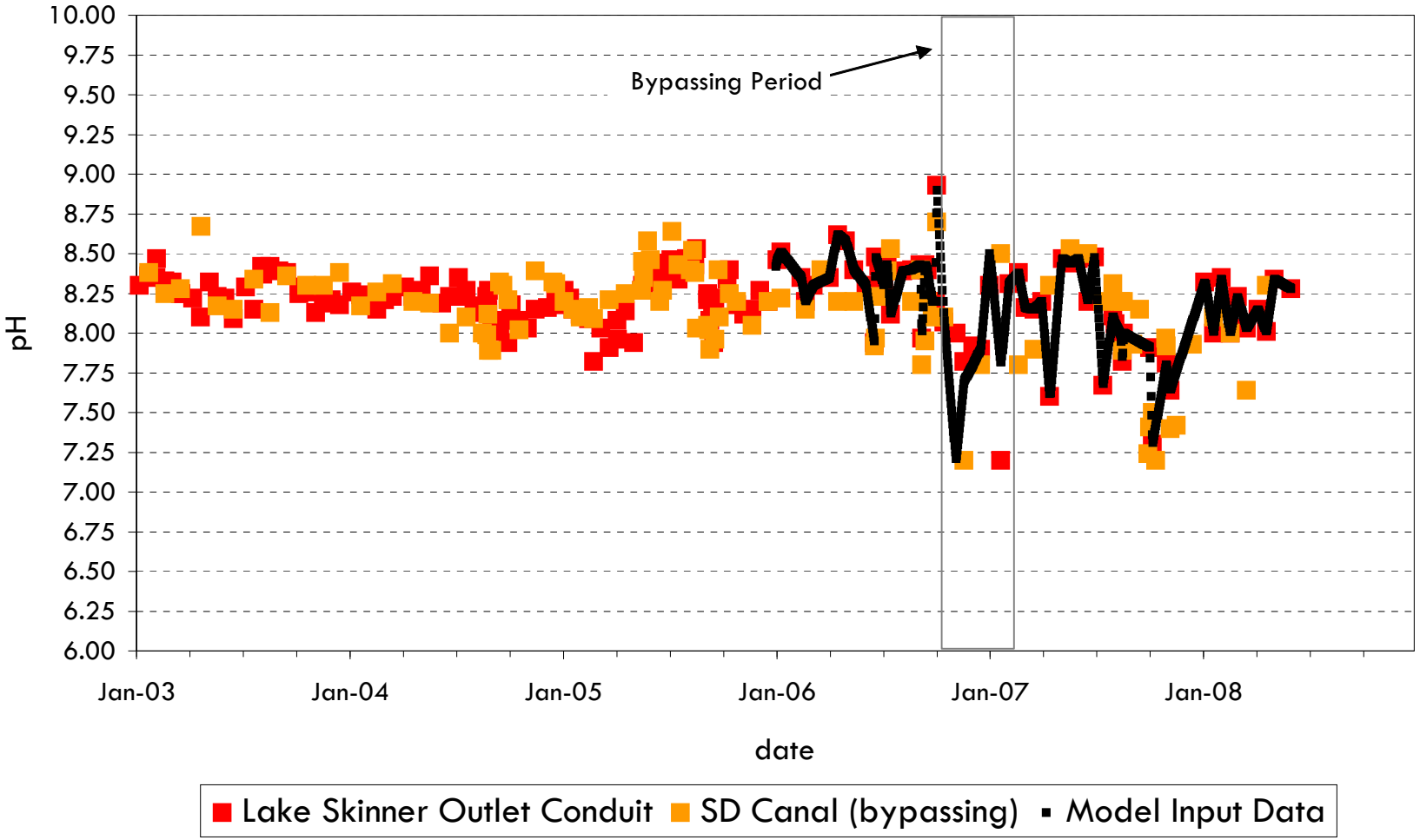

FSI V094005
May 01, 2012

Figure C-29

FLOW SCIENCE®

San Vicente Reservoir

Runoff Inflow Ammonia

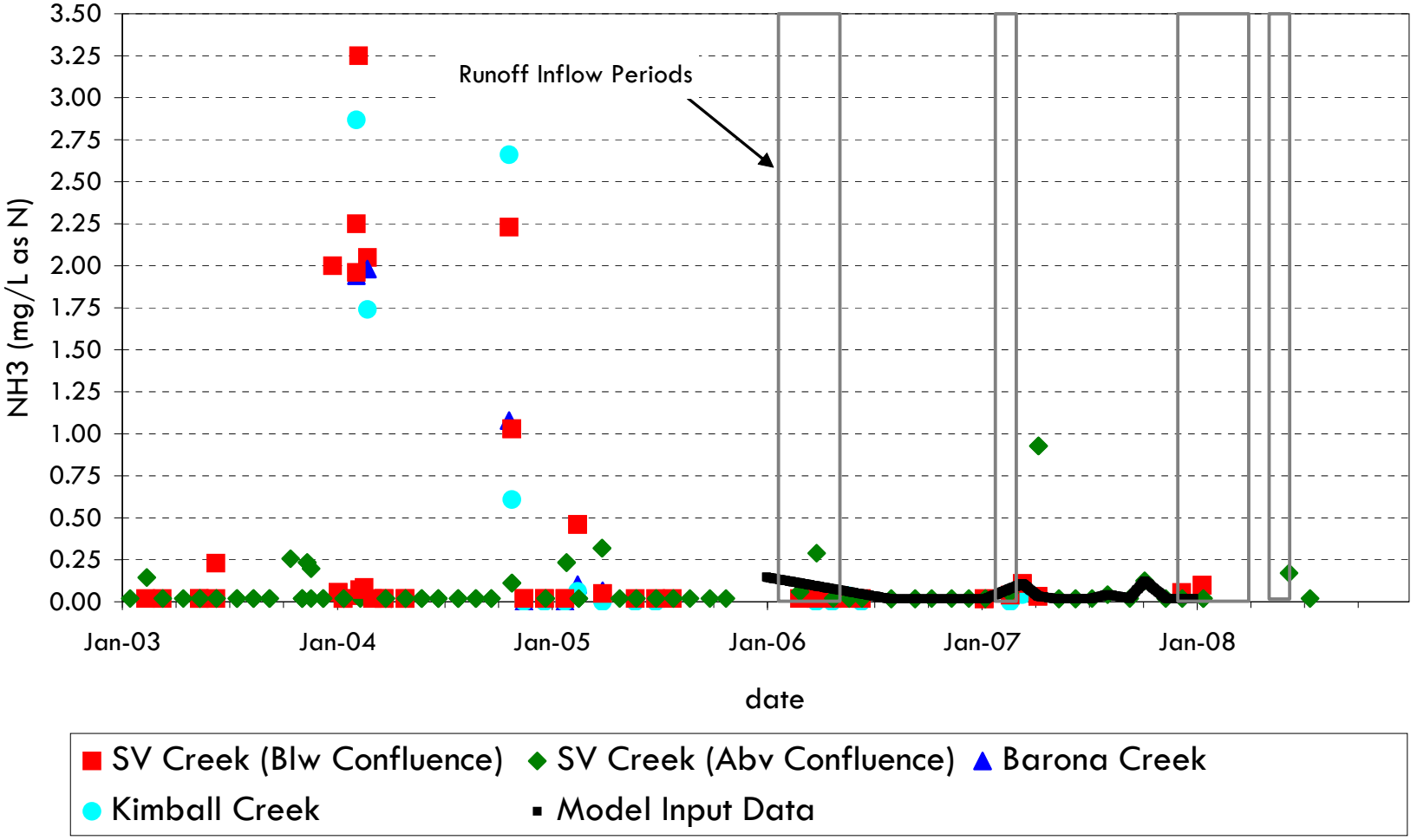

FSI V094005
May 01, 2012

Figure C-30

FLOW SCIENCE®

San Vicente Reservoir

Runoff Inflow Nitrate

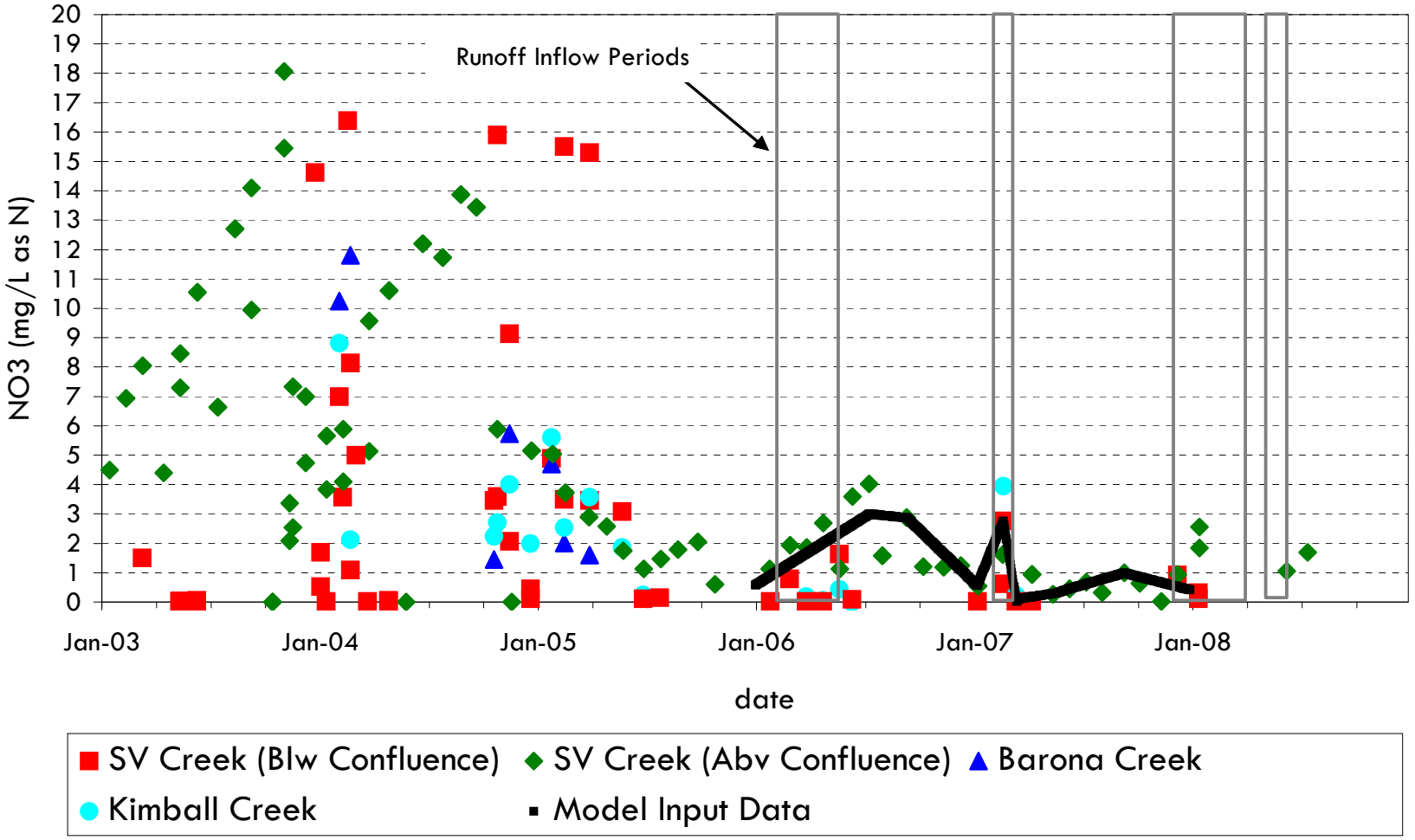

FSI V094005
May 01, 2012

Figure C-31

FLOW SCIENCE®

San Vicente Reservoir

Runoff Inflow Total Nitrogen

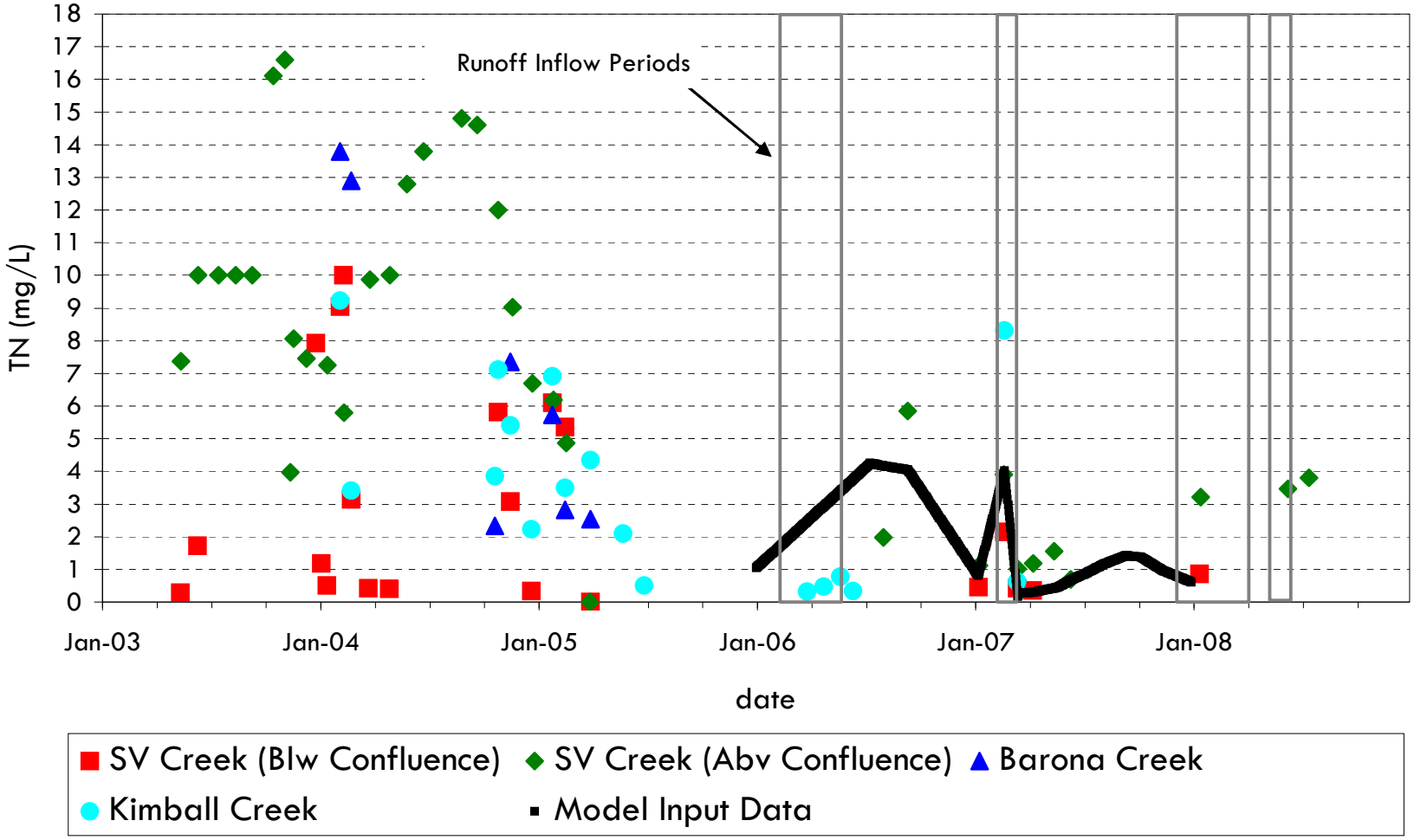

FSI V094005
May 01, 2012

Figure C-32

FLOW SCIENCE®

San Vicente Reservoir

Runoff Inflow Ortho-Phosphate

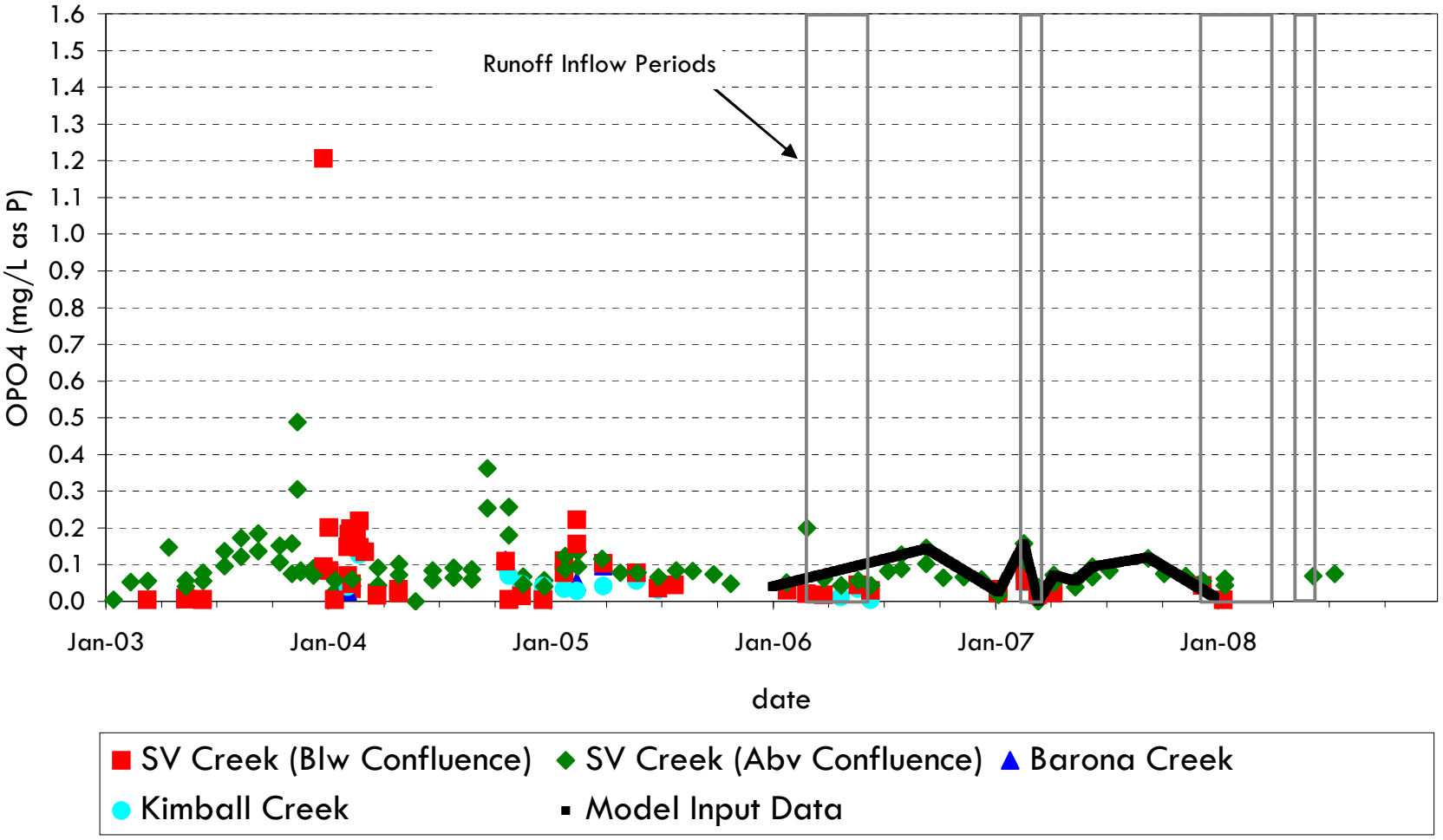

FSI V094005
May 01, 2012

Figure C-33

FLOW SCIENCE®

San Vicente Reservoir

Runoff Inflow Total Phosphorus

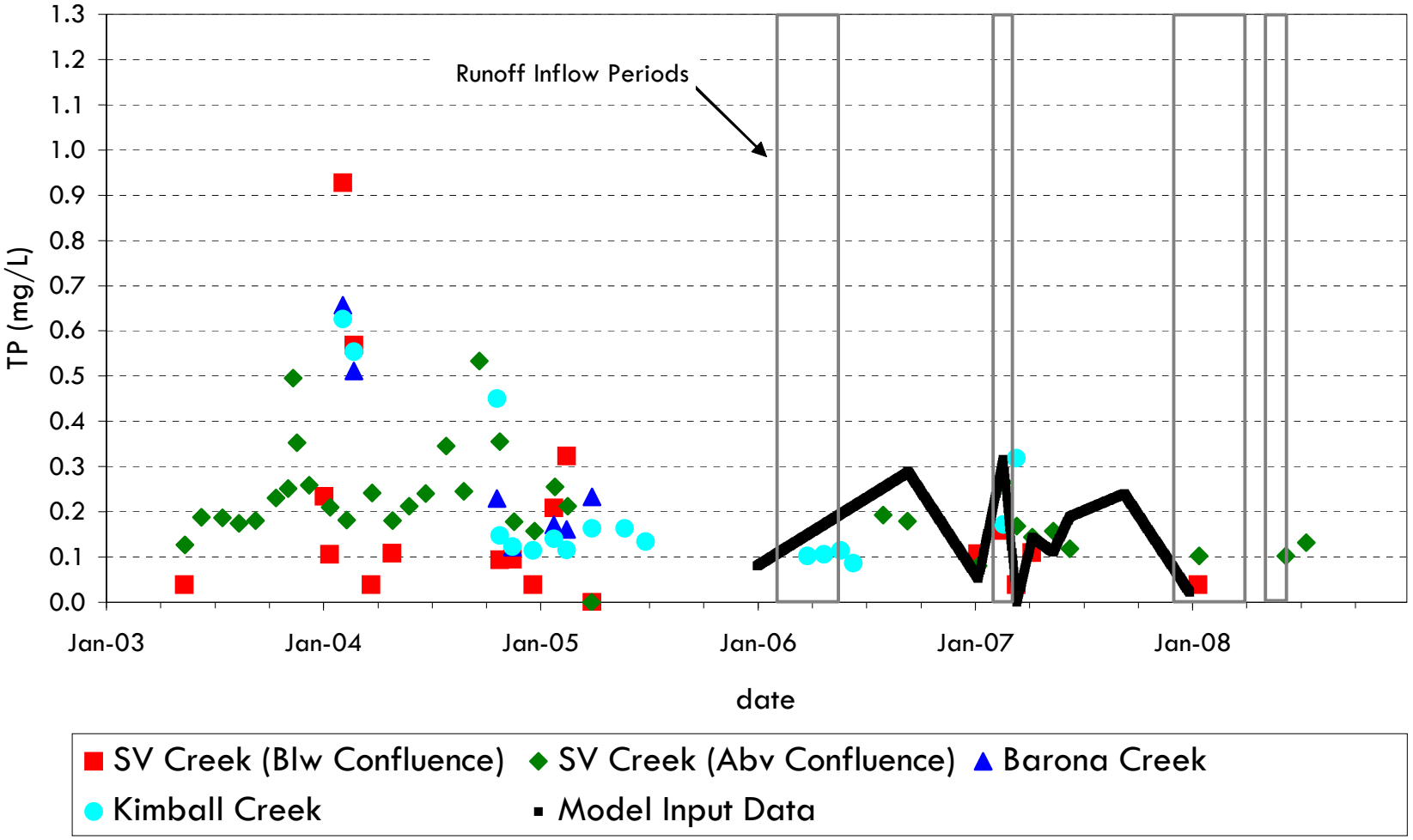

FSI V094005
May 01, 2012

Figure C-34

FLOW SCIENCE®

San Vicente Reservoir

Runoff Inflow Dissolved Oxygen

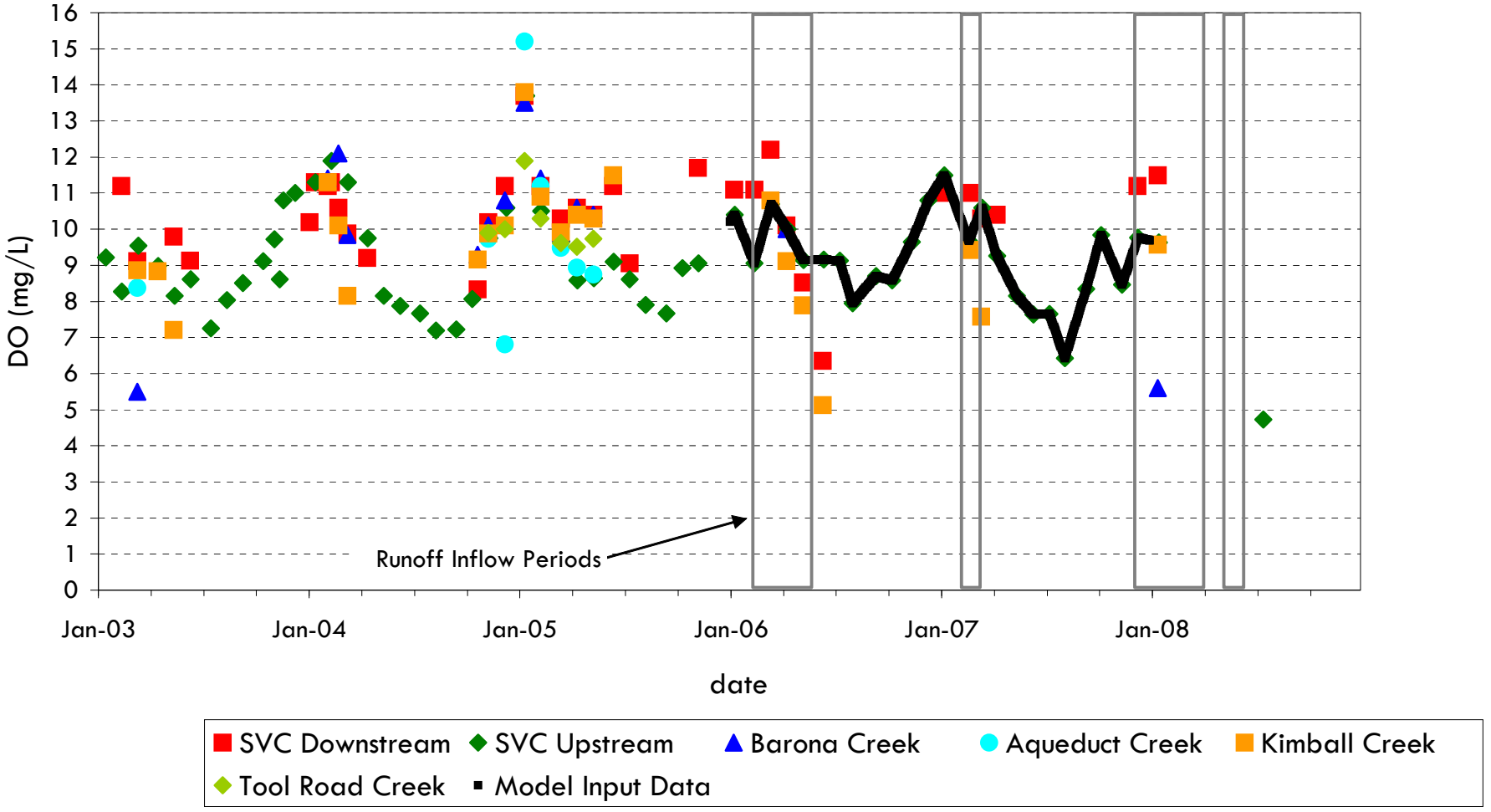

FSI V094005
May 01, 2012

Figure C-35

FLOW SCIENCE®

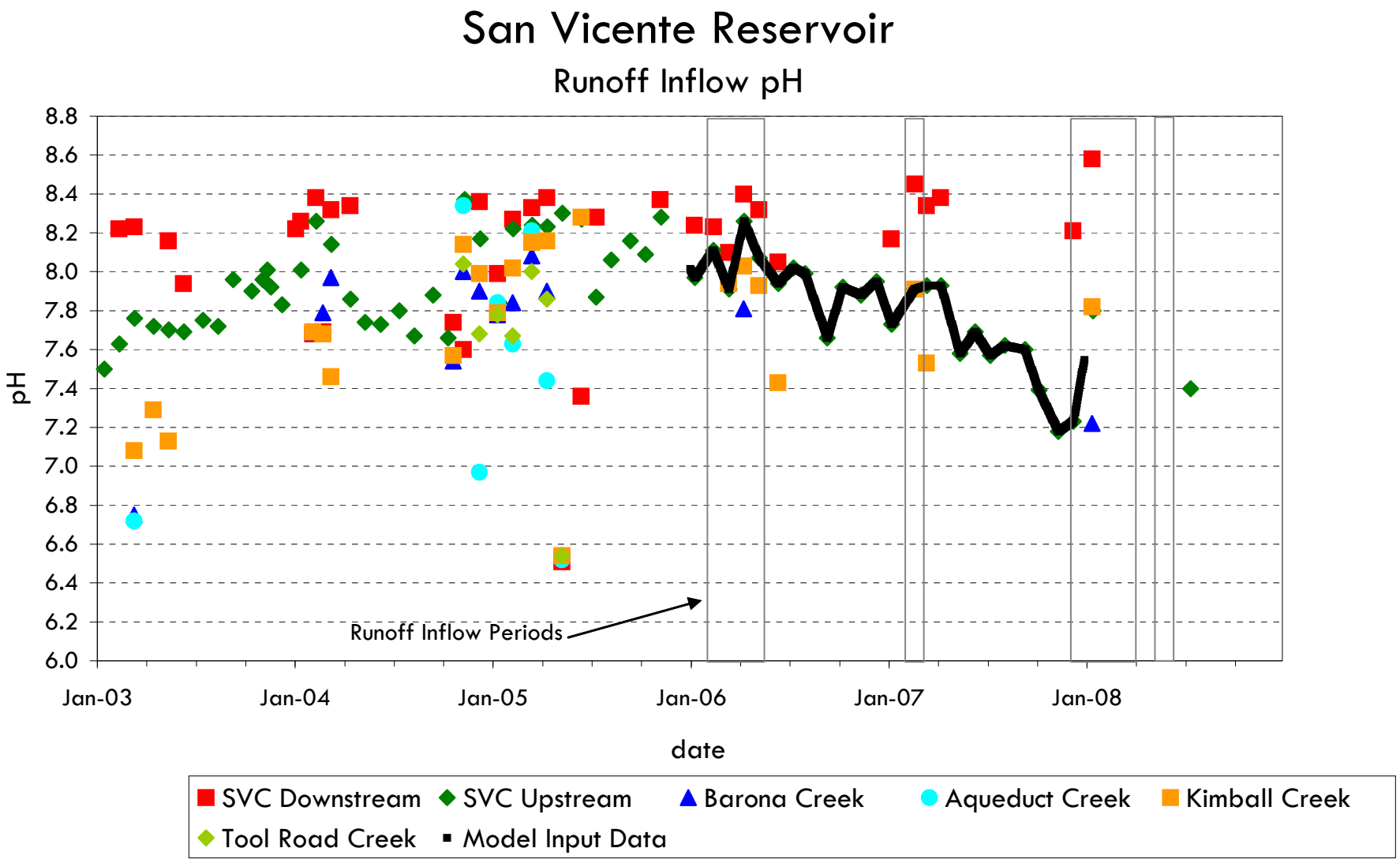

FSI V094005
May 01, 2012

Figure C-36

FLOW SCIENCE®

City of San Diego
Water Quality Laboratory
Sutherland Reservoir Station A Data
January 01, 2006 thru December 31, 2007

Sample Date	Nitrate (mg/L)	Total Nitrogen (mg/L)	Ortho-phosphate (mg/L)	Total Phosphorus (mg/L)
9-Jan-06	< 0.4	0.869	0.253	0.103
6-Apr-06	**< 0.4**	**0.578**	**< 0.2**	**0.109**
10-Jul-06	N/A	0.522	N/A	< 0.078
5-Oct-06	N/A	0.3	N/A	< 0.078
11-Jan-07	< 0.4	0.823	< 0.2	0.264
5-Apr-07	**N/A**	**0.62**	**N/A**	**< 0.078**
9-Jul-07	N/A	0.639	N/A	< 0.078
1-Oct-07	**< 0.4**	**0.493**	**< 0.2**	**< 0.078**
11-Jan-08	< 0.4	0.946	N/A	< 0.078
7-Apr-08	< 0.4	0.779	< 0.2	< 0.078
7-Jul-08	< 0.4	0.363	< 0.2	< 0.078

San Vicente Reservoir

Sutherland Reservoir Dissolved Oxygen Near Outlet (El 1940 ft)

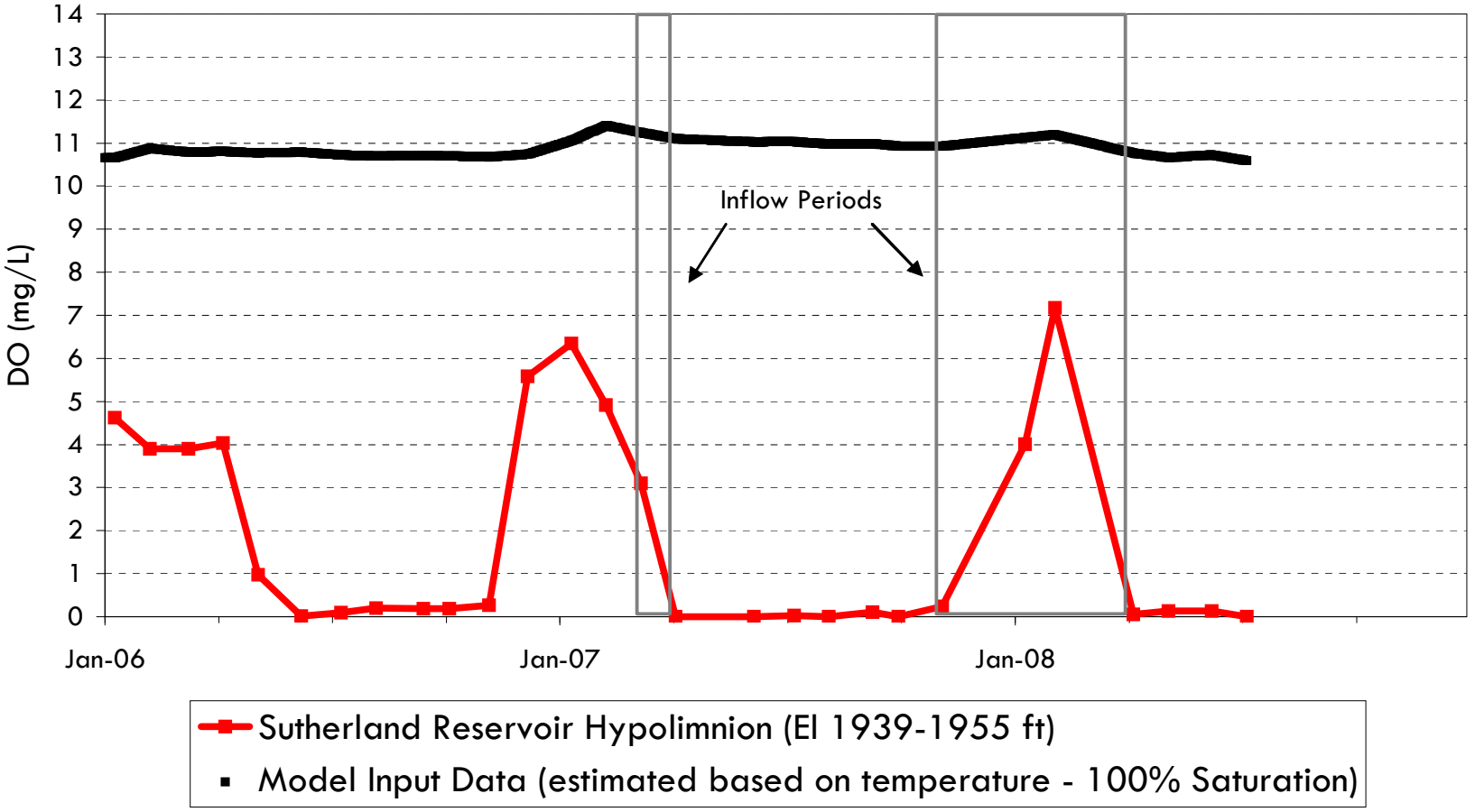

FSI V094005
May 01, 2012

Figure C-38

FLOW SCIENCE®

San Vicente Reservoir

Sutherland Reservoir pH Near Outlet (El 1940 ft)

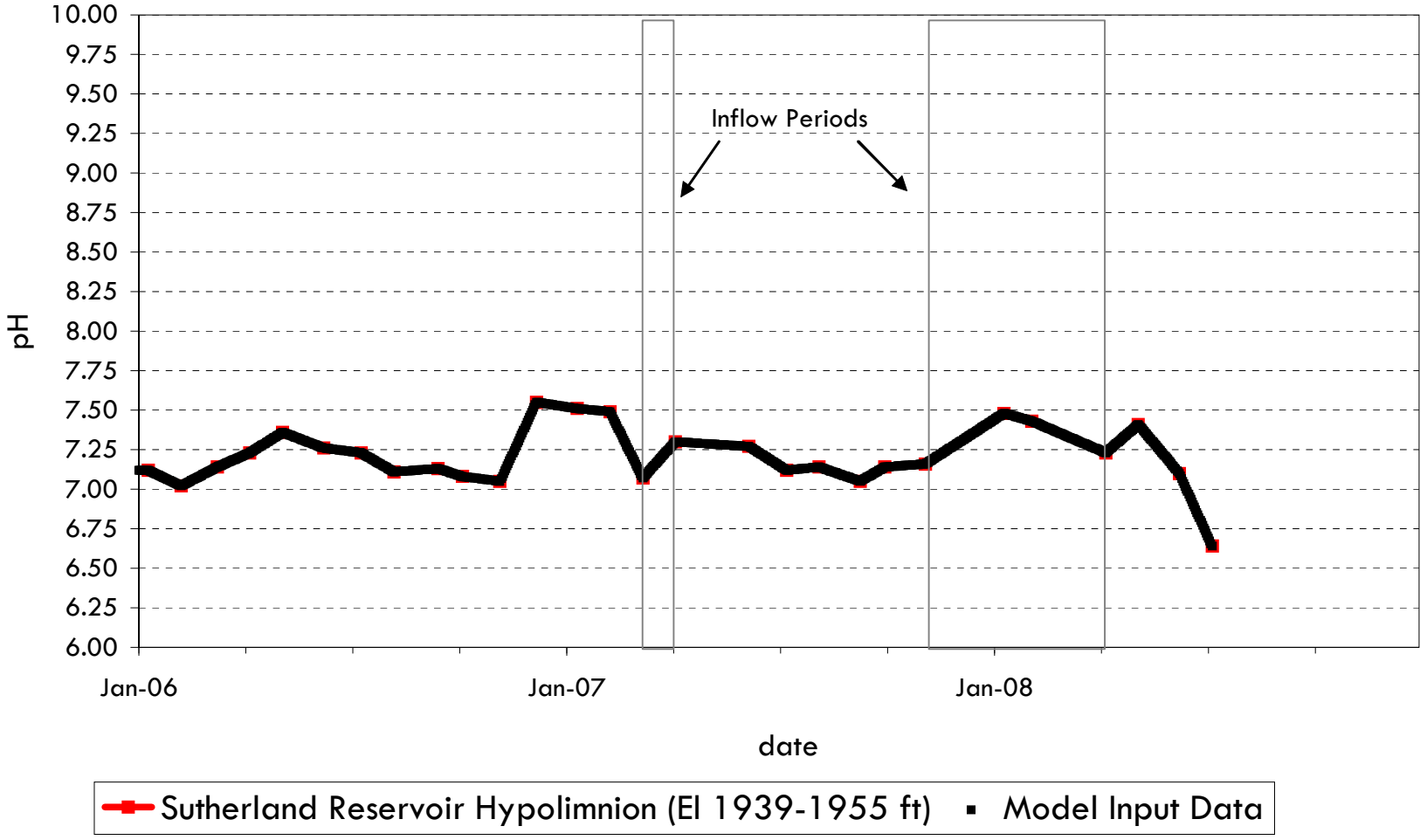

FSI V094005
May 01, 2012

Figure C-39

FLOW SCIENCE®

San Vicente Reservoir

Sutherland Reservoir Chlorophyll a Near Outlet (El 1940 ft)

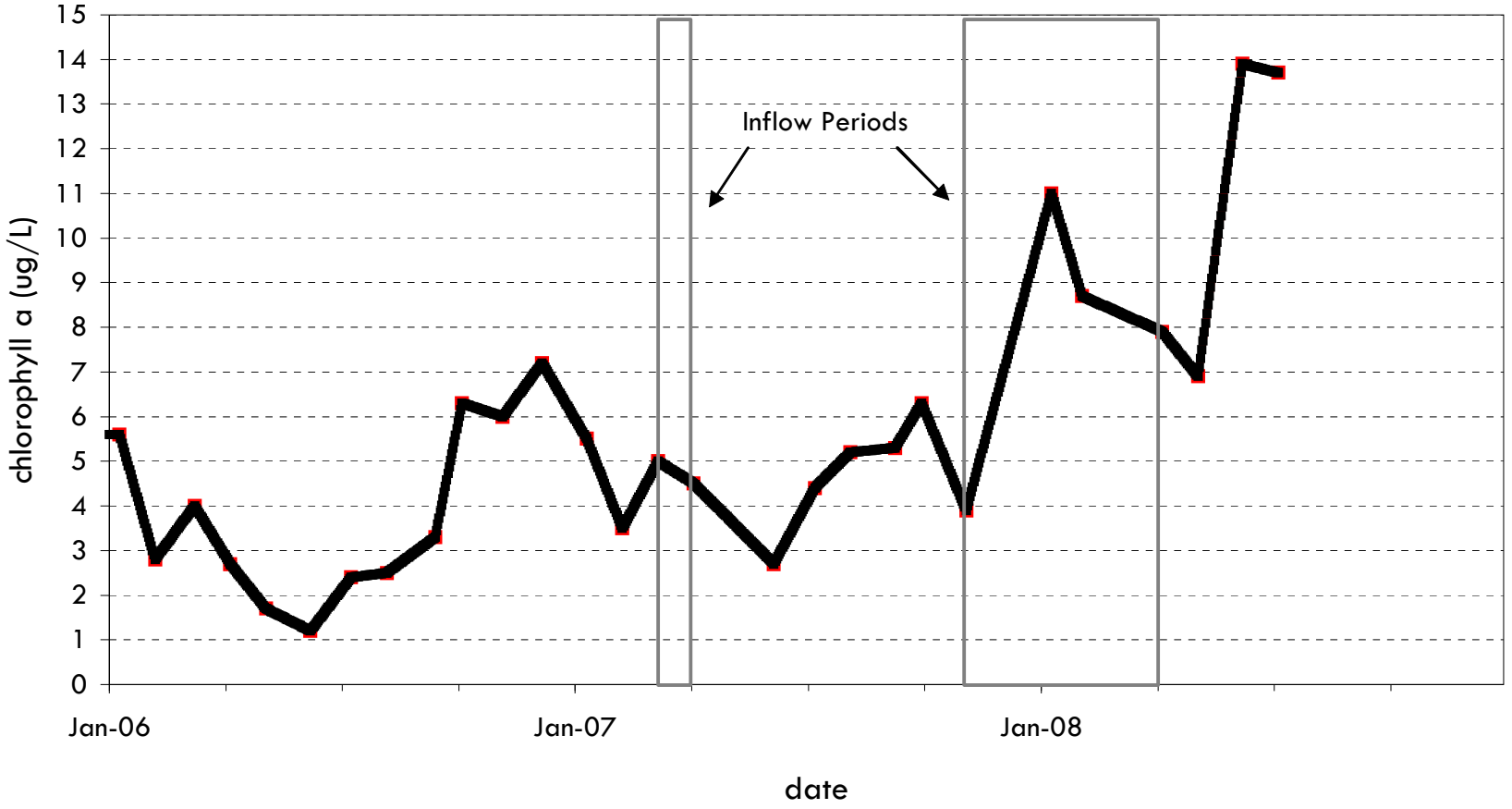

FSI V094005
May 01, 2012

Figure C-40

FLOW SCIENCE®

APPENDIX D

LIST OF ANIMATIONS

INSTRUCTIONS FOR INSTALLING AND USING FRAMER TO VIEW ANIMATION FILES

Installation of Framer

Copy the files from the CD(s) to a directory on your computer.

Running Framer

1) In the Start Menu, choose "run." In this window, type "framer.exe." This should open a "Framer Open File" window, in which you find the proper directory and choose the file that you wish to view.

2) Commands for running the animation files are in the toolbar in the upper left corner of the framer window.

LIST OF ANIMATIONS

1) Appendix D_SVR_Aqueduct_Tracer.rm

Flow Science Incorporated
420 Neff Avenue, Suite 230, Harrisonburg, VA 22801
(540) 442-8433 • FAX (540) 442-8863

Water Purification Demonstration Project: Limnology and Reservoir Detention Study of San Vicente Reservoir - Hydrodynamic Modeling Study

Prepared for
City of San Diego
600 B Street, Suite 600,
San Diego, CA 92101

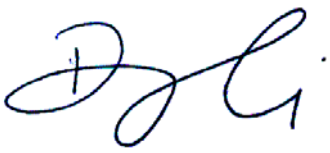

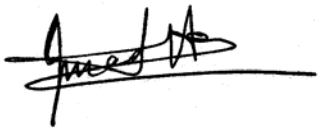

Prepared By
Li Ding, Ph.D., P.E. (VA)
Senior Engineer

Reviewed By
Imad A. Hannoun, Ph.D., P.E. (VA)
President

Reviewed By
E. John List, Ph.D., P.E. (CA)
Principal Consultant

FSI V094005
May 01, 2012

Table of Contents

SUMMARY **1**

1. INTRODUCTION **8**

1.1 Background 8
1.2 Description of the SVR Model 9
1.3 hydrodynamic Effects of SVR expansion 10
1.4 TECHNICAL MEMORANDUM organization 11

2. STUDY OBJECTIVES AND APPROACH **12**

2.1 study objectives 12
2.2 Approach 12

3. SCENARIO MODELING RESULTS **14**

3.1 BASE CASE Scenario 14
3.2 No Purified water scenario 18
3.3 extended drought and emergency drawdown scenarios 19
3.4 Comparison of various purified water INLET locations 24
3.4.1 Evaluation Under the Base Case Operating Conditions *25*
3.4.2 Evaluation Under the Extended Drought Operating Conditions *26*

4. CONCLUSIONS **28**

5. REFERENCES **33**

6. GLOSSARY **34**

FIGURES **37**

APPENDIX A **A-1**

APPENDIX B **B-1**

List of Tables

Table S1 Modeled Operating Scenarios
Table S2 Simulations Conducted for Examining Various Purified Water Inlet Locations
Table S3 Summary of Simulation Results Using Various Purified Water Inlet Locations
Table 1 Monthly Reservoir Inflow and Outflow Volumes for Base Operating Scenario
Table 2 Available Withdrawal Elevations on Proposed Reservoir Outlet Tower
Table 3 Summary of 24-hour Conservative Tracer Simulation Results for the Base Case
Table 4 Monthly Reservoir Inflow and Outflow Volumes for No Purified Water Scenario
Table 5 Monthly Reservoir Inflow and Outflow Volumes for the Extended Drought Scenario
Table 6 Monthly Reservoir Inflow and Outflow Volumes for the Emergency Drawdown Scenario
Table 7 Summary of 24-hour Conservative Tracer Simulation Results for the Extended Drought Scenario
Table 8 Summary of 24-hour Conservative Tracer Simulation Results for the Emergency Drawdown Scenario
Table 9 Summary of 24-hour Conservative Tracer Simulation Results for Various Purified Water Inlet Locations under Base Case Conditions
Table 10 Summary of 24-hour Conservative Tracer Simulation Results for Various Purified Water Inlet Locations under the Extended Drought Conditions

List of Figures

Figure 1 Map of San Vicente Reservoir
Figure 2 SVR Hydrodynamic Grid
Figure 3 SVR Hydrodynamic Model Calibration Results – Station A Water Temperature Comparison
Figure 4 SVR Hydrodynamic Model Calibration Results – Station A – Conductivity Comparison
Figure 5 SVR Hydrodynamic Model Calibration Results - 1995 Winter Tracer Study
Figure 6 SVR Hydrodynamic Model Calibration Results – 1995 Summer Tracer Study
Figure 7 Comparison of Existing and Expanded Reservoir – Simulated Water Temperature at Station A
Figure 8 Comparison of Existing and Expanded Reservoir – Simulated Conductivity at Station A
Figure 9 Base Case: Purified Water Inflow Temperature
Figure 10 Base Case: Simulated Water Temperature and Conductivity at Station A
Figure 11 Base Case: Contours of Simulated Temperature and Decaying Tracer
Figure 12 Base Case: Simulated Decaying Tracer at the Reservoir Outlet Tower
Figure 13 Base Case: Simulated 24-hour Conservative Tracer Concentrations in Reservoir Outflow
Figure 14 Comparison of Base Case and No Purified Water Scenario – Simulated Water Temperature at Station A
Figure 15 Comparison of Base Case and No Purified Water Scenario – Simulated Conductivity at Station A
Figure 16 Inflow and Outflow Rates of Base Case, Extended Drought and Emergency Drawdown Scenarios
Figure 17 Water Volumes of Base Case, Extended Drought and Emergency Drawdown Scenarios
Figure 18 Comparison of Base Case, Extended Drought and Emergency Drawdown Scenarios – Simulated Water Temperature at Station A
Figure 19 Comparison of Base Case, Extended Drought and Emergency Drawdown Scenarios – Simulated Conductivity at Station A
Figure 20 Comparison of Base Case, Extended Drought and Emergency Drawdown Scenarios – Simulated Decaying Tracer Concentrations in the Reservoir Outflow
Figure 21 Extended Drought Scenario Simulated 24-hour Conservative Tracer Concentrations in the Reservoir Outflow
Figure 22 Emergency Drawdown Scenario Simulated 24-hour Conservative Tracer Concentrations in the Reservoir Outflow
Figure 23 Map of the Modeled Purified Water Inlet Locations

Figure 24 Comparison of Reservoir Outflow Decaying Tracer Concentrations from Different Purified Water Inlet Locations Under Base Case Operating Scenario
Figure 25 Comparison of Reservoir Outflow Tracer Concentrations from Different Purified Water Inlet Locations Under Base Case Operating Scenario
Figure 26 Comparison of Reservoir Outflow 24-hour Conservative Tracer Concentrations from Different Purified Water Inlet Locations Under Base Case Operating Scenario
Figure 27 Comparison of Reservoir Outflow 24-hour Conservative Tracer Concentrations from Different Purified Water Inlet Locations Under Base Case Operating Scenario
Figure 28 Comparison of Reservoir Outflow 24-hour Conservative Tracer Concentrations from Different Purified Water Inlet Locations Under Base Case Operating Scenario
Figure 29 Comparison of Reservoir Outflow 24-hour Conservative Tracer Concentrations from Different Purified Water Inlet Locations Under Base Case Operating Scenario
Figure 30 Comparison of Reservoir Outflow 24-hour Conservative Tracer Concentrations from Different Purified Water Inlet Locations Under Base Case Operating Scenario
Figure 31 Comparison of Reservoir Outflow Decaying Tracer Concentrations from Different Purified Water Inlet Locations Under Extended Drought Scenario
Figure 32 Comparison of Reservoir Outflow 24-hour Conservative Tracer Concentrations from Different Purified Water Inlet Locations Under Extended Drought
Figure 33 Comparison of Reservoir Outflow 24-hour Conservative Tracer Concentrations from Different Purified Water Inlet Locations Under Extended Drought Scenario
Figure 34 Comparison of Reservoir Outflow 24-hour Conservative Tracer Concentrations from Different Purified Water Inlet Locations Under Extended Drought Scenario
Figure 35 Comparison of Reservoir Outflow 24-hour Conservative Tracer Concentrations from Different Purified Water Inlet Locations Under Extended Drought Scenario
Figure 36 Comparison of Reservoir Outflow 24-hour Conservative Tracer Concentrations from Different Purified Water Inlet Locations Under Extended Drought Scenario
Figure 37 Comparison of Reservoir Outflow 24-hour Conservative Tracer Concentrations from Different Purified Water Inlet Locations Under Extended Drought Scenario

SUMMARY

BACKGROUND

San Vicente Reservoir (SVR) is located near Lakeside, California, and is used as a source of drinking water supply by the City of San Diego (City), its owner and operator. The reservoir currently has a capacity of about 90,000 acre-feet (see **Figure 1**). It is undergoing an enlargement that will raise the dam 117 feet and increase the reservoir's storage to 247,000 acre-feet at the spillway level (or 242,000 acre-feet at the maximum operation level). The City is considering an option to augment SVR supply by bringing advanced purified recycled water (*i.e.,* purified water) from the advanced water purification facility to SVR. The purified water would be blended with other water in the reservoir. The current project – the Water Purification Demonstration Project (Demonstration Project) – will not actually put any purified water into the reservoir; rather it will study and model the reservoir augmentation process. A component of the Demonstration Project is the Limnology and Reservoir Detention Study of San Vicente Reservoir (Limnology Study).

As part of the Limnology Study, Flow Science Incorporated (FSI) has developed a three-dimensional water quality model that is used to evaluate hydrodynamic and water quality effects of using purified water to augment SVR. After the model was developed, its results were compared to existing field data and documented in the Calibration Technical Memorandum (TM) submitted to the City in 2010 (FSI, 2010). The Calibration TM has been peer-reviewed by the National Water Research Institute Independent Advisory Panel (NWRIIAP) that was assembled for the review of the City's Demonstration Project. After implementing suggestions proposed by the NWRIIAP, the model was deemed by NWRIIAP to be "an effective and robust tool, for 1) simulating thermoclines and hydrodynamics of the San Vicente Reservoir; 2) assessing biological water quality for nutrients; 3) assessing options for the purified water inlet location" (NWRI, 2010).

HYDRODYNAMIC EFFECTS OF RESERVOIR EXPANSION

In order to understand the background conditions where purified water will be stored, the hydrodynamic changes due to the expansion prior to adding purified water were first examined. This was accomplished by running a simulation that uses the same reservoir conditions (climate, inflow and outflow parameters etc.) as the 2006-2007 calibration simulation except for using a higher initial reservoir volume that is close to a full pool. The results from this simulation were compared against those from the original calibration simulation. Based on the comparisons, the following conclusions can be drawn:

- The expanded reservoir is predicted to start stratifying in about March of each year. In the spring and summer, the stratification will intensify. In the fall, the thermocline will start deepening appreciably until the reservoir becomes fully mixed in late fall or early winter. As a result, the reservoir is predicted to be stratified from about March to December, and will be destratified from December to February.

- Reservoir expansion will increase the volume of the hypolimnion but will have a negligible effect on the thermocline depth when the reservoir is stratified. Both surface and bottom reservoir temperatures are expected to remain unchanged due to increased water depth.

RESULTS FOR VARIOUS OPERATING SCENARIOS USING THE DESIGN PURIFIED WATER INLET LOCATION

The main objectives of this study were to use the calibrated and validated SVR computer model to determine the effectiveness of SVR as an environmental buffer and barrier for purified water introduced into SVR, and to evaluate any hydrodynamic changes in SVR induced by the purified water. To achieve these goals, reservoir simulations were conducted to evaluate a number of proposed future reservoir operating scenarios. Firstly, a Base Case simulation was performed to evaluate SVR under expected typical future conditions. This scenario considered a reservoir under median expected storage and normal expected operations. After that, a case was considered whereby no purified water is introduced in the reservoir, enabling a quantification of the effects of purified water addition on the reservoir behavior. Further scenarios were modeled to consider somewhat extreme operations: a scenario with an extended drought and another with emergency drawdown. These scenarios and associated annual flow volumes from various sources are listed in **Table S-1**. The simulations discussed in this section all utilized the Design Purified Water Inlet Location (see **Figure 1** for the location) as the point of release for purified water flow into SVR. Port #2 at the reservoir outlet tower structure was used for all water withdrawals from the reservoir throughout this study.

In these simulations various hypothetical tracers were added to the purified water inflow to illustrate the transport and mixing of the purified water within the reservoir. In particular, decaying tracers (decay rate of 1 log per month, *i.e.*, a reduction in concentration by a factor of 10 per month) were used to study the dilution and inactivation of potential pathogens entering the reservoir and to evaluate the ability of the reservoir to reduce pathogen concentrations before they reach the reservoir outlet. The decaying tracer was continuously released with the purified water inflow at a constant

concentration throughout the entire modeling period. In addition, hypothetical conservative (that is, non-decaying) tracers were added to the purified water inflow in order to simulate the potential effects of elevated concentrations of chemical constituents in the purified water entering SVR after "excursion events" at the water purification facility. These conservative tracers were tracked to determine the dilution and lag time provided by the reservoir (*i.e.*, the time interval between the release of the tracer and peak reservoir outflow concentration). In all simulations, such tracers were added to the reservoir's inflow over a 24-hour period and were thus referred to as 24-hour conservative tracers.

Table S-1. Modeled Operating Scenarios[1,2]

Operating Scenarios	Description	Initial /Final Reservoir Volume (acre-feet)	Annual Purified Water Inflow (acre-feet/year)	Annual Aqueduct inflow (acre-feet/year)	Annual Reservoir Outflow (acre-feet/year)
Base Case	median expected storage and normal expected operations	155,000 /155,000	15,000	3,000	19,000
No Purified Water	no purified water additions and an equal reduction in reservoir outflow	155,000 /155,000	0	3,000	4,000
Extended Drought	a hypothetical two-year drought situation	155,000 /100,000	15,000	3,000	48,000
Emergency Drawdown[3]	a situation where a total of 66,000 acre-feet water is withdrawn from the reservoir in January and February of Year 2 and the reservoir is subsequently refilled by adding 66,000 acre-feet water from the Aqueduct between March and July in Year 2	200,000 /200,000	15,000	69,000	85,000

Note: 1. There are no water transfers from Sutherland Reservoir into SVR.
2. Runoff flow rate is 4,500 acre-feet/year for all scenarios.
3. The table lists the flow volumes for Year 2 for this scenario. Flow volumes for Year 1 are the same as those for the Base Case.

Based on the simulation results, the following conclusions and observations are made for the Base Case:

- The addition of purified water in the expanded reservoir is predicted to slightly deepen the thermocline (*e.g.,* by less than 3 ft in September) and reduce conductivity in the reservoir (compared to the Calibration Run).

- The purified water generally has a lower density (lower conductivity and higher temperature) than the ambient reservoir water. This will cause the purified water to initially spread along the surface of the reservoir near the purified water inlet location. In the stratified reservoir period (typically March to December), the purified water will rapidly mix within the entire epilimnion. As the thermocline gradually deepens, the purified water will gradually approach successively lower ports on the reservoir outlet tower.

- In the unstratified period (December to February), the purified water is predicted to initially flow along the reservoir's surface, but then it will quickly mix over the entire depth, achieving rapid dilution over the entire reservoir volume.

- The proposed withdrawal strategy at SVR will generally utilize deeper ports (Port #2 was considered to be the open port throughout this investigation). Since the purified water will generally flow into the reservoir above the thermocline in the stratified period, it is predicted to typically take several weeks or months for newly released purified water to appear at the reservoir outlet, after undergoing large dilution (*i.e.*, achieving a dilution of at least 2,000). In the reservoir destratified period, the simulations indicate that the purified water can appear at the reservoir outlet within days or weeks after release, but only after undergoing significant dilution (*i.e.*, achieving a dilution of at least 2,000).

- For a decaying tracer released with the purified water (a surrogate for pathogens), the reservoir outflow from the reservoir is predicted to achieve at least a 2-log reduction[1] (100:1 reduction in concentration) in the unstratified period. In the stratified period, the reservoir will provide significantly higher reductions (as high as 9 logs; that is, a 1 trillion reduction).

[1] A log reduction is defined as a 10-fold reduction.

- For a 24-hour conservative tracer that enters the reservoir the simulations indicate that a dilution of at least 2,000 can be obtained in the reservoir outflow.

In the following, conclusions and observations for the Extended Drought and Emergency Drawdown scenarios are listed based on the simulation results. It should be noted that the release dates of the 24-hour conservative tracers for these two scenarios are different from those for the Base Case. The selection of 24-hour conservative tracer release dates for Extended Drought and Emergency Drawdown scenarios was based on identifying critical periods in which the highest reservoir outflow concentrations are most likely to occur (the timings for the 24-hour conservative tracer release for the Base Case were distributed more evenly over the year). From our understanding of the variations in 24-hour conservative tracer release concentrations in the Base Case, the most critical periods are expected to meet the following three conditions: 1) the reservoir is almost or fully mixed vertically; 2) the reservoir water volume is at a minimum; and 3) the occurrence of Santa Ana wind events (events where prevailing winds are expected to rapidly drive purified water introduced at the east side of the reservoir directly toward the reservoir outlet located near the southwest end of the reservoir).

- For a decaying tracer in the purified water inflow under the Extended Drought scenario, the analyses indicate that the reservoir can achieve a 2-log reduction in tracer concentration in the unstratified period and significantly higher values (typically 4-8 log reduction) for the remainder of the year. The minimum predicted dilution and its corresponding lag time for a 24-hour conservative tracer are about 900 and 5 days, respectively, and occurs at the end of Year Two when the reservoir volume is lowest.

- For a decaying tracer in the purified water inflow under the Emergency Drawdown scenario, the results indicate that the reservoir can achieve a 2-log reduction in the unstratified period and significantly higher values (typically 4-10 log reduction) for the remainder of the year. The minimum predicted dilution and its corresponding lag time for a 24-hour conservative tracer are about 1,400 and 8 days, respectively. The minimum predicted dilution here is higher than those obtained from both the Base Case and the Extended Drought scenarios, a result of the larger reservoir volume considered in the Emergency Drawdown Scenario during the winter months.

EFFECT OF PURIFIED WATER INLET LOCATION

Various purified water inlet locations were also evaluated under various operating conditions to examine the effects of varying the purified water inlet location. A total of four different purified water inlet locations were considered under the Base Case operating scenario. These are: the Design Purified Water Inlet Location, Existing Aqueduct Purified Water Inlet Location, New Aqueduct Purified Water Inlet Location, and Barona Arm Purified Water Inlet Location. The Design and New Aqueduct Purified Water Inlet Locations were further evaluated under the Extended Drought operating scenario. All simulations conducted for varying the purified water inlet locations are listed in **Table S-2** and results for the decaying tracer and 24-hour conservative tracers from these simulations are presented in **Table S-3**. Note that the release dates of the 24-hour conservative tracers for these runs are different from those for the runs listed in **Table S-1**.

Based on the simulation results, the conclusions and observations on the effects of varying the purified water inlet location are summarized as follows:

- In the stratified season, utilizing different inlet locations to introduce purified water into SVR is predicted to have little effect on both the decaying and 24-hour conservative tracer concentrations in the reservoir outflow under all scenarios considered (*i.e.*, Base Case and Extend Drought Scenarios).

- For the Design, Existing Aqueduct and Barona Arm Purified Water Inlet Locations, moving the purified water inlet location closer to the reservoir outlet is predicted to generally (but not always) result in slightly higher values in the reservoir outflow concentrations for both the decaying and 24-hour conservative tracers during the unstratified period. However, a minimum 2-log reduction for the decaying tracer and a minimum predicted dilution of 909 for the 24-hour conservative tracer are achieved under all scenarios considered (*i.e.*, Base Case and Extended Drought Scenarios). The lag times for the 24-hour conservative tracer range from 5 to 276 days.

- For the New Aqueduct Purified Water Inlet Location, the modeling shows higher peak concentration values for a 24-hour conservative tracer release in the reservoir outflow in the unstratified period than other purified water inlet locations due to its proximity to the reservoir outlet structure. The minimum achieved dilution is found to be about 385 for the Base Case and 200 for the Extend Drought scenario. The corresponding lag times are typically less than 2 days.

Table S-2. Simulations Conducted for Examining Various Purified Water Inlet Locations

Operating Scenario	Purified Water Inlet Location
Base Case	Design Purified Water Inlet Location
	New Aqueduct Purified Water Inlet Location
	Existing Aqueduct Purified Water Inlet Location
	Barona Arm Purified Water Inlet Location
Extended Drought	Design Purified Water Inlet Location
	New Aqueduct Purified Water Inlet Location

Table S-3. Summary of Simulation Results Using Various Purified Water Inlet Locations

Inlet Location	Operating Scenarios	Minimum Reduction for the Decaying Tracer	Lowest Minimum Dilution for 24-hour Conservative Tracers	Minimum Lag Time[1]
Design Purified Water Inlet Location	Base Case	2-log Reduction	2222	14 days
	Extended Drought	2-log Reduction	909	5 days
Existing Aqueduct Purified Water Inlet Location	Base Case	2-log Reduction	1000	10 days
Barona Arm Purified Water Inlet Location	Base Case	2-log Reduction	1923	39 days
New Aqueduct Purified Water Inlet Location	Base Case	Near 2-log Reduction	385	0.8 days
	Extended Drought	Near 2-log Reduction	196	1.3 days

Note: 1. The minimum lag time does not necessarily correspond to the 24-hour conservative tracer released that results in lowest minimum dilution

1. INTRODUCTION

1.1 BACKGROUND

San Vicente Reservoir (SVR) is located near Lakeside, California, and is used as a drinking water supply by the City of San Diego (City), its owner and operator (**Figure 1**). The reservoir currently has a capacity of about 90,000 acre-feet. It is undergoing an enlargement that will raise the dam by 117 feet and increase the reservoir's storage to 247,000 acre-feet at the spillway level (or 242,000 acre-feet at the maximum operation level).

A water reuse project, entitled Reservoir Augmentation, is being studied by the City. If implemented at full-scale, Reservoir Augmentation would bring advanced purified recycled water (*i.e.,* purified water) from the advanced water purification facility to SVR via a pipeline. The purified water would be blended with other water in the reservoir. The current project – the Water Purification Demonstration Project (Demonstration Project) – will not actually put any purified water into the reservoir; rather it will study and model the Reservoir Augmentation process. A component of the Demonstration Project is the Limnology and Reservoir Detention Study of San Vicente Reservoir (Limnology Study).

As part of the Limnology Study, Flow Science Incorporated (FSI) has developed a three-dimensional water quality model that is used to evaluate hydrodynamic and water quality effects of using purified water to augment SVR. After the model was developed, its results were compared to existing field data and documented in the Calibration Technical Memorandum (TM) submitted to the City in 2010 (FSI, 2010). The Calibration TM has been peer-reviewed by the National Water Research Institute Independent Advisory Panel (NWRIIAP) that was assembled for the review of the City's Demonstration Project. The model was deemed by NWRIIAP, with some fine-tuning, as "an effective and robust tool, for 1) simulating thermoclines and hydrodynamics of the San Vicente Reservoir; 2) assessing biological water quality for nutrients; 3) assessing options for the purified water inlet location" (NWRI, 2010). After the review, all the suggestions by NWRIIAP on fine-tuning the model have been addressed or implemented. Findings and results from the Calibration TM that are relevant to the work presented here are summarized in the next section.

This Technical Memorandum focuses on using the calibrated and validated SVR hydrodynamic model to evaluate the dilution, mixing, and circulation of the purified water in the expanded SVR under various projected reservoir operating scenarios. The detailed results include establishing dilution for purified water in the reservoir; assessing the potential for short-circuiting of purified water between the purified water inlet location and the dam outlet structure; and evaluating various potential purified water

reservoir inlet locations. This work has been performed by Flow Science Incorporated (FSI) of Pasadena, California, under contract to the City of San Diego, California. It is noted that another report that focuses on reservoir water quality (as opposed to hydrodynamics and mixing, which is the focus of this TM) within SVR will be forthcoming.

1.2 DESCRIPTION OF THE SVR MODEL

The three-dimensional SVR model consists of two coupled computer models that simulate both the hydrodynamics and water quality of SVR. These two models are the Estuary Lake and Coastal Ocean DYnamics Model (ELCOM) for hydrodynamic simulation and the Computational Aquatic Ecosystem DYnamics Model (CAEDYM) for water quality simulation. ELCOM requires the user to define boundary conditions, physical inputs, meteorological inputs, and bathymetry in a grid structure. The output from ELCOM consists of predictions for water velocities, temperature, salinity (*i.e.*, conductivity), and concentrations of decaying or conservative tracers in space and time within the body of water. CAEDYM is the water quality module that can be coupled to ELCOM. CAEDYM simulates changes in dissolved oxygen (DO), nutrients, organic matter, pH and chlorophyll *a*. ELCOM can be run independently of CAEDYM, as is the case for the work presented in this report, but CAEDYM requires the use of ELCOM. The coupled models are used to study the spatial and temporal relationships between physical, biological, and chemical variables in SVR. Details on ELCOM and CAEDYM can be found in **Appendix A**.

The modeling domain includes both the existing reservoir as well as the proposed expanded reservoir (**Figure 1**). A grid with a horizontal resolution of 50 × 50 m is used in this investigation – similar to the grid used in the calibration (**Figure 2**). A variable grid size was used in the vertical dimension with a grid size of 1.64 ft (0.5 m) near the surface and expanding in size with depth. This variable size grid enables the highest resolution in regions of steep gradients, while maintaining the execution time of the model within a reasonable span. The calibration was conducted for the two-year period of 2006 and 2007. The input data required by the calibration were either based on the measured data or derived from these data. ELCOM requires limited calibration effort in that the physical aspects of water movements in reservoirs are fairly well understood.

The calibrated model shows good agreement with the measured data for both water temperature and conductivity. The Calibration TM presents various comparisons between model and data. In the following, we discuss the highlights of the Calibration TM. For example, the onset and duration of thermal stratification as well as the deepening rate of the thermocline were predicted accurately by the model (**Figure 3**). In particular both the data and model show that winter water temperatures in the fully mixed reservoir are nearly uniform in the vertical direction at a value near 12 ^{o}C to 13 ^{o}C. By

April, increased solar radiation warms the water surface up to 17 ^{o}C to 18 ^{o}C and thermal stratification starts to develop. This process intensifies and by summer (July through September) the surface temperatures have risen to as high as 28 ^{o}C, while the temperature in the hypolimnion remains nearly unchanged at the winter temperature of 12 ^{o}C to 13 ^{o}C. This large temperature difference indicates that a strong vertical stratification is established in the lake. The thermocline is well defined and located at a depth ranging from 30 to 40 ft as shown in **Figure 3** for both the model and the data. In the fall, surface water temperatures steadily decrease due to reduced solar radiation. This generates convective plumes, which combined with more effective wind mixing, deepens the thermocline to a depth of 60 ft by November. The stratification continues to weaken until the reservoir totally destratifies and becomes fully mixed at the end of the year or beginning of the following year. The variation of conductivity in the reservoir was also well captured by the model (**Figure 4**).

After the model was calibrated, a validation was performed to compare the model against the results of previous tracer field studies. The field studies involved two separate episodes of tracer release in the reservoir (winter 1995 and summer 1995, FSI, 1995). The field studies clearly showed the impacts of stratification (or lack thereof) on the mixing and dispersion of the tracer. The ELCOM model was capable of replicating the main features of the tracer study (**Figures 5** and **6**). In particular, the model was capable of replicating the sinking of the inflow in the winter and its dispersion with time, as well as capturing the magnitude of the dilution (**Figure 5)**. In the summer, the model accurately predicted the insertion of the inflow at the level of the thermocline (**Figure 6)** and the gradual horizontal dispersion and dilution of the inflowing tracer. This validation provides verification and assurance that the model performance is reliable and accurate. Other results of the validation are discussed in the Calibration TM (FSI, 2010).

In conclusion, the SVR model is capable of replicating the stratification, concentration of tracers, as well as water movement in the reservoir. The simulation results are generally in good agreement with the field measurements. Thus the model provides "an effective and robust tool, for simulating thermoclines and hydrodynamics of the San Vicente Reservoir" and for "assessing options for the purified water inlet location" (findings from NWRIIAP, NWRI, 2010). The further ability of the model in "assessing biological water quality for nutrients" will be the subject of a subsequent Technical Memorandum.

1.3 HYDRODYNAMIC EFFECTS OF SVR EXPANSION

The existing SVR has a capacity of 90,000 acre-feet and is currently undergoing an expansion to 247,000 acre-feet that will be completed in 2013. The expanded SVR may then be used to store and dilute purified water from the advanced water purification facility. Thus, it is useful to study hydrodynamic changes due to the expansion prior to

adding purified water and understand the background conditions where purified water will be stored. This was accomplished by running a simulation that uses the same reservoir conditions (climate, inflow and outflow parameters etc.) as the 2006-2007 calibration simulation except for using a higher initial reservoir volume that is close to a full pool. The results from this simulation were compared against those from the original calibration simulation and differences between these two simulations were examined.

Figure 7 shows a comparison of water temperature for the existing reservoir (*i.e.*, the original calibration simulation) and the expanded reservoir (*i.e.*, the calibration simulation with a higher initial reservoir volume). The depth and deepening rate of the thermocline are fairly similar between these two simulations, indicating that the reservoir expansion will cause no major changes in the thickness of the epilimnion and the volume of the epilimnion is somewhat larger, but mostly because of the increase in surface area. However, the thickness and volume of the hypolimnion will be significantly larger for the expanded reservoir. With a larger hypolimnion, the expanded reservoir will destratify a few days later than the existing reservoir in the late fall.

Figure 8 shows a conductivity comparison between the existing and expanded reservoir. Note that conductivity is used to represent salinity in the reservoir throughout this report. As shown, the conductivity decreases in the spring of 2006 for the existing reservoir, a result of the low-conductivity levels from the Aqueduct inflow. For the expanded reservoir, the footprint of the low-conductivity Aqueduct inflow is attenuated in the early spring of 2006 because the Aqueduct inflow mixes with a significantly larger volume of water in the expanded reservoir. This shows that, compared to the existing reservoir, the expanded reservoir will provide a larger buffer that attenuates the effects of fluctuations in the inflow on the water quality in the reservoir. Other than in the spring of 2006, there is little difference in simulated conductivity between the expanded and existing reservoir.

In summary, the reservoir expansion is predicted to cause little change in the temperature, epilimnion depth and water conductivity in the reservoir but it will significantly enlarge the hypolimnion and provide a larger volume of water for dilution.

1.4 TECHNICAL MEMORANDUM ORGANIZATION

This TM provides a detailed description of hydrodynamic effects of discharging purified water into the reservoir, based on the SVR modeling results. **Chapter 2** of the report describes the study objectives and approach. **Chapter 3** presents details of the hydrodynamic simulation results. Conclusions and discussion are provided in **Chapter 4**.

2. STUDY OBJECTIVES AND APPROACH

2.1 STUDY OBJECTIVES

SVR provides a large volume of water for dilution of the repurified water, as well as a storage place where natural assimilation can occur. By holding water for several years on average, the reservoir acts as a settling basin, as well as provides a medium where potential pathogens can decay. In the case of potential spikes in concentration of chemical constituents in the purified water inflow resulting from "excursion events" at the advanced water purification facility, the reservoir also serves as an environmental barrier between the advanced water purification facility upstream and the drinking water treatment facility downstream. The reservoir acts as a barrier in two important ways. First, it offers a large volume of water for dilution and blending of incoming water. Second, the reservoir provides a lag time between the inflows and outflows.

The objectives of this study are to use the calibrated and validated SVR computer model to determine the effectiveness of SVR as an environmental buffer and barrier for purified water and to evaluate hydrodynamic changes in SVR induced by the addition of purified water. Specifically, answers to the following four questions are sought using the SVR model:

- Does purified water cause any hydrodynamic changes in the reservoir?
- Does the reservoir provide a robust year-round pathogen barrier?
- Does the reservoir provide substantial mixing and blending to reduce the effects of potential spikes in concentration of chemical constituents in the purified water inflow resulting from "excursion events" at the advanced water purification facility?
- Does the purified water inlet location within the reservoir affect the above findings?

2.2 APPROACH

To address the aforementioned questions, an analysis approach has been developed in conjunction with the City. It includes using decaying and conservative tracers as surrogates for pathogen and chemical constituents in the purified water to examine the fate and dilution of such constituents that flow into SVR. To achieve that, various tracers were added at specified times to the purified water inflow at a nominal concentration of 100. The movement of purified water in the reservoir is then visually illustrated by

following the contours of the tracer concentration. The dilution achieved by purified water at any location can be obtained by dividing the source tracer concentration (*i.e.*, 100) by the simulated tracer concentration at that location.

It is noted here that the released tracers employed in this study consisted of two types. The first type of tracer was used to simulate viral pathogens that are known to decay with time. As suggested by Welch (2011) and accepted by the NWRIIAP, a first-order exponential decay function with a decay rate of one log per month (half life = 9 days, or decay by a factor of 10 each month) was used to represent a reasonable and conservative method for estimating pathogen decay at SVR. The decaying tracer was continuously released in the purified water inflow at a nominal constant concentration of 100 throughout the whole two-year modeling period. A second type of tracer was used to simulate non-decaying constituents in the purified water that may inadvertently enter the reservoir as a result of a potential excursion event at the advanced water purification facility. In the simulation, such tracers were added to the reservoir's inflow over a 24-hour period and were considered to be conservative (that is, non-decaying). They are thus referred to as 24-hour conservative tracers hereafter.

The specific approaches and methodologies adopted to answer the four questions stated above are the following:

- Comparison of simulated reservoir water temperature and conductivity under various reservoir operation scenarios to examine hydrodynamic changes in the reservoir.

- Comparison of concentrations of the decaying tracer in the reservoir outflow under various reservoir operating scenarios to determine pathogen reduction in the reservoir outflow.

- Selecting critical dates during both the stratified and unstratified periods for the release of the 24-hour conservative tracer (*i.e.*, releasing a conservative tracer for 24 hour period) and then examining the corresponding concentrations and peaking times of these tracers in the reservoir outflow. This allows the calculation of the dilution and lag time provided by the reservoir.

- Comparison of concentrations of decaying and 24-hour conservative tracers in the reservoir outflow originating from different potential purified water inlet locations. This allows the optimal selection of the location where the purified water may be introduced in the reservoir.

3. SCENARIO MODELING RESULTS

In order to help understand the behavior of the reservoir in future conditions if purified water is introduced into SVR, several modeling scenarios were performed. The parameters for these modeling scenarios were determined in collaboration between the City, its consultants, and Flow Science, and based on information provided by the San Diego County Water Authority (SDCWA) about the expected operational schemes for SVR. Firstly, a Base Case simulation was performed to evaluate SVR under expected typical future conditions. This scenario considered a reservoir under median expected storage and normal expected operations. After that, a case was considered whereby no purified water is introduced in the reservoir, enabling a quantification of the effects of purified water addition on the reservoir behavior. Further scenarios were modeled to consider somewhat extreme operations: a scenario with an extended drought and another with emergency drawdown. All preceding operating scenarios utilized the Design Purified Water Inlet Location (see Figure 1 for the location) as the point of release for purified water flow into SVR. Port #2 at the reservoir outlet tower structure was used for all water withdrawals from the reservoir throughout this study. Finally, four alternate inlet locations for the purified water at SVR were evaluated. In the following, we discuss the results of each of these scenarios.

3.1 BASE CASE SCENARIO

The Base Case simulated a two-year period and used the same 2006-2007 meteorological data, Aqueduct inflow water quality data, and other modeling parameters as used in the Calibration, except for the initial reservoir volume, introduction of purified water, and modified inflow and outflow rates as discussed below. The real-world wind data used as inputs for the model included several Santa Ana Wind events that occurred in the winter of each simulated year. The City provided the initial reservoir volume, inflow and outflow rates for the Base Case. The initial reservoir volume for the Base Case is considered to be near the median of the expected future conditions with a volume of 155,000 acre-feet (determined in conjunction with SDCWA). It is considered that the daily flow for all inflows and outflows is constant throughout each month and that there are no water transfers from Sutherland Reservoir into SVR. A new surface inflow, purified water inflow, was added to represent incoming purified water from the advanced water purification facility at an annual rate of 15,000 acre-feet/year. The monthly inflow and outflow volumes for the Base Case are listed in **Table 1**. The purified water inlet for the Base Case is located at the "Design Purified Water Inlet Location" shown in **Figure 1**. As suggested by the City, the multi-year averages of weekly water temperatures at North City Water Reclamation Plant were used to characterize the purified water temperature (**Figure 9**). The salinity of the purified water was considered to be constant at 100 ppm. The available withdrawal elevations on the proposed reservoir outlet are

listed in **Table 2**. In all the simulations presented herein, Port #2 was used for all water withdrawals from the reservoir.

Table 1. Monthly Reservoir Inflow and Outflow Volumes for Base Case Operating Scenario

Month	Aqueduct Inflow (acre-feet)	Runoff Inflow (acre-feet)	Purified Water Inflow (acre-feet)	Withdrawal (acre-feet)
Jan-Year 1	0	0	1440	0
Feb-Year 1	0	1,500	1590	0
Mar-Year 1	0	1,500	1480	0
Apr-Year 1	1,000	1,500	1350	0
May-Year 1	1,000	0	1230	0
Jun-Year 1	1,000	0	1090	0
Jul-Year 1	0	0	900	2200
Aug-Year 1	0	0	1020	4200
Sep-Year 1	0	0	1090	4200
Oct-Year 1	0	0	1120	4200
Nov-Year 1	0	0	1210	4200
Dec-Year 1	0	0	1480	0
Jan-Year 2	0	0	1440	0
Feb-Year 2	0	1,500	1590	0
Mar-Year 2	0	1,500	1480	0
Apr-Year 2	1,000	1,500	1350	0
May-Year 2	1,000	0	1230	0
Jun-Year 2	1,000	0	1090	0
Jul-Year 2	0	0	900	2200
Aug-Year 2	0	0	1020	4200
Sep-Year 2	0	0	1090	4200
Oct-Year 2	0	0	1120	4200
Nov-Year 2	0	0	1210	4200
Dec-Year 2	0	0	1480	0

Table 2. Available Withdrawal Elevations on Proposed Reservoir Outlet Tower

Port	Withdrawal Elevation
6	733 ft
5	708 ft
4	683 ft
3	653 ft
2	623 ft
1	593 ft

Figure 10 shows time-sequenced profiles of simulated temperature and conductivity at Station A (see **Figure 1** for Station A location) for the Base Case. In general, simulated temperatures from the Base Case are similar to those from the Calibration (**Figure 3**) in terms of range of temperature and the development and vertical location of the thermocline. The main difference between the Base Case and the Calibration is the larger hypolimnion in the larger reservoir. The simulated conductivity values for the Base case vary between 740 and 820 µS/cm and are lower than those from the calibration (*i.e.*, 740 – 880 µS/cm). This reduction is mainly due to year-round inflow of purified water with relatively low conductivity.

Figure 11 presents contours of the temperature and decaying tracer along a profile path joining the Design Purified Water Inlet Location to the reservoir outlet near the dam (See **Figure 1** for the path). On the left hand side of **Figure 11** are three snapshots of the temperature contours on 7/1 and 11/30 of Year 1 as well as 1/8 of Year 2. On the right hand side of the figure are decaying tracer concentration contours on the same date. As shown in the top frame, a strong temperature stratification exists on 7/1. At that time, the highest concentrations of the decaying tracer are above the thermocline. This is a result of the fact that the purified water has a lower density than the ambient reservoir water (combination of elevated temperature and lower salinity than the ambient). The purified water initially flows near the surface and then is quickly mixed throughout the epilimnion. While there is some horizontal gradient in tracer concentration, the values above the thermocline are nearly uniform. As the thermocline deepens (11/30 of Year 1), the decaying tracer persists in the entire epilimnion albeit at a lower concentration (due to larger volume in the epilimnion). The concentrations of tracer in the hypolimnion are very low. When the lake completely destratifies (1/8 of Year 2), the decaying tracer concentration is nearly uniform throughout the reservoir. The animations in **Appendix B** show the above phenomena on a daily cycle. Note that the animations are not included in this copy of the report and the reader can contact the City to obtain the animations if needed.

Figure 12 shows the time series of simulated decaying tracer concentrations at all available withdrawal levels (*i.e.*, ports) at the reservoir outlet tower. It should be noted

that water was only withdrawn from Port #2 and the other ports were closed during the simulation. However, it is believed that concentrations sampled at the other ports (aside from Port #2) would approximately represent the reservoir outflow concentrations if that sampled port was open and actually used for withdrawal. Also note that the y-axis in **Figure 12** features a logarithmic scale. This means, for example, with the initial purified water tracer concentration set at 100, a reservoir outflow tracer concentration at 10^{-4} represents a 6-log reduction in concentration (*i.e.*, a million-fold reduction in concentration).

As shown in **Figure 12** and in the animations in **Appendix B**, Port #5, the shallowest port, is generally located inside the epilimnion in which the incoming purified water initially resides. The decaying tracer concentrations at Port #5 remain close to 1 (2-log reduction, this is equivalent to a 100:1 reduction) throughout the simulation period. At Port #1, the deepest port on the reservoir outlet tower, decaying tracer concentrations are generally similar to those at Port #5 during the destratified winter periods, but gradually decrease at the approximate rate of 1-log per month after the onset of stratification (when Port #1 is in the hypolimnion).

As discussed above, the thermocline in the summer months serves as a barrier to inhibit mixing between the epilimnion and hypolimnion. Thus the hypolimnion becomes isolated from the newly added purified water. As a result, hypolimnetic decaying tracer concentrations drop at a rate of 1-log per month throughout the stratified period. When the deepening thermocline reaches the elevation of Port #1 in late fall or early winter, tracer concentrations rise sharply to the level present in the epilimnion. The variation patterns of tracer concentrations at other ports are similar to those at Port #1. The main difference lies in the timing when the tracer concentrations start to rise: a shallower port exhibits an earlier rise in the decaying tracer concentrations in the fall. For reservoir outflow from Port #2, the simulation results show that decaying tracer achieves a 6-log reduction during the summer months and at least a 2-log reduction for the rest of the year.

Figure 13 shows the reservoir outflow concentrations of simulated releases of 24-hour conservative tracers. The tracer releases occurred on 2/1, 4/1, 7/1, 10/1 and 12/30 in the first year of the simulation period and each release lasted for 24 hours. The general trend for all tracers is that concentrations in the reservoir outflow remain very low until the thermocline reaches the level of Port #2. Subsequently, the concentrations rise quickly to a fixed level and stay near that level for the rest of the simulation period (the fixed concentration level can be estimated by considering that the tracer is well mixed in the layer above the port). Details on the maximum tracer concentration as well as the lag time to reach the maximum after release are listed in **Table 3**.

The maximum concentrations for all 24-hour conservative tracers released with purified water remain below 0.05 in the reservoir outflow, indicating a minimum dilution

of 2,000 prior to withdrawal at Port #2 (minimum dilution is computed as the initial concentration, 100 in this case, divided by the maximum observed concentration). The shortest lag time between the release of the 24-hour conservative tracer and peak reservoir outflow concentration (*i.e.*, lag time) is about 31 days and occurs for the tracer released on 12/30, Year 1, a period of reservoir destratification. The longest lag time is about 276 days and corresponds to the tracer released in early spring when the thermocline begins to form. This implies that the time it takes for purified water tracer to reach the reservoir outflow is more controlled by vertical mixing than by horizontal advection and dispersion.

Table 3. Summary of 24-hour Conservative Tracer Simulation Results for the Base Case

Date of Release	Reservoir Outflow Peak Tracer Concentration (%) / Minimum Dilution	Lag Time* (days)
2/1, Year 1	0.037 / 2703	49
4/1, Year 1	0.045 / 2222	276
7/1, Year 1	0.031 / 3226	185
10/1, Year 1	0.037 / 2703	93
12/30, Year 1	0.030 / 3333	31

Note: * Lag Time – time interval between the start of tracer release and occurrence of a concentration peak in the reservoir outflow at Port #2.

3.2 NO PURIFIED WATER SCENARIO

A scenario with no purified water addition was investigated. The inputs for this scenario are similar to those for the Base Case scenario, except for no purified water additions and an equal reduction in reservoir outflow volume. **Table 4** presents the monthly water volumes of inflows and outflow for the No Purified Water scenario. The purpose of conducting this simulation was, by comparing results with the Base Case, to evaluate the hydrodynamic effects of purified water addition on the expanded SVR.

Figures 14 and **15** show comparisons between the Base Case and No Purified Water scenarios for temperature and conductivity, respectively. Note that we use elevation as y-axis in all the figures hereafter to allow labeling the port elevations. The temperature patterns are fairly similar between these two scenarios with similar thermocline development patterns. However, note that the thermocline is slightly deeper for the Base Case (*e.g.*, less than 3 ft in September), a result of adding water in the epilimnion. Without addition of low-conductivity purified water, conductivity is higher for the No Purified Water scenario, especially in the epilimnion (**Figure 15**).

Table 4. Monthly Reservoir Inflow and Outflow Volumes for No Purified Water Scenario

Month	Aqueduct Inflow (acre-feet)	Runoff Inflow (acre-feet)	Purified Water Inflow (acre-feet)	Withdrawal (acre-feet)
Jan-Year 1	0	0	0	0
Feb-Year 1	0	1500	0	0
Mar-Year 1	0	1500	0	0
Apr-Year 1	1000	1500	0	0
May-Year 1	1000	0	0	0
Jun-Year 1	1000	0	0	0
Jul-Year 1	0	0	0	800
Aug-Year 1	0	0	0	800
Sep-Year 1	0	0	0	800
Oct-Year 1	0	0	0	800
Nov-Year 1	0	0	0	800
Dec-Year 1	0	0	0	0
Jan-Year 2	0	0	0	0
Feb-Year 2	0	1500	0	0
Mar-Year 2	0	1500	0	0
Apr-Year 2	1000	1500	0	0
May-Year 2	1000	0	0	0
Jun-Year 2	1000	0	0	0
Jul-Year 2	0	0	0	800
Aug-Year 2	0	0	0	800
Sep-Year 2	0	0	0	800
Oct-Year 2	0	0	0	800
Nov-Year 2	0	0	0	800
Dec-Year 2	0	0	0	0

3.3 EXTENDED DROUGHT AND EMERGENCY DRAWDOWN SCENARIOS

The Extended Drought scenario represents a hypothetical multi-year drought situation where a large and constant volume of water is withdrawn monthly from the reservoir without importing additional water (as compared to the Base Case) to refill the reservoir. **Table 5** lists the monthly inflow and outflow water volumes for this scenario while **Figure 16** shows an inflow and outflow rate comparison between this scenario and the

Base Case. Under the Extended Drought scenario, the volume of water stored in SVR decreases steadily throughout the modeling period from an initial 155,000 acre-feet to slightly below 100,000 acre-feet at the end of the simulation (**Figure 17**). This corresponds to a WSEL (water surface elevation) reduction from 710 ft to about 660 ft. In comparison, the volume of water stored in SVR for the Base Case remains above the initial volume of 155,000 acre-feet and reaches as high as about 170,000 acre-feet (WSEL of about 720 ft) in the middle of the simulation year (**Figure 17**).

Table 5. Monthly Reservoir Inflow and Outflow Volumes for the Extended Drought Scenario

Month	Aqueduct Inflow (acre-feet)	Runoff Inflow (acre-feet)	Purified Water Inflow (acre-feet)	Withdrawal (acre-feet)
Jan-Year 1	0	0	1440	4000
Feb-Year 1	0	1500	1590	4000
Mar-Year 1	0	1500	1480	4000
Apr-Year 1	1000	1500	1350	4000
May-Year 1	1000	0	1230	4000
Jun-Year 1	1000	0	1090	4000
Jul-Year 1	0	0	900	4000
Aug-Year 1	0	0	1020	4000
Sep-Year 1	0	0	1090	4000
Oct-Year 1	0	0	1120	4000
Nov-Year 1	0	0	1210	4000
Dec-Year 1	0	0	1480	4000
Jan-Year 2	0	0	1440	4000
Feb-Year 2	0	1500	1590	4000
Mar-Year 2	0	1500	1480	4000
Apr-Year 2	1000	1500	1350	4000
May-Year 2	1000	0	1230	4000
Jun-Year 2	1000	0	1090	4000
Jul-Year 2	0	0	900	4000
Aug-Year 2	0	0	1020	4000
Sep-Year 2	0	0	1090	4000
Oct-Year 2	0	0	1120	4000
Nov-Year 2	0	0	1210	4000
Dec-Year 2	0	0	1480	4000

The Emergency Drawdown scenario simulates a situation where a large volume of water is withdrawn from the reservoir in January and February of Year 2 and the reservoir is subsequently refilled by adding water from the Aqueduct between March and July in Year 2. The monthly inflow and outflow rates for this scenario are listed in **Table 6** and are plotted against flow rates from the Base Case and Extended Drought scenario in **Figure 16**. The volume of water stored in SVR over the two-year simulation period under this scenario (as well as the Base Case and Extended Drought) is plotted in **Figure 17**. Note that the initial volume of the Emergency Drawdown scenario is set at 200,000 acre-feet (WSEL of about 738 ft) compared to an initial volume for the Base Case and Extended Drought scenarios of 155,000 acre-feet (WSEL of about 710 ft). During the emergency drawdown period, the reservoir water volume is reduced to about 140,000 acre-feet (WSEL of 690 ft). It then climbs rapidly to above 200,000 acre-feet during the refill period.

The purified water inlet location used for both the Extended Drought and Emergency Drawdown scenarios is the "Design Purified Water Inlet Location" (see **Figure 1**), the same as that for the Base Case.

A comparison of simulated water temperature between the Base Case, Extended Drought, and Emergency Drawdown scenarios is shown in **Figure 18**. All three scenarios have a generally similar epilimnion thickness and thermocline deepening rate. A notable exception is the emergence of a thick epilimnion for the Emergency Drawdown scenario in the spring of the second year, a result of the influx of a large amount of inflow into the epilimnion in a short period of time. Since the epilimnion thickness is generally unchanged amongst these three scenarios, the *elevation* of the thermocline is mostly determined by the WSEL. For example, as a result of the steady decrease in WSEL for the Extended Drought scenario, the thermocline reaches the elevation of Port #2 in early September in Year 2 compared to mid-October for the Base Case. For the Emergency Drawdown scenario, the thermocline reaches the elevation of Port #2 in mid-December, a result of the higher WSEL.

A comparison of simulated conductivity between the Base Case, Extended Drought, and Emergency Drawdown scenarios is shown in **Figure 19**. Note that the values of conductivity in the purified water are lower than those in the Aqueduct water. Thus, the levels of conductivity in the reservoir are elevated in Year 2 of the Emergency Drawdown scenario compared to the other two scenarios, a result of using a large volume of Aqueduct water to refill the reservoir after the emergency drawdown. During the rest of simulation period, the conductivity is fairly similar among these three scenarios.

Table 6. Monthly Reservoir Inflow and Outflow Volumes for the Emergency Drawdown Scenario

Month	Aqueduct Inflow (acre-feet)	Runoff Inflow (acre-feet)	Purified Water Inflow (acre-feet)	Withdrawal (acre-feet)
Jan-Year 1	0	0	1440	0
Feb-Year 1	0	1500	1590	0
Mar-Year 1	0	1500	1480	0
Apr-Year 1	1000	1500	1350	0
May-Year 1	1000	0	1230	0
Jun-Year 1	1000	0	1090	0
Jul-Year 1	0	0	900	2200
Aug-Year 1	0	0	1020	4200
Sep-Year 1	0	0	1090	4200
Oct-Year 1	0	0	1120	4200
Nov-Year 1	0	0	1210	4200
Dec-Year 1	0	0	1480	0
Jan-Year 2	0	0	1440	33000
Feb-Year 2	0	1500	1590	33000
Mar-Year 2	19000	1500	1480	0
Apr-Year 2	15000	1500	1350	0
May-Year 2	12000	0	1230	0
Jun-Year 2	12000	0	1090	0
Jul-Year 2	11000	0	900	2200
Aug-Year 2	0	0	1020	4200
Sep-Year 2	0	0	1090	4200
Oct-Year 2	0	0	1120	4200
Nov-Year 2	0	0	1210	4200
Dec-Year 2	0	0	1480	0

Figure 20 shows a comparison of decaying tracer concentrations in the reservoir outflow at Port #2 between the Base Case, Extended Drought and Emergency Drawdown scenarios. In general, all three scenarios show many similarities: tracer concentrations are highest during the destratified winter period with at least a 2-log reduction, steadily decreasing in the summer due to decay, and rise sharply once the thermocline reaches the elevation of the reservoir outlet port. The main difference between these scenarios is the timing of the rise in reservoir outflow tracer concentration. As discussed previously, the

timing of the thermocline reaching the open reservoir outlet mainly depends on the WSEL: the higher the WSEL, the later is the rise. As such, the Extended Drought scenario has the earliest rise, followed by the Base Case then the Emergency drawdown scenario.

Simulated 24-hour conservative tracer concentrations in the reservoir outflow are shown in **Figures 21** and **22** for the Extended Drought and Emergency Drawdown scenarios respectively. It should be noted that the release dates of the 24-hour conservative tracers for these two scenarios are different from those for the Base Case. The selection of 24-hour conservative tracer release dates for these scenarios was based on identifying critical periods in which the highest reservoir outflow concentrations are most likely to occur (the timings for the 24-hour conservative tracer release for the Base Case were distributed more evenly over the year). From our understanding of the variations in 24-hour conservative tracer release concentrations in the Base Case, the critical periods are most likely to occur when the reservoir is near to, or fully, mixed and the water volume in the reservoir is at the lowest. In addition, Santa Ana winds, a wind event where strong and extremely dry east and northeast winds prevail in Southern California, are expected to rapidly drive purified water introduced at the east side of the reservoir directly toward the reservoir outlet located near the west end of the reservoir. Such an event could minimize dilution and lag time between the time when the water enters the reservoir and the time it reaches the reservoir outlet. Thus, the most critical periods are expected to meet the following three conditions: 1) the reservoir is almost or fully mixed vertically; 2) the reservoir water volume is at a minimum; and 3) the occurrence of Santa Ana wind events.

FSI conducted an analysis of meteorological data at SVR to identify Santa Ana wind events. Based on the analysis and the discussion above, the six 24-hour conservative tracer release dates were considered to be: 12/2 of Year 1, 1/6, 1/14, 1/21, 11/29 and 12/2 of Year 2 for the Extended Drought scenario (note that two release dates at the end of Year 2 were chosen for this scenario due to the lower WSEL at the end of Year 2). For the Emergency Drawdown scenario the dates were 12/2 of Year 1, 1/6, 1/14, 1/21, 2/20 and 2/25 of Year 2.

Figures 21 and **22** present simulated reservoir outflow concentrations for all 24-hour conservative tracer releases. The results are also summarized in **Tables 7** and **8**. For the Extended Drought scenario, the maximum observed concentrations at the outflow range from about 0.03 to 0.11, reflecting a minimum dilution range between 900 and 2,700. The smallest dilution occurs for the 24-hour conservative tracer released on 12/2 of Year 2 when the reservoir volume is near the low end of the range. The lag time ranges from 5 to 25 days. For the Emergency Drawdown scenario, the maximum observed concentrations at the outflow range from about 0.03 to 0.07, reflecting a minimum dilution of about 1,400 to 3,000. The lag time ranges from 8 to 120 days.

Table 7. Summary of 24-hour Conservative Tracer Simulation Results for the Extended Drought Scenario

Date of Release	Reservoir Outflow Peak Tracer Concentration (%) / Minimum Dilution	Lag Time* (days)
12/2, Year 1	0.077 / 1299	11
1/6, Year 2	0.034 / 2941	25
1/14, Year 2	0.037 / 2703	37
1/21, Year 2	0.058 / 1724	8
11/29, Year 2	0.11 / 909	5
12/2, Year 2	0.11 / 909	9

Note: * Lag Time – time interval between the start of tracer release and occurrence of tracer concentration peak in the reservoir outflow at Port #2.

Table 8. Summary of 24-hour Conservative Tracer Simulation Results for the Emergency Drawdown Scenario

Date of Release	Reservoir Outflow Peak Tracer Concentration (%) / Minimum Dilution	Lag Time* (days)
12/2, Year 1	0.043 / 2326	31
1/6, Year 2	0.023 / 4348	33
1/14, Year 2	0.025 / 4000	32
1/21, Year 2	0.042 / 2381	8
2/20, Year 2	0.072 / 1388	8
2/25, Year 2	0.031 / 3226	120

Note: * Lag Time – time interval between the start of tracer release and occurrence of tracer concentration peak in the reservoir outflow at Port #2.

3.4 COMPARISON OF VARIOUS PURIFIED WATER INLET LOCATIONS

All simulations discussed prior to this section utilized the "Design Purified Water Inlet Location" as the point of release for purified water flow into SVR. This section focuses on evaluating other potential purified water inlet locations and investigating the location impact on dilution and mixing under different reservoir operating scenarios. A total of four purified water inlet locations were considered under the Base Case operating scenario. Two of these four locations were further evaluated under the Extended Drought operating scenario.

3.4.1 Evaluation Under Base Case Operating Conditions

Four purified water inlet locations were considered under the Base Case operating scenario. These are: Design Purified Water Inlet Location, Existing Aqueduct Purified Water Inlet Location, New Aqueduct Purified Water Inlet Location, and Barona Arm Purified Water Inlet Location. These four locations are illustrated in **Figure 23**. As shown, the Barona Arm Purified Water Inlet Location is the furthest from the reservoir outlet and the New Aqueduct Purified Water Inlet Location is the nearest to the reservoir outlet.

A comparison of decaying tracer reservoir outflow concentrations for tracers released into these four purified water inlet locations is shown in **Figure 24**. The decaying tracer concentrations in the reservoir outflow are fairly similar for all purified water inlet locations. The Barona Arm Purified Water Inlet Location, the furthest from the reservoir outlet, produces slightly lower reservoir outflow tracer concentrations than the other three purified water inlet locations. On the other hand, the New Aqueduct Purified Water Inlet Location, the release point nearest to the reservoir outlet, produces slightly higher reservoir outflow concentrations than the other three. Overall, the differences in reservoir outflow concentrations between different purified water inlet locations are relatively small. All purified water inlet locations can achieve a 6-log reduction in concentration in the summer months and near a 2-log reduction in the destratified period.

Comparison of the 24-hour conservative tracer concentrations in the reservoir outflow for releases at various purified water inlet locations are presented in **Figures 25 – 30** and results are summarized in **Table 9**. **Figure 25** shows that, for a 24-hour conservative tracer released during the destratified period, the New Aqueduct Purified Water Inlet Location features the shortest lag time for the tracer to reach the reservoir outlet. Furthermore, the New Aqueduct Purified Water Inlet location has the highest concentration and lowest minimum dilution at the reservoir outlet. It is noted, however, that the minimum dilution for the New Aqueduct Purified Water Inlet location is over 1,200 (maximum concentration of 0.08).

For releases between April and October, the purified water inlet location has very little effect on the 24-hour conservative tracer concentration at the reservoir outlet, as shown in **Figures 26 – 28**. This finding is a result of the thermocline isolating the reservoir outflow from the purified water during the stratified season regardless of the purified water inlet location. The 24-hour conservative tracers released during the summer do not reach the reservoir outflow until the following late fall when the reservoir is nearly well mixed.

For the 1/5 and 1/15 of Year 2 tracer releases, the results shown in **Figures 29** and **30** indicate that the New Aqueduct Purified Water Inlet Location features the highest

concentrations and lowest minimum dilutions, followed by the Existing Aqueduct Purified Water Inlet Location, Design Purified Water Inlet Location, and Barona Arm Purified Water Inlet Location. Note that the main differences between the various scenarios during these unstratified periods occur in the first few days after tracer release.

As indicated in **Table 9**, minimum dilutions achieved in the reservoir outflow for these releases range from 385 to 3,448 and the lag times vary from 0.8 to 276 days. The purified water inlet location nearest to the reservoir outlet, the New Aqueduct Purified Water Inlet Location, produces the highest peak concentration (*i.e.*, 0.26, corresponding to a dilution of 385) in the reservoir outflow and the peak reaches the reservoir outflow within two days.

Table 9. Summary of 24-hour Conservative Tracer Simulation Results for Various Purified Water Inlet Locations Under Base Case Conditions

Date of Release	Design Purified Water Inlet Location		Existing Aqueduct Purified Water Inlet Location		New Aqueduct Purified Water Inlet Location		Barona Arm Purified Water Inlet Location	
	C/D*	LT**	C/D	LT	C/D	LT	C/D	LT
1/30 Year 1	0.030 / 3333	51	0.038/ 2632	27	0.081/ 1235	0.8	0.033/ 3030	39
4/1 Year 1	0.045 / 2222	276	0.038/ 2632	275	0.042/ 2381	271	0.052/ 1923	271
7/1 Year 1	0.036 / 2778	178	0.034/ 2941	180	0.032/ 3125	182	0.037/ 2703	180
10/1 Year 1	0.037/ 2703	93	0.041/ 2439	88	0.038/ 2632	87	0.045/ 2222	88
1/5 Year 2	0.033/ 3030	17	0.10/ 1000	10	0.26/ 385	1.5	0.030/ 3333	87
1/15 Year 2	0.031/ 3226	14	0.079/ 1266	10	0.13/ 769	0.8	0.029/ 3448	188

Note: * C/D – Reservoir outflow peak tracer concentration (%) / Minimum Dilution
** LT –lag time in days between the start of tracer release and occurrence of tracer concentration peak in the reservoir outflow Port #2.

3.4.2 Evaluation Under the Extended Drought Operating Conditions

The Design Purified Water Inlet Location and the New Aqueduct Purified Water Inlet Locations were further evaluated under the Extended Drought Operating Scenario. **Figure 31** shows a comparison of reservoir outflow decaying tracer concentrations for

tracer releases at these two purified water inlet locations. In general, the concentrations are fairly similar, but as expected the New Aqueduct Purified Water Inlet Location (location nearest to the reservoir outlet) produces slightly higher concentrations overall.

Figures 32-37 show comparisons of the 24-hour conservative tracer in the reservoir outflow for these two locations. The results are also summarized in **Table 10**. As shown in **Table 10,** the maximum concentrations are higher (and minimum dilutions therefore lower) for the New Aqueduct Purified Water Inlet Location. The maximum concentration and minimum dilution at the reservoir outlet are about 0.51 and 196, respectively, and occur for the 24-hour tracer release on 12/2, Year 2. It is noted that several days after release, any effect of the purified water inlet location has become negligible. Also note that in this analysis, all the purified water 24-hour conservative tracers were released in the destratified period. It is expected that little differences in dilutions between purified water inlet locations would be observed for 24-hour conservative tracers released in the stratified period.

Table 10. Summary of 24-hour Conservative Tracer Simulation Results for Various Purified Water Inlet Locations under the Extended Drought Conditions

Date of Release	Design Purified Water Inlet Location		New Aqueduct Purified Water Inlet Location	
	C/D*	LT**	C/D	LT
12/2, Year 1	0.077 /1299	11	0.15 /667	6
1/6, Year 2	0.034 /2941	25	0.19 /526	1.5
1/14, Year 2	0.037 /2703	37	0.25 /400	1.8
1/21, Year 2	0.058 /1724	8	0.24 /417	1.8
11/25, Year 2	0.11 /909	5	0.47 /213	2.5
12/2, Year 2	0.11 /909	9	0.51 /196	1.3

Note: * C/D – Reservoir outflow peak tracer concentration (%) / Minimum Dilution
** T – time lag in days between the start of tracer release and occurrence of tracer concentration peak in the reservoir outflow at Port #2.

4. CONCLUSIONS

The objectives of this study were to use the calibrated and validated SVR computer model to determine the effectiveness of SVR as an environmental buffer and barrier for purified water introduced into SVR, and to evaluate any hydrodynamic changes in SVR induced by the purified water. To achieve these goals, reservoir simulations were conducted to evaluate a number of proposed future reservoir operating scenarios.

First, the model was used to determine the impacts of reservoir expansion on mixing and dilution in the reservoir, without the introduction of any purified water. The model was then used to investigate the effects of the purified water addition on the general hydrodynamics of the reservoir for several different operational scenarios:

- Base Case ---- This scenario considered a reservoir under median expected storage and normal expected operations. The initial reservoir volume for the Base Case is set at 155,000 acre-feet. The annual flow rates for Aqueduct inflow, Runoff, purified water inflow and dam withdrawal are 3,000, 4,500, 15,000 and 19,000 acre-feet/year respectively. There are no water transfers from Sutherland Reservoir into SVR.

- No Purified Water ---- The inputs for this scenario are similar to those for the Base Case scenario, except for no purified water additions and an equal reduction in reservoir outflow. The initial reservoir volume for this scenario is set at 155,000 acre-feet. The annual flow rates for Aqueduct inflow, Runoff, purified water inflow and dam withdrawal are 3,000, 4,500, 0 and 4,000 acre-feet/year respectively. There are no water transfers from Sutherland Reservoir into SVR.

- Extended Drought ---- This scenario represents a hypothetical two-year drought situation where a large and constant volume of water is withdrawn monthly from the reservoir without importing additional water (as compared to the Base Case) to refill the reservoir. The initial reservoir volume for this scenario is set at 155,000 acre-feet. The annual flow rates for Aqueduct inflow, Runoff, purified water inflow and dam withdrawal are 3,000, 4,500, 15,000 and 48,000 acre-feet/year respectively. There are no water transfers from Sutherland Reservoir into SVR. The volume of water stored in SVR at the end of the two-year simulation period is about 100,000 acre-feet.

- Emergency Drawdown ---- The Emergency Drawdown scenario simulates a situation where a total of 66,000 acre-feet water is withdrawn from the reservoir in January and February of Year 2 and the reservoir is subsequently refilled by adding 66,000 acre-feet water from the Aqueduct between March

and July in Year 2. The rest of flow rates for all inflows and outflows are the same as the Base Case. The initial reservoir volume for this scenario is set at 200,000 acre-feet.

Note that all preceding simulations utilized the Design Purified Water Inlet Location as the point of release of purified water flow into SVR. Port #2 was used for all water withdrawals from the reservoir throughout this investigation.

In these simulations various hypothetical tracers were added to the purified water inflow to illustrate the transport and mixing of the purified water within the reservoir. In particular, decaying tracers (decay rate of 1 log per month, *i.e.*, a reduction in concentration by a factor of 10 per month) were used to study the dilution and inactivation of potential pathogens entering the reservoir and to evaluate the ability of the reservoir to reduce pathogen concentrations before they reach the reservoir outlet. The decaying tracer was continuously released with the purified water inflow at a constant concentration throughout the entire modeling period. In addition, hypothetical conservative (that is, non-decaying) tracers were added to the purified water inflow in order to simulate the potential effects of elevated concentrations of chemical constituents in the purified water entering SVR after "excursion events" at the water purification facility. These conservative tracers were tracked to determine the dilution and lag time provided by the reservoir (*i.e.*, the time interval between the release of the tracer and peak reservoir outflow concentration). In all simulations, such tracers were added to the reservoir's inflow over a 24-hour period and were thus referred to as 24-hour conservative tracers.

Finally, various purified water inlet locations were also evaluated under various operating conditions to examine the effects of varying the purified water inlet location. A total of four different purified water inlet locations were considered under the Base Case operating scenario. These are: the Design Purified Water Inlet Location, Existing Aqueduct Purified Water Inlet Location, New Aqueduct Purified Water Inlet Location, and Barona Arm Purified Water Inlet Location. The Design and New Aqueduct Purified Water Inlet Locations were further evaluated under the Extended Drought operating scenario.

Based on the simulation results, the following conclusions and observations are made:

GENERAL CONCLUSIONS ON RESERVOIR EXPANSION

- The expanded reservoir is predicted to start stratifying in about March of each year. In the spring and summer, the stratification will intensify. In the fall, the thermocline will start deepening appreciably until the reservoir becomes fully mixed in late fall or early winter. As a result, the reservoir is predicted

to be stratified from about March to December, and will be destratified from December to February.

- Reservoir expansion will increase the volume of the hypolimnion but will have a negligible effect on the thermocline depth when the reservoir is stratified. Both surface and bottom reservoir temperatures are expected to remain unchanged due to increased water depth.

CONCLUSIONS FOR BASE CASE (DESIGN PURIFIED WATER INLET LOCATION)

- Under the Base Case scenario, the addition of purified water in the expanded reservoir is predicted to slightly deepen the thermocline (*e.g.,* by less than 3 ft in September) and reduce conductivity in the reservoir (compared to the Calibration Run).

- The purified water generally has a lower density (lower conductivity and higher temperature) than the ambient reservoir water. This will cause the purified water to initially spread along the surface of the reservoir near the purified water inlet location. In the stratified reservoir period (typically March to December), the purified water will rapidly mix within the entire epilimnion. As the thermocline gradually deepens, the purified water will gradually approach successively lower ports on the reservoir outlet tower.

- In the unstratified period (December to February), the purified water is predicted to initially flow along the reservoir's surface, but then it will quickly mix over the entire depth, achieving rapid dilution over the entire reservoir volume.

- The proposed withdrawal strategy at SVR will generally utilize deeper ports (Port #2 was considered to be the open port throughout this investigation). Since the purified water will generally flow into the reservoir above the thermocline in the stratified period, it is predicted to typically take several weeks or months for newly released purified water to appear at the reservoir outlet, after undergoing large dilution (*i.e.*, achieving a dilution of at least 2,000). In the reservoir destratified period, the simulations indicate that the purified water can appear at the reservoir outlet within days or weeks after release, but only after undergoing significant dilution (*i.e.*, achieving a dilution of at least 2,000).

- For a decaying tracer released with the purified water (a surrogate for pathogens), the reservoir outflow from the reservoir is predicted to achieve at least a 2-log reduction[2] (100:1 reduction in concentration) in the unstratified period. In the stratified period, the reservoir will provide significantly higher reductions (as high as 9 logs; that is, a 1 trillion reduction).

- For a 24-hour conservative tracer that enters the reservoir the simulations indicate that a dilution of at least 2,000 can be obtained in the reservoir outflow.

CONCLUSIONS FOR EXTENDED DROUGHT & EMERGENCY DRAWDOWN SCENARIOS (DESIGN PURIFIED WATER INLET LOCATION)

- For a decaying tracer in the purified water inflow under the Extended Drought scenario, the analyses indicate that the reservoir can achieve a 2-log reduction in tracer concentration in the unstratified period and significantly higher values (typically 4-8 log reduction) for the remainder of the year. The minimum predicted dilution and its corresponding lag time for a 24-hour conservative tracer are about 900 and 5 days, respectively, and occurs at the end of Year Two when the reservoir volume is lowest.

- For a decaying tracer in the purified water inflow under the Emergency Drawdown scenario, the results indicate that the reservoir can achieve a 2-log reduction in the unstratified period and significantly higher values (typically 4-10 log reduction) for the remainder of the year. The minimum predicted dilution and its corresponding lag time for a 24-hour conservative tracer are about 1,400 and 8 days, respectively. The minimum predicted dilution here is higher than those obtained from both the Base Case and the Extended Drought scenarios, a result of the larger reservoir volume considered in the Emergency Drawdown Scenario during the winter months.

[2] A log reduction is defined as a 10-fold reduction.

EFFECT OF THE PURIFIED WATER INLET LOCATION

- In the stratified season, utilizing different inlet locations to introduce purified water into SVR is predicted to have little effect on both the decaying and 24-hour conservative tracer concentrations in the reservoir outflow under all scenarios considered (*i.e.*, Base Case and Extend Drought Scenarios).

- For the Design, Existing Aqueduct and Barona Arm Purified Water Inlet Locations, moving the purified water inlet location closer to the reservoir outlet is predicted to generally (but not always) result in slightly higher values in the reservoir outflow concentrations for both the decaying and 24-hour conservative tracers during the unstratified period. However, a minimum 2-log reduction for the decaying tracer and a minimum predicted dilution of 909 for the 24-hour conservative tracer are achieved under all scenarios considered (*i.e.*, Base Case and Extended Drought Scenarios). The lag times for the 24-hour conservative tracer range from 5 to 276 days.

- For the New Aqueduct Purified Water Inlet Location, the modeling shows higher peak concentration values for a 24-hour conservative tracer release in the reservoir outflow in the unstratified period than other purified water inlet locations due to its proximity to the reservoir outlet structure. The minimum achieved dilution is found to be about 385 for the Base Case and 200 for the Extend Drought scenario. The corresponding lag times are typically less than 2 days.

5. REFERENCES

City of San Diego (2008). "IPR Description for BOR Grant 122208 MS," obtained from Jeffery Pasek of the City of San Diego through e-mail on December 23, 2008.

Flow Science Incorporated (1995). "San Vicente Water Reclamation Project: Results of Tracer Studies, prepared for Montgomery Watson", FSI Project No. P941003, Pasadena, CA.

Flow Science Incorporated (2010). "Reservoir Augmentation Demonstration Project: Limnology and Reservoir Detention Study of San Vicente Reservoir – Calibration of the Water Quality Model", FSI Project No. V094005, Pasadena, CA.

National Water Research Institute (2010). "Findings and Recommendations of the Limnology and Reservoir Subcommittee Meeting for the Reservoir Augmentation Demonstration Project's 'Limnology and Reservoir Detention Study of the San Vicente Reservoir' " Memorandum from NWRI Independent Advisory Panel for the City of San Diego's Indirect Potable Reuse/Reservoir Augmentation Demonstration Project, June 7, 2010.

Welch, M.R. (2011). "Potential Pathogen Inactivation at San Vicente Reservoir", dated May, 2011 and submitted to the City of San Diego.

6. GLOSSARY

Advanced Water Purification Facility: The demonstration facility located at the North City Water Reclamation Plant. The facility is considered "advanced" because of the high level of treatment utilizing reverse osmosis and advanced oxidation.

Blending: Mixing or combining one water source with another such as purified water with raw water sources.

Conductivity: see "Salinity".

Constituent: In water, a constituent is a dissolved chemical element or compound or a suspended material that is carried in the water.

Drought: A defined period of time when rainfall and runoff in a geographic area are much less than average.

Epilimnion: Natural thermal stratification exists for much of the year in almost all temperate lakes and reservoirs and creates three vertical zones. The upper, warmer water is called the epilimnion, the deeper, colder water is called the hypolimnion, whereas the middle portion separating these two layers, where the rate of vertical temperature change is greatest, is called the metalimnion, or thermocline.

Excursion events at the advanced purification facility: Events in which the water quality of the recycled water into the advanced purification facility deviates from the normal or expected conditions. They result in that the final outflow from the advanced purification facility may contain chemical constituents at higher level than normal concentrations when no such events occur.

Hypolimnion: see "epilimnion".

Pathogens: Disease-causing organisms. The general groupings of pathogens are viruses, bacteria, protozoa, and fungi.

Periods of mixing: Periods when water temperatures become vertically uniform in the water body and they generally occur in the winter.

Purified water: Recycled water that has been treated to an advanced level beyond tertiary treatment, so that it can be added to water supplies ultimately used for drinking water. The treatment includes membrane filtration with microfiltration or ultrafiltration, reverse osmosis (RO), and advanced oxidation that consists of disinfection with

ultraviolet light (UV) and hydrogen peroxide (H_2O_2). Purified water may be released into a groundwater basin or surface water reservoir that supplies water to a drinking water treatment facility.

Purified water inflow: Purified water that is transported from the advanced purified water treatment facility to the SVR.

Purified water inlet: Point of release in the SVR for purified water inflow. Note that the purified water is assumed to be released at the surface of the SVR.

Recycled water: Water that originated from homes, businesses and drains as municipal wastewater and has undergone a high level of treatment at a reclamation facility so that it can be beneficially reused for a variety of purposes. This is the water that comes into the AWP Facility.

Reservoir: A manmade lake or tank used to collect and store water.

Reservoir augmentation: The process of adding purified water to a surface water reservoir. The purified water undergoes advanced treatment (membrane filtration, reverse osmosis and UV disinfection/advanced oxidation). The purified water is then blended with untreated water in a reservoir. The blended water is then treated and disinfected at a conventional drinking water treatment plant and is distributed into the drinking water delivery system. Also known as "surface water augmentation."

Reservoir outflow: The flow withdrawal through the opening port located at the outlet structure near the dam.

Reservoir outlet: The opening port at the outlet structure near the dam. In this study, the opening port is assumed to be Port #2.

Salinity: The concentration of mineral salts dissolved in water. Salinity may be measured by weight (total dissolved solids or TDS) or by electrical conductivity. Salinity and TDS are both measures of the amount of salt dissolved in water, and the terms are often used interchangeably. Generally, salinity is used when referring to water with a lot of salt (*e.g.*, seawater), whereas TDS is used to refer to water with little salt (*e.g.*, freshwater).

Storage: Water held in a reservoir for later use.

Surface water: Water located on the Earth's surface, in a river, stream, lake, pond or surface water reservoir.

Thermocline: see "epilimnion".

Water Purification Demonstration Project (Demonstration Project): The second phase of the City of San Diego's Water Reuse Program. During this test phase the Advanced Water Purification Facility will operate for approximately one year and will produce 1 million gallons of purified water per day. A study of the San Vicente Reservoir is being conducted to test the key functions of reservoir augmentation and to determine the viability of a full-scale project. No purified water will be sent to the reservoir during the demonstration phase.

Water Measurement Terms

Milligrams per liter (mg/L) ***also known as parts per million (ppm):*** A measurement describing the amount of a substance (such as a mineral, chemical or contaminant) in a liter of water; a unit used to measure concentration of water constituents (parts of something per million parts of water). One part per million is equal to one milligram per liter. (This term is becoming obsolete as instruments measure smaller concentrations.) This is equivalent to one drop of water diluted into 50 liters (roughly the fuel tank capacity of a compact car) or about thirty seconds out of a year.

Acre-foot (AF): A unit of water commonly used in the water industry to measure large volumes of water. It equals the volume of water required to cover one acre to a depth of one foot. An acre-foot is 325,851 gallons (43,560 cubic feet) and is considered enough water to meet the needs of two families of four with a house and yard for one year.

µS/cm: A basic unit of water conductivity. It stands for microSiemens per meter. Distilled water has a conductivity in the range of 0.5 to 3 µS/cm. The conductivity of rivers in the United States generally ranges from 50 to 1500 µS/cm.

FIGURES

Map of San Vicente Reservoir

Plan View of Existing and Expanded Reservoir and Inflow/Outflow Locations

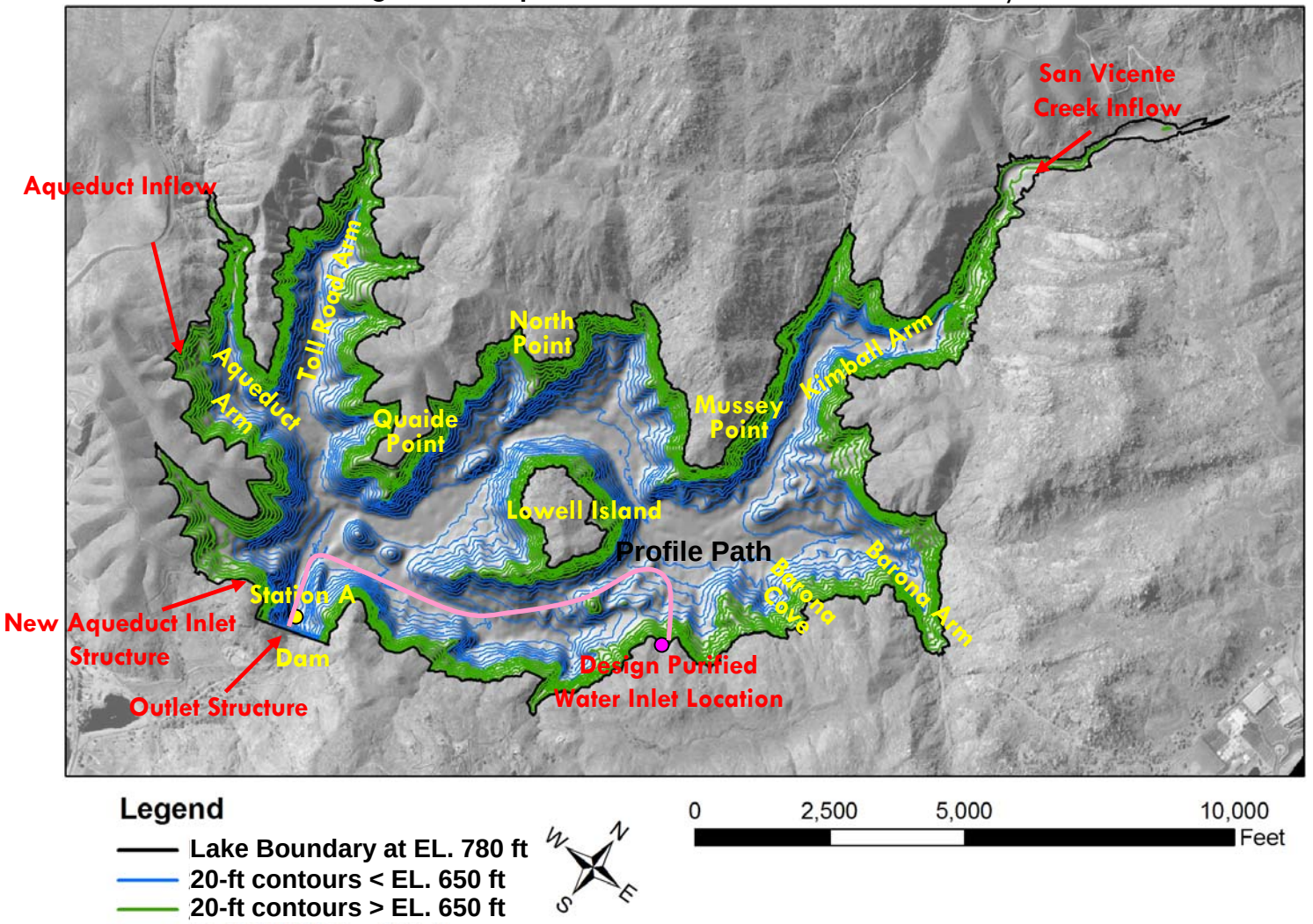

FSI V094005
May 01, 2012

Figure 1

FLOW SCIENCE®

SVR Hydrodynamic Model Grid

(Grid Size = 50 m)

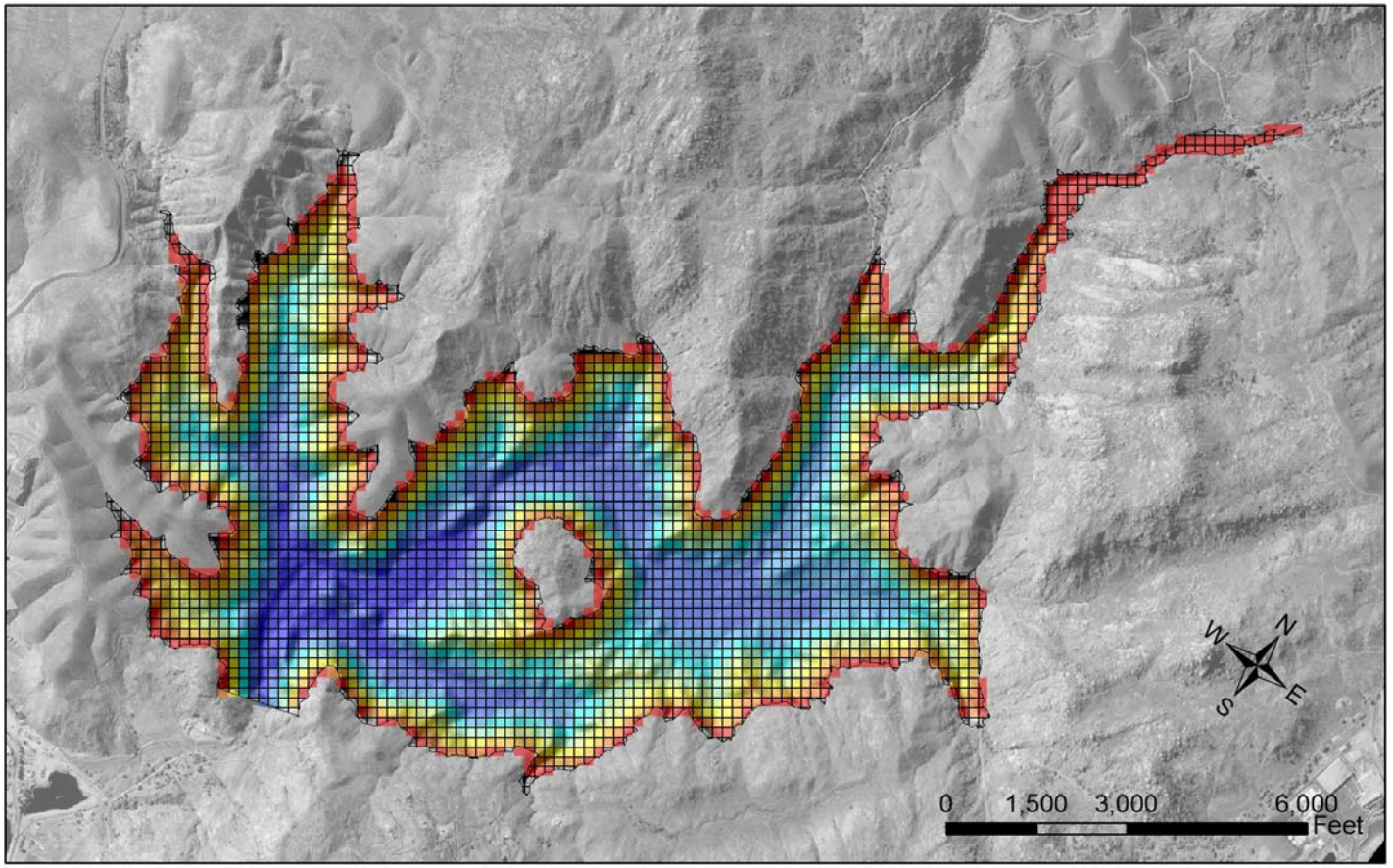

Legend

Lake Boundary at 780 ft

Elevation (ft)

480 - 510
511 - 540
541 - 569
570 - 599
600 - 629
630 - 659
660 - 689
690 - 718
719 - 748
749 - 778

Figure 2

FSI V094005
May 01, 2012

FLOW SCIENCE®

SVR Hydrodynamic Model Calibration Results

Station A – Water Temperature Comparison

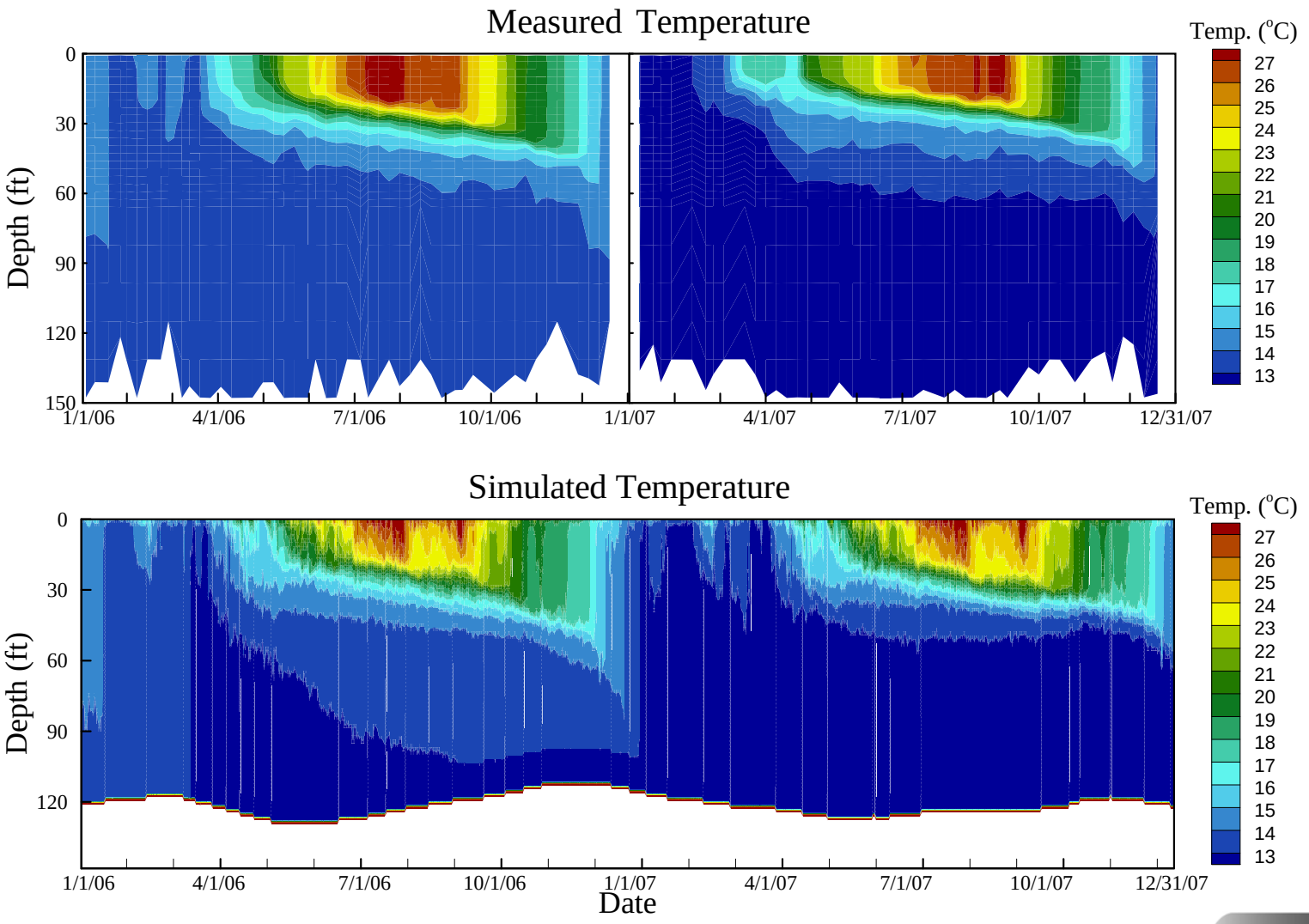

Figure 3

FSI V094005
May 01, 2012

FLOW SCIENCE®

SVR Hydrodynamic Model Calibration Results

Station A – Conductivity Comparison

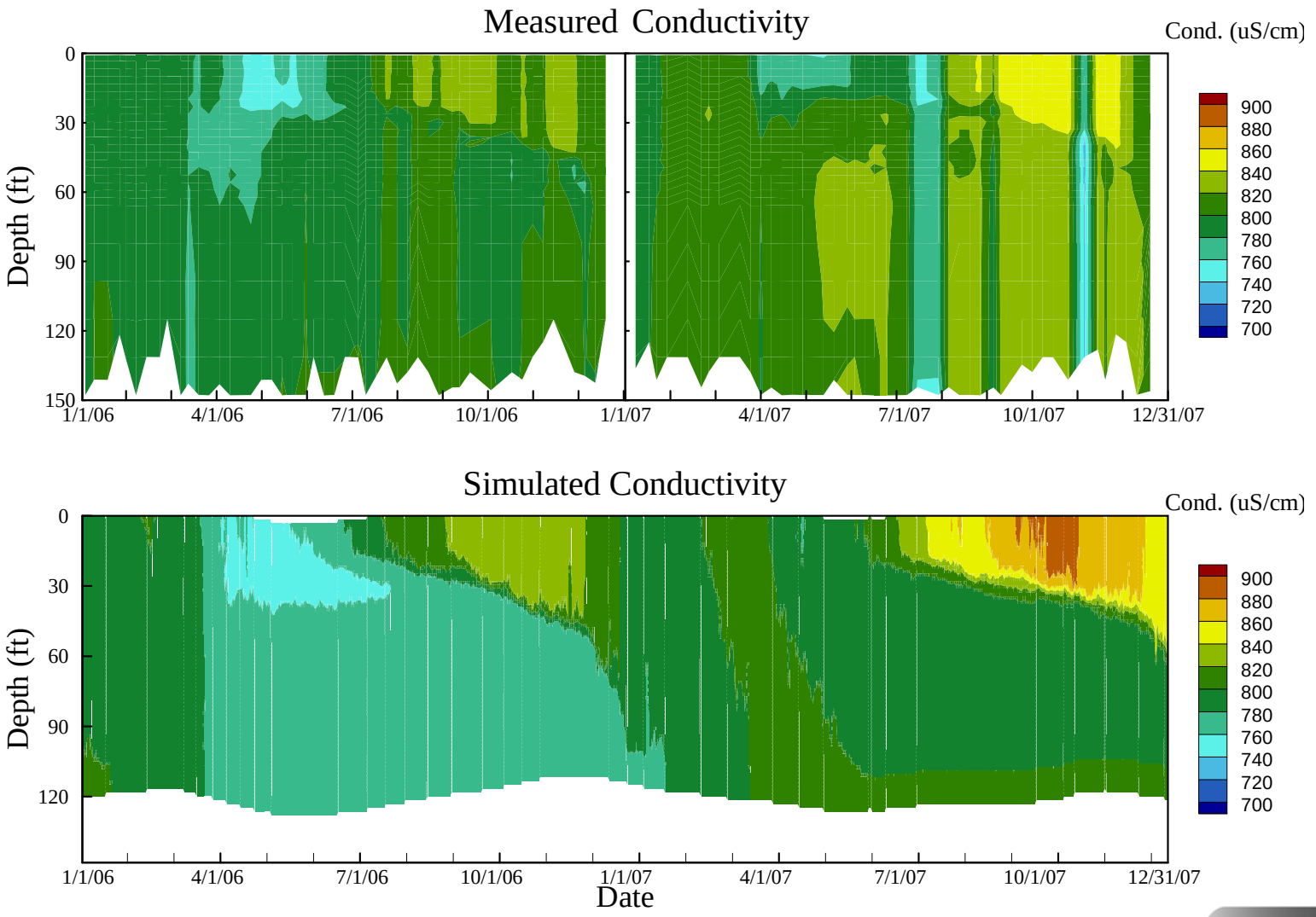

Figure 4

FSI V094005
May 01, 2012

FLOW SCIENCE®

SVR Hydrodynamic Model Calibration Results

1995 Winter Tracer Study – Measured versus Simulated Lanthanum Concentrations

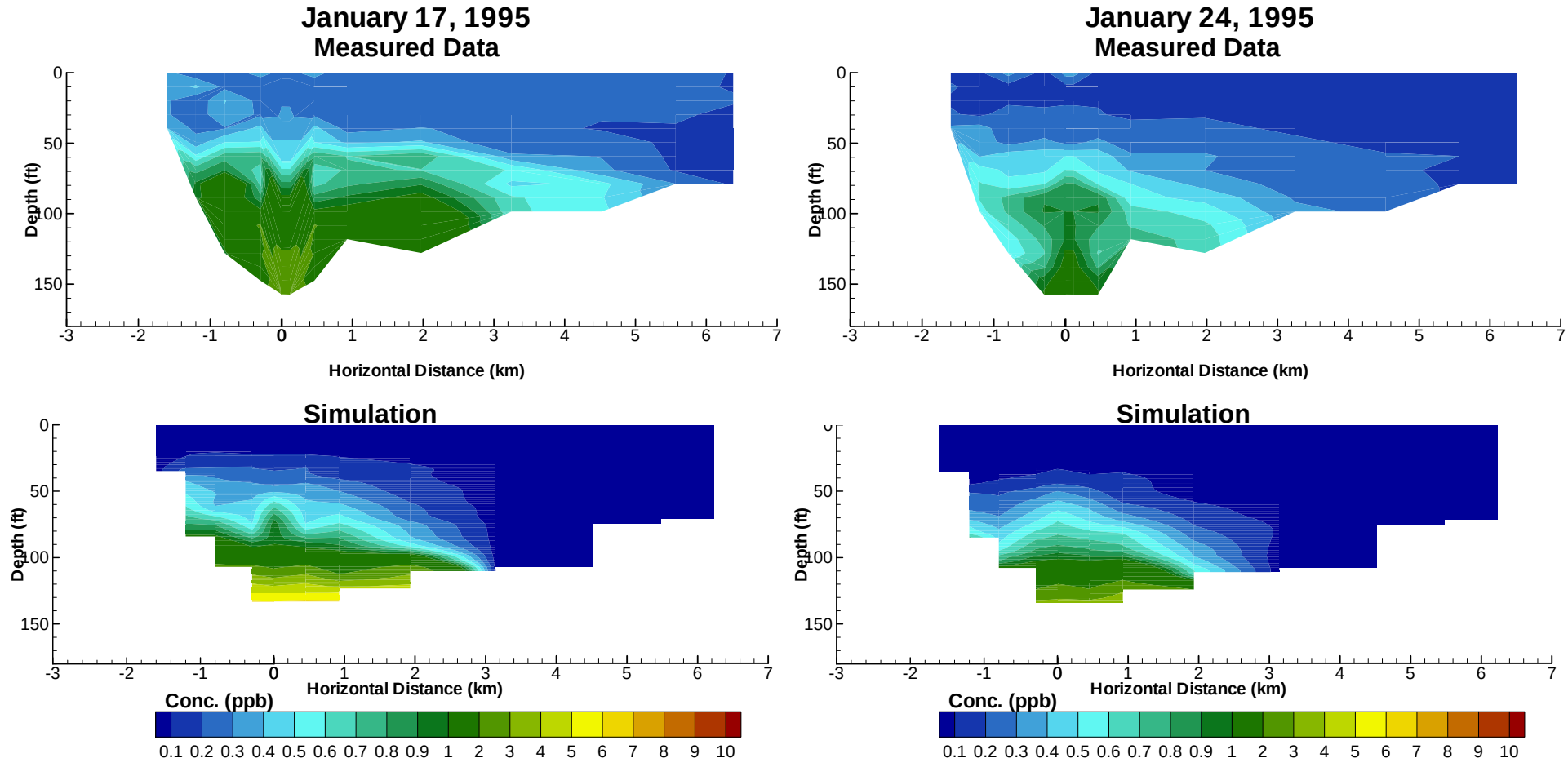

FSI V094005
May 01, 2012

Figure 5

FLOW SCIENCE®

SVR Hydrodynamic Model Calibration Results

1995 Summer Tracer Study – Measured versus Simulated Lanthanum Concentrations

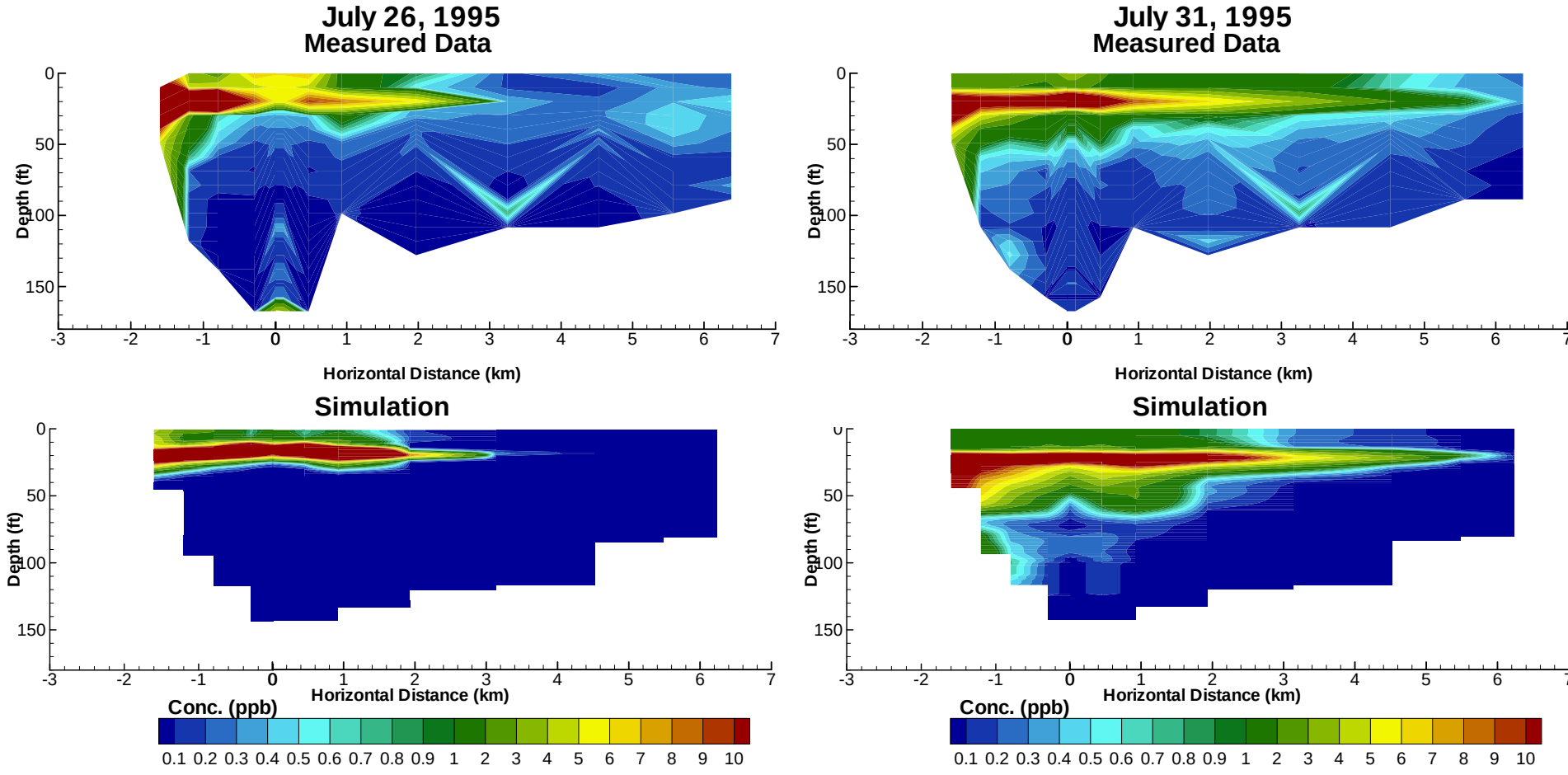

FSI V094005
May 01, 2012

Figure 6

FLOW SCIENCE®

Comparison of Existing and Expanded Reservoir

Simulated Water Temperature at Station A

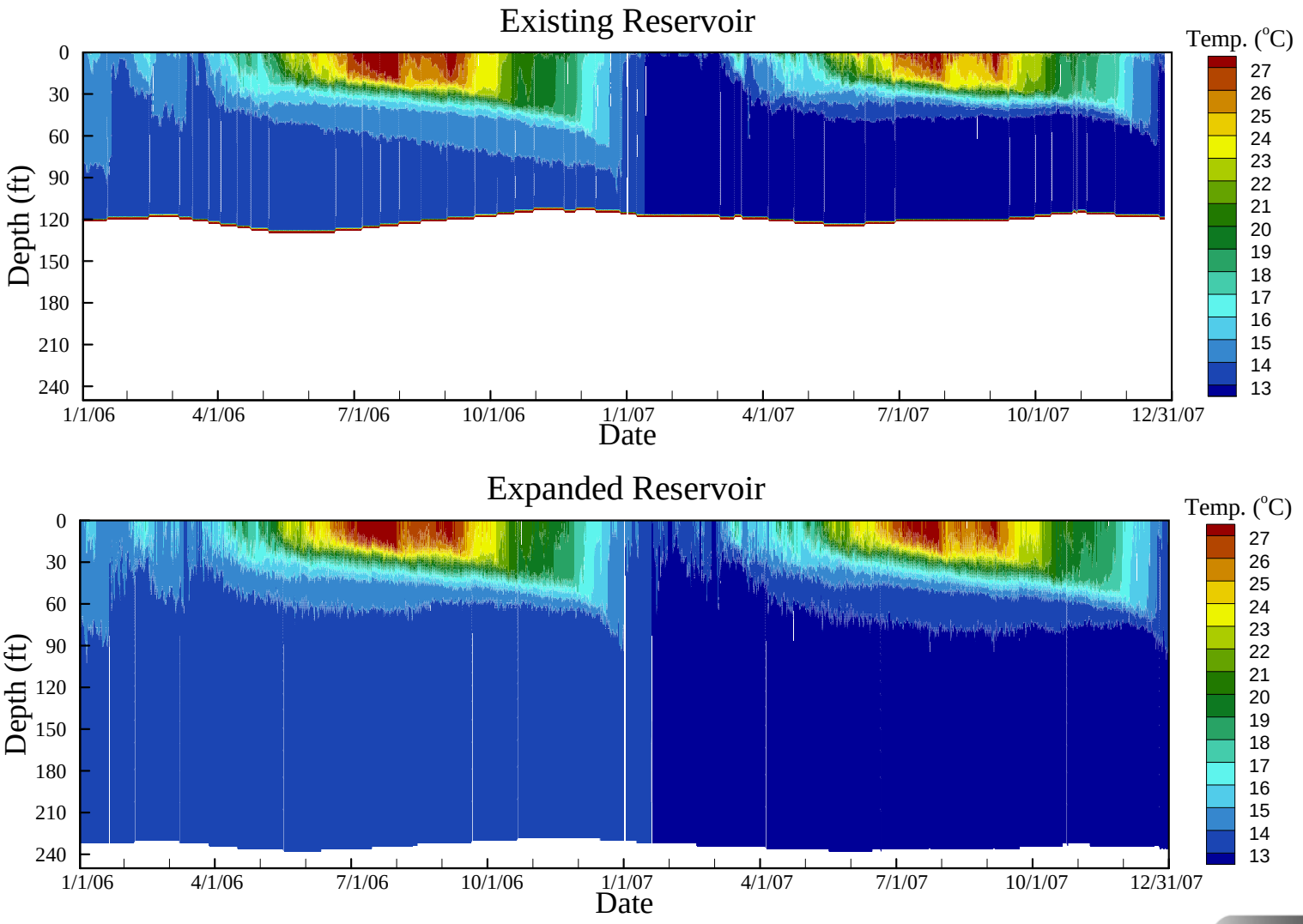

Figure 7

FSI V094005
May 01, 2012

FLOW SCIENCE®

Comparison of Existing and Expanded Reservoir

Simulated Conductivity at Station A

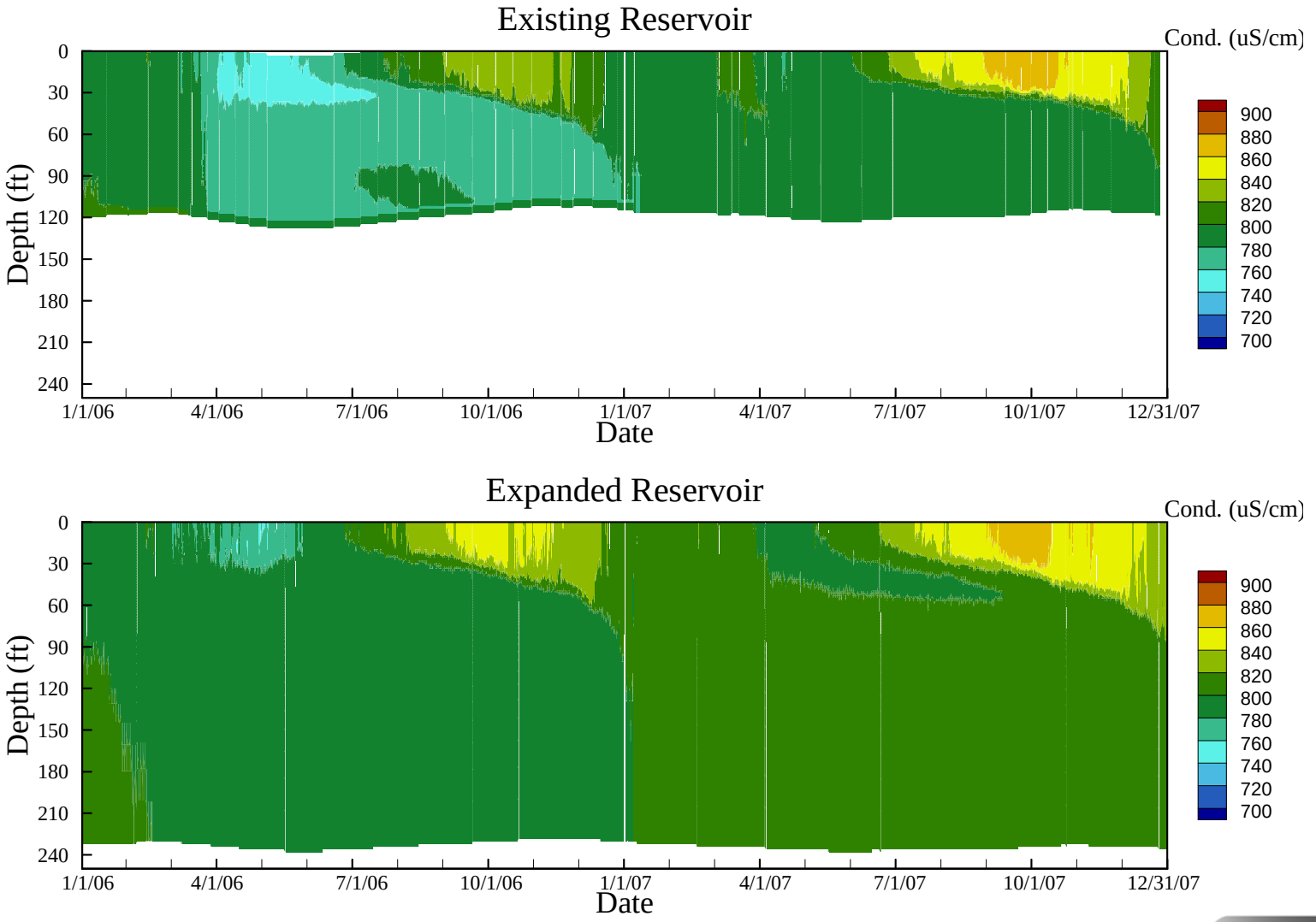

Figure 8

FSI V094005
May 01, 2012

FLOW SCIENCE®

Base Case: Purified Water Inflow Temperature

(Using multi-year averages of weekly water temperatures at North City Water Reclamation Plant; Provided by the City)

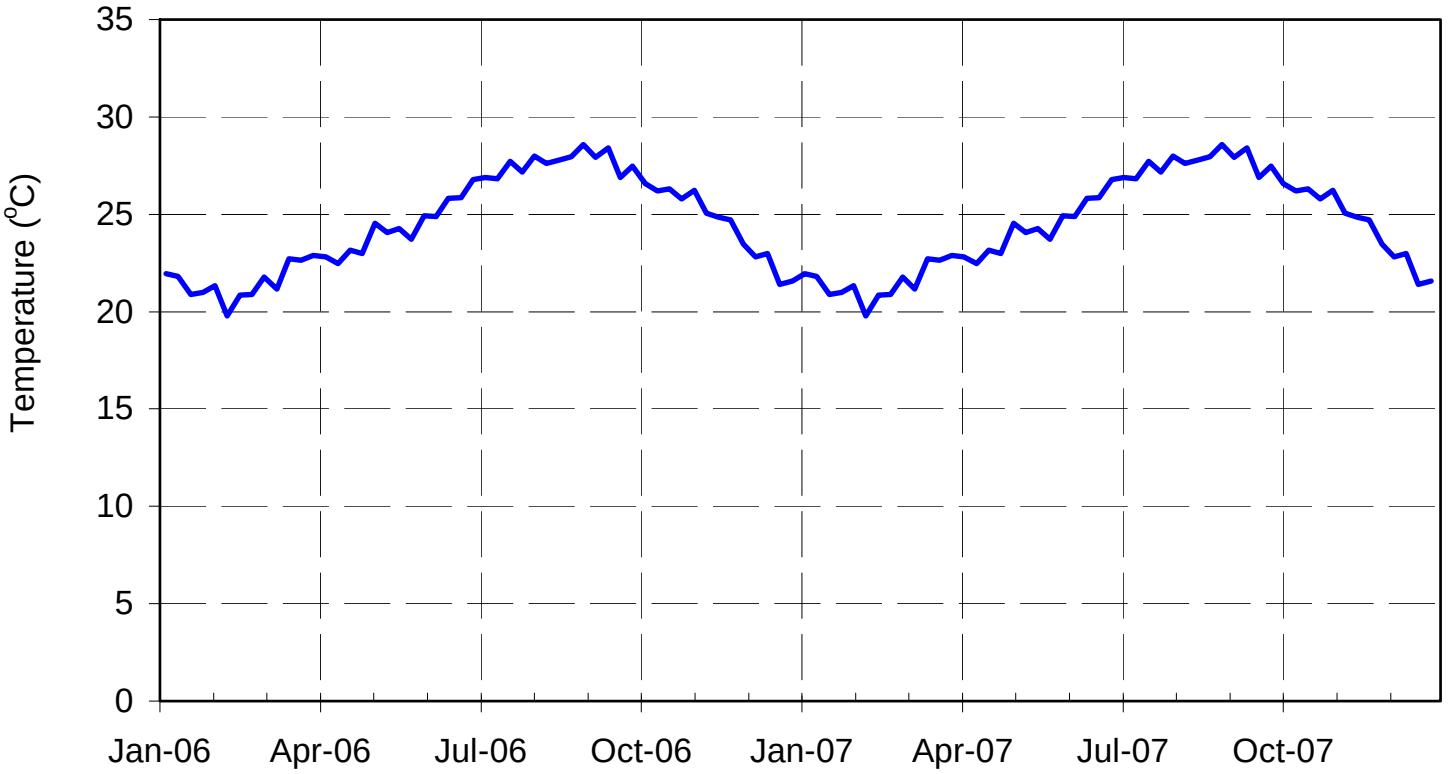

FSI V094005
May 01, 2012

Figure 9

FLOW SCIENCE®

Base Case: Simulated Water Temperature and Conductivity at Station A

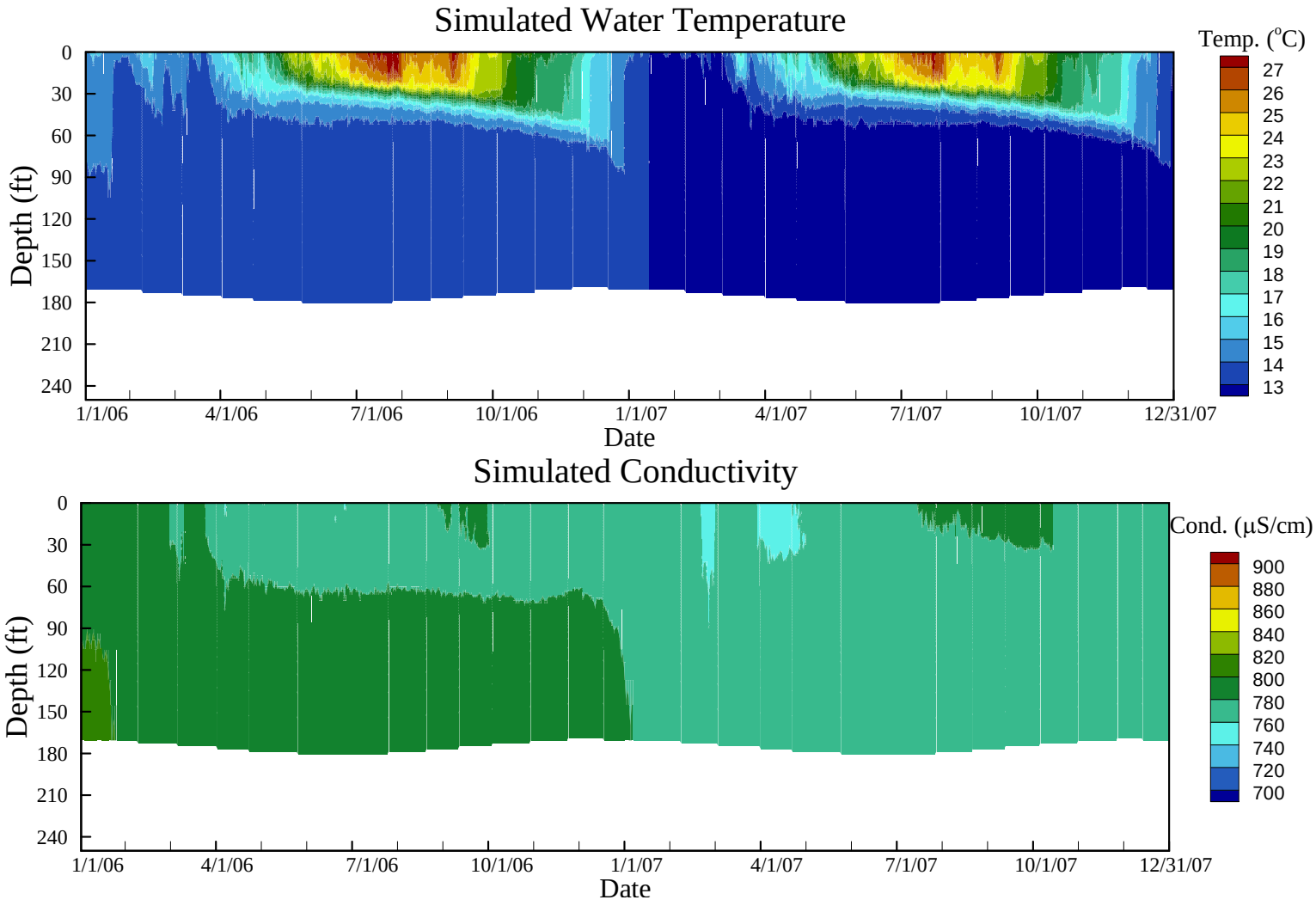

FSI V094005
May 01, 2012

Figure 10

FLOW SCIENCE®

Base Case: Contours of Simulated Temperature and Decaying Tracer

(Initial Inflow Concentration = 100%; Decay Rate = One Log Reduction Per Month)

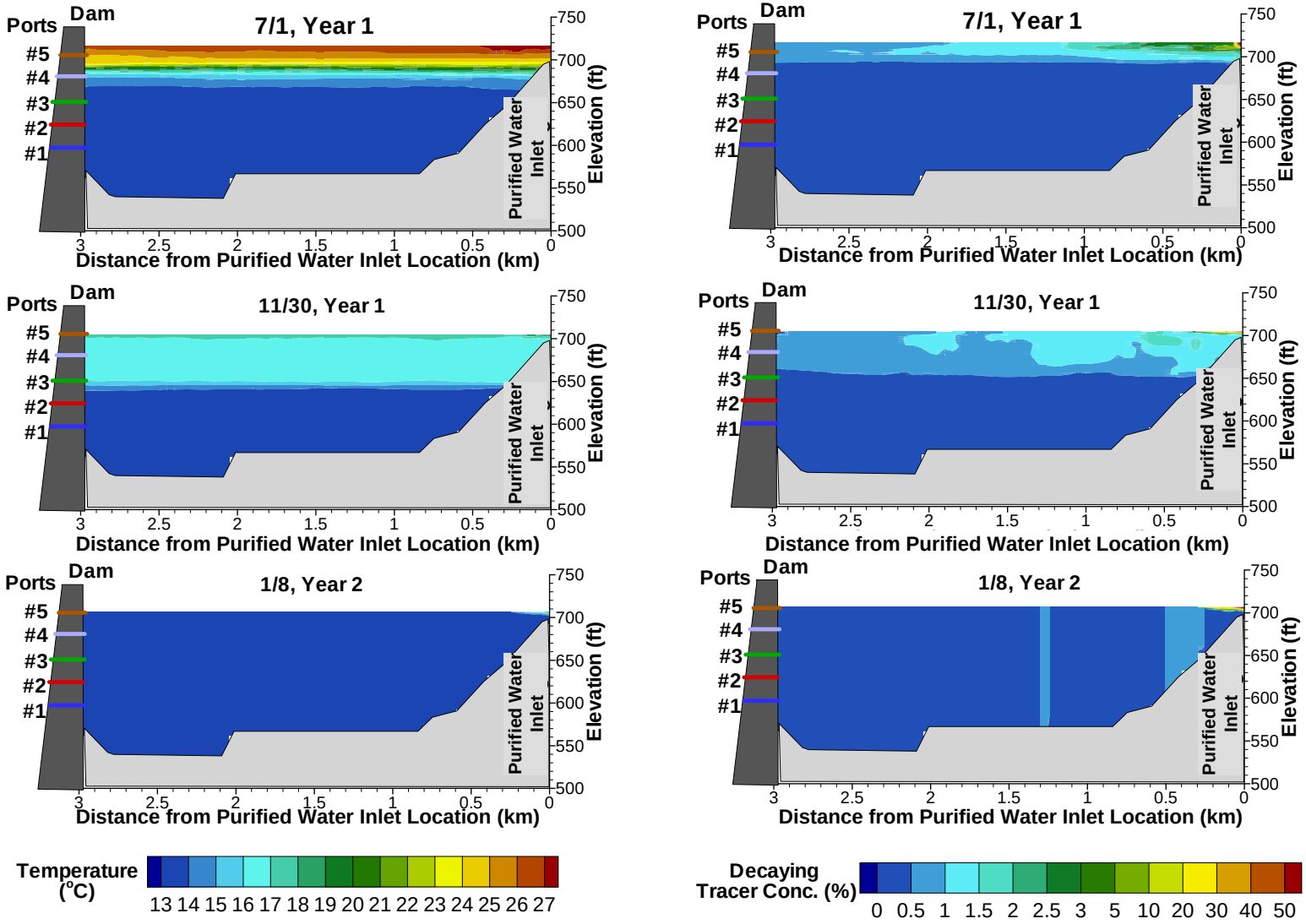

FSI V094005
May 01, 2012

Figure 11

FLOW SCIENCE®

Base Case: Simulated Decaying Tracer at the Reservoir Outlet Tower

(Initial Inflow Concentration = 100%; Decay Rate = One Log Reduction Per Month)

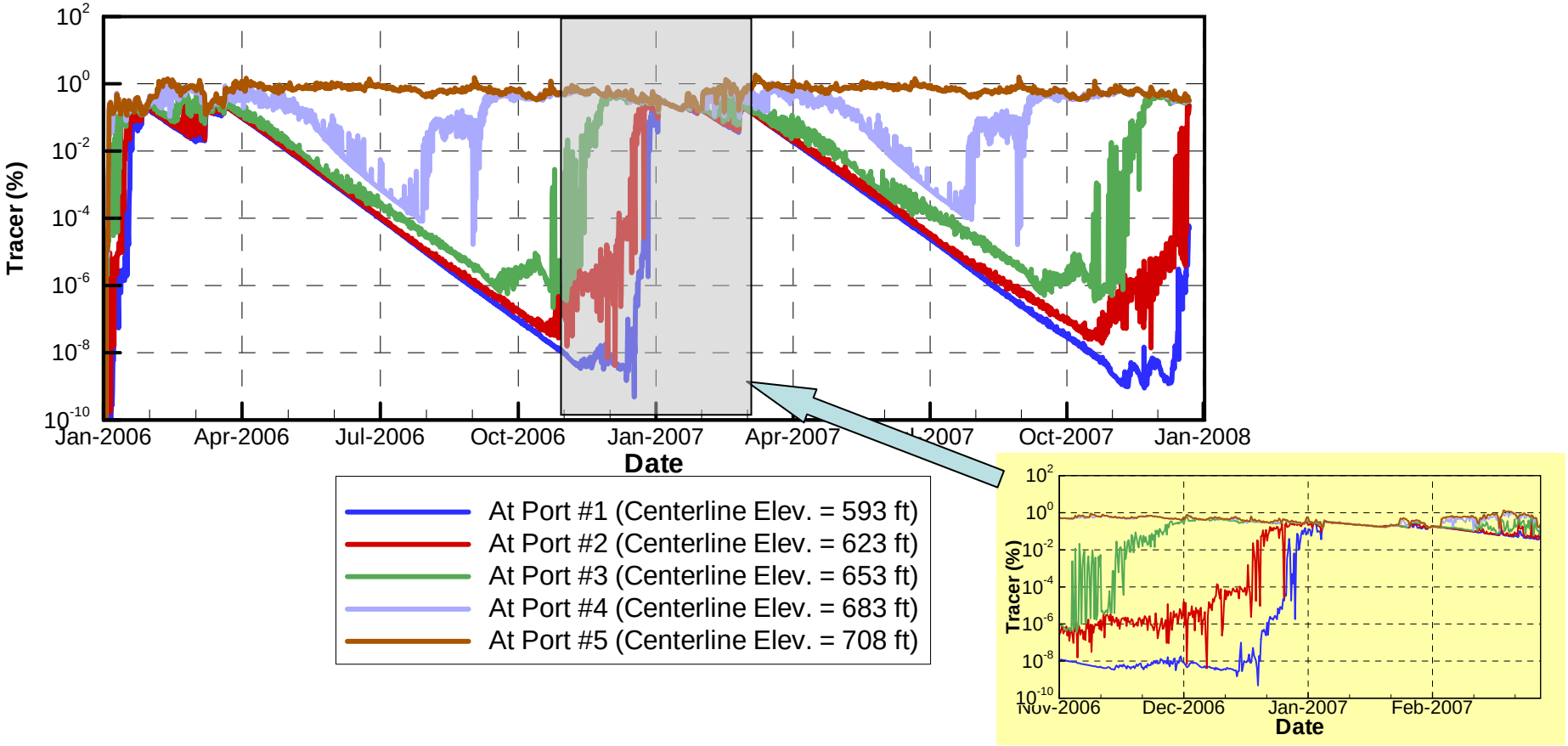

FSI V094005
May 01, 2012

Figure 12

FLOW SCIENCE®

Base Case: Simulated 24-hour Conservative Tracer Concentrations in Reservoir Outflow*

(Initial Inflow Concentration = 100%; Open Port #2)

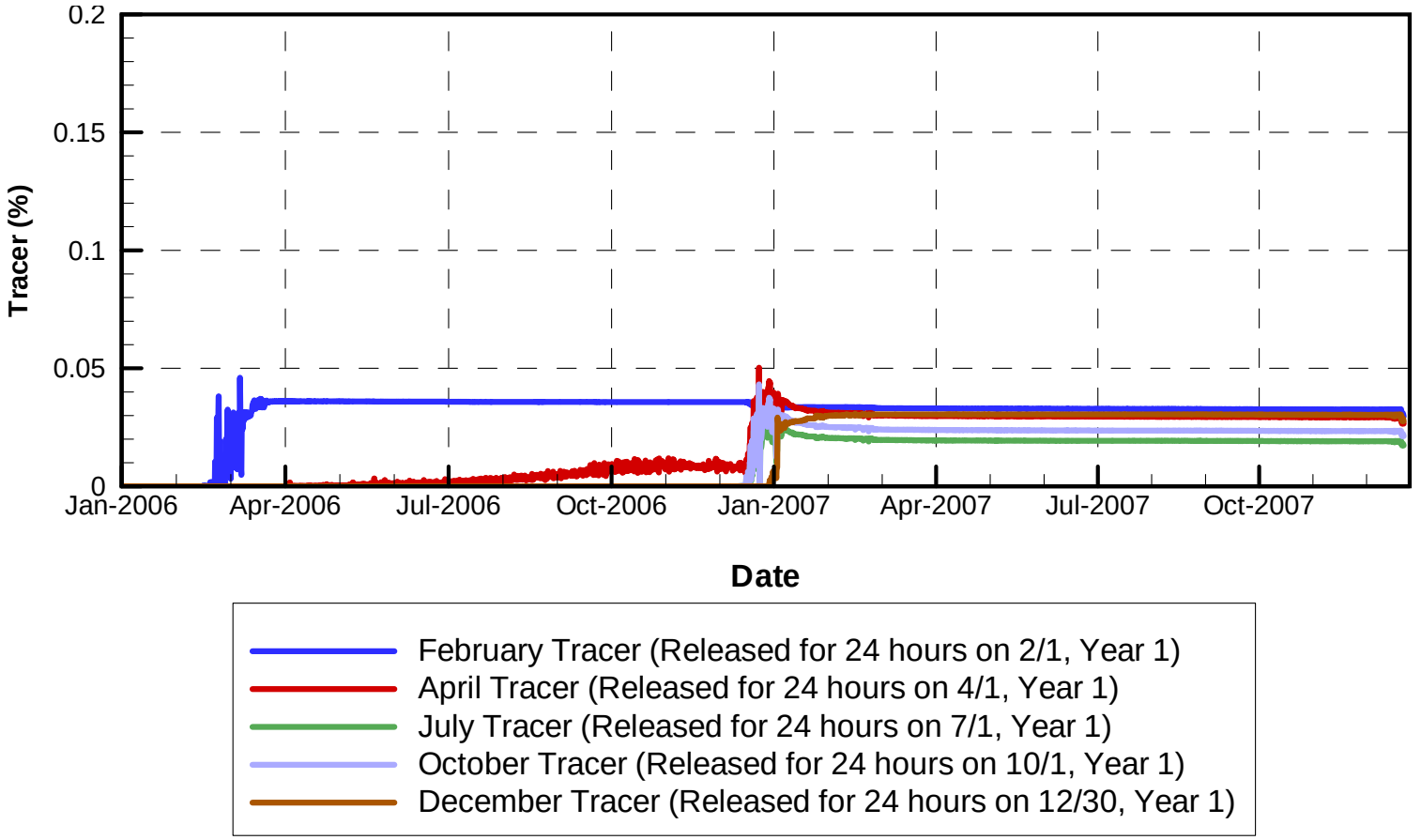

* Concentrations of trace within the reservoir at the outlet tower at the depth of the outlet port

Comparison of Base Case and No Purified Water Scenario

Simulated Water Temperature at Station A

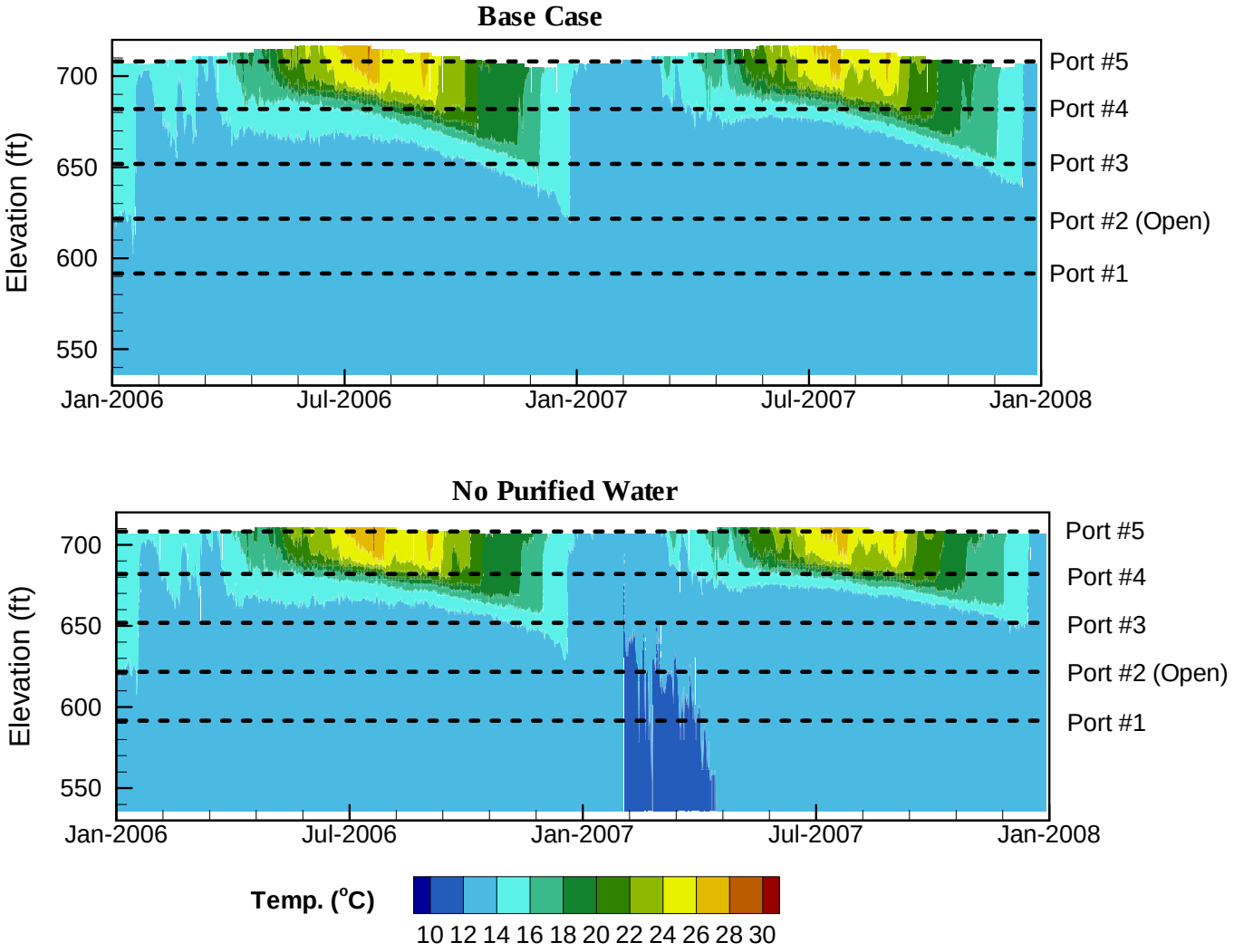

* Note that y-axis in this figure is elevation in ft for allowing labels of the port elevations in the figure

FSI V094005
May 01, 2012

Figure 14

FLOW SCIENCE®

Comparison of Base Case and No Purified Water Scenario

Simulated Conductivity at Station A

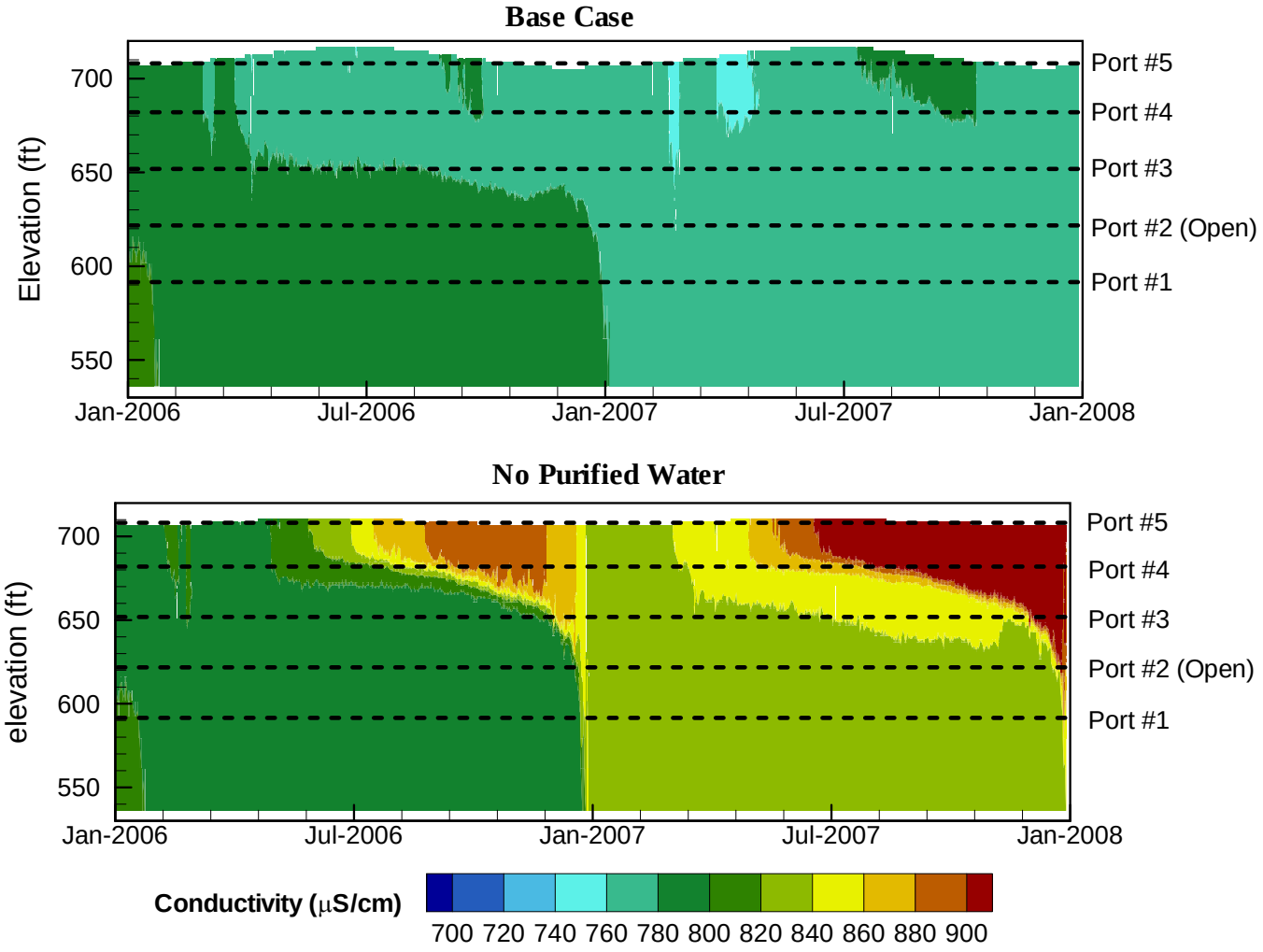

* Note that y-axis in this figure is elevation in ft for allowing labels of the port elevations in the figure

Figure 15

FLOW SCIENCE®

Inflow and Outflow Rates of Base Case, Extended Drought and Emergency Drawdown Scenarios

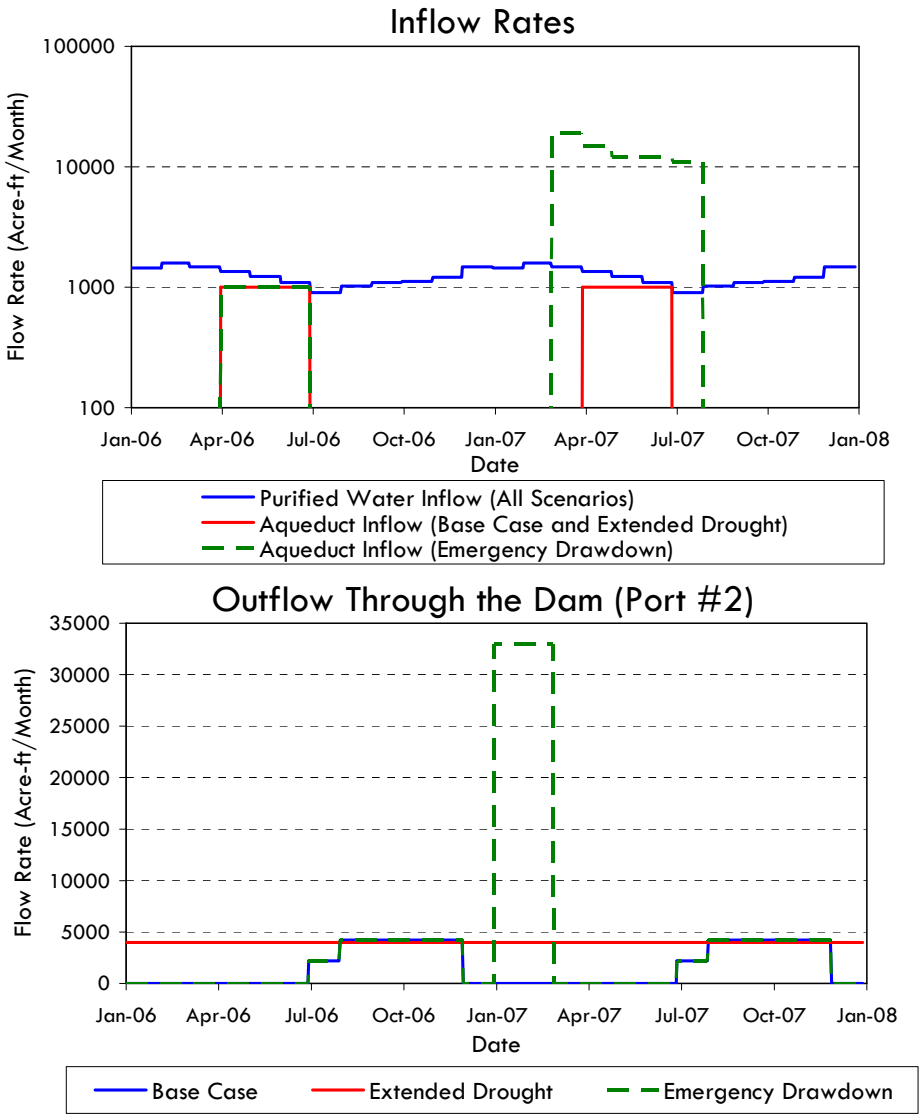

Figure 16

FSI V094005
May 01, 2012

FLOW SCIENCE®

Water Volumes of Base Case, Extended Drought and Emergency Drawdown Scenarios

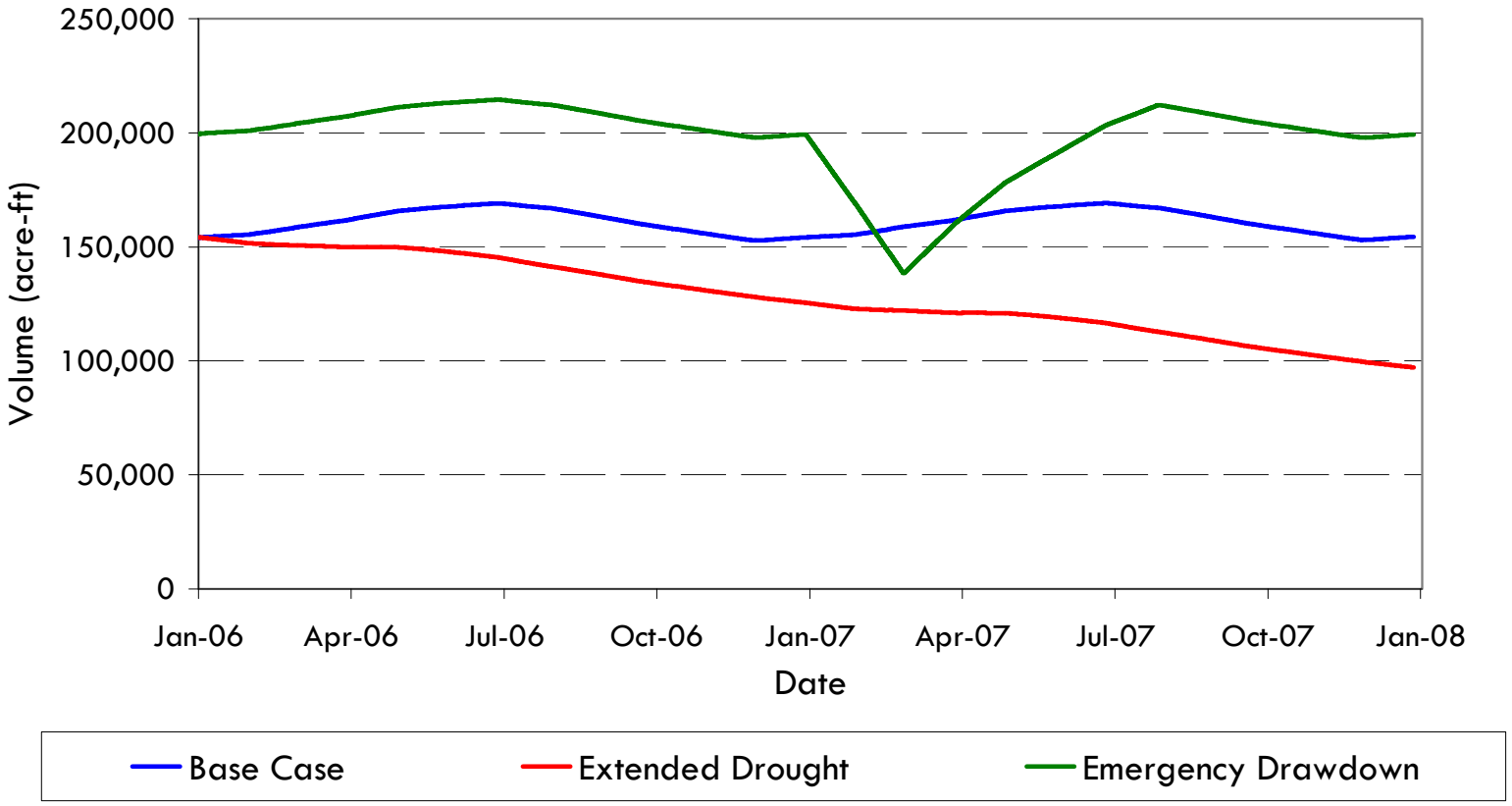

FSI V094005
May 01, 2012

Figure 17

FLOW SCIENCE®

Comparison of Base Case, Extended Drought and Emergency Drawdown Scenarios

Simulated Water Temperature at Station A

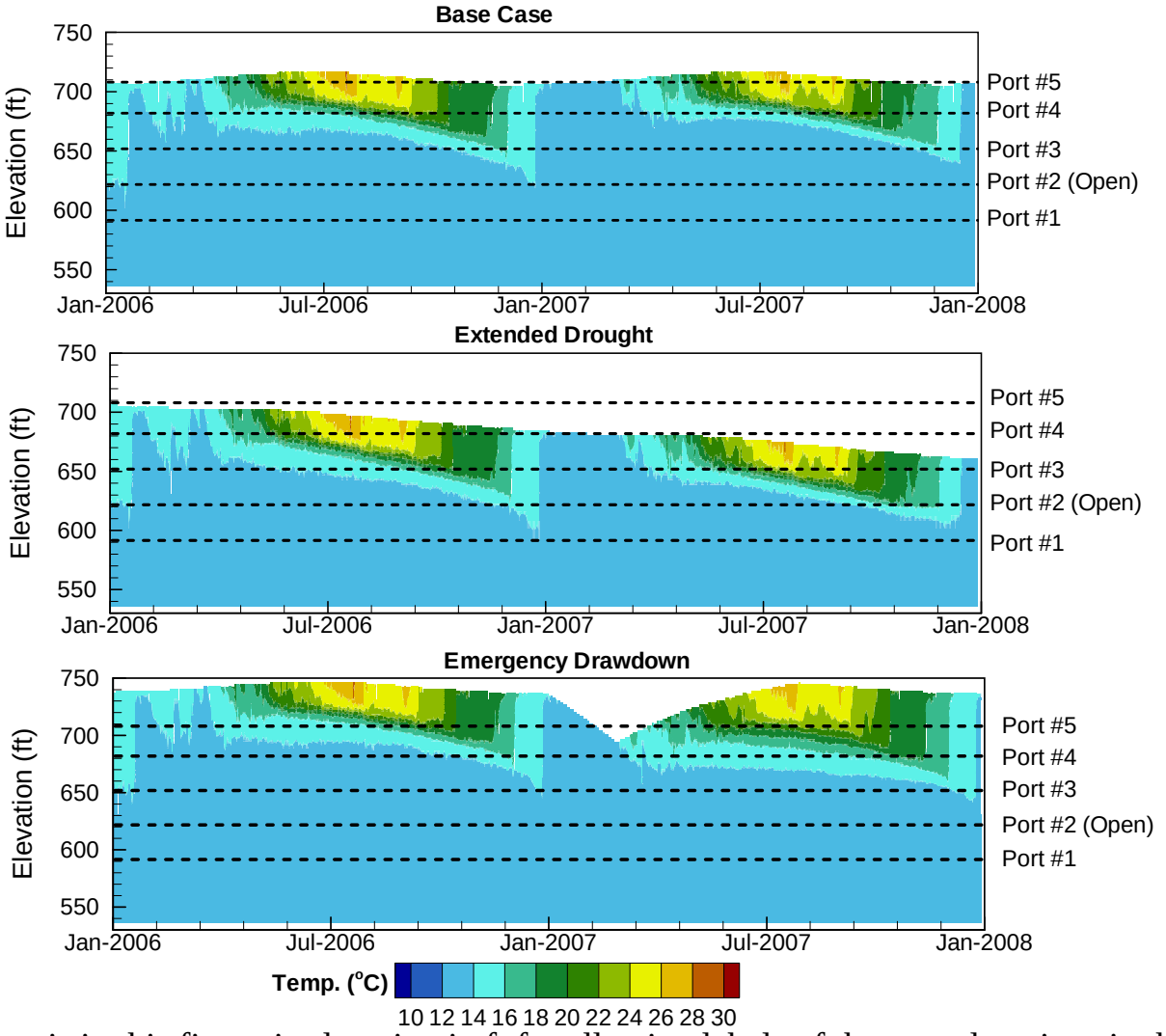

* Note that y-axis in this figure is elevation in ft for allowing labels of the port elevations in the figure

Figure 18

FLOW SCIENCE®

Comparison of Base Case, Extended Drought and Emergency Drawdown Scenarios

Simulated Conductivity at Station A

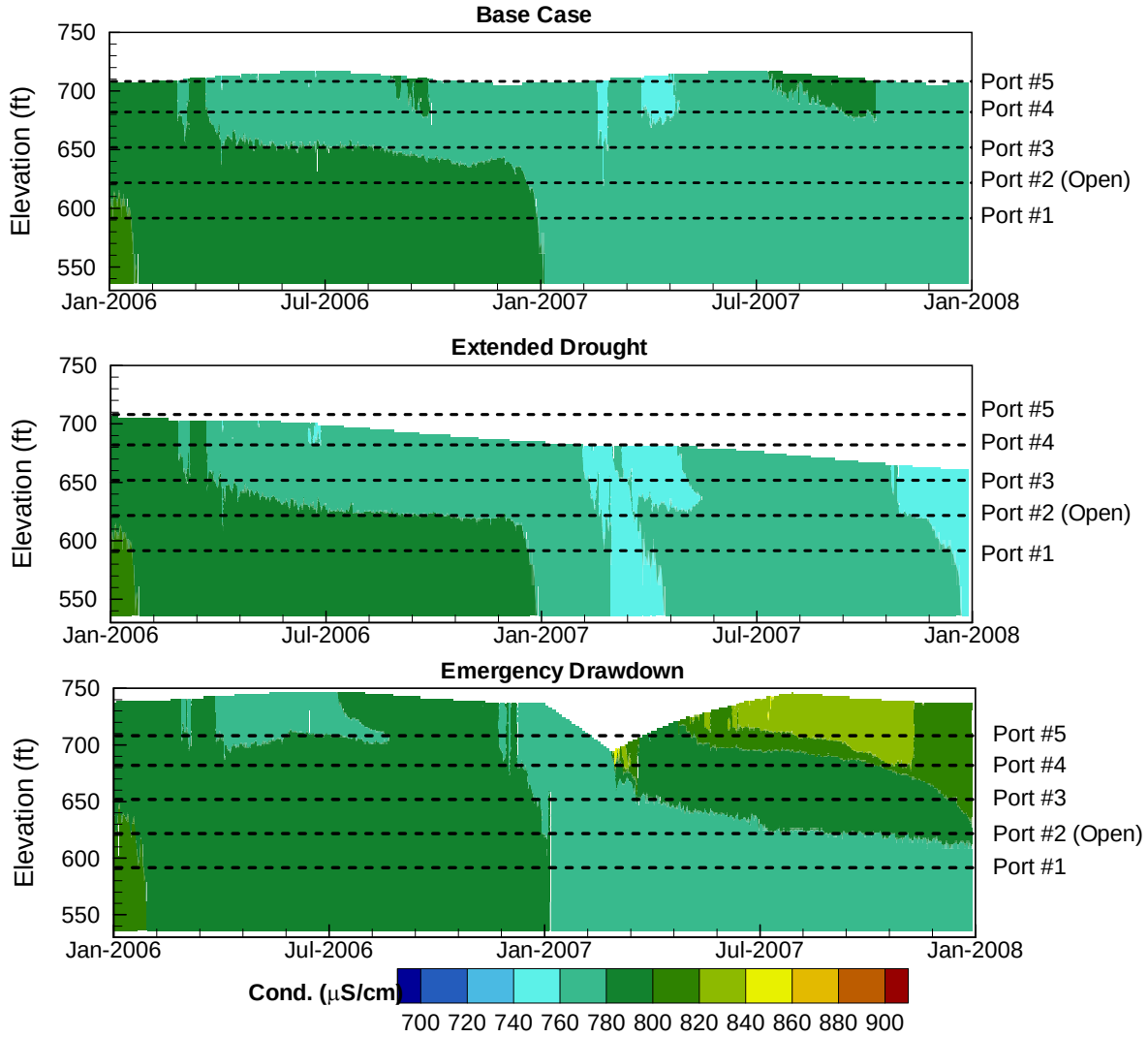

* Note that y-axis in this figure is elevation in ft for allowing labels of the port elevations in the figure

Figure 19

FLOW SCIENCE®

Comparison of Base Case, Extended Drought and Emergency Drawdown Scenarios

Simulated Decaying Tracer Concentrations in the Reservoir Outflow*

(Open Port #2; Initial Inflow Concentration = 100%; Decay Rate = One Log Reduction Per Month)

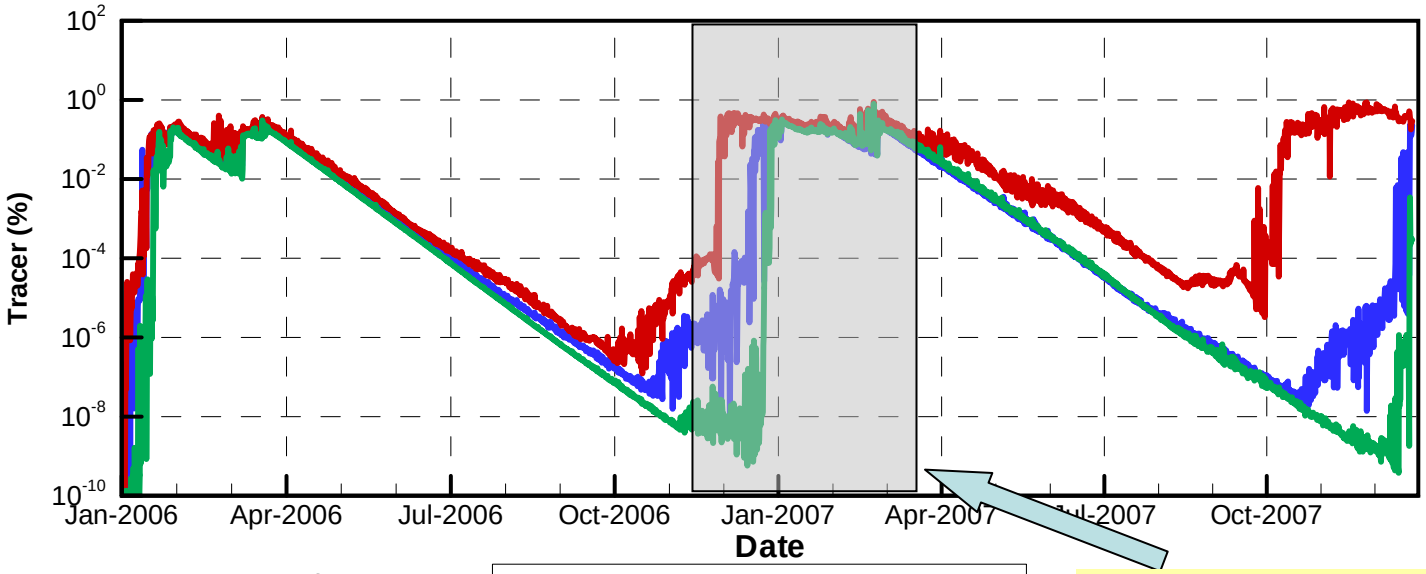

* Concentrations of tracer within the reservoir at the outlet tower at the depth of the open outlet port

Base Case
Extended Drought
Emergency Drawdown

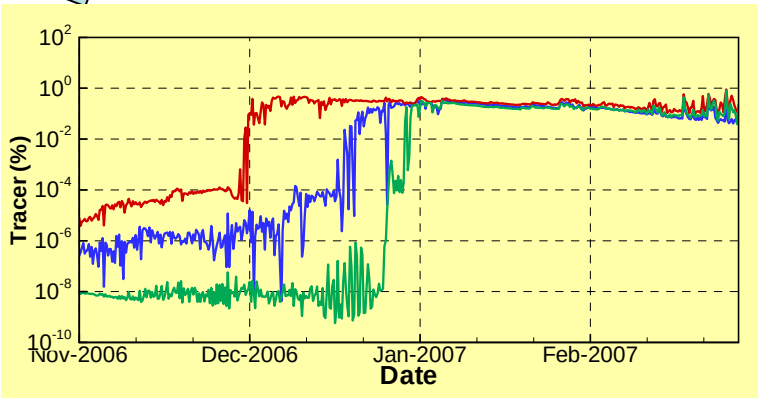

FSI V094005
May 01, 2012

Figure 20

FLOW SCIENCE®

Extended Drought Scenario Simulated 24-hour Conservative Tracer Concentrations in the Reservoir Outflow*

(Open Port #2; Initial Inflow Concentration = 100%)

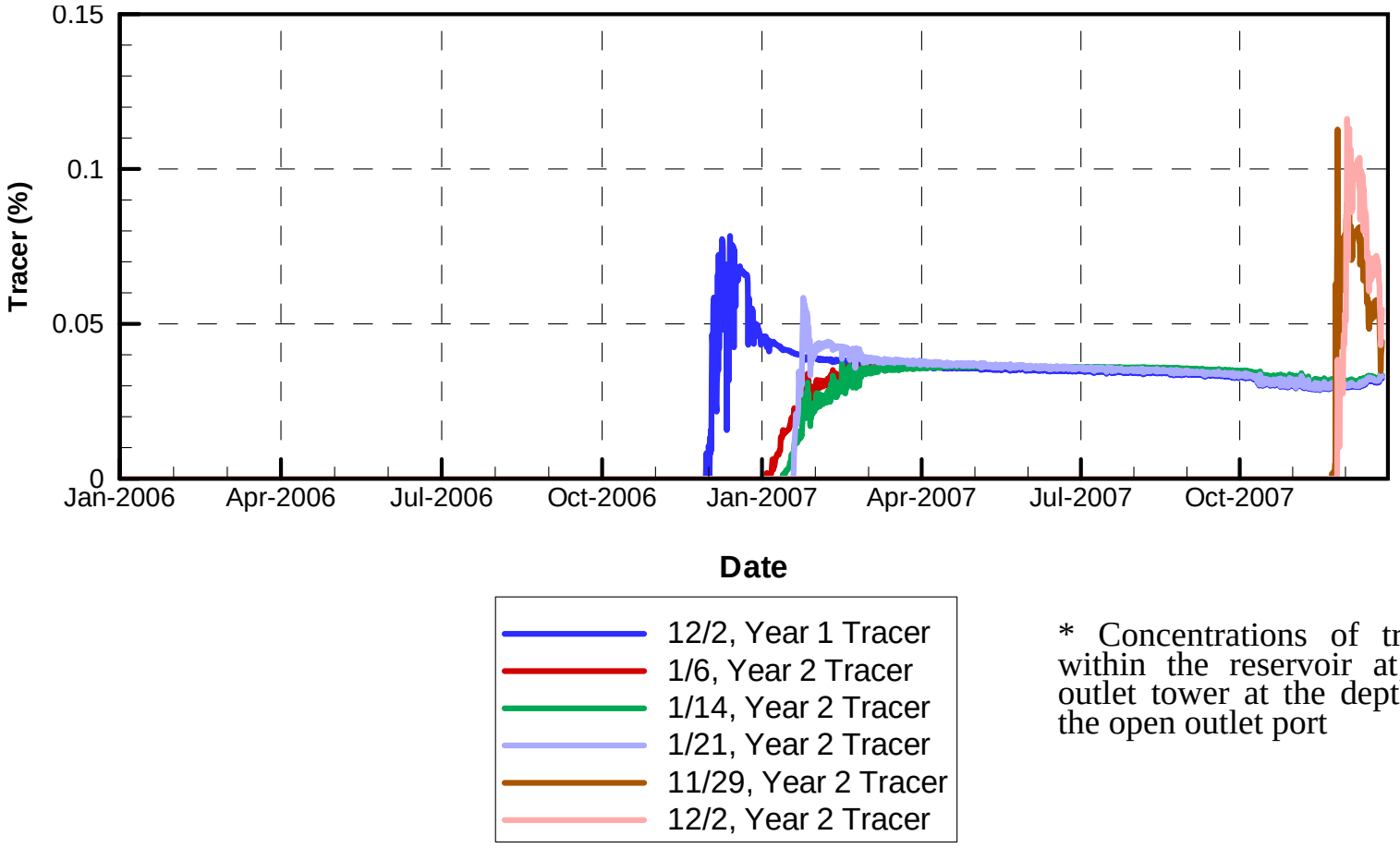

* Concentrations of tracer within the reservoir at the outlet tower at the depth of the open outlet port

FSI V094005
May 01, 2012

Figure 21

FLOW SCIENCE®

Emergency Drawdown Scenario Simulated 24-hour Conservative Tracer Concentrations in the Reservoir Outflow*

(Open Port #2; Initial Inflow Concentration = 100%)

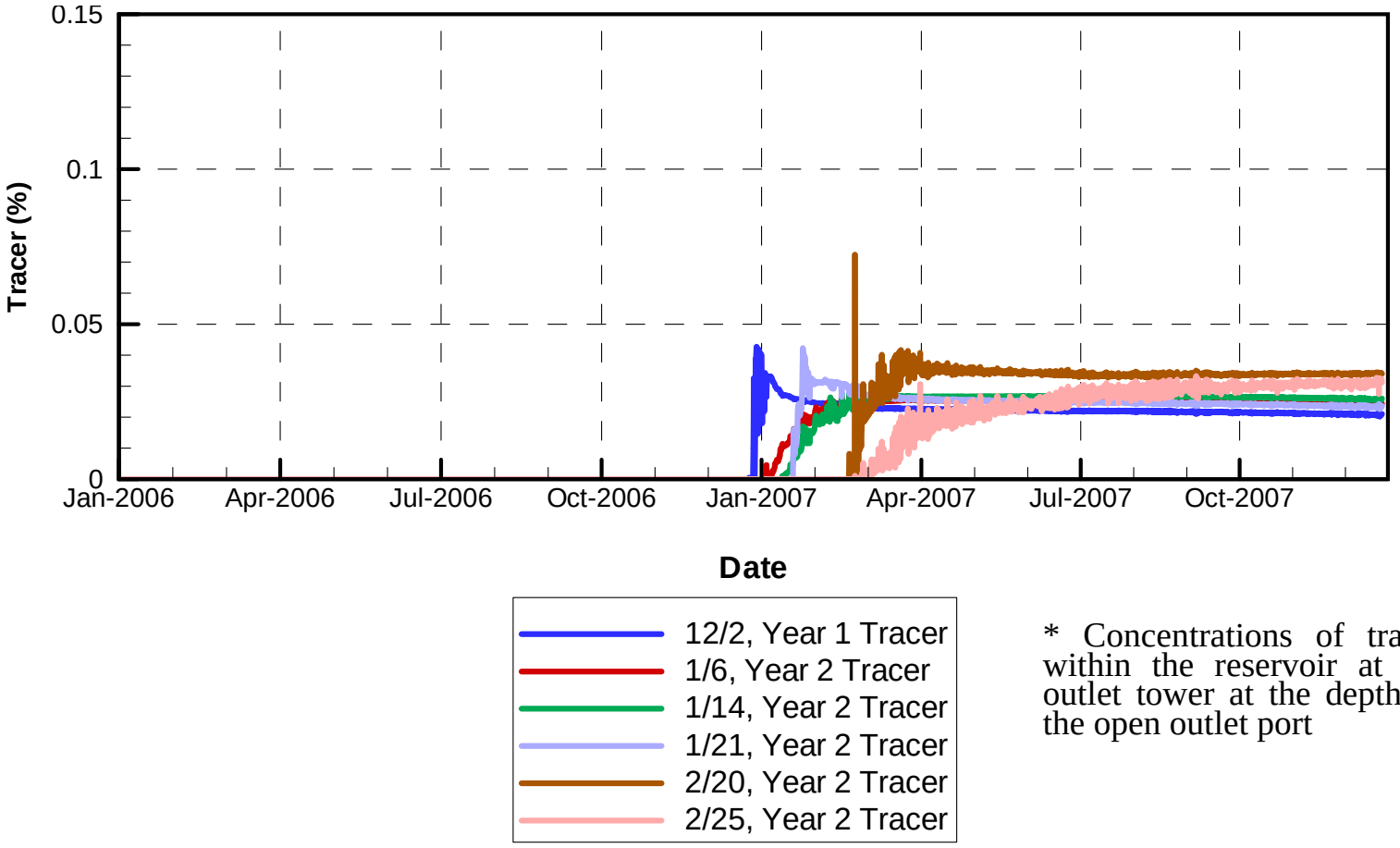

* Concentrations of tracer within the reservoir at the outlet tower at the depth of the open outlet port

FSI V094005
May 01, 2012

Figure 22

FLOW SCIENCE®

Map of Modeled Purified Water Inlet Locations

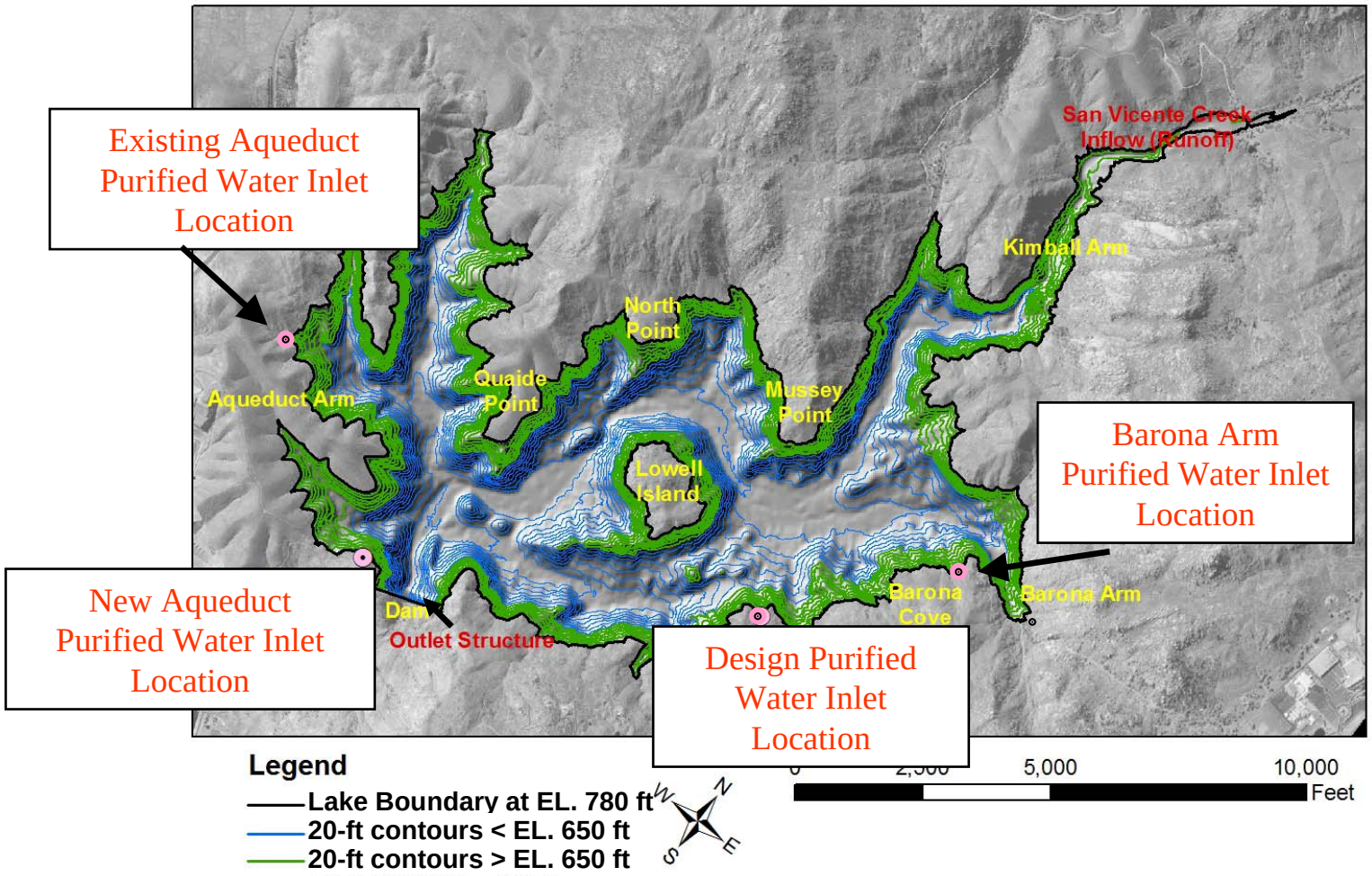

FSI V094005
May 01, 2012

Figure 23

FLOW SCIENCE®

Comparison of Reservoir Outflow Decaying Tracer Concentrations* from Different Purified Water Inlet Locations Under Base Case Operating Scenario

(Open Port #2; Initial Inflow Concentration = 100%;
Decay Rate = One Log Reduction Per Month)

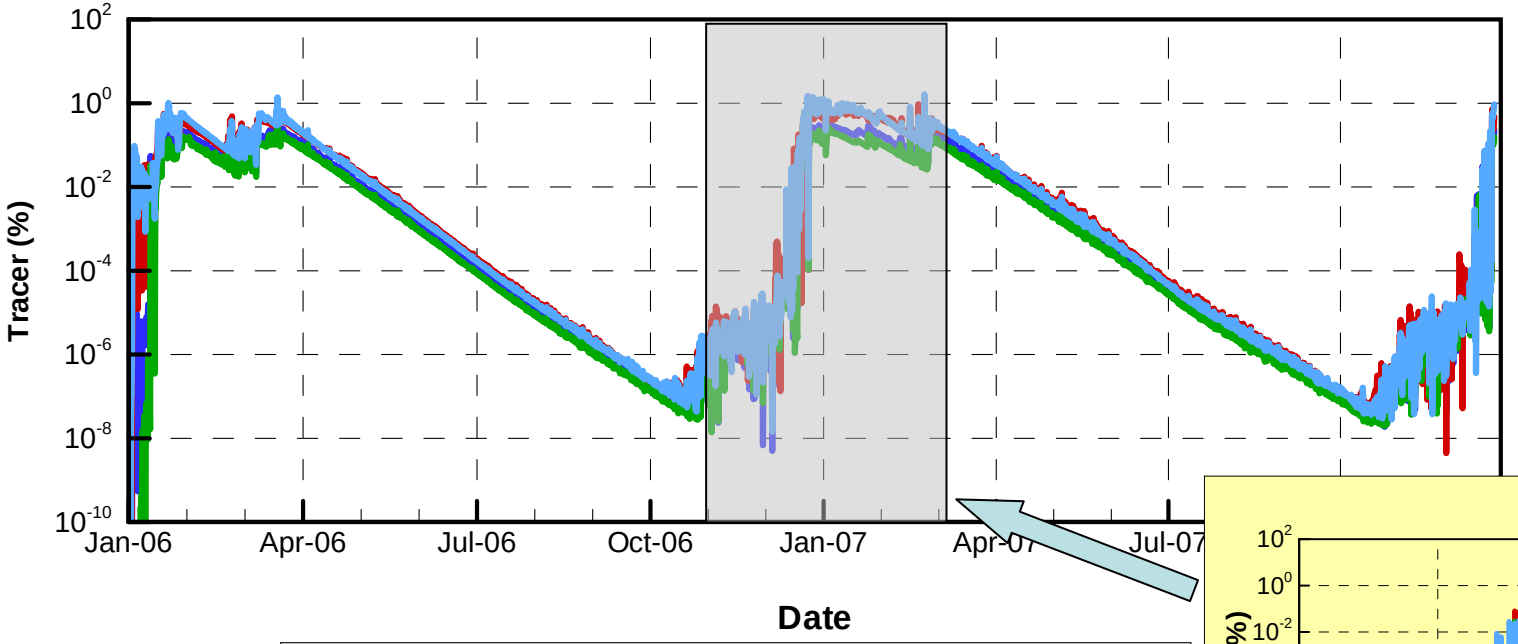

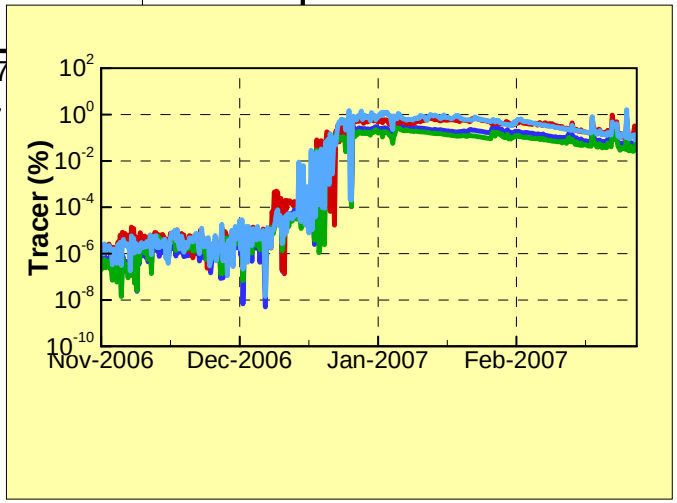

* Concentrations of tracer within the reservoir at the outlet tower at the depth of the open outlet port.

Figure 24

FSI V094005
May 01, 2012

Comparison of Reservoir Outflow 24-hour Conservative Tracer Concentrations* from Different Purified Water Inlet Locations Under Base Case Operating Scenario

Tracer Released on 1/30, Year 1 for 24 hours

(Open Port #2; Initial Inflow Concentration = 100%)

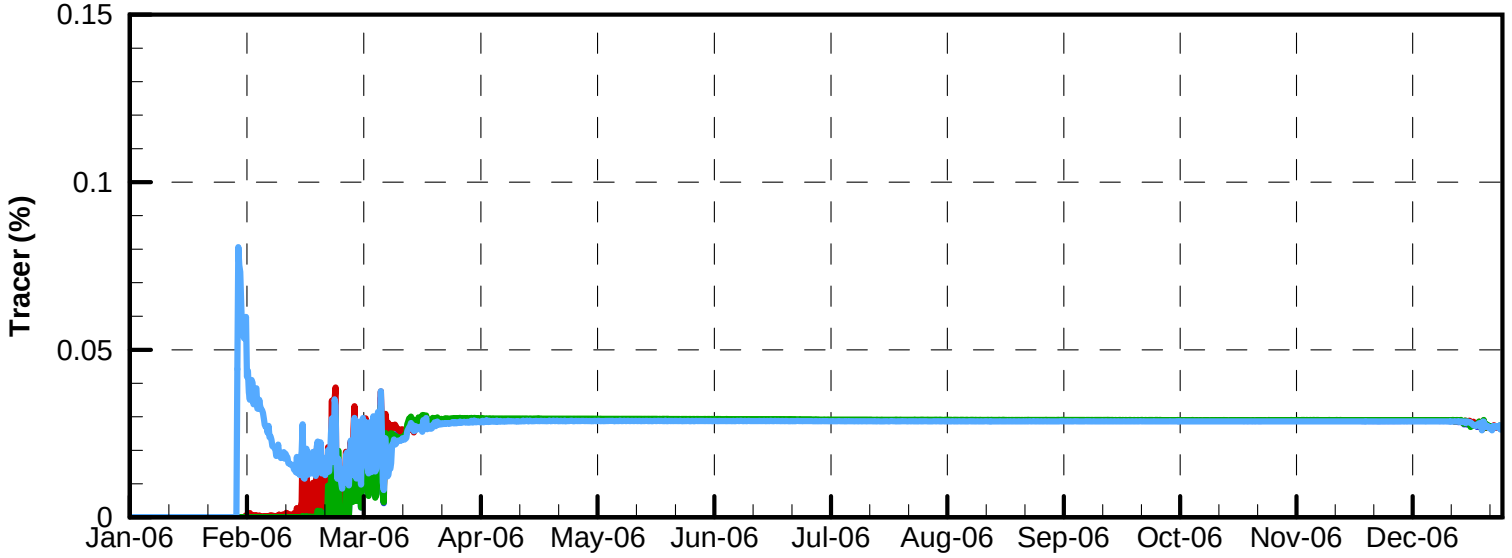

* Concentrations of tracer within the reservoir at the outlet tower at the depth of the open outlet port

Figure 25

FSI V094005
May 01, 2012

FLOW SCIENCE®

Comparison of Reservoir Outflow 24-hour Conservative Tracer Concentrations* from Different Purified Water Inlet Locations Under Base Case Operating Scenario

Tracer released on 4/1, Year 1 for 24 hours

(Open Port #2; Initial Inflow Concentration = 100%)

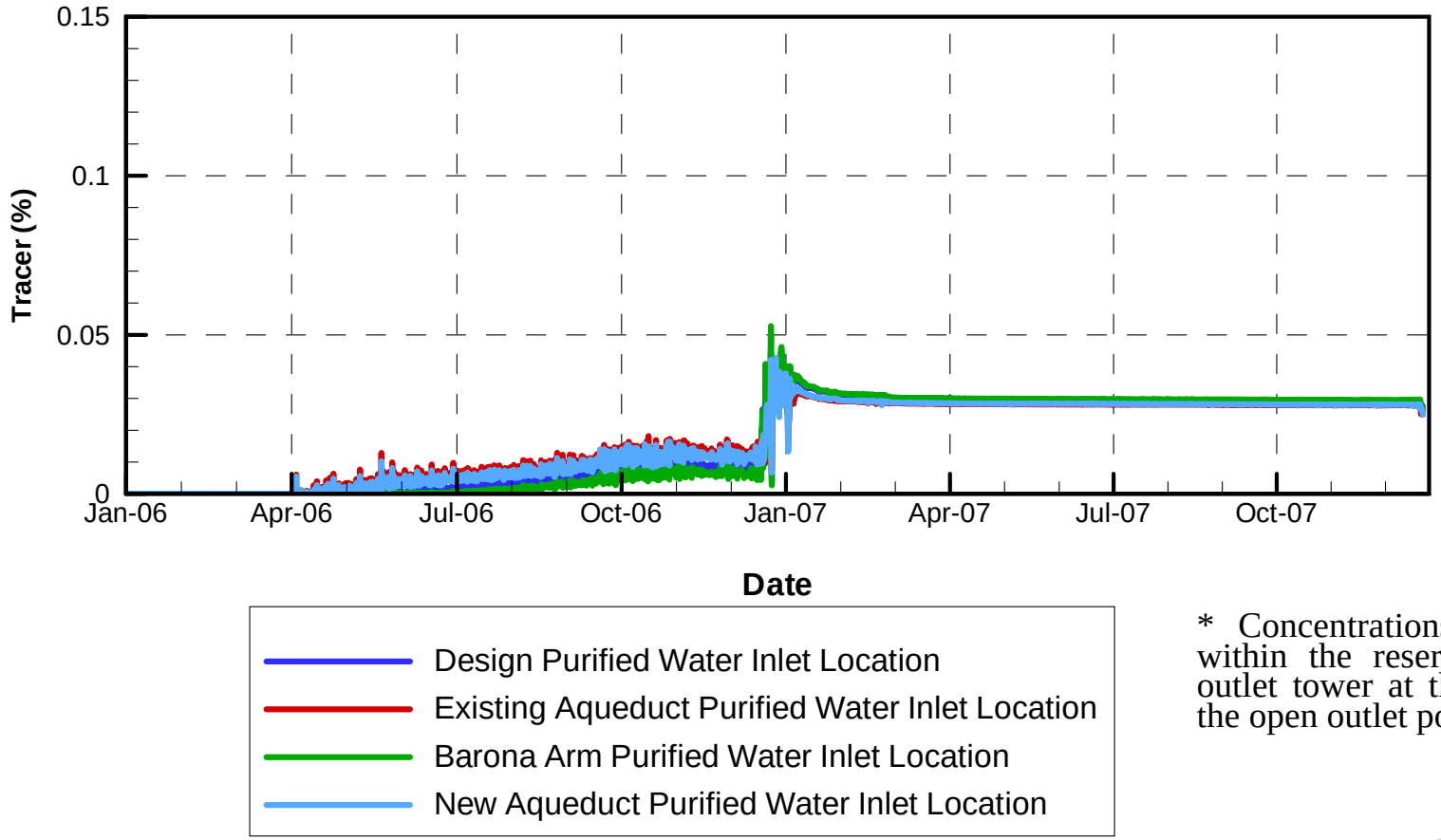

* Concentrations of tracer within the reservoir at the outlet tower at the depth of the open outlet port

Figure 26

FSI V094005
May 01, 2012

FLOW SCIENCE®

Comparison of Reservoir Outflow 24-hour Conservative Tracer Concentrations* from Different Purified Water Inlet Locations Under Base Case Operating Scenario

Tracer released on 7/1, Year 1 for 24 hours

(Open Port #2; Initial Inflow Concentration = 100%)

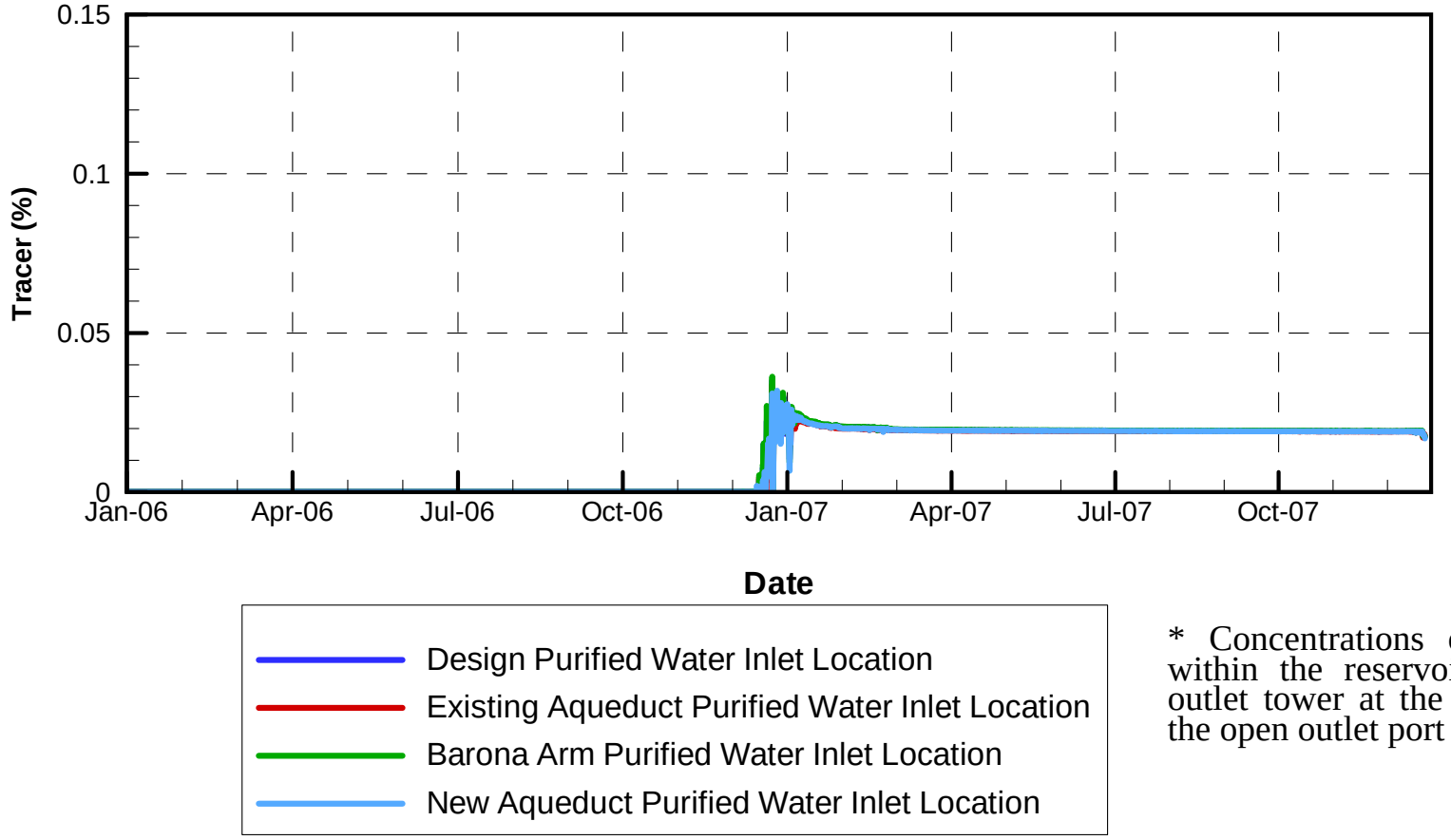

* Concentrations of tracer within the reservoir at the outlet tower at the depth of the open outlet port

FSI V094005
May 01, 2012

Figure 27

FLOW SCIENCE®

Comparison of Reservoir Outflow 24-hour Conservative Tracer Concentrations* from Different Purified Water Inlet Locations Under Base Case Operating Scenario

Tracer released on 10/1, Year 1 for 24 hours

(Open Port #2; Initial Inflow Concentration = 100%)

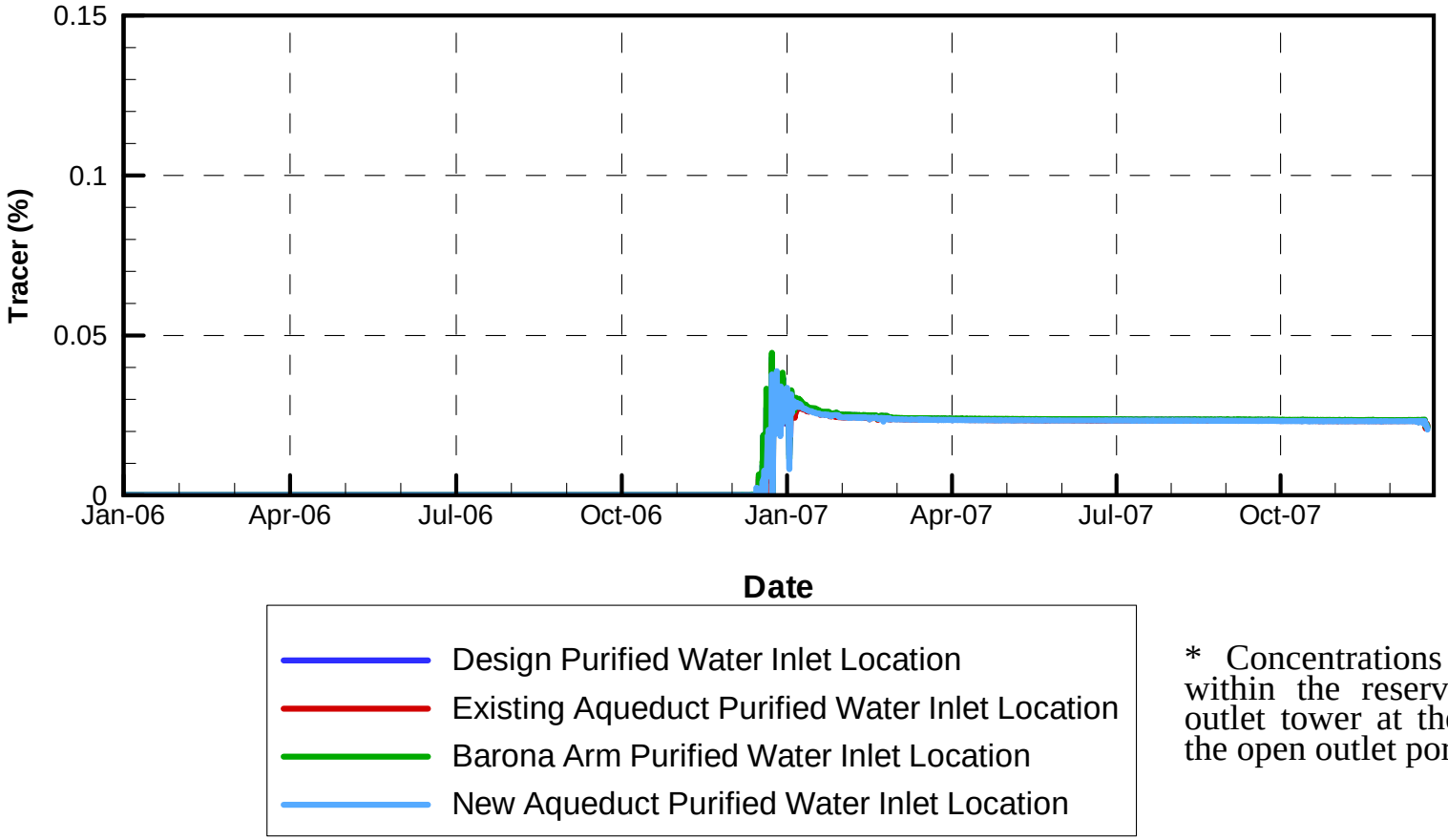

* Concentrations of tracer within the reservoir at the outlet tower at the depth of the open outlet port

FSI V094005
May 01, 2012

Figure 28

FLOW SCIENCE®

Comparison of Reservoir Outflow 24-hour Conservative Tracer Concentrations* from Different Purified Water Inlet Locations Under Base Case Operating Scenario

Tracer released on 1/5, Year 2 for 24 hours

(Open Port #2; Initial Inflow Concentration = 100%)

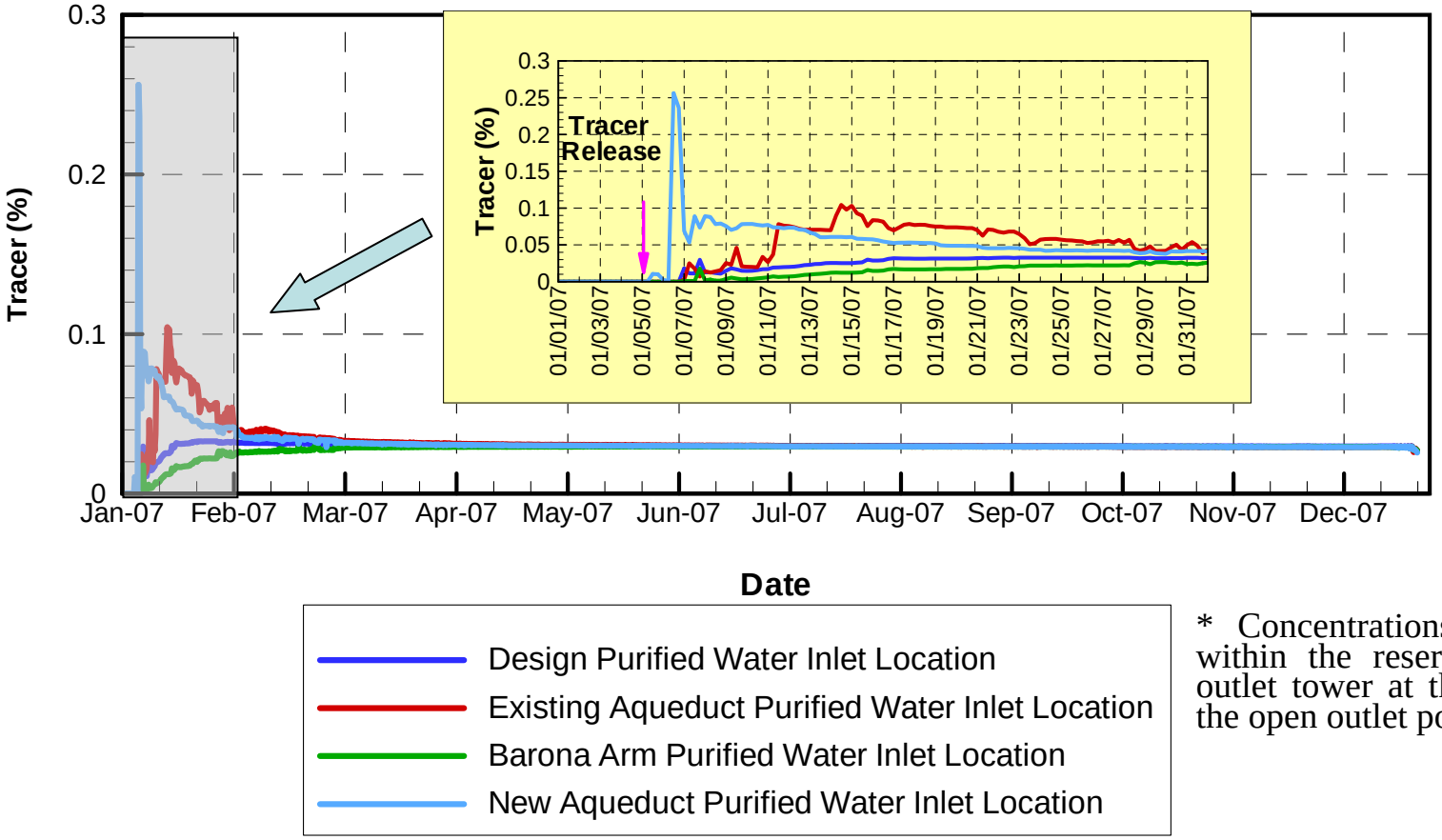

* Concentrations of tracer within the reservoir at the outlet tower at the depth of the open outlet port

Figure 29

FSI V094005
May 01, 2012

FLOW SCIENCE®

Comparison of Reservoir Outflow 24-hour Conservative Tracer Concentrations* from Different Purified Water Inlet Locations Under Base Case Operating Scenario

Tracer released on 1/15, Year 2 for 24 hours

(Open Port #2; Initial Inflow Concentration = 100%)

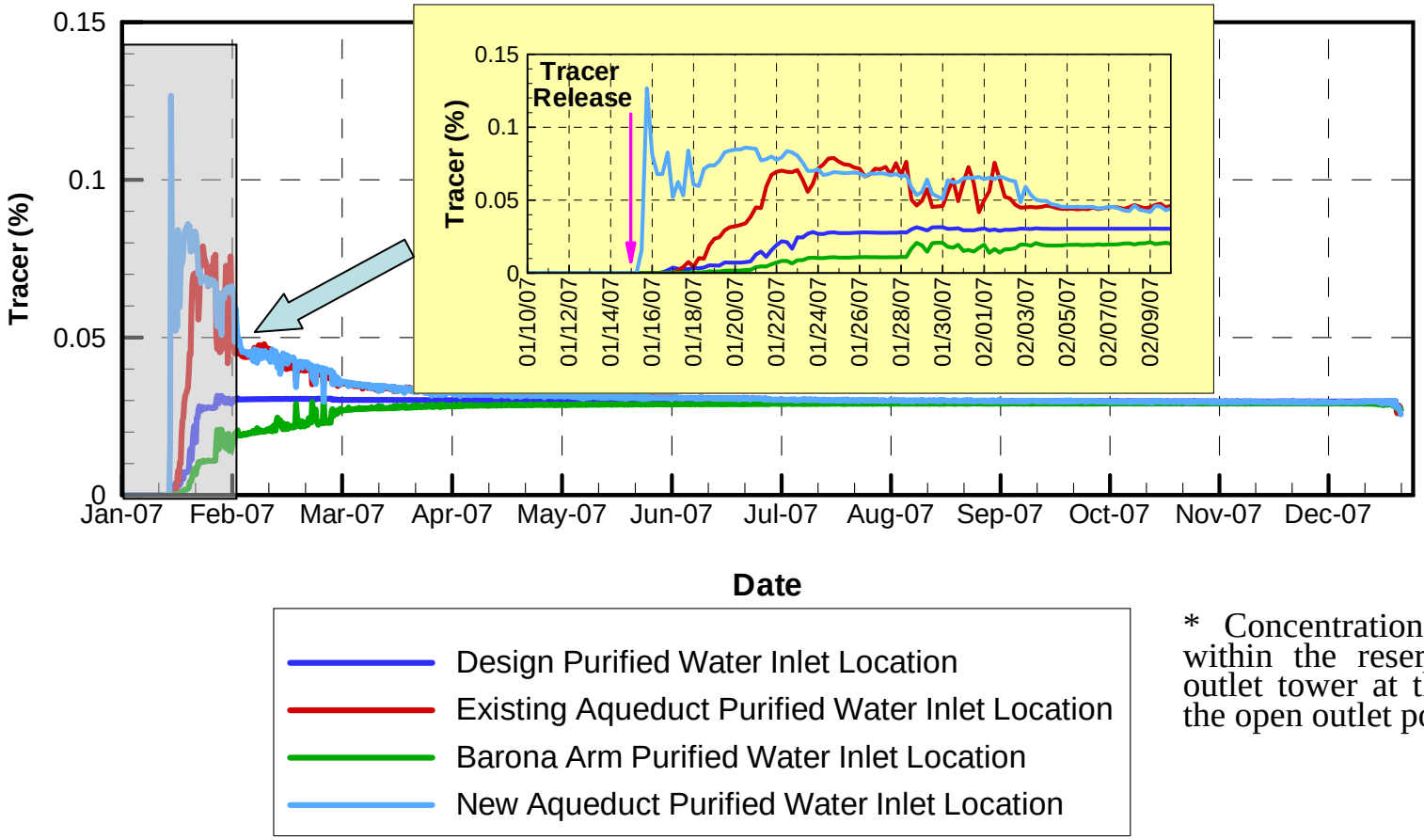

* Concentrations of tracer within the reservoir at the outlet tower at the depth of the open outlet port

Figure 30

FSI V094005
May 01, 2012

FLOW SCIENCE®

Comparison of Reservoir Outflow 24-hour Decaying Tracer Concentrations* from Different Purified Water Inlet Locations Under Extended Drought Scenario

(Open Port #2; Initial Inflow Concentration = 100%;
Decay Rate = One Log Reduction Per Month)

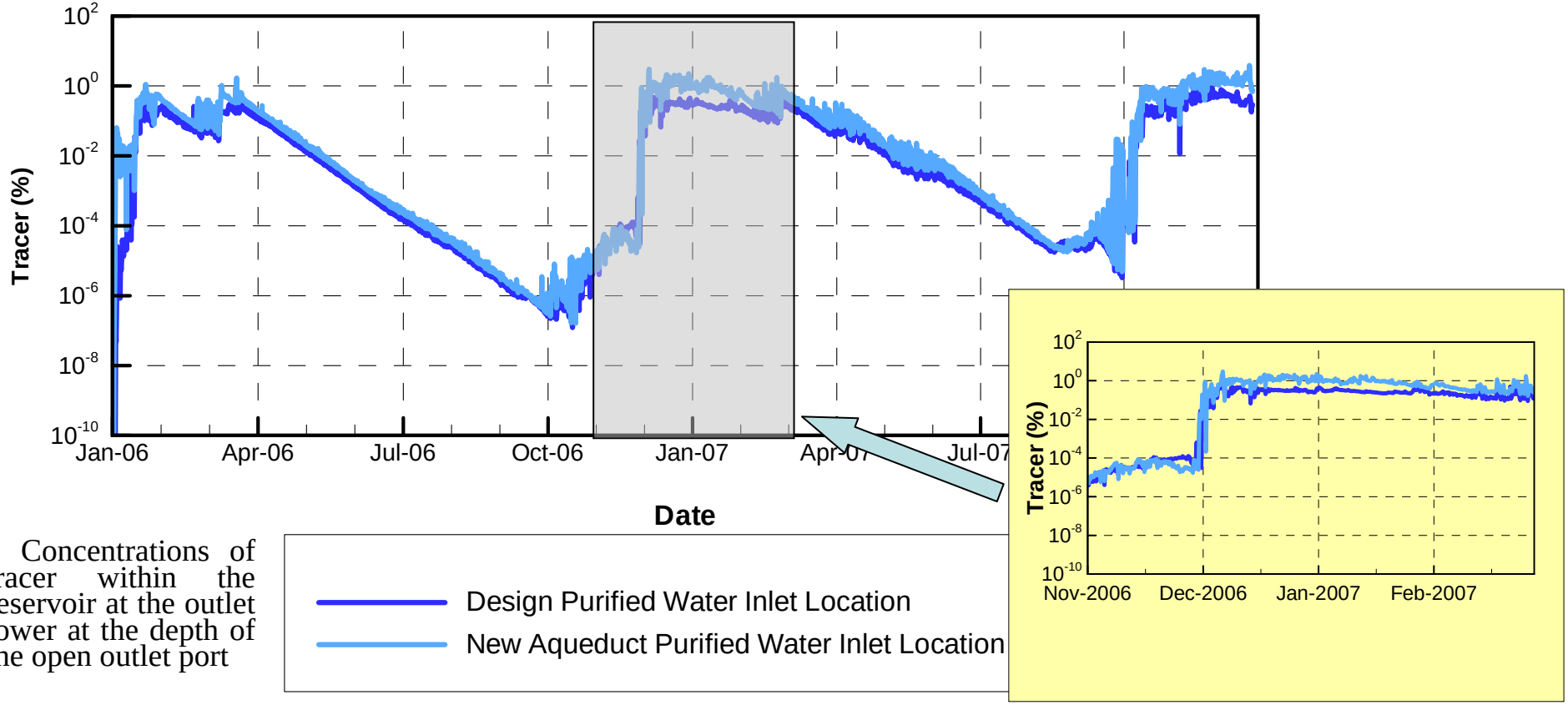

* Concentrations of tracer within the reservoir at the outlet tower at the depth of the open outlet port

FSI V094005
May 01, 2012

Figure 31

FLOW SCIENCE®

Comparison of Reservoir Outflow 24-hour Conservative Tracer Concentrations* from Different Purified Water Inlet Locations Under Extended Drought Scenario

Tracer Released on 12/2, Year 1 for 24 hours

(Open Port #2; Initial Inflow Concentration = 100%)

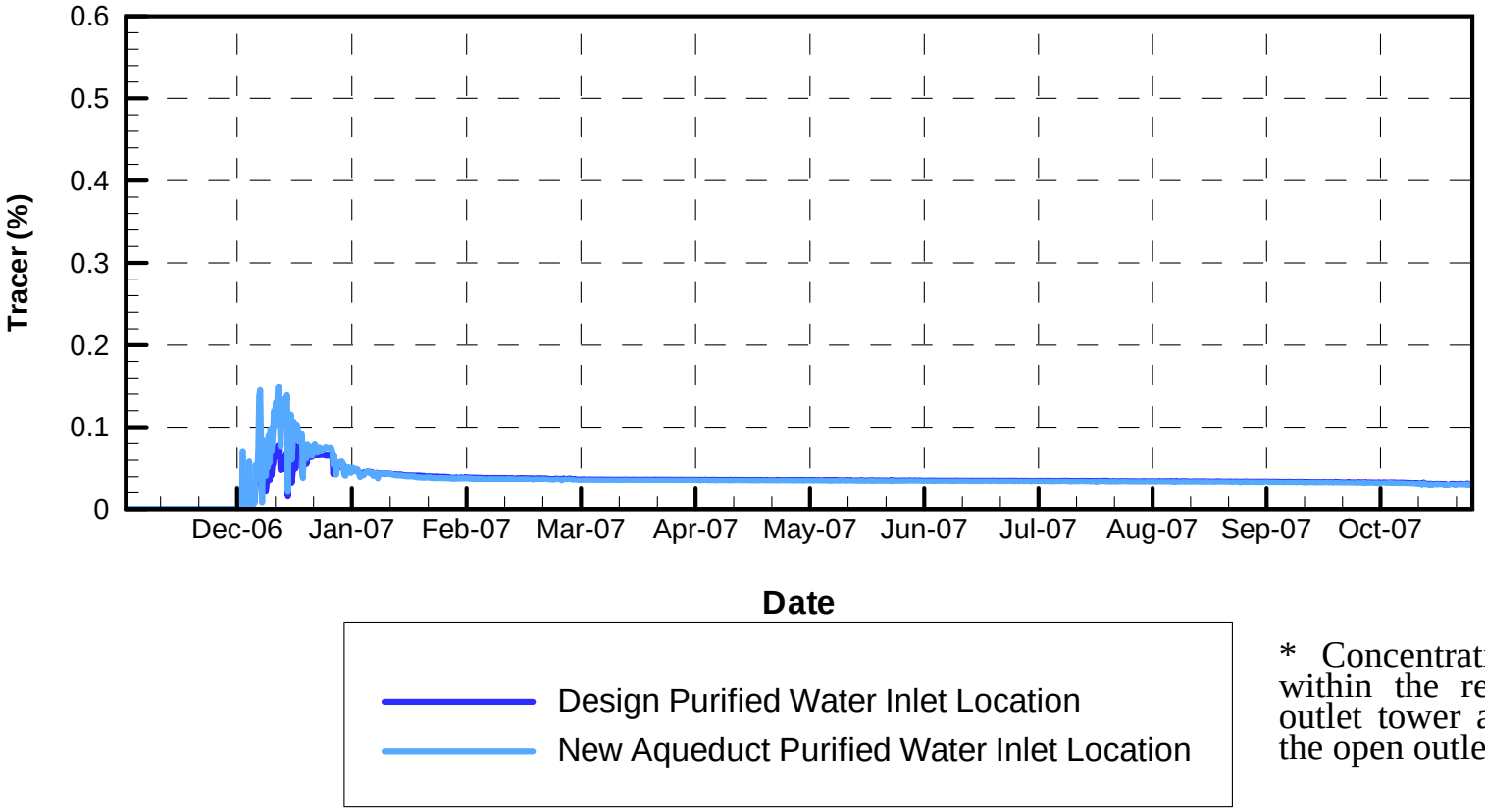

* Concentrations of tracer within the reservoir at the outlet tower at the depth of the open outlet port

FSI V094005
May 01, 2012

Figure 32

FLOW SCIENCE®

Comparison of Reservoir Outflow 24-hour Conservative Tracer Concentrations* from Different Purified Water Inlet Locations Under Extended Drought Scenario

Tracer Released on 1/6, Year 2 for 24 hours

(Open Port #2; Initial Inflow Concentration = 100%)

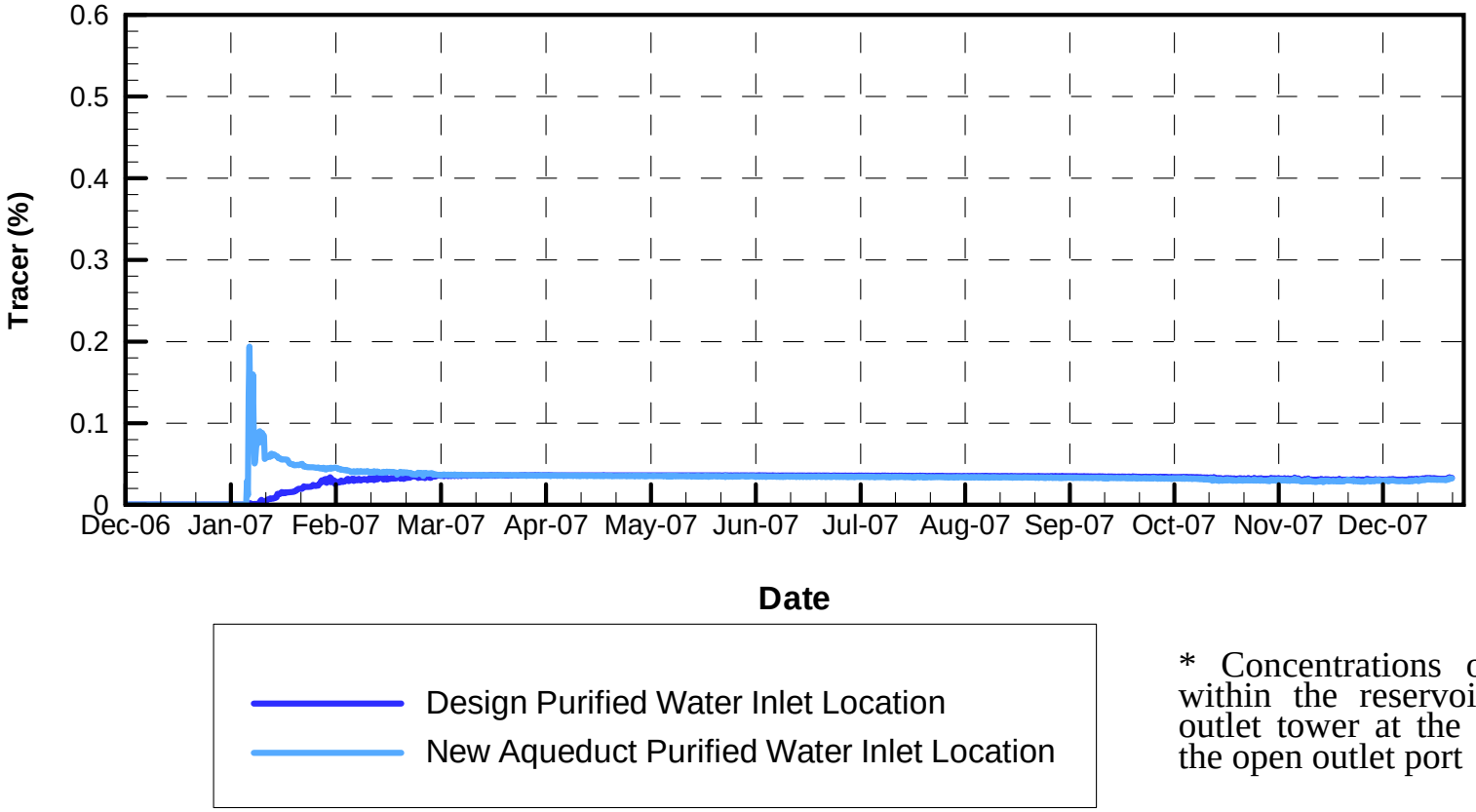

* Concentrations of tracer within the reservoir at the outlet tower at the depth of the open outlet port

FSI V094005
May 01, 2012

Figure 33

FLOW SCIENCE®

Comparison of Reservoir Outflow 24-hour Conservative Tracer Concentrations* from Different Purified Water Inlet Locations Under Extended Drought Scenario

Tracer Released on 1/14, Year 2 for 24 hours

(Open Port #2; Initial Inflow Concentration = 100%)

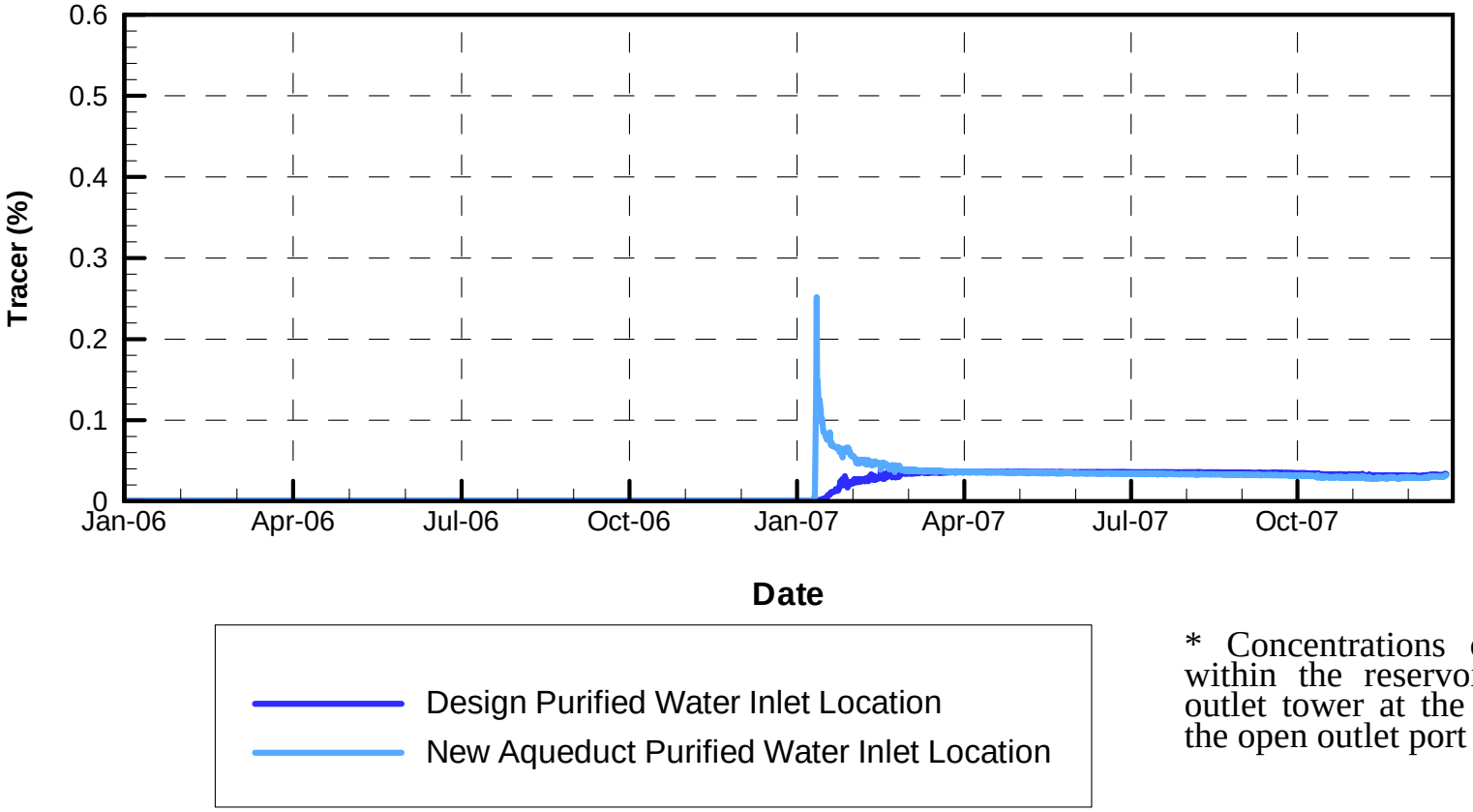

* Concentrations of tracer within the reservoir at the outlet tower at the depth of the open outlet port

FSI V094005
May 01, 2012

Figure 34

FLOW SCIENCE®

Comparison of Reservoir Outflow 24-hour Conservative Tracer Concentrations* from Different Purified Water Inlet Locations Under Extended Drought Scenario

Tracer Released on 1/21, Year 2 for 24 hours

(Open Port #2; Initial Inflow Concentration = 100%)

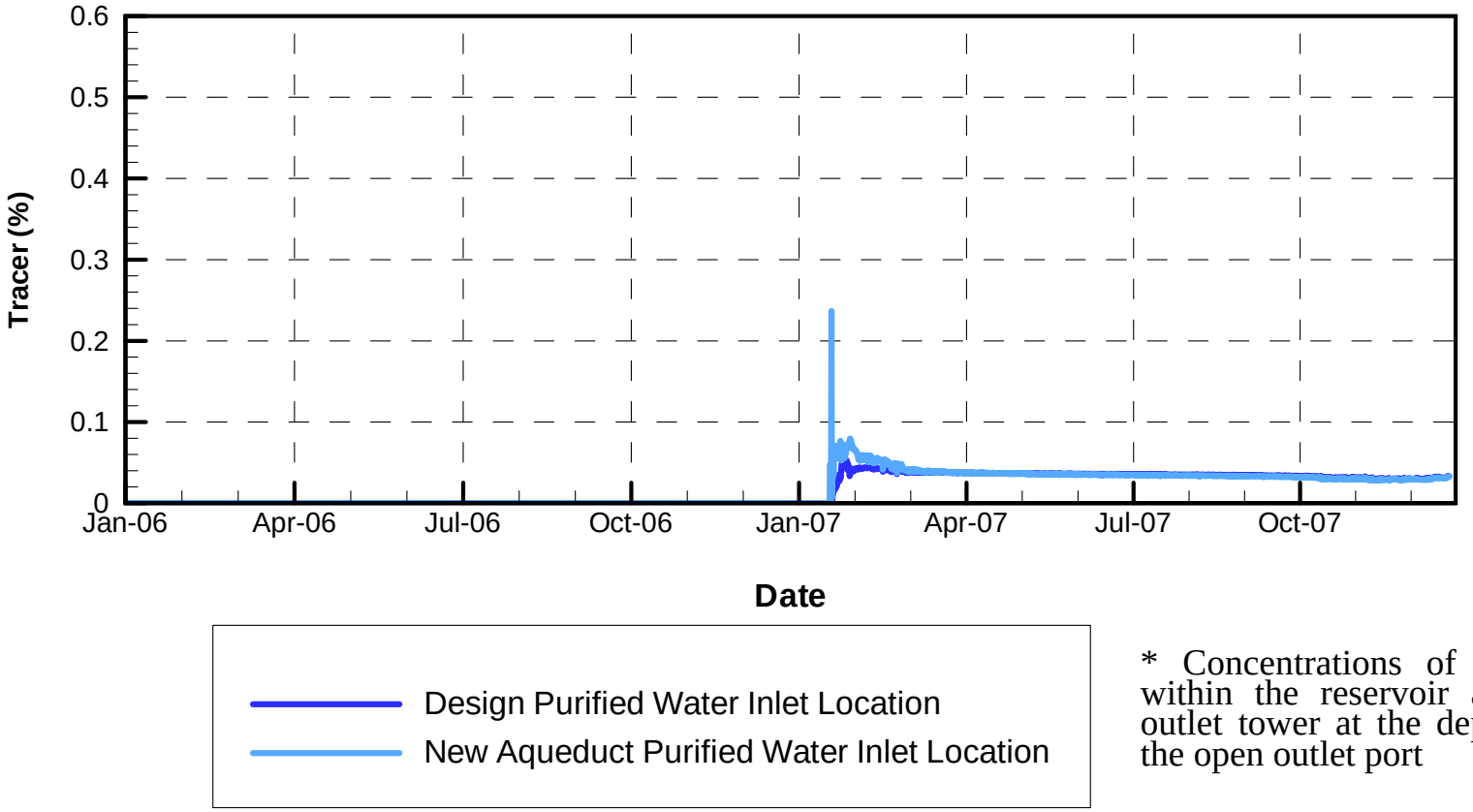

* Concentrations of tracer within the reservoir at the outlet tower at the depth of the open outlet port

FSI V094005
May 01, 2012

Figure 35

FLOW SCIENCE®

Comparison of Reservoir Outflow 24-hour Conservative Tracer Concentrations* from Different Purified Water Inlet Locations Under Extended Drought Scenario

Tracer Released on 11/29, Year 2 for 24 hours

(Open Port #2; Initial Inflow Concentration = 100%)

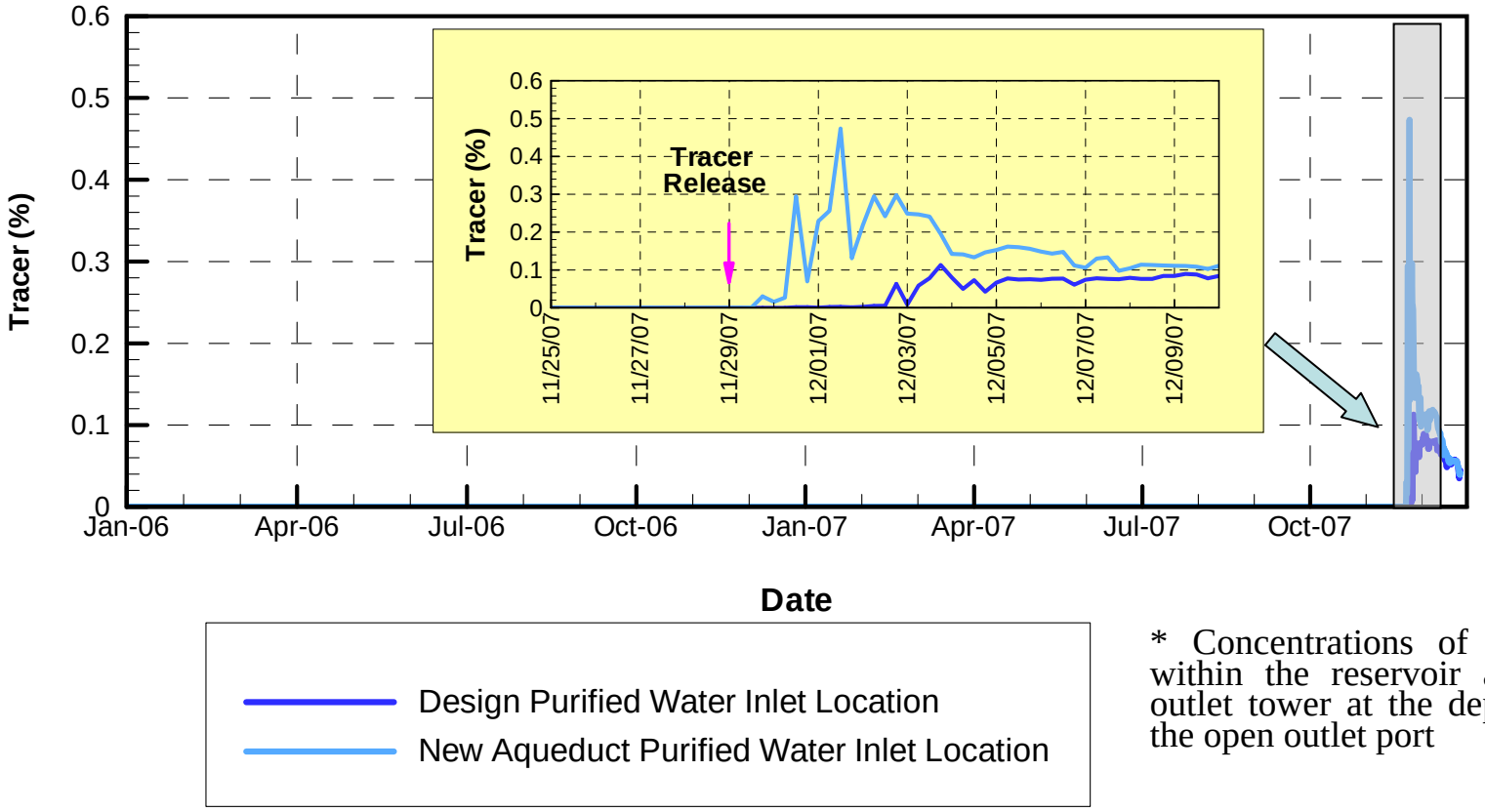

* Concentrations of tracer within the reservoir at the outlet tower at the depth of the open outlet port

FSI V094005
May 01, 2012

Figure 36

FLOW SCIENCE®

Comparison of Reservoir Outflow 24-hour Conservative Tracer Concentrations* from Different Purified Water Inlet Locations Under Extended Drought Scenario

Tracer Released on 12/2, Year 2 for 24 hours

(Open Port #2; Initial Inflow Concentration = 100%)

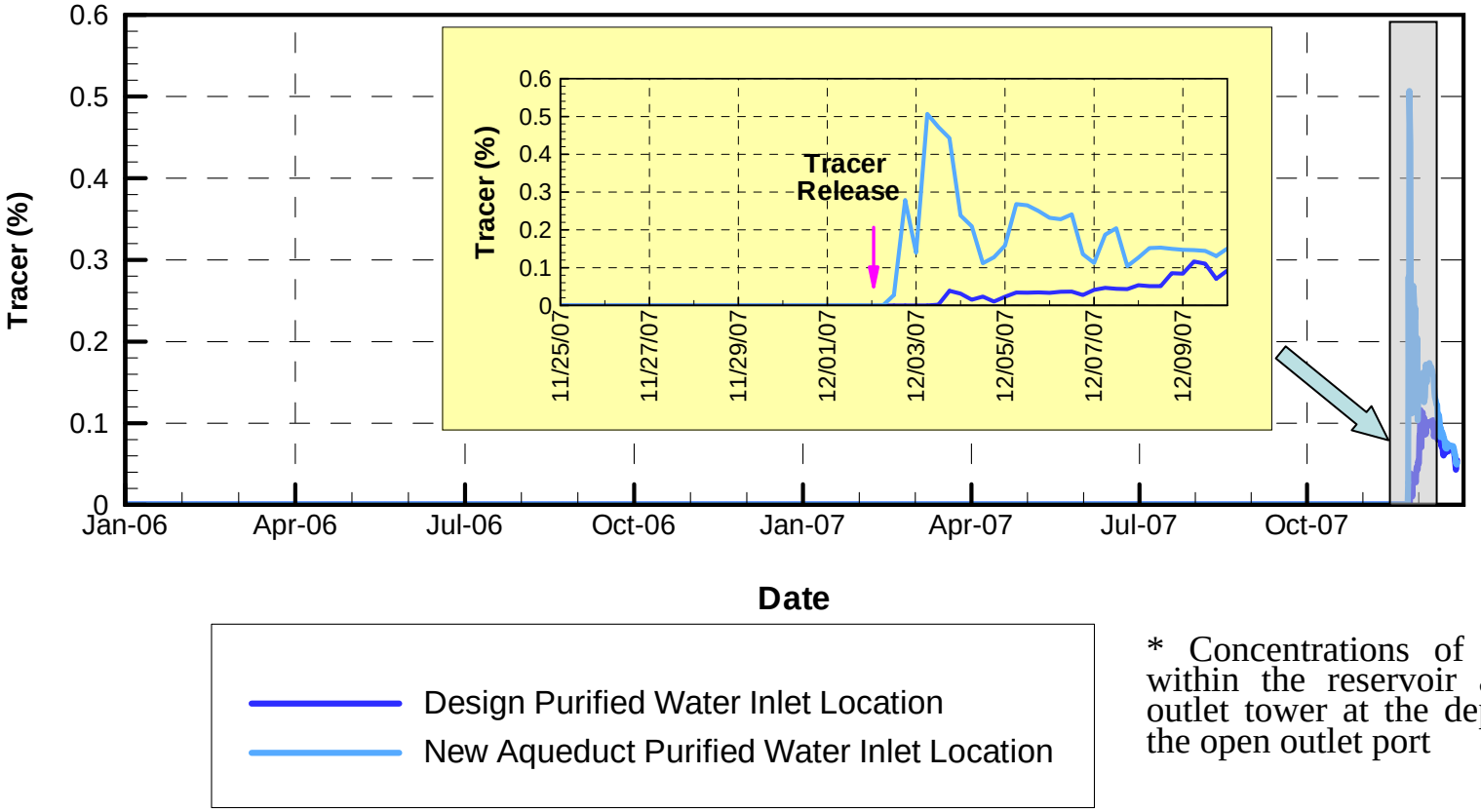

* Concentrations of tracer within the reservoir at the outlet tower at the depth of the open outlet port

FSI V094005
May 01, 2012

Figure 37

FLOW SCIENCE®

APPENDIX A

Description of ELCOM/CAEDYM/Visual Plumes Models and Evidence of Validation

DESCRIPTION OF ELCOM/CAEDYM MODELS AND EVIDENCE OF VALIDATION

The coupling of biogeochemical and hydrodynamic processes in numerical simulations is a fundamental tool for research and engineering studies of water quality in coastal oceans, estuaries, lakes, and rivers. A modeling system for aquatic ecosystems has been developed that combines a three-dimensional hydrodynamic simulation method with a suite of water quality modules that compute interactions between biological organisms and the chemistry of their nutrient cycles. This integrated approach allows for the feedback and coupling between biogeochemical and hydrodynamic systems so that a complete representation of all appropriate processes can be included in an analysis. The hydrodynamic simulation code is the Estuary Lake and Coastal Ocean Model (ELCOM) and the biogeochemical model is the Computational Aquatic Ecosystem Dynamics Model (CAEDYM).

The purpose of this appendix is to demonstrate that ELCOM and CAEDYM are accepted models that have been systematically tested and debugged, and then successfully validated in numerous applications. A history of the models is provided, followed by an outline of the general model methodology and evolution that emphasizes the basis of the ELCOM/ CAEDYM codes in previously validated models and research. Then the process of code development, testing, and validation of ELCOM/CAEDYM is detailed. Specific model applications are described to illustrate how the ELCOM/CAEDYM models have been applied to coastal oceans, estuaries, lakes, and rivers throughout the world and the results successfully validated against field data. Finally, a general description of the governing equations, numerical models, and processes used in the models is provided along with an extensive bibliography of supporting material.

A comprehensive description of the equations and methods used in the models is provided in the "Estuary Lake and Coastal Ocean Model: ELCOM v2.2 Science Manual" by Hodges and Dallimore (2006), "Estuary Lake and Coastal Ocean Model: ELCOM v2.2 User Manual" by Hodges and Dallimore (2007), "Computational Aquatic Ecosystem Dynamics Model: CAEDYM: v2.2 Science Manual" by Hipsey, Romero, Antenucci and Hamilton (2005), and the "Computational Aquatic Ecosystem Dynamics Model: CAEDYM: v2.2 User Manual" by Hipsey, Romero, Antenucci and Hamilton (2005).

A.1.1 MODEL HISTORY

The ELCOM/CAEDYM models were originally developed at the Centre for Water Research (CWR) at the University of Western Australia, although the hydrodynamics

code ELCOM is an outgrowth of a hydrodynamic model developed earlier by Professor Vincenzo Casulli in Italy and now in use at Stanford University under the name TRIM-3D. The CAEDYM model was essentially developed at CWR as an outgrowth of earlier water quality modules used in the one-dimensional model, Dynamic Reservoir Simulation Model - Water Quality (DYRESM-WQ, Hamilton and Schladow, 1997).

The original ELCOM/CAEDYM models, as developed by CWR, were implemented in Fortran 90 (with F95 extensions) on a UNIX computer system platform. In 2001, the codes for both models were ported to a personal computer (PC) platform through an extensive recompiling and debugging effort by Flow Science Incorporated (Flow Science) in Pasadena, California. Since then, Flow Science has updated the PC version of the code several times when new versions of the code have been released by CWR.

A.1.2 MODEL METHODOLOGY

ELCOM is a three-dimensional numerical simulation code designed for practical numerical simulation of hydrodynamics and thermodynamics for inland and coastal waters. The code links seamlessly with the CAEDYM biogeochemical model undergoing continuous development at CWR, as shown graphically in **Figure A.1**. The

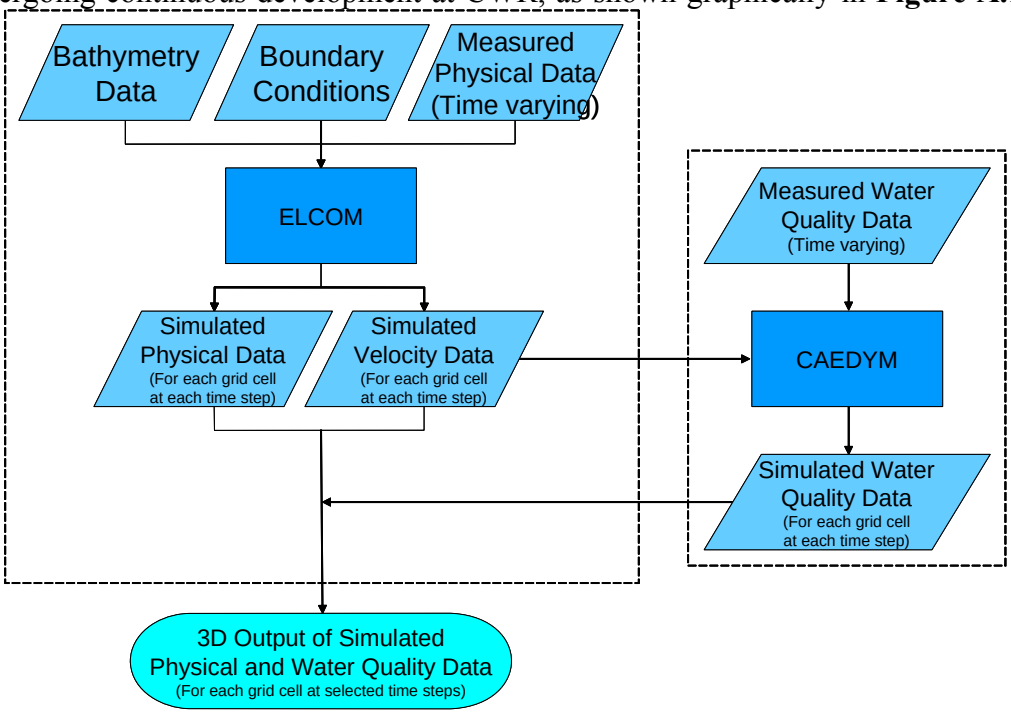

Figure A.1 Flow chart showing the integration of the linked ELCOM/CAEDYM models.

combination of the two codes provides three-dimensional simulation capability for examination of changes in water quality that arise from anthropogenic changes in either quality of inflows or reservoir operations.

The numerical method used in ELCOM is based on the TRIM-3D model scheme of Casulli and Cheng (1992) with adaptations made to improve accuracy, scalar conversion, numerical diffusion, and implementation of a mixed-layer model. The ELCOM model also extends the TRIM-3D scheme by including conservative advection of scalars. The unsteady Reynolds-averaged, Navier-Stokes equations, and the scalar transport equations serve as the basis of ELCOM. The pressure distribution is assumed hydrostatic and density changes do not impact the inertia of the fluid (the Boussinesq approximation), but are considered in the fluid body forces. There is an eddy-viscosity approximation for the horizontal turbulence correlations that represent the turbulent momentum transfer. Vertical momentum transfer is handled by a Richardson number-based diffusion coefficient. Since numerical diffusion generally dominates molecular processes, molecular diffusion in the vertical direction is neglected in ELCOM.

Both ELCOM and TRIM-3D are three-dimensional, computational fluid dynamics (CFD) models. CFD modeling is a validated and well-established approach to solving the equations of fluid motions in a variety of disciplines. Prior to the development of TRIM-3D, there were difficulties in modeling density-stratified flows and such flows required special numerical methods. With TRIM-3D, Casulli and Cheng (1992) developed the first such successful method to model density-stratified flows, such as occur in the natural environment. Since then, TRIM-3D has been validated by numerous publications. ELCOM is based on the same proven method, but incorporates additional improvements as described above. Furthermore, the ELCOM model is based on governing equations and numerical algorithms that have been used in the past (*e.g.,* in validated models such as TRIM-3D), and have been validated in refereed publications. For example:

- The hydrodynamic algorithms in ELCOM are based on the Euler-Lagrange method for advection of momentum with a conjugate gradient solution for the free-surface height (Casulli and Cheng, 1992).

- The free-surface evolution is governed by vertical integration of the continuity equation for incompressible flow applied to the kinematic boundary condition (*e.g.*, Kowalik and Murty, 1993).

- The numerical scheme is a semi-implicit solution of the hydrostatic Navier-Stokes equations with a quadratic Euler-Lagrange, or semi-Lagrangian (Staniforth and Côté, 1991).

- Passive and active scalars (*i.e.,* tracers, salinity, and temperature) are advected using a conservative ULTIMATE QUICKEST discretization (Leonard, 1991). The ULTIMATE QUICKEST approach has been implemented in two-dimensional format and demonstration of its effectiveness in estuarine flows has been documented by Lin and Falconer (1997).

- Heat exchange is governed by standard bulk transfer models found in the literature (*e.g.*, Smooch and DeVries, 1980; Imberger and Patterson, 1981; Jacquet, 1983).

- The vertical mixing model is based on an approach derived from the mixing energy budgets used in one-dimensional lake modeling as presented in Imberger and Patterson (1981), Spigel et al (1986), and Imberger and Patterson (1990). Furthermore, Hodges presents a summary of validation using laboratory experiments of Stevens and Imberger (1996). This validation exercise demonstrates the ability of the mixed-layer model to capture the correct momentum input to the mixed-layer and reproduce the correct basin-scale dynamics, even while boundary-induced mixing is not directly modeled.

- The wind momentum model is based on a mixed-layer model combined with a model for the distribution of momentum over depth (Imberger and Patterson, 1990).

The numerical approach and momentum and free surface discretization used in ELCOM are defined in more detail in Hodges, Imberger, Saggio, and Winters (1999). Similarly, the water quality processes and methodology used in CAEDYM are described in more detail in Hamilton and Schladow (1997). Further technical details on ELCOM and CAEDYM are provided in Sections 0 and 0 below.

A.1.3 VALIDATION AND APPLICATION OF ELCOM/CAEDYM

Since initial model development, testing and validation of ELCOM and/or CAEDYM have been performed and numerous papers on model applications have been presented, written, and/or published as described in more detail below. In summary:

- ELCOM solves the full three-dimensional flow equations with small approximations.

- ELCOM/CAEDYM was developed, tested, and validated over a variety of test cases and systems by CWR.

- Papers on ELCOM/CAEDYM algorithms, methodology, and applications have been published in peer reviewed journals such as the *Journal of Geophysical Research*, the *Journal of Fluid Mechanics*, the *Journal of Hydraulic Engineering*, the *International Journal for Numerical Methods in Fluids*, and *Limnology and Oceanography*.

- ELCOM/CAEDYM was applied by Flow Science to Lake Mead, Nevada. As part of this application, mass balances were verified and results were presented to a model review panel over a two-year period. The model review panel, the National Park Service, the United States Bureau of Reclamation, the Southern Nevada Water Authority, and the Clean Water Coalition (a consortium of water and wastewater operators in the Las Vegas, Nevada, region) all accepted the ELCOM/CAEDYM model use and validity.

- There are numerous applications of ELCOM/CAEDYM in the literature that compare the results to data, as summarized in Section 0.

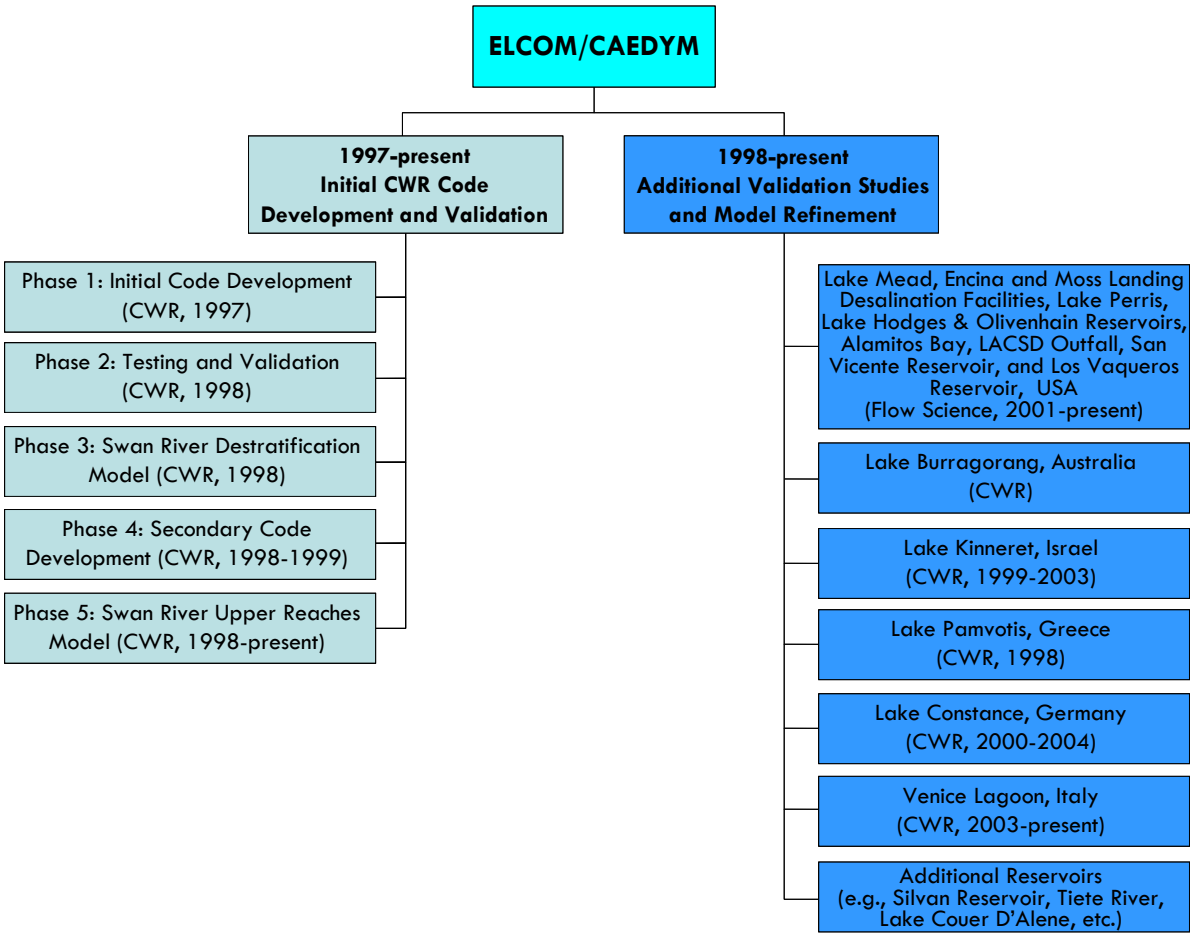

Figure A.2 ELCOM/CAEDYM code development, testing, validation, and applications by CWR and Flow Science Incorporated.

The process of code development, testing, and validation of ELCOM/CAEDYM by CWR, and the ongoing validation and refinement of the codes through further application of the models are detailed in the following subsections. The major components of the development, testing, and validation process are summarized in **Figure A.2**.

A.1.3.1 CWR Code Development, Testing, and Validation

Initial development of the code by CWR occurred from March through December 1997 (Phase 1), followed by a period of testing and validation from January through April 1998 (Phases 2 and 3). Secondary code development by CWR occurred from September 1998 through February 1999 (Phase 4). Testing and validation were

performed over a variety of test cases and systems to ensure that all facets of the code were tested. In addition, Phase 5 modeling of the Swan River since 1998 has been used to gain a better understanding of the requirements and limitations of the model (Hodges et al, 1999).

A.1.3.1.1 *Phase 1: Initial Code Development*

The ELCOM code was initially conceived by CWR as a Fortran 90/95 adaptation of the TRIM-3D model of Casulli and Cheng (1992) in order to: 1) link directly to the CAEDYM water quality module developed concurrently at CWR and 2) provide a basis for future development in a modern programming language. Although written in Fortran 77, TRIM-3D is considered a state-of-the-art numerical model for estuarine applications using a semi-implicit discretization of the Reynolds-averaged hydrostatic Navier-Stokes equations and an Euler-Lagrange method for momentum and scalar transport.

During development of ELCOM, it became clear that additional improvements to the TRIM-3D algorithm were required for accurate solution of density-stratified flows in estuaries. After the basic numerical algorithms were written in Fortran 90, subroutine-by-subroutine debugging was performed to ensure that each subroutine produced the expected results. Debugging and testing of the entire model used a series of test cases that exercised the individual processes in simplified geometries. This included test cases for the functioning of the open boundary condition (tidal forcing), surface wave propagation, internal wave propagation, scalar transport, surface thermodynamics, density underflows, wind-driven circulations, and flooding/drying of shoreline grid cells. Shortcomings identified in the base numerical algorithms were addressed during secondary code development (Phase 4).

Towards the end of the initial code development, ELCOM/CAEDYM were coupled and test simulations were run to calibrate the ability of the models to work together on some simplified problems. Results showing the density-driven currents induced by phytoplankton shading were presented at the Second International Symposium on Ecology and Engineering (Hodges and Herzfeld, 1997). Further details of modeling of density-driven currents due to combinations of topographic effects and phytoplankton shading were presented at a joint meeting of the American Geophysical Union (AGU) and the American Society of Limnology and Oceanography (ASLO) by Hodges et al. (1998), and at a special seminar at Stanford University (Hodges 1998). Additionally, presentations by Hamilton (1997), Herzfeld et al. (1997), and Herzfeld and Hamilton (1998) documented the concurrent development of the CAEDYM ecological model.

A.1.3.1.2 *Phase 2: Testing and Validation*

The simplified geometry tests of Phase I revealed deficiencies in the TRIM-3D algorithm including the inability of the TRIM-3D Euler-Lagrange method (ELM) to provide conservative transport of scalar concentrations (e.g., salinity and temperature). Thus, a variety of alternate scalar transport methods were tested, with the best performance being a flux-conservative implementation of the ULTIMATE filter applied to third-order QUICKEST discretization based on the work of Leonard (1991).

Model testing and validation against simple test cases was again undertaken. In addition, a simulation of a winter underflow event in Lake Burragorang in New South Wales, Australia, was performed to examine the ability of the model to capture a density underflow in complex topography in comparison to field data taken during the inflow event. These tests showed that the ability to model underflows is severely constrained by the cross-channel grid resolution.

A.1.3.1.3 *Phase 3: Swan River Destratification Model*

Phase 3 involved examining a linked ELCOM/CAEDYM destratification model of the Swan River system during a period of destratification in 1997 when intensive field monitoring had been conducted. The preliminary results of this work were presented at the Swan-Canning Estuary Conference (Hertzfeld *et al,* 1998). More comprehensive results were presented at the Western Australian Estuarine Research Foundation (WAERF) Community Forum (Imberger, 1998).

A.1.3.1.4 *Phase 4: Secondary Code Development*

In conducting the Phase 3 Swan River destratification modeling, it became clear to CWR that long-term modeling of the salt-wedge propagation would require a better model for mixing dynamics than presently existed. Thus, the availability of an extensive field data set for Lake Kinneret, Israel, led to its use as a test case for development of an improved mixing algorithm for stratified flows (Hodges *et al*, 1999).

A further problem appeared in the poor resolution of momentum terms using the linear ELM discretization (i.e., as used in the original TRIM-3D method). Since the conservative ULTIMATE QUICKEST method (used for scalar transport, see Phase 1 above) does not lend itself to efficient use for discretization of momentum terms in a semi-implicit method, a quadratic ELM approach was developed for more accurate discretization of the velocities.

A.1.3.1.5 *Phase 5: Swan River Upper Reaches Model*

Phases 1-4 developed and refined the ELCOM code for accurate modeling of three-dimensional hydrodynamics where the physical domain is well resolved. Phase 5 is an ongoing process of model refinement that concentrates on developing a viable approach to modeling longer-term evolution hydrodynamics and water quality in the Swan River where fine-scale resolution of the domain is not practical. The Swan River application is also used for ongoing testing and calibration of the CAEDYM water quality module.

The Swan River estuary is located on the Swan Coastal Plain, Western Australia. It is subject to moderate to high nutrient loads associated with urban and agricultural runoff and suffered from *Microcystis aeruginosa* blooms in January 2000. In an effort to find a viable means of conducting seasonal to annual simulations of the Swan River that retain the fundamental along-river physics and the cross-channel variability in water quality parameters, CWR has developed and tested ELCOM/CAEDYM extensively. A progress report by Hodges et al (1999) indicates that ELCOM is capable of accurately reproducing the hydrodynamics of the Swan River over long time scales with a reasonable computational time.

Furthermore, studies conducted by Robson and Hamilton (2002) proved that ELCOM/CAEDYM accurately reproduced the unusual hydrodynamic circumstances that occurred in January 2000 after a record maximum rainfall, and predicted the magnitude and timing of the *Microcystis* bloom. These studies show that better identification and monitoring procedures for potentially harmful phytoplankton species could be established with ELCOM/CAEDYM and will assist in surveillance and warnings for the future.

A.1.3.2 Model Applications

In addition to the initial code development, testing, and validation by CWR, numerous other applications of ELCOM/CAEDYM have been developed by CWR and validated against field data. Additionally, Flow Science has applied ELCOM/CAEDYM extensively at Lake Mead (USA) and validated the results against measured data. The results of numerous ELCOM/CAEDYM model applications are presented below.

A.1.3.2.1 *Lake Mead (Nevada, USA)*

An ELCOM/CAEDYM model of Boulder Basin, Lake Mead near Las Vegas, Nevada, was used to evaluate alternative discharge scenarios for inclusion in an Environmental Impact Statement (EIS) for the Clean Water Coalition (CWC), a

consortium of water and wastewater operators in the Las Vegas region. **Figure A.3** is a cut-away of the three-dimensional model grid used for Boulder Basin, showing the varying grid spacing in the vertical direction.

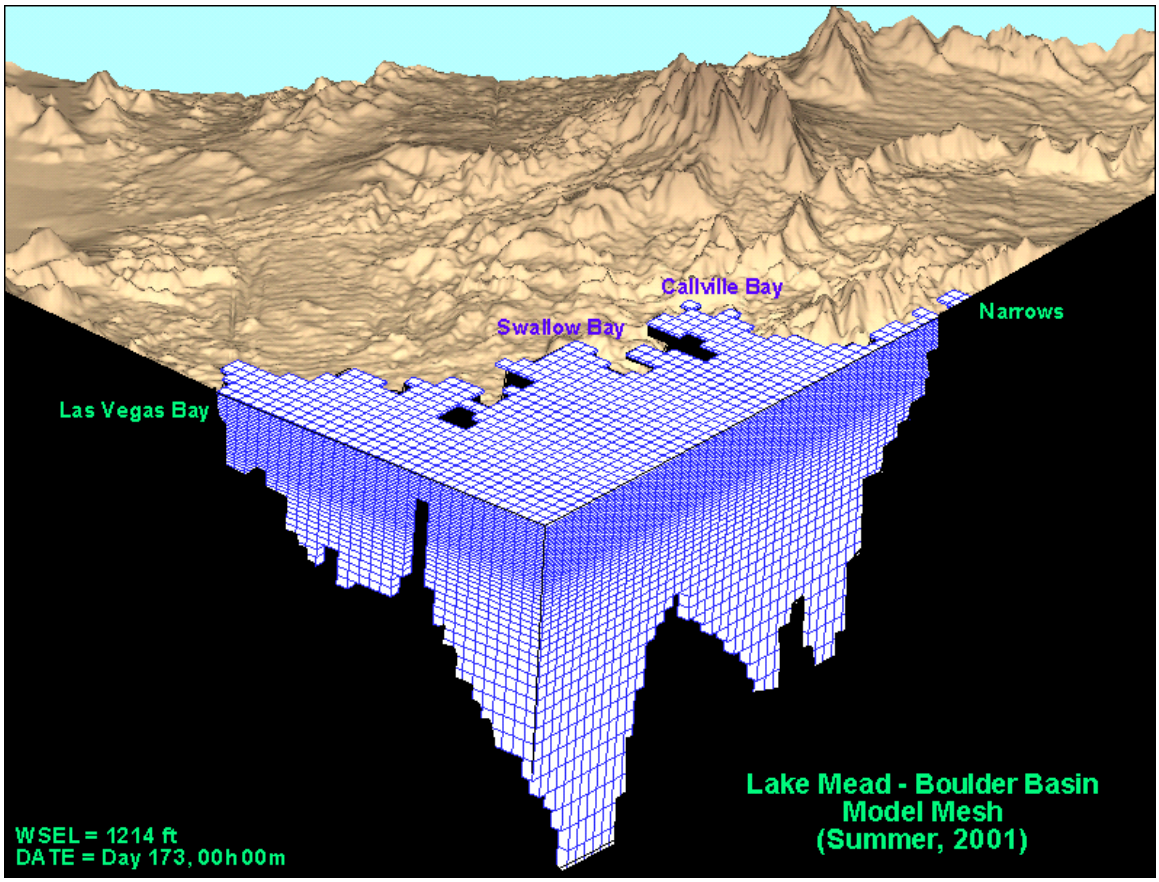

Figure A.3 Model grid for Lake Mead Boulder Basin model.

As part of the EIS process, a model review panel met monthly for two years to review the validation of the ELCOM/CAEDYM model, its calibration against field data, and its application. The modeling committee approved the use of the model. Subsequently, a scientific Water Quality Advisory Panel concluded that the ELCOM/CAEDYM model was applicable and acceptable. The members of the Water Quality Advisory Panel were diverse and included Jean Marie Boyer, Ph.D., P.E. (Water Quality Specialist/Modeler, Hydrosphere), Chris Holdren, Ph.D., CLM (Limnologist, United States Bureau of Reclamation), Alex Horne, Ph.D. (Ecological Engineer, University of California Berkeley), and Dale Robertson, Ph.D. (Research Hydrologist, United States Geological

Survey). More specifically, the Water Quality Advisory Panel agreed on the following findings:

- The ELCOM/CAEDYM model is appropriate for the project.
- There are few three-dimensional models available for reservoirs. ELCOM is one of the best hydrodynamic models and has had good success in the Boulder Basin of Lake Mead and other systems.
- The ELCOM model accurately simulates most physical processes.
- The algorithms used in CAEDYM are widely accepted (a biological consultant, Professor David Hamilton of The University of Waikato, New Zealand, was retained to review the CAEDYM coefficients and algorithms).

The Boulder Basin ELCOM/CAEDYM model was calibrated against four years of measured data for numerous physical and water quality parameters including temperature, salinity, conductivity, dissolved oxygen, pH, nutrients (nitrogen and phosphorus), chlorophyll *a*, perchlorate, chloride, sulfate, bromide, and total organic carbon. Detailed results of this calibration and the subsequent evaluation of alternative discharge scenarios were made available in late 2005 in the CWC EIS that was being prepared for this project. An example of the calibration results for chlorophyll *a* for 2002 is presented in **Figure A.4** below. In this figure, simulated concentrations are compared against field data measured in the lake by the United States Bureau of Reclamation (USBR) and the City of Las Vegas (COLV).

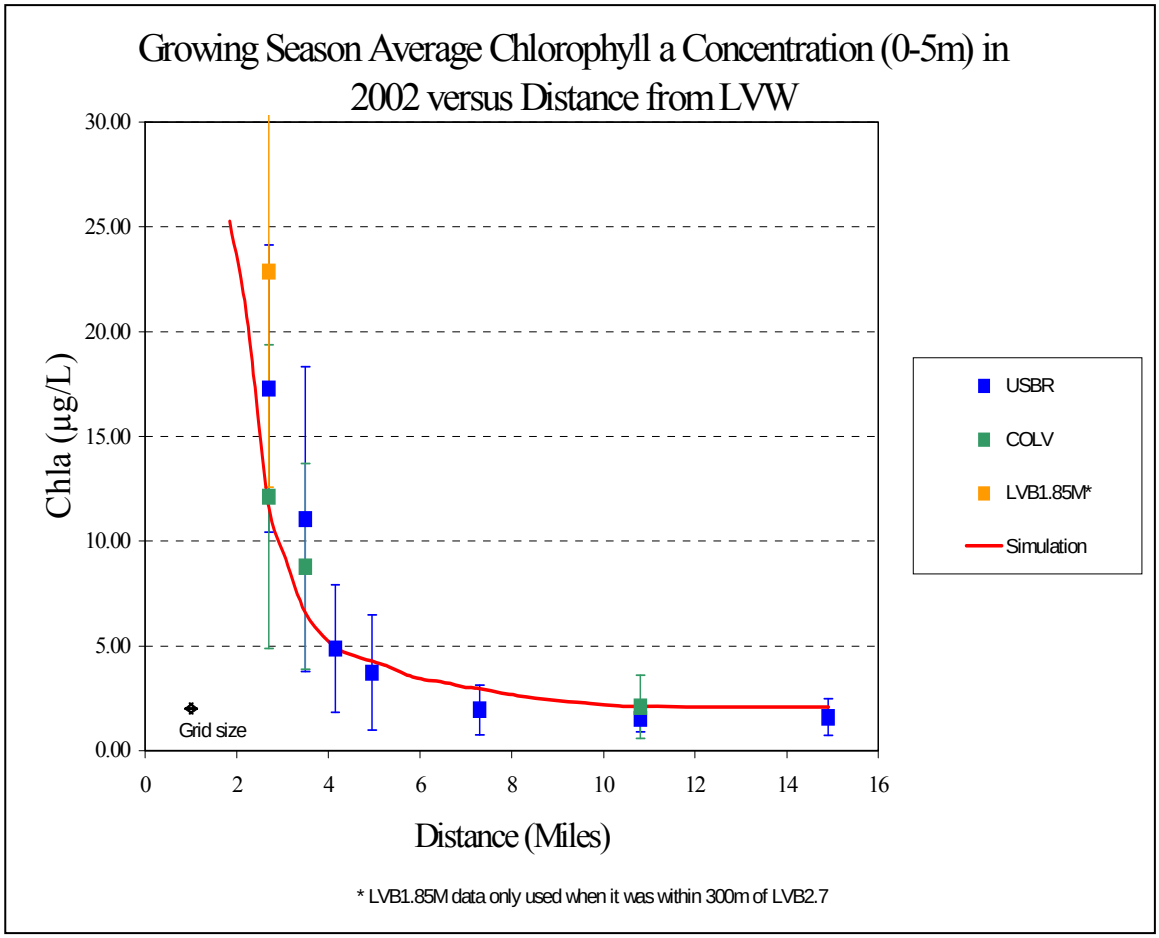

Figure A.4 ELCOM/CAEDYM calibration results for chlorophyll a in Boulder Basin for 2002 as a function of distance from the inflow at Las Vegas Wash.

Most recently, the original Boulder Basin model was extended to include all of Lake Mead, including the Overton Arm and Gregg Basin. The extended whole lake ELCOM/CAEDYM model has been calibrated against nine (9) years of data for use in informing design and operations management decisions. Specifically, the model has been used to simulate temperature (including stratification patterns), salinity, conductivity, dissolved oxygen, nutrients, chlorophyll *a* (as a surrogate for algae), perchlorate, total organic carbon, bromide, and suspended solids. **Figure A.5** below shows the extent of the expanded whole lake domain and the calibration results for conductivity for February 2005.

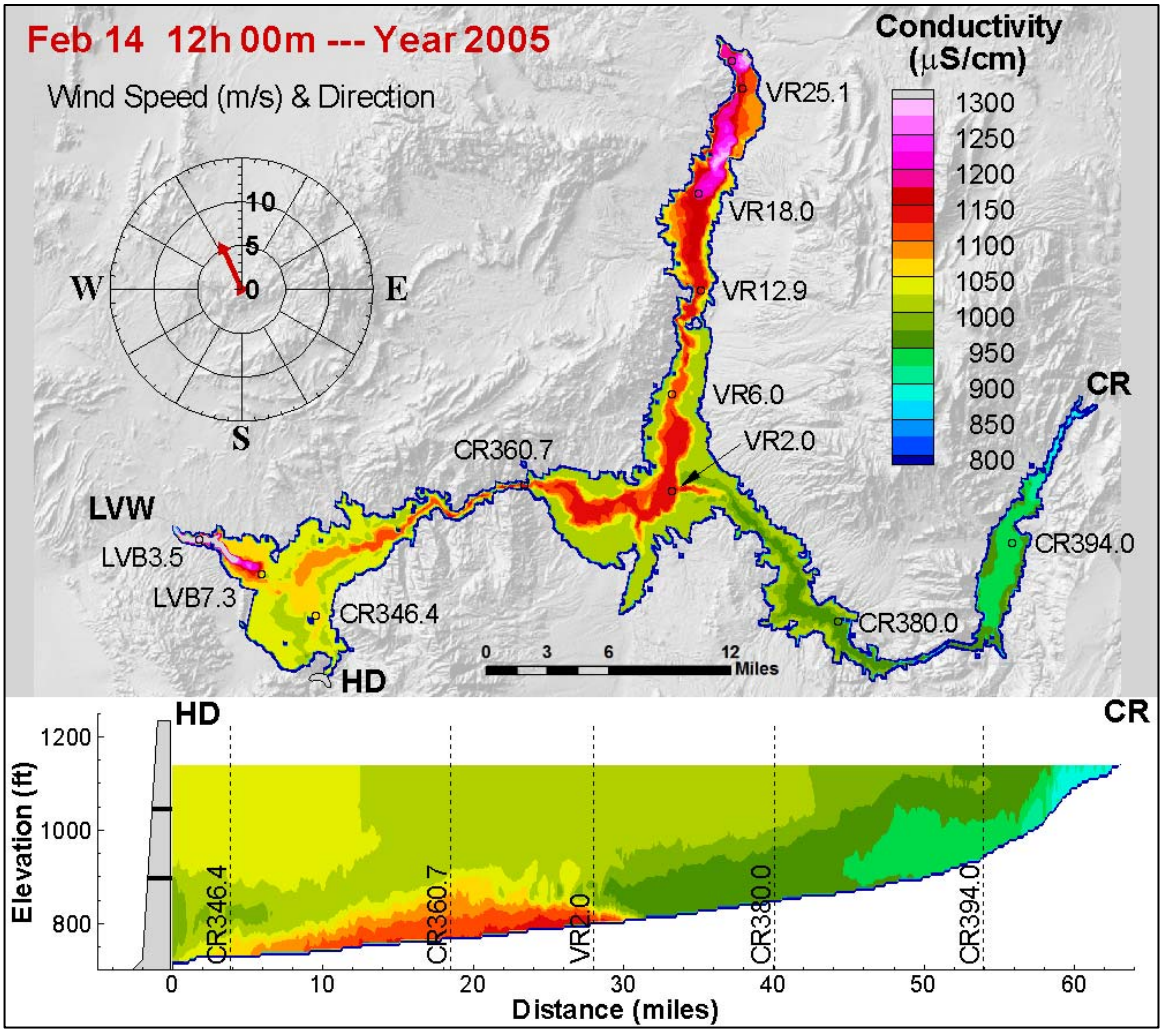

Figure A.5 ELCOM/CAEDYM calibration results for conductivity in the Lake Mead Whole Lake Model (including plan view of entire lake and cross-section from Hoover Dam to the mouth of the Colorado River).

ELCOM/CAEDYM model of the entire Lake Mead is being continually updated and calibrated on approximately a yearly basis, with funding having been provided by the CWC, the Southern Nevada Water Authority, and the National Park Service. These various stakeholders have demonstrated a long term commitment to maintaining the model because it has proven to be a worthy and successful tool. Additional funding for

ELCOM/CAEDYM modeling of the impacts of climate change on Lake Mead is being provided by the USBR under the WaterSMART grant program.

A.1.3.2.2*Lake Burragorang (New South Wales, Australia)*

ELCOM was applied and validated for Lake Burragorang in order to rapidly assess the potential impacts on water quality during an underflow event (CWR). Underflows usually occur during the winter when inflow water temperature is low compared to the reservoir. This causes the upheaval of hypolimnetic water at the dam wall, and as a result it transports nutrient rich waters into the euphotic zone.

The thermal dynamics during the underflow event were reproduced accurately by ELCOM for the case with idealized bathymetry data with coarse resolutions (straightened curves and rotating the lake in order to bypass the resolution problem), but not for the simulation with the complex, actual bathymetry. This is because the model tests showed that the ability to model underflows is severely constrained by the cross-channel grid resolution. When the cross-channel direction is poorly resolved at bends and curves, an underflow is unable to propagate downstream without a significant loss of momentum. Nevertheless, the simulations with the coarse idealized domain certainly can be used as aids and tools to visualize the behavior of reservoirs. Particularly, ELCOM was able to capture the traversal of the underflow down the length of Lake Burragorang and then had sufficient momentum to break against the wall causing the injection of underflow waters into the epilimnion near the dam. This simulated dynamic was in agreement with what was measured in the field.

A.1.3.2.3*Lake Kinneret (Israel)*

ELCOM was applied to model basin-scale internal waves that are seen in Lake Kinneret, Israel, since understanding of basin-scale internal waves behaviors provide valuable information on mixing and transport of nutrients below the wind-mixed layer in stratified lakes. In studies done by Hodges et al. (1999) and Laval et al (2003), the ELCOM simulation results were compared with field data under summer stratification conditions to identify and illustrate the spatial structure of the lowest-mode basin-scale Kelvin and Poincare waves that provide the largest two peaks in the internal wave energy spectra. The results demonstrated that while ELCOM showed quantitative differences in the amplitude and steepness of the waves as well as in the wave phases, the basin-scale waves were resolved very well by ELCOM. In particular, the model captures the qualitative nature of the peaks and troughs in the thermocline and the depth of the wind-mixed layer at relatively coarse vertical grid resolutions (Hodges et al, 1999).

A.1.3.2.4 *Lake Pamvotis (Greece)*

ELCOM/CAEDYM was applied to Lake Pamvotis, a moderately sized (22 km^2), shallow (4 m average depth) lake located in northwest Greece. Since the lake has undergone eutrophication over the past 40 years, many efforts are directed at understanding the characteristics of the lake and developing watershed management and restoration plans.

Romero and Imberger (1999) simulated Lake Pamvotis over a one month period during May to June, 1998, and compared the simulated thermal and advective dynamics of the lake with data obtained from a series of field experiments. The simulation results over-predicted heating; however, diurnal fluctuations in thermal structures were similar to those measured. Since the meteorological site was sheltered from the winds, the wind data used in the simulation was believed to be too low, causing insufficient evaporative heat-loss and subsequent over-heating by ELCOM. An increase in the wind speed by a factor of three gave temperature profiles in agreement with the field data. Moreover, the study demonstrated that the model is capable of predicting the substantial diurnal variations in the intensity and direction of both vertical and horizontal velocities. Romero and Imberger were also able to illustrate the functionality of ELCOM when coupled to the water quality model, CAEDYM, and confirmed that the model could be used to evaluate the effect of various strategies to improve poor water quality in localized areas in the lake.

A.1.3.2.5 *Lake Constance (Germany, Austria, Switzerland)*

Appt (2000) and Appt et al. (2004) applied ELCOM to characterize the internal wave structures and motions in Lake Constance [Bodensee] since internal waves are a key factor in understanding the transport mechanisms for chemical and biological processes in a stratified lake such as Lake Constance. Lake Constance is an important source of drinking water and a major tourism destination for its three surrounding countries of Germany, Austria, and Switzerland. Due to anthropogenic activities and climatic changes, Lake Constance water quality has deteriorated and its ecosystem has changed.

It was shown that ELCOM was able to reproduce the dominant internal wave and major hydrodynamic processes occurring in Lake Constance. For instance, three types of basin-scale waves were found to dominate the wave motion: the vertical mode-one Kelvin wave, the vertical mode-one Poincare waves, and a vertical mode-two Poincare wave. Moreover, an upwelling event was also reproduced by ELCOM suggesting that the width and length ratio of the basin, spatial variations in the wind, and Coriolis effects play critical roles in the details of the upwelling event. This on-going research has shown

that ELCOM can be used as a tool to predict and understand hydrodynamics and water quality in lakes.

A.1.3.2.6 *Venice Lagoon (Italy)*

ELCOM/CAEDYM is being used to develop a hydrodynamic and sediment transport model of Venice Lagoon, Italy, since future gate closures at the mouth of the lagoon are likely to impact flushing patterns. This project is an integral part of the Venice Gate Projects in Italy that was launched in May 2003 to prevent flooding.

ELCOM was validated for the tidal amplitude and phase using the data obtained from 12 tidal stations located throughout the lagoon (Yeates, 2004). Remaining tasks include model validation of temperature, salinity, and velocity against measurements made in the major channels of the lagoon.

A.1.3.2.7 *Silvan Reservoir (Australia)*

ELCOM is currently being applied to reproduce the circulation patterns observed in Silvan Reservoir, Australia, during a field experiment that was conducted in March 2004 to determine the transport pathways in the lake. This experiment confirmed the upwelling behavior of the lake and the strong role of the inflows in creating hydraulic flows in the reservoir (Antenucci, 2004).

A.1.3.2.8 *Billings and Barra Bonita Reservoirs (Brazil)*

ELCOM/CAEDYM is being applied to Billings and Barra Bonita Reservoirs in Brazil. Billings Reservoir is an upstream reservoir that feeds Barra Bonita via the Tiete River. The objective of the project is to develop an integrated management tool for these reservoirs and river reaches for use in the future planning of water resource utilization in Sao Paulo, Brazil (Romero and Antenucci, 2004).

A.1.3.2.9 *Lake Coeur D'Alene (Idaho, USA)*

ELCOM/CAEDYM is being applied to investigate the trade-off between reducing heavy metal concentrations and a potential increase in eutrophication due to remediation procedures in Lake Coeur D'Alene, Idaho. In order to investigate heavy metal fate and transport, CAEDYM is being improved further to include heavy metals and a feedback loop to phytoplankton based on metal toxicity (Antenucci, 2004).

A.1.3.2.10 *Seawater Desalination at Encina (California, USA)*

Flow Science conducted ELCOM modeling in 2004-2006 for a proposed desalination facility to be sited adjacent to the Encina Power Plant in Carlsbad, California. The proposed Encina facility involved source water taken from inside Agua Hedionda Lagoon and discharge of brines with the power plant cooling water via a surface channel across the beach south of the lagoon mouth. Flow Science used both a fine grid model to simulate water quality and dilution local to the intake and outfall and a larger grid model to simulate the effect of treated wastewater discharges and ocean currents and tides in the ocean near the lagoon. For the Encina study, Flow Science also used ELCOM to predict mixing in the vicinity of the plant discharge. The study area encompassed about 100 square miles of the ocean and also included some inland lagoons. The model resolved various tidal conditions and plant operating scenarios. The model compared favorably to existing oceanic data in the vicinity of the discharge.

A.1.3.2.11 *Moss Landing Desalination Project (California, USA)*

Flow Science applied ELCOM to simulate the flow and mixing in the entire Monterey Bay, including Elkhorn Slough. The purpose of the modeling was to evaluate the impacts of the proposed Moss Landing Desalination facility on receiving waters. The desalination facility was proposed to utilize a nearby existing power plant intake in Moss Landing Harbor and discharge to the ocean via the power plant's existing outfall, which is a submerged outfall located in Monterey Bay offshore of the harbor entrance. The ELCOM model resolved the details of the mixing in the vicinity of the power plant/desalination facility combined discharge. The model results compared favorably to existing measured water quality parameters. The results were used to determine compliance with water quality regulations for the combined outfall. The study was performed in 2004-2006.

A.1.3.2.12 *Lake Perris (California, USA)*

In 2005, ELCOM was applied to Lake Perris in order to compare the impacts of several recreational use strategies on measured fecal coliform concentrations at the reservoir outlet tower. The physical results of the simulation were validated against measured temperature and salinity data over a one-year period. The comparison of fecal coliform concentrations against measured data was fair due to a lack of data describing the timing and magnitude of loading and the settling and re-suspension of fecal matter.

The ELCOM model was expanded in 2006-2007 to include CAEDYM in order to evaluate the performance of a proposed hypolimnetic oxygenation system and observed

water quality benefits. The model was calibrated against two years of historical data and used to assess the magnitude and extent of oxygenation in the hypolimnion as a result of system operation. Impacts on dissolved oxygen concentrations and nutrient dynamics and algal production potential (as represented by chlorophyll *a*) were also evaluated, and recommendations were provided for final design of the system. The project has not yet been constructed due to seismic safety risks with the dam that must first be addressed.

A.1.3.2.13 *Lake Hodges and Olivenhain Reservoir (California, USA)*

The San Diego County Water Authority (SDCWA) is planning a tunnel connection between Lake Hodges and Olivenhain Reservoir. The tunnel and an associated hydroelectric turbine will allow for operation of the two reservoirs as part of a pumped storage project. Due to the difference in water quality between the two reservoirs, the SDCWA was concerned that the planned pumped storage project could adversely impact water quality in Olivenhain Reservoir. In order to evaluate the water quality impacts of the planned pumped storage operations on Olivenhain Reservoir, Flow Science developed a coupled ELCOM model of the two reservoirs in 2007-2008 to simulate temperature and salinity and several tracers in order to characterize the extent of mixing of the pumped storage inflow water from Lake Hodges within Olivenhain Reservoir and the percentages of Lake Hodges and Olivenhain Reservoir water throughout each reservoir due to the pumped storage operations and subsequent mixing.

A.1.3.2.14 *Lower San Gabriel River, Intake Channel, and Alamitos Bay (California, USA)*

The Los Angeles Department of Water and Power (LADWP) Haynes Generating Station (HnGS) and AES Generating Station (AES) each utilize three outfalls located on the east and west bank of the Lower San Gabriel River, respectively, and discharge cooling water to the Lower San Gabriel River Flood Control Channel (LSGR). Flow Science conducted ELCOM modeling from 2003-2010 to evaluate the mixing of flows within the river channel and found that, under typical operating conditions, the cooling water discharges form a "barrier" between freshwater from the upstream river channel and ocean water downstream of the LSGR. Both modeling and field work (conducted by others) confirmed that the net direction of flow downstream of HnGS and AES is downstream, even during flood tide conditions. Flow Science's modeling also evaluated temperature, salinity, and mixing in the LSGR for a wide range of potential future conditions and for hypothetical conditions in which both HnGS and AES cooling water flows are removed from the LSGR. Water quality in the adjacent Alamitos Bay, which is strongly influenced by flushing induced by cooling water flows from HnGS and AES, was also evaluated using ELCOM. In addition, Flow Science used CAEDYM to evaluate

nutrient concentrations, algae, and dissolved oxygen within the Bay for a range of actual and potential future operating conditions. The HnGS Intake Channel (which connects Alamitos Bay to HnGS) was also evaluated with ELCOM/CAEDYM.

Results of the Flow Science analyses have been used by LADWP in NPDES permit discussions with the Regional Water Board, in CEQA evaluations supporting the potential future repowering of HnGS Units 5 and 6, and in comments on the State's draft Once-Through Cooling (OTC) policy.

A.1.3.2.15 *Joint Water Pollution Control Plant Outfall Evaluation (California, USA)*

The Sanitation Districts of Los Angeles County (LACSD) are conducting a detailed study to evaluate the feasibility of a proposed new ocean outfall to carry treated wastewater from the Joint Water Pollution Control Plant (JWPCP) in Carson, California, to an ocean discharge location off the southern California coast near the Palos Verdes and San Pedro Shelves. As part of the Feasibility Study, Flow Science developed an ELCOM model in 2007 to evaluate the impact of this proposed ocean outfall. The near-field effluent discharge model, NRFIELD2, coupled with the far field hydrodynamic model, ELCOM, was used to simulate the mixing and determine the concentrations of a conservative effluent tracer and various indicator bacteria (assuming no chlorination). The coupled model was validated using measured current and temperature data in the vicinity of the potential discharge sites. The water quality impacts of five proposed diffuser discharge sites were evaluated, and the modeling results will be used by LACSD to estimate concentrations of indicator bacteria at selected locations at the shore and inshore regions that would result from a discharge without chlorination. Ongoing ELCOM modeling will be performed to assist LACSD in selecting a preferred diffuser location. An example of the simulated effluent tracer concentrations during summer for one of the potential diffuser sites is presented in **Figure A.6** below.

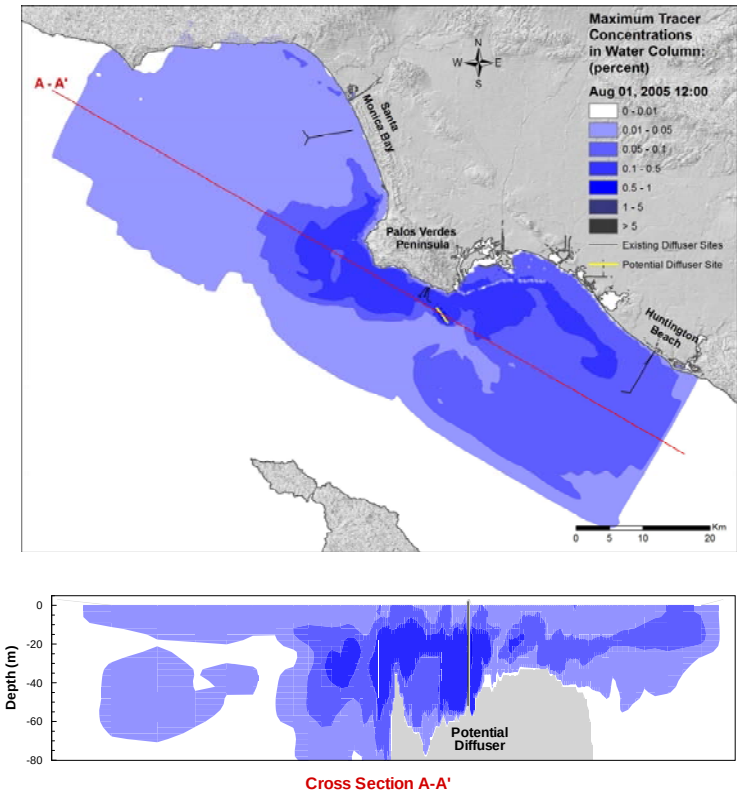

Figure A.6 Plan and section views of ELCOM simulated effluent tracer concentrations from proposed diffuser Site 1 in summer (August 1, 2005).

A.1.3.2.16 *San Vicente Reservoir (California, USA)*

Flow Science is assisting the City of San Diego in assessing the mixing and dilution potential resulting from the potential injection of highly treated effluent into San Vicente Reservoir. In 2010, Flow Science developed an ELCOM/CAEDYM model to assess the mixing and dispersion properties in San Vicente Reservoir as well as a field program to validate the modeling. The ELCOM/CAEDYM model includes temperature, salinity, conductivity, dissolved oxygen, nutrients, chlorophyll *a* (as a surrogate for algae), and multiple tracers. The model provides an accurate three-dimensional representation of water quality within the reservoir. The model was calibrated for the reservoir at its

current capacity against two years of historical data. The calibrated model has since been applied to the expanded reservoir to evaluate the impacts of the advanced water treatment (AWT) water. The model is being used to predict water quality conditions in the future enlarged reservoir and will also be used to help manage water quality in the enlarged reservoir once it is filled. The work is being reviewed by an expert panel being overseen by the National Water Research Institute. The panel is expected to complete its review and accept the use of the modeling.

A.1.3.2.17 *Los Vaqueros Reservoir (California, USA)*

In conjunction with the Contra Costa Water District (CCWD), Flow Science developed a three-dimensional ELCOM/CAEDYM model of Los Vaqueros Reservoir beginning in 2006 that is capable of providing an accurate, three-dimensional representation of water quality including temperature, salinity/TDS, nutrients and algae. The ELCOM model was calibrated against two years of historical data and validated against four years of data, while the CAEDYM model was calibrated for four years of historical data. **Figure A.7** shows a comparison of the measured versus simulated annual and growing season average chlorophyll *a* concentrations which show very good agreement. In ongoing work, Flow Science is using the ELCOM/CAEDYM model to evaluate the water quality of the reservoir under future conditions where the impounding dam is raised. This will expand the capacity of the reservoir from 100,000 acre-ft to 160,000 acre ft. The water quality model is being used to determine the changes in outflow water quality resulting from the expansion and to provide preliminary design recommendations for the inlet/outlet facilities with respect to improving water quality.

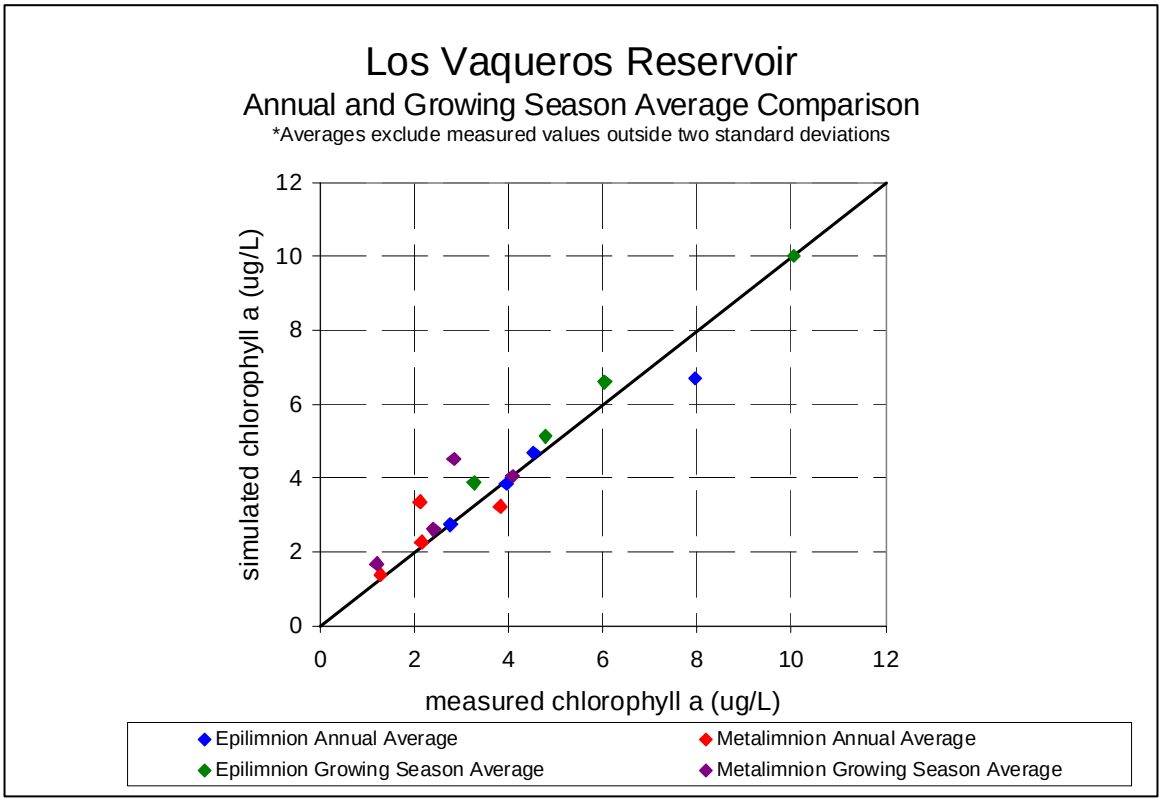

Figure A.7 Comparison of simulated ELCOM/CAEDYM results and measured chlorophyll *a* data for 2006-2009.

A.1.3.2.18 *Other Applications*

Other ELCOM/CAEDYM applications and development in on-going research at CWR include:

- Plume dynamics and horizontal dispersion (Marmion Marine Park, Australia).
- Inflow and pathogen dynamics (Helena, Myponga and Sugarloaf Reservoirs, Australia).
- Mixing and dissipation in stratified environments (Tone River, Japan, and Brownlee Reservoir, USA).

- Tidally forced estuaries and coastal lagoons (Marmion Marine Park and Barbamarco Lagoon, Italy).

- Three-dimensional circulation induced by wind and convective exchange (San Roque Reservoir, Argentina, and Prospect Reservoir, Australia).

- Sea-surface temperature fluctuation and horizontal circulation (Adriatic Sea).

- Response of bivalve mollusks to tidal forcing (Barbamarco Lagoon, Italy).

A.1.4 TECHNICAL DESCRIPTION OF ELCOM

As outlined above, ELCOM solves the unsteady, viscous Navier-Stokes equations for incompressible flow using the hydrostatic assumption for pressure. ELCOM can simulate the hydrodynamics and thermodynamics of a stratified system, including baroclinic effects, tidal forcing, wind stresses, heat budget, inflows, outflows, and transport of salt, heat and passive scalars. Through coupling with the CAEDYM water quality module, ELCOM can be used to simulate three-dimensional transport and interactions of flow physics, biology, and chemistry. The hydrodynamic algorithms in ELCOM are based upon the proven semi-Lagrangian method for advection of momentum with a conjugate-gradient solution for the free-surface height (Casulli and Cheng, 1992) and a conservative ULTIMATE QUICKEST transport of scalars (Leonard, 1991). This approach is advantageous for geophysical-scale simulations since the time step can be allowed to exceed the Courant-Friedrichs-Lewy (CFL) condition for the velocity without producing instability or requiring a fully-implicit discretization of the Navier-Stokes equations.

A.1.4.1 Governing Equations

Significant governing equations and approaches used in ELCOM include:

- Three-dimensional simulation of hydrodynamics (unsteady Reynolds-averaged Navier-Stokes equations).

- Advection and diffusion of momentum, salinity, temperature, tracers, and water quality variables.

- Hydrostatic approximation for pressure.

- Boussinesq approximation for density effects.

- Surface thermodynamics module accounts for heat transfer across free surface.
- Wind stress applied at the free surface.
- Dirichlet boundary conditions on the bottom and sides.

A.1.4.2Numerical Method

Significant numerical methods used in ELCOM include:

- Finite-difference solution on staggered-mesh Cartesian grid.
- Implicit volume-conservative solution for free-surface position.
- Semi-Lagrangian advection of momentum allows time steps with CFL > 1.0.
- Conservative ULTIMATE QUICKEST advection of temperature, salinity, and tracers.
- User-selectable advection methods for water quality scalars using upwind, QUICKEST, or semi-Lagrangian to allow trade-offs between accuracy and computational speed.
- Solution mesh is Cartesian and allows non-uniformity (i.e. stretching) in horizontal and vertical directions.

The implementation of the semi-Lagrangian method in Fortran 90 includes sparse-grid mapping of three-dimensional space into a single vector for fast operation using array-processing techniques. Only the computational cells that contain water are represented in the single vector so that memory usage is minimized. This allows Fortran 90 compiler parallelization and vectorization without platform-specific modification of the code. A future extension of ELCOM will include dynamic pressure effects to account for nonlinear dynamics of internal waves that may be lost due to the hydrostatic approximation.

Because the spatial scales in a turbulent geophysical flow may range from the order of millimeters to kilometers, it is presently impossible to conduct a Direct Navier-Stokes (DNS) solution of the equations of motion (i.e. an exact solution of the equations). Application of a numerical grid and a discrete time step to a simulation of a geophysical domain is implicitly a filtering operation that limits the resolution of the equations.

Numerical models (or closure schemes) are required to account for effects that cannot be resolved for a particular grid or time step. There are four areas of modeling in the flow physics: (l) turbulence and mixing, (2) heat budgets, (3) hydrodynamic boundary conditions, and (4) sediment transport.

A.1.4.3 Turbulence Modeling and Mixing

ELCOM presently uses uniform fixed eddy viscosity as the turbulence closure scheme in the horizontal plane (in future versions a Smagorinsky 1963 closure scheme will be implemented to represent subgrid-scale turbulence effects as a function of the resolves large-scale strain-rates). These methods are the classic "eddy viscosity" turbulence closure. With the implementation of the Smagorinsky closure, future extensions will allow the eddy-viscosity to be computed on a local basis to allow improvements in modeling local turbulent events and flow effects of biological organisms (e.g., drag induced by macroalgae or seagrass).

In the present code, the user has the option to extend the eddy-viscosity approach to the vertical direction by setting different vertical eddy-viscosity coefficients for each grid layer. However, in a stratified system, this does not adequately account for vertical turbulent mixing that may be suppressed or enhanced by the stratification (depending on the stability of the density field and the magnitude of the shear stress). To model the effect of density stratification on turbulent mixing the CWR has developed a closure model based on computation of a local Richardson number to scale. The latter is generally smaller than the time step used in geophysical simulations, so the mixing is computed in a series of partial time steps. When the mixing time-scale is larger than the simulation time step, the mixing ratio is reduced to account for the inability to obtain mixing on very short time scales. This model has the advantage of computing consistent mixing effects without regard to the size of the simulation time-step (i.e. the model produces mixing between cells that is purely a function of the physics and not the numerical step size).

A.1.4.4 Heat Budget

The heat balance at the surface is divided into short-wave (penetrative) radiation and a heat budget for surface heat transfer effects. The surface heat budget requires user input of the net loss or gain through conduction, convection, and long wave radiation in the first grid layer beneath the free surface. The short wave range is modeled using a user-prescribed input of solar radiation and an exponential decay with depth that is a function of a bulk extinction coefficient (a Beer's law formulation for radiation absorption). This coefficient is the sum of individual coefficients for the dissolved

organics ("gilvin"), phytoplankton biomass concentration, suspended solids, and the water itself. The extinction coefficients can either be computed in the water quality module (CAEDYM) or provided as separate user input.

A.1.4.5 Hydrodynamic Boundary Conditions

The hydrodynamic solution requires that boundary conditions on the velocity must be specified at each boundary. There are six types of boundary conditions: (1) free surface, (2) open edge, (3) inflow-outflow, (4) no-slip, (5) free-slip, and (6) a Chezy-Manning boundary stress model (the latter is presently not fully implemented). For the free surface, the stress due to wind and waves is required. The user can either input the wind/wave stress directly, or use a model that relates the surface stress to the local wind speed and direction *via* a bulk aerodynamic drag coefficient. Open boundaries (e.g. tidal inflow boundaries for estuaries) require the user to supply the tidal signature to drive the surface elevation. Transport across open boundaries is modeled by enforcing a Dirichlet condition on the free-surface height and allowing the inflow to be computed from the barotropic gradient at the boundary. Inflow-outflow boundary conditions (e.g. river inflows) are Dirichlet conditions that specify the flow either at a particular boundary location *or inside the domain*. Allowing an inflow-outflow boundary condition to be specified for an interior position (i.e. as a source or sink) allows the model to be used for sewage outfalls or water outlets that may not be located on a land boundary. Land boundaries can be considered zero velocity (no-slip), zero-flux (free-slip) or, using a Chezy-Manning model, assigned a computed stress.

A.1.4.6 Sediment Transport

While sediment transport is fundamentally an issue of flow physics, the algorithms for the sediment transport are more conveniently grouped with the water quality algorithms in CAEDYM. Settling of suspended particulate matter is computed using Stokes law to obtain settling velocities for the top and bottom of each affected grid cell. This allows the net settling flux in each cell to be computed. A two-layer sediment model has been developed that computes resuspension, deposition, flocculation, and consolidation of sediment based on (1) the shear stress at the water/sediment interface, (2) the type of sediment (cohesive/non-cohesive), and (3) the thickness of the sediment layer. Determination of the shear stress at the water/sediment interface requires the computation of bottom shear due to current, wind, and waves. A model has been developed to account for the effects of small-scale surface waves that cannot be resolved on a geophysical-scale grid. This model computes the theoretical wave height and period for small-scale surface waves from the wind velocity, water depth, and domain fetch. From these, the wavelength and orbital velocities are calculated. The wave-induced shear

stress at the bottom boundary resulting from the wave orbital velocities is combined with a model for the current-induced shear stress to obtain the total bottom shear that effects sediment resuspension. The cohesiveness of the sediment determines the critical shear stresses that are necessary to resuspend or deposit the sediments. A model of consolidation of the sediments is used to remove lower sediment layers from the maximum mass that may be resuspended.

A.1.5 TECHNICAL DESCRIPTION OF CAEDYM

CAEDYM is an outgrowth of previous CWR water quality modules in DYRESM-WQ and the Estuary Lake Model - Water Quality (ELMO-WQ) codes. CAEDYM is designed as a set of subroutine modules that can be directly coupled with one, two, or three-dimensional hydrodynamic "drivers", catchment surface hydrological models, or groundwater models. Additionally, it can be used in an uncoupled capacity with specification of velocity, temperature, and salinity distributions provided as input files rather than as part of a coupled computation. The user can specify the level of complexity in biogeochemical process representation so both simple and complex interactions can be studied. Direct coupling to a hydrodynamic driver (e.g. ELCOM) allows CAEDYM to operate on the same spatial and temporal scales as the hydrodynamics. This permits feedbacks from CAEDYM into ELCOM for water quality effects such as changes in light attenuation or effects of macroalgae accumulation on bottom currents. **Figure A.8** shows an illustration of the interactions of modeled parameters in CAEDYM. Being an “N-P-Z” (nutrient-phytoplankton-zooplankton) model, CAEDYM can be used to assess eutrophication. Unlike the traditional general ecosystem model, CAEDYM serves as a species- or group-specific model (i.e. resolves various phytoplankton species). Furthermore, oxygen dynamics and several other state variables are included in CAEDYM.

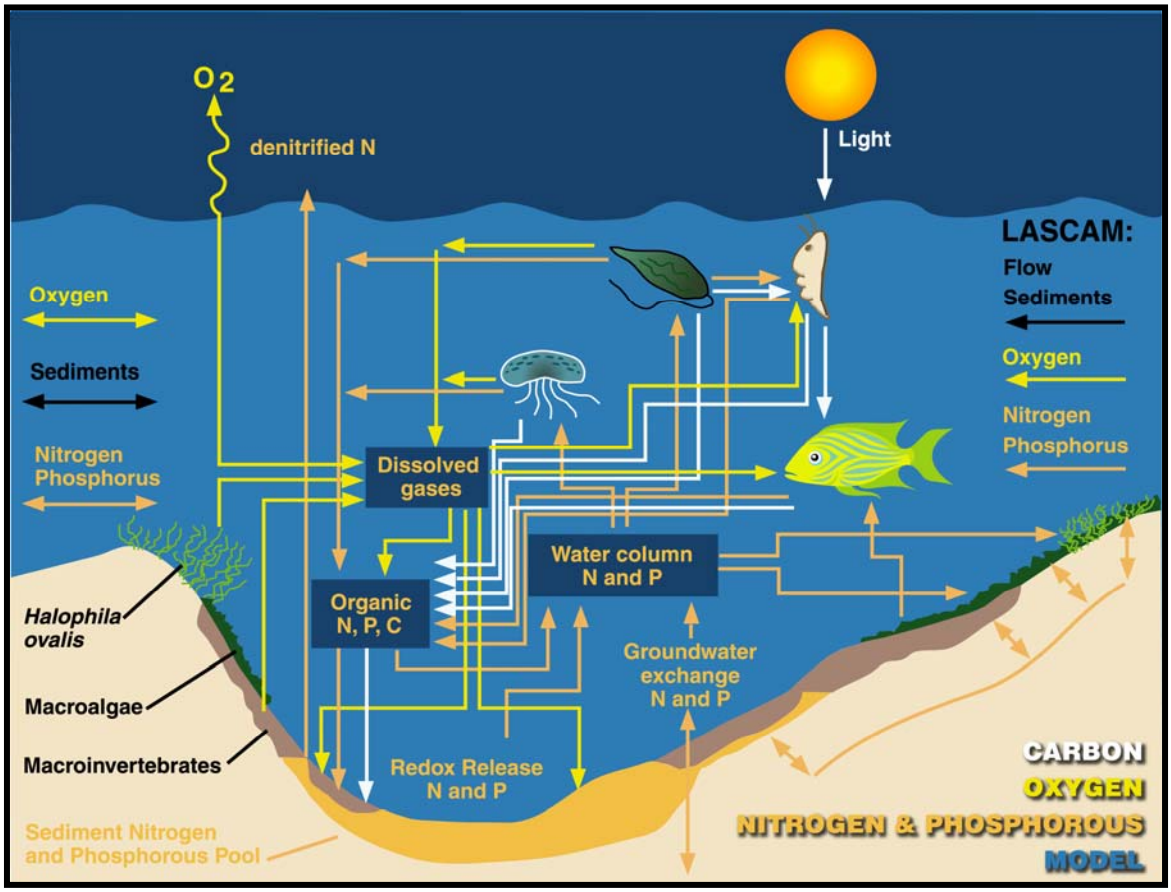

Figure A.8 Illustration of interactions of modeled parameters in CAEDYM.

The representation of biogeochemical processes in ecological models has, historically, been treated in a simple manner. In fact, the pioneering work on modeling marine ecosystems (Riley et al, 1949; Steel, 1962) is still used as a template for many of the models that are currently used (Hamilton and Schladow, 1997). The level of sophistication and process representation included in CAEDYM is of a level hitherto unseen in any previous aquatic ecosystem model. This enables many different components of the system to be examined, as well as providing a better representation of the dynamic response of the ecology to major perturbations to the system (e.g. the response to various management strategies). **Figure A.9** shows the major state variables included in the CAEDYM model. Using CAEDYM to aid in management decisions and system understanding requires (1) a high level of process representation, (2) process

interactions and species differentiation of several state variables, and (3) applicability over a spectrum of spatial and temporal scales. The spectrum of scales relates to the need for managers to assess the effects of temporary events, such as anoxia at specific

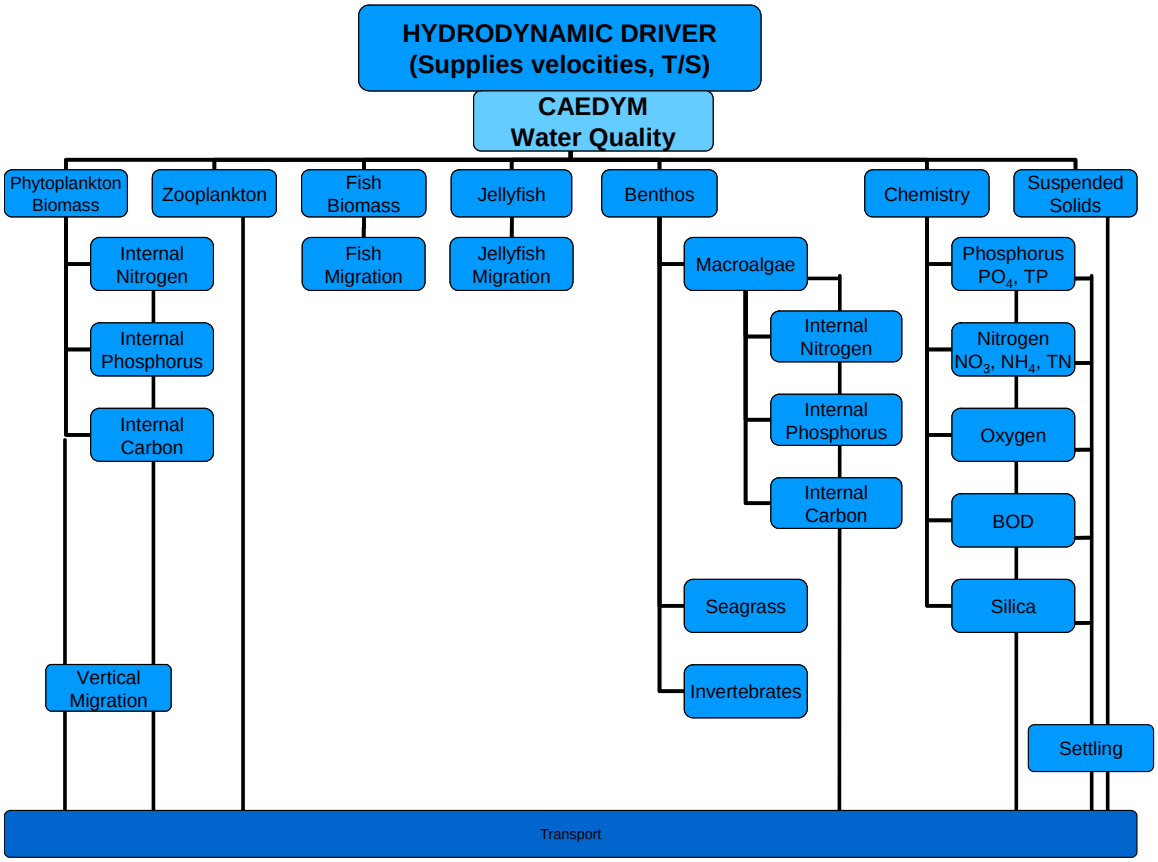

Figure A.9 Major state variables included in the CAEDYM model.

locations, through to understanding long-term changes that may occur over seasons or years. There is considerable flexibility in the time step used for the ecological component. Long time steps (relative to the hydrodynamic advective scale) may be used to reduce the frequency of links to ELCOM when long-term (i.e. seasonal or annual) simulations are run.

A.1.5.1 Biological Model

The biological model used in CAEDYM consists of seven phytoplankton groups, five zooplankton groups, six fish groups, four macroalgae groups and three invertebrate groups, as well as models of seagrass and jellyfish. This set will be expanded as biological models are developed, tested, and calibrated to field data. There is flexibility for the user in choosing which species to include in a simulation. Vertical migration is simulated for motile and non-motile phytoplankton, and fish are migrated throughout the model domain according to a migration function based on their mortality. A weighted grazing function is included for zooplankton feeding on phytoplankton and fish feeding on zooplankton. The biomass grazed is related to both food availability and preference of the consumer for its food supply. Improved temperature, respiration and light limitation functions have been developed to represent the environmental response of the organisms. The benthic processes included a self-shading component and beach wrack function for macroalgae, sediment bioturbation and nutrient cycling by polychaetes, and effects of seagrass on sediment oxygen status.

In particular, the seven phytoplankton groups modeled are dinoflagellates, freshwater diatoms, marine/estuarine diatoms, freshwater cyanobacteria, marine estuarine cyanobacteria, chlorophytes, and cryptophytes. Phytoplankton biomass is represented in terms of chlorophyll *a*. Phytoplankton concentrations are affected by the following processes:

- Temperature growth function
- Light limitation
- Nutrient limitation by phosphorus and nitrogen (and when diatoms are considered, silica)
- Loss due to respiration, natural mortality, excretion, and grazing
- Salinity response
- Vertical migration and settling

A.1.5.2 Nutrients, Metals, and Oxygen Dynamics

The transport and chemical cycling of nutrients is an important part of simulating the interaction of biological organisms in an ecosystem. CAEDYM includes as state variables the following:

- Nutrients (dissolved inorganic phosphorus, total phosphorus, total nitrogen, ammonium nitrate, and silica).
- Dissolved oxygen and biochemical oxygen demand.
- Metals (dissolved and particulate forms of iron and manganese).
- Suspended sediment (the particulate and colloidal fractions).
- pH

The model incorporates oxygen dynamics and nutrient cycling in both the sediments and water column. A sediment pool of organic detritus and inorganic sediments, both of which may be resuspended into the water column, is included. Redox-mediated release of dissolved nutrients is simulated from the sediments to the water column.

Processes included in the water and sediment oxygen dynamics include:

- Atmospheric exchange (Wanninkhof, 1992).
- Oxygen production and consumption through phytoplankton, macroalgae, and seagrass/macrophyte photosynthesis and respiration, respectively.
- Utilization of dissolved oxygen due to respiration of higher organisms such as zooplankton and fish and due to photosynthesis and respiration in jellyfish
- Water column consumption of oxygen during nitrification.
- Biochemical oxygen demand due to mineralization of organic matter in the water column and in the sediments.

Oxygen flux from the water column to the sediments, sediment oxygen demand (SOD), as developed from Fick's law of diffusion.

The last two processes are used together with a sediment porosity and diffusion coefficient (Ullman and Aller, 1982) in order to define the depth of the toxic layer in the sediments.

Nutrient processes included in the sediment and water column dynamics include:

- Phytoplankton nutrient uptake, with provision for luxury storage of nutrients.
- Release of dissolved inorganic nutrients from phytoplankton excretion.
- Excretion of nutrients as fecal material by zooplankton.
- Nitrification and denitrification by bacterial mediated action.
- Generation of inorganic nutrients from organic detritus.
- Transfer of nutrients through the food chain (e.g. phytoplankton--zooplankton--fish).
- Uptake of nutrients by macroalgae and seagrasses.
- Adsorption/desorption of nutrients from inorganic suspended sediments.
- Sediment/water transfer of nutrients (*via* such processes as sediment resuspension, sedimentation, redox-mediated nutrient release, and bioturbation).

In essence, CAEDYM represents the type of interactive processes that occur amongst the ecological and chemical components in the aquatic ecosystem. As a broad generalization, one component of the system cannot be manipulated or changed within the model without affecting other components of the system. Similarly in nature, changing an integral component in the aquatic system will have wide-ranging and follow-on effects on many of the other system components. CAEDYM is designed to have the complexity and flexibility to be able to handle the continuum of responses that will be elicited as components of a system that are manipulated. Thus, the model represents a valuable tool to examine responses under changed conditions, as for example, when new approaches to managing an ecosystem are adopted.

A.2 DESCRIPTION OF ELCOM/CAEDYM/VISUAL PLUMES (ECP)

A.2.1 INTRODUCTION

Outfalls are commonly used to discharge treated effluent into open waters. The hydrodynamics of an effluent discharged through an outfall can be conceptualized as a mixing process occurring in two separate regions: a near-field region and a far-field region. In the near-field region the effluent generally experiences a significant amount of mixing, and dilution occurs very rapidly. In this region, the initial jet characteristics of momentum flux, buoyancy flux, flow rate, as well as outfall geometry greatly influence the effluent trajectory and degree of mixing (Fischer et al, 1979). As the effluent plume travels further away from the source, the source characteristics become less important and the far-field region is attained. Mixing of the effluent plume in this region is caused by spatial and temporal variations of ambient velocity fields and dilution generally occurs slowly over a long distance, but may be rapid if there is a high degree of turbulence in the environment.

Due to different dominant temporal and spatial scales of flow velocity and effluent concentration in the near and far field region, a complete model that accounts for all important spatial and temporal scales in both the near-field and far-field regions is not feasible. Instead, these two regions are usually treated by separate models termed the near-field model and the far-field model respectively.

The near-field model has been under intensive study from the 1950s through the early 1990s. Thorough reviews of these studies are provided by Fischer et al. (1979), Baumgartner et al. (1994), and Roberts et al. (1989 a, b, c). These studies have produced a number of near-field models that were verified by both field and laboratory data. Among them, Visual Plumes (VP or PLUMES), endorsed by the U.S. Environmental Protection Agency (USEPA), is the most popular model and has been widely used by regulatory agencies and outfall designers to estimate the near-field dilution.

A variety of models can be used to model far-field mixing processes. These include ELCOM/ CAEDYM, Princeton Ocean Model (POM), and MIT General Circulation Model (MITGCM). All of these models obtain a velocity field from the numerical calculation of the equations of motion and account for influences by tide, wind stress, and pressure gradient due to free surface gradients (barotropic) or density gradients (baroclinic). Given the velocity field, the pollutant concentration field is

typically obtained by solving the Eulerian advective diffusion equation in three dimensions or by using the Lagrangian particle-tracking method.

In simple water bodies with well-defined uni-directional current regimes, the use of near-field models alone may suffice to evaluate a design of an outfall discharge that meets regulations. However, in regions with multiple current regimes (inertial, tide, wind, and buoyancy driven) and with large pollutant loadings, especially where several sources may interact, near-field models must be supplemented by far-field transport and water quality models. The latter are capable of prediction, over a greater distance in the water body, of the concentration distributions for different pollutants, nutrients, and other bio-chemical parameters. They do not, however, have the high spatial resolution that is required to predict near-field mixing processes. Thus, a coupled approach is necessary. In the following sections, a method of coupling the near-field model PLUMES and the far-field model ELCOM/CAEDYM is discussed. The coupled code is referred to as ELCOM/CAEDYM/PLUMES (ECP). Note that there is no standard procedure for the coupling of near and far field models and the coupling procedure varies from code to code mainly because of the different code structures among all of the near-field and far-field models.

A.2.2 NEAR-FIELD MODEL – PLUMES

PLUMES is an interface program that contains the near-field models such as the Roberts, Snyder, and Baumgartner model (RSB) and UM and CORnell MIXing Zone Expert System (CORMIX) (Baumgartner et al., 1994). In ECP, the UM model is chosen to simulate near-field dilution. The UM model is an integral near-field model that uses one-dimensional conservation equations for mass, momentum, salinity and temperature, to model the growth of the plume once the effluent has left the port. Assumptions are made about the shape of the plume and the distribution of pollutant concentration within the plume. Several mechanisms of entrainment such as aspirated, forced, and turbulent diffusion are considered. Both positively and negatively buoyant plumes, single source and multi-port diffuser configurations can be modeled. Model outputs include average dilution, centerline dilution, and horizontal distance of the effluent plume. The major limitation of UM lies in the assumption of an infinite receiving water body, similar to all other available integral-type models (e.g. RSB model). Thus, UM should only be used for deep-water outfalls without boundary interactions. More details on UM and PLUMES can be found in Baumgartner et al. (1994).

A.2.3 FAR-FIELD MODEL – ELCOM/CAEDYM

ELCOM is a three-dimensional hydrodynamic model for lakes and reservoirs and is used to predict the velocity, temperature, and salinity distribution in natural water bodies subjected to external environmental forcing, such as wind stress, surface heating, or cooling. Through coupling with the CAEDYM water quality module, ELCOM can be used to simulate three dimensional transport and interactions of flow physics, biology, and chemistry. ELCOM/CAEDYM is the chosen far-field model in ECP.

A.2.4 COUPLING PLUMES AND ELCOM/CAEDYM

The adopted coupling procedure is based on four steps: ambient conditions modeling, near-field modeling, coupling of near-field and far-field models, and far-field modeling.

1. Ambient conditions modeling

   The near-field model, UM, needs the input of ambient conditions such as the prevailing velocity, temperature, and salinity profiles in the vicinity of the outfall. These profiles are extracted from the ELCOM/CAEDYM simulation at the beginning of a time step at a vertical column of grid cells containing or overlapping the diffuser (the "Diffuser Cell Column" in **Figure A.10**). The depth of the diffuser is also updated based on the surface elevation at that time step.

2. Near-field modeling

   The UM model is applied at each time step using the ambient conditions extracted from ELCOM/CAEDYM. Furthermore, effluent data is obtained from input files for ELCOM/CAEDYM, and the diffuser geometry is specified in the input file called "diffuser_config.dat." The UM model is modified to consider the trapping or surfacing of the plume as the end of the near-field region. The computed average dilution along the trajectory of the plume is then stored for the following coupling step.

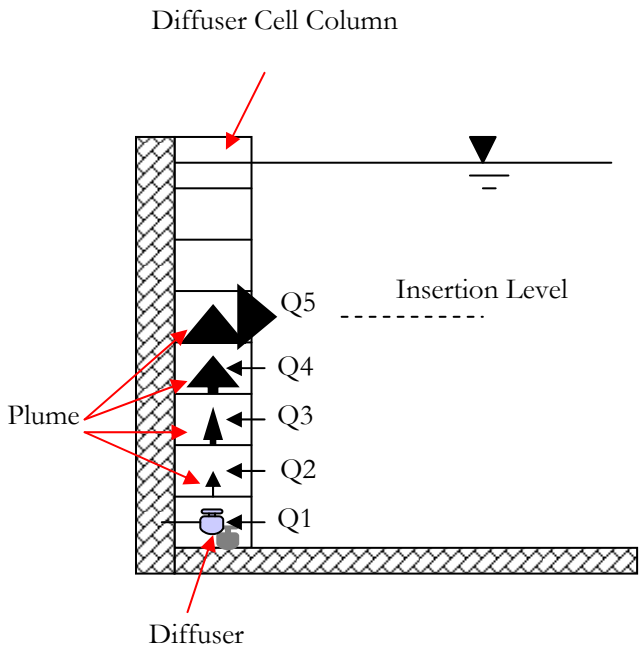

Figure A.10 Schematic of coupling procedure for near-field and far-field models.

3. Coupling of near-field and far-field models

After identifying the "Diffuser Cell Column" (**Figure A.10**), the dilution in each of the cells along this column can be calculated from the linear interpolation of results from UM. Water is then withdrawn from each of these cells based on the dilution occurring in the cell. This withdrawn water is then mixed with the effluent to form the effluent plume and passed to the cell above. Finally, the diluted effluent is then inserted into the cell where the UM model indicates the occurrence of trapping or surfacing (**Figure A.10**). Flow rate, temperature, salinity, and tracer concentrations within this inserted inflow are determined by mass conservation.

4. Far-field modeling

ELCOM/CAEDYM treats the previous coupling process as a series of outflows and inflows along the "Diffuser Cell Column" and proceeds with its time-marching far-field simulation for the time step. Steps 1 - 4 are then repeated for the next time step until the simulation ends.

A.2.5 VERIFICATION OF ECP

The UM model was originally written in TURBO PASCAL and was converted into FORTRAN and included in ECP. The comparison between the results from UM of PLUMES and UM of ECP shows an exact match (**Figure A.11**) and the conversion of the UM model is verified.

Output from UM Model of PLUMES

depth (m)	dilution (m)	horiz dis	
50.000	1.000	0.000	
49.761	1.971	0.005	
49.311	3.913	0.035	
48.585	7.797	0.127	
47.525	15.566	0.327	
46.035	31.104	0.696	
45.928	32.424	0.725	merging
43.228	62.180	1.529	
37.335	124.335	3.385	
25.609	248.651	7.517	
22.323	285.625	8.893	trap level
15.436	395.624	12.750	begin overlap, dilution
	overestimated		
14.308	442.027	13.760	surface hit

Output from UM Model of ECP

depth (m)	dilution (m)	horiz dis	
50.000	1.000	0.000	
49.761	1.971	0.005	
49.311	3.913	0.035	
48.585	7.797	0.127	
47.525	15.566	0.327	
46.035	31.104	0.696	
45.928	32.424	0.725	merging
43.228	62.180	1.529	
37.335	124.335	3.385	
25.609	248.651	7.517	
22.323	285.625	8.893	trap level
15.436	395.624	12.750	begin overlap, dilution
	overestimated		
14.308	442.027	13.760	surface hit

Figure A.11 Comparison of outputs from UM of PLUMES and ECP

Mass conservation within ECP was tested by simulating an idealized lake with a single outfall (inflow) and no outflow. Total mass of both a conservative tracer and total phosphorus (TP) in the lake was calculated at each time step and compared with a similar simulation using ELCOM/CAEDYM (where the outfall was treated as a single inflow). Less than 0.1% difference was found for the conservative tracer and less than 1% difference was found for TP at the end of a one-year simulation. These small differences indicate that mass conservation within the ECP code is comparable to that of ELCOM/CAEDYM.

The accuracy of ECP can also be qualitatively evaluated by simulating the behavior of a plume under stratified and unstratified ambient conditions. **Figure A.12** shows that ECP correctly predicts surfacing of the plume under unstratified conditions and the level of insertion of the plume under stratified conditions.

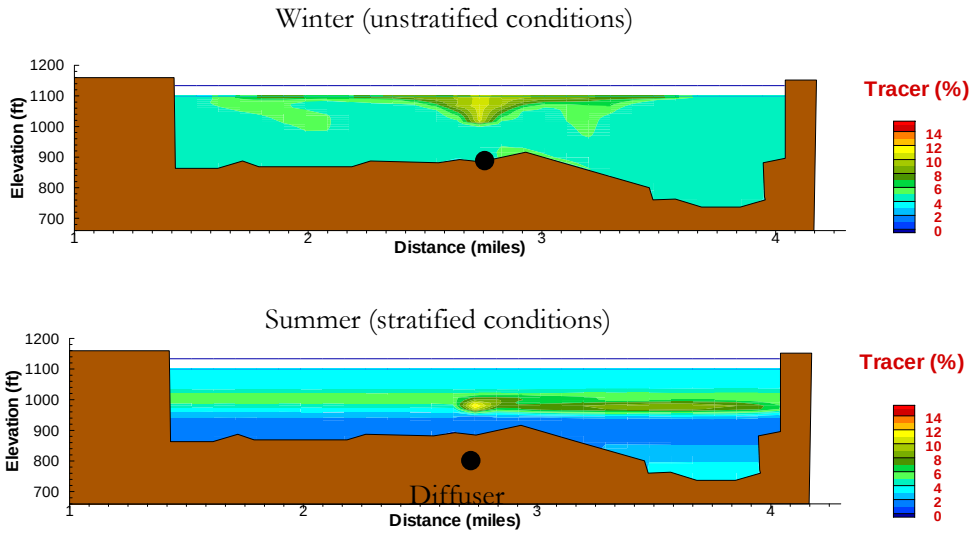

Figure A.12 Comparison of tracer concentrations released from an outfall under stratified and unstratified conditions using ECP.

A.3 BIBLIOGRAPHY

A.3.1 REFERENCED IN TEXT

Amorocho, J. and DeVries, J.J. (1980). "A new evaluation of the wind stress coefficient over water surfaces," Journal of Geophysical Research, 85:433-442.

Antenucci, Jason (2004). "Tracing Short-Circuiting Potential," from CWR Models: Bytes and Nybbles, Autumn 2004, Issue 10, page 2.

Antenucci, Jason (2004). "New Metals Model for CAEDYM," from CWR Services: Bytes and Nybbles, December 2004, Issue 11, page 1.

Appt, Jochen (January 2000), "Review on the modeling of short period internal waves in lakes with focus on Lake Constance," Pfaffenwaldring 61, D-70550 Stuttgart, Universität Stuttgart, Institut für Hydraulik und Grandmaster, Stuttgart.

Appt, J., Imberger, J., Kobus, H. (2004), "Basin-scale motion in stratified Upper Lake Constance," Limnology and Oceanography, 49(4), 919-933

Baumgartner, D. J., Frick, W. E. & Roberts, P. J. W. (1994), Dilution Models for Effluent Discharges (3rd ed.), *United States Environmental Protection Agency (EPA/600/R-94/086).*

Casulli, Vincenzo and Cheng, Ralph T. (1992), "Semi-implicit finite difference methods for three-dimensional shallow water flow," *International Journal for Numerical Methods in Fluids*, **15**, 629-48.

CWR, "Limnological Study of Lake Burragorang," Centre For Water Research, The University of Western Australia, Chapter 4 excerpt from report, pp. 104-126.

Fischer, H.B., List, E.J., Koh, R.C.Y., Imberger, J. & Brooks, N.H. (1979), Mixing in Inland and Coastal Waters, *Academic Press, New York*

Hamilton, D. (1997). "An integrated ecological model for catchment hydrology and water quality for the Swan and Canning Rivers," presented at the 2nd International Symposium on Ecology and Engineering, 10-12 November 1997, Freemantle, Australia. IAHR Eco-Hydraulics section.

Hamilton, D.P. and S.G. Schladow (1997), "Prediction of water quality in lakes and reservoirs: Part I: Model description," *Ecological Modelling, 96*, 91-110.

Herzfeld, M. and Hamilton, D. (1998), "A computational aquatic ecosystem dynamics model for the Swan River," *EOS Trans. AGU*, **79**(1), Ocean Sciences Meet. Suppl. OS11P-02.

Herzfeld, M.; Hodges, B.R.; and Hamilton, D. (1998), "Modelling the Swan River on small temporal and spatial scales," The Swan Canning Estuary conference, York, Australia, Apr., 1998.

Herzfeld, M.; Hamilton, D.; and Hodges, B.R. (1997), "Reality vs. management: The role of ecological numerical models," *2nd International Symposium on Ecology and Engineering*, 10-12 November 1997, Fremantle, Australia, IAHR Eco-Hydraulics section.

Hipsey, M.R., Romero, J.R., Antenucci, J.P. and Hamilton, D. (2005) "Computational Aquatic Ecosystem Dynamics Model: CAEDYM: v2.2 Science Manual", Centre for Water Research, The University of Western Australia.

Hipsey, M.R., Romero, J.R., Antenucci, J.P. and Hamilton, D. (2005) "Computational Aquatic Ecosystem Dynamics Model: CAEDYM: v2.2 User Manual", Centre for Water Research, The University of Western Australia.

Hodges, B.R. (1998), "Hydrodynamics of differential heat absorption," *Environmental Mechanics Laboratory Seminar*, Dept. of Civil Eng., Stanford University, Feb. 1998.

Hodges, B.R. and Dallimore C (2006), "Estuary Lake and Coastal Ocean Model: ELCOM v2.2 Science Manual", Centre for Water Research, The University of Western Australia.

Hodges, B.R. and Dallimore C (2007), "Estuary Lake and Coastal Ocean Model: ELCOM v2.2 User Manual", Centre for Water Research, The University of Western Australia.

Hodges, B.R. and Herzfeld, M. (1997), "Coupling of hydrodynamics and water quality for numerical simulations of Swan River," *2nd International Symposium on Ecology and Engineering*, 10-12 November, Fremantle, Australia, IAHR Eco-Hydraulics section.

Hodges, B.R.; Herzfeld, M.; Winters, K.; and Hamilton, D. (1998), "Coupling of hydrodynamics and water quality in numerical simulations," *EOS Trans. AGU*, **79**(1), Ocean Sciences Meet. Suppl. OS11P-01.

Hodges, B.R., Imberger, J., Saggio, A., and K. Winters (1999), "Modeling basin-scale internal waves in a stratified lake," *Limnology and Oceanography*), **45**(7), 1603-20.

Hodges, B.R., Yue, N., and Bruce, L. (May 27, 1999), "Swan River hydrodynamic model progress report," Centre For Water Research, The University of Western Australia, 14pp.

Jacquet, J. (1983). "Simulation of the thermal regime of rivers," In Orlob, G.T., editor, Mathematical Modeling of Water Quality: Streams, Lakes and Reservoirs, pages 150-176. Wiley-Interscience.

Kowalik, Z. and Murty, T.S. (1993). "Numerical Modeling of Ocean Dynamics," World Scientific.

Laval, B., Imberger, J., Hodges, B.R., and Stocker, R. (2003), "Modeling circulation in lakes: spatial and temporal variations," Limnology and Oceanography 48(3), 983-994.

Leonard, B.P. (1991), "The ULTIMATE conservative difference scheme applied to unsteady one-dimensional advection," *Computational Methods in Applied Mechanics and Engineering*, **88**, 17-74.

Lin, B. and Falconer, R.A. (1997). "Tidal flow and transport modeling using ULTIMATE QUICKEST," Journal of Hydraulic Engineering, 123:303-314.

Roberts, P.J.W., Snyder, W.H. & Baumgartner, D.J. (1989a), Ocean Outfalls I, Submerged wastefield formation, *J. Hydraulic Engineering*, **115**, 1-25

Roberts, P.J.W., Snyder, W.H. & Baumgartner, D.J. (1989b), Ocean Outfalls II, Spatial evolution of submerged wastefield, *J. Hydraulic Engineering*, **115**, 26-48

Roberts, P.J.W., Snyder, W.H. & Baumgartner, D.J. (1989c), Ocean Outfalls III, Effect of diffuser design on submerged wastefield, *J. Hydraulic Engineering*, **115**, 49-70

Robson, B.J. and Hamilton, D. P. (2002). "Three-Dimensional Modeling of a Microcystis bloom event in a Western Australian Estuary." Centre For Water Research, The University of Western Australia, 491- 496 pp.

Romero, J.R. and Antenucci, J. (2004). "The Tiete River: Supply for Sao Paolo, Brazil," from CWR Models: Bytes and Nybbles, Autumn 2004, Issue 10, page 4.

Romero, J.R. and Imberger, J. (1999). "Lake Pamvotis Project-Final report", ED report WP 1364 JR, Centre for Water Research, Crawley, Western Australia, Australia.

Spigel, R.H.; Imberger, J.; and Rayner, K.N. (1986), "Modeling the diurnal mixed layer," *Limnology and Oceanography,* **31**, 533-56.

Staniforth, A. and Côté, J. (1991). "Semi-Lagrangian integration schemes for atmospheric models – a review," Monthly Weather Review, 119:2206-2223.

Stevens, C. and Imberger, J. (1996). "The initial response of a stratified lake to a surface shear stress," Journal of Fluid Mechanics, 312:39-66.

Ullman, W.J. and R.C. Aller (1982), "Diffusion coefficients in nearshore marine sediments," *Limnol. Oceanogr., 27*, 552-556.

Wanninkhof, R. (1992), "Relationship between wind speed and gas exchange over the ocean," *J. Geophys. Res., 97(C5)*, 7373-7382.

Yeates, Peter (2004). "ELCOM in the Venice Lagoon," from CWR Models: Bytes and Nybbles, Autumn 2004, Issue 10, page 2.

A.3.2 SUPPLEMENTAL REFERENCES

(November 1999), "Course notes, Computational aquatic ecosystem dynamics model, CAEDYM, Special introduction work session," TTF/3/Nov99, Centre for Water Research, University of Western Australia, 51pp.

(January 2000), "Course notes, Estuary & lake computer model, ELCOM, Special introduction training session," TTF/3/JAN2000, Centre for Water Research, University of Western Australia, 21pp+app.

(January 21, 2000) "Instructions for the use of the graphical user interface *modeler* in the configuration & visualization of DYRESM-CAEDYM," Draft version 2, 42pp.

Antenucci, J. and Imberger, J. (1999), "Seasonal development of long internal waves in a strongly stratified lake: Lake Kinneret," *Journal of Geophysical Research* (in preparation).

Antenucci, J. and Imberger, J. (2000), "Observation of high frequency internal waves in a large stratified lake," *5th International Symposium on Stratified Flows, (ISSF5)*, Vancouver, July 2000, **1**, 271-6.

Bailey, M.B. and Hamilton, D.H. (1997), "Wind induced sediment re-suspension: a lake wide model," *Ecological Modeling*, **99**, 217-28.

Burling, M.; Pattiaratchi, C.; and Ivey, G. (1996), "Seasonal dynamics of Shark Bay, Western Australia," *3rd National AMOS Conference*, 5-7 February 1996, University of Tasmania, Hobart, 128.

Chan, C.U.; Hamilton, D.P.; and Robson, B.J. (2001), "Modeling phytoplankton succession and biomass in a seasonal West Australian estuary," *Proceedings, SIL Congress XXVIII* (in press).

Chan, T. and Hamilton, D.P. (2001), "The effect of freshwater flow on the succession and biomass of phytoplankton in a seasonal estuary," *Marine and Freshwater Research* (in press).

De Silva, I.P.D.; Imberger, J.; and Ivey, G.N. (1997), "Localized mixing due to a breaking internal wave ray at a sloping bed," *Journal of Fluid Mechanics,* **350**, 1-27.

Eckert, W.; Imberger, J.; and Saggio, A. (1999), "Biogeochemical evolution in response to physical forcing in the water column of a warm monomictic lake," *Limnology and Oceanography* (submitted).

Gersbach, G.; Pattiaratchi, C.; Pearce, A.; and Ivey, G. (1996), "The summer dynamics of the oceanography of the south-west coast of Australia – The Capes current" *3rd National AMOS Conference*, 5-7 February 1996, University of Tasmania, Hobart, 132.

Hamilton, D.P. (1996), "An ecological model of the Swan River estuary: An integrating tool for diverse ecological and physico-chemical studies," *INTECOL's V International Wetlands Conference 1996 "Wetlands for the Future,"* September 1996, Perth, Australia.

Hamilton, D.P.; Chan, T.; Hodges, B.R.; Robson, B.J.; Bath, A.J.; and Imberger, J. (1999), "Animating the interactions of physical, chemical and biological processes to understand the dynamics of the Swan River Estuary," Combined Australian-New Zealand Limnology Conference, Lake Taupo.

Hamilton, D.P. (2000), "Record summer rainfall induces first recorded major cyanobacterial bloom in the Swan River," *The Environmental Engineer*, **1**(1), 25.

Hamilton, D.; Hodges, B.; Robson, B.; and Kelsey, P. (2000), "Why a freshwater blue-green algal bloom occurred in an estuary: the Microcystis bloom in the Swan River Estuary in 2000," Western Australian Marine Science Conference 2000, Path, Western Australia.

Hamilton, D.P.; Chan, T.; Robb, M.S.; Pattiaratchi, C.B.; Herzfeld, M.; and Hodges, B. (2001), "Physical effects of artificial destratification in the upper Swan River Estuary," *Hydrological Processes*.

Heinz, G.; Imberger, J.; and Schimmele, M. (1990), "Vertical mixing in Überlinger See, western part of Lake Constance," *Aquat. Sci.,* **52**, 256-68.

Herzfeld, M. (1996), "Sea surface temperature and circulation in the Great Australian bight," Ph.D. Thesis, School of Earth Science, Flinders University, South Australia.

Herzfeld, M. and Hamilton, D. (1997), "A computational aquatic ecosystem dynamics model for the Swan River, Western Australia," *MODSIM '97, International Congress on Modeling and Simulation Proceedings*, 8-11 December, 1997, University of Tasmania, Hobart, **2**, 663-8.

Herzfeld, Michael (May 28, 1999), "Computational aquatic ecosystem dynamics model (CAEDYM), An ecological water quality model designed for coupling with hydrodynamic drivers, Programmer's guide," Centre for Water Research, The University of Western Australia, Nedlands, Australia, 133pp.

Hodges, Ben R. (July 1991), "Pressure-driven flow through an orifice for two stratified, immiscible liquids," M.S. thesis, The George Washington University, School of Engineering and Applied Science.

Hodges, Ben R. (March 1997), "Numerical simulation of nonlinear free-surface waves on a turbulent open-channel flow," Ph.D. dissertation, Stanford University, Dept. of Civil Engineering.

Hodges, Ben R. (June 9, 1998), "Heat budget and thermodynamics at a free surface: Some theory and numerical implementation (revision 1.0c)," Working manuscript, Centre for Water Research, The University of Western Australia, 14pp.

Hodges, Ben R. (1999), "Numerical techniques in CWR-ELCOM," Technical report, Centre for Water Research, The University of Western Australia. (in preparation)

Hodges, Ben R. (2000), "Recirculation and equilibrium displacement of the thermocline in a wind-driven stratified lake," *5th International Symposium on Stratified Flows, (ISSF5)*, Vancouver, July 2000, **1**, 327-30.

Hodges, B.R., Herzfeld, M., and Hamilton, D. (1998), "A computational aquatic ecosystem dynamics model for the Swan River," *EOS Trans. AGU*, **79**(1), Ocean Sciences Meet. Suppl. OS11P-02.

Hodges, B.; Herzfeld, M.; Winters, K.; and Hamilton, D. (1998), "Interactions of a surface gravity waves and a sheared turbulent current," *EOS Trans. AGU*, **79**(1), Ocean Sciences Meet. Suppl. OS53.

Hodges, B.R. and Street, R.L. (1999), "On simulation of turbulent nonlinear free-surface flow," *Journal of Computational Physics*, **151**, 425-57.

Hodges, B.R.; Imberger, J.; Laval, B.; and Appt, J. (2000), "Modeling the hydrodynamics of stratified lakes," *Fourth International conference on HydroInformatics*, Iowa Institute of Hydraulic Research, Iowa City, 23-27 July 2000.

Hodges, B.R. and Imberger, J. (2001), "Simple curvilinear method for numerical methods of open channels," *Journal of Hydraulic Engineering*, **127**(11), 949-58.

Hodges, Ben R. and Street, Robert L. (1996), "Three-dimensional, nonlinear, viscous wave interactions in a sloshing tank," *Proceedings of the Fluid Engineering Summer Meeting 1996*, Vol. **3**, FED-Vol. **238**, ASME, 361-7.

Hodges, Ben R. and Street, Robert L. (1998), "Wave-induced enstrophy and dissipation in a sheared turbulent current," *Proceedings of the Thirteenth Australian fluid Mechanics Conference*, M.C. Thompson and K. Hourigan (eds.), Monash University, Melbourne, Australia, 13-18 December 1998, Vol. **2**, 717-20.

Hodges, B.R., Street, R.L., and Zang, Y. (1996), "A method for simulation of viscous, non-linear, free-surface flows," *Twentieth Symposium on Naval Hydrodynamics*, National Academy Press, 791-809.

Hollan, E. (1998), "Large inflow-driven vortices in Lake Constance," in J. Imberger (ed.), *Physical Processes in Lakes and Oceans. Coastal and Estuarine Studies,* **54,** American Geophysical Union, 123-36.

Hollan, E.; Hamblin, P.F.; and Lehn, H. (1990), "Long-term modeling of stratification in Large Lakes: Application to Lake Constance," in: Tilzer, M.M. and C. Serruya (eds.). *Large Lakes, Ecological Structure and Function***,** Berlin: Springer Verlag, 107-24.

Horn, D.A.; Imberger, J.; and Ivey, G.N. (1999), "Internal solitary waves in lakes – a closure problem for hydrostatic models," *Proceedings of 'Aha Halikoa Hawaiian Winter Workshop*, January 19-22, 1999, University of Hawaii, Manoa.

Horn, D.A.; Imberger, J.; and Ivey, G.N. (1999), "The degeneration of large-scale interfacial gravity waves in lakes," under consideration for publication in *Journal of Fluid Mechanics*.

Horn, D.A.; Imberger, J.; Ivey, G.N.; and Redekopp, L.G. (2000), "A weakly nonlinear model of long internal waves in lakes," *5th International Symposium on Stratified Flows, (ISSF5)*, Vancouver, July 2000, **1**, 331-6.

Imberger, J. (1985), "The diurnal mixed layer," *Limnology and Oceanography,* **30**(4), 737-70.

Imberger, J. (1985), "Thermal characteristics of standing waters: an illustration of dynamic processes," *Hydrobiologia,* **125,** 7-29.

Imberger, J. (1994), "Mixing and transport in a stratified lake," Preprints of *Fourth International Stratified on Flows Symposium*, Grenoble, France, June-July 1994, **3** 1-29.

Imberger, J. (1994), "Transport processes in lakes: a review," in R. Margalef (ed.), *Limnology Now: A Paradigm of Planetary Problems,* Elsevier Science, 99-193.

Imberger, J. (1998), "Flux paths in a stratified lake: A review," in J. Imberger (ed.), *Physical Processes in Lakes and Oceans. Coastal and Estuarine Studies,* **54,** American Geophysical Union, 1-18.

Imberger, J. (1998), "How does the estuary work?" WAERF Community Forum, 25 July 1998, The University of Western Australia.

Imberger, J.; Berman, T; Christian, R.R.; Sherr, E.B.; Whitney, D.E.; Pomeroy, L.R.; Wiegert, R.G.; and Wiebe, W.J. (1983), "The influence of water motion on the distribution and transport of materials in a salt marsh estuary," *Limnology and Oceanography*, **28**, 201-14.

Imberger, J. and Hamblin, P.F. (1982), "Dynamics of lakes, reservoirs, and cooling ponds," *Journal of Fluid Mechanics,* **14**, 153-87.

Imberger, J. and Head, R. (1994), "Measurement of turbulent properties in a natural system," reprinted from *Fundamentals and Advancements in Hydraulic Measurements and Experimentation*.

Imberger, J. and Ivey, G.N. (1991), "On the nature of turbulence in a stratified fluid. Part II: Application to lakes," *Journal of Physical Oceanography,* **21**(5), 659-80.

Imberger, J. and Ivey, G.N. (1993), "Boundary mixing in stratified reservoirs," *Journal of Fluid Mechanics,* **248**, 477-91.

Imberger, J. and Patterson, J.C. (1981), "A dynamic reservoir simulation model – DYRESM: 5," In H.B. Fischer (ed.) *Transport Models for Inland and Coastal Waters,* Academic Press, 310-61.

Imberger, J. and Patterson, J.C. (1990), "Physical limnology," In: *Advances in Applied Mechanics,* **27**, 303-475.

Ivey, G.N. and Corcos, G.M. (1982), "Boundary mixing in a stratified fluid," *Journal of Fluid Mechanics,* **121**, 1-26.

Ivey, G.N. and Imberger, J. (1991), "On the nature of turbulence in a stratified fluid. Part I: The energetics of mixing," *Journal of Physical Oceanography,* **21**(5), 650-8.

Ivey, G.N.; Imberger, J.; and Koseff, J.R. (1998), "Buoyancy fluxes in a stratified fluid," in J. Imberger (ed.), *Physical Processes in Lakes and Oceans. Coastal and Estuarine Studies,* **54,** American Geophysical Union, 377-88.

Ivey, G.N.; Taylor, J.R.; and Coates, M.J. (1995), "Convectively driven mixed layer growth in a rotating, stratified fluid," *Deep-Sea Research I.,* **42**(3), 331-49.

Ivey, G.N.; Winters, K.B; and De Silva; I.P.D. (1998), "Turbulent mixing in an internal wave energized benthic boundary layer on a slope," submitted to *Journal of Fluid Mechanics*.

Jandaghi Alaee, M.; Pattiaratchi, C.; and Ivey, G. (1996), "The three-dimensional structure of an island wake," *8th International Biennial Conference. Physics of Estuaries and coastal Seas (PECS)* 9-11 September 1996, the Netherlands, 177-9.

Javam, A; Teoh, S.G.; Imberger, J.; and Ivey, G.N. (1998), "Two intersecting internal wave rays: a comparison between numerical and laboratory results," in J. Imberger (ed.), *Physical Processes in Lakes and Oceans. Coastal and Estuarine Studies***, 54,** American Geophysical Union, 241-50.

Kurup, R.; Hamilton, D.P.; and Patterson, J.C. (1998), "Modeling the effects of seasonal flow variations on the position of a salt wedge in a microtidal estuary," Estuarine Coastal *and Shelf Science*, **47**(2), 191-208.

Kurup, R.G.; Hamilton, D.P.; and Phillips, R.L. (2000), "Comparison of two 2-dimensional, laterally averaged hydrodynamic model applications to the Swan River Estuary," *Mathematics and Computers in Simulation*, **51**(6), 627-39.

Laval, B.; Hodges, B.R.; and Imberger, J. (2000), "Numerical diffusion in stratified lake," *5th International Symposium on Stratified Flows, (ISSF5)*, Vancouver, July 2000, **1**, 343-8.

Lemckert, C. and Imberger, J. (1995), "Turbulent benthic boundary layers in fresh water lakes," Iutam Symposium on Physical Limnology, Broome, Australia, 409-22.

Maiss, M.; Imberger, J.; and Münnich, K.O. (1994), "Vertical mixing in Überlingersee (Lake Constance) traced by SF6 and heat," *Aquat. Sci.,* **56**(4), 329-47.

Michallet, H. and Ivey, G.N. (1999), "Experiments on mixing due to internal solitary waves breaking on uniform slopes," *Journal of Geophysical Research,* **104**, 13467-78.

Nehru, A; Eckert, W.; Ostrovosky, I.; Geifman, J.; Hadas, O.; Malinsky-Rushansky, N.; Erez, J.; and Imberger, J. (1999), "The physical regime and the respective biogeochemical processes in Lake Kinneret lower water mass," *Limnology and Oceanography***,** (in press).

Ogihara, Y.; Zic, K.; Imberger, J.; and Armfield, S. (1996), "A parametric numerical model for lake hydrodynamics," *Ecological Modeling,* **86**, 271-6.

Patterson, J.C; Hamblin, P.F.; and Imberger, J. (1984), "Classification and dynamic simulation of the vertical density structure of lakes," *Limnology and Oceanography,* **29**(4), 845-61.

Pattiaratchi, C.; Backhaus, J.; Abu Shamleh, B.; Jandaghi Alaee, M.; Burling, M.; Gersbach, G.; Pang, D.; and Ranasinghe, R. (1996), "Application of a three-dimensional numerical model for the study of coastal phenomena in south-western Australia," *Proceedings of the Ocean & Atmosphere Pacific International Conference*, Adelaide, October 1995, 282-7.

Riley, G.A., H. Stommel and D.F. Bumpus, "Quantitative ecology of the plankton of the Western North Atlantic," *Bull. Bingham Oceanogr. Coll., 12(3)*, 1-69, 1949.

Robson, B.J.; Hamilton, D.P.; Hodges, B.R.; and Kelsey, P. (2000), "Record summer rainfall induces a freshwater cyanobacterial bloom in the Swan River Estuary," *Australian Limnology Society Annual Congress*, Darwin, 2000.

Saggio, A. and Imberger, J. (1998), "Internal wave weather in a stratified lake," *Limnology and Oceanography,* **43**, 1780-95.

Schladow, S.G. (1993), "Lake destratification by bubble-plume systems: Design methodology," *Journal of Hydraulic Engineering*, **119**(3), 350-69.

Smagorinsky, J. (1963) "General circulation experiments with the primitive equations, ´*Monthly Weather Review, 91*, 99-152.

Spigel, R.H. and Imberger, J. (1980), "The classification of mixed-layer dynamics in lakes of small to medium size," *Journal of Physical Oceanography,* **10**, 1104-21.

Steele, J.H. (1962), "Environmental control of photosynthesis in the sea," *Limnol. Oceanogr., 7*, 137-150.

Taylor, J.R. (1993), "Turbulence and mixing in the boundary layer generated by shoaling internal waves," *Dynamics of Atmospheres and Oceans,* **19**, 233-58.

Thorpe, S.A. (1995), "Some dynamical effects of the sloping sides of lakes," *IUTAM Symposium on Physical Limnology*, Broome, Australia, 215-30.

Thorpe, S.A. (1998), "Some dynamical effects of internal waves and the sloping sides of lakes," in J. Imberger (ed.), *Physical Processes in Lakes and Oceans. Coastal and Estuarine Studies,* **54,** American Geophysical Union, 441-60.

Thorpe, S.A. and Lemmin, U. (1999), "Internal waves and temperature fronts on slops," *Annales Geophysicae,* **17**(9), 1227-34.

Unlauf, L; Wang, Y.; and Hutter, K. (1999), "Comparing two topography-Following primitive equation models for lake circulation," *Journal of Computational Physics*, **153**, 638-59.

Winter, K.B. and Seim, H.E. (1998), "The role of dissipation and mixing in exchange flow through a contracting channel," submitted to *Journal of Fluid Mechanics*.

Winter, K.B.; Seim, H.E.; and Finnigan, T.D. (1998), "Simulation of non-hydrostatic, density-stratified flow in irregular domains," submitted to *International Journal of Numerical Methods in Fluids*.

Zhu, S. and Imberger, J. (1994) "A three-dimensional numerical model of the response of the Australian North West Shelf to tropical cyclones," in: *J. Austral. Math. Soc. Ser.***, B 36,** 64-100.

APPENDIX B

ANIMATIONS

INSTRUCTIONS FOR INSTALLING AND USING FRAMER TO VIEW ANIMATION FILES

Installation of Framer

Copy the files from the CD(s) to a directory on your computer.

Running Framer

1) In the Start Menu, choose "run." In this window, type "framer.exe." This should open a "Framer Open File" window, in which you find the proper directory and choose the file that you wish to view.

2) Commands for running the animation files are in the toolbar in the upper left corner of the framer window.

LIST OF ANIMATIONS

1) SVR_BaseCase_Temperature.rm: Animation of predicted water temperature for the Base Case

2) SVR_BaseCase_DecayingTracer.rm: Animation of predicted decaying tracer concentration for the Base Case

3) SVR_Extended_Drought_DecayingTracer.rm: Animation of predicted decaying tracer concentration for the Extended Drought scenario

4) SVR_Emergency_Drawdown_DecayingTracer.rm: Animation of predicted decaying tracer concentration for the Emergency Drawdown scenario

5) SVR_DesignLocation_BaseCase_DecayingTracer.rm: Animation of predicted decaying tracer concentration using Design Purified Water Inlet Location under the Base Case operating scenario

6) SVR_BaronaArm_BaseCase_DecayingTracer.rm: Animation of predicted decaying tracer concentration using Barona Arm Purified Water Location under the Base Case operating scenario

7) SVR_CurrentAqueduct_BaseCase_DecayingTracer.rm: Animation of predicted decaying tracer concentration using Current Aqueduct Purified Water Inlet Location under the Base Case operating scenario

8) SVR_NewAqueduct_BaseCase_DecayingTracer.rm: Animation of predicted decaying tracer concentration using New Aqueduct Purified Water Inlet Location under the Base Case operating scenario

9) SVR_DesignLocation_ExtendedDrought_DecayingTracer.rm: Animation of predicted decaying tracer concentration using Design Purified Water Inlet Location under the Extended Drought operating scenario

10) SVR_NewAqueduct_ExtendedDrought_DecayingTracer.rm: Animation of predicted decaying tracer concentration using New Aqueduct Purified Water Inlet Location under the Extended Drought operating scenario

Flow Science Incorporated
420 Neff Avenue, Suite 230, Harrisonburg, VA 22801
(540) 442-8433 • FAX (540) 442-8863

Water Purification Demonstration Project: Limnology and Reservoir Detention Study of San Vicente Reservoir – Nutrient and Algae Modeling Results

Prepared for
City of San Diego
600 B Street, Suite 600,
San Diego, CA 92101

Prepared By
Li Ding, Ph.D., P.E. (VA)
Senior Engineer

Reviewed By
Imad A. Hannoun, Ph.D., P.E. (VA)
President

Reviewed By
E. John List, Ph.D., P.E. (CA)
Principal Consultant

FSI V094005
May 01, 2012

Table of Contents

SUMMARY **1**

1. INTRODUCTION **6**

1.1 Background 6
1.2 the SVR Model 7
1.2.1 General Description of the SVR Model 7
1.2.2 Model Calibration/Validation 8
1.2.2.1 Hydrodynamic (ELCOM) Calibration/Validation 8
1.2.2.2 Water Quality (CAEDYM) Calibration 9
1.3 Summary of hydrodynamic results in TM #2 10
1.4 Approach and Report organization 11

2. EFFECTS OF RESERVOIR EXPANSION **12**

2.1 comparison of modeling results 12
2.2 nutrient Loadings 15

3. MODELING RESULTS FOR FUTURE CONDITONS **18**

3.1 modeling scenarios 18
3.1.1 Base Case 18
3.1.2 No Purified Water Scenario 19
3.2 Comparison Of Modeling Results 22
3.3 Nutrient Loadings 25

4. CONCLUSIONS AND DISCUSSION **28**

5. REFERENCES **32**

6. GLOSSARY **33**

FIGURES **36**

APPENDIX A **A-1**

List of Tables

Table S-1	Summary of Bottom Anoxia Occurrence for Existing Case and Expanded Reservoir Case
Table S-2	Summary of Simulated DO, Chlorophyll a and Secchi Depth for Modeling Scenarios
Table 1	Summary of Bottom Anoxia Occurrence for Existing Case and Expanded Reservoir Case
Table 2	Predicted Volume of Water under Anoxic Conditions in the Existing Case and Expanded Reservoir Case
Table 3	Estimated Annual Phosphorus Loadings for the Existing and Expanded Reservoir
Table 4	Estimated Annual Nitrogen Loadings for the E-xisting and Expanded Reservoir
Table 5	Monthly Reservoir Inflow and Outflow Volumes for Base Case Operating Scenario
Table 6	Available Withdrawal Elevations on Proposed Reservoir Outlet Tower
Table 7	Purified Water Inflow Water Quality Parameters
Table 8	Monthly Reservoir Inflow and Outflow Volumes for No Purified Water Scenario
Table 9	Modeled Operating Scenarios
Table 10	Summary of Simulated Do, Chlorophyll *a* and Secchi Depth for Modeling Scenarios
Table 11	Annual SRP Loadings
Table 12	Annual TP Loadings
Table 13	Annual (NO_3+NH_4)-N Loadings
Table 14	Annual TN Loadings

List of Figures

Figure 1 Map of San Vicente Reservoir
Figure 2 ELCOM-CAEDYM Schematic of Processes Modeled in ELCOM-CAEDYM
Figure 3 SVR Water Quality Model Grid
Figure 4 SVR Water Quality Model Calibration Results – Station A – Water Temperature Comparison
Figure 5 SVR Water Quality Model Calibration Results – Station A – DO Comparison
Figure 6 SVR Water Quality Model Calibration Results – Station A – Secchi Depth Comparison
Figure 7 Aqueduct Inflow Nutrient Concentrations
Figure 8 Comparison of Existing Case and Expanded Reservoir Case – Simulated Temperature at Station A
Figure 9 Comparison of Existing Case and Expanded Reservoir Case – Simulated DO at Station A
Figure 10 Comparison of Existing Case and Expanded Reservoir Case – Simulated Surface and Bottom DO at Station A
Figure 11 Comparison of Existing Case and Expanded Reservoir Case – Simulated Surface and Bottom Ammonia (as N) at Station A
Figure 12 Comparison of Existing Case and Expanded Reservoir Case – Simulated Surface and Bottom Nitrate (as N) at Station A
Figure 13 Comparison of Existing Case and Expanded Reservoir Caser – Simulated Surface and Bottom TN at Station A
Figure 14 Comparison of Existing Case and Expanded Reservoir Case – Simulated Surface and Bottom SRP at Station A
Figure 15 Comparison of Existing Case and Expanded Reservoir Case – Simulated Surface and Bottom TP at Station A
Figure 16 Comparison of Existing Case and Expanded Reservoir Case – Simulated Surface Chlorophyll *a* at Station A
Figure 17 Comparison of Existing Case and Expanded Reservoir Case – Simulated Secchi Depth at Station A
Figure 18 Comparison of Existing Case and Expanded Reservoir Case – Simulated Surface and Bottom pH at Station A
Figure 19 Purified Water and Aqueduct Inflow Rates of Existing Case, No Purified Water and Base Case Scenarios
Figure 20 Reservoir Water Volumes for Existing Case, No Purified Water and Base Case Scenarios
Figure 21 Comparison of Existing Case, No Purified Water and Base Case Scenarios – Simulated Water Temperature at Station A

Figure 22 Comparison of Existing Case, No Purified Water and Base Case Scenarios – Simulated Surface and Bottom DO at Station A
Figure 23 Comparison of Existing Case, No Purified Water and Base Case Scenarios – Simulated Surface and Bottom Nitrate (as N) at Station A
Figure 24 Comparison of Existing Case, No Purified Water and Base Case Scenarios – Simulated Surface and Bottom Ammonia (as N) at Station A
Figure 25 Comparisons of Existing Case, No Purified Water and Base Case Scenarios – Simulated Surface and Bottom Total Nitrogen at Station A
Figure 26 Comparison of Existing Case, No Purified Water and Base Case Scenarios – Simulated Surface and Bottom SRP at Station A
Figure 27 Comparison of Existing Case, No Purified Water and Base Case Scenarios – Simulated Surface and Bottom TP at Station A
Figure 28 Comparison of Existing Case, No Purified water and Base Case Scenarios – Simulated Surface Chlorophyll *a* at Station A
Figure 29 Comparison of Existing Case, No Purified Water and Base Case Scenarios – Secchi Depth at Station A
Figure 30 Comparison of Existing Case, No Purified Water and Base Case Scenarios – Simulated Surface and Bottom pH at Station A

SUMMARY

San Vicente Reservoir (SVR) is located near Lakeside, California, and is used as a source of drinking water supply by the City of San Diego (City), its owner and operator. The reservoir currently has a capacity of about 90,000 acre-feet (see Figure 1). It is undergoing an expansion that will raise the dam 117 feet (ft) and increase the reservoir's storage to 247,000 acre-feet at the spillway level (or 242,000 acre-feet at the maximum operation level). The City is considering an option to augment SVR supply by bringing advanced purified recycled water (*i.e.*, purified water) from the advanced water purification facility to SVR. The purified water would be blended with other water in the reservoir. The current project – the Water Purification Demonstration Project (Demonstration Project) – will not actually put any purified water into the reservoir; rather it will study and model the reservoir augmentation process. A component of the Demonstration Project is the Limnology and Reservoir Detention Study of San Vicente Reservoir (Limnology Study).

As part of the Limnology Study, Flow Science Incorporated (FSI) has developed a three-dimensional water quality model that is used to evaluate hydrodynamic and water quality effects of using purified water to augment SVR. After the model was developed, its results were compared to existing field data and documented in a Technical Memorandum (TM #1) submitted to the City in 2010 (FSI, 2010). The TM #1 has been peer-reviewed by the National Water Research Institute Independent Advisory Panel (NWRIIAP) that was assembled for the review of the City's Demonstration Project. After implementing suggestions proposed by the NWRIIAP, the model was deemed by NWRIIAP to be "an effective and robust tool, for 1) simulating thermoclines and hydrodynamics of the San Vicente Reservoir; 2) assessing biological water quality for nutrients; 3) assessing options for the purified water inlet location" (NWRIIAP, 2010).

Upon completion of the SVR model calibration and validation, FSI conducted simulations of purified water delivery to the expanded SVR under various projected future operating conditions using the calibrated/validated model. The simulation results and findings are presented in two separate Technical Memorandums (TM #2 and TM #3). The TM #2 summarizes the hydrodynamic aspects of the modeling results and was submitted to the City on November 28, 2011. This report, TM #3, focuses on the water quality aspects of the modeling results and findings, with emphasis on nutrients (phosphorus and nitrogen), dissolved oxygen (DO), and algal concentration levels. The water quality parameters evaluated include chlorophyll *a* (a surrogate measure of algal growth), DO, pH, nitrate as N, ammonia as N, Total Nitrogen (TN), Soluble Reactive Phosphorus (SRP), Total Phosphorus (TP) and Secchi depth.

The goal of this work is to determine the effects of purified water delivery on the reservoir's water quality under anticipated future conditions in the expanded reservoir.

Because both the reservoir expansion and augmentation with purified water are expected to affect the reservoir water quality, a two-step approach was taken in this study to examine the water quality effects caused by the reservoir expansion and argumentation, respectively.

RESERVOIR EXPANSION

First, the SVR model was used to determine the effects of the reservoir expansion on water quality, without the introduction of any purified water. This was accomplished by performing a simulation (referred to as Expanded Reservoir Case) that uses the same reservoir conditions (climate, inflow and outflow volumes and concentrations etc.) as the 2006 - 2007 calibration simulation (*i.e.*, Existing Case), except for using a higher initial reservoir volume that is set at 155,000 acre-feet (median expected future storage). The results from the Expanded Reservoir Case were compared against those from the Existing Case. The differences between the results of these two simulations demonstrate the effects of the expansion on the reservoir's water quality in the absence of any purified water discharge to the reservoir.

Based on the results of these two simulations, the following conclusions and observations on the effects of the reservoir expansion can be made:

- As evidenced in **Table S-1**, the reservoir expansion is predicted to extend the duration of the hypolimnetic anoxia by an average of 27 days per year (from 189 days per year to 216 days per year) and enlarge the volume of water under anoxic condition by at least two fold.

- The reservoir expansion will produce lower surface chlorophyll *a* concentrations and higher Secchi depths *(i.e.*, better water clarity) in the reservoir. It is predicted that the annual average chlorophyll *a* concentration will decrease from 5.8 micrograms per liter (µg/L) to 3.4 µg/L and the annual average Secchi depth will increase from 3.2 meters (m) to 4.7 m after the expansion.

- Based on a nutrient loading calculation, the internal nutrient loadings *(i.e.*, nutrients released from sediment) are larger than all external loadings combined over the two-year modeling period for both the Existing Case and Expanded Reservoir Case. Meanwhile, the reservoir expansion is predicted to lead to a significant increase in sediment nutrient release, likely due to the larger hypolimnetic bottom area and extended hypolimnetic anoxia period. However, despite the significantly higher sediment release, surface TN concentrations are actually lower after the reservoir expansion, a result of the significantly larger volume of water for the Expanded Reservoir Case. The resulting lower nutrient concentrations are believed to be one of the main factors that lead to lower surface

chlorophyll *a* concentrations for the Expanded Reservoir Case (compared to the Existing Reservoir Case).

Table S-1. Summary of Bottom Anoxia[1] Occurrence for Existing Case and Expanded Reservoir Case

Simulation	Days Under Anoxia: Total Days (Percentage)[2]	Average Surface Chlorophyll *a* (µg/L)	Average Secchi Depth (m)
Existing Case	189 (52%)	5.8	3.2
Expanded Reservoir Case	216 (59%)	3.4	4.7

Notes:1. Anoxia is defined here as the bottom DO less than 0.5 mg/L
2. Both the total number of days and percentage under anoxia are yearly values averaged over the two-year simulation period.

FUTURE OPERATING CONDITIONS

After the effects of the reservoir expansion were determined, the model was used to examine the water quality in the expanded reservoir under future operating conditions both with and without purified water augmentation. Specifically, the following two future scenarios were simulated:

- Base Case (includes purified water inflow) ---- This scenario considered an expanded reservoir under median expected storage and expected future operations. The initial reservoir volume for the Base Case is set at 155,000 acre-feet. The following annual flow rates were assumed: for aqueduct inflow 3,000 acre-feet/year (a-f/y); runoff 4,500 a-f/y; purified water inflow 15,000 a-f/y; and dam withdrawal 19,000 a-f/y, with no water transfers from Sutherland Reservoir into SVR.

- No Purified Water ---- The inputs for this scenario are similar to those for the Base Case scenario, except for no purified water additions and an equal reduction in reservoir outflow. The initial reservoir volume for this scenario is set at 155,000 acre-feet. The annual flow rates for aqueduct inflow, runoff, purified water inflow and dam withdrawal are 3,000, 4,500, 0 and 4,000 acre-feet/year respectively. There are no water transfers from Sutherland Reservoir into SVR.

Results from the Base Case and No Purified Water scenarios were compared against those obtained from the Existing Case simulations (*i.e*., no reservoir expansion). Based on the simulation results, the following conclusions and observations on the effects of the purified water and future operating conditions are made:

- The hypolimnetic anoxia period is predicted to last an average of 189 days per year for the Existing Case (**Table S-2**). For the No Purified Water scenario, the hypolimnetic anoxia period is predicted to increase to 207 days per year, an addition of 18 days per year. Adding purified water into the reservoir under future operating conditions (*i.e.*, Base Case) will further extend the average duration of the hypolimnetic anoxia period by 8 days, to a total of 215 days per year.

- The No Purified Water scenario produces lower algae levels *(i.e.*, lower surface chlorophyll *a* concentrations) and higher Secchi depths (*i.e.*, better water clarity) compared to the Existing Case. For example, the annual average chlorophyll *a* concentration and Secchi depth are predicted to be 5.8 µg/L and 3.2 m respectively for the Existing Case (**Table S-2**). By comparison, the annual average chlorophyll *a* concentration and Secchi depth are predicted to be 3.1 µg/L and 4.8 m, respectively, for the No Purified Water scenario in the expanded reservoir. This is a reduction of 2.7 µg/L for the average chlorophyll *a* concentration and an increase of 1.6 m for the average Secchi depth compared to the Existing Case.

- The Base Case scenario also produces lower algae levels *(i.e.*, lower surface chlorophyll *a* concentrations) and higher Secchi depths (*i.e.*, better water clarity) compared to the Existing Case. The Base Case is predicted to produce 3.7 µg/L for the annual average chlorophyll *a* concentration and 4.3 m for the annual average Secchi depth (**Table S-2**). This is a reduction of 2.1 µg/L for the average chlorophyll *a* concentration and an increase of 1.1 m for the average Secchi depth compared to the Existing Case.

- Nutrient loading calculations show that nutrient sediment release constitutes a significant portion of all nutrient loadings into SVR for all future scenarios as well as the Existing Case. The future operating scenarios (*i.e.*, Base Case and No Purified Water) produce sediment nutrient loadings significantly larger than those for the Existing Case, likely a result of the larger hypolimnetic bottom area and extended hypolimnetic anoxia period. However, despite the significantly higher sediment release for the future operating scenarios, surface TN concentrations are actually lower for the future scenarios compared to the Existing Reservoir Case, a result of the larger volume of water in the expanded reservoir. The resulting

lower nutrient concentrations are believed to be one of the main factors that lead to lower surface chlorophyll *a* concentrations for the future operating scenarios (compared to the Existing Reservoir Case).

- Nutrient limitation in SVR can be affected by various factors including the nutrient loadings from all the inflows and the sediments. As a result, nutrient limitation at any point may vary based on existing conditions. However, note that the N:P ratio of the purified water is expected to reach about 159, indicating that algal growth in the future reservoir may tend to become more phosphorus-limited.

Table S-2. Summary of Simulated DO, Chlorophyll *a* and Secchi Depth for Modeling Scenarios

Operating Scenarios	Days Under Anoxia[1]: Total Days (Percentage)[2]	Average Surface Chlorophyll *a* (µg/L)	Average Secchi Depth (m)
Existing Case	189 (52%)	5.8	3.2
No Purified Water	207 (57%)	3.1	4.8
Base Case	215 (59%)	3.7	4.3

Notes: 1. Anoxia is defined here as the bottom DO less than 0.5 mg/L.
2. Both the total days and percentage under anoxia are yearly values averaged over the two-year simulation period.

1. INTRODUCTION

1.1 BACKGROUND

San Vicente Reservoir (SVR) is located near Lakeside, California, and is used as a drinking water supply by the City of San Diego (City), its owner and operator (**Figure 1**). The reservoir currently has a capacity of about 90,000 acre-feet. It is undergoing an expansion that will raise the dam by 117 feet and increase the reservoir's storage to 247,000 acre-feet at the spillway level (or 242,000 acre-feet at the maximum operation level). The reservoir expansion is scheduled to be completed in 2013.

In the meantime, a water reuse project, entitled Reservoir Augmentation, is being studied by the City. If implemented at full-scale, Reservoir Augmentation would bring advanced purified recycled water (*i.e.*, purified water) from the advanced water purification facility to the expanded SVR via a pipeline. The purified water would be blended with other water in the reservoir. The current project – the Water Purification Demonstration Project (Demonstration Project) – will not actually put any purified water into the reservoir; rather it will study and model the Reservoir Augmentation process. A component of the Demonstration Project is the Limnology and Reservoir Detention Study of San Vicente Reservoir (Limnology Study).

As part of the Limnology Study, Flow Science Incorporated (FSI) has developed a three-dimensional computer model that is used to evaluate hydrodynamic and water quality effects of using purified water to augment SVR. After the model was developed, its results were compared to existing field data and documented in a Technical Memorandum (TM #1) submitted to the City in 2010 (FSI, 2010). The TM #1 has been peer-reviewed by the National Water Research Institute Independent Advisory Panel (NWRIIAP) that was assembled for the review of the City's Demonstration Project. The model was deemed by NWRIIAP, with some fine-tuning, as "an effective and robust tool, for 1) simulating thermoclines and hydrodynamics of the San Vicente Reservoir; 2) assessing biological water quality for nutrients; 3) assessing options for the purified water inlet location" (NWRIIAP, 2010). After the review, all the suggestions by NWRIIAP on fine-tuning the model have been addressed or implemented. Findings and results from the TM #1 that are relevant to the work presented here are summarized in the next section.

Upon completion of the SVR model calibration and validation, FSI conducted simulations of purified water release to the expanded reservoir under various projected future operating conditions using the calibrated/validated model. The simulation results and findings are presented in two separate Technical Memorandums (TM #2 and TM #3). The TM #2 summarizes the hydrodynamic aspects of the modeling results and was submitted to the City on November 28, 2011. The highlights of TM#2 are included in the

next section. This current report, TM #3, focuses on the water quality aspects of the modeling results and findings with emphasis on nutrients (phosphorus and nitrogen), DO, and algal concentration levels. The water quality parameters evaluated include chlorophyll *a* (a surrogate measure of algal growth), DO, pH, nitrate as N, ammonia as N, Total Nitrogen (TN), Soluble Reactive Phosphorus (SRP), Total Phosphorus (TP) and Secchi depth.

This work has been performed by Flow Science Incorporated (FSI) of Pasadena, California, under contract to the City of San Diego, California.

1.2 THE SVR MODEL

1.2.1 General Description of the SVR Model

The three-dimensional SVR model consists of two coupled computer models that simulate both the hydrodynamics and water quality of SVR. These two models are the Estuary Lake and Coastal Ocean DYnamics Model (ELCOM) for hydrodynamic simulation and the Computational Aquatic Ecosystem DYnamics Model (CAEDYM) for water quality simulation. ELCOM requires the user to define boundary conditions, physical inputs, meteorological inputs, and bathymetry in a grid structure. The output from ELCOM consists of predictions for water velocities, temperature, salinity (*i.e.*, conductivity), and concentrations of decaying or conservative tracers in space and time within the body of water. CAEDYM is a suite of water quality modules that compute interactions between biological organisms and the chemistry of their nutrient cycles (**Figure 2**). It is coupled with ELCOM to simulate the biochemical parameters of an aquatic ecosystem including carbon, nitrogen, phosphorus, silicon, organic matter, DO, pH, inorganic suspended solids, metals, carbon, fish and chlorophyll *a*. In this study, we focus on simulation results for nutrients (*i.e.*, nitrogen and phosphorus), DO and algae in the expanded SVR. Detailed information and technical descriptions concerning ELCOM and CAEDYM are included in **Appendix A**.

The SVR modeling domain includes both the existing reservoir as well as the proposed expanded reservoir (**Figure 1**). A grid with a horizontal resolution of 100 × 100 m is used in this study – similar to the grid used in the water quality calibration (**Figure 3**). It should be noted that the horizontal grid used in the water quality simulation is coarser than the grid used in the hydrodynamic simulation (*i.e.*, 50 × 50 m in resolution) in order to ensure a reasonable computational time. The vertical grid used in the water quality simulation is the same as that used in the hydrodynamic simulation, with a grid size of 1.64 ft (0.5 m) near the surface and expanding in size with depth. A test has been conducted (and presented in TM #1) to evaluate the accuracy of the coarse grid in simulating temperature and conductivity. It concluded that using either the fine or coarse grids will result in almost identical predicted conductivity and temperature

profiles. Therefore, it is appropriate to use the coarse grid in the water quality simulation to ensure adequate model resolution and reasonable model run times.

1.2.2 Model Calibration/Validation

The model calibration was conducted for the two-year period of 2006 and 2007. The input data required by the calibration were either based on the measured data or derived from these data. Various comparisons between model and data are presented in the TM #1 and they include temperature, conductivity, DO, pH, nutrients (nitrogen and phosphorus), chlorophyll *a* and Secchi depth. In the following, we discuss the highlights of TM #1.

1.2.2.1 Hydrodynamic (ELCOM) Calibration/Validation

The calibrated/validated ELCOM model shows good agreement with the measured data for both water temperature and conductivity. For example, the onset and duration of thermal stratification as well as the deepening rate of the thermocline were predicted accurately by the model (**Figure 4**). In particular both the field data and model show that winter water temperatures in the fully mixed reservoir were nearly uniform in the vertical direction at a value near 12 ^{o}C to 13 ^{o}C. By April, increased solar radiation warmed the water surface up to 17 ^{o}C to 18 ^{o}C and thermal stratification started to develop. This process intensified and by summer (July through September) the surface temperatures had risen to as high as 28 ^{o}C, while the temperature in the hypolimnion remained nearly unchanged at the winter temperature of 12 ^{o}C to 13 ^{o}C. This large temperature difference between surface and bottom indicates that a strong vertical stratification was established in the lake. The thermocline was well defined and located at a depth ranging from approximately 30 to 40 ft, as shown in **Figure 4** for both the model and the data. In the fall, surface water temperatures steadily decreased due to reduced solar radiation and cooler air temperatures. This generated convective plumes within the reservoir, which combined with more effective wind mixing, deepened the thermocline to a depth of 60 ft by November. The stratification continued to weaken until the reservoir totally destratified and became well mixed at the end of the year, or at the beginning of the following year. The variation of conductivity in the reservoir was also well captured by the model (see Figures 18-20 in TM #1 for the calibration results in conductivity).

After the ELCOM model was calibrated, a validation was performed to compare the model against the results of previous tracer field studies. The validation shows that the model was capable of replicating the main features of the tracer study. This provides verification and assurance that the model performance is reliable and accurate in simulating hydrodynamics in the reservoir.

1.2.2.2 Water Quality (CAEDYM) Calibration

For all the simulated water quality parameters, the calibrated CAEDYM model shows overall good agreement with measured data. For example, both field data and simulation show that DO concentrations at the surface remained high throughout the years as a result of both the supply of oxygen directly from the atmosphere and of oxygen produced by photosynthetic activity near the surface (**Figure 5**). At high rates of photosynthesis, oxygen production by algae exceeded the diffusion of oxygen out of the system and this resulted in occasional oxygen supersaturation in the spring of 2006 and 2007. At the beginning of the simulation period, DO near the bottom of the reservoir was near saturation levels, a result of strong vertical mixing in the winter period. However, during the spring and summer, strong stratification at SVR inhibited vertical mixing and the DO at the bottom was quickly depleted by the decay of organic material (primarily algae cells) settling through the water column and organic matter in the sediments (*i.e.*, Sediment Oxygen Demand or SOD). The water in the hypolimnion became anoxic (defined as DO < 0.5 milligrams per liter [mg/L] herein) in the spring and anoxia lasted through the fall for both years, until the reservoir became destratified in the winter. **Figure 5** shows that the simulated DO concentrations captured the major trends in the measured DO concentrations, including the onset, duration, and magnitude of anoxia in the hypolimnion, the hypolimnetic DO decay rate in the spring, and the high surface DO concentrations resulting from algae blooms.

The available in-reservoir chlorophyll *a* data were qualitatively measured using a fluorometer that had not been calibrated. The calibration of chlorophyll *a* was conducted indirectly through comparisons with measured Secchi depth (**Figure 6**). Note that the formula used to derive Secchi depths using surface chlorophyll *a* concentrations is presented in the figure and this formula was also used in this study to obtain Secchi depths in all scenarios presented here. As shown in **Figure 6**, the Secchi depths from the calibration match fairly well with the measured Secchi depths, indicating a reasonably good calibration for chlorophyll *a*.

In conclusion, the SVR model is capable of capturing both the hydrodynamic features and the water quality variations in the reservoir. The simulation results are generally in good agreement with the field measurements. Thus the model provides "an effective and robust tool, for simulating thermoclines and hydrodynamics of the San Vicente Reservoir" and for "assessing biological water quality for nutrients" (findings from NWRIIAP, 2010). For more details of the calibration/validation refer to TM #1 (FSI, 2010).

1.3 SUMMARY OF HYDRODYNAMIC RESULTS IN TM #2

TM #2 presented the hydrodynamic results of various projected future operating scenarios for the expanded SVR. In particular, simulation results for temperature, conductivity and tracers are included in TM #2 for evaluation of reservoir hydrodynamics. Note that TM #2 has been peer-reviewed by NWRIIAP, which concluded that "the modeling is sufficiently predictive for purposes of evaluating the input of advanced treated recycled water" (NWRIIAP, 2012). In the simulations presented in TM #2, various hypothetical tracers were added to the purified water inflow to illustrate dilution, mixing and transport of the purified water within the reservoir. In particular, decaying tracers were used to study the dilution and inactivation of potential pathogens entering the reservoir; conservative tracers (*i.e.*, non-decaying) were used to simulate potential effects of elevated concentrations of chemical constituents in the purified water entering SVR after "excursion events" at the water purification facility.

Based on the simulation results, several key conclusions for the reservoir hydrodynamics were drawn in TM #2 and are listed here:

- Reservoir expansion will increase the volume of the hypolimnion but will have a negligible effect on overall temperature variation patterns as well as the thermocline depth during stratified periods.

- For all simulated future operating scenarios, decaying tracer concentrations in the reservoir outflow are predicted to achieve a 2-log reduction (100:1 reduction in concentration) in the unstratified period and significantly higher reductions (at least 4 logs; that is, a 10,000:1 reduction) in the stratified period.

- The minimum predicted dilution in the reservoir outflow for conservative tracers is about 900:1 for all simulated future operating scenarios.

- Moving the purified water inlet location closer to the reservoir outlet is predicted to generally (but not always) result in slightly higher values in the reservoir outflow concentrations for both the decaying and conservative tracers during the unstratified period. During the stratified period, different purified water inlet locations have little effect on decaying and conservative tracer concentrations in the reservoir outflow.

1.4 APPROACH AND REPORT ORGANIZATION

The goal of the work presented here is to determine the effects of purified water on the reservoir's water quality under anticipated future operating conditions in the expanded reservoir. Both the reservoir expansion and augmentation with purified water are expected to affect the reservoir water quality. Thus, a two-step approach was taken with the intent of examining the effects caused by each of these two changes. First, water quality effects caused solely by the reservoir expansion are investigated in **Chapter 2** by comparing results from two simulations that are different in the initial reservoir water volume, but otherwise identical. In **Chapter 3**, the water quality of the expanded reservoir under future operating conditions is examined, both with and without purified water augmentation to demonstrate the combined effects of argumentation and expansion under future operating conditions. Finally, conclusions and discussion are provided in **Chapter 4**.

2. EFFECTS OF RESERVOIR EXPANSION

The existing SVR has a capacity of 90,000 acre-feet and is currently undergoing an expansion to a capacity of 247,000 acre-feet that will be completed in 2013. Absent the Reservoir Augmentation project, SVR will be filled with imported water, local runoff, and water transferred from Sutherland Reservoir. Should the Reservoir Augmentation project go forward, the purified water would substitute for some of the imported water. The purified water would be diluted with other water stored in the reservoir. It is expected that the reservoir expansion alone could cause changes in the reservoir water quality. Thus, it is useful to investigate these anticipated changes in order to understand the future baseline conditions in the expanded reservoir. This was accomplished by performing a simulation that uses the same reservoir conditions (climate, inflow and outflow parameters etc.) as the 2006 - 2007 calibration simulation, except for using a higher initial reservoir volume that is set at 155,000 acre-ft (median expected future storage, see **Table 1**). This simulation is referred to herein as the Expanded Reservoir Case and the results from this simulation are compared to those from the original calibration in the unexpanded reservoir (henceforth referred as the Existing Case). The differences between the Existing Case and Expanded Reservoir Case therefore demonstrate the effects of the reservoir's expansion on water quality under the same operating conditions.

It should be noted that the nutrient levels in all the existing inflows to SVR are highly variable. **Figure 7** shows an example of nutrient levels in one of the main inflows to SVR, the aqueduct inflow, during the modeling period. The highest concentration of TN, for example, is almost four times that of the lowest concentration. This is expected to lead to variable nutrient and algae levels in the reservoir.

2.1 COMPARISON OF MODELING RESULTS

Figure 8 shows a comparison of simulated water temperatures from the Existing Case and Expanded Reservoir Case. The depth and deepening rate of the thermocline are fairly similar between these two simulations, indicating that the reservoir expansion will cause no major changes in the thickness of the epilimnion. Note that the volume of the epilimnion is somewhat larger for the Expanded Reservoir Case, mostly a result of the increase in the reservoir's surface area. However, the thickness and volume of the hypolimnion will be significantly larger for the Expanded Reservoir Case. With a larger hypolimnion, the reservoir from the Expanded Reservoir Case is predicted to destratify in the late fall or early winter a few days later than that from the Existing Case.

Table 1. Summary of Bottom Anoxia[1] Occurrence for Existing Case and Expanded Reservoir Case

Simulation	Year	Initial Reservoir Volume (acre-feet)	Bottom Anoxia Period	Days Under Anoxia: Total Days (Percentage)[2]	Average Surface Chlorophyll *a* (µg/L)	Average Secchi Depth (m)
Existing Case	2006	64,000	1/1 – 1/15 7/10 – 12/14	189 (52%)	5.8	3.2
	2007	60,000	6/8 – 12/28			
Expanded Reservoir Case	2006	155,000	1/1 – 1/19 6/21 – 12/23	216 (59%)	3.4	4.7
	2007	149,000	5/21 – 12/31			

Notes:1. Anoxia is defined here as the bottom DO less than 0.5 mg/L
2. Both the total number of days and percentage under anoxia are yearly values averaged over the two-year simulation period.

Figure 9 shows contours of simulated DO from the Existing Case and Expanded Reservoir Case at Station A (see **Figure 1** for Station A location). Time series of simulated surface and bottom DO at the same station are presented in **Figure 10**. As shown, the simulated DO exhibits similar patterns between the Existing Case and Expanded Reservoir Case. At the surface, DO concentrations are relatively high due to the oxygen replenishment from the atmosphere and algal production. At the bottom, DO concentrations steadily decrease during the stratified period because of algae decay and SOD, then rise sharply during the unstratified period as vertical mixing transports surface water with high DO towards the bottom.

Despite the similarities in overall DO profiles, reservoir expansion produces a few changes in DO concentrations in the reservoir as well. First, reservoir expansion significantly increases the volume of water under anoxic condition. **Table 2** lists volumes of water under an anoxic condition on several selected days during the two-year simulation period for both the Existing Case and the Expanded Reservoir Case. It shows that the volume of water under an anoxic condition in the Expanded Reservoir Case is at least twice and sometimes five times, as large as for the Existing Case. Secondly, during the unstratified period, DO concentrations in the Expanded Reservoir Case are predicted to be lower than those in the Existing Case. This is a result of the increased reservoir depth and the somewhat slower destratification rate for the Expanded Reservoir Case. This is one of the factors that lead to the predicted early onset of hypolimnetic anoxia for the Expanded Reservoir Case. For example, the hypolimnetic anoxia period starts on 6/21 in 2006 for the Expanded Reservoir Case compared to 7/10 for the Existing Case. Finally, the reservoir expansion delays destratification and prolongs the duration of hypolimnetic anoxia in the reservoir. In the Existing Case in 2006, the hypolimnetic

anoxia period is predicted to end on 12/14. In the Expanded Reservoir Case, the hypolimnetic anoxia period is predicted to end on 12/23, a delay of 9 days. Overall, the hypolimnetic anoxia period from the Existing Case consists of 52% of the time per year on average, which is equivalent to 189 days per year (**Table 1**). With the reservoir expansion, the reservoir experiences hypolimnetic anoxia for 59% of the time or for 216 days per year on average. Thus, given the same operating conditions the reservoir expansion is predicted to extend the hypolimnetic anoxia period by an average of 27 days per year.

Table 2. Predicted Volume of Water under Anoxic Conditions in the Existing Case and Expanded Reservoir Case

Date	Existing Case (acre-ft)	Expanded Reservoir Case (acre-ft)
8/1/06	15,900	48,000
10/1/06	17,600	64,600
12/1/06	15,900	82,300
8/1/07	25,000	57,600
10/1/07	32,500	66,500
12/1/07	24,000	82,300

Note: The volume of water under an anoxic condition is defined as the layer with DO less than 0.5 mg/L

Predicted time series of ammonia (as N), nitrate (as N), TN, SRP and TP at the surface and bottom of the reservoir are presented in **Figures 11 - 15**. Note that TN (TP) is defined as the sum of all particulate and soluble forms of nitrogen (phosphorus). Except for nitrate, all nutrients behave in a similar fashion. At the surface, nutrient concentrations (nitrogen and phosphorus) are generally low during the spring and summer due to algal consumption, and are generally high during the unstratified period when surface water is mixed with the nutrient-rich hypolimnion. At the bottom, nutrient concentrations (except for nitrate) generally show an opposite trend from surface nutrient concentrations: they rise during the stratified period as a result of sediment nutrient release and fall sharply during the unstratified period after being mixed with the surface water in which nutrients are depleted by algae. For nitrate, variation patterns are different from those displayed by other nutrient components. Nitrate levels are low in the summer and high in the winter at both the surface and the bottom (**Figure 12**). In the summer, algal growth consumes most of surface nitrate and the hypolimnetic anoxic condition leads to the loss of the bottom nitrate through denitrification or conversion to ammonia. In the winter, large influxes of nitrate from surface runoff and aqueduct inflow are mostly responsible for the rise in nitrate concentration at the surface and bottom within the reservoir.

Figure 16 shows predicted time series of surface chlorophyll *a* concentrations and **Figure 17** shows time series of Secchi depths derived from simulated chlorophyll *a*. Both figures indicate that the reservoir expansion will lower surface chlorophyll *a* levels and increases Secchi depth in the reservoir. **Table 1** lists predicted annual averages of surface chlorophyll *a* concentration and Secchi depth. With the expansion, the annual average surface chlorophyll *a* concentration is predicted to decrease from 5.8 µg/L to 3.4 µg/L, a 41% reduction in annual algal growth. This leads to a 47% increase in the annual average Secchi depth after expansion; the annual average Secchi depth increases from 3.2 m for the Existing Case to 4.7 m for the Expanded Reservoir Case.

A comparison of simulated pH between the Existing Case and Expanded Reservoir Case is presented in **Figure 18.** As shown, the pH is fairly similar for both simulations.

2.2 NUTRIENT LOADINGS

Phosphorus and nitrogen loadings have been computed for all inflows to SVR, as well as estimated for sediment release for both the Existing Case and Expanded Reservoir Case (**Tables 3** and **4**). The external nutrient loadings (*i.e.*, loadings from inflows) are calculated as the product of water inflow rate and the associated nutrient concentrations. The model does not directly output the total nutrient loadings from the sediments (*i.e.*, internal loadings). However, an order-of-magnitude estimate was computed for the sediment nutrient loading by multiplying the hypolimnetic volume of the reservoir by the rise in nutrient concentration at the reservoir bottom. Nutrient fluxes by atmospheric deposition are considered to be negligible.

As shown in **Tables 3** and **4**, estimated sediment nutrient loadings constitute a significant portion of the total nutrient loadings to the reservoir. In fact, the reservoir is calculated to receive more nutrients from the sediments than those from all inflows combined over the two-year modeling period. For example, in the Expanded Reservoir Case, the sediments release calculations shows about 26.6 tons TP over the two-year period and the total TP loading from all inflows is calculated to be 9.2 tons over the same period. In the Existing Case, the calculated sediment TP loading and the sum of all inflow TP loadings are 11.7 and 9.2 tons, respectively, over the two-year period.

In general, the limiting factor for algal growth is considered to be nitrogen if N:P < 10 and phosphorus if N:P > 10 (Horne and Goldman, 1994). From **Tables 3** and **4**, the ratios of TN:TP total loadings for the Existing Reservoir and Expanded Reservoir range from 3-6, indicating algal growth is likely limited by nitrogen in the reservoir. Note, however, that the inflow water quality is very variable and depends on both the water source and seasonality so the nutrient limitation at any specific instant may vary.

Tables 3 and **4** also show that the estimated total amount of nutrients released by sediments are generally larger in the Expanded Reservoir Case than in the Existing Case, partly a result of the larger hypolimnetic bottom area and extended hypolimnetic anoxia period for the Expanded Reservoir Case. The sediments are estimated to release a total of 26.6 tons TP over the two-year period in the Expanded Reservoir Case, more than twice of that in the Existing Case (*i.e.*, 11.7 tons TP). For TN, the estimated sediment release in the anoxic period is 80.6 tons for the Expanded Reservoir Case, almost three times the amount for the Existing Case (*i.e.*, 27.6 tons).

In conclusion, the reservoir expansion is predicted to slightly extend the duration of the hypolimnetic anoxia and enlarge the volume of water under anoxic condition. The reservoir expansion also produces lower surface chlorophyll *a* concentrations and higher Secchi depth *(i.e.*, more water clarity). Based on a nutrient loading calculation, the internal nutrient loadings *(i.e.*, sediment release) are larger than all external loadings combined over the two-year modeling period for both the Existing Case and Expanded Reservoir Case. Meanwhile, the reservoir expansion leads to an increase in sediment nutrient release due to the larger hypolimnetic bottom area and extended hypolimnetic anoxia period. However, despite the significantly higher sediment release, surface TN concentrations are actually lower after the reservoir expansion (**Figure 13**), a result of the significantly larger volume of water for the Expanded Reservoir Case. The resulting lower nutrient concentrations are believed to be one of the main factors that lead to lower surface chlorophyll a concentrations for the Expanded Reservoir Case (compared to the Existing Reservoir Case).

Table 3. Estimated Annual Phosphorus Loadings[1] for the Existing and Expanded Reservoir

Sources	SRP				TP			
	Existing Case		Expanded Reservoir Case		Existing Case		Expanded Reservoir Case	
	2006	2007	2006	2007	2006	2007	2006	2007
Purified Water	0	0	0	0	0	0	0	0
Runoff	0.1	0.8	0.1	0.8	2.9	3.3	2.9	3.3
Aqueduct Inflow	0.7	0.5	0.7	0.5	1.7	1.3	1.7	1.3
Sediment Release	9.0	2.6	19.5	7.0	9.0	2.7	19.5	7.1
Total Loadings	9.8	3.9	20.3	8.3	13.6	7.3	24.1	11.7

Note: 1. All units for loadings are in tons/year (*i.e.*, 2000 lbs/year)

Table 4. Estimated Annual Nitrogen Loadings[1] for the Existing and Expanded Reservoir

Sources	(NO_3 +NH_4) as N				TN			
	Existing Case		Expanded Reservoir Case		Existing Case		Expanded Reservoir Case	
	2006	2007	2006	2007	2006	2007	2006	2007
Purified Water	0	0	0	0	0	0	0	0
Runoff	3.4	5.4	3.4	5.4	4.8	7.6	4.8	7.6
Aqueduct Inflow	14.6	15.5	14.6	15.5	22.4	21.1	22.4	21.1
Sediment Release	13.2	14.3	61.8	17.7	13.3	14.3	61.9	18.7
Total Loadings	31.2	35.2	79.8	38.6	40.5	43.0	89.1	46.4

Note: 1. All units for loadings are in tons/year (*i.e.*, 2000 lbs/year)

3. MODELING RESULTS FOR FUTURE CONDITIONS

3.1 MODELING SCENARIOS

Two scenarios have been modeled to evaluate the water quality in the expanded reservoir under future operating conditions. The first scenario considered the expected typical future conditions with purified water at median expected storage and normal expected operations, and is referred to herein as the Base Case. The second scenario addresses the expanded reservoir under future operating conditions but with no added purified water, referred to herein as No Purified Water. This latter case is identical to the Base Case except no purified water is introduced into the reservoir (with a compensating equal reduction in outflow).

The comparison of these two future scenarios enables a quantification of the effects of purified water addition on the expanded reservoir behavior under future operating conditions. The parameters for these two modeling scenarios were determined in collaboration between the City, its consultants, and Flow Science, and are based on information provided by the San Diego County Water Authority (SDCWA) about the expected future operational schemes for SVR. The Base Case utilized the Design Purified Water Inlet Location (see **Figure 1** for the location) as the point of release for purified water inflow into SVR. The two scenarios considered Port #2 at the reservoir outlet tower structure to be the open port for all water withdrawals from the reservoir. It should be noted that hydrodynamic results of the modeling for these two scenarios are included in the TM #2 (FSI, 2011) and are not included here. Only the results of the water quality analyses are presented in this report, focusing on DO, nutrients, chlorophyll *a* and Secchi depth. In the following, details of each of these two modeling scenarios are discussed.

3.1.1 Base Case

The Base Case simulated a two-year period of reservoir operations and used the same 2006 - 2007 meteorological data, aqueduct inflow water quality data, runoff water quality data, and other modeling parameters as used in the Existing Case, except for the initial reservoir volume, introduction of purified water, and modified inflow and outflow rates as discussed below. Note also that the measured wind data used as inputs for the model included several Santa Ana Wind events that occurred in the winter of each simulated year.

The City provided the initial reservoir volume and inflow and outflow rates for the Base Case. The initial reservoir volume for the Base Case is considered to be near the median of the expected future conditions with a volume of 155,000 acre-feet (determined

in conjunction with SDCWA). It is considered that the daily inflows and outflows will be constant throughout each month and it was also assumed that there would be no water transfers from Sutherland Reservoir into SVR in the modeling period. For the Base Case, a new surface inflow, the purified water inflow, was added to represent incoming purified water from the advanced water purification facility at an annual rate of 15,000 a-f/y. The detailed monthly inflow and outflow volumes for each source for the Base Case are listed in **Table 5**. The available withdrawal elevations on the proposed reservoir outlet are listed in **Table 6** and Port #2 was used for all water withdrawals from the reservoir. The multi-year averages of weekly water temperatures at North City Water Reclamation Plant were used to characterize the purified water temperature and the salinity of the purified water was considered to be constant at 100 parts per million (ppm).

The water quality for the purified water inflow was determined by analyzing water quality field data measured in the effluent from the advanced water purification facility (these data are available separately). After consulting with the City and analyzing the effluent data, FSI provided the final values for water quality of purified water used in the simulations. These are listed in **Table 7** as well as the nutrient concentrations for other inflows. Note that particulate and organic nutrients are considered to be negligible in the purified water. Thus, the concentration of TN in the purified water is 0.78 mg/L, the sum of ammonia, nitrate and nitrite in the purified water; the concentration of TP in the purified water is 0.004 mg/L and equal to the concentration of SRP.

3.1.2 No Purified Water Scenario

The data inputs for the No Purified Water scenario are similar to those for the Base Case scenario, except for no purified water additions and an equal reduction in reservoir outflow volume (to obtain similar reservoir storage volumes). The purpose of conducting this simulation was, by comparison with the Base Case, to evaluate the water quality effects of the purified water addition on the expanded SVR. **Table 8** presents the monthly water volumes of inflows and outflow for the No Purified Water scenario.

Table 5. Monthly Reservoir Inflow and Outflow Volumes for Base Case Operating Scenario

Month	Aqueduct Inflow (acre-feet)	Runoff Inflow (acre-feet)	Purified Water Inflow (acre-feet)	Withdrawal (acre-feet)
Jan-Year 1	0	0	1440	0
Feb-Year 1	0	1,500	1590	0
Mar-Year 1	0	1,500	1480	0
Apr-Year 1	1,000	1,500	1350	0
May-Year 1	1,000	0	1230	0
Jun-Year 1	1,000	0	1090	0
Jul-Year 1	0	0	900	2200
Aug-Year 1	0	0	1020	4200
Sep-Year 1	0	0	1090	4200
Oct-Year 1	0	0	1120	4200
Nov-Year 1	0	0	1210	4200
Dec-Year 1	0	0	1480	0
Jan-Year 2	0	0	1440	0
Feb-Year 2	0	1,500	1590	0
Mar-Year 2	0	1,500	1480	0
Apr-Year 2	1,000	1,500	1350	0
May-Year 2	1,000	0	1230	0
Jun-Year 2	1,000	0	1090	0
Jul-Year 2	0	0	900	2200
Aug-Year 2	0	0	1020	4200
Sep-Year 2	0	0	1090	4200
Oct-Year 2	0	0	1120	4200
Nov-Year 2	0	0	1210	4200
Dec-Year 2	0	0	1480	0

Table 6. Available Withdrawal Elevations on Proposed Reservoir Outlet Tower

Port	Withdrawal Elevation
6	733 ft
5	708 ft
4	683 ft
3	653 ft
2	623 ft
1	593 ft

Table 7. Inflow Water Quality Parameters

Water Quality Parameter	Purified Water	Aqueduct Inflow	Runoff
$(NO_3 + NO_2) - N$ (mg/L)	0.64	0.12 – 0.47	0.02 – 3.00
$NH_4 - N$ (mg/L)	0.14	0.02 – 0.09	0.02 – 0.15
TN (mg/L)	0.78	0.17 – 0.68	0.18 – 4.22
SRP (mg/L)	0.004	0.009 – 0.031	0.007 – 0.16
TP (mg/L)	0.004	0.024 – 0.081	0.022 – 0.32

Table 8. Monthly Reservoir Inflow and Outflow Volumes for No Purified Water Scenario

Month	Aqueduct Inflow (acre-feet)	Runoff Inflow (acre-feet)	Purified Water Inflow (acre-feet)	Withdrawal (acre-feet)
Jan-Year 1	0	0	0	0
Feb-Year 1	0	1500	0	0
Mar-Year 1	0	1500	0	0
Apr-Year 1	1000	1500	0	0
May-Year 1	1000	0	0	0
Jun-Year 1	1000	0	0	0
Jul-Year 1	0	0	0	800
Aug-Year 1	0	0	0	800
Sep-Year 1	0	0	0	800
Oct-Year 1	0	0	0	800
Nov-Year 1	0	0	0	800
Dec-Year 1	0	0	0	0
Jan-Year 2	0	0	0	0
Feb-Year 2	0	1500	0	0
Mar-Year 2	0	1500	0	0
Apr-Year 2	1000	1500	0	0
May-Year 2	1000	0	0	0
Jun-Year 2	1000	0	0	0
Jul-Year 2	0	0	0	800
Aug-Year 2	0	0	0	800
Sep-Year 2	0	0	0	800
Oct-Year 2	0	0	0	800
Nov-Year 2	0	0	0	800
Dec-Year 2	0	0	0	0

3.2 COMPARISON OF MODELING RESULTS

In this section, results from the Base Case are compared with those from the Existing Case and No Purified Water scenarios. **Figure 19** provides a comparison of inflow rates among the Existing Case, No Purified Water and Base Case. **Figure 20** shows a comparison of reservoir water volume during the two-year modeling period for these

three scenarios. The main differences in flow rate and water volume among the scenarios are summarized in **Table 9**.

Table 9. Modeled Operating Scenarios

Operating Scenarios	Description	Initial Reservoir Volume (acre-feet)	Annual Purified Water Inflow (acre-feet/year)	Annual Aqueduct inflow (acre-feet/year)	Annual Reservoir Outflow (acre-feet/year)
Existing Case[1] (06/07)	existing conditions during 2006 - 2007	64,000 /60,000	0	27,018 /30,810	28,417 /22,185
No Purified Water[2]	no purified water additions and an equal reduction in reservoir outflow	155,000	0	3,000	4,000
Base Case[2]	median expected storage and normal expected operations	155,000	15,000	3,000	19,000

Notes: 1. The total volume of runoff and water transfers from Sutherland is 1,556 acre-feet for 2006 and 5,902 acre-feet for 2007.
2. Runoff flow rate is 4,500 acre-feet/year and there are no water transfers from Sutherland Reservoir into SVR.

Figure 21 shows a comparison of simulated water temperature among the Existing Case, No Purified Water scenario, and Base Case at Station A. Note that the vertical axis in all figures hereafter is defined as elevation (and not depth) to allow labeling of the reservoir outlet port elevations. The temperature patterns are fairly similar among all three scenarios with similar thermocline development patterns. However, since the reservoir is significantly shallower in the Existing Case, the destratification in the winter appears to occur earlier in that case than in the other two scenarios. A comparison between the Base Case and the No Purified Water scenario shows that the thermocline is slightly deeper for the Base Case (*e.g.*, little less than 3 ft deeper in September), a result of adding purified water in the epilimnion.

A comparison of simulated surface and bottom DO among the Existing Case, No Purified Water, and Base Case is shown in **Figure 22**. **Table 10** lists the hypolimnetic anoxia period of these three scenarios. The hypolimnetic anoxia period is predicted to last an average of 189 days per year (or 52% of the time in a year) for the Existing Case. For the future No Purified Water scenario, the hypolimnetic anoxia period increases to 207 days per year, an addition of 18 days per year. Adding purified water into the reservoir under future operating conditions (*i.e.*, Base Case) further extends the average duration of the hypolimnetic anoxia period by 8 days, to a total of 215 days per year.

Table 10. Summary of Simulated DO, Chlorophyll *a* and Secchi Depth for Modeling Scenarios

Operating Scenarios	Year	Initial Reservoir Volume (acre-feet)	Bottom Anoxia Period	Days Under Anoxia: Total Days (Percentage)[2]	Average Surface Chlorophyll *a* (µg/L)	Average Secchi Depth (m)
Existing Case	2006	64,000	1/1 – 1/15 7/10 – 12/14	189 (52%)	5.8	3.2
	2007	60,000	6/8 – 12/28			
No Purified Water	2006	155,000	1/1 – 1/21 6/25 – 12/23	207 (57%)	3.1	4.8
	2007	155,000	6/5 – 12/31			
Base Case	2006	155,000	1/1 – 1/24 6/23 – 12/31	215 (59%)	3.7	4.3
	2007	155,000	1/1, 6/3 – 12/31			

Notes: 1. Anoxia is defined here as the bottom DO less than 0.5 mg/L.
2. Both the total days and percentage under anoxia are yearly values averaged over the two-year simulation period.

Figures 23 - 27 show comparisons for nitrate, ammonia, TN, SRP and TP among the Existing Case, Base Case and No Purified Water scenarios. In general, the Base Case and No Purified Water scenarios show similarities in variation trends and both are somewhat different from the Existing Case in overall patterns (mostly a result of different inflow/outflow sources and temporal patterns). The Base Case generally shows slightly higher nitrogen concentrations (**Figures 23 - 25**) and slightly lower phosphorus concentrations (**Figures 26** and **27**) than the No Purified Water scenario. This is a result of year-round inflow of purified water with relatively high nitrogen levels and low phosphorus levels.

Comparisons of simulated surface chlorophyll *a* concentrations and derived Secchi depths among the Existing Case, Base Case and No Purified Water are shown in **Figures 28** and **29** respectively. As shown, variation patterns for the Base Case and No Purified Water (*i.e.*, two future operating scenarios) resemble each other and the Base Case shows slightly higher chlorophyll *a* levels and slightly lower Secchi depths. In contrast, the Existing Case features significantly higher algal levels and lower Secchi depths than the Base Case or No Purified Water scenarios. In addition, the temporal variations in chlorophyll *a* concentration and Secchi depth for the Existing Case are different from the future operating scenarios, likely because of significant differences in the timing and magnitude of nutrient loadings between these scenarios.

Annual average surface chlorophyll *a* concentration and Secchi depth are listed in **Table 10** for all three scenarios. The annual chlorophyll *a* concentration and Secchi depth are predicted to be 5.8 µg/L and 3.2 m respectively for the Existing Case. In comparison, the annual average chlorophyll *a* concentration and Secchi depth are 3.1 µg/L and 4.8 m respectively for the No Purified Water scenario. This is a reduction of 2.7 µg/L for the average chlorophyll *a* concentration and an increase of 1.6 m for the average Secchi depth when the operating conditions change from the Existing Case to the No Purified Water scenario in the expanded reservoir. Meanwhile, the Base Case is predicted to produce 3.7 µg/L for the annual average chlorophyll *a* concentration and 4.3 m for the annual average Secchi depth. This is a reduction of 2.1 µg/L for the annual average chlorophyll *a* concentration and an increase of 1.1 m for the annual average Secchi depth compared to the Existing Case. This indicates that both the No Purified Water scenario and Base Case are predicted to produce lower algal levels *(i.e.*, lower surface chlorophyll *a* concentrations) and higher water clarity (*i.e.*, high Secchi depths) compared to the Existing Case.

A comparison of simulated pH among the Existing Case, Base Case and No Purified Water scenarios is presented in **Figure 30.** As shown, the pH is fairly similar for all three runs.

3.3 NUTRIENT LOADINGS

Tables 11 – 14 present, respectively, the nutrient loadings for SRP, TP, the sum of nitrate and ammonia, and TN, for the Existing Case, Base Case and No Purified Water scenarios.

For phosphorus (**Tables 11** and **12**), the loadings from the sediments are generally larger than other loadings and consist of 30 - 90% of all phosphorus loadings into SVR. Both the Base Case and No Purified Water scenarios produce sediment nutrient loadings that are twice as large as those from the Existing Case, likely a result of the larger hypolimnetic bottom area and extended hypolimnetic anoxia period. There is little difference in the sediment releases between the Base Case and No Purified Water scenarios.

For nitrogen (**Tables 13** and **14),** the loadings from the sediments are significant as well and consist of about 30 – 80% of all nitrogen loadings into SVR. Sediment nutrient loadings are generally higher for the future scenarios (*i.e.*, Base Case and No Purified Water scenarios) than the Existing Case.

However, despite the significantly higher sediment release for the future operating scenarios, surface TN concentrations are actually lower for the future scenarios compared to the Existing Reservoir Case (**Figure 25**), a result of the larger volume of water in the

expanded reservoir. The resulting lower nutrient concentrations are believed to be one of the main factors that lead to lower surface chlorophyll a concentrations for the future operating scenarios (compared to the Existing Reservoir Case).

It is noted that the N:P ratio (*i.e.*, calculated as the ratio of the TN loading to TP loading in this case) in the purified water, the major inflow to SVR in the Base Case, is about 159. As shown, this overall ratio for the reservoir can be affected by many factors including the nutrient loadings from inflows as well as sediments. However, given the extremely high N:P ratio of the purified water inflow, algal growth in the future reservoir may tend to become more phosphorus-limited.

Table 11. Annual SRP Loadings[1]

Sources	Existing Case		No Purified Water		Base Case	
	2006	2007	2006	2007	2006	2007
Purified Water	0	0	0	0	0.1	0.1
Runoff	0.1	0.8	0.5	0.5	0.5	0.5
Aqueduct Inflow	0.7	0.5	0.1	0.1	0.1	0.1
Sediment Release[2]	9.0	2.6	19.4	7.0	19.4	7.0
Total Loadings	9.8	3.9	20.0	7.6	20.1	7.7

Note: 1. All units for the loadings are in tons/year *(i.e.*, 2000 lbs/year)

Table 12. Annual TP Loadings[1]

Sources	Existing Case		No Purified Water		Base Case	
	2006	2007	2006	2007	2006	2007
Purified Water	0	0	0	0	0.1	0.1
Runoff	2.9	3.3	0.9	0.9	0.9	0.9
Aqueduct Inflow	1.7	1.3	0.2	0.1	0.2	0.1
Sediment Release[2]	9.0	2.7	19.4	7.0	19.4	7.0
Total Loadings	13.6	7.3	20.5	8.0	20.6	8.1

Note: 1. All units for the loadings are in tons/year *(i.e.*, 2000 lbs/year)

Table 13. Annual (NO_3+NH_4)-N Loadings[1]

Sources	Existing Case		No Purified Water		Base Case	
	2006	2007	2006	2007	2006	2007
Purified Water	0	0	0	0	15.9	15.9
Runoff	3.4	5.4	9.9	6.4	9.9	6.4
Aqueduct Inflow	14.6	15.5	1.1	1.7	1.1	1.7
Sediment Release[2]	13.2	14.3	60.1	14.2	68.9	23.0
Total Loadings	31.2	35.2	71.1	22.3	95.8	47.0

Note: 1. All units for the loadings are in tons/year *(i.e.,* 2000 lbs/year)

Table 14. Annual TN Loadings[1]

Sources	Existing Case		No Purified Water		Base Case	
	2006	2007	2006	2007	2006	2007
Purified Water	0	0	0	0	15.9	15.9
Runoff	4.8	7.6	14.0	9.1	14.0	9.1
Aqueduct Inflow	22.4	21.1	1.3	2.1	1.3	2.1
Sediment Release[2]	13.3	14.3	60.1	14.2	68.9	23.0
Total Loadings	40.5	43.0	75.4	25.4	100.1	50.1

Note: 1. All units for the loadings are in tons/year *(i.e.,* 2000 lbs/year)

4. CONCLUSIONS AND DISCUSSION

The objectives of this study were to use the calibrated and validated SVR ELCOM/CAEDYM water quality model to evaluate the effects of purified water on water quality in the expanded SVR. To achieve these goals, a two-step approach was taken to examine the effects caused by the reservoir expansion and augmentation with purified water, respectively. This work focused on water quality results for nutrients DO, and algal growth.

RESERVOIR EXPANSION

First, the model was used to determine the effects of the reservoir expansion on water quality, without the introduction of any purified water. This was accomplished by performing a simulation that uses the same reservoir conditions (climate, inflow and outflow volumes and concentrations etc.) as the 2006 - 2007 calibration simulation (Existing Case), except for using a higher initial reservoir volume that is set at 155,000 acre-feet (median expected future storage). The results from this simulation (Expanded Reservoir Case) were compared against those obtained from the Existing Case simulation. The differences between the results of these two simulations demonstrate the effects of the expansion on the reservoir's water quality.

Based on the results of these two simulations, the following conclusions and observations on the effects of the reservoir expansion can be made:

- The reservoir expansion is predicted to extend the duration of the hypolimnetic anoxia by an average of 27 days per year (from 189 days per year to 216 days per year) and enlarge the volume of water under anoxic condition by at least two fold.

- The reservoir expansion will produce lower surface chlorophyll *a* concentrations and higher Secchi depths *(i.e.*, better water clarity) in the reservoir. It is predicted that the annual average chlorophyll *a* concentration will decrease from 5.8 µg/L to 3.4 µg/L and the annual average Secchi depth will increase from 3.2 m to 4.7 m after the expansion.

- Based on a nutrient loading calculation, the internal nutrient loadings *(i.e.*, nutrients released from sediment) are larger than all external loadings combined over the two-year modeling period for both the Existing Case and Expanded Reservoir Case. Meanwhile, the reservoir expansion is predicted to lead to a significant increase in sediment nutrient release, likely due to the larger hypolimnetic bottom area and extended hypolimnetic anoxia period. However, despite the significantly higher sediment release, surface TN concentrations are actually lower after the reservoir expansion, a result of the significantly larger

volume of water for the Expanded Reservoir Case. The resulting lower nutrient concentrations are believed to be one of the main factors that lead to lower surface chlorophyll *a* concentrations for the Expanded Reservoir Case (compared to the Existing Reservoir Case).

FUTURE OPERATING CONDITIONS

After the effects of the reservoir expansion were determined, the model was used to examine the water quality in the expanded reservoir under future operating conditions both with and without purified water augmentation. Specifically, the following two future scenarios were simulated:

- Base Case (includes purified water inflow) ---- This scenario considered an expanded reservoir under median expected storage and expected future operations. The initial reservoir volume for the Base Case is set at 155,000 acre-feet. The following annual inflow rates were assumed: for aqueduct inflow 3,000 a-f/y; runoff 4,500 a-f/y; purified water inflow 15,000 a-f/y; and dam withdrawal 19,000 a-f/y, with no water transfers from Sutherland Reservoir into SVR.

- No Purified Water ---- The inputs for this scenario are similar to those for the Base Case scenario, except for no purified water additions and an equal reduction in reservoir outflow. The initial reservoir volume for this scenario is set at 155,000 acre-feet. The annual rates for aqueduct inflow, runoff, purified water inflow and dam withdrawal are 3,000, 4,500, 0 and 4,000 a-f/y respectively. There are no water transfers from Sutherland Reservoir into SVR.

Results from the Base Case and No Purified Water scenarios were compared against those obtained from the Existing Case simulations (*i.e.*, no reservoir expansion). The purpose is to quantify the water quality effects of purified water by comparing the Base Case against the No Purified Water scenario, and to evaluate the effects of future operating conditions in the expanded reservoir (prior to adding purified water) by comparing the No Purified Water scenario against the Existing Case.

Based on the simulation results, the following conclusions and observations on the effects of the purified water and future operating conditions are made:

- The hypolimnetic anoxia period is predicted to last an average of 189 days per year for the Existing Case. For the No Purified Water scenario, the hypolimnetic anoxia period is predicted to increase to 207 days per year, an addition of 18 days per year. Adding purified water into the reservoir under

future operating conditions (*i.e.*, Base Case) will further extend the average duration of the hypolimnetic anoxia period by 8 days, to a total of 215 days per year.

- The No Purified Water scenario produces lower algae levels *(i.e.*, lower surface chlorophyll *a* concentrations) and higher Secchi depths (*i.e.*, better water clarity) compared to the Existing Case. For example, the annual average chlorophyll *a* concentration and Secchi depth are predicted to be 5.8 µg/L and 3.2 m respectively for the Existing Case. By comparison, the annual average chlorophyll *a* concentration and Secchi depth are predicted to be 3.1 µg/L and 4.8 m, respectively, for the No Purified Water scenario in the expanded reservoir. This is a reduction of 2.7 µg/L for the average chlorophyll *a* concentration and an increase of 1.6 m for the average Secchi depth compared to the Existing Case.

- The Base Case scenario also produces lower algae levels *(i.e.*, lower surface chlorophyll *a* concentrations) and higher Secchi depths (*i.e.*, better water clarity) compared to the Existing Case. The Base Case is predicted to produce 3.7 µg/L for the annual average chlorophyll *a* concentration and 4.3 m for the annual average Secchi depth. This is a reduction of 2.1 µg/L for the average chlorophyll *a* concentration and an increase of 1.1 m for the average Secchi depth compared to the Existing Case.

- Nutrient loading calculations show that nutrient sediment release constitutes a significant portion of all nutrient loadings into SVR for all future scenarios as well as the Existing Case. The future operating scenarios (*i.e.*, Base Case and No Purified Water) produce sediment nutrient loadings significantly larger than those for the Existing Case, likely a result of the larger hypolimnetic bottom area and extended hypolimnetic anoxia period. However, despite the significantly higher sediment release for the future operating scenarios, surface TN concentrations are actually lower for the future scenarios compared to the Existing Reservoir Case, a result of the larger volume of water in the expanded reservoir. The resulting lower nutrient concentrations are believed to be one of the main factors that lead to lower surface chlorophyll *a* concentrations for the future operating scenarios (compared to the Existing Reservoir Case).

- Nutrient limitation in SVR can be affected by various factors including the nutrient loadings from all the inflows and the sediments. As a result, nutrient limitation at any point may vary based on existing conditions. However, note that the N:P ratio of the purified water is expected to reach about 159,

indicating that algal growth in the future reservoir may tend to become more phosphorus-limited.

5. REFERENCES

City of San Diego (2008). "IPR Description for BOR Grant 122208 MS," obtained from Jeffery Pasek of the City of San Diego through e-mail on December 23, 2008.

Flow Science Incorporated (2010). "Reservoir Augmentation Demonstration Project: Limnology and Reservoir Detention Study of San Vicente Reservoir – Calibration of the Water Quality Model", FSI Project No. V094005, Pasadena, CA.

Flow Science Incorporated (2011). "Water Purification Demonstration Project: Limnology and Reservoir Detention Study of San Vicente Reservoir – Hydrodynamic Modeling Study", FSI Project No. V094005, Pasadena, CA.

Horne, A.J. and C.R. Goldman (1994). "Limnology (Second Edition)", Published by McGraw-Hill, Inc. ISBN 0-07-023673-9.

National Water Research Institute (2010). "Findings and Recommendations of the Limnology and Reservoir Subcommittee Meeting for the Reservoir Augmentation Demonstration Project's 'Limnology and Reservoir Detention Study of the San Vicente Reservoir' " Memorandum from NWRI Independent Advisory Panel for the City of San Diego's Indirect Potable Reuse/Reservoir Augmentation Demonstration Project, June 7, 2010.

National Water Research Institute (2012). "Findings and Recommendations of the Limnology and Reservoir Subcommittee Meeting for the Reservoir Augmentation Demonstration Project's 'Limnology and Reservoir Detention Study of the San Vicente Reservoir' " Memorandum from NWRI Independent Advisory Panel for the City of San Diego's Indirect Potable Reuse/Reservoir Augmentation Demonstration Project, January 5, 2012.

6. GLOSSARY

Advanced Water Purification Facility: The demonstration facility located at the North City Water Reclamation Plant. The facility is considered "advanced" because of the high level of treatment utilizing reverse osmosis and advanced oxidation.

Blending: Mixing or combining one water source with another such as purified water with raw water sources.

Conductivity: See "Salinity".

Constituent: In water, a constituent is a dissolved chemical element or compound or a suspended material that is carried in the water.

Drought: A defined period of time when rainfall and runoff in a geographic area are much less than average.

Epilimnion: Natural thermal stratification exists for much of the year in almost all temperate lakes and reservoirs and creates three vertical zones. The upper, warmer water is called the epilimnion, the deeper, colder water is called the hypolimnion, whereas the middle portion separating these two layers, where the rate of vertical temperature change is greatest, is called the metalimnion, or thermocline.

Excursion events at the advanced purification facility: Events in which the water quality of the recycled water into the advanced purification facility deviates from the normal or expected conditions. They result in the final outflow from the advanced purification facility may contain chemical constituents at higher level than normal concentrations when no such events occur.

Hypolimnion: See "epilimnion".

Pathogens: Disease-causing organisms. The general groupings of pathogens are viruses, bacteria, protozoa, and fungi.

Periods of mixing: Periods when water temperatures become vertically uniform in the water body and they generally occur in the winter.

Purified water: Recycled water that has been treated to an advanced level beyond tertiary treatment, so that it can be added to water supplies ultimately used for drinking water. The treatment includes membrane filtration with microfiltration or ultrafiltration, reverse osmosis (RO), and advanced oxidation that consists of disinfection with

ultraviolet light (UV) and hydrogen peroxide (H_2O_2). Purified water may be released into a groundwater basin or surface water reservoir that supplies water to a drinking water treatment facility.

Purified water inflow: Purified water that is transported from the advanced purified water treatment facility to SVR.

Purified water inlet: Point of release in SVR for purified water inflow. Note that the purified water is assumed to be released at the surface of SVR.

Recycled water: Water that originated from homes, businesses and drains as municipal wastewater and has undergone a high level of treatment at a reclamation facility so that it can be beneficially reused for a variety of purposes. This is the water that comes into the AWP Facility.

Reservoir: A manmade lake or tank used to collect and store water.

Reservoir augmentation: The process of adding purified water to a surface water reservoir. The purified water undergoes advanced treatment (membrane filtration, reverse osmosis and UV disinfection/advanced oxidation). The purified water is then blended with untreated water in a reservoir. The blended water is then treated and disinfected at a conventional drinking water treatment plant and is distributed into the drinking water delivery system. Also known as "surface water augmentation."

Reservoir outflow: The flow withdrawal through the opening port located at the outlet structure near the dam.

Reservoir outlet: The opening port at the outlet structure near the dam. In this study, the opening port is assumed to be Port #2.

Salinity: The concentration of mineral salts dissolved in water. Salinity may be measured by weight (total dissolved solids or TDS) or by electrical conductivity. Salinity and TDS are both measures of the amount of salt dissolved in water, and the terms are often used interchangeably. Generally, salinity is used when referring to water with a lot of salt (*e.g.*, seawater), whereas TDS is used to refer to water with little salt (*e.g.*, freshwater).

Storage: Water held in a reservoir for later use.

Soluble Reactive Phosphorus (SRP): A measure of orthophosphate, the filterable (soluble, inorganic) fraction of phosphorus, the form directly taken up by plant cells.

Surface water: Water located on the Earth's surface, in a river, stream, lake, pond or surface water reservoir.

Thermocline: See "epilimnion".

Total Nitrogen (TN): A measure of all the forms of nitrogen, dissolved or particulate, that are found in a sample.

Total Phosphorus (TP): A measure of all the forms of phosphorus, dissolved or particulate, that are found in a sample.

Water Purification Demonstration Project (Demonstration Project): The second phase of the City of San Diego's Water Reuse Program. During this test phase the Advanced Water Purification Facility will operate for approximately one year and will produce 1 million gallons of purified water per day. A study of the San Vicente Reservoir is being conducted to test the key functions of reservoir augmentation and to determine the viability of a full-scale project. No purified water will be sent to the reservoir during the demonstration phase.

Water Measurement Terms

Milligrams per liter (mg/L) ***also known as parts per million (ppm):*** A measurement describing the amount of a substance (such as a mineral, chemical or contaminant) in a liter of water; a unit used to measure concentration of water constituents (parts of something per million parts of water). One part per million is equal to one milligram per liter. (This term is becoming obsolete as instruments measure smaller concentrations.) This is equivalent to one drop of water diluted into 50 liters (roughly the fuel tank capacity of a compact car) or about thirty seconds out of a year.

Acre-foot (AF): A unit of water commonly used in the water industry to measure large volumes of water. It equals the volume of water required to cover one acre to a depth of one foot. An acre-foot is 325,851 gallons (43,560 cubic feet) and is considered enough water to meet the needs of two families of four with a house and yard for one year.

Micrograms per liter (µg/L) also known as parts per billion (ppb): A frequently used measurement for water concentration (parts of something per billion parts of water). One part per billion is equivalent to one second of time in 32 years or one drop of water in a swimming pool. One thousand parts per billion is equal to one part per million.

FIGURES

Map of San Vicente Reservoir

Plan View of Existing and Expanded Reservoir and Inflow/Outflow Locations

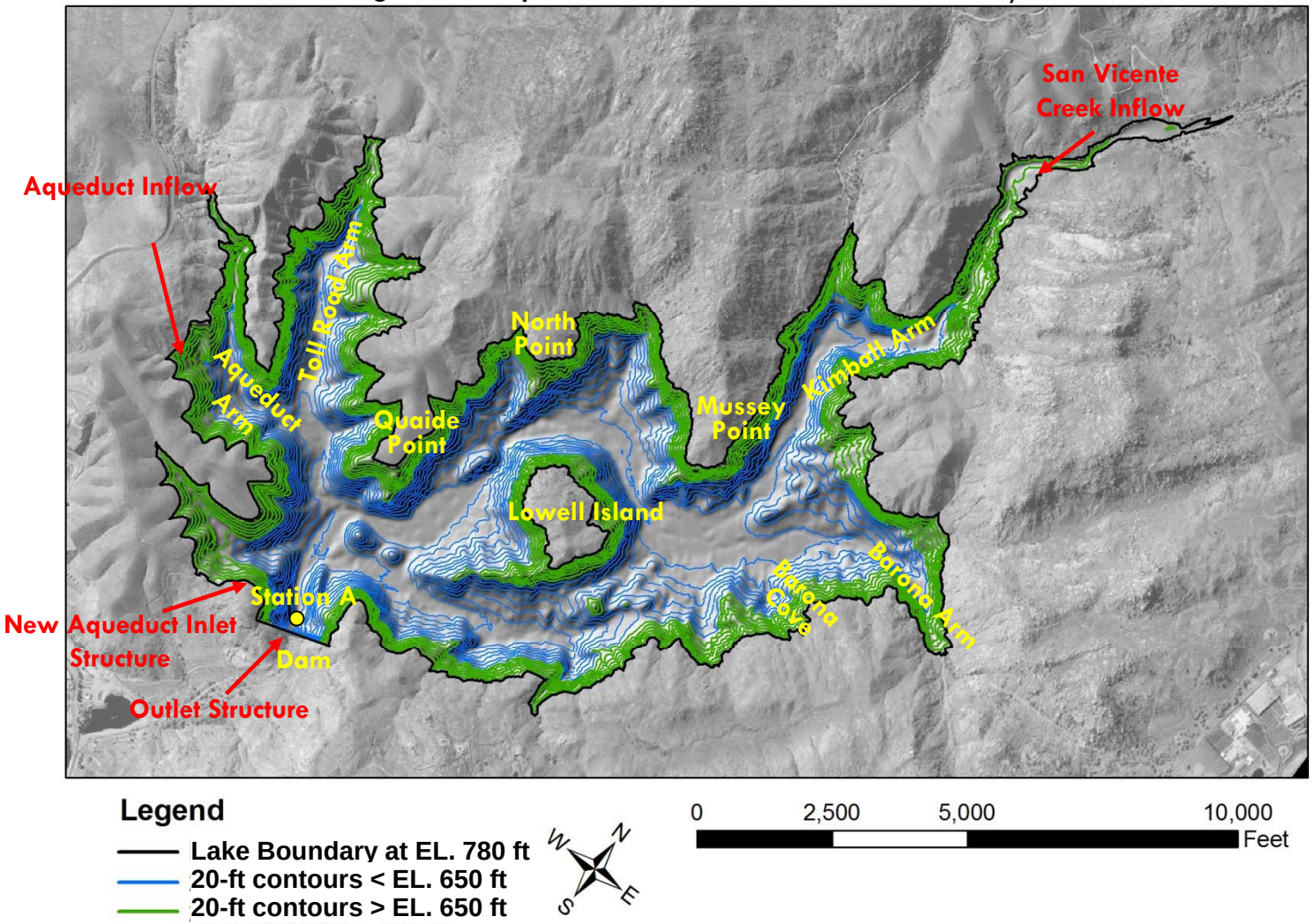

FSI V094005
May 01, 2012

Figure 1

FLOW SCIENCE®

ELCOM-CAEDYM

Schematic of Processes Modeled in ELCOM-CAEDYM

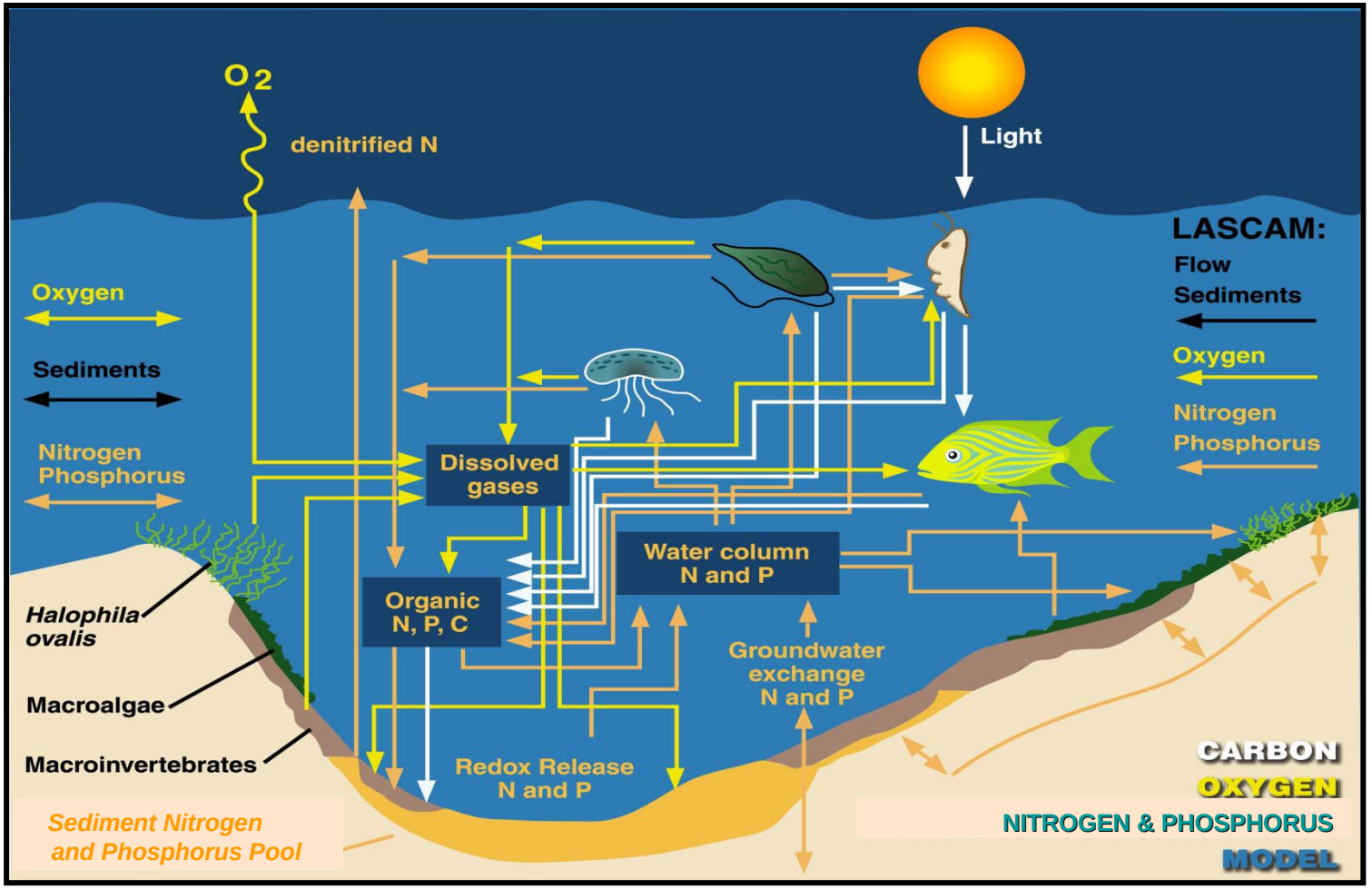

FSI V094005
May 01, 2012

Figure 2

FLOW SCIENCE®

SVR Water Quality Model Grid

(Grid Size = 100 m)

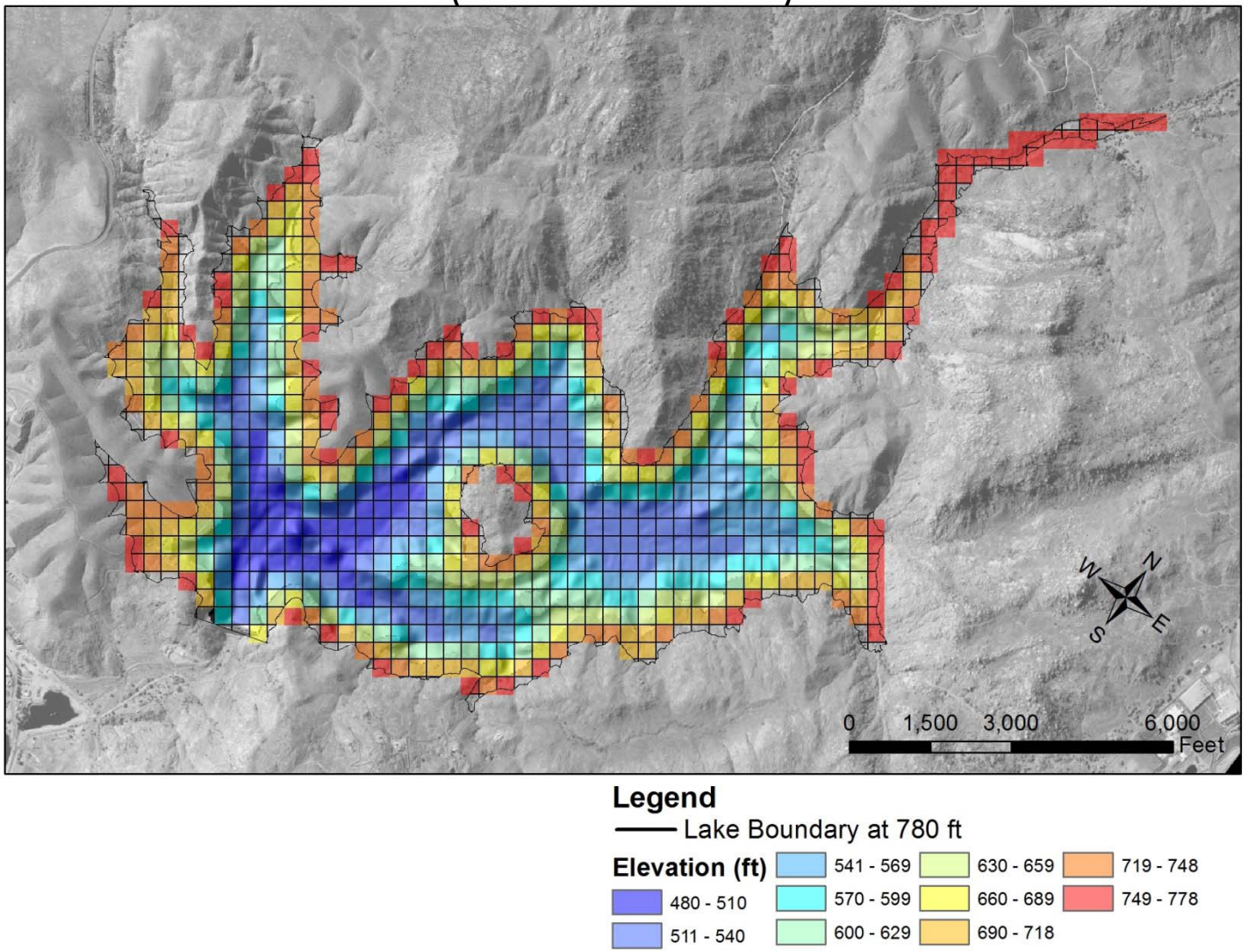

Figure 3

FSI V094005
May 01, 2012

FLOW SCIENCE®

SVR Water Quality Model Calibration Results

Station A – Water Temperature Comparison

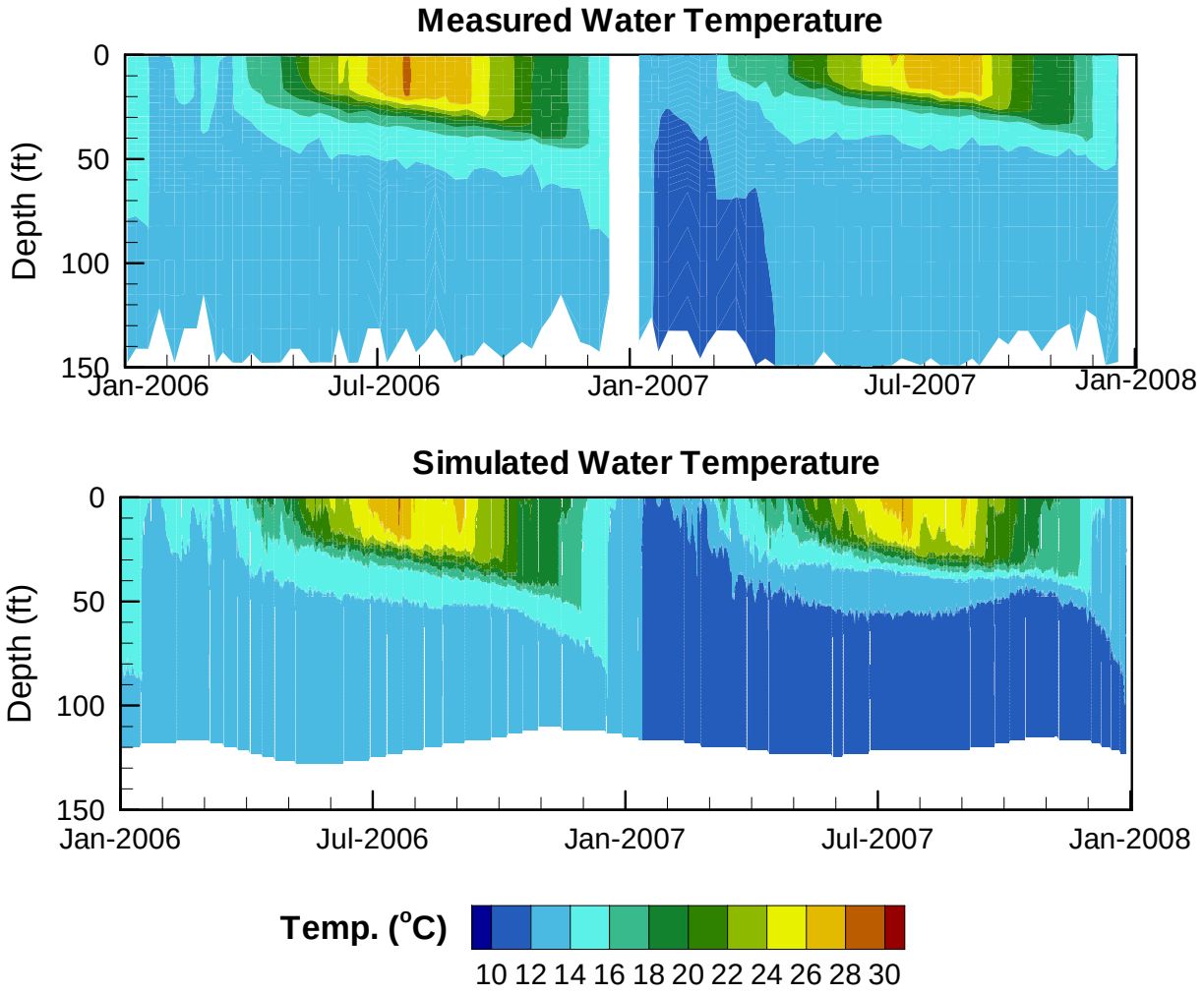

Figure 4

FLOW SCIENCE®

SVR Water Quality Model Calibration Results

Station A – Dissolved Oxygen Comparison

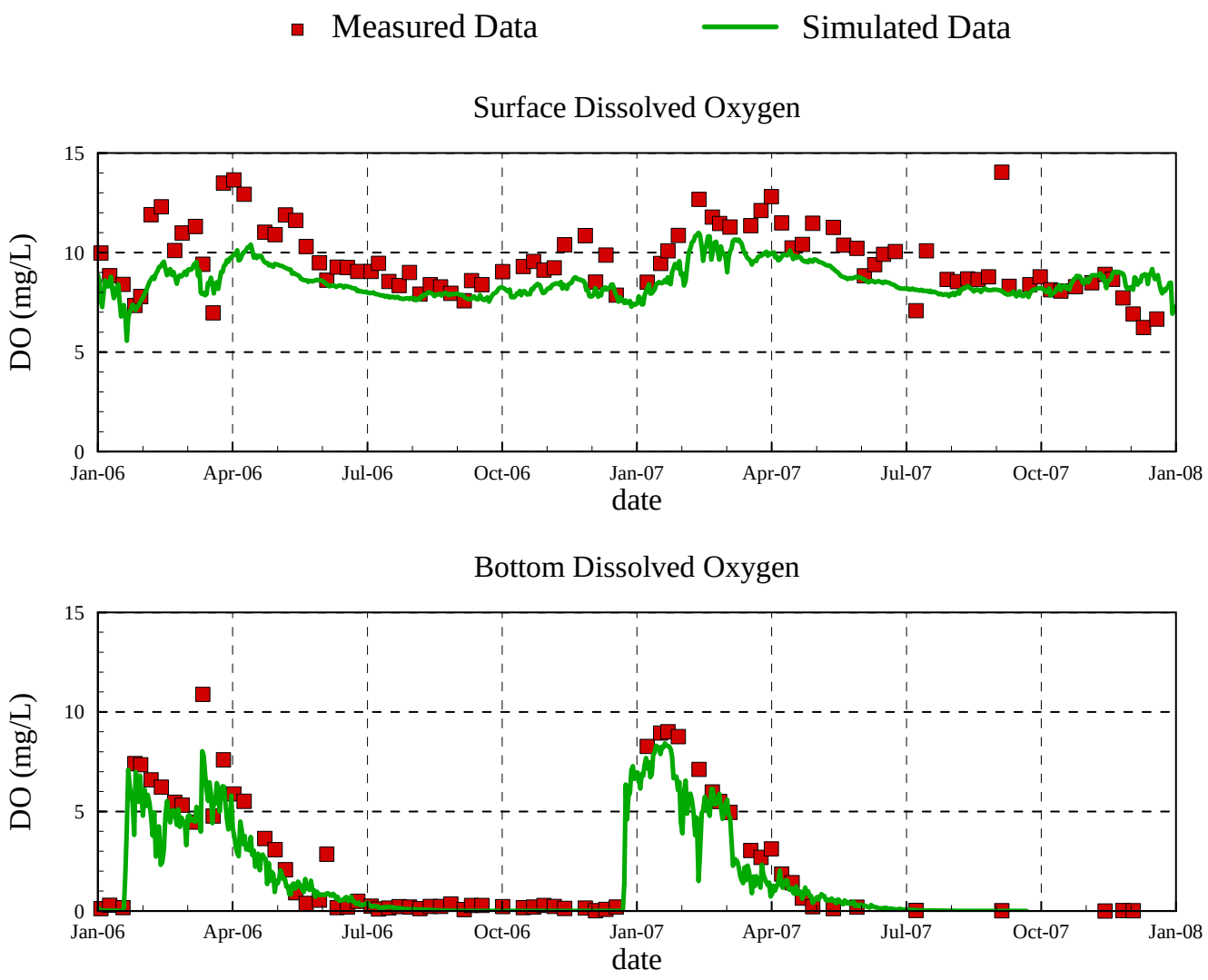

Figure 5

FSI V094005
May 01, 2012

FLOW SCIENCE®

SVR Water Quality Model Calibration Results

Station A – Secchi Depth Comparison

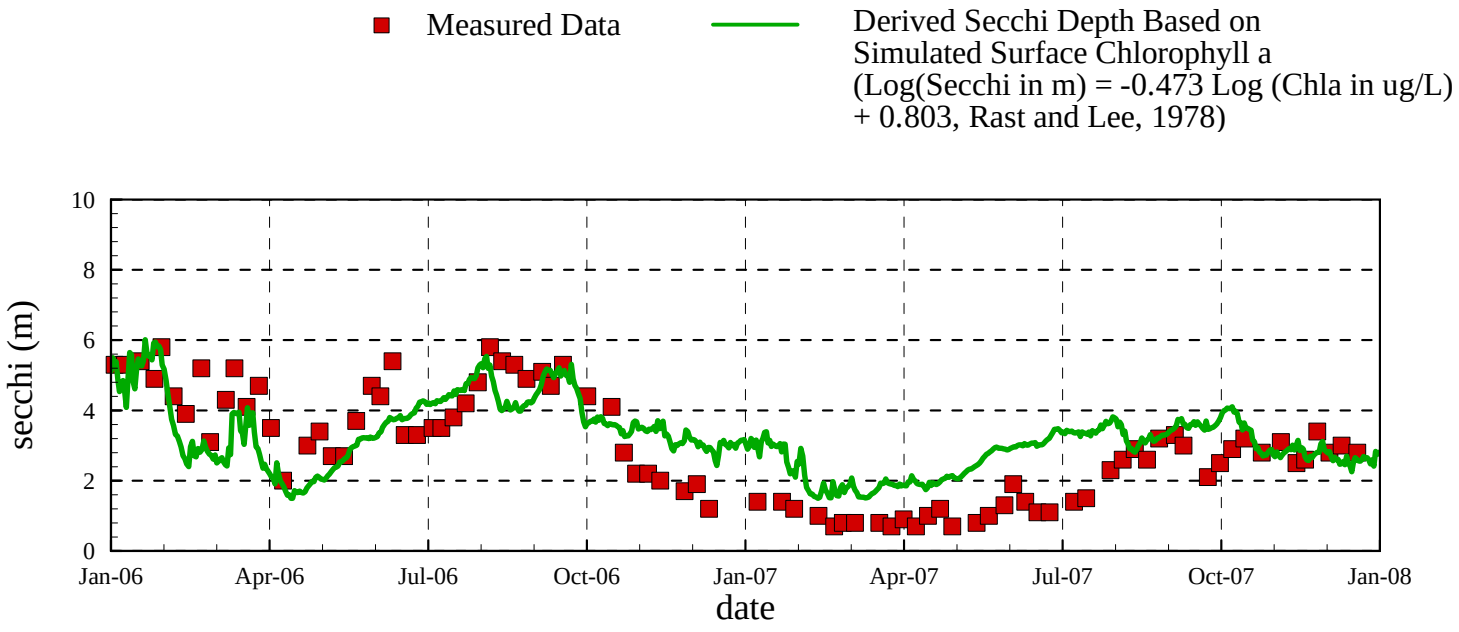

FSI V094005
May 01, 2012

Figure 6

FLOW SCIENCE®

Aqueduct Inflow Nutrient Concentrations

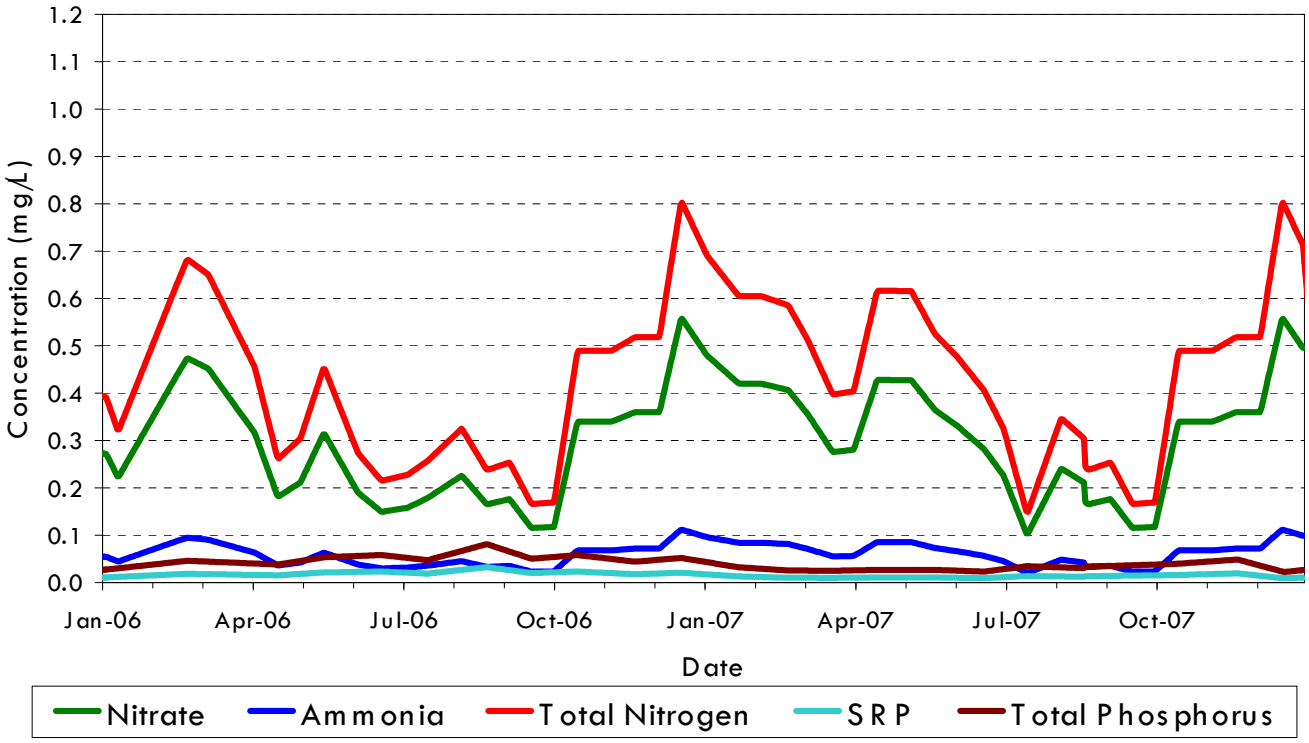

FSI V094005
May 01, 2012

Figure 7

FLOW SCIENCE®

Comparison of Existing Case and Expanded Reservoir Case

Simulated Temperature at Station A

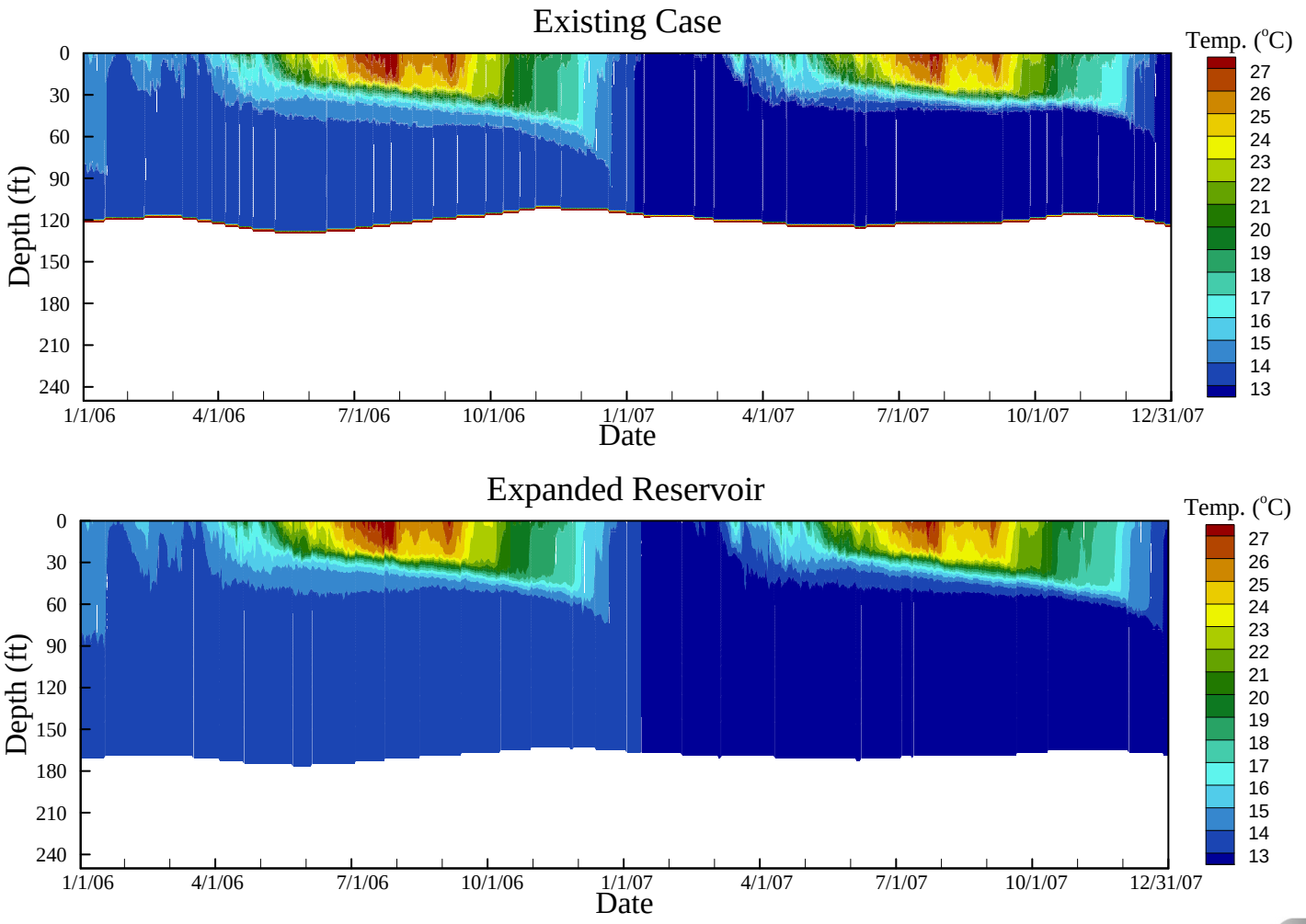

Figure 8

FSI V094005
May 01, 2012

FLOW SCIENCE®

Comparison of Existing Case and Expanded Reservoir Case

Simulated Dissolved Oxygen at Station A

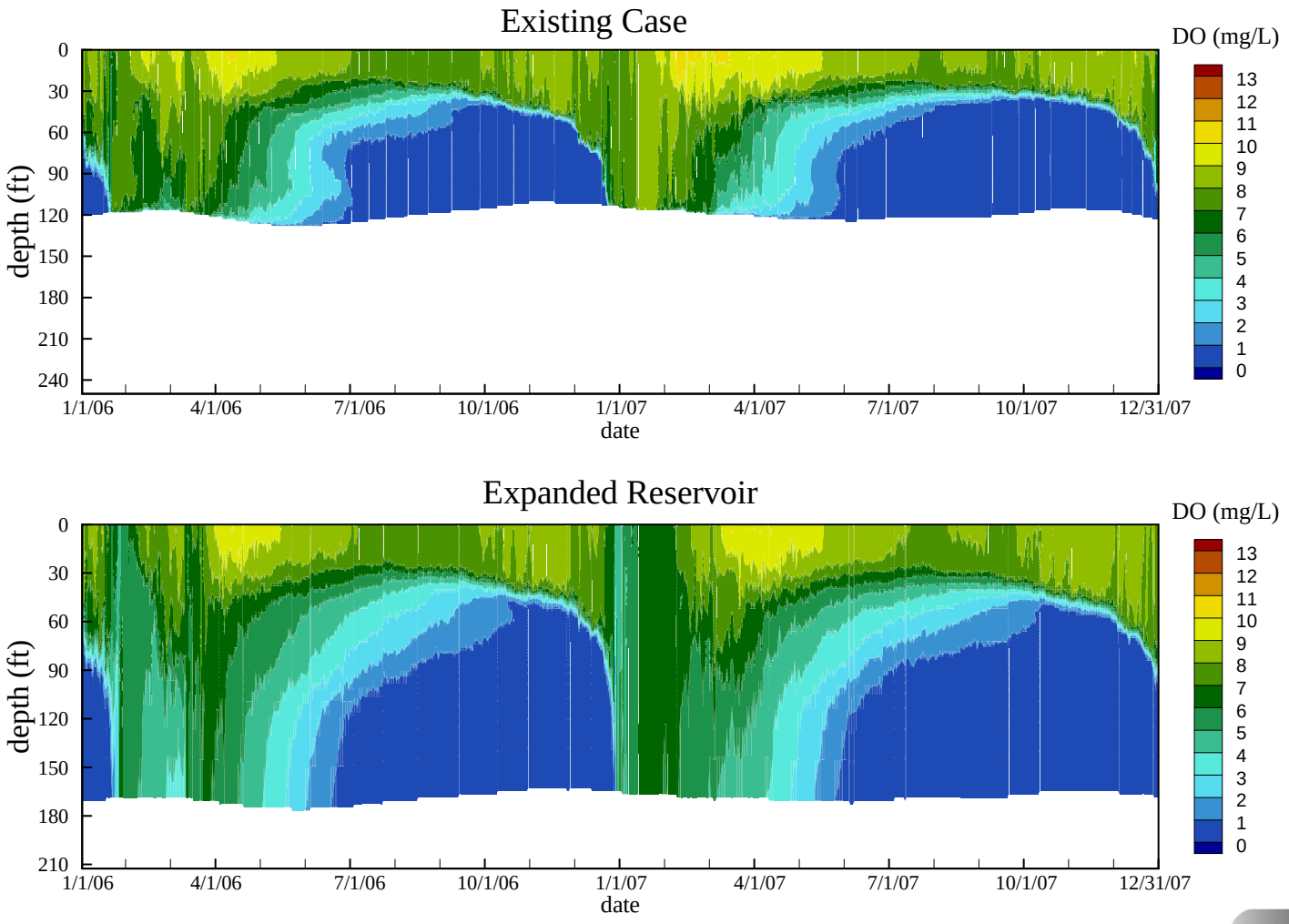

Figure 9

FSI V094005
May 01, 2012

FLOW SCIENCE®

Comparison of Existing Case and Expanded Reservoir Case

Simulated Surface and Bottom Dissolved Oxygen at Station A

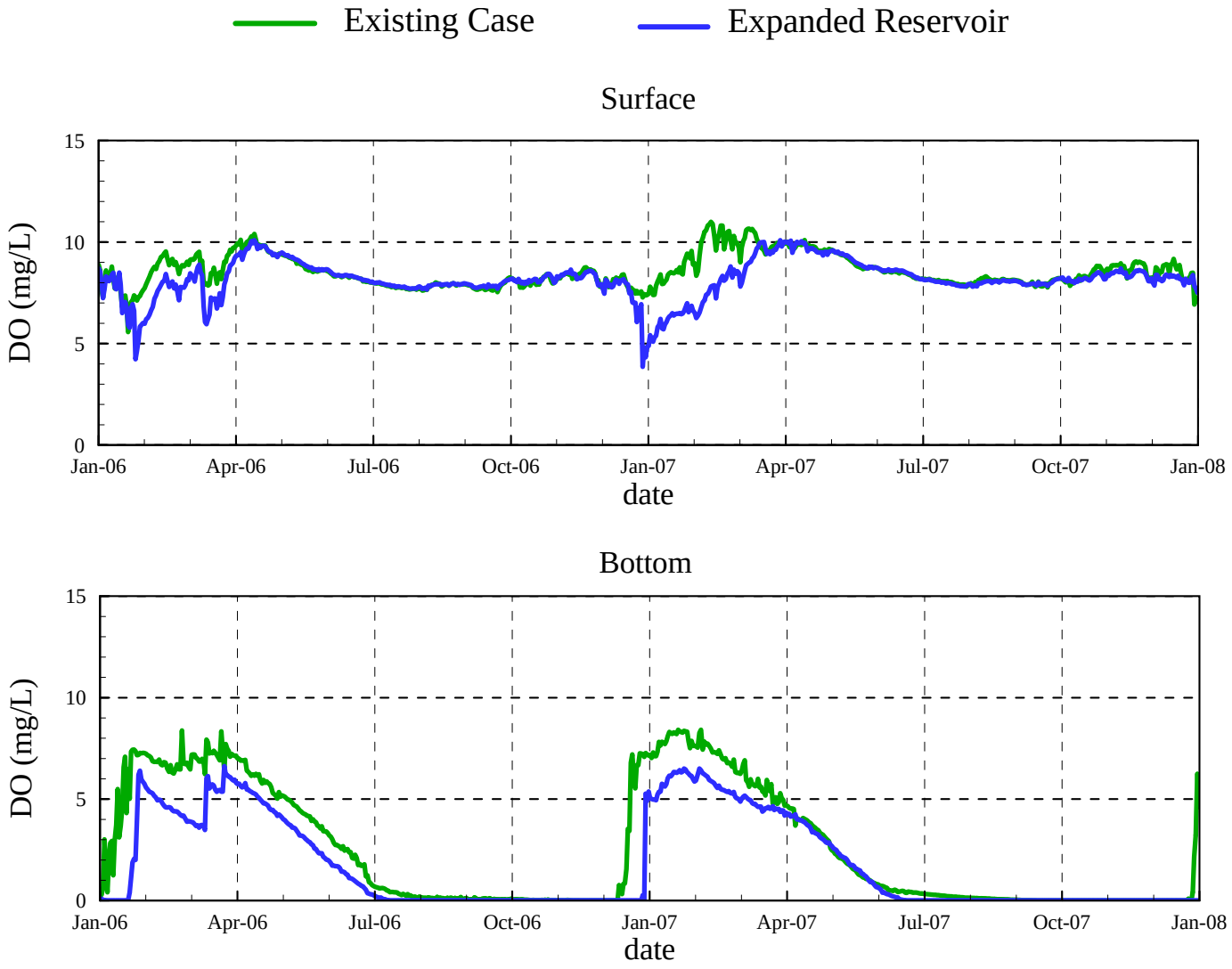

Figure 10

FSI V094005
May 01, 2012

FLOW SCIENCE®

Comparison of Existing Case and Expanded Reservoir Case

Simulated Surface and Bottom Ammonia (as N) at Station A

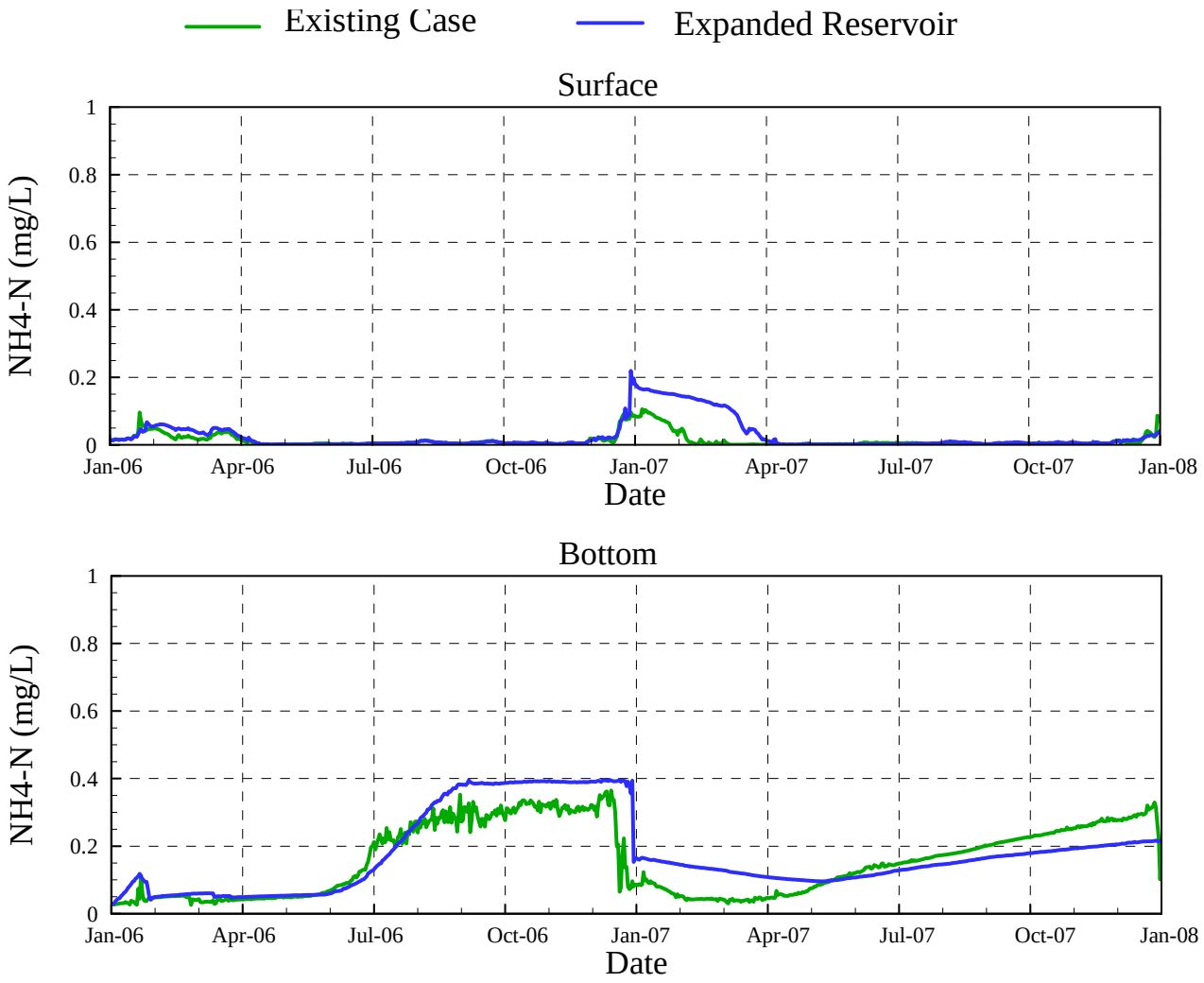

Figure 11

FSI V094005
May 01, 2012

FLOW SCIENCE®

Comparison of Existing Case and Expanded Reservoir Case

Simulated Surface and Bottom Nitrate (as N) at Station A

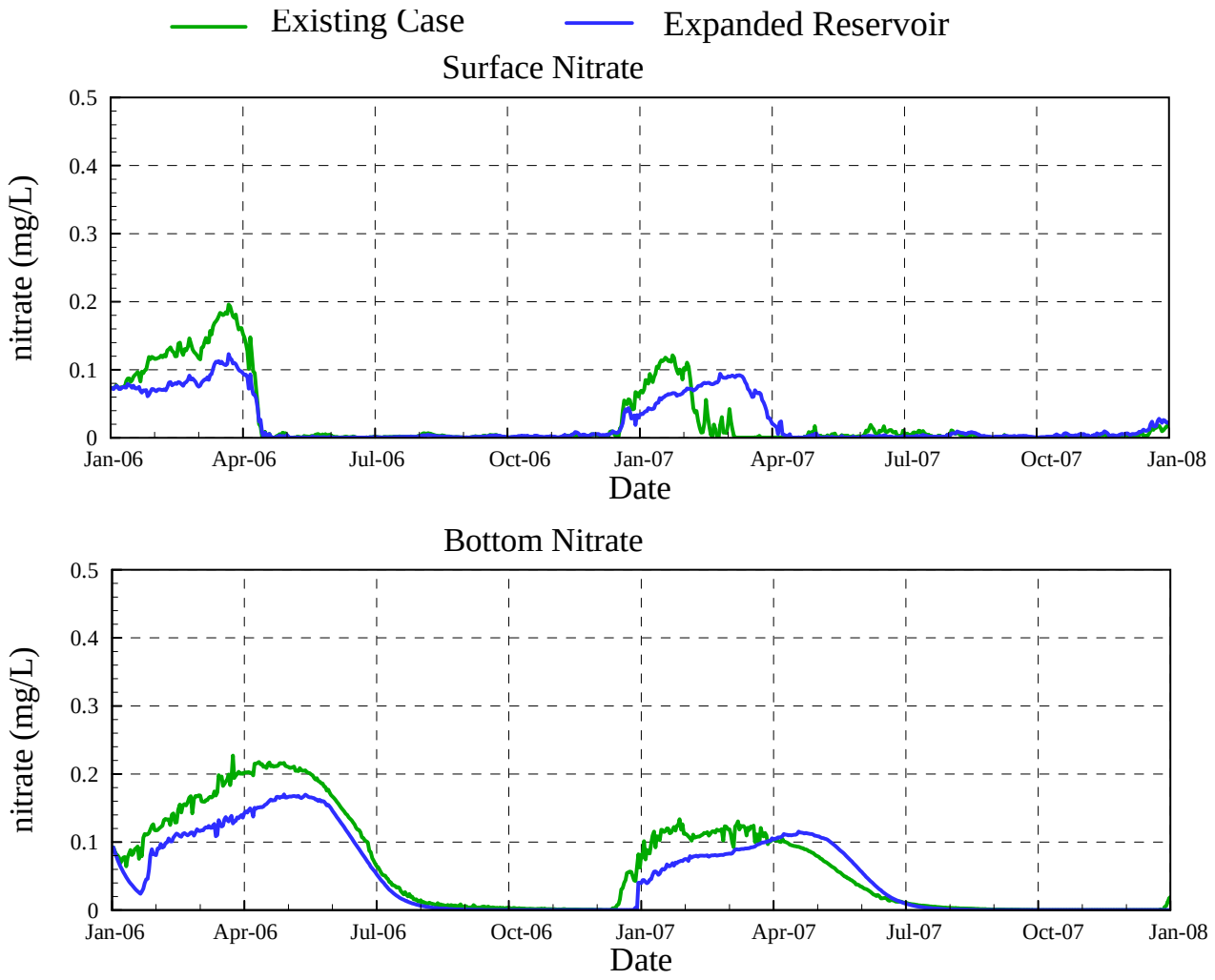

Figure 12

FSI V094005
May 01, 2012

FLOW SCIENCE®

Comparison of Existing Case and Expanded Reservoir Case

Simulated Surface and Bottom TN at Station A

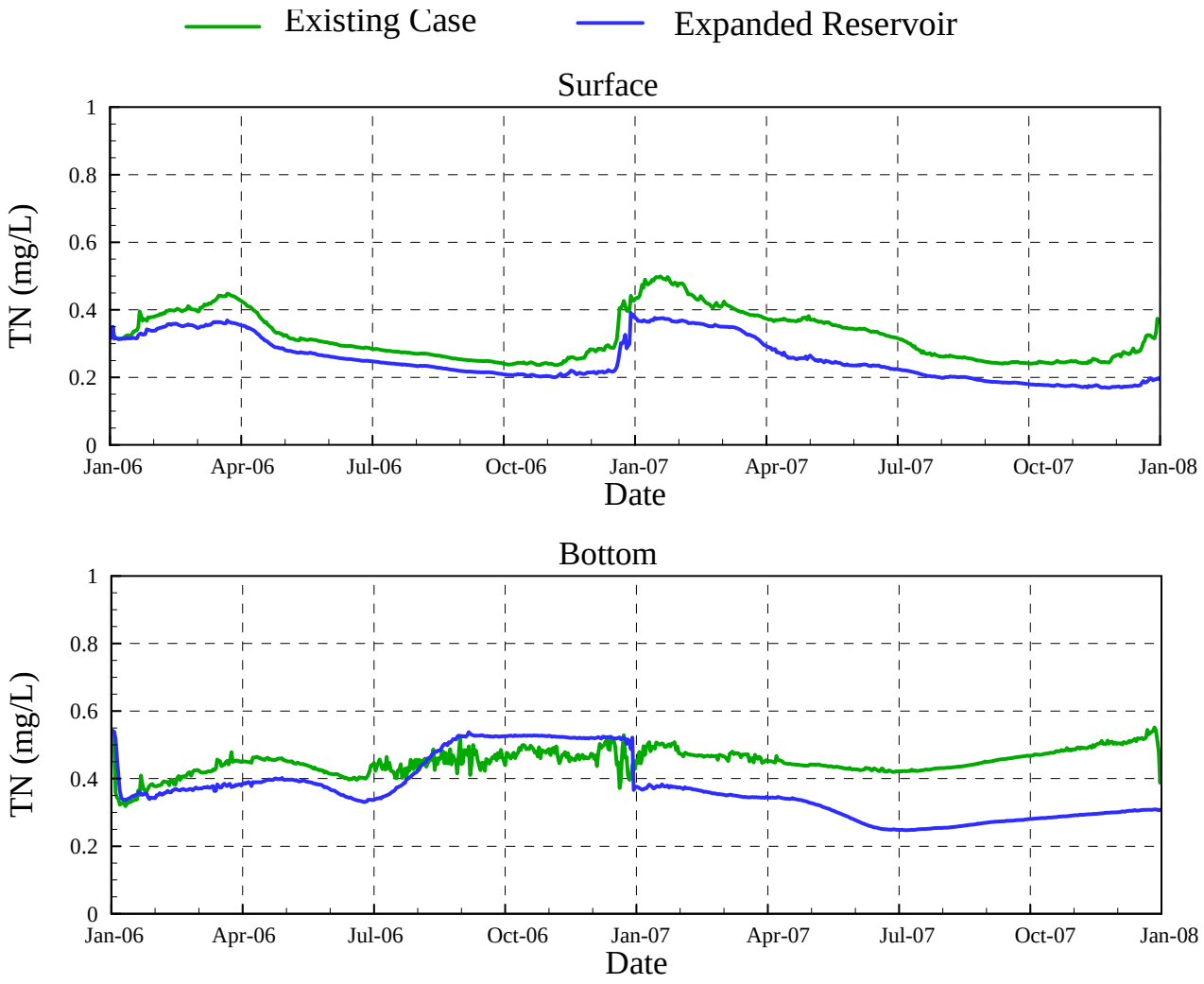

Figure 13

FSI V094005
May 01, 2012

FLOW SCIENCE®

Comparison of Existing Case and Expanded Reservoir Case

Simulated Surface and Bottom SRP at Station A

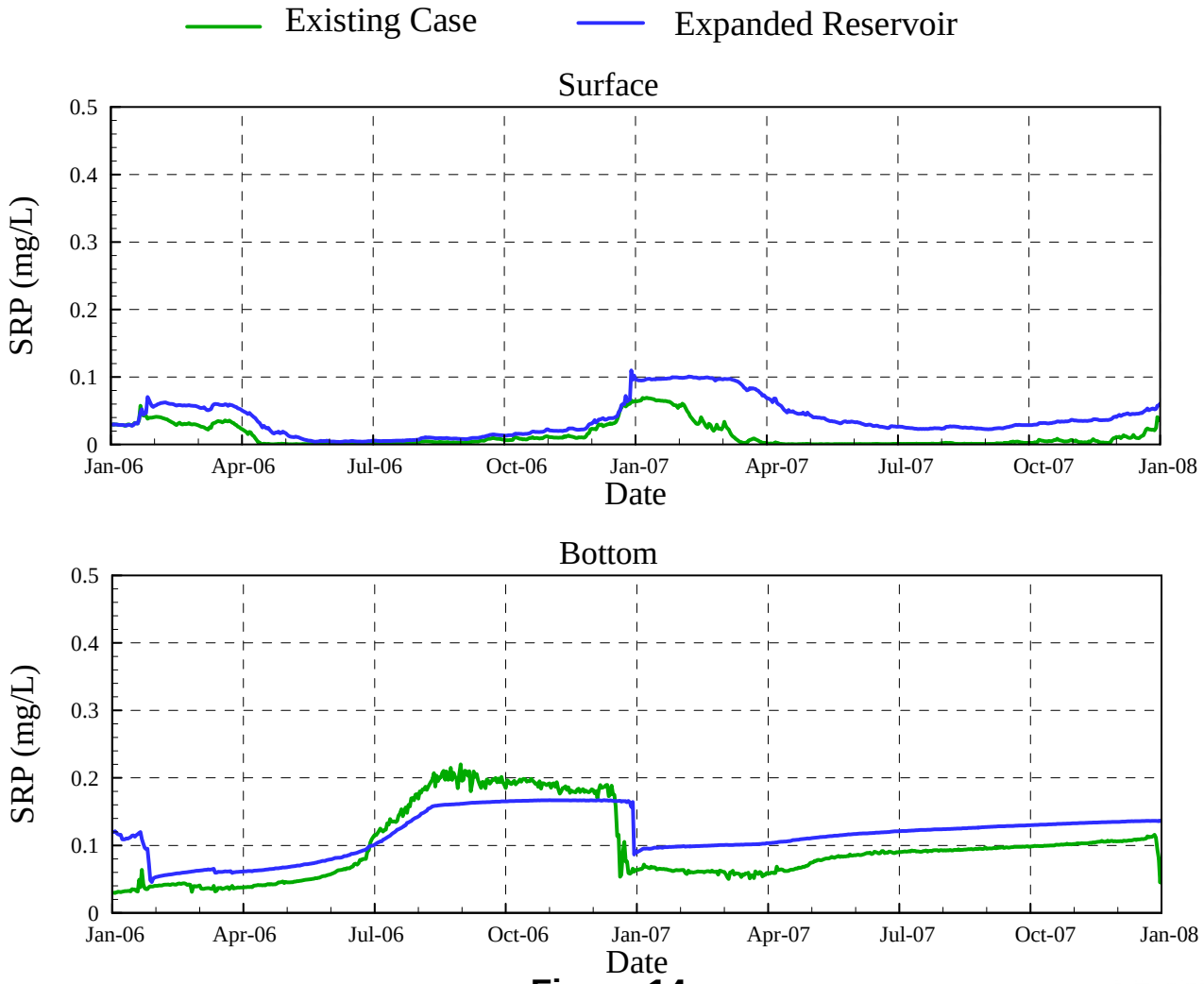

Figure 14

FLOW SCIENCE®

Comparison of Existing Case and Expanded Reservoir Case

Simulated Surface and Bottom TP at Station A

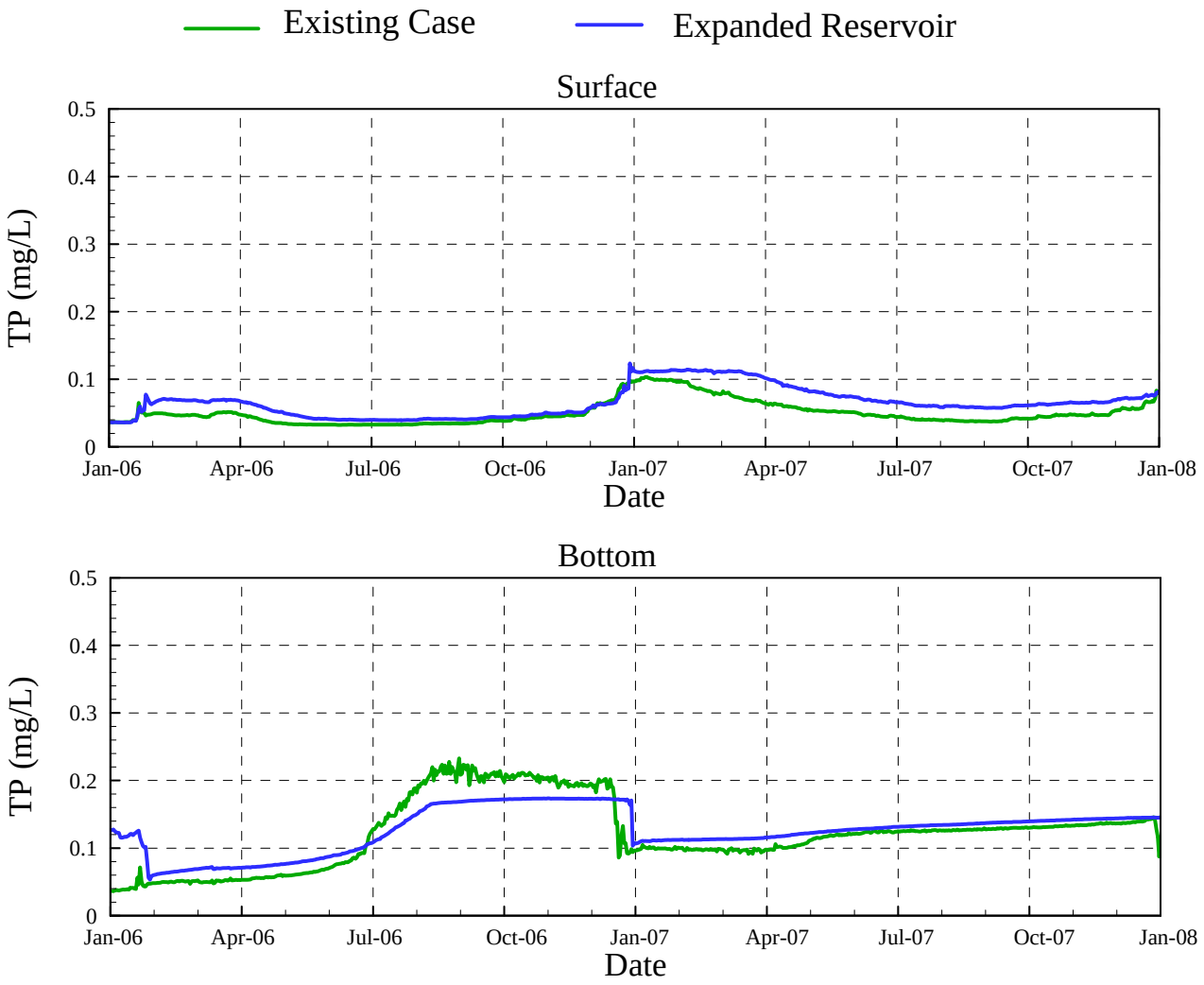

Figure 15

FSI V094005
May 01, 2012

FLOW SCIENCE®

Comparison of Existing Case and Expanded Reservoir Case

Simulated Surface Chlorophyll a at Station A

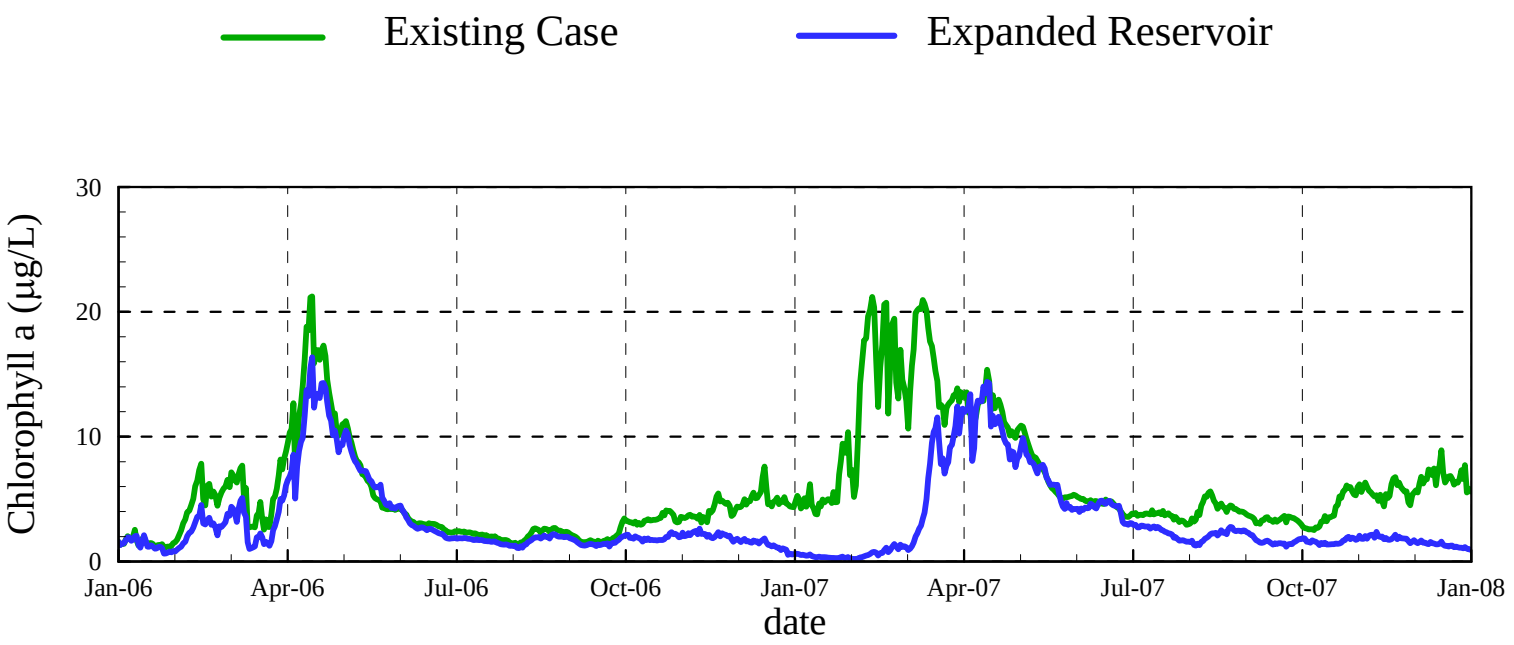

FSI V094005
May 01, 2012

Figure 16

FLOW SCIENCE®

Comparison of Existing Case and Expanded Reservoir Case

Simulated Secchi Depth at Station A

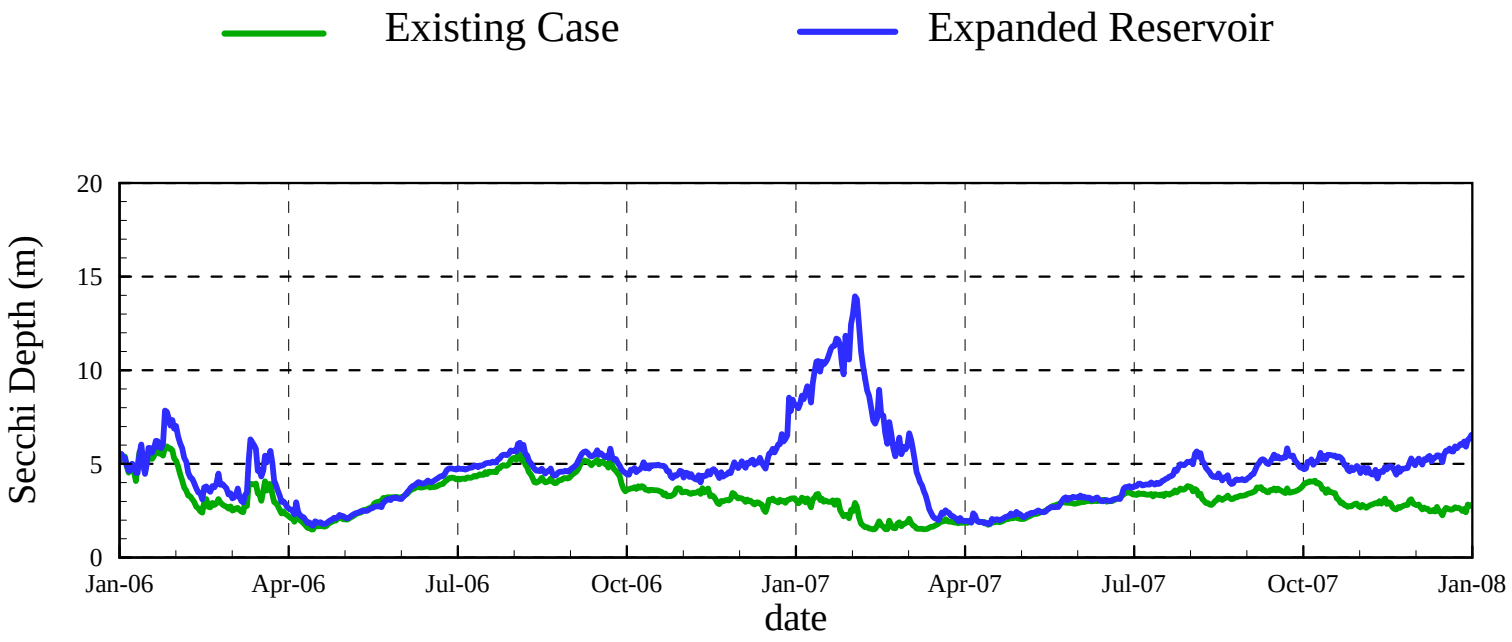

FSI V094005
May 01, 2012

Figure 17

FLOW SCIENCE®

Comparison of Existing Case and Expanded Reservoir Case

Simulated Surface and Bottom pH at Station A

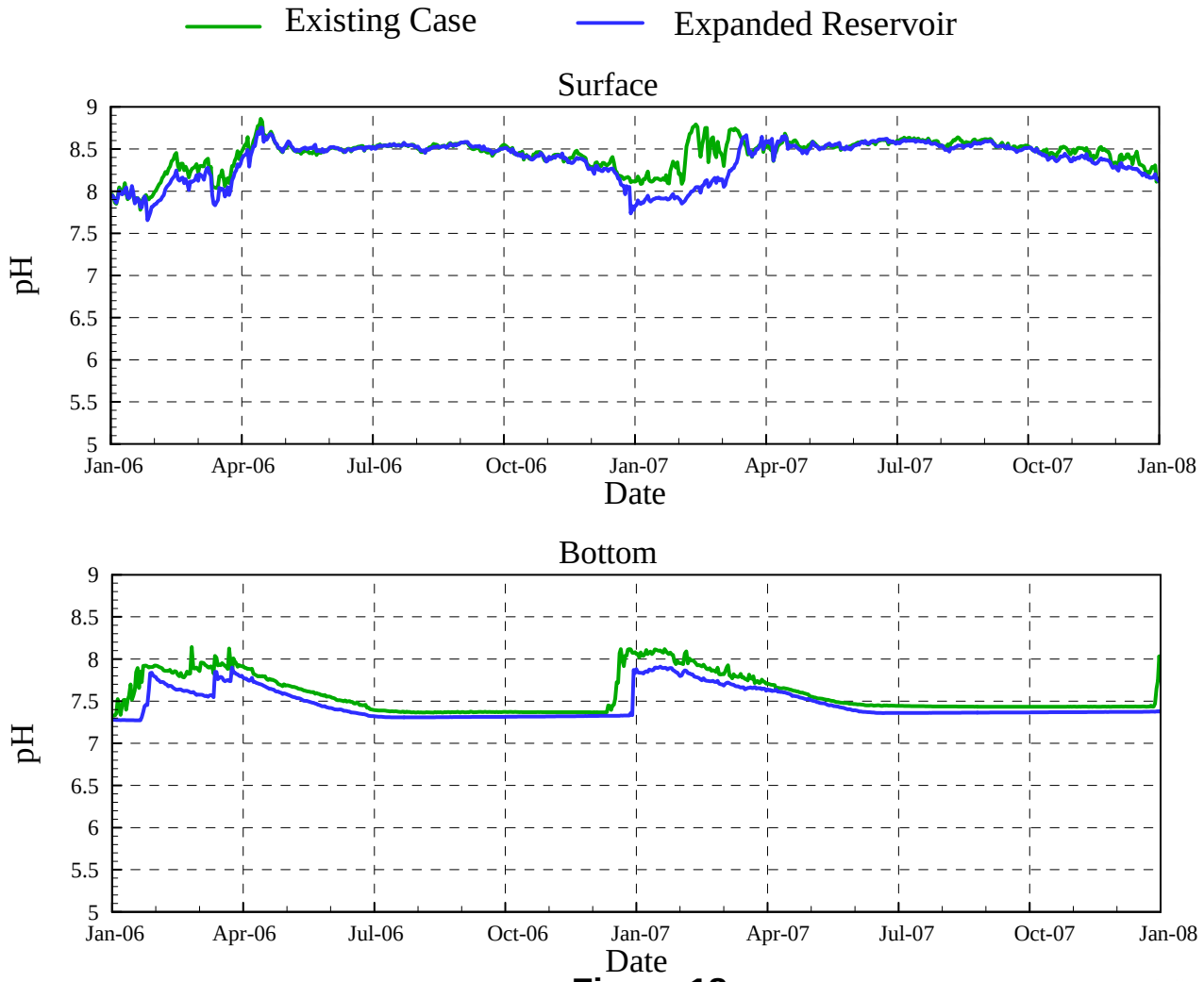

Figure 18

FSI V094005
May 01, 2012

FLOW SCIENCE®

Purified Water and Aqueduct Inflow Rates of Existing Case, No Purified Water and Base Case Scenarios

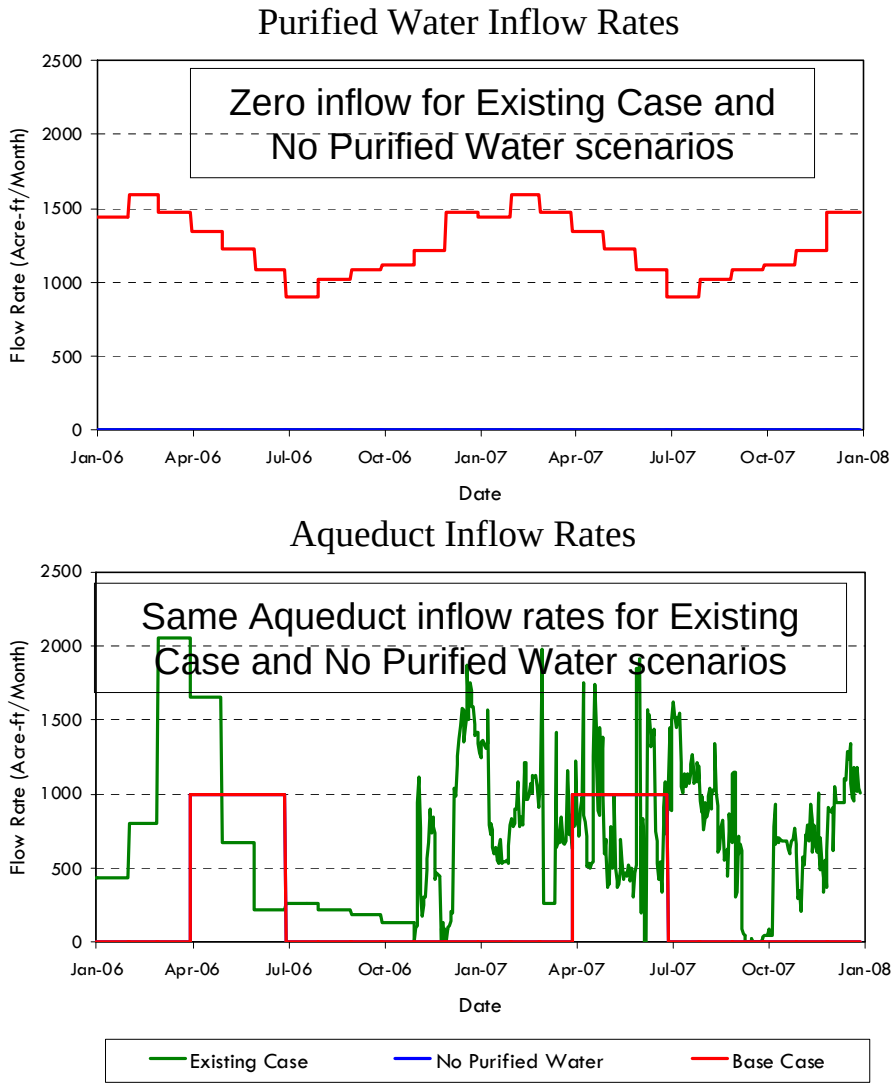

FSI V094005
May 01, 2012

Figure 19

FLOW SCIENCE®

Reservoir Water Volumes for Existing Case, No Purified Water and Base Case Scenarios

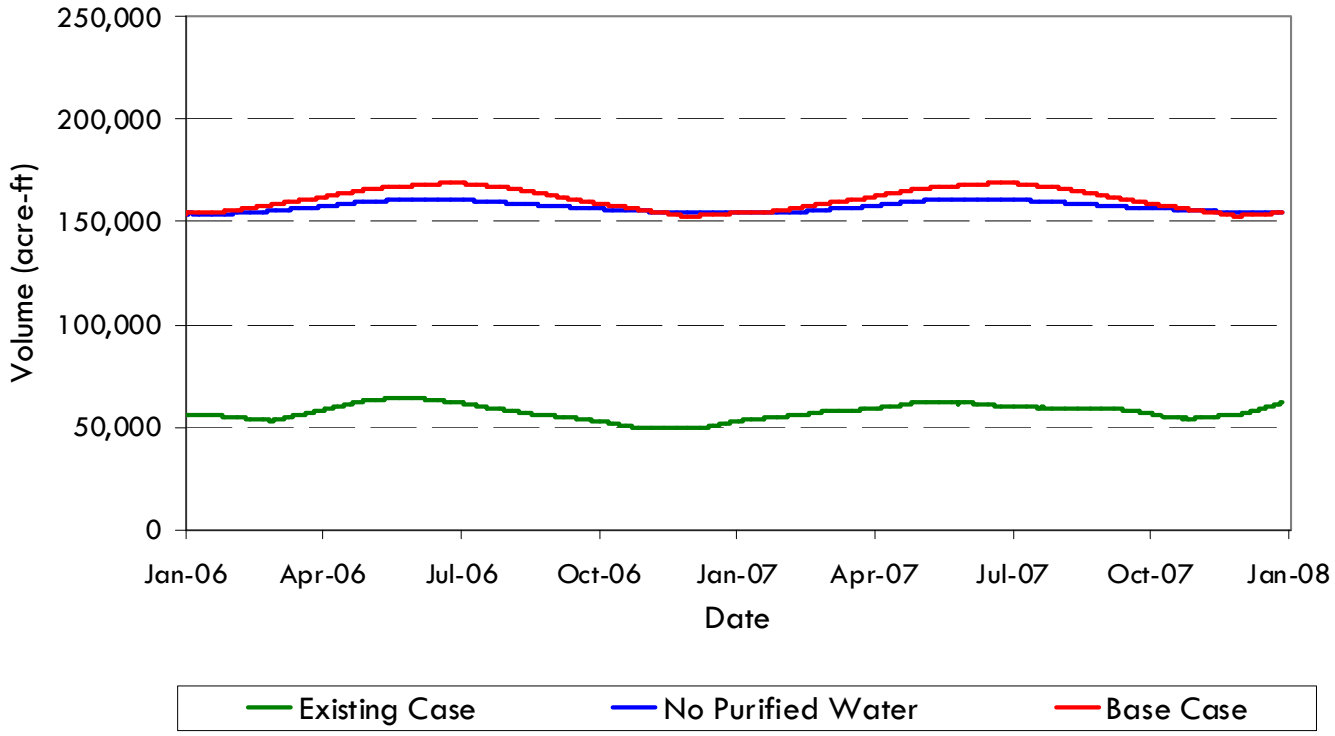

FSI V094005
May 01, 2012

Figure 20

FLOW SCIENCE®

Comparison of Existing Case, No Purified Water and Base Case Scenarios

Simulated Water Temperature at Station A

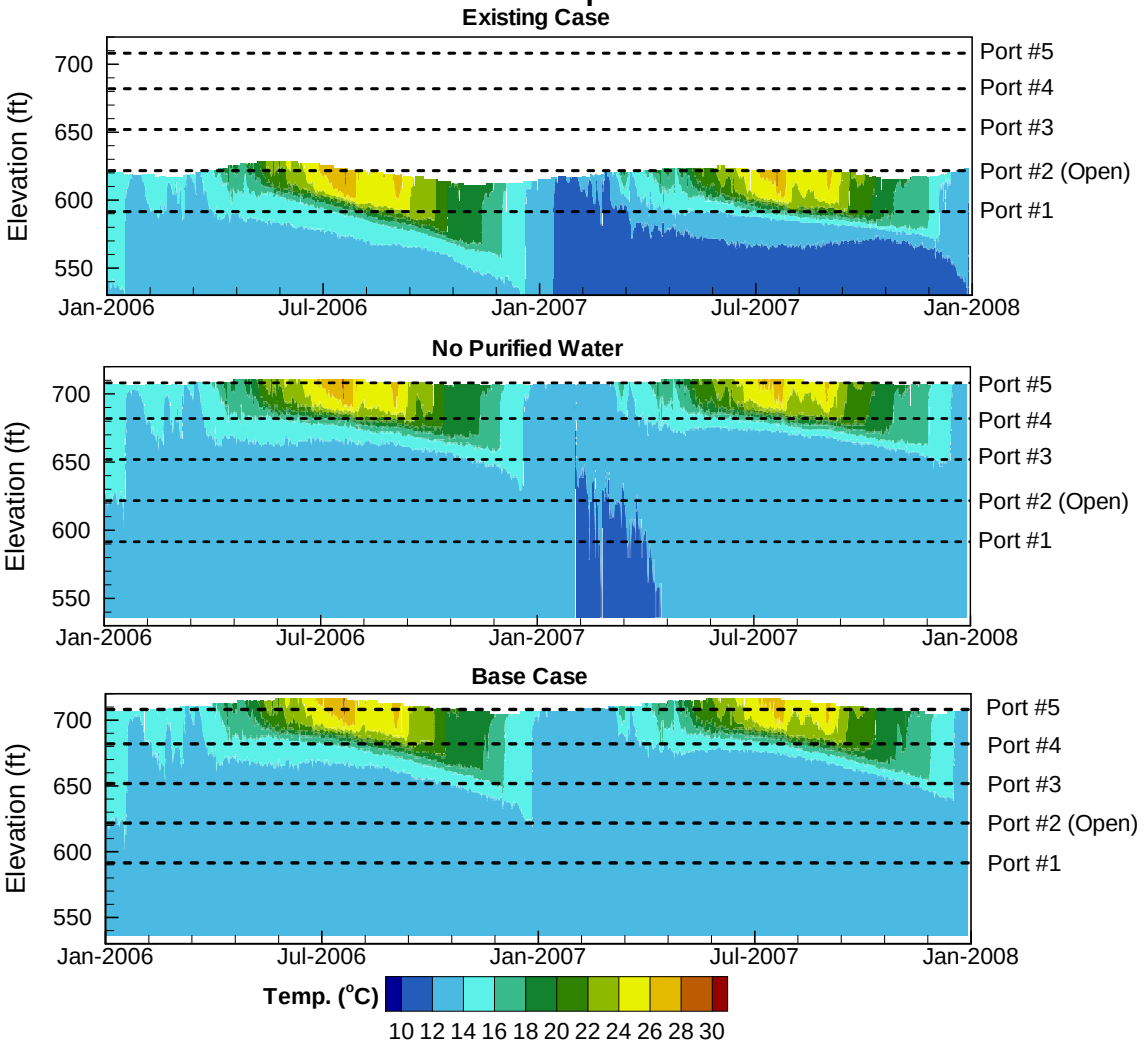

FSI V094005
May 01, 2012

Figure 21

FLOW SCIENCE®

Comparison of Existing Case, No Purified Water and Base Case Scenarios

Simulated Surface and Bottom Dissolved Oxygen at Station A

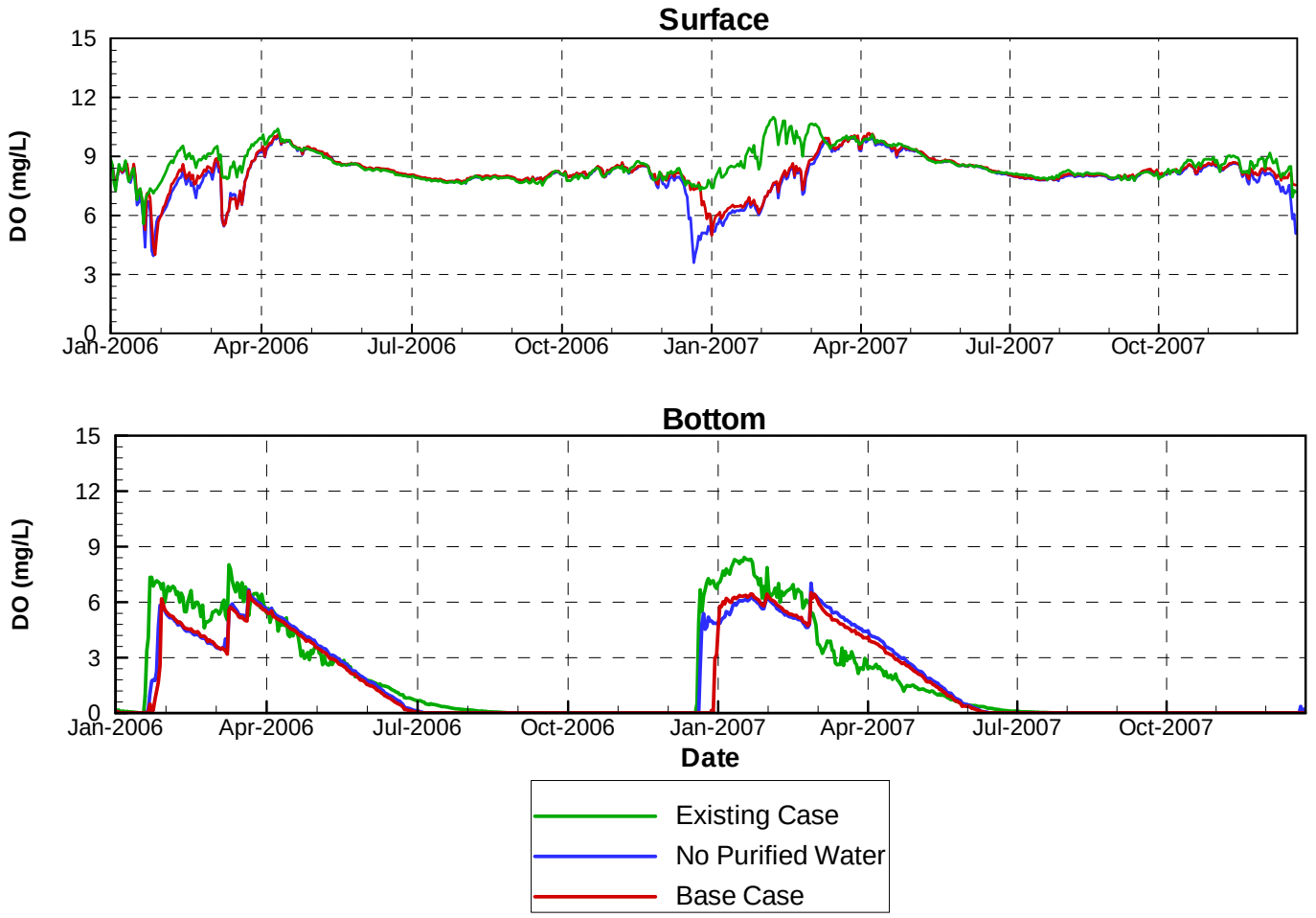

Figure 22

FSI V094005
May 01, 2012

FLOW SCIENCE®

Comparison of Existing Case, No Purified Water and Base Case Scenarios

Simulated Surface and Bottom Nitrate (as N) at Station A

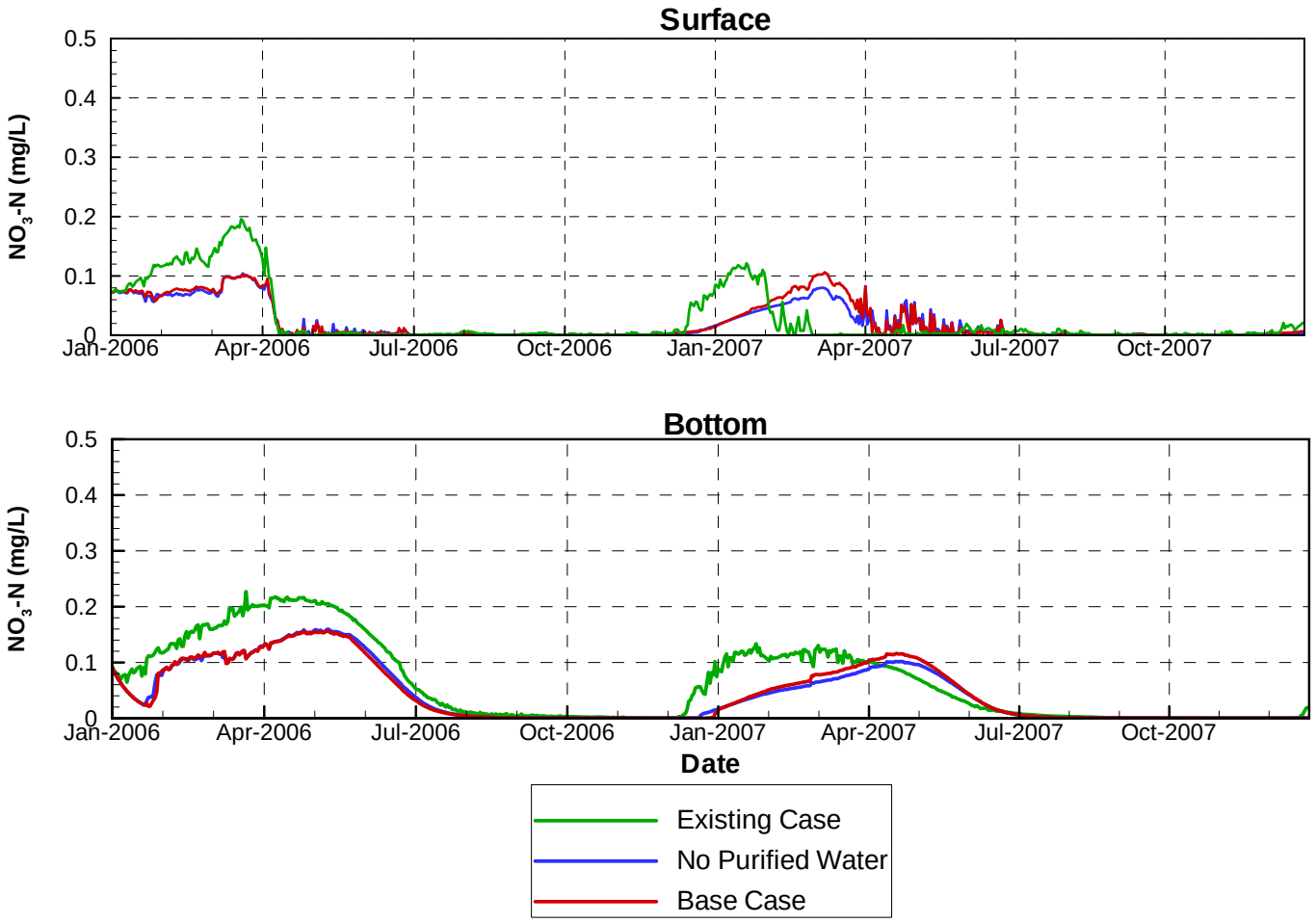

FSI V094005
May 01, 2012

Figure 23

FLOW SCIENCE®

Comparison of Existing Case, No Purified Water and Base Case Scenarios

Simulated Surface and Bottom Ammonia (as N) at Station A

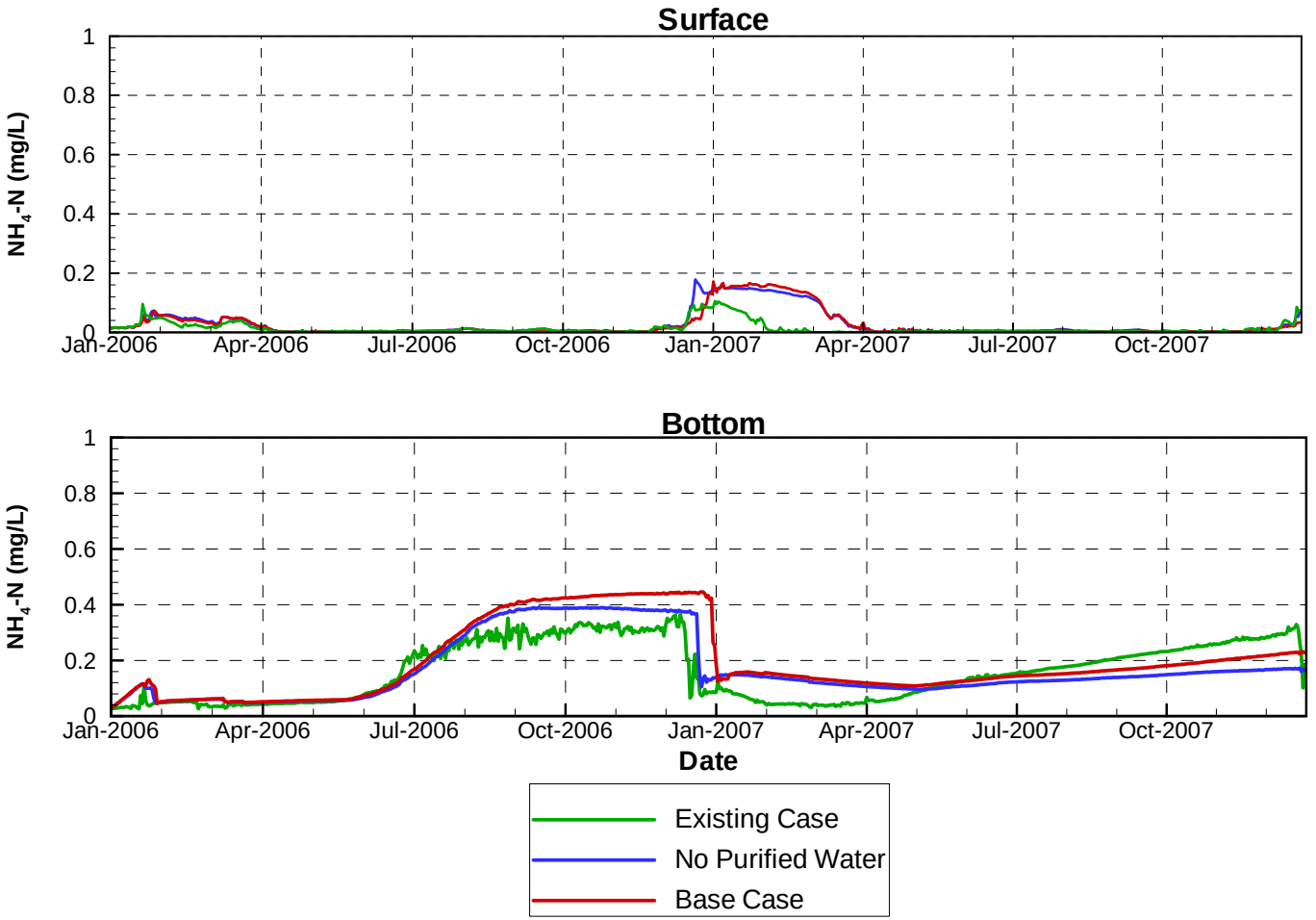

Figure 24

FSI V094005
May 01, 2012

FLOW SCIENCE®

Comparison of Existing Case, No Purified Water and Base Case Scenarios

Simulated Surface and Bottom Total Nitrogen at Station A

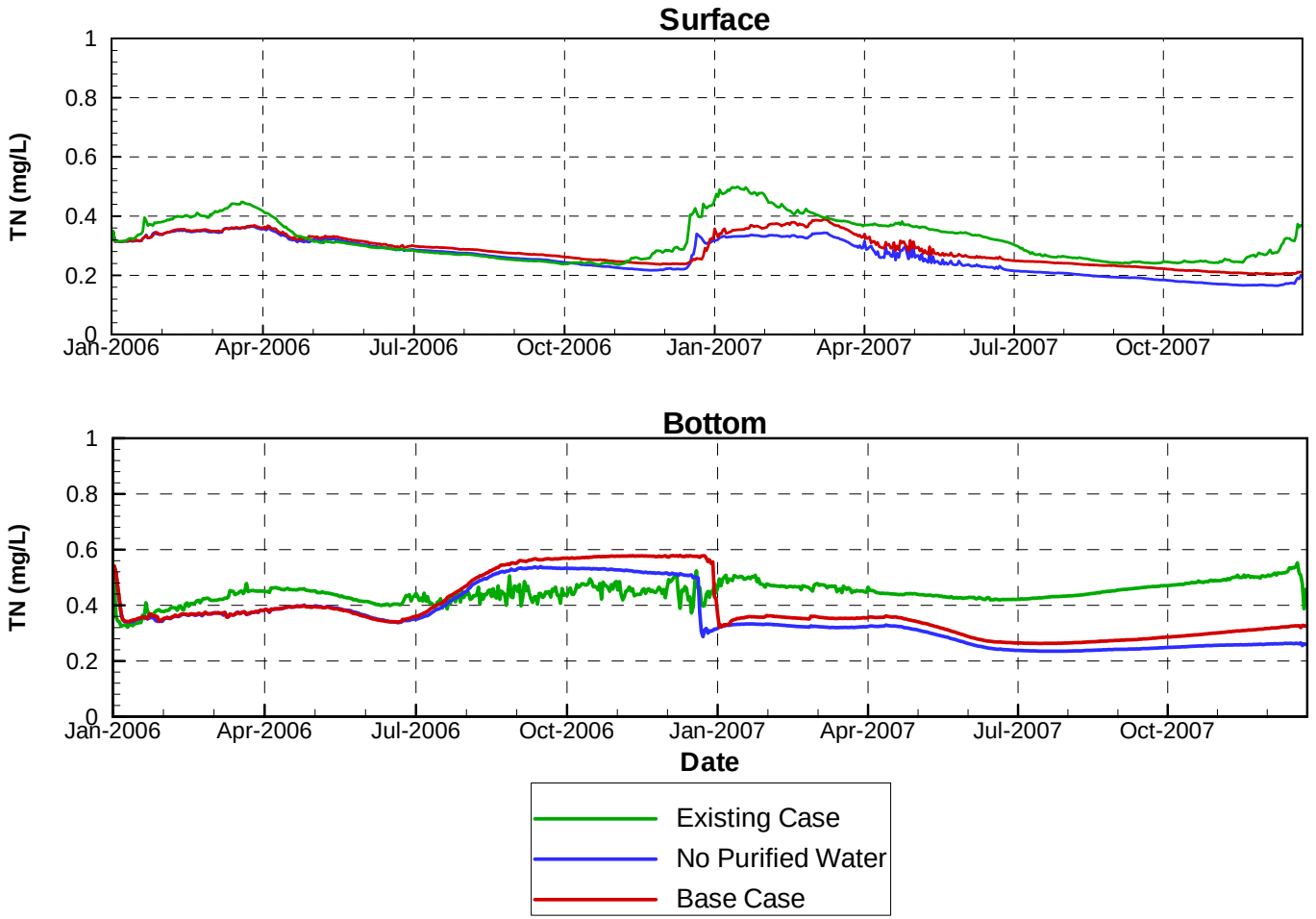

Figure 25

FSI V094005
May 01, 2012

FLOW SCIENCE®

Comparison of Existing Case, No Purified Water and Base Case Scenarios

Simulated Surface and Bottom SRP at Station A

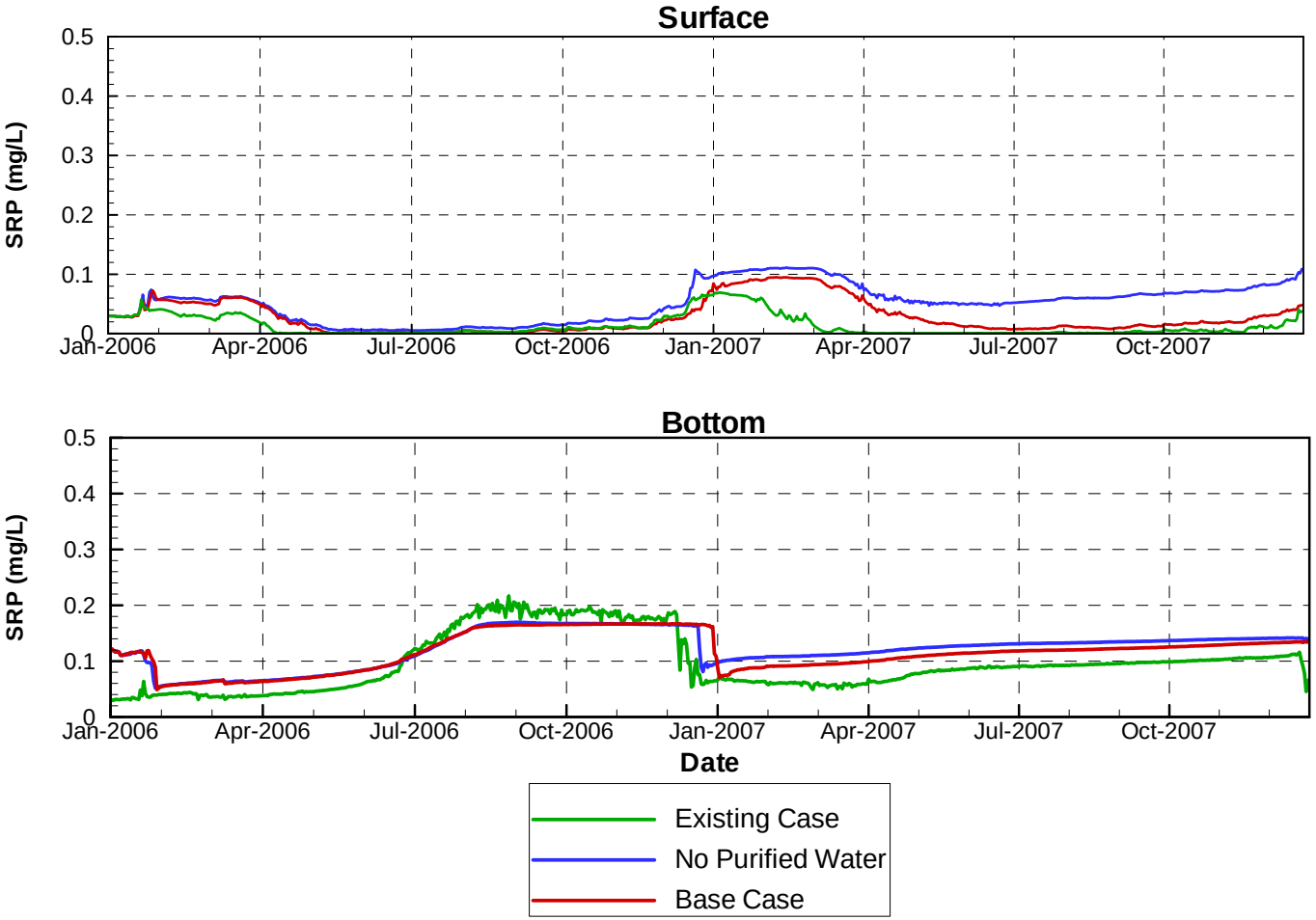

Figure 26

FLOW SCIENCE®

Comparison of Existing Case, No Purified Water and Base Case Scenarios

Simulated Surface and Bottom TP at Station A

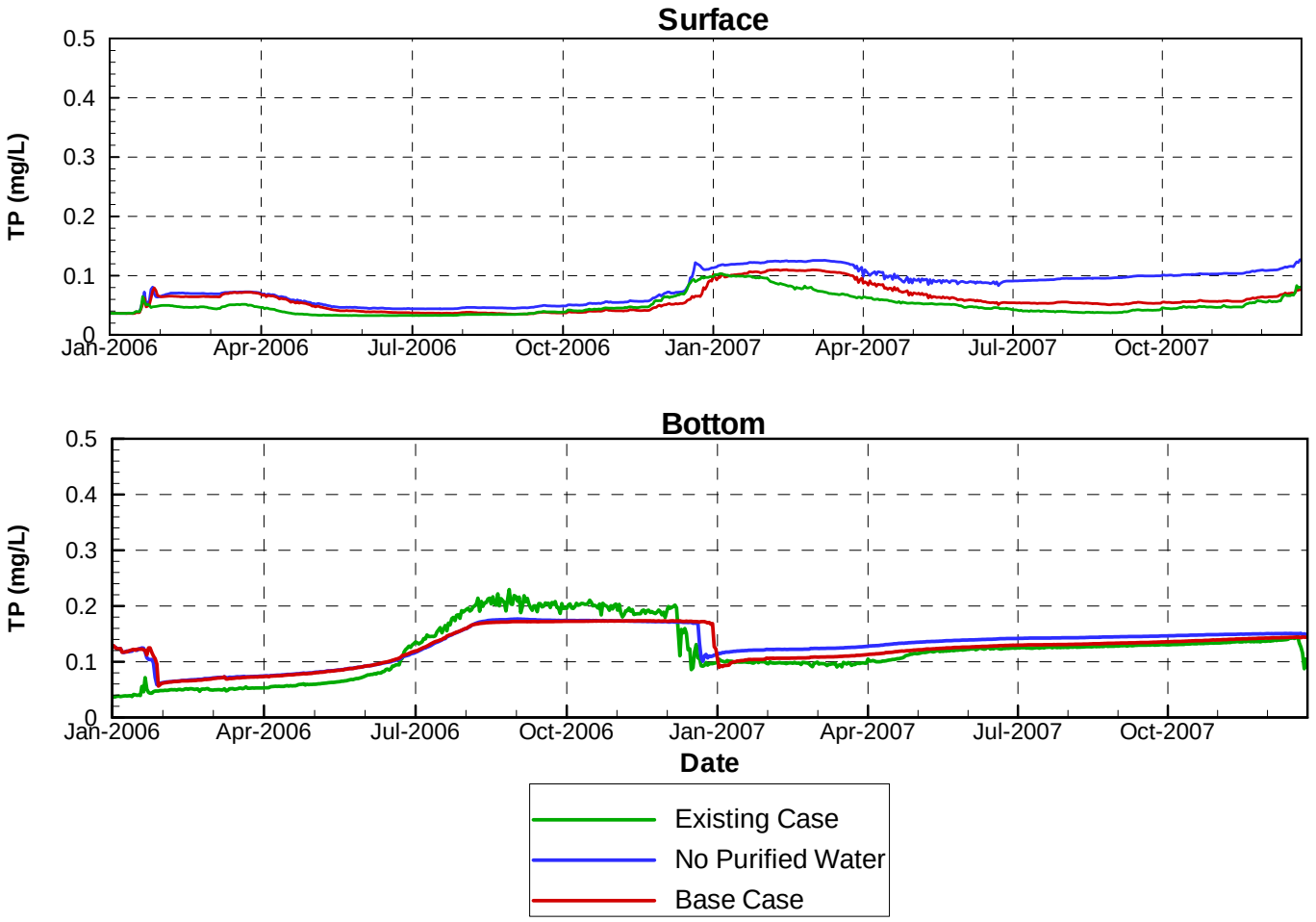

Figure 27

FSI V094005
May 01, 2012

FLOW SCIENCE®

Comparison of Existing Case, No Purified Water and Base Case Scenarios

Simulated Surface Chlorophyll *a* at Station A

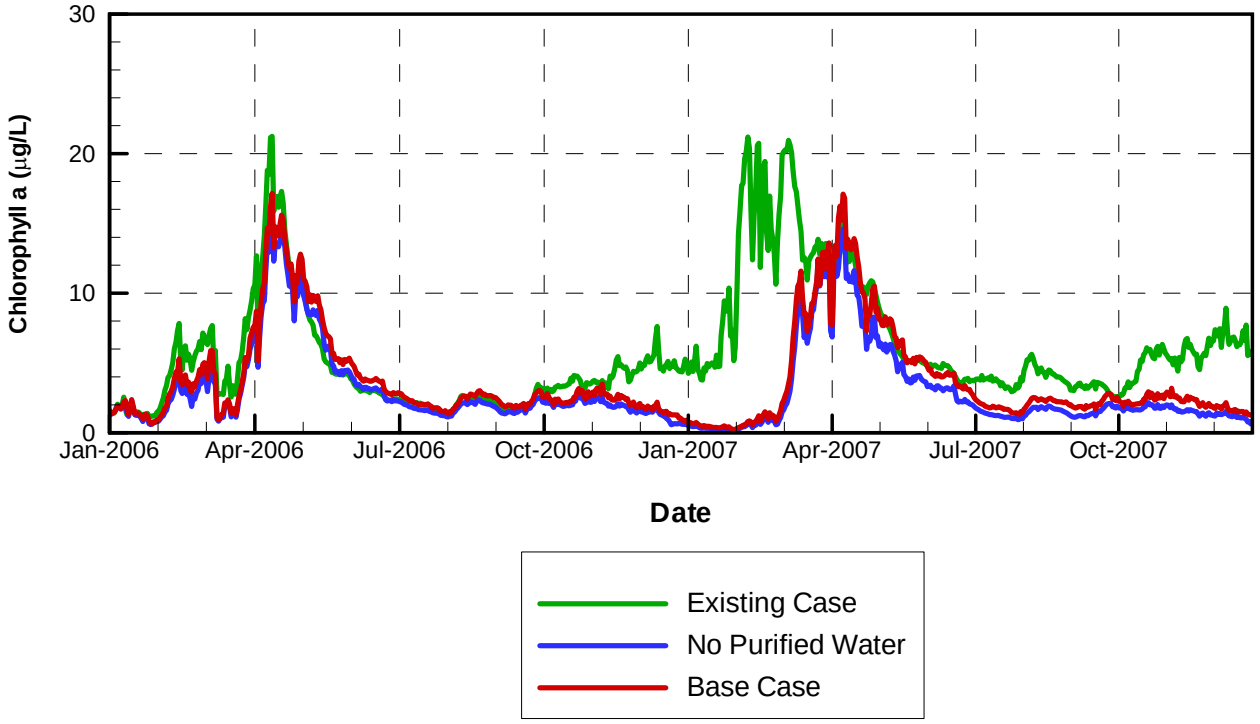

FSI V094005
May 01, 2012

Figure 28

FLOW SCIENCE®

Comparison of Existing Case, No Purified Water and Base Case Scenarios

Secchi Depth at Station A

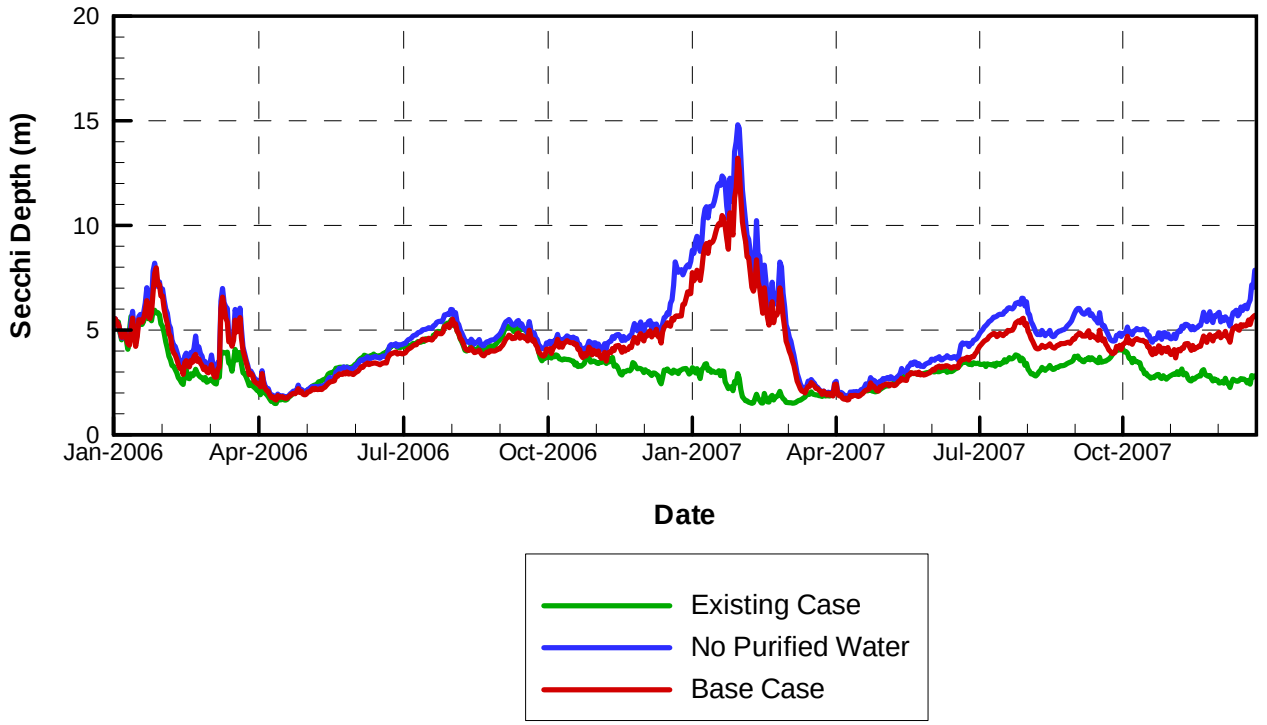

FSI V094005
May 01, 2012

Figure 29

FLOW SCIENCE®

Comparison of Existing Case, No Purified Water and Base Case Scenarios

Simulated Surface and Bottom pH at Station A

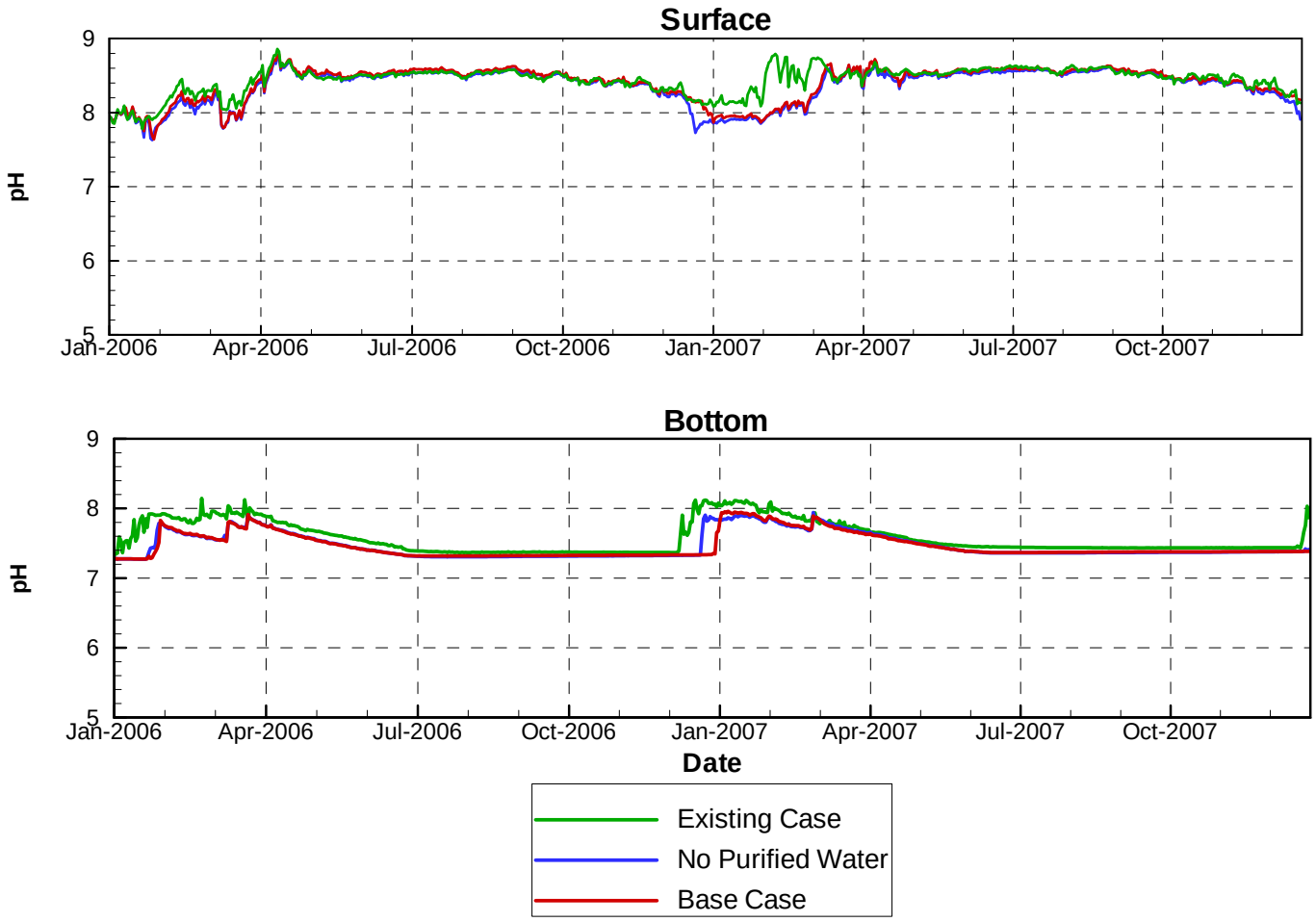

Figure 30

FSI V094005
May 01, 2012

FLOW SCIENCE®

APPENDIX A

Description of ELCOM/CAEDYM/Visual Plumes Models and Evidence of Validation

DESCRIPTION OF ELCOM/CAEDYM MODELS AND EVIDENCE OF VALIDATION

The coupling of biogeochemical and hydrodynamic processes in numerical simulations is a fundamental tool for research and engineering studies of water quality in coastal oceans, estuaries, lakes, and rivers. A modeling system for aquatic ecosystems has been developed that combines a three-dimensional hydrodynamic simulation method with a suite of water quality modules that compute interactions between biological organisms and the chemistry of their nutrient cycles. This integrated approach allows for the feedback and coupling between biogeochemical and hydrodynamic systems so that a complete representation of all appropriate processes can be included in an analysis. The hydrodynamic simulation code is the Estuary Lake and Coastal Ocean Model (ELCOM) and the biogeochemical model is the Computational Aquatic Ecosystem Dynamics Model (CAEDYM).

The purpose of this appendix is to demonstrate that ELCOM and CAEDYM are accepted models that have been systematically tested and debugged, and then successfully validated in numerous applications. A history of the models is provided, followed by an outline of the general model methodology and evolution that emphasizes the basis of the ELCOM/ CAEDYM codes in previously validated models and research. Then the process of code development, testing, and validation of ELCOM/CAEDYM is detailed. Specific model applications are described to illustrate how the ELCOM/CAEDYM models have been applied to coastal oceans, estuaries, lakes, and rivers throughout the world and the results successfully validated against field data. Finally, a general description of the governing equations, numerical models, and processes used in the models is provided along with an extensive bibliography of supporting material.

A comprehensive description of the equations and methods used in the models is provided in the "Estuary Lake and Coastal Ocean Model: ELCOM v2.2 Science Manual" by Hodges and Dallimore (2006), "Estuary Lake and Coastal Ocean Model: ELCOM v2.2 User Manual" by Hodges and Dallimore (2007), "Computational Aquatic Ecosystem Dynamics Model: CAEDYM: v2.2 Science Manual" by Hipsey, Romero, Antenucci and Hamilton (2005), and the "Computational Aquatic Ecosystem Dynamics Model: CAEDYM: v2.2 User Manual" by Hipsey, Romero, Antenucci and Hamilton (2005).

A.1.1 MODEL HISTORY

The ELCOM/CAEDYM models were originally developed at the Centre for Water Research (CWR) at the University of Western Australia, although the hydrodynamics

code ELCOM is an outgrowth of a hydrodynamic model developed earlier by Professor Vincenzo Casulli in Italy and now in use at Stanford University under the name TRIM-3D. The CAEDYM model was essentially developed at CWR as an outgrowth of earlier water quality modules used in the one-dimensional model, Dynamic Reservoir Simulation Model - Water Quality (DYRESM-WQ, Hamilton and Schladow, 1997).

The original ELCOM/CAEDYM models, as developed by CWR, were implemented in Fortran 90 (with F95 extensions) on a UNIX computer system platform. In 2001, the codes for both models were ported to a personal computer (PC) platform through an extensive recompiling and debugging effort by Flow Science Incorporated (Flow Science) in Pasadena, California. Since then, Flow Science has updated the PC version of the code several times when new versions of the code have been released by CWR.

A.1.2 MODEL METHODOLOGY

ELCOM is a three-dimensional numerical simulation code designed for practical numerical simulation of hydrodynamics and thermodynamics for inland and coastal waters. The code links seamlessly with the CAEDYM biogeochemical model undergoing continuous development at CWR, as shown graphically in **Figure A.1**. The

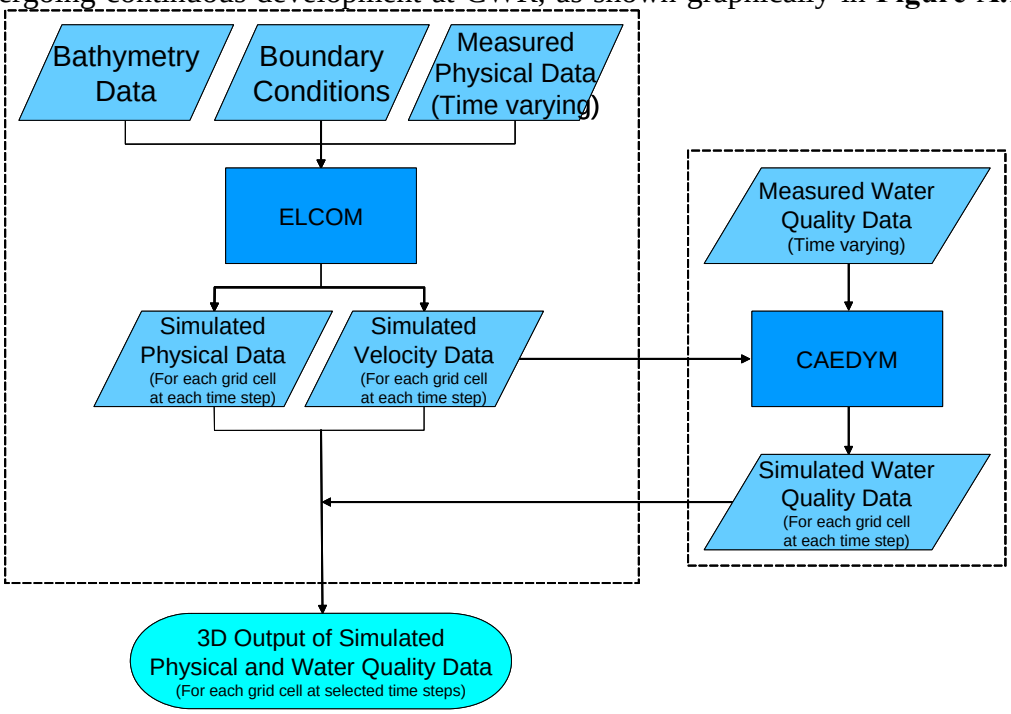

Figure A.1 Flow chart showing the integration of the linked ELCOM/CAEDYM models.

combination of the two codes provides three-dimensional simulation capability for examination of changes in water quality that arise from anthropogenic changes in either quality of inflows or reservoir operations.

The numerical method used in ELCOM is based on the TRIM-3D model scheme of Casulli and Cheng (1992) with adaptations made to improve accuracy, scalar conversion, numerical diffusion, and implementation of a mixed-layer model. The ELCOM model also extends the TRIM-3D scheme by including conservative advection of scalars. The unsteady Reynolds-averaged, Navier-Stokes equations, and the scalar transport equations serve as the basis of ELCOM. The pressure distribution is assumed hydrostatic and density changes do not impact the inertia of the fluid (the Boussinesq approximation), but are considered in the fluid body forces. There is an eddy-viscosity approximation for the horizontal turbulence correlations that represent the turbulent momentum transfer. Vertical momentum transfer is handled by a Richardson number-based diffusion coefficient. Since numerical diffusion generally dominates molecular processes, molecular diffusion in the vertical direction is neglected in ELCOM.

Both ELCOM and TRIM-3D are three-dimensional, computational fluid dynamics (CFD) models. CFD modeling is a validated and well-established approach to solving the equations of fluid motions in a variety of disciplines. Prior to the development of TRIM-3D, there were difficulties in modeling density-stratified flows and such flows required special numerical methods. With TRIM-3D, Casulli and Cheng (1992) developed the first such successful method to model density-stratified flows, such as occur in the natural environment. Since then, TRIM-3D has been validated by numerous publications. ELCOM is based on the same proven method, but incorporates additional improvements as described above. Furthermore, the ELCOM model is based on governing equations and numerical algorithms that have been used in the past (*e.g.*, in validated models such as TRIM-3D), and have been validated in refereed publications. For example:

- The hydrodynamic algorithms in ELCOM are based on the Euler-Lagrange method for advection of momentum with a conjugate gradient solution for the free-surface height (Casulli and Cheng, 1992).

- The free-surface evolution is governed by vertical integration of the continuity equation for incompressible flow applied to the kinematic boundary condition (*e.g.*, Kowalik and Murty, 1993).

- The numerical scheme is a semi-implicit solution of the hydrostatic Navier-Stokes equations with a quadratic Euler-Lagrange, or semi-Lagrangian (Staniforth and Côté, 1991).

- Passive and active scalars (*i.e.*, tracers, salinity, and temperature) are advected using a conservative ULTIMATE QUICKEST discretization (Leonard, 1991). The ULTIMATE QUICKEST approach has been implemented in two-dimensional format and demonstration of its effectiveness in estuarine flows has been documented by Lin and Falconer (1997).

- Heat exchange is governed by standard bulk transfer models found in the literature (*e.g.*, Smooch and DeVries, 1980; Imberger and Patterson, 1981; Jacquet, 1983).

- The vertical mixing model is based on an approach derived from the mixing energy budgets used in one-dimensional lake modeling as presented in Imberger and Patterson (1981), Spigel et al (1986), and Imberger and Patterson (1990). Furthermore, Hodges presents a summary of validation using laboratory experiments of Stevens and Imberger (1996). This validation exercise demonstrates the ability of the mixed-layer model to capture the correct momentum input to the mixed-layer and reproduce the correct basin-scale dynamics, even while boundary-induced mixing is not directly modeled.

- The wind momentum model is based on a mixed-layer model combined with a model for the distribution of momentum over depth (Imberger and Patterson, 1990).

The numerical approach and momentum and free surface discretization used in ELCOM are defined in more detail in Hodges, Imberger, Saggio, and Winters (1999). Similarly, the water quality processes and methodology used in CAEDYM are described in more detail in Hamilton and Schladow (1997). Further technical details on ELCOM and CAEDYM are provided in Sections **Error! Reference source not found.** and **Error! Reference source not found.** below.

A.1.3 VALIDATION AND APPLICATION OF ELCOM/CAEDYM

Since initial model development, testing and validation of ELCOM and/or CAEDYM have been performed and numerous papers on model applications have been presented, written, and/or published as described in more detail below. In summary:

- ELCOM solves the full three-dimensional flow equations with small approximations.

- ELCOM/CAEDYM was developed, tested, and validated over a variety of test cases and systems by CWR.

- Papers on ELCOM/CAEDYM algorithms, methodology, and applications have been published in peer reviewed journals such as the *Journal of Geophysical Research*, the *Journal of Fluid Mechanics*, the *Journal of Hydraulic Engineering*, the *International Journal for Numerical Methods in Fluids*, and *Limnology and Oceanography*.

- ELCOM/CAEDYM was applied by Flow Science to Lake Mead, Nevada. As part of this application, mass balances were verified and results were presented to a model review panel over a two-year period. The model review panel, the National Park Service, the United States Bureau of Reclamation, the Southern Nevada Water Authority, and the Clean Water Coalition (a consortium of water and wastewater operators in the Las Vegas, Nevada, region) all accepted the ELCOM/CAEDYM model use and validity.

- There are numerous applications of ELCOM/CAEDYM in the literature that compare the results to data, as summarized in Section **Error! Reference source not found.**.

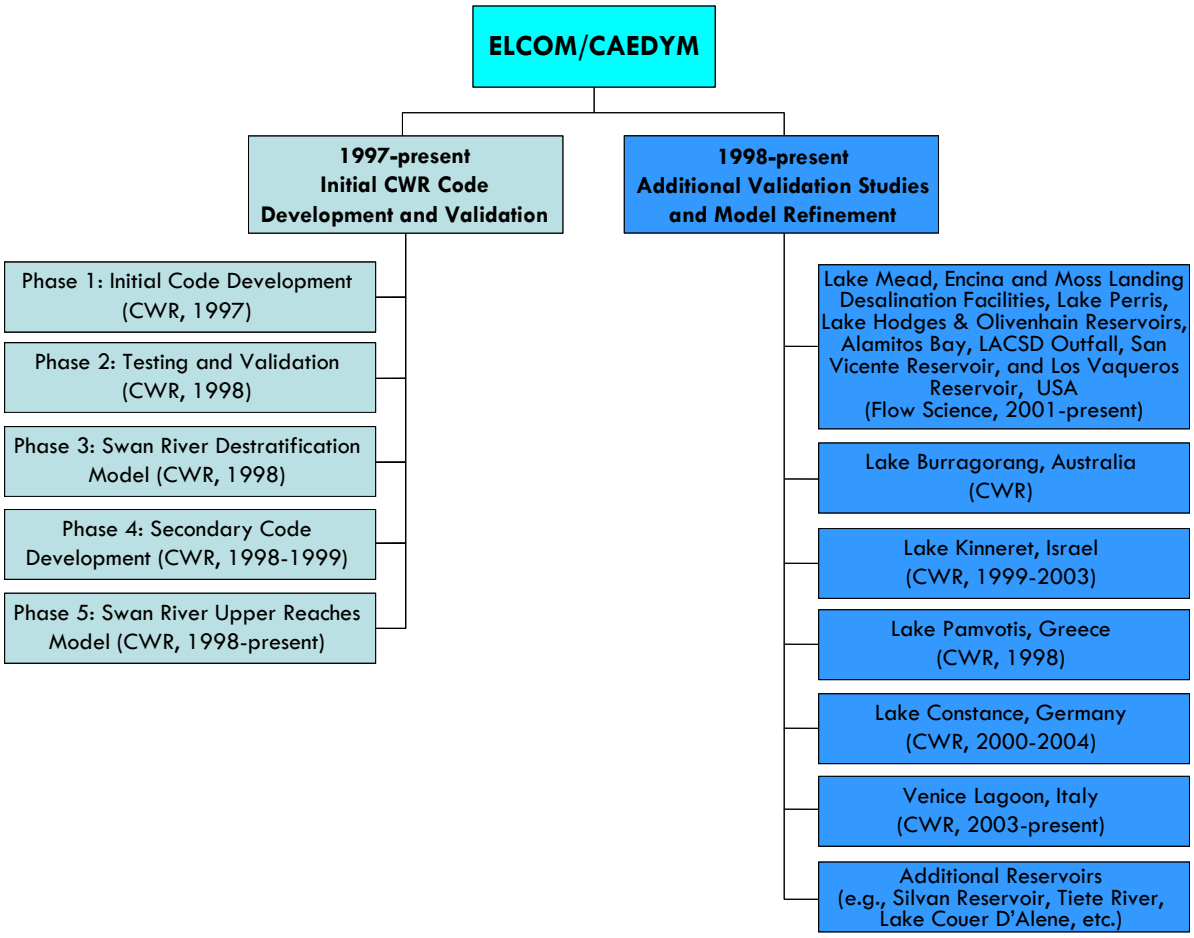

Figure A.2 ELCOM/CAEDYM code development, testing, validation, and applications by CWR and Flow Science Incorporated.

The process of code development, testing, and validation of ELCOM/CAEDYM by CWR, and the ongoing validation and refinement of the codes through further application of the models are detailed in the following subsections. The major components of the development, testing, and validation process are summarized in **Figure A.2**.

A.1.3.1 CWR Code Development, Testing, and Validation

Initial development of the code by CWR occurred from March through December 1997 (Phase 1), followed by a period of testing and validation from January through April 1998 (Phases 2 and 3). Secondary code development by CWR occurred from September 1998 through February 1999 (Phase 4). Testing and validation were

performed over a variety of test cases and systems to ensure that all facets of the code were tested. In addition, Phase 5 modeling of the Swan River since 1998 has been used to gain a better understanding of the requirements and limitations of the model (Hodges et al, 1999).

A.1.3.1.1 *Phase 1: Initial Code Development*

The ELCOM code was initially conceived by CWR as a Fortran 90/95 adaptation of the TRIM-3D model of Casulli and Cheng (1992) in order to: 1) link directly to the CAEDYM water quality module developed concurrently at CWR and 2) provide a basis for future development in a modern programming language. Although written in Fortran 77, TRIM-3D is considered a state-of-the-art numerical model for estuarine applications using a semi-implicit discretization of the Reynolds-averaged hydrostatic Navier-Stokes equations and an Euler-Lagrange method for momentum and scalar transport.

During development of ELCOM, it became clear that additional improvements to the TRIM-3D algorithm were required for accurate solution of density-stratified flows in estuaries. After the basic numerical algorithms were written in Fortran 90, subroutine-by-subroutine debugging was performed to ensure that each subroutine produced the expected results. Debugging and testing of the entire model used a series of test cases that exercised the individual processes in simplified geometries. This included test cases for the functioning of the open boundary condition (tidal forcing), surface wave propagation, internal wave propagation, scalar transport, surface thermodynamics, density underflows, wind-driven circulations, and flooding/drying of shoreline grid cells. Shortcomings identified in the base numerical algorithms were addressed during secondary code development (Phase 4).

Towards the end of the initial code development, ELCOM/CAEDYM were coupled and test simulations were run to calibrate the ability of the models to work together on some simplified problems. Results showing the density-driven currents induced by phytoplankton shading were presented at the Second International Symposium on Ecology and Engineering (Hodges and Herzfeld, 1997). Further details of modeling of density-driven currents due to combinations of topographic effects and phytoplankton shading were presented at a joint meeting of the American Geophysical Union (AGU) and the American Society of Limnology and Oceanography (ASLO) by Hodges et al. (1998), and at a special seminar at Stanford University (Hodges 1998). Additionally, presentations by Hamilton (1997), Herzfeld et al. (1997), and Herzfeld and Hamilton (1998) documented the concurrent development of the CAEDYM ecological model.

A.1.3.1.2*Phase 2: Testing and Validation*

The simplified geometry tests of Phase I revealed deficiencies in the TRIM-3D algorithm including the inability of the TRIM-3D Euler-Lagrange method (ELM) to provide conservative transport of scalar concentrations (e.g., salinity and temperature). Thus, a variety of alternate scalar transport methods were tested, with the best performance being a flux-conservative implementation of the ULTIMATE filter applied to third-order QUICKEST discretization based on the work of Leonard (1991).

Model testing and validation against simple test cases was again undertaken. In addition, a simulation of a winter underflow event in Lake Burragorang in New South Wales, Australia, was performed to examine the ability of the model to capture a density underflow in complex topography in comparison to field data taken during the inflow event. These tests showed that the ability to model underflows is severely constrained by the cross-channel grid resolution.

A.1.3.1.3*Phase 3: Swan River Destratification Model*

Phase 3 involved examining a linked ELCOM/CAEDYM destratification model of the Swan River system during a period of destratification in 1997 when intensive field monitoring had been conducted. The preliminary results of this work were presented at the Swan-Canning Estuary Conference (Hertzfeld *et al*, 1998). More comprehensive results were presented at the Western Australian Estuarine Research Foundation (WAERF) Community Forum (Imberger, 1998).

A.1.3.1.4*Phase 4: Secondary Code Development*

In conducting the Phase 3 Swan River destratification modeling, it became clear to CWR that long-term modeling of the salt-wedge propagation would require a better model for mixing dynamics than presently existed. Thus, the availability of an extensive field data set for Lake Kinneret, Israel, led to its use as a test case for development of an improved mixing algorithm for stratified flows (Hodges *et al*, 1999).

A further problem appeared in the poor resolution of momentum terms using the linear ELM discretization (*i.e.*, as used in the original TRIM-3D method). Since the conservative ULTIMATE QUICKEST method (used for scalar transport, see Phase 1 above) does not lend itself to efficient use for discretization of momentum terms in a semi-implicit method, a quadratic ELM approach was developed for more accurate discretization of the velocities.

A.1.3.1.5 *Phase 5: Swan River Upper Reaches Model*

Phases 1-4 developed and refined the ELCOM code for accurate modeling of three-dimensional hydrodynamics where the physical domain is well resolved. Phase 5 is an ongoing process of model refinement that concentrates on developing a viable approach to modeling longer-term evolution hydrodynamics and water quality in the Swan River where fine-scale resolution of the domain is not practical. The Swan River application is also used for ongoing testing and calibration of the CAEDYM water quality module.

The Swan River estuary is located on the Swan Coastal Plain, Western Australia. It is subject to moderate to high nutrient loads associated with urban and agricultural runoff and suffered from *Microcystis aeruginosa* blooms in January 2000. In an effort to find a viable means of conducting seasonal to annual simulations of the Swan River that retain the fundamental along-river physics and the cross-channel variability in water quality parameters, CWR has developed and tested ELCOM/CAEDYM extensively. A progress report by Hodges et al (1999) indicates that ELCOM is capable of accurately reproducing the hydrodynamics of the Swan River over long time scales with a reasonable computational time.

Furthermore, studies conducted by Robson and Hamilton (2002) proved that ELCOM/CAEDYM accurately reproduced the unusual hydrodynamic circumstances that occurred in January 2000 after a record maximum rainfall, and predicted the magnitude and timing of the *Microcystis* bloom. These studies show that better identification and monitoring procedures for potentially harmful phytoplankton species could be established with ELCOM/CAEDYM and will assist in surveillance and warnings for the future.

A.1.3.2 Model Applications

In addition to the initial code development, testing, and validation by CWR, numerous other applications of ELCOM/CAEDYM have been developed by CWR and validated against field data. Additionally, Flow Science has applied ELCOM/CAEDYM extensively at Lake Mead (USA) and validated the results against measured data. The results of numerous ELCOM/CAEDYM model applications are presented below.

A.1.3.2.1 *Lake Mead (Nevada, USA)*

An ELCOM/CAEDYM model of Boulder Basin, Lake Mead near Las Vegas, Nevada, was used to evaluate alternative discharge scenarios for inclusion in an Environmental Impact Statement (EIS) for the Clean Water Coalition (CWC), a

consortium of water and wastewater operators in the Las Vegas region. **Figure A.3** is a cut-away of the three-dimensional model grid used for Boulder Basin, showing the varying grid spacing in the vertical direction.

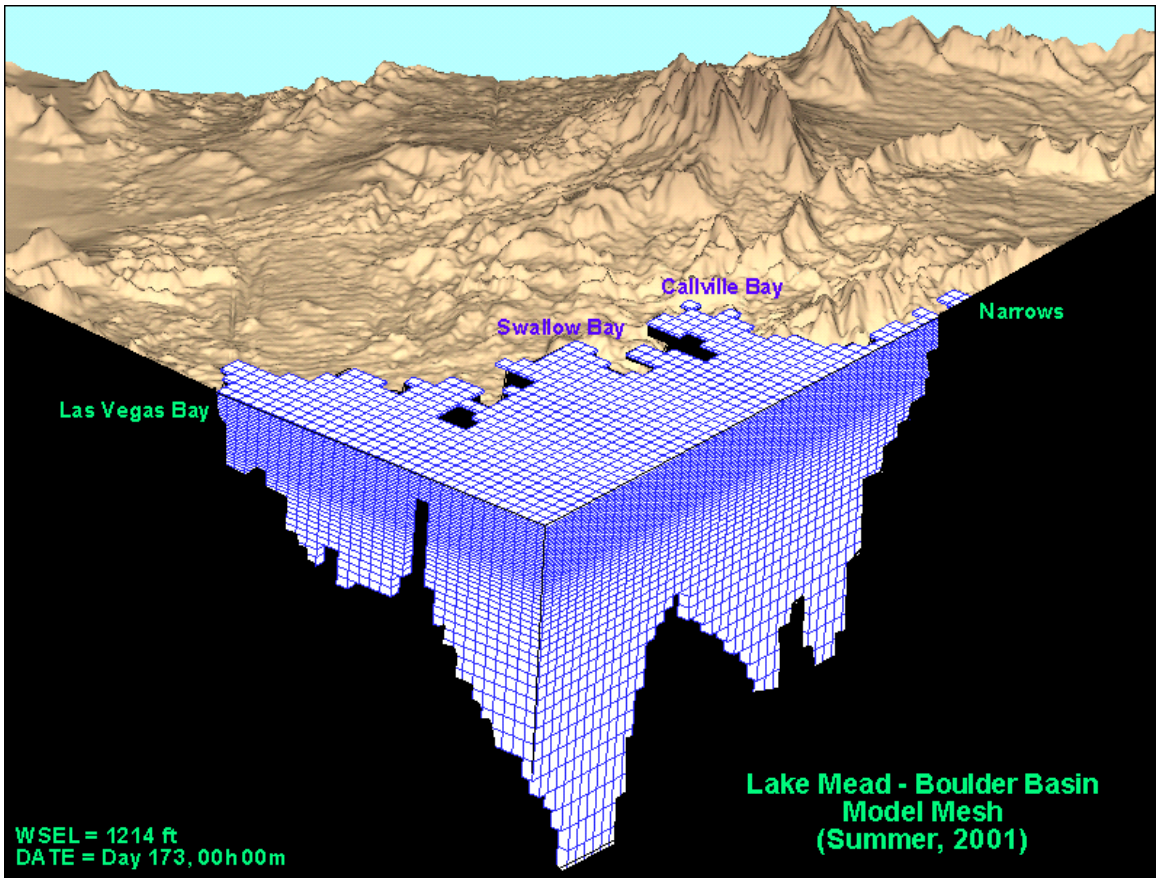

Figure A.3 Model grid for Lake Mead Boulder Basin model.

As part of the EIS process, a model review panel met monthly for two years to review the validation of the ELCOM/CAEDYM model, its calibration against field data, and its application. The modeling committee approved the use of the model. Subsequently, a scientific Water Quality Advisory Panel concluded that the ELCOM/CAEDYM model was applicable and acceptable. The members of the Water Quality Advisory Panel were diverse and included Jean Marie Boyer, Ph.D., P.E. (Water Quality Specialist/Modeler, Hydrosphere), Chris Holdren, Ph.D., CLM (Limnologist, United States Bureau of Reclamation), Alex Horne, Ph.D. (Ecological Engineer, University of California Berkeley), and Dale Robertson, Ph.D. (Research Hydrologist, United States Geological

Survey). More specifically, the Water Quality Advisory Panel agreed on the following findings:

- The ELCOM/CAEDYM model is appropriate for the project.
- There are few three-dimensional models available for reservoirs. ELCOM is one of the best hydrodynamic models and has had good success in the Boulder Basin of Lake Mead and other systems.
- The ELCOM model accurately simulates most physical processes.
- The algorithms used in CAEDYM are widely accepted (a biological consultant, Professor David Hamilton of The University of Waikato, New Zealand, was retained to review the CAEDYM coefficients and algorithms).

The Boulder Basin ELCOM/CAEDYM model was calibrated against four years of measured data for numerous physical and water quality parameters including temperature, salinity, conductivity, dissolved oxygen, pH, nutrients (nitrogen and phosphorus), chlorophyll *a*, perchlorate, chloride, sulfate, bromide, and total organic carbon. Detailed results of this calibration and the subsequent evaluation of alternative discharge scenarios were made available in late 2005 in the CWC EIS that was being prepared for this project. An example of the calibration results for chlorophyll *a* for 2002 is presented in **Figure A.4** below. In this figure, simulated concentrations are compared against field data measured in the lake by the United States Bureau of Reclamation (USBR) and the City of Las Vegas (COLV).

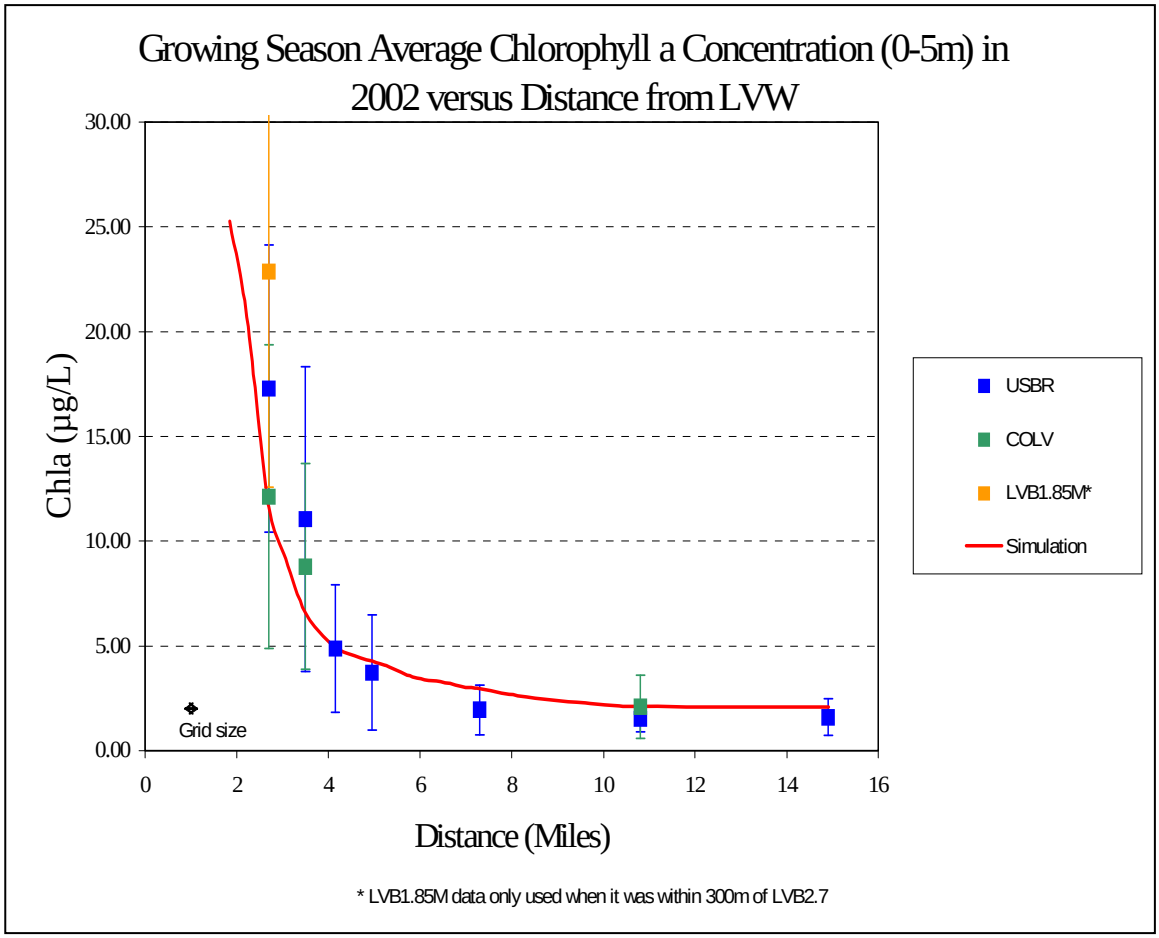

Figure A.4 ELCOM/CAEDYM calibration results for chlorophyll a in Boulder Basin for 2002 as a function of distance from the inflow at Las Vegas Wash.

Most recently, the original Boulder Basin model was extended to include all of Lake Mead, including the Overton Arm and Gregg Basin. The extended whole lake ELCOM/CAEDYM model has been calibrated against nine (9) years of data for use in informing design and operations management decisions. Specifically, the model has been used to simulate temperature (including stratification patterns), salinity, conductivity, dissolved oxygen, nutrients, chlorophyll *a* (as a surrogate for algae), perchlorate, total organic carbon, bromide, and suspended solids. **Figure A.5** below shows the extent of the expanded whole lake domain and the calibration results for conductivity for February 2005.

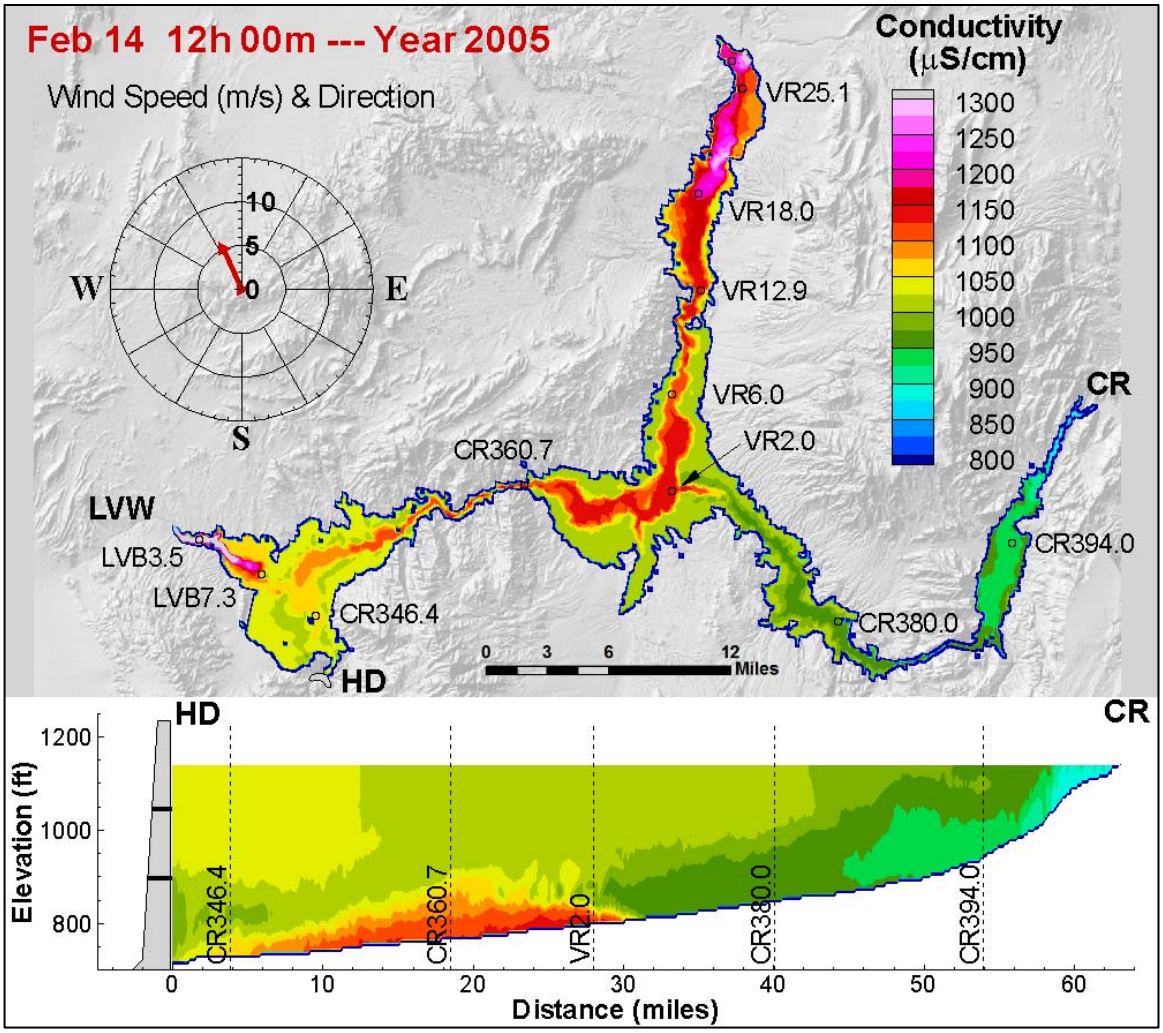

Figure A.5 ELCOM/CAEDYM calibration results for conductivity in the Lake Mead Whole Lake Model (including plan view of entire lake and cross-section from Hoover Dam to the mouth of the Colorado River).

ELCOM/CAEDYM model of the entire Lake Mead is being continually updated and calibrated on approximately a yearly basis, with funding having been provided by the CWC, the Southern Nevada Water Authority, and the National Park Service. These various stakeholders have demonstrated a long term commitment to maintaining the model because it has proven to be a worthy and successful tool. Additional funding for

ELCOM/CAEDYM modeling of the impacts of climate change on Lake Mead is being provided by the USBR under the WaterSMART grant program.

A.1.3.2.2*Lake Burragorang (New South Wales, Australia)*

ELCOM was applied and validated for Lake Burragorang in order to rapidly assess the potential impacts on water quality during an underflow event (CWR). Underflows usually occur during the winter when inflow water temperature is low compared to the reservoir. This causes the upheaval of hypolimnetic water at the dam wall, and as a result it transports nutrient rich waters into the euphotic zone.

The thermal dynamics during the underflow event were reproduced accurately by ELCOM for the case with idealized bathymetry data with coarse resolutions (straightened curves and rotating the lake in order to bypass the resolution problem), but not for the simulation with the complex, actual bathymetry. This is because the model tests showed that the ability to model underflows is severely constrained by the cross-channel grid resolution. When the cross-channel direction is poorly resolved at bends and curves, an underflow is unable to propagate downstream without a significant loss of momentum. Nevertheless, the simulations with the coarse idealized domain certainly can be used as aids and tools to visualize the behavior of reservoirs. Particularly, ELCOM was able to capture the traversal of the underflow down the length of Lake Burragorang and then had sufficient momentum to break against the wall causing the injection of underflow waters into the epilimnion near the dam. This simulated dynamic was in agreement with what was measured in the field.

A.1.3.2.3*Lake Kinneret (Israel)*

ELCOM was applied to model basin-scale internal waves that are seen in Lake Kinneret, Israel, since understanding of basin-scale internal waves behaviors provide valuable information on mixing and transport of nutrients below the wind-mixed layer in stratified lakes. In studies done by Hodges et al. (1999) and Laval et al (2003), the ELCOM simulation results were compared with field data under summer stratification conditions to identify and illustrate the spatial structure of the lowest-mode basin-scale Kelvin and Poincare waves that provide the largest two peaks in the internal wave energy spectra. The results demonstrated that while ELCOM showed quantitative differences in the amplitude and steepness of the waves as well as in the wave phases, the basin-scale waves were resolved very well by ELCOM. In particular, the model captures the qualitative nature of the peaks and troughs in the thermocline and the depth of the wind-mixed layer at relatively coarse vertical grid resolutions (Hodges et al, 1999).

A.1.3.2.4 *Lake Pamvotis (Greece)*

ELCOM/CAEDYM was applied to Lake Pamvotis, a moderately sized (22 km^2), shallow (4 m average depth) lake located in northwest Greece. Since the lake has undergone eutrophication over the past 40 years, many efforts are directed at understanding the characteristics of the lake and developing watershed management and restoration plans.

Romero and Imberger (1999) simulated Lake Pamvotis over a one month period during May to June, 1998, and compared the simulated thermal and advective dynamics of the lake with data obtained from a series of field experiments. The simulation results over-predicted heating; however, diurnal fluctuations in thermal structures were similar to those measured. Since the meteorological site was sheltered from the winds, the wind data used in the simulation was believed to be too low, causing insufficient evaporative heat-loss and subsequent over-heating by ELCOM. An increase in the wind speed by a factor of three gave temperature profiles in agreement with the field data. Moreover, the study demonstrated that the model is capable of predicting the substantial diurnal variations in the intensity and direction of both vertical and horizontal velocities. Romero and Imberger were also able to illustrate the functionality of ELCOM when coupled to the water quality model, CAEDYM, and confirmed that the model could be used to evaluate the effect of various strategies to improve poor water quality in localized areas in the lake.

A.1.3.2.5 *Lake Constance (Germany, Austria, Switzerland)*

Appt (2000) and Appt et al. (2004) applied ELCOM to characterize the internal wave structures and motions in Lake Constance [Bodensee] since internal waves are a key factor in understanding the transport mechanisms for chemical and biological processes in a stratified lake such as Lake Constance. Lake Constance is an important source of drinking water and a major tourism destination for its three surrounding countries of Germany, Austria, and Switzerland. Due to anthropogenic activities and climatic changes, Lake Constance water quality has deteriorated and its ecosystem has changed.

It was shown that ELCOM was able to reproduce the dominant internal wave and major hydrodynamic processes occurring in Lake Constance. For instance, three types of basin-scale waves were found to dominate the wave motion: the vertical mode-one Kelvin wave, the vertical mode-one Poincare waves, and a vertical mode-two Poincare wave. Moreover, an upwelling event was also reproduced by ELCOM suggesting that the width and length ratio of the basin, spatial variations in the wind, and Coriolis effects play critical roles in the details of the upwelling event. This on-going research has shown

that ELCOM can be used as a tool to predict and understand hydrodynamics and water quality in lakes.

A.1.3.2.6 *Venice Lagoon (Italy)*

ELCOM/CAEDYM is being used to develop a hydrodynamic and sediment transport model of Venice Lagoon, Italy, since future gate closures at the mouth of the lagoon are likely to impact flushing patterns. This project is an integral part of the Venice Gate Projects in Italy that was launched in May 2003 to prevent flooding.

ELCOM was validated for the tidal amplitude and phase using the data obtained from 12 tidal stations located throughout the lagoon (Yeates, 2004). Remaining tasks include model validation of temperature, salinity, and velocity against measurements made in the major channels of the lagoon.

A.1.3.2.7 *Silvan Reservoir (Australia)*

ELCOM is currently being applied to reproduce the circulation patterns observed in Silvan Reservoir, Australia, during a field experiment that was conducted in March 2004 to determine the transport pathways in the lake. This experiment confirmed the upwelling behavior of the lake and the strong role of the inflows in creating hydraulic flows in the reservoir (Antenucci, 2004).

A.1.3.2.8 *Billings and Barra Bonita Reservoirs (Brazil)*

ELCOM/CAEDYM is being applied to Billings and Barra Bonita Reservoirs in Brazil. Billings Reservoir is an upstream reservoir that feeds Barra Bonita via the Tiete River. The objective of the project is to develop an integrated management tool for these reservoirs and river reaches for use in the future planning of water resource utilization in Sao Paulo, Brazil (Romero and Antenucci, 2004).

A.1.3.2.9 *Lake Coeur D'Alene (Idaho, USA)*

ELCOM/CAEDYM is being applied to investigate the trade-off between reducing heavy metal concentrations and a potential increase in eutrophication due to remediation procedures in Lake Coeur D'Alene, Idaho. In order to investigate heavy metal fate and transport, CAEDYM is being improved further to include heavy metals and a feedback loop to phytoplankton based on metal toxicity (Antenucci, 2004).

A.1.3.2.10 *Seawater Desalination at Encina (California, USA)*

Flow Science conducted ELCOM modeling in 2004-2006 for a proposed desalination facility to be sited adjacent to the Encina Power Plant in Carlsbad, California. The proposed Encina facility involved source water taken from inside Agua Hedionda Lagoon and discharge of brines with the power plant cooling water via a surface channel across the beach south of the lagoon mouth. Flow Science used both a fine grid model to simulate water quality and dilution local to the intake and outfall and a larger grid model to simulate the effect of treated wastewater discharges and ocean currents and tides in the ocean near the lagoon. For the Encina study, Flow Science also used ELCOM to predict mixing in the vicinity of the plant discharge. The study area encompassed about 100 square miles of the ocean and also included some inland lagoons. The model resolved various tidal conditions and plant operating scenarios. The model compared favorably to existing oceanic data in the vicinity of the discharge.

A.1.3.2.11 *Moss Landing Desalination Project (California, USA)*

Flow Science applied ELCOM to simulate the flow and mixing in the entire Monterey Bay, including Elkhorn Slough. The purpose of the modeling was to evaluate the impacts of the proposed Moss Landing Desalination facility on receiving waters. The desalination facility was proposed to utilize a nearby existing power plant intake in Moss Landing Harbor and discharge to the ocean via the power plant's existing outfall, which is a submerged outfall located in Monterey Bay offshore of the harbor entrance. The ELCOM model resolved the details of the mixing in the vicinity of the power plant/desalination facility combined discharge. The model results compared favorably to existing measured water quality parameters. The results were used to determine compliance with water quality regulations for the combined outfall. The study was performed in 2004-2006.

A.1.3.2.12 *Lake Perris (California, USA)*

In 2005, ELCOM was applied to Lake Perris in order to compare the impacts of several recreational use strategies on measured fecal coliform concentrations at the reservoir outlet tower. The physical results of the simulation were validated against measured temperature and salinity data over a one-year period. The comparison of fecal coliform concentrations against measured data was fair due to a lack of data describing the timing and magnitude of loading and the settling and re-suspension of fecal matter.

The ELCOM model was expanded in 2006 - 2007 to include CAEDYM in order to evaluate the performance of a proposed hypolimnetic oxygenation system and observed

water quality benefits. The model was calibrated against two years of historical data and used to assess the magnitude and extent of oxygenation in the hypolimnion as a result of system operation. Impacts on dissolved oxygen concentrations and nutrient dynamics and algal production potential (as represented by chlorophyll *a*) were also evaluated, and recommendations were provided for final design of the system. The project has not yet been constructed due to seismic safety risks with the dam that must first be addressed.

A.1.3.2.13 *Lake Hodges and Olivenhain Reservoir (California, USA)*

The San Diego County Water Authority (SDCWA) is planning a tunnel connection between Lake Hodges and Olivenhain Reservoir. The tunnel and an associated hydroelectric turbine will allow for operation of the two reservoirs as part of a pumped storage project. Due to the difference in water quality between the two reservoirs, the SDCWA was concerned that the planned pumped storage project could adversely impact water quality in Olivenhain Reservoir. In order to evaluate the water quality impacts of the planned pumped storage operations on Olivenhain Reservoir, Flow Science developed a coupled ELCOM model of the two reservoirs in 2007-2008 to simulate temperature and salinity and several tracers in order to characterize the extent of mixing of the pumped storage inflow water from Lake Hodges within Olivenhain Reservoir and the percentages of Lake Hodges and Olivenhain Reservoir water throughout each reservoir due to the pumped storage operations and subsequent mixing.

A.1.3.2.14 *Lower San Gabriel River, Intake Channel, and Alamitos Bay (California, USA)*

The Los Angeles Department of Water and Power (LADWP) Haynes Generating Station (HnGS) and AES Generating Station (AES) each utilize three outfalls located on the east and west bank of the Lower San Gabriel River, respectively, and discharge cooling water to the Lower San Gabriel River Flood Control Channel (LSGR). Flow Science conducted ELCOM modeling from 2003-2010 to evaluate the mixing of flows within the river channel and found that, under typical operating conditions, the cooling water discharges form a “barrier” between freshwater from the upstream river channel and ocean water downstream of the LSGR. Both modeling and field work (conducted by others) confirmed that the net direction of flow downstream of HnGS and AES is downstream, even during flood tide conditions. Flow Science’s modeling also evaluated temperature, salinity, and mixing in the LSGR for a wide range of potential future conditions and for hypothetical conditions in which both HnGS and AES cooling water flows are removed from the LSGR. Water quality in the adjacent Alamitos Bay, which is strongly influenced by flushing induced by cooling water flows from HnGS and AES, was also evaluated using ELCOM. In addition, Flow Science used CAEDYM to evaluate

nutrient concentrations, algae, and dissolved oxygen within the Bay for a range of actual and potential future operating conditions. The HnGS Intake Channel (which connects Alamitos Bay to HnGS) was also evaluated with ELCOM/CAEDYM.

Results of the Flow Science analyses have been used by LADWP in NPDES permit discussions with the Regional Water Board, in CEQA evaluations supporting the potential future repowering of HnGS Units 5 and 6, and in comments on the State's draft Once-Through Cooling (OTC) policy.

A.1.3.2.15 *Joint Water Pollution Control Plant Outfall Evaluation (California, USA)*

The Sanitation Districts of Los Angeles County (LACSD) are conducting a detailed study to evaluate the feasibility of a proposed new ocean outfall to carry treated wastewater from the Joint Water Pollution Control Plant (JWPCP) in Carson, California, to an ocean discharge location off the southern California coast near the Palos Verdes and San Pedro Shelves. As part of the Feasibility Study, Flow Science developed an ELCOM model in 2007 to evaluate the impact of this proposed ocean outfall. The near-field effluent discharge model, NRFIELD2, coupled with the far field hydrodynamic model, ELCOM, was used to simulate the mixing and determine the concentrations of a conservative effluent tracer and various indicator bacteria (assuming no chlorination). The coupled model was validated using measured current and temperature data in the vicinity of the potential discharge sites. The water quality impacts of five proposed diffuser discharge sites were evaluated, and the modeling results will be used by LACSD to estimate concentrations of indicator bacteria at selected locations at the shore and inshore regions that would result from a discharge without chlorination. Ongoing ELCOM modeling will be performed to assist LACSD in selecting a preferred diffuser location. An example of the simulated effluent tracer concentrations during summer for one of the potential diffuser sites is presented in **Figure A.6** below.

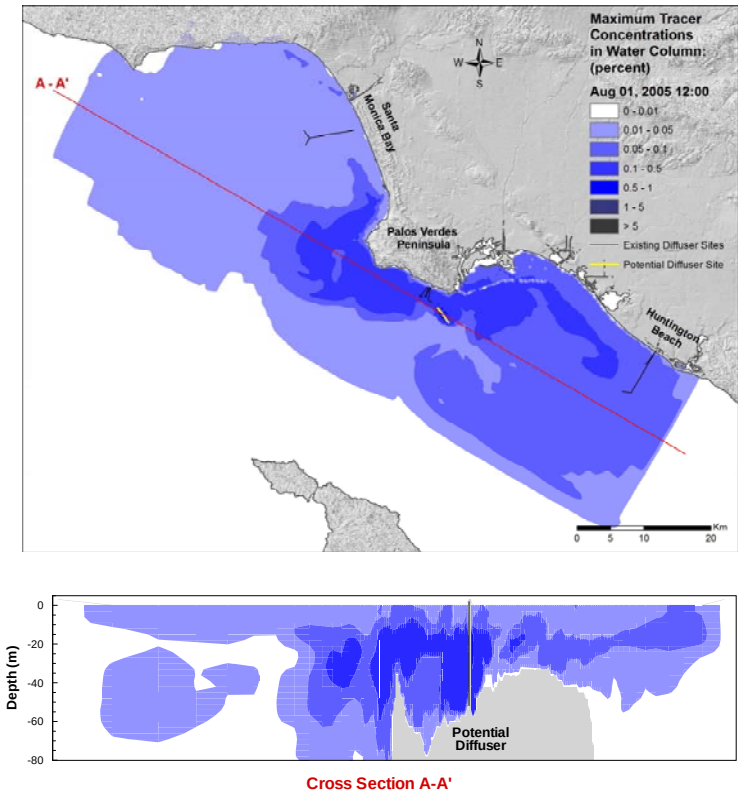

Figure A.6 Plan and section views of ELCOM simulated effluent tracer concentrations from proposed diffuser Site 1 in summer (August 1, 2005).

A.1.3.2.16 *San Vicente Reservoir (California, USA)*

Flow Science is assisting the City of San Diego in assessing the mixing and dilution potential resulting from the potential injection of highly treated effluent into San Vicente Reservoir. In 2010, Flow Science developed an ELCOM/CAEDYM model to assess the mixing and dispersion properties in San Vicente Reservoir as well as a field program to validate the modeling. The ELCOM/CAEDYM model includes temperature, salinity, conductivity, dissolved oxygen, nutrients, chlorophyll *a* (as a surrogate for algae), and multiple tracers. The model provides an accurate three-dimensional representation of water quality within the reservoir. The model was calibrated for the reservoir at its

current capacity against two years of historical data. The calibrated model has since been applied to the expanded reservoir to evaluate the impacts of the advanced water treatment (AWT) water. The model is being used to predict water quality conditions in the future enlarged reservoir and will also be used to help manage water quality in the enlarged reservoir once it is filled. The work is being reviewed by an expert panel being overseen by the National Water Research Institute. The panel is expected to complete its review and accept the use of the modeling.

A.1.3.2.17 *Los Vaqueros Reservoir (California, USA)*

In conjunction with the Contra Costa Water District (CCWD), Flow Science developed a three-dimensional ELCOM/CAEDYM model of Los Vaqueros Reservoir beginning in 2006 that is capable of providing an accurate, three-dimensional representation of water quality including temperature, salinity/TDS, nutrients and algae. The ELCOM model was calibrated against two years of historical data and validated against four years of data, while the CAEDYM model was calibrated for four years of historical data. **Figure A.7** shows a comparison of the measured versus simulated annual and growing season average chlorophyll *a* concentrations which show very good agreement. In ongoing work, Flow Science is using the ELCOM/CAEDYM model to evaluate the water quality of the reservoir under future conditions where the impounding dam is raised. This will expand the capacity of the reservoir from 100,000 acre-ft to 160,000 acre ft. The water quality model is being used to determine the changes in outflow water quality resulting from the expansion and to provide preliminary design recommendations for the inlet/outlet facilities with respect to improving water quality.

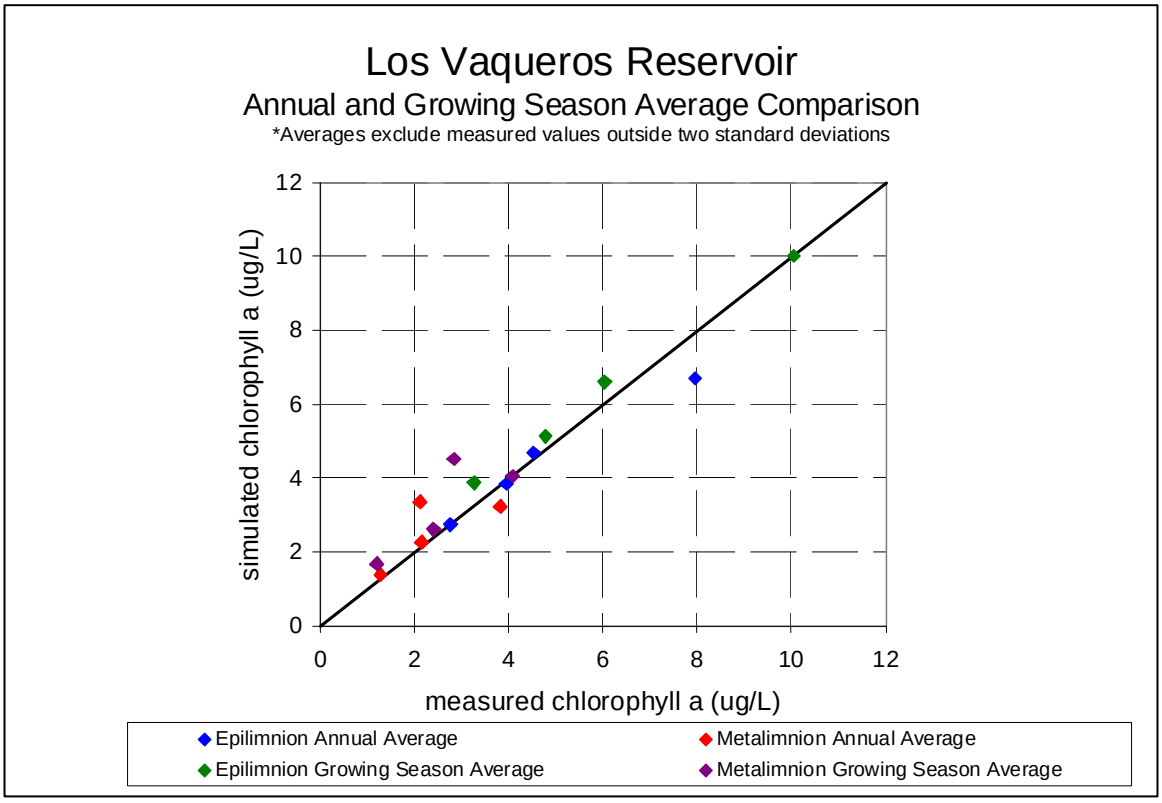

Figure A.7 Comparison of simulated ELCOM/CAEDYM results and measured chlorophyll *a* data for 2006-2009.

A.1.3.2.18 *Other Applications*

Other ELCOM/CAEDYM applications and development in on-going research at CWR include:

- Plume dynamics and horizontal dispersion (Marmion Marine Park, Australia).
- Inflow and pathogen dynamics (Helena, Myponga and Sugarloaf Reservoirs, Australia).
- Mixing and dissipation in stratified environments (Tone River, Japan, and Brownlee Reservoir, USA).

- Tidally forced estuaries and coastal lagoons (Marmion Marine Park and Barbamarco Lagoon, Italy).

- Three-dimensional circulation induced by wind and convective exchange (San Roque Reservoir, Argentina, and Prospect Reservoir, Australia).

- Sea-surface temperature fluctuation and horizontal circulation (Adriatic Sea).

- Response of bivalve mollusks to tidal forcing (Barbamarco Lagoon, Italy).

A.1.4 TECHNICAL DESCRIPTION OF ELCOM

As outlined above, ELCOM solves the unsteady, viscous Navier-Stokes equations for incompressible flow using the hydrostatic assumption for pressure. ELCOM can simulate the hydrodynamics and thermodynamics of a stratified system, including baroclinic effects, tidal forcing, wind stresses, heat budget, inflows, outflows, and transport of salt, heat and passive scalars. Through coupling with the CAEDYM water quality module, ELCOM can be used to simulate three-dimensional transport and interactions of flow physics, biology, and chemistry. The hydrodynamic algorithms in ELCOM are based upon the proven semi-Lagrangian method for advection of momentum with a conjugate-gradient solution for the free-surface height (Casulli and Cheng, 1992) and a conservative ULTIMATE QUICKEST transport of scalars (Leonard, 1991). This approach is advantageous for geophysical-scale simulations since the time step can be allowed to exceed the Courant-Friedrichs-Lewy (CFL) condition for the velocity without producing instability or requiring a fully-implicit discretization of the Navier-Stokes equations.

A.1.4.1 Governing Equations

Significant governing equations and approaches used in ELCOM include:

- Three-dimensional simulation of hydrodynamics (unsteady Reynolds-averaged Navier-Stokes equations).

- Advection and diffusion of momentum, salinity, temperature, tracers, and water quality variables.

- Hydrostatic approximation for pressure.

- Boussinesq approximation for density effects.

- Surface thermodynamics module accounts for heat transfer across free surface.
- Wind stress applied at the free surface.
- Dirichlet boundary conditions on the bottom and sides.

A.1.4.2 Numerical Method

Significant numerical methods used in ELCOM include:

- Finite-difference solution on staggered-mesh Cartesian grid.
- Implicit volume-conservative solution for free-surface position.
- Semi-Lagrangian advection of momentum allows time steps with CFL > 1.0.
- Conservative ULTIMATE QUICKEST advection of temperature, salinity, and tracers.
- User-selectable advection methods for water quality scalars using upwind, QUICKEST, or semi-Lagrangian to allow trade-offs between accuracy and computational speed.
- Solution mesh is Cartesian and allows non-uniformity (*i.e.* stretching) in horizontal and vertical directions.

The implementation of the semi-Lagrangian method in Fortran 90 includes sparse-grid mapping of three-dimensional space into a single vector for fast operation using array-processing techniques. Only the computational cells that contain water are represented in the single vector so that memory usage is minimized. This allows Fortran 90 compiler parallelization and vectorization without platform-specific modification of the code. A future extension of ELCOM will include dynamic pressure effects to account for nonlinear dynamics of internal waves that may be lost due to the hydrostatic approximation.

Because the spatial scales in a turbulent geophysical flow may range from the order of millimeters to kilometers, it is presently impossible to conduct a Direct Navier-Stokes (DNS) solution of the equations of motion (*i.e.* an exact solution of the equations). Application of a numerical grid and a discrete time step to a simulation of a geophysical domain is implicitly a filtering operation that limits the resolution of the equations.

Numerical models (or closure schemes) are required to account for effects that cannot be resolved for a particular grid or time step. There are four areas of modeling in the flow physics: (l) turbulence and mixing, (2) heat budgets, (3) hydrodynamic boundary conditions, and (4) sediment transport.

A.1.4.3 Turbulence Modeling and Mixing

ELCOM presently uses uniform fixed eddy viscosity as the turbulence closure scheme in the horizontal plane (in future versions a Smagorinsky 1963 closure scheme will be implemented to represent subgrid-scale turbulence effects as a function of the resolves large-scale strain-rates). These methods are the classic "eddy viscosity" turbulence closure. With the implementation of the Smagorinsky closure, future extensions will allow the eddy-viscosity to be computed on a local basis to allow improvements in modeling local turbulent events and flow effects of biological organisms (e.g., drag induced by macroalgae or seagrass).

In the present code, the user has the option to extend the eddy-viscosity approach to the vertical direction by setting different vertical eddy-viscosity coefficients for each grid layer. However, in a stratified system, this does not adequately account for vertical turbulent mixing that may be suppressed or enhanced by the stratification (depending on the stability of the density field and the magnitude of the shear stress). To model the effect of density stratification on turbulent mixing the CWR has developed a closure model based on computation of a local Richardson number to scale. The latter is generally smaller than the time step used in geophysical simulations, so the mixing is computed in a series of partial time steps. When the mixing time-scale is larger than the simulation time step, the mixing ratio is reduced to account for the inability to obtain mixing on very short time scales. This model has the advantage of computing consistent mixing effects without regard to the size of the simulation time-step (*i.e.* the model produces mixing between cells that is purely a function of the physics and not the numerical step size).

A.1.4.4 Heat Budget

The heat balance at the surface is divided into short-wave (penetrative) radiation and a heat budget for surface heat transfer effects. The surface heat budget requires user input of the net loss or gain through conduction, convection, and long wave radiation in the first grid layer beneath the free surface. The short wave range is modeled using a user-prescribed input of solar radiation and an exponential decay with depth that is a function of a bulk extinction coefficient (a Beer's law formulation for radiation absorption). This coefficient is the sum of individual coefficients for the dissolved

organics ("gilvin"), phytoplankton biomass concentration, suspended solids, and the water itself. The extinction coefficients can either be computed in the water quality module (CAEDYM) or provided as separate user input.

A.1.4.5 Hydrodynamic Boundary Conditions

The hydrodynamic solution requires that boundary conditions on the velocity must be specified at each boundary. There are six types of boundary conditions: (1) free surface, (2) open edge, (3) inflow-outflow, (4) no-slip, (5) free-slip, and (6) a Chezy-Manning boundary stress model (the latter is presently not fully implemented). For the free surface, the stress due to wind and waves is required. The user can either input the wind/wave stress directly, or use a model that relates the surface stress to the local wind speed and direction *via* a bulk aerodynamic drag coefficient. Open boundaries (e.g. tidal inflow boundaries for estuaries) require the user to supply the tidal signature to drive the surface elevation. Transport across open boundaries is modeled by enforcing a Dirichlet condition on the free-surface height and allowing the inflow to be computed from the barotropic gradient at the boundary. Inflow-outflow boundary conditions (e.g. river inflows) are Dirichlet conditions that specify the flow either at a particular boundary location *or inside the domain*. Allowing an inflow-outflow boundary condition to be specified for an interior position (*i.e.* as a source or sink) allows the model to be used for sewage outfalls or water outlets that may not be located on a land boundary. Land boundaries can be considered zero velocity (no-slip), zero-flux (free-slip) or, using a Chezy-Manning model, assigned a computed stress.

A.1.4.6 Sediment Transport

While sediment transport is fundamentally an issue of flow physics, the algorithms for the sediment transport are more conveniently grouped with the water quality algorithms in CAEDYM. Settling of suspended particulate matter is computed using Stokes law to obtain settling velocities for the top and bottom of each affected grid cell. This allows the net settling flux in each cell to be computed. A two-layer sediment model has been developed that computes resuspension, deposition, flocculation, and consolidation of sediment based on (1) the shear stress at the water/sediment interface, (2) the type of sediment (cohesive/non-cohesive), and (3) the thickness of the sediment layer. Determination of the shear stress at the water/sediment interface requires the computation of bottom shear due to current, wind, and waves. A model has been developed to account for the effects of small-scale surface waves that cannot be resolved on a geophysical-scale grid. This model computes the theoretical wave height and period for small-scale surface waves from the wind velocity, water depth, and domain fetch. From these, the wavelength and orbital velocities are calculated. The wave-induced shear

stress at the bottom boundary resulting from the wave orbital velocities is combined with a model for the current-induced shear stress to obtain the total bottom shear that effects sediment resuspension. The cohesiveness of the sediment determines the critical shear stresses that are necessary to resuspend or deposit the sediments. A model of consolidation of the sediments is used to remove lower sediment layers from the maximum mass that may be resuspended.

A.1.5 TECHNICAL DESCRIPTION OF CAEDYM

CAEDYM is an outgrowth of previous CWR water quality modules in DYRESM-WQ and the Estuary Lake Model - Water Quality (ELMO-WQ) codes. CAEDYM is designed as a set of subroutine modules that can be directly coupled with one, two, or three-dimensional hydrodynamic "drivers", catchment surface hydrological models, or groundwater models. Additionally, it can be used in an uncoupled capacity with specification of velocity, temperature, and salinity distributions provided as input files rather than as part of a coupled computation. The user can specify the level of complexity in biogeochemical process representation so both simple and complex interactions can be studied. Direct coupling to a hydrodynamic driver (e.g. ELCOM) allows CAEDYM to operate on the same spatial and temporal scales as the hydrodynamics. This permits feedbacks from CAEDYM into ELCOM for water quality effects such as changes in light attenuation or effects of macroalgae accumulation on bottom currents. **Figure A.8** shows an illustration of the interactions of modeled parameters in CAEDYM. Being an “N-P-Z” (nutrient-phytoplankton-zooplankton) model, CAEDYM can be used to assess eutrophication. Unlike the traditional general ecosystem model, CAEDYM serves as a species- or group-specific model (*i.e.* resolves various phytoplankton species). Furthermore, oxygen dynamics and several other state variables are included in CAEDYM.

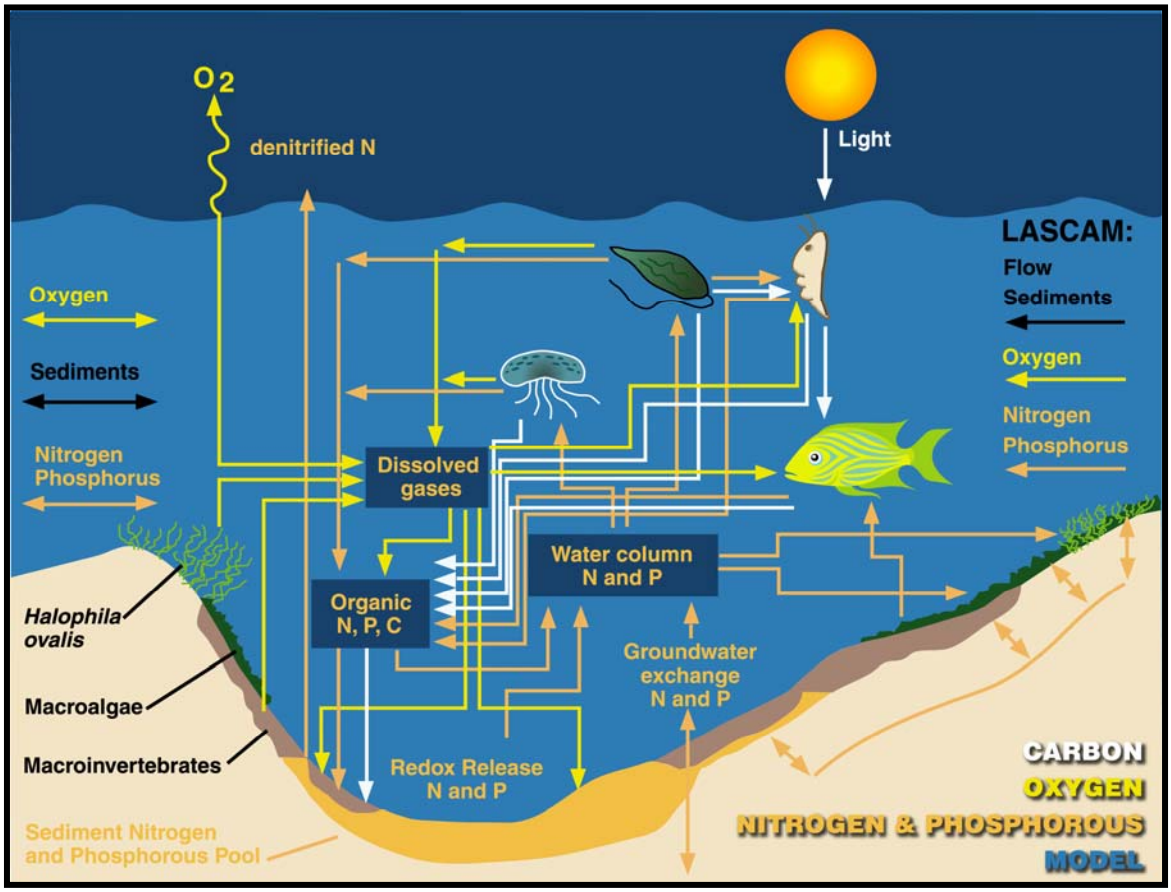

Figure A.8 Illustration of interactions of modeled parameters in CAEDYM.

The representation of biogeochemical processes in ecological models has, historically, been treated in a simple manner. In fact, the pioneering work on modeling marine ecosystems (Riley et al, 1949; Steel, 1962) is still used as a template for many of the models that are currently used (Hamilton and Schladow, 1997). The level of sophistication and process representation included in CAEDYM is of a level hitherto unseen in any previous aquatic ecosystem model. This enables many different components of the system to be examined, as well as providing a better representation of the dynamic response of the ecology to major perturbations to the system (e.g. the response to various management strategies). **Figure A.9** shows the major state variables included in the CAEDYM model. Using CAEDYM to aid in management decisions and system understanding requires (1) a high level of process representation, (2) process

interactions and species differentiation of several state variables, and (3) applicability over a spectrum of spatial and temporal scales. The spectrum of scales relates to the need for managers to assess the effects of temporary events, such as anoxia at specific

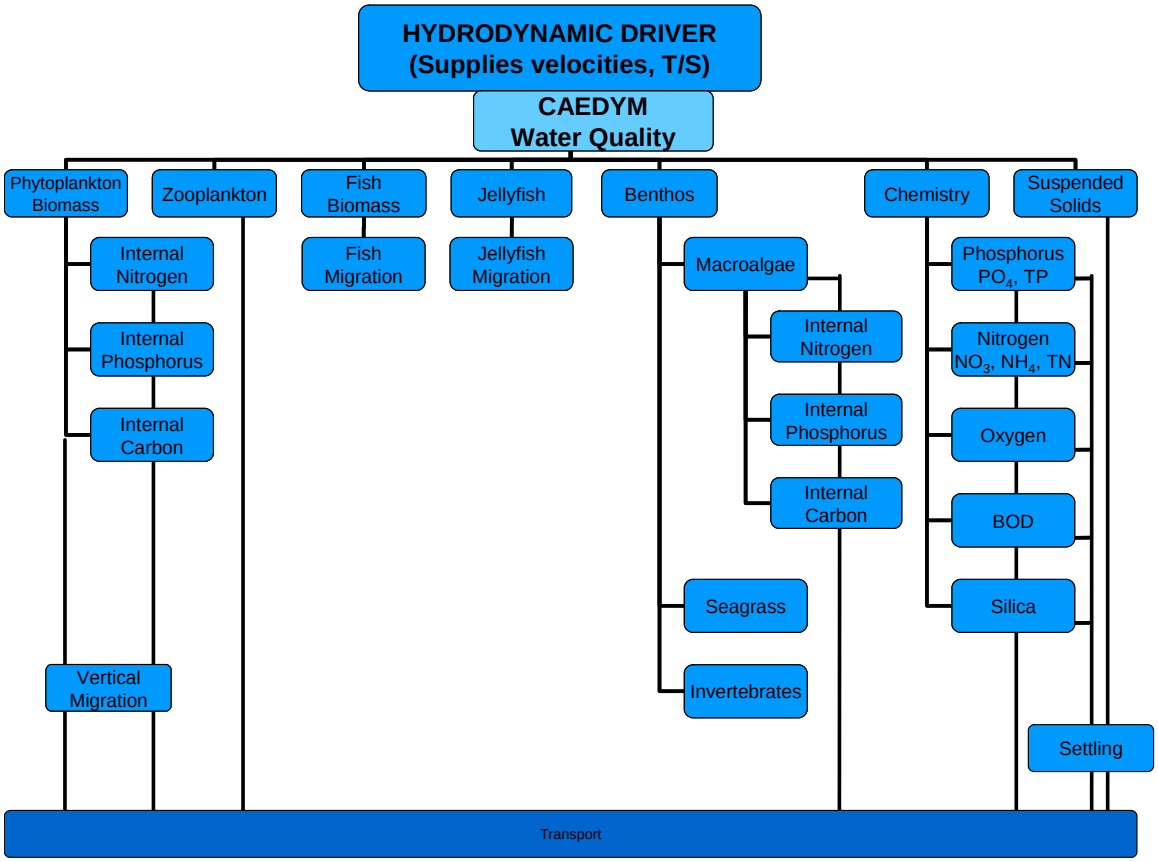

Figure A.9 Major state variables included in the CAEDYM model.

locations, through to understanding long-term changes that may occur over seasons or years. There is considerable flexibility in the time step used for the ecological component. Long time steps (relative to the hydrodynamic advective scale) may be used to reduce the frequency of links to ELCOM when long-term (*i.e.* seasonal or annual) simulations are run.

A.1.5.1 Biological Model

The biological model used in CAEDYM consists of seven phytoplankton groups, five zooplankton groups, six fish groups, four macroalgae groups and three invertebrate groups, as well as models of seagrass and jellyfish. This set will be expanded as biological models are developed, tested, and calibrated to field data. There is flexibility for the user in choosing which species to include in a simulation. Vertical migration is simulated for motile and non-motile phytoplankton, and fish are migrated throughout the model domain according to a migration function based on their mortality. A weighted grazing function is included for zooplankton feeding on phytoplankton and fish feeding on zooplankton. The biomass grazed is related to both food availability and preference of the consumer for its food supply. Improved temperature, respiration and light limitation functions have been developed to represent the environmental response of the organisms. The benthic processes included a self-shading component and beach wrack function for macroalgae, sediment bioturbation and nutrient cycling by polychaetes, and effects of seagrass on sediment oxygen status.

In particular, the seven phytoplankton groups modeled are dinoflagellates, freshwater diatoms, marine/estuarine diatoms, freshwater cyanobacteria, marine estuarine cyanobacteria, chlorophytes, and cryptophytes. Phytoplankton biomass is represented in terms of chlorophyll *a*. Phytoplankton concentrations are affected by the following processes:

- Temperature growth function
- Light limitation
- Nutrient limitation by phosphorus and nitrogen (and when diatoms are considered, silica)
- Loss due to respiration, natural mortality, excretion, and grazing
- Salinity response
- Vertical migration and settling

A.1.5.2 Nutrients, Metals, and Oxygen Dynamics

The transport and chemical cycling of nutrients is an important part of simulating the interaction of biological organisms in an ecosystem. CAEDYM includes as state variables the following:

- Nutrients (dissolved inorganic phosphorus, total phosphorus, total nitrogen, ammonium nitrate, and silica).
- Dissolved oxygen and biochemical oxygen demand.
- Metals (dissolved and particulate forms of iron and manganese).
- Suspended sediment (the particulate and colloidal fractions).
- pH

The model incorporates oxygen dynamics and nutrient cycling in both the sediments and water column. A sediment pool of organic detritus and inorganic sediments, both of which may be resuspended into the water column, is included. Redox-mediated release of dissolved nutrients is simulated from the sediments to the water column.

Processes included in the water and sediment oxygen dynamics include:

- Atmospheric exchange (Wanninkhof, 1992).
- Oxygen production and consumption through phytoplankton, macroalgae, and seagrass/macrophyte photosynthesis and respiration, respectively.
- Utilization of dissolved oxygen due to respiration of higher organisms such as zooplankton and fish and due to photosynthesis and respiration in jellyfish
- Water column consumption of oxygen during nitrification.
- Biochemical oxygen demand due to mineralization of organic matter in the water column and in the sediments.

Oxygen flux from the water column to the sediments, sediment oxygen demand (SOD), as developed from Fick's law of diffusion.

The last two processes are used together with a sediment porosity and diffusion coefficient (Ullman and Aller, 1982) in order to define the depth of the toxic layer in the sediments.

Nutrient processes included in the sediment and water column dynamics include:

- Phytoplankton nutrient uptake, with provision for luxury storage of nutrients.
- Release of dissolved inorganic nutrients from phytoplankton excretion.
- Excretion of nutrients as fecal material by zooplankton.
- Nitrification and denitrification by bacterial mediated action.
- Generation of inorganic nutrients from organic detritus.
- Transfer of nutrients through the food chain (e.g. phytoplankton--zooplankton--fish).
- Uptake of nutrients by macroalgae and seagrasses.
- Adsorption/desorption of nutrients from inorganic suspended sediments.
- Sediment/water transfer of nutrients (*via* such processes as sediment resuspension, sedimentation, redox-mediated nutrient release, and bioturbation).

In essence, CAEDYM represents the type of interactive processes that occur amongst the ecological and chemical components in the aquatic ecosystem. As a broad generalization, one component of the system cannot be manipulated or changed within the model without affecting other components of the system. Similarly in nature, changing an integral component in the aquatic system will have wide-ranging and follow-on effects on many of the other system components. CAEDYM is designed to have the complexity and flexibility to be able to handle the continuum of responses that will be elicited as components of a system that are manipulated. Thus, the model represents a valuable tool to examine responses under changed conditions, as for example, when new approaches to managing an ecosystem are adopted.

A.2 DESCRIPTION OF ELCOM/CAEDYM/VISUAL PLUMES (ECP)

A.2.1 INTRODUCTION

Outfalls are commonly used to discharge treated effluent into open waters. The hydrodynamics of an effluent discharged through an outfall can be conceptualized as a mixing process occurring in two separate regions: a near-field region and a far-field region. In the near-field region the effluent generally experiences a significant amount of mixing, and dilution occurs very rapidly. In this region, the initial jet characteristics of momentum flux, buoyancy flux, flow rate, as well as outfall geometry greatly influence the effluent trajectory and degree of mixing (Fischer et al, 1979). As the effluent plume travels further away from the source, the source characteristics become less important and the far-field region is attained. Mixing of the effluent plume in this region is caused by spatial and temporal variations of ambient velocity fields and dilution generally occurs slowly over a long distance, but may be rapid if there is a high degree of turbulence in the environment.

Due to different dominant temporal and spatial scales of flow velocity and effluent concentration in the near and far field region, a complete model that accounts for all important spatial and temporal scales in both the near-field and far-field regions is not feasible. Instead, these two regions are usually treated by separate models termed the near-field model and the far-field model respectively.

The near-field model has been under intensive study from the 1950s through the early 1990s. Thorough reviews of these studies are provided by Fischer et al. (1979), Baumgartner et al. (1994), and Roberts et al. (1989 a, b, c). These studies have produced a number of near-field models that were verified by both field and laboratory data. Among them, Visual Plumes (VP or PLUMES), endorsed by the U.S. Environmental Protection Agency (USEPA), is the most popular model and has been widely used by regulatory agencies and outfall designers to estimate the near-field dilution.

A variety of models can be used to model far-field mixing processes. These include ELCOM/ CAEDYM, Princeton Ocean Model (POM), and MIT General Circulation Model (MITGCM). All of these models obtain a velocity field from the numerical calculation of the equations of motion and account for influences by tide, wind stress, and pressure gradient due to free surface gradients (barotropic) or density gradients (baroclinic). Given the velocity field, the pollutant concentration field is

typically obtained by solving the Eulerian advective diffusion equation in three dimensions or by using the Lagrangian particle-tracking method.

In simple water bodies with well-defined uni-directional current regimes, the use of near-field models alone may suffice to evaluate a design of an outfall discharge that meets regulations. However, in regions with multiple current regimes (inertial, tide, wind, and buoyancy driven) and with large pollutant loadings, especially where several sources may interact, near-field models must be supplemented by far-field transport and water quality models. The latter are capable of prediction, over a greater distance in the water body, of the concentration distributions for different pollutants, nutrients, and other bio-chemical parameters. They do not, however, have the high spatial resolution that is required to predict near-field mixing processes. Thus, a coupled approach is necessary. In the following sections, a method of coupling the near-field model PLUMES and the far-field model ELCOM/CAEDYM is discussed. The coupled code is referred to as ELCOM/CAEDYM/PLUMES (ECP). Note that there is no standard procedure for the coupling of near and far field models and the coupling procedure varies from code to code mainly because of the different code structures among all of the near-field and far-field models.

A.2.2 NEAR-FIELD MODEL – PLUMES

PLUMES is an interface program that contains the near-field models such as the Roberts, Snyder, and Baumgartner model (RSB) and UM and CORnell MIXing Zone Expert System (CORMIX) (Baumgartner et al., 1994). In ECP, the UM model is chosen to simulate near-field dilution. The UM model is an integral near-field model that uses one-dimensional conservation equations for mass, momentum, salinity and temperature, to model the growth of the plume once the effluent has left the port. Assumptions are made about the shape of the plume and the distribution of pollutant concentration within the plume. Several mechanisms of entrainment such as aspirated, forced, and turbulent diffusion are considered. Both positively and negatively buoyant plumes, single source and multi-port diffuser configurations can be modeled. Model outputs include average dilution, centerline dilution, and horizontal distance of the effluent plume. The major limitation of UM lies in the assumption of an infinite receiving water body, similar to all other available integral-type models (e.g. RSB model). Thus, UM should only be used for deep-water outfalls without boundary interactions. More details on UM and PLUMES can be found in Baumgartner et al. (1994).

A.2.3 FAR-FIELD MODEL – ELCOM/CAEDYM

ELCOM is a three-dimensional hydrodynamic model for lakes and reservoirs and is used to predict the velocity, temperature, and salinity distribution in natural water bodies subjected to external environmental forcing, such as wind stress, surface heating, or cooling. Through coupling with the CAEDYM water quality module, ELCOM can be used to simulate three dimensional transport and interactions of flow physics, biology, and chemistry. ELCOM/CAEDYM is the chosen far-field model in ECP.

A.2.4 COUPLING PLUMES AND ELCOM/CAEDYM

The adopted coupling procedure is based on four steps: ambient conditions modeling, near-field modeling, coupling of near-field and far-field models, and far-field modeling.

1. Ambient conditions modeling

   The near-field model, UM, needs the input of ambient conditions such as the prevailing velocity, temperature, and salinity profiles in the vicinity of the outfall. These profiles are extracted from the ELCOM/CAEDYM simulation at the beginning of a time step at a vertical column of grid cells containing or overlapping the diffuser (the "Diffuser Cell Column" in **Figure A.10**). The depth of the diffuser is also updated based on the surface elevation at that time step.

2. Near-field modeling

   The UM model is applied at each time step using the ambient conditions extracted from ELCOM/CAEDYM. Furthermore, effluent data is obtained from input files for ELCOM/CAEDYM, and the diffuser geometry is specified in the input file called "diffuser_config.dat." The UM model is modified to consider the trapping or surfacing of the plume as the end of the near-field region. The computed average dilution along the trajectory of the plume is then stored for the following coupling step.

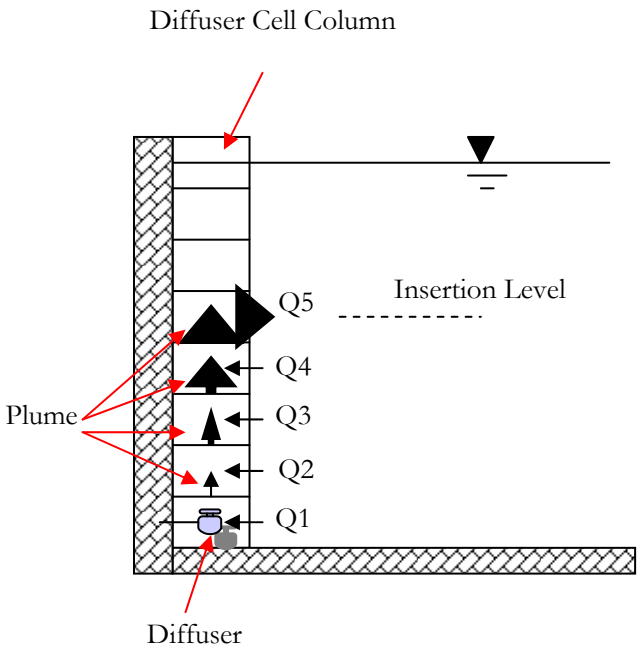

Figure A.10 Schematic of coupling procedure for near-field and far-field models.

3. Coupling of near-field and far-field models

After identifying the "Diffuser Cell Column" (**Figure A.10**), the dilution in each of the cells along this column can be calculated from the linear interpolation of results from UM. Water is then withdrawn from each of these cells based on the dilution occurring in the cell. This withdrawn water is then mixed with the effluent to form the effluent plume and passed to the cell above. Finally, the diluted effluent is then inserted into the cell where the UM model indicates the occurrence of trapping or surfacing (**Figure A.10**). Flow rate, temperature, salinity, and tracer concentrations within this inserted inflow are determined by mass conservation.

4. Far-field modeling

ELCOM/CAEDYM treats the previous coupling process as a series of outflows and inflows along the "Diffuser Cell Column" and proceeds with its time-marching far-field simulation for the time step. Steps 1 - 4 are then repeated for the next time step until the simulation ends.

A.2.5 VERIFICATION OF ECP

The UM model was originally written in TURBO PASCAL and was converted into FORTRAN and included in ECP. The comparison between the results from UM of PLUMES and UM of ECP shows an exact match (**Figure A.11**) and the conversion of the UM model is verified.

Output from UM Model of PLUMES

depth (m)	dilution (m)	horiz dis	
50.000	1.000	0.000	
49.761	1.971	0.005	
49.311	3.913	0.035	
48.585	7.797	0.127	
47.525	15.566	0.327	
46.035	31.104	0.696	
45.928	32.424	0.725	merging
43.228	62.180	1.529	
37.335	124.335	3.385	
25.609	248.651	7.517	
22.323	285.625	8.893	trap level
15.436	395.624	12.750	begin overlap, dilution
	overestimated		
14.308	442.027	13.760	surface hit

Output from UM Model of ECP

depth (m)	dilution (m)	horiz dis	
50.000	1.000	0.000	
49.761	1.971	0.005	
49.311	3.913	0.035	
48.585	7.797	0.127	
47.525	15.566	0.327	
46.035	31.104	0.696	
45.928	32.424	0.725	merging
43.228	62.180	1.529	
37.335	124.335	3.385	
25.609	248.651	7.517	
22.323	285.625	8.893	trap level
15.436	395.624	12.750	begin overlap, dilution
	overestimated		
14.308	442.027	13.760	surface hit

Figure A.11 Comparison of outputs from UM of PLUMES and ECP

Mass conservation within ECP was tested by simulating an idealized lake with a single outfall (inflow) and no outflow. Total mass of both a conservative tracer and total phosphorus (TP) in the lake was calculated at each time step and compared with a similar simulation using ELCOM/CAEDYM (where the outfall was treated as a single inflow). Less than 0.1% difference was found for the conservative tracer and less than 1% difference was found for TP at the end of a one-year simulation. These small differences indicate that mass conservation within the ECP code is comparable to that of ELCOM/CAEDYM.

The accuracy of ECP can also be qualitatively evaluated by simulating the behavior of a plume under stratified and unstratified ambient conditions. **Figure A.12** shows that ECP correctly predicts surfacing of the plume under unstratified conditions and the level of insertion of the plume under stratified conditions.

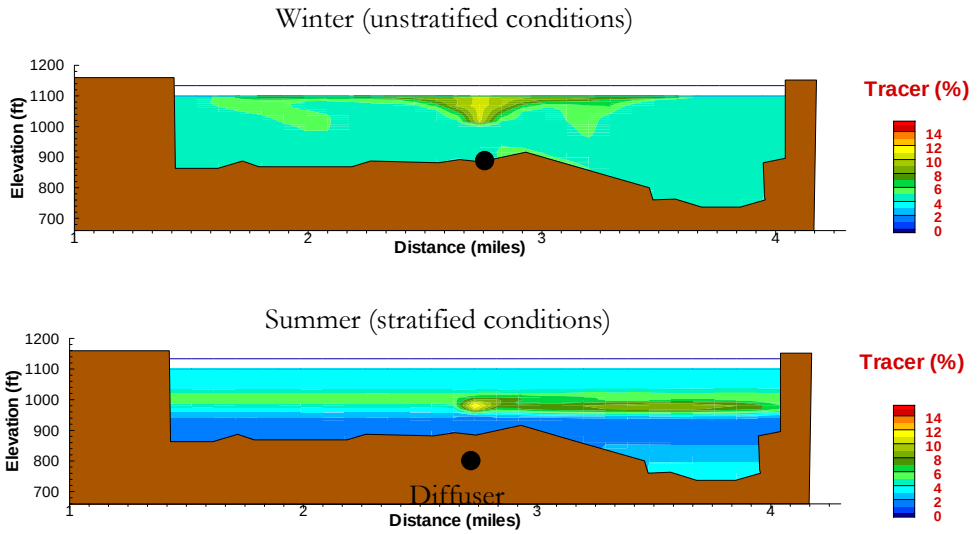

Figure A.12 Comparison of tracer concentrations released from an outfall under stratified and unstratified conditions using ECP.

A.3 BIBLIOGRAPHY

A.3.1 REFERENCED IN TEXT

Amorocho, J. and DeVries, J.J. (1980). "A new evaluation of the wind stress coefficient over water surfaces," Journal of Geophysical Research, 85:433-442.

Antenucci, Jason (2004). "Tracing Short-Circuiting Potential," from CWR Models: Bytes and Nybbles, Autumn 2004, Issue 10, page 2.

Antenucci, Jason (2004). "New Metals Model for CAEDYM," from CWR Services: Bytes and Nybbles, December 2004, Issue 11, page 1.

Appt, Jochen (January 2000), "Review on the modeling of short period internal waves in lakes with focus on Lake Constance," Pfaffenwaldring 61, D-70550 Stuttgart, Universität Stuttgart, Institut für Hydraulik und Grandmaster, Stuttgart.

Appt, J., Imberger, J., Kobus, H. (2004), "Basin-scale motion in stratified Upper Lake Constance," Limnology and Oceanography, 49(4), 919-933

Baumgartner, D. J., Frick, W. E. & Roberts, P. J. W. (1994), Dilution Models for Effluent Discharges (3rd ed.), *United States Environmental Protection Agency (EPA/600/R-94/086).*

Casulli, Vincenzo and Cheng, Ralph T. (1992), "Semi-implicit finite difference methods for three-dimensional shallow water flow," *International Journal for Numerical Methods in Fluids*, **15**, 629-48.

CWR, "Limnological Study of Lake Burragorang," Centre For Water Research, The University of Western Australia, Chapter 4 excerpt from report, pp. 104-126.

Fischer, H.B., List, E.J., Koh, R.C.Y., Imberger, J. & Brooks, N.H. (1979), Mixing in Inland and Coastal Waters, *Academic Press, New York*

Hamilton, D. (1997). "An integrated ecological model for catchment hydrology and water quality for the Swan and Canning Rivers," presented at the 2nd International Symposium on Ecology and Engineering, 10-12 November 1997, Freemantle, Australia. IAHR Eco-Hydraulics section.

Hamilton, D.P. and S.G. Schladow (1997), "Prediction of water quality in lakes and reservoirs: Part I: Model description," *Ecological Modelling, 96*, 91-110.

Herzfeld, M. and Hamilton, D. (1998), "A computational aquatic ecosystem dynamics model for the Swan River," *EOS Trans. AGU*, **79**(1), Ocean Sciences Meet. Suppl. OS11P-02.

Herzfeld, M.; Hodges, B.R.; and Hamilton, D. (1998), "Modelling the Swan River on small temporal and spatial scales," The Swan Canning Estuary conference, York, Australia, Apr., 1998.

Herzfeld, M.; Hamilton, D.; and Hodges, B.R. (1997), "Reality vs. management: The role of ecological numerical models," *2nd International Symposium on Ecology and Engineering*, 10-12 November 1997, Fremantle, Australia, IAHR Eco-Hydraulics section.

Hipsey, M.R., Romero, J.R., Antenucci, J.P. and Hamilton, D. (2005) "Computational Aquatic Ecosystem Dynamics Model: CAEDYM: v2.2 Science Manual", Centre for Water Research, The University of Western Australia.

Hipsey, M.R., Romero, J.R., Antenucci, J.P. and Hamilton, D. (2005) "Computational Aquatic Ecosystem Dynamics Model: CAEDYM: v2.2 User Manual", Centre for Water Research, The University of Western Australia.

Hodges, B.R. (1998), "Hydrodynamics of differential heat absorption," *Environmental Mechanics Laboratory Seminar*, Dept. of Civil Eng., Stanford University, Feb. 1998.

Hodges, B.R. and Dallimore C (2006), "Estuary Lake and Coastal Ocean Model: ELCOM v2.2 Science Manual", Centre for Water Research, The University of Western Australia.

Hodges, B.R. and Dallimore C (2007), "Estuary Lake and Coastal Ocean Model: ELCOM v2.2 User Manual", Centre for Water Research, The University of Western Australia.

Hodges, B.R. and Herzfeld, M. (1997), "Coupling of hydrodynamics and water quality for numerical simulations of Swan River," *2nd International Symposium on Ecology and Engineering*, 10-12 November, Fremantle, Australia, IAHR Eco-Hydraulics section.

Hodges, B.R.; Herzfeld, M.; Winters, K.; and Hamilton, D. (1998), "Coupling of hydrodynamics and water quality in numerical simulations," *EOS Trans. AGU*, **79**(1), Ocean Sciences Meet. Suppl. OS11P-01.

Hodges, B.R., Imberger, J., Saggio, A., and K. Winters (1999), "Modeling basin-scale internal waves in a stratified lake," *Limnology and Oceanography*), **45**(7), 1603-20.

Hodges, B.R., Yue, N., and Bruce, L. (May 27, 1999), "Swan River hydrodynamic model progress report," Centre For Water Research, The University of Western Australia, 14pp.

Jacquet, J. (1983). "Simulation of the thermal regime of rivers," In Orlob, G.T., editor, Mathematical Modeling of Water Quality: Streams, Lakes and Reservoirs, pages 150-176. Wiley-Interscience.

Kowalik, Z. and Murty, T.S. (1993). "Numerical Modeling of Ocean Dynamics," World Scientific.

Laval, B., Imberger, J., Hodges, B.R., and Stocker, R. (2003), "Modeling circulation in lakes: spatial and temporal variations," Limnology and Oceanography 48(3), 983-994.

Leonard, B.P. (1991), "The ULTIMATE conservative difference scheme applied to unsteady one-dimensional advection," *Computational Methods in Applied Mechanics and Engineering*, **88**, 17-74.

Lin, B. and Falconer, R.A. (1997). "Tidal flow and transport modeling using ULTIMATE QUICKEST," Journal of Hydraulic Engineering, 123:303-314.

Roberts, P.J.W., Snyder, W.H. & Baumgartner, D.J. (1989a), Ocean Outfalls I, Submerged wastefield formation, *J. Hydraulic Engineering*, **115**, 1-25

Roberts, P.J.W., Snyder, W.H. & Baumgartner, D.J. (1989b), Ocean Outfalls II, Spatial evolution of submerged wastefield, *J. Hydraulic Engineering*, **115**, 26-48

Roberts, P.J.W., Snyder, W.H. & Baumgartner, D.J. (1989c), Ocean Outfalls III, Effect of diffuser design on submerged wastefield, *J. Hydraulic Engineering*, **115**, 49-70

Robson, B.J. and Hamilton, D. P. (2002). "Three-Dimensional Modeling of a Microcystis bloom event in a Western Australian Estuary." Centre For Water Research, The University of Western Australia, 491- 496 pp.

Romero, J.R. and Antenucci, J. (2004). "The Tiete River: Supply for Sao Paolo, Brazil," from CWR Models: Bytes and Nybbles, Autumn 2004, Issue 10, page 4.

Romero, J.R. and Imberger, J. (1999). "Lake Pamvotis Project-Final report", ED report WP 1364 JR, Centre for Water Research, Crawley, Western Australia, Australia.

Spigel, R.H.; Imberger, J.; and Rayner, K.N. (1986), "Modeling the diurnal mixed layer," *Limnology and Oceanography*, **31**, 533-56.

Staniforth, A. and Côté, J. (1991). "Semi-Lagrangian integration schemes for atmospheric models – a review," Monthly Weather Review, 119:2206-2223.

Stevens, C. and Imberger, J. (1996). "The initial response of a stratified lake to a surface shear stress," Journal of Fluid Mechanics, 312:39-66.

Ullman, W.J. and R.C. Aller (1982), "Diffusion coefficients in nearshore marine sediments," *Limnol. Oceanogr., 27,* 552-556.

Wanninkhof, R. (1992), "Relationship between wind speed and gas exchange over the ocean," *J. Geophys. Res., 97(C5),* 7373-7382.

Yeates, Peter (2004). "ELCOM in the Venice Lagoon," from CWR Models: Bytes and Nybbles, Autumn 2004, Issue 10, page 2.

A.3.2 SUPPLEMENTAL REFERENCES

(November 1999), "Course notes, Computational aquatic ecosystem dynamics model, CAEDYM, Special introduction work session," TTF/3/Nov99, Centre for Water Research, University of Western Australia, 51pp.

(January 2000), "Course notes, Estuary & lake computer model, ELCOM, Special introduction training session," TTF/3/JAN2000, Centre for Water Research, University of Western Australia, 21pp+app.

(January 21, 2000) "Instructions for the use of the graphical user interface *modeler* in the configuration & visualization of DYRESM-CAEDYM," Draft version 2, 42pp.

Antenucci, J. and Imberger, J. (1999), "Seasonal development of long internal waves in a strongly stratified lake: Lake Kinneret," *Journal of Geophysical Research* (in preparation).

Antenucci, J. and Imberger, J. (2000), "Observation of high frequency internal waves in a large stratified lake," *5th International Symposium on Stratified Flows, (ISSF5)*, Vancouver, July 2000, **1**, 271-6.

Bailey, M.B. and Hamilton, D.H. (1997), "Wind induced sediment re-suspension: a lake wide model," *Ecological Modeling*, **99**, 217-28.

Burling, M.; Pattiaratchi, C.; and Ivey, G. (1996), "Seasonal dynamics of Shark Bay, Western Australia," *3rd National AMOS Conference*, 5-7 February 1996, University of Tasmania, Hobart, 128.

Chan, C.U.; Hamilton, D.P.; and Robson, B.J. (2001), "Modeling phytoplankton succession and biomass in a seasonal West Australian estuary," *Proceedings, SIL Congress XXVIII* (in press).

Chan, T. and Hamilton, D.P. (2001), "The effect of freshwater flow on the succession and biomass of phytoplankton in a seasonal estuary," *Marine and Freshwater Research* (in press).

De Silva, I.P.D.; Imberger, J.; and Ivey, G.N. (1997), "Localized mixing due to a breaking internal wave ray at a sloping bed," *Journal of Fluid Mechanics*, **350**, 1-27.

Eckert, W.; Imberger, J.; and Saggio, A. (1999), "Biogeochemical evolution in response to physical forcing in the water column of a warm monomictic lake," *Limnology and Oceanography* (submitted).

Gersbach, G.; Pattiaratchi, C.; Pearce, A.; and Ivey, G. (1996), "The summer dynamics of the oceanography of the south-west coast of Australia – The Capes current" *3rd National AMOS Conference*, 5-7 February 1996, University of Tasmania, Hobart, 132.

Hamilton, D.P. (1996), "An ecological model of the Swan River estuary: An integrating tool for diverse ecological and physico-chemical studies," *INTECOL's V International Wetlands Conference 1996 "Wetlands for the Future,"* September 1996, Perth, Australia.

Hamilton, D.P.; Chan, T.; Hodges, B.R.; Robson, B.J.; Bath, A.J.; and Imberger, J. (1999), "Animating the interactions of physical, chemical and biological processes to understand the dynamics of the Swan River Estuary," Combined Australian-New Zealand Limnology Conference, Lake Taupo.

Hamilton, D.P. (2000), "Record summer rainfall induces first recorded major cyanobacterial bloom in the Swan River," *The Environmental Engineer*, **1**(1), 25.

Hamilton, D.; Hodges, B.; Robson, B.; and Kelsey, P. (2000), "Why a freshwater blue-green algal bloom occurred in an estuary: the Microcystis bloom in the Swan River Estuary in 2000," Western Australian Marine Science Conference 2000, Path, Western Australia.

Hamilton, D.P.; Chan, T.; Robb, M.S.; Pattiaratchi, C.B.; Herzfeld, M.; and Hodges, B. (2001), "Physical effects of artificial destratification in the upper Swan River Estuary," *Hydrological Processes*.

Heinz, G.; Imberger, J.; and Schimmele, M. (1990), "Vertical mixing in Überlinger See, western part of Lake Constance," *Aquat. Sci.*, **52**, 256-68.

Herzfeld, M. (1996), "Sea surface temperature and circulation in the Great Australian bight," Ph.D. Thesis, School of Earth Science, Flinders University, South Australia.

Herzfeld, M. and Hamilton, D. (1997), "A computational aquatic ecosystem dynamics model for the Swan River, Western Australia," *MODSIM '97, International Congress on Modeling and Simulation Proceedings*, 8-11 December, 1997, University of Tasmania, Hobart, **2**, 663-8.

Herzfeld, Michael (May 28, 1999), "Computational aquatic ecosystem dynamics model (CAEDYM), An ecological water quality model designed for coupling with hydrodynamic drivers, Programmer's guide," Centre for Water Research, The University of Western Australia, Nedlands, Australia, 133pp.

Hodges, Ben R. (July 1991), "Pressure-driven flow through an orifice for two stratified, immiscible liquids," M.S. thesis, The George Washington University, School of Engineering and Applied Science.

Hodges, Ben R. (March 1997), "Numerical simulation of nonlinear free-surface waves on a turbulent open-channel flow," Ph.D. dissertation, Stanford University, Dept. of Civil Engineering.

Hodges, Ben R. (June 9, 1998), "Heat budget and thermodynamics at a free surface: Some theory and numerical implementation (revision 1.0c)," Working manuscript, Centre for Water Research, The University of Western Australia, 14pp.

Hodges, Ben R. (1999), "Numerical techniques in CWR-ELCOM," Technical report, Centre for Water Research, The University of Western Australia. (in preparation)

Hodges, Ben R. (2000), "Recirculation and equilibrium displacement of the thermocline in a wind-driven stratified lake," *5th International Symposium on Stratified Flows, (ISSF5)*, Vancouver, July 2000, **1**, 327-30.

Hodges, B.R., Herzfeld, M., and Hamilton, D. (1998), "A computational aquatic ecosystem dynamics model for the Swan River," *EOS Trans. AGU*, **79**(1), Ocean Sciences Meet. Suppl. OS11P-02.

Hodges, B.; Herzfeld, M.; Winters, K.; and Hamilton, D. (1998), "Interactions of a surface gravity waves and a sheared turbulent current," *EOS Trans. AGU*, **79**(1), Ocean Sciences Meet. Suppl. OS53.

Hodges, B.R. and Street, R.L. (1999), "On simulation of turbulent nonlinear free-surface flow," *Journal of Computational Physics*, **151**, 425-57.

Hodges, B.R.; Imberger, J.; Laval, B.; and Appt, J. (2000), "Modeling the hydrodynamics of stratified lakes," *Fourth International conference on HydroInformatics*, Iowa Institute of Hydraulic Research, Iowa City, 23-27 July 2000.

Hodges, B.R. and Imberger, J. (2001), "Simple curvilinear method for numerical methods of open channels," *Journal of Hydraulic Engineering*, **127**(11), 949-58.

Hodges, Ben R. and Street, Robert L. (1996), "Three-dimensional, nonlinear, viscous wave interactions in a sloshing tank," *Proceedings of the Fluid Engineering Summer Meeting 1996*, Vol. **3**, FED-Vol. **238**, ASME, 361-7.

Hodges, Ben R. and Street, Robert L. (1998), "Wave-induced enstrophy and dissipation in a sheared turbulent current," *Proceedings of the Thirteenth Australian fluid Mechanics Conference*, M.C. Thompson and K. Hourigan (eds.), Monash University, Melbourne, Australia, 13-18 December 1998, Vol. **2**, 717-20.

Hodges, B.R., Street, R.L., and Zang, Y. (1996), "A method for simulation of viscous, non-linear, free-surface flows," *Twentieth Symposium on Naval Hydrodynamics*, National Academy Press, 791-809.

Hollan, E. (1998), "Large inflow-driven vortices in Lake Constance," in J. Imberger (ed.), *Physical Processes in Lakes and Oceans. Coastal and Estuarine Studies*, **54,** American Geophysical Union, 123-36.

Hollan, E.; Hamblin, P.F.; and Lehn, H. (1990), "Long-term modeling of stratification in Large Lakes: Application to Lake Constance," in: Tilzer, M.M. and C. Serruya (eds.). *Large Lakes, Ecological Structure and Function***,** Berlin: Springer Verlag, 107-24.

Horn, D.A.; Imberger, J.; and Ivey, G.N. (1999), "Internal solitary waves in lakes – a closure problem for hydrostatic models," *Proceedings of 'Aha Halikoa Hawaiian Winter Workshop*, January 19-22, 1999, University of Hawaii, Manoa.

Horn, D.A.; Imberger, J.; and Ivey, G.N. (1999), "The degeneration of large-scale interfacial gravity waves in lakes," under consideration for publication in *Journal of Fluid Mechanics*.

Horn, D.A.; Imberger, J.; Ivey, G.N.; and Redekopp, L.G. (2000), "A weakly nonlinear model of long internal waves in lakes," *5th International Symposium on Stratified Flows, (ISSF5)*, Vancouver, July 2000, **1**, 331-6.

Imberger, J. (1985), "The diurnal mixed layer," *Limnology and Oceanography,* **30**(4), 737-70.

Imberger, J. (1985), "Thermal characteristics of standing waters: an illustration of dynamic processes," *Hydrobiologia,* **125,** 7-29.

Imberger, J. (1994), "Mixing and transport in a stratified lake," Preprints of *Fourth International Stratified on Flows Symposium,* Grenoble, France, June-July 1994, **3** 1-29.

Imberger, J. (1994), "Transport processes in lakes: a review," in R. Margalef (ed.), *Limnology Now: A Paradigm of Planetary Problems,* Elsevier Science, 99-193.

Imberger, J. (1998), "Flux paths in a stratified lake: A review," in J. Imberger (ed.), *Physical Processes in Lakes and Oceans. Coastal and Estuarine Studies,* **54,** American Geophysical Union, 1-18.

Imberger, J. (1998), "How does the estuary work?" WAERF Community Forum, 25 July 1998, The University of Western Australia.

Imberger, J.; Berman, T; Christian, R.R.; Sherr, E.B.; Whitney, D.E.; Pomeroy, L.R.; Wiegert, R.G.; and Wiebe, W.J. (1983), "The influence of water motion on the distribution and transport of materials in a salt marsh estuary," *Limnology and Oceanography*, **28**, 201-14.

Imberger, J. and Hamblin, P.F. (1982), "Dynamics of lakes, reservoirs, and cooling ponds," *Journal of Fluid Mechanics,* **14**, 153-87.

Imberger, J. and Head, R. (1994), "Measurement of turbulent properties in a natural system," reprinted from *Fundamentals and Advancements in Hydraulic Measurements and Experimentation*.

Imberger, J. and Ivey, G.N. (1991), "On the nature of turbulence in a stratified fluid. Part II: Application to lakes," *Journal of Physical Oceanography,* **21**(5), 659-80.

Imberger, J. and Ivey, G.N. (1993), "Boundary mixing in stratified reservoirs," *Journal of Fluid Mechanics,* **248**, 477-91.

Imberger, J. and Patterson, J.C. (1981), "A dynamic reservoir simulation model – DYRESM: 5," In H.B. Fischer (ed.) *Transport Models for Inland and Coastal Waters,* Academic Press, 310-61.

Imberger, J. and Patterson, J.C. (1990), "Physical limnology," In: *Advances in Applied Mechanics,* **27**, 303-475.

Ivey, G.N. and Corcos, G.M. (1982), "Boundary mixing in a stratified fluid," *Journal of Fluid Mechanics,* **121**, 1-26.

Ivey, G.N. and Imberger, J. (1991), "On the nature of turbulence in a stratified fluid. Part I: The energetics of mixing," *Journal of Physical Oceanography,* **21**(5), 650-8.

Ivey, G.N.; Imberger, J.; and Koseff, J.R. (1998), "Buoyancy fluxes in a stratified fluid," in J. Imberger (ed.), *Physical Processes in Lakes and Oceans. Coastal and Estuarine Studies,* **54,** American Geophysical Union, 377-88.

Ivey, G.N.; Taylor, J.R.; and Coates, M.J. (1995), "Convectively driven mixed layer growth in a rotating, stratified fluid," *Deep-Sea Research I.,* **42**(3), 331-49.

Ivey, G.N.; Winters, K.B; and De Silva; I.P.D. (1998), "Turbulent mixing in an internal wave energized benthic boundary layer on a slope," submitted to *Journal of Fluid Mechanics*.

Jandaghi Alaee, M.; Pattiaratchi, C.; and Ivey, G. (1996), "The three-dimensional structure of an island wake," *8th International Biennial Conference. Physics of Estuaries and coastal Seas (PECS)* 9-11 September 1996, the Netherlands, 177-9.

Javam, A; Teoh, S.G.; Imberger, J.; and Ivey, G.N. (1998), "Two intersecting internal wave rays: a comparison between numerical and laboratory results," in J. Imberger (ed.), *Physical Processes in Lakes and Oceans. Coastal and Estuarine Studies***, 54,** American Geophysical Union, 241-50.

Kurup, R.; Hamilton, D.P.; and Patterson, J.C. (1998), "Modeling the effects of seasonal flow variations on the position of a salt wedge in a microtidal estuary," Estuarine Coastal *and Shelf Science*, **47**(2), 191-208.

Kurup, R.G.; Hamilton, D.P.; and Phillips, R.L. (2000), "Comparison of two 2-dimensional, laterally averaged hydrodynamic model applications to the Swan River Estuary," *Mathematics and Computers in Simulation,* **51**(6), 627-39.

Laval, B.; Hodges, B.R.; and Imberger, J. (2000), "Numerical diffusion in stratified lake," *5th International Symposium on Stratified Flows, (ISSF5)*, Vancouver, July 2000, **1**, 343-8.

Lemckert, C. and Imberger, J. (1995), "Turbulent benthic boundary layers in fresh water lakes," Iutam Symposium on Physical Limnology, Broome, Australia, 409-22.

Maiss, M.; Imberger, J.; and Münnich, K.O. (1994), "Vertical mixing in Überlingersee (Lake Constance) traced by SF6 and heat," *Aquat. Sci.*, **56**(4), 329-47.

Michallet, H. and Ivey, G.N. (1999), "Experiments on mixing due to internal solitary waves breaking on uniform slopes," *Journal of Geophysical Research*, **104**, 13467-78.

Nehru, A; Eckert, W.; Ostrovosky, I.; Geifman, J.; Hadas, O.; Malinsky-Rushansky, N.; Erez, J.; and Imberger, J. (1999), "The physical regime and the respective biogeochemical processes in Lake Kinneret lower water mass," *Limnology and Oceanography*, (in press).

Ogihara, Y.; Zic, K.; Imberger, J.; and Armfield, S. (1996), "A parametric numerical model for lake hydrodynamics," *Ecological Modeling*, **86**, 271-6.

Patterson, J.C; Hamblin, P.F.; and Imberger, J. (1984), "Classification and dynamic simulation of the vertical density structure of lakes," *Limnology and Oceanography*, **29**(4), 845-61.

Pattiaratchi, C.; Backhaus, J.; Abu Shamleh, B.; Jandaghi Alaee, M.; Burling, M.; Gersbach, G.; Pang, D.; and Ranasinghe, R. (1996), "Application of a three-dimensional numerical model for the study of coastal phenomena in south-western Australia," *Proceedings of the Ocean & Atmosphere Pacific International Conference*, Adelaide, October 1995, 282-7.

Riley, G.A., H. Stommel and D.F. Bumpus, "Quantitative ecology of the plankton of the Western North Atlantic," *Bull. Bingham Oceanogr. Coll., 12(3)*, 1-69, 1949.

Robson, B.J.; Hamilton, D.P.; Hodges, B.R.; and Kelsey, P. (2000), "Record summer rainfall induces a freshwater cyanobacterial bloom in the Swan River Estuary," *Australian Limnology Society Annual Congress*, Darwin, 2000.

Saggio, A. and Imberger, J. (1998), "Internal wave weather in a stratified lake," *Limnology and Oceanography*, **43**, 1780-95.

Schladow, S.G. (1993), "Lake destratification by bubble-plume systems: Design methodology," *Journal of Hydraulic Engineering*, **119**(3), 350-69.

Smagorinsky, J. (1963) "General circulation experiments with the primitive equations, ´*Monthly Weather Review*, *91*, 99-152.

Spigel, R.H. and Imberger, J. (1980), "The classification of mixed-layer dynamics in lakes of small to medium size," *Journal of Physical Oceanography,* **10**, 1104-21.

Steele, J.H. (1962), "Environmental control of photosynthesis in the sea," *Limnol. Oceanogr., 7*, 137-150.

Taylor, J.R. (1993), "Turbulence and mixing in the boundary layer generated by shoaling internal waves," *Dynamics of Atmospheres and Oceans,* **19**, 233-58.

Thorpe, S.A. (1995), "Some dynamical effects of the sloping sides of lakes," *IUTAM Symposium on Physical Limnology*, Broome, Australia, 215-30.

Thorpe, S.A. (1998), "Some dynamical effects of internal waves and the sloping sides of lakes," in J. Imberger (ed.), *Physical Processes in Lakes and Oceans. Coastal and Estuarine Studies,* **54,** American Geophysical Union, 441-60.

Thorpe, S.A. and Lemmin, U. (1999), "Internal waves and temperature fronts on slops," *Annales Geophysicae,* **17**(9), 1227-34.

Unlauf, L; Wang, Y.; and Hutter, K. (1999), "Comparing two topography-Following primitive equation models for lake circulation," *Journal of Computational Physics,* **153**, 638-59.

Winter, K.B. and Seim, H.E. (1998), "The role of dissipation and mixing in exchange flow through a contracting channel," submitted to *Journal of Fluid Mechanics*.

Winter, K.B.; Seim, H.E.; and Finnigan, T.D. (1998), "Simulation of non-hydrostatic, density-stratified flow in irregular domains," submitted to *International Journal of Numerical Methods in Fluids*.

Zhu, S. and Imberger, J. (1994) "A three-dimensional numerical model of the response of the Australian North West Shelf to tropical cyclones," in: *J. Austral. Math. Soc. Ser.***, B 36,** 64-100.

Flow Science Incorporated
723 East Green Street , Pasadena, CA 91101
(626) 304-1134 • FAX (626) 304-9427

San Vicente Reservoir Proposed Water Quality Monitoring Program

Prepared for
City of San Diego
600 B Street, Suite 600,
San Diego, CA 92101

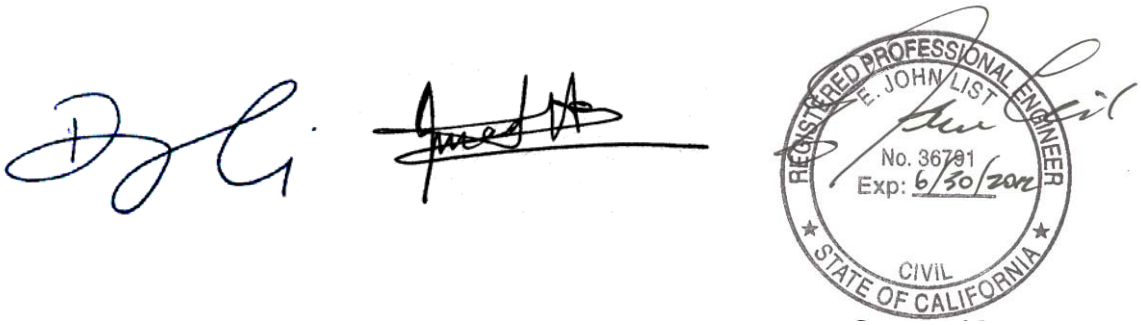

Prepared By
Li Ding, Ph.D., P.E. (VA)
Senior Engineer

Reviewed By
Imad A. Hannoun, Ph.D., P.E. (VA)
President

Reviewed By
E. John List, Ph.D., P.E. (CA)
Principal Consultant

FSI V094005
July 10, 2012

Table of Contents

1. INTRODUCTION 1

2. SVR MONITORING PLAN 3

2.1 Inflow Monitoring 5
2.2 Outflow Monitoring 9
2.3 In-Reservoir Monitoring 11
2.4 Metorological Monitoring 15

3. SPECIAL STUDIES 17

3.1 sutherland reservoir water quality 17
3.2 algal dynamics studies 17
3.3 sediment oxygen demand and nutrient release 17
3.4 tracer studies of purified water water 18

4. DATA ANALYSIS 19

4.1 Analysis of Pre IPR/RA Project Data 19
4.2 Yearly Analysis of Post IPR/RA Project Data 19

5. REFERENCES 21

FIGURES 22

List of Tables

Table 1 SVR Monitoring Sites
Table 2 Inflow Monitoring – Basic Plan
Table 3 Inflow Monitoring – Optimal Plan
Table 4 Outflow Monitoring – Basic Plan
Table 5 Outflow Monitoring – Optimal Plan
Table 6 In-reservoir Monitoring – Basic Plan
Table 7 In-reservoir Monitoring – Optimal Plan
Table 8 Meteorological Data – Basic and Optimal Plan

List of Figures

Figure 1 Location Map of San Vicente Reservoir Monitoring Stations

1. INTRODUCTION

San Vicente Reservoir (SVR) is located near Lakeside, California, and is used as a source of drinking water supply by the City of San Diego (City), its owner and operator. The reservoir currently has a capacity of about 90,000 acre-feet (see **Figure 1**). It is undergoing an expansion that will raise the dam 117 feet and increase the reservoir's storage capacity to 247,000 acre-feet at the spillway level. The City is considering an option to augment the SVR supply by bringing advanced treated recycled water (*i.e.*, purified water) from an advanced water purification facility to SVR; *i.e.* an Indirect Potable Reuse / Reservoir Augmentation (IPR/RA) project. The purified water would be blended with other water in the reservoir. The current project – the Water Purification Demonstration Project (Demonstration Project) – will not actually put any purified water into the reservoir; rather it will study and model the reservoir augmentation process. A component of the Demonstration Project is the Limnology and Reservoir Detention Study of San Vicente Reservoir (Limnology Study).

As part of the Limnology Study, Flow Science Incorporated (FSI) has developed a numerical three-dimensional water quality model that is used to evaluate hydrodynamic and water quality effects of using purified water to augment SVR. After the model was developed its results were compared to existing field data. The results of this analysis were documented in a Technical Memorandum (TM #1) submitted to the City in 2010 (FSI, 2010). TM #1 has been peer-reviewed by the National Water Research Institute Independent Advisory Panel (IAP) that was assembled for the review of the City's Demonstration Project. After implementing suggestions proposed by the IAP, the model was deemed by IAP to be "an effective and robust tool, for 1) simulating thermoclines and hydrodynamics of the San Vicente Reservoir; 2) assessing biological water quality for nutrients; 3) assessing options for the purified water inlet location" (IAP, 2010).

Upon completion of the SVR model calibration and validation, FSI conducted simulations of purified water delivery to the expanded SVR under various projected future operating conditions using the calibrated and validated model. The simulation results and findings are presented in two separate Technical Memorandums (TM #2 and TM #3). TM #2 summarizes the hydrodynamic aspects of the modeling results and was submitted to the City on November 28, 2011 (FSI, 2011). TM #3 focuses on the water quality aspects of the modeling results and findings, with emphasis on nutrients (phosphorus and nitrogen), dissolved oxygen (DO), and algal productivity, and was submitted to the City on February 24, 2012 (FSI, 2012). Both TM#2 and TM#3 have been peer-reviewed by the IAP.

If SVR is augmented by purified water in the future, the three-dimensional model developed for the Limnology Study is expected to provide a tool for evaluating various reservoir management options, assessing residence time and dilution of the purified water within SVR, determining optimal reservoir operations for maximizing water quality, and

minimizing any potential short-circuiting between the inlet and outlet. It is expected that the model will be updated on a yearly basis using new data collected each year. In order to update the model and maintain it as a tool for assessing reservoir water quality and operations, data collection in the reservoir, as well as its inflows and outflows, will be needed. The goal of this document is to provide an outline of an initial reservoir monitoring plan to obtain these necessary data. Another goal of the monitoring plan is to identify monitoring efforts that may be needed to enhance water treatability and address future water quality regulatory issues. It is anticipated that this monitoring plan will be refined based on initial monitoring results and yet to be established regulatory requirements.

This memorandum is organized in four sections. Section 1 is this Introduction. Section 2 identifies the ongoing future data needs that are required to support the goals of the IPR/RA project. Such needs are deemed either "basic" or "optimal". Basic data needs refer to the minimum level of information required to support the goals of the project and future modeling. Optimal data needs define some additional monitoring efforts that may be required to support analysis of future regulatory issues, and to further enhance the water quality modeling ability.

Section 3 of this document identifies some special studies or monitoring efforts that are needed to enhance our understanding of the reservoir. Such studies are typically of short and limited duration. The specific goals of such studies are to clarify various reservoir mixing and water quality processes that can enhance the operational efficiency of the reservoir.

Section 4 of this document identifies data compilation and analysis needs that are necessary to the continuing success of the modeling effort and the understanding of water quality in the reservoir. A key proposed task is the compilation and archiving of all historical and future data (as they become available) into a central repository. After the data are archived, data analysis will be performed to identify various water quality trends. It is also recommended that a yearly data analysis report be issued as part of the future data collection effort.

2. SVR MONITORING PLAN

The SVR monitoring plan will include periodic sampling and measurement of physical, chemical, and biological parameters for inflows, outflows, and at in-reservoir locations. It also includes on-site measurements of meteorological data. Two alternate monitoring plans are proposed to match differing goals, resources, and funding. The "basic" monitoring plan is intended to meet minimum requirements for achieving the monitoring plan goals, while the "optimal" monitoring plan can provide a more comprehensive database to further improve understanding of the reservoir's limnology and enhance the water quality model with additional resources. The "optimal" monitoring plan is essentially an expanded version of the "basic" plan, but involves monitoring at more locations and reservoir depths, as well as more water quality parameters at a higher frequency.

Based on previous experience with modeling and analysis of historical data, the main interest in the spatial variability of water quality is expected to be along a path (i.e., a transect) connecting the location of the purified water discharge into the reservoir and the dam, as well as the path connecting San Vicente Creek (a main stream inflow with additional water transfer from Sutherland reservoir) and the dam. This expected variability was considered in selecting the in-reservoir monitoring stations. **Table 1** provides a list of proposed monitoring stations at the inflow locations, outflow locations, and in the reservoir. A map of these station locations is shown in **Figure 1**. It is noted that many of these stations have been monitored either routinely, or as part of the tracer studies that were performed in 1995 (FSI, 1995).

The selection of monitoring parameters depends on anticipated water quality issues. The important water quality parameters for SVR include metals, DO, nutrients (*i.e.*, phosphorus and nitrogen) and associated biological productivity. Some additional physical, chemical, and biological parameters will also be measured to help with the basic understanding of the reservoir. Meteorological data are needed as they are important drivers for the water quality model.

The monitoring plan is divided into four categories: inflow monitoring, outflow monitoring, in-reservoir monitoring, and meteorological monitoring. The "optimal" and "basic" plans are proposed for each category and are discussed in greater detail in the following sections.

Table 1. SVR Monitoring Sites

Site #	Abbreviation	Type	Location	Notes
1	BAR	Inflow Station	Barona Creek	
2	SNC	Inflow Station	San Vicente Creek	Includes the water transfer from Sutherland
3	KIM	Inflow Station	Kimball Creek	Also known as West Fork San Vicente Creek
4	TOL	Inflow Station	Toll Road Creek	
5	AQA	Inflow Station	Aqueduct Creek	Aqueduct Creek is a natural water course. It is not to be confused with the First San Diego Aqueduct, which conveys imported water.
6	AQW	Inflow Station	The First San Diego Aqueduct	The imported water through the First San Diego Aqueduct
7	PWI	Inflow Station	Purified Water Inflow	Optional, can be replaced by using flow rate and water quality measured at the APWF effluent
8	SVPL	Outflow Station	Dam outflow	San Vicente Pipeline #1 downstream of dam
9	SVA	In-reservoir Station	Lat: 32.9129 Lon: -116.0250	Near the Dam, the original Station A currently sampled by the city
10	SVC	In-reservoir Station	Lat: 32.9225 Lon: -116.9221	Main body of the reservoir to the west of Lowell Island
11	SVG	In-reservoir Station	Lat: 32.9295 Lon: -116.9071	Main body of the reservoir to the east of Lowell Island
12	SVH	In-reservoir Station	Lat: 32.9400 Lon: -116.9097	In Kimball Arm and near the largest surface stream inflow, San Vicente Creek
13	SVN	In-reservoir Station	Lat: 32.9201 Lon: -116.9131	Near the Design Purified Water Inlet Location
14	SVWX East	Meteorological Station	On the east side of Lowell Island	Meteorology Station
15	SVWX West	Meteorological Station	On the west side of Lowell Island	Meteorology Station

2.1 INFLOW MONITORING

There are five surface streams that flow into SVR: Barona Creek, San Vicente Creek, Kimball Creek, Toll Road Creek, and Aqueduct Creek (Aqueduct Creek is different from the imported water inflow through the First San Diego Aqueduct). In addition, the imported water flows into SVR through the First San Diego Aqueduct (**Figure 1**). The water transfer from Sutherland Reservoir enters SVR through San Vicente Creek. Monitoring these inflows for water quantity and quality will be required in order to provide important input data for future modeling and water and nutrient loading calculations.

The list of suggested inflow monitoring parameters, locations, and monitoring frequency is provided in **Table 2** for the "basic" monitoring plan. Field measurements for parameters such as temperature and DO should be done *in situ* using a sonde (such as a YSI or Hydrolab profiler). For parameters that require laboratory analysis (such as nutrients, please refer to **Table 2**), discrete grab samples are required. Such samples would then be preserved and transferred to a laboratory for analysis. The purpose for monitoring certain parameters, listed in the table for reference, includes the need for model input, model verification, or water treatability. In the "basic" monitoring plan, the *in situ* measurements at the First San Diego Aqueduct (AQW) and San Vicente Creek (SNC) are suggested to be done continuously *i.e.*, daily or hourly results because the flows at these sites are more or less continuous and there is a man-made structure to locate autonomous monitoring equipment. The other four inflows (BAR, KIM, TOL, and AQA) have highly variable flows and are located in steep rocky natural channels. It is not possible to deploy autonomous monitoring equipment at these sites and each monitoring event is necessarily a stand-alone visit. It is suggested that monitoring be done monthly at these four creek inflows. For parameters that require laboratory analysis, monthly grab sampling is suggested for all inflow sites. This sampling frequency provides a modest resolution of the water quality's temporal variation in the inflows with relatively less resources required and a lower cost.

During wet-weather events (*i.e.*, storms), both flow and nutrient loadings may be large and highly variable. Thus, both flows and nutrient levels in the inflow need to be monitored during representative wet-weather events to characterize flow and nutrient loadings. A study of available historic precipitation data shows that there are a total of 8 days with daily precipitation greater than 0.5 inch between 10/26/2004 and 1/1/2008, a period of on-site precipitation data available to the authors, and they account for 10% of the total number of days with precipitation during this period. For the monitoring plan, it is suggested that a wet-weather event be defined as an event with expected daily precipitation greater than 0.5 inch. On average, it can be expected to have about two forecasted wet-weather events per year. It is suggested for the "basic" monitoring plan that up to two wet-weather events per year be monitored on an hourly basis. The specific parameters required to be monitored during wet-weather events for the "basic" monitoring plan are listed in **Table 2**. An alternative to the

hourly sampling of the inflows during wet-weather events is to use a flow-weighted composite sampling method. This involves using an autosampler to capture representative flow-weighted composite samples during wet-weather events. Details on this method can be found in Paulsen *et al*. (2011).

Table 2. Inflow Monitoring – Basic Plan

Parameter	Units	Preferred Detection Limit	Location	Frequency	Parameter Type	Purpose
Flow	cfs	±0.5	6 Locations[2]	Daily or monthly[1,3]	In-situ	Model Input
Temperature	°C	±0.10	6 Locations[2]	Daily or monthly[1,3]	In-situ	Model Input
Dissolved Oxygen [DO]	mg/L	±0.20	6 Locations[2]	Daily or monthly[1,3]	In-situ	Model Input
pH	N/A	±0.20	6 Locations[2]	Daily or monthly[1,3]	In-situ	Model Input
Oxidation-Reduction Potential [ORP]	mV	±20	6 Locations[2]	Daily or monthly[1,3]	In-situ	Model Input
Electrical Conductivity [EC]	mS/cm	±0.5%	6 Locations[2]	Daily or monthly[1,3]	In-situ	Model Input
Specific Conductance	mS/cm	±0.01	6 Locations[2]	Daily or monthly[1,3]	In-situ	Model Input
Total Dissolved Solids [TDS]	mg/L	±1	6 Locations[2]	Daily[1] or monthly[1,3]	In-situ	Model Input
Total Nitrogen [TN]	mg/L	0.05	6 Locations[2]	Monthly[1]	Grab Sample	Model Input
Total Phosphorus [TP]	mg/L	0.01	6 Locations[2]	Monthly[1]	Grab Sample	Model Input
Nitrate [NO_3]	mg/L	0.05	6 Locations[2]	Monthly[1]	Grab Sample	Model Input
Nitrite [NO_2]	mg/L	0.05	6 Locations[2]	Monthly[1]	Grab Sample	Model Input
Ammonia [NH_4]	mg/L	0.02	6 Locations[2]	Monthly[1]	Grab Sample	Model Input
Orthophosphate [PO_4]	mg/L	0.01	6 Locations[2]	Monthly[1]	Grab Sample	Model Input
SRP	mg/L	0.01	6 Locations[2]	Monthly[1]	Grab Sample	Model Input
TOC	mg/L	0.01	6 Locations[2]	Monthly[1]	Grab Sample	Model Input
Iron [Fe]	mg/L	0.01	6 Locations[2]	Monthly	Grab Sample	Treatability
Sodium [Na]	mg/L	0.01	6 Locations[2]	Monthly	Grab Sample	Treatability
Potassium [K]	mg/L	0.1	6 Locations[2]	Monthly	Grab Sample	Treatability
Manganese [Mn]	mg/L	0.01	6 Locations[2]	Monthly	Grab Sample	Treatability

Parameter	Units	Preferred Detection Limit	Location	Frequency	Parameter Type	Purpose
Calcium [Ca]	mg/L	0.01	6 Locations[2]	Monthly	Grab Sample	Treatability
Magnesium [Mg]	mg/L	0.01	6 Locations[2]	Monthly	Grab Sample	Treatability
Carbonate [CO_3]	mg/L	0.01	6 Locations[2]	Monthly	Grab Sample	Treatability
Bicarbonate [HCO_3]	mg/L	0.01	6 Locations[2]	Monthly	Grab Sample	Treatability
Alkalinity	mg/L	0.01	6 Locations[2]	Monthly	Grab Sample	Treatability
Sulfate [SO_4]	mg/L	0.1	6 Locations[2]	Monthly	Grab Sample	Treatability
Chloride [Cl]	mg/L	0.1	6 Locations[2]	Monthly	Grab Sample	Treatability
TDS	mg/L	10	6 Locations[2]	Monthly	Grab Sample	Model Input
Chlorophyll *a*	µg/L	1	6 Locations[2]	Monthly	Grab Sample	Model Input
Phycocyanin	µg/L	1	6 Locations[2]	Monthly	Grab Sample	Treatability

Notes: 1. Hourly sampling and measurements for up to two wet-weather events (*i.e.*, daily precipitation greater than 0.5 inch) per year.
2. BAR, SNC, KIM, TOL, AQA, AQW.
3. Daily at SNC and AQW; monthly at BAR, KIM, TOL, and AQA

Table 3 lists the "optimal" monitoring plan for the inflows. The main difference between the "basic" and "optimal" monitoring plan is that the "optimal" monitoring plan suggests increasing monitoring frequency for all of the parameters that require laboratory analysis from monthly to twice monthly and to increase stand-alone monitoring visits to the four creeks [BAR, KIM, TOL, and AQA] from monthly to twice per month. This will improve resolution of water quality temporal variation in the inflows. In addition, the "optimal" monitoring plan suggests monitoring all *in situ* parameters and parameters that require laboratory analysis on an hourly basis for all wet-weather events (*i.e.*, daily precipitation greater than 0.5 inch).

Table 3. Inflow Monitoring – Optimal Plan

Parameter	Units	Preferred Detection Limit	Location	Frequency	Parameter Type	Purpose
Flow	cfs	±0.5	7 Locations[2]	Daily or twice per month[1,3]	In-situ	Model Input
Temperature	°C	±0.10	7 Locations[2]	Daily or twice per month[1,3]	In-situ	Model Input

Parameter	Units	Preferred Detection Limit	Location	Frequency	Parameter Type	Purpose
Dissolved Oxygen [DO]	mg/L	±0.20	7 Locations[2]	Daily or twice per month[1,3]	In-situ	Model Input
pH	N/A	±0.20	7 Locations[2]	Daily or twice per month[1,3]	In-situ	Model Input
Oxidation-Reduction Potential [ORP]	mV	±20	7 Locations[2]	Daily or twice per month[1,3]	In-situ	Model Input
Electrical Conductivity [EC]	mS/cm	±0.5%	7 Locations[2]	Daily or twice per month[1,3]	In-situ	Model Input
Specific Conductance	mS/cm	±0.01	7 Locations[2]	Daily or twice per month[1,3]	In-situ	Model Input
Total Dissolved Solids [TDS]	mg/L	±1	7 Locations[2]	Daily or twice per month[1,3]	In-situ	Model Input
Total Nitrogen [TN]	mg/L	0.05	7 Locations[2]	Twice per month[1]	Grab Sample	Model Input
Total Phosphorus [TP]	mg/L	0.01	7 Locations[2]	Twice per month[1]	Grab Sample	Model Input
Nitrate [NO_3]	mg/L	0.05	7 Locations[2]	Twice per month[1]	Grab Sample	Model Input
Nitrite [NO_2]	mg/L	0.05	7 Locations[2]	Twice per month[1]	Grab Sample	Model Input
Ammonia [NH4]	mg/L	0.02	7 Locations[2]	Twice per month[1]	Grab Sample	Model Input
Orthophosphate [PO_4]	mg/L	0.01	7 Locations[2]	Twice per month[1]	Grab Sample	Model Input
SRP	mg/L	0.01	7 Locations[2]	Twice per month[1]	Grab Sample	Model Input
TOC	mg/L	0.01	7 Locations[2]	Twice per month[1]	Grab Sample	Model Input
Iron [Fe]	mg/L	0.01	7 Locations[2]	Twice per month[1]	Grab Sample	Treatability
Sodium [Na]	mg/L	0.01	7 Locations[2]	Twice per month[1]	Grab Sample	Treatability
Potassium [K]	mg/L	0.1	7 Locations[2]	Twice per month[1]	Grab Sample	Treatability

Parameter	Units	Preferred Detection Limit	Location	Frequency	Parameter Type	Purpose
Manganese [Mn]	mg/L	0.01	7 Locations[2]	Twice per month[1]	Grab Sample	Treatability
Calcium [Ca]	mg/L	0.01	7 Locations[2]	Twice per month[1]	Grab Sample	Treatability
Magnesium [Mg]	mg/L	0.01	7 Locations[2]	Twice per month[1]	Grab Sample	Treatability
Carbonate [CO3]	mg/L	0.01	7 Locations[2]	Twice per month[1]	Grab Sample	Treatability
Bicarbonate [HCO3]	mg/L	0.01	7 Locations[2]	Twice per month[1]	Grab Sample	Treatability
Alkalinity	mg/L	0.01	7 Locations[2]	Twice per month[1]	Grab Sample	Treatability
Sulfate [SO4]	mg/L	0.1	7 Locations[2]	Twice per month[1]	Grab Sample	Treatability
Chloride [Cl]	mg/L	0.1	7 Locations[2]	Twice per month[1]	Grab Sample	Treatability
TDS	mg/L	10	7 Locations[2]	Twice per month[1]	Grab Sample	Model Verification
Chlorophyll *a*	µg/L	1	7 Locations[2]	Twice per month[1]	Grab Sample	Model Verification
Phycocyanin	µg/L	1	7 Locations[2]	Twice per month[1]	Grab Sample	Treatability

Notes: 1. Hourly sampling and measurements for all wet-weather events (i.e., daily precipitation greater than 0.5 inch) at BAR, SNC, KIM, TOL and AQA.
2. BAR, SNC, KIM, TOL, AQA, AQW, PWI.
3. Daily at SNC, AQW and PWI; monthly at BAR, KIM, TOL, and AQA

2.2 OUTFLOW MONITORING

The only outflow from SVR is the water withdrawn through the intake structure at the dam. Keeping an accurate record of port opening history and monitoring daily outflow rate is essential for modeling accuracy. Water temperature is relatively easy to measure and can be used to verify the accuracy of port opening records. Thus, the open ports, water temperature, and outflow rates are suggested to be monitored for the "basic" monitoring plan (**Table 4**). For the "optimal" monitoring plan, a list of water quality parameters (**Table 5**) is suggested to be monitored to enhance the modeling effort and provide information for the reservoir operation management and water treatability for downstream water treatment plant.

Table 4. Outflow Monitoring – Basic Plan

Parameter	Units	Preferred Detection Limit	Location	Frequency	Parameter Type	Purpose
Open Ports			SVPL		In-situ	Model Input
Temperature	^{o}C	±0.10	SVPL	Daily	In-situ	Model Verification
Flow	cfs	±0.5	SVPL	Daily	In-situ	Model Input

Table 5. Outflow Monitoring – Optimal Plan

Parameter	Units	Preferred Detection Limit	Location	Frequency	Parameter Type	Purpose
Open Ports			SVPL		In-situ	Model Input
Temperature	^{o}C	±0.10	SVPL	Daily	In-situ	Model Verification
Dissolved Oxygen [DO]	mg/L	±0.20	SVPL	Daily	In-situ	Model Verification
pH	N/A	±0.20	SVPL	Daily	In-situ	Model Verification
Oxidation-Reduction Potential [ORP]	mV	±20	SVPL	Daily	In-situ	Model Verification
Electrical Conductivity [EC]	mS/cm	±0.5%	SVPL	Daily	In-situ	Model Verification
Specific Conductance	mS/cm	±0.01	SVPL	Daily	In-situ	Model Verification
Total Dissolved Solids [TDS]	mg/L	±1	SVPL	Daily	In-situ	Model Verification
Flow	cfs	±0.5	SVPL	Daily	In-situ	Model Verification
Total Nitrogen [TN]	mg/L	0.05	SVPL	Twice per month	Grab Sample	Model Verification
Total Phosphorus [TP]	mg/L	0.01	SVPL	Twice per month	Grab Sample	Model Verification
Nitrate [NO_3]	mg/L	0.05	SVPL	Twice per month	Grab Sample	Model Verification
Nitrite [NO_2]	mg/L	0.05	SVPL	Twice per month	Grab Sample	Model Verification
Ammonia [NH4]	mg/L	0.02	SVPL	Twice per month	Grab Sample	Model Verification
Orthophosphate [PO_4]	mg/L	0.01	SVPL	Twice per month	Grab Sample	Model Verification

Parameter	Units	Preferred Detection Limit	Location	Frequency	Parameter Type	Purpose
SRP	mg/L	0.01	SVPL	Twice per month	Grab Sample	Model Verification
TOC	mg/L	0.01	SVPL	Twice per month	Grab Sample	Model Verification
Iron [Fe]	mg/L	0.01	SVPL	Twice per month	Grab Sample	Treatability
Sodium [Na]	mg/L	0.01	SVPL	Twice per month	Grab Sample	Treatability
Potassium [K]	mg/L	0.1	SVPL	Twice per month	Grab Sample	Treatability
Manganese [Mn]	mg/L	0.01	SVPL	Twice per month	Grab Sample	Treatability
Calcium [Ca]	mg/L	0.01	SVPL	Twice per month	Grab Sample	Treatability
Magnesium [Mg]	mg/L	0.01	SVPL	Twice per month	Grab Sample	Treatability
Carbonate [CO3]	mg/L	0.01	SVPL	Twice per month	Grab Sample	Treatability
Bicarbonate [HCO3]	mg/L	0.01	SVPL	Twice per month	Grab Sample	Treatability
Alkalinity	mg/L	0.01	SVPL	Twice per month	Grab Sample	Model Treatability
Sulfate [SO4]	mg/L	0.1	SVPL	Twice per month	Grab Sample	Treatability
Chloride [Cl]	mg/L	0.1	SVPL	Twice per month	Grab Sample	Treatability
TDS	mg/L	10	SVPL	Twice per month	Grab Sample	Model Verification
Chlorophyll *a*	µg/L	1	SVPL	Twice per month	Grab Sample	Model Verification
Phycocyanin	µg/L	1	SVPL	Twice per month	Grab Sample	Treatability

2.3 IN-RESERVOIR MONITORING

The "basic" monitoring plan suggests measuring water temperature, pH, DO, ORP, EC, specific conductance, and TDS profiles every one meter vertically in the top 30 meters, then every five meters to the bottom using a sonde (**Table 6**). This will provide adequate resolution across the thermocline. Chlorophyll *a* and phycocyanin only need to be measured

using top five meter composite samples. For other grab sample parameters to be analyzed in the laboratory, the "basic" monitoring plan suggests that they be measured at the surface and bottom, as well as at the elevations of all the submerged intake tower ports. It is also suggested that the above mentioned parameters be monitored on a monthly frequency at two in-reservoir monitoring stations: SVA and SVN. These locations are recommended because they correspond to locations close to the outlet and purified water inlet, respectively.

The "optimal" monitoring plan will increase the monitoring frequency from monthly to twice monthly (**Table 7**), providing a more detailed view of the in-reservoir water quality. It also suggests monitoring these parameters at five in-reservoir stations so a more detailed spatial view of the reservoir can be developed and compared to the model. Grab sample parameters that require laboratory analysis are suggested to be monitored at the surface, bottom, and every 10 meters in between, to provide better vertical spatial resolution. The "optimal" monitoring plan also proposes to measure the cell count and biomass of different algal species in the reservoir to study the dominant algal species within the reservoir. It is suggested that a fluorometer be attached to the sonde to measure *in vivo* chlorophyll *a* profiles to provide information on the vertical distribution of algae. Note that the fluorometer should be calibrated and verified before and during the deployment following the protocol from the manufacturer.

Table 6. In-reservoir Monitoring – Basic Plan

Parameter	Units	Preferred Detection Limit	Location	Frequency	Parameter Type	Purpose	Sampling Depth
Depth	m	±0.01	SVA, SVN	Monthly	In-situ	Model Verification	Multiple[1]
Temperature	°C	±0.10	SVA, SVN	Monthly	In-situ	Model Verification	Multiple[1]
Dissolved Oxygen [DO]	mg/L	±0.20	SVA, SVN	Monthly	In-situ	Model Verification	Multiple[1]
pH	N/A	±0.20	SVA, SVN	Monthly	In-situ	Model Verification	Multiple[1]
Oxidation-Reduction Potential [ORP]	mV	±20	SVA, SVN	Monthly	In-situ	Model Verification	Multiple[1]
Electrical Conductivity [EC]	mS/cm	±0.5%	SVA, SVN	Monthly	In-situ	Model Verification	Multiple[1]
Specific Conductance	mS/cm	±0.01	SVA, SVN	Monthly	In-situ	Model Verification	Multiple[1]
Total Dissolved Solids [TDS]	mg/L	±1	SVA, SVN	Monthly	In-situ	Model Verification	Multiple[1]
Chlorophyll *a* using profiling fluorometer	µg/L	1	SVA, SVN	Monthly	In-situ	Model Verification	Multiple[1]
Phycocyanin using profiling fluorometer	µg/L	1	SVA, SVN	Monthly	In-situ	Model Verification	Multiple[1]
Secchi Depth	m		SVA, SVN	Monthly	In-situ	Model Verification	

Parameter	Units	Preferred Detection Limit	Location	Frequency	Parameter Type	Purpose	Sampling Depth
Total Nitrogen [TN]	mg/L	0.05	SVA, SVN	Monthly	Grab Sample	Model Verification	Multiple[2]
Total Phosphorus [P]	mg/L	0.01	SVA, SVN	Monthly	Grab Sample	Model Verification	Multiple[2]
Nitrate [NO_3]	mg/L	0.05	SVA, SVN	Monthly	Grab Sample	Model Verification	Multiple[2]
Nitrite [NO_2]	mg/L	0.05	SVA, SVN	Monthly	Grab Sample	Model Verification	Multiple[2]
Ammonia [NH4]	mg/L	0.02	SVA, SVN	Monthly	Grab Sample	Model Verification	Multiple[2]
Orthophosphate [PO_4]	mg/L	0.01	SVA, SVN	Monthly	Grab Sample	Model Verification	Multiple[2]
SRP	mg/L	0.01	SVA, SVN	Monthly	Grab Sample	Model Verification	Multiple[2]
TOC	mg/L	0.01	SVA, SVN	Monthly	Grab Sample	Model Verification	Multiple[2]
Iron [Fe]	mg/L	0.01	SVA, SVN	Monthly	Grab Sample	Treatability	Multiple[2]
Sodium [Na]	mg/L	0.01	SVA, SVN	Monthly	Grab Sample	Treatability	Multiple[2]
Potassium [K]	mg/L	0.1	SVA, SVN	Monthly	Grab Sample	Treatability	Multiple[2]
Manganese [Mn]	mg/L	0.01	SVA, SVN	Monthly	Grab Sample	Treatability	Multiple[2]
Calcium [Ca]	mg/L	0.01	SVA, SVN	Monthly	Grab Sample	Treatability	Multiple[2]
Magnesium [Mg]	mg/L	0.01	SVA, SVN	Monthly	Grab Sample	Treatability	Multiple[2]
Carbonate [CO3]	mg/L	0.01	SVA, SVN	Monthly	Grab Sample	Treatability	Multiple[2]
Bicarbonate [HCO3]	mg/L	0.01	SVA, SVN	Monthly	Grab Sample	Treatability	Multiple[2]
Alkalinity	mg/L	0.01	SVA, SVN	Monthly	Grab Sample	Treatability	Multiple[2]
Sulfate [SO4]	mg/L	0.1	SVA, SVN	Monthly	Grab Sample	Treatability	Multiple[2]
Chloride [Cl]	mg/L	0.1	SVA, SVN	Monthly	Grab Sample	Treatability	Multiple[2]
TDS	mg/L	10	SVA, SVN	Monthly	Grab Sample	Model Verification	Multiple[2]
Chlorophyll *a*	µg/L	1	SVA, SVN	Monthly	Grab Sample/	Model Verification	Top 5 m composite
Phycocyanin	µg/L	1	SVA, SVN	Monthly	Grab Sample	Treatability	Top 5 m composite

Notes: 1. Sample every one meter in the top 30 meter water and every five meters for the rest water column.

2. Sample at Surface, Bottom, and at the elevations of all the submerged intake tower ports.

Table 7. In-reservoir Monitoring – Optimal Plan

Parameter	Units	Preferred Detection Limit	Location	Frequency	Parameter Type	Purpose	Sampling Depth
Depth	m	±0.01	5 Locations[3]	Twice per month	In-situ	Model Verification	Multiple[1]
Temperature	°C	±0.10	5 Locations[3]	Twice per month	In-situ	Model Verification	Multiple[1]
Dissolved Oxygen [DO]	mg/L	±0.20	5 Locations[3]	Twice per month	In-situ	Model Verification	Multiple[1]
pH	N/A	±0.20	5 Locations[3]	Twice per month	In-situ	Model Verification	Multiple[1]
Oxidation-Reduction Potential [ORP]	mV	±20	5 Locations[3]	Twice per month	In-situ	Model Verification	Multiple[1]
Electrical Conductivity [EC]	mS/cm	±0.5%	5 Locations[3]	Twice per month	In-situ	Model Verification	Multiple[1]
Specific Conductance	mS/cm	±0.01	5 Locations[3]	Twice per month	In-situ	Model Verification	Multiple[1]
Total Dissolved Solids [TDS]	mg/L	±1	5 Locations[3]	Twice per month	In-situ	Model Verification	Multiple[1]
Chlorophyll *a* using profiling fluorometer	µg/L	1	5 Locations[3]	Twice per month	In-situ	Model Verification	Multiple[1]
Phycocyanin using profiling fluorometer	µg/L	1	5 Locations[3]	Twice per month	In-situ	Model Verification	Multiple[1]
Secchi Depth	m		5 Locations[3]	Twice per month	In-situ	Model Verification	
Total Nitrogen [TN]	mg/L	0.05	5 Locations[3]	Twice per month	Grab Sample	Model Verification	Multiple[2]
Total Phosphorus [TP]	mg/L	0.01	5 Locations[3]	Twice per month	Grab Sample	Model Verification	Multiple[2]
Nitrate [NO_3]	mg/L	0.05	5 Locations[3]	Twice per month	Grab Sample	Model Verification	Multiple[2]
Nitrite [NO_2]	mg/L	0.05	5 Locations[3]	Twice per month	Grab Sample	Model Verification	Multiple[2]
Ammonia [NH4]	mg/L	0.02	5 Locations[3]	Twice per month	Grab Sample	Model Verification	Multiple[2]
Orthophosphate [PO_4]	mg/L	0.01	5 Locations[3]	Twice per month	Grab Sample	Model Verification	Multiple[2]
SRP	mg/L	0.01	5 Locations[3]	Twice per month	Grab Sample	Model Verification	Multiple[2]
TOC	mg/L	0.01	5 Locations[3]	Twice per month	Grab Sample	Model Verification	Multiple[2]
Iron [Fe]	mg/L	0.01	5 Locations[3]	Twice per month	Grab Sample	Treatability	Multiple[2]
Sodium [Na]	mg/L	0.01	5 Locations[3]	Twice per month	Grab Sample	Treatability	Multiple[2]

Parameter	Units	Preferred Detection Limit	Location	Frequency	Parameter Type	Purpose	Sampling Depth
Potassium [K]	mg/L	0.1	5 Locations[3]	Twice per month	Grab Sample	Treatability	Multiple[2]
Manganese [Mn]	mg/L	0.01	5 Locations[3]	Twice per month	Grab Sample	Treatability	Multiple[2]
Calcium [Ca]	mg/L	0.01	5 Locations[3]	Twice per month	Grab Sample	Treatability	Multiple[2]
Magnesium [Mg]	mg/L	0.01	5 Locations[3]	Twice per month	Grab Sample	Treatability	Multiple[2]
Carbonate [CO3]	mg/L	0.01	5 Locations[3]	Twice per month	Grab Sample	Treatability	Multiple[2]
Bicarbonate [HCO3]	mg/L	0.01	5 Locations[3]	Twice per month	Grab Sample	Treatability	Multiple[2]
Alkalinity	mg/L	0.01	5 Locations[3]	Twice per month	Grab Sample	Treatability	Multiple[2]
Sulfate [SO4]	mg/L	0.1	5 Locations[3]	Twice per month	Grab Sample	Treatability	Multiple[2]
Chloride [Cl]	mg/L	0.1	5 Locations[3]	Twice per month	Grab Sample	Treatability	Multiple[2]
TDS	mg/L	10	5 Locations[3]	Twice per month	Grab Sample	Model Verification	Multiple[2]
Chlorophyll *a*	µg/L	1	5 Locations[3]	Twice per month	Grab Sample	Model Verification	Top 5 m composite
Phycocyanin	µg/L	1	5 Locations[3]	Twice per month	Grab Sample	Treatability	Top 5 m composite
Algae Species Cell count and Biomass			5 Locations[3]	Twice per month	Grab Sample	Model Verification	Top 5 m composite

Notes:
1. Sample every one meter in the top 30 meter water and every five meters for the rest water column.
2. Sample at Surface, Bottom, and every 10 meters in between.
3. SVA, SVC, SVG, SVH and SVN.

2.4 METEOROLOGICAL MONITORING

Monitoring meteorological data is commonly done by instruments that automatically measure and record the data at a pre-defined frequency. There is no difference between the "basic" and "optimal" plans for meteorological monitoring. Two meteorological stations are proposed for SVR: one on the east side of Lowell Island and the other on the west side of Lowell Island. This arrangement is suggested in order to capture the wind variation on the windward and leeward sides of the island. It is expected that the western station will provide

more representative wind data when the wind is blowing from the west, and similarly when the wind is predominantly from the east.

Table 8. Meteorological Data – Basic and Optimal Plan

Parameter	Units	Preferred Detection Limit	Location	Frequency	Parameter Type	Purpose
Air Temperature	^{o}C	±0.10	SVWX East, SVWX West	every 15 minutes	In-situ	Model Input
Barometric Pressure	mBar	±0.10	SVWX East, SVWX West	every 15 minutes	In-situ	Model Input
Relative Humidity	%	±3%	SVWX East, SVWX West	every 15 minutes	In-situ	Model Input
Wind Velocity	m/s	±3%	SVWX East, SVWX West	every 15 minutes	In-situ	Model Input
Wind Direction	deg true	±3%	SVWX East, SVWX West	every 15 minutes	In-situ	Model Input
Precipitation	Mm	±4%	SVWX East, SVWX West	every 15 minutes	In-situ	Model Input
Solar Irradiance	w/m^2	±5%	SVWX East, SVWX West	every 15 minutes	In-situ	Model Input
Photosynthetically active radiation	$Umol/s/ m^2$	±5%	SVWX East, SVWX West	every 15 minutes	In-situ	Model Input

3. SPECIAL STUDIES

Section 2 discussed the ongoing data needs to help support the modeling effort, water treatability, and analysis of potential regulatory issues. In this section, we identify some short-term investigations that can enhance our understanding of various reservoir processes.

3.1 SUTHERLAND RESERVOIR WATER QUALITY

In Section 2, routine monitoring of San Vicente Creek, which transports water from Sutherland Reservoir into SVR, is discussed and outlined. Aside from routine monitoring of the creek, it is suggested that a special study be conducted to better identify the water quality in Sutherland Reservoir. In this study, monthly water quality samples will be performed for a period of 12 months. The parameters to be measured would include vertical profiles using a sonde (temperature, DO, pH, ORP, EC, specific conductance, and TDS). Furthermore, samples at three different elevations (surface, bottom, and at the outlet level) should be collected and analyzed for the parameters listed as "grab sample" in **Table 2** on monthly basis.; except that Chlorophyll *a* and Phycocyanin only need to be sampled in the top 5 m. The goal of such a study is to understand the reservoir's water quality over a yearly cycle, and to identify whether water transfer timing can be optimized to maximize water quality in SVR.

3.2 ALGAL DYNAMICS STUDIES

Laboratory and in-lake studies can provide valuable information for modeling algal dynamics. In particular, the in-situ determinations of nutrient uptake rates by algae, as well as the rate of algal growth, are important for accurate modeling of algal dynamics (Tietjen, 2011). It is suggested that a one-time study of algal growth dynamics be conducted to determine the main relationships between nutrient uptake and algal growth in the reservoir.

3.3 SEDIMENT OXYGEN DEMAND AND NUTRIENT RELEASE

Sediment oxygen demand is an important feature in determining water quality in SVR. As the sediments utilize oxygen in the hypolimnetic waters, the DO eventually gets depleted. After DO depletion, various nutrients are released from the sediments, and may contribute a significant source for subsequent algal growth. As a result, the determination of sediment oxygen demand as well as sediment nutrient release rates is important. Such a study was completed in the 1990s (Buetel, 2001, and Buetel, *et al,* 2007), but a similar follow up study is recommended after the reservoir expansion.

3.4 TRACER STUDIES OF PURIFIED WATER

If required for demonstration purposes, tracer studies can be conducted to demonstrate the fate, mixing, and dilution of the purified water inflow. These studies will be similar to the 1995 tracer studies that were performed wherein a tracer is injected in the inflow for a short duration (approximately 24 hours). The concentration of the tracer within the lake at various stations and depths would then be measured. From the results, the dilution of the tracer can be computed, as well as the residence time distribution. At least two such studies are envisioned: one during the stratified season (late spring or summer), and another during the winter turnover period, when the purified water is expected to rapidly mix within the reservoir.

4. DATA COMPILATION AND ANALYSIS

The purpose of this task is to gather all historical and future data, compile it into a database, and analyze the data with the purpose of discerning any trends. The following tasks are envisioned.

4.1 ANALYSIS OF PRE IPR/RA PROJECT DATA

This task assesses all water quality data gathered before the IPR/RA project is operational. As part of this task, all pertinent historical water quality data will be gathered and compiled in a suitable database. The database format should allow for easy manipulation of the data. After the database is established, it is recommended that a detailed data analysis be performed to include:

- An analysis of historical trends for all available inflow and in-reservoir water quality parameters, including temperature, TDS, nutrients, DO, and chlorophyll *a*. There should be a review of data integrity to include a data set clean up, if needed. Various data trends should be identified and examined. The analysis should include plotting parameters of concern and producing summary charts and tables that will help assess the reservoir water quality.
- A statistical analysis of various data to determine seasonal, yearly, and multi-year data trends. Identify any relationships between inflow and in-reservoir water quality trends. Determine the range of variation and identify the maximum, minimum and standard deviation of various water quality parameters, such as DO, chlorophyll *a*, Secchi depth, and temperature.
- A determination whether the statistics can indicate a shift in the reservoir's water quality between the old and expanded reservoir.
- Construction of a water and nutrient budget (phosphorus and nitrogen) on a yearly basis.
- Preparation of an extensive data analysis report.

4.2 YEARLY ANALYSIS OF POST IPR/RA PROJECT DATA

This task assesses water quality data gathered subsequent to the IPR/RA project becoming operational. It is suggested that, if the IPR/RA project is implemented in SVR, the various water quality data obtained under Sections 2 and 3 be appended to the data set on a yearly (or shorter time frame) basis. The data should be reviewed and any data integrity issues identified and corrected. On a yearly basis, it is expected that the following tasks would be performed.

- Analysis of all available inflow and in-reservoir water quality parameters, including temperature, TDS, nutrients, DO, and chlorophyll *a*. There should be a review of data integrity to include clean up of the data set if needed. Data trends should be identified and examined. The analysis should include plotting various water quality parameters and the production of summary charts and tables that will help assess the reservoir water quality.
- A statistical analysis of available data and a comparison of the particular year to the historical reservoir trend. Identify any relationships between inflow and in-reservoir water quality trends. Determine the range of variation and identify the maximum, minimum and standard deviation of various water quality parameters, such as DO, chlorophyll *a*, Secchi depth, temperature etc.
- A determination if statistics can indicate a shift in the reservoir's water quality between pre and post IPR/RA project.
- Construction of a yearly water and nutrient budget (phosphorus and nitrogen).
- A comparison of data to model predictions.
- A determination if model or data adjustments are needed to improve our reservoir understanding.

The expected layout of the table of contents of a typical yearly report would be as follows:

1. Introduction and purpose of monitoring
2. Summary of measured data
3. Overall assessment of data quality
4. Actions needed to correct or clean up data set
5. Detailed presentation of the data set (figures, tables, etc.)
6. Trend analysis of data set
7. Nutrient and water budget
8. Statistical parameters obtained from data set
9. Comparison of current data to data from previous years
10. Detailed comparison to model predictions
11. Recommendations for changes in future monitoring or modeling
12. Conclusions

5. REFERENCES

Buetel, M, I. Hannoun, J. Pasek, and K.B. Kavenaugh. (2007) "Evaluation of Hypolimnetic Oxygen Demand in a Large Eutrophic Raw Water Reservoir, San Vicente Reservoir, California". J. Environ. Eng. 133:130-138.

Beutel, M. (2001). "San Vicente Reservoir: Sediment-Water Interface Study" dated July 2001 and submitted to the San Diego Water Department.

Flow Science Incorporated (1995). "San Vicente Water Reclamation Project: Results of Tracer Studies, prepared for Montgomery Watson," FSI Project. P941003, Pasadena, CA.

Flow Science Incorporated (2010). "Reservoir Augmentation Demonstration Project: Limnology and Reservoir Detention Study of San Vicente Reservoir – Calibration of the Water Quality Model", FSI Project V094005, Pasadena, CA.

Flow Science Incorporated (2011). "Water Purification Demonstration Project: Limnology and Reservoir Detention Study of San Vicente Reservoir – Hydrodynamic Modeling Study", FSI Project V094005, Pasadena, CA.

Flow Science Incorporated (2012). "Water Purification Demonstration Project: Limnology and Reservoir Detention Study of San Vicente Reservoir – Nutrient and Algae Modeling Results", FSI Project V094005, Pasadena, CA.

National Water Research Institute (2010). "Findings and Recommendations of the Limnology and Reservoir Subcommittee Meeting for the Reservoir Augmentation Demonstration Project's 'Limnology and Reservoir Detention Study of the San Vicente Reservoir' " Memorandum from NWRI Independent Advisory Panel for the City of San Diego's Indirect Potable Reuse/Reservoir Augmentation Demonstration Project, June 7, 2010.

Paulsen S.C., G. Goteti, B.K. Kelly, and V. K. Yoon (2011). " Automated Flow-Weighted Composite Sampling of Stormwater Runoff in Ventura County, CA", presented at 2011 WEFTEC workshop.

Tietjen T. (2011). "Assessing the Impact of Changes in Phosphorus Concentrations on Phytoplankton Biomass in Boulder Basin, Lake Mead", presented at 2011 North American Lake Management Society Symposium.

FIGURES

Map of San Vicente Reservoir Monitoring Stations

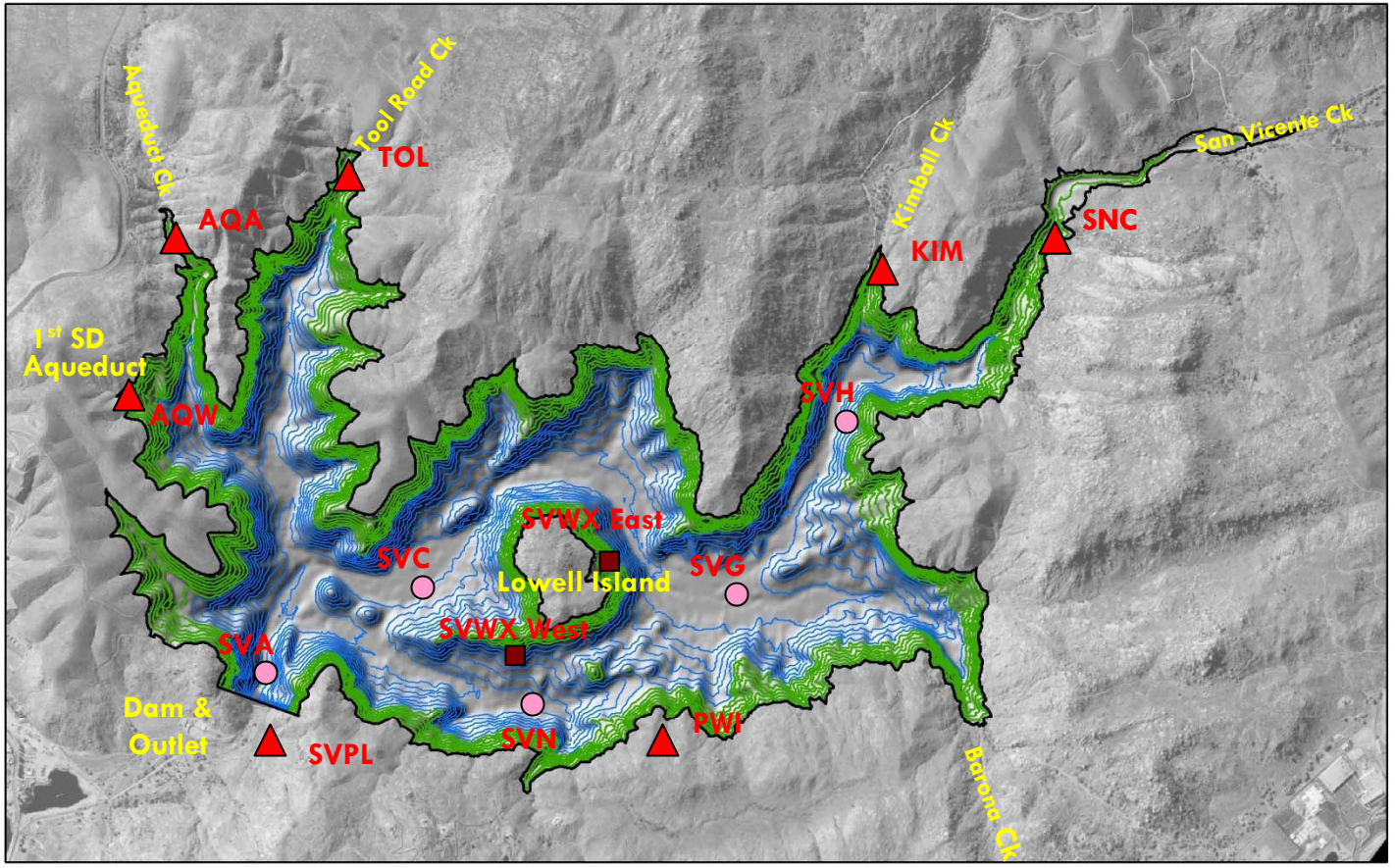

FSI V094005
July10, 2012

Figure 1

FLOW SCIENCE®